HEINRICH HEINE
UNIVERSITÄT DÜSSELDORF

Understanding the mechanism of SOS1 interactions and activation towards RAS GTPases

Dissertation

This dissertation is submitted
for the degree of the Doctor of Philosophy
to the Faculty of Mathematics and Natural Sciences
at the Heinrich-Heine-University Düsseldorf

Presented by
Neda Sadat Kazemein Jasemi

from Kermanshah, Iran

Düsseldorf, April

2021

HEINRICH HEINE
UNIVERSITÄT DÜSSELDORF

Verstehen des Mechanismus der SOS1-Interaktionen und der Aktivierung in Richtung RAS GTPases

Dissertation

zur Erlangung des Doktorgrades
der Mathematisch-Naturwissenschaftlichen Fakultät
der Heinrich-Heine-Universität Düsseldorf

vorgelegt von
Neda Sadat Kazemein Jasemi

aus Kermanshah, Iran

Düsseldorf, April

2021

Aus dem Institut für Biochemie und Molekularbiologie II
der Heinrich-Heine-Universität Düsseldorf

Gedruckt mit der Genehmigung der
Mathematisch-Naturwissenschaftlichen Fakultät der
Heinrich-Heine-Universität Düsseldorf

Referent: Prof. Dr. Reza Ahmadian
Korreferent: Prof. Dr. George Groth
Tag der mündlichen Prüfung: 2021

‘The only true wisdom is knowing you know nothing’

Socrates

Table of contents

List of figures

Summary

The RAS superfamily is a large group of GTP binding proteins, which share a common conserved G domain. They are divided into five families, including RHO, RAS, RAB, ARF, and RAN. RAS signalling is mediated *via* their physical interaction with two regulator families, GEFs (Guanine nucleotide exchange factors) and GAPs (GTPase activating proteins), and a large number of downstream effectors. GEFs accelerate the RAS activation reaction *via* GDP/GTP exchange and GAPs increase the rate of GTP hydrolysis reaction. Among all RAS GEFs in the human genome, SOS1 is the best studied RAS activator. SOS1 exists in an auto-inhibited structure in the cytoplasm due to the inter-domain interactions. Its activation takes place through its recruitment to the plasma membrane *via* GRB2 adaptor protein. This interaction occurs *via* SH3 domains of GRB2 with the proline-rich domain of SOS1. Although SOS1-GRB2 interaction is the critical step in SOS1 activation, still the biochemical mechanism of the interaction is not well understood. Here, we shed light on the SOS1-GRB2 interaction and proposed an allosteric regulation of GRB2-SOS1 interaction that is controlled by GRB2 interaction with the activated receptor at the plasma membrane. GRB2 is not the only SH3-containing protein that interacts with SOS1. SOS1 comprises more than 10 proline-rich motifs. Thus, we hypothesized that there must be other SH3-containing proteins that interact with and regulate SOS1. Therefore, we characterized the interaction of SH3 domains in the human genome with proline-rich motifs of SOS1. We proved the interaction of already reported SOS1 binding partners by clarifying the exact binding sites and also introduced new binding partners of SOS1 including SPD2A, ARHGAP12, OBSCN, RIMBP3, and SORBS1.

RHO-specific GDP-dissociation inhibitor 1 (GDI1), a different type of small GTPase regulator, binds to isoprenylated RHO GTPases and extracts them from the membrane. The mechanism and structural specificity of GDI1 remained unclear. This study provided unprecedented mechanistic details about the GDI1 function towards RHO GTPases, especially RAC1. Accordingly, membrane release of RHO GTPases by GDI1 underlies a 3-step mechanism: (1) A non-specific association of GDI with switch regions of the RHO GTPases; (2) an electrostatic switch determining the interaction specificity between the C-terminal polybasic region of RHO GTPases and two distinct negatively charged clusters of GDI1; (3) a non-specific displacement of geranylgeranyl moiety from the membrane and its sequestration into a hydrophobic cleft, effectively shielding it from the aqueous milieu. This study unambiguously challenges the paradigm of RAC1 regulation by GDI1. Besides understanding the GDI interaction, we identified and characterized the first small molecule RHO GDI1 inhibitor as a pseudo-natural product (NP) termed Rhonin. Our data revealed that Rhonin inhibits binding of the GDI1 to RHO GTPases and consequently inhibits signal transduction through a non-canonical Hedgehog pathway.

Active, GTP-bound RAS proteins selectively interact with downstream effectors and transmit signals towards multiple pathways to control diverse cellular processes, such as proliferation, differentiation and apoptosis. RAS effectors mainly are RAS association (RA) or RAS binding (RB) domain-containing proteins. Here, we investigated in-depth the specificity of the interaction of different RAS proteins with the RA domain family, called RASSFs. We found novel interactions between RRAS1, RIT1, and RALA and RASSF7, RASSF9, and RASSF1, respectively, which were systematically explored in sequence-structure-property relationship analysis, and validated by mutational analysis. These data provided a set of distinct functional properties and putative biological roles that should now be investigated in the cellular context. Mutations in RAS genes were not only found in cancers but also developmental disorders, including Noonan syndrome

(NS). We showed that the NS-causing RRAS2 variants affect highly conserved residues localized around the nucleotide binding pocket of the GTPase and are predicted to variably affect diverse aspects of RRAS2 biochemical behaviour, including nucleotide binding, GTP hydrolysis, and interaction with the effectors. Additionally, all pathogenic variants increase activation of the MAPK cascade and variably impact cell morphology and cytoskeletal rearrangement.

Zusammenfassung

Die RAS-Superfamilie ist eine große Gruppe von GTP-bindenden Proteinen, die eine gemeinsame konservierte G-Domäne teilen. Sie wird in fünf Familien unterteilt, darunter RHO, RAS, RAB, ARF und RAN. Die RAS-Signaltransduktion wird über die physikalische Interaktion mit den zwei Regulator Familien, GEFs (Guanin-Nukleotid-Austauschfaktoren) und GAPs (GTPase-aktivierende Proteine), und einer großen Anzahl von nachgeschalteten Effektoren vermittelt. GEFs beschleunigen die RAS-Aktivierungsreaktion über GDP/GTP-Austausch und GAPs erhöhen die Rate der GTP-Hydrolyse Reaktion. Unter allen RAS-GEFs im menschlichen Genom ist SOS1 der am besten untersuchte RAS-Aktivator. SOS1 existiert in einer autoinhibierten Struktur im Zytoplasma, aufgrund von Inter-Domänen Interaktionen. SOS1 Aktivierung erfolgt durch die Rekrutierung an die Plasmamembran über das Adaptorprotein GRB2. Diese Interaktion erfolgt über die SH3-Domänen von GRB2 mit der Prolin-reichen Domäne von SOS1. Obwohl die SOS1-GRB2-Interaktion der kritische Schritt in der SOS1-Aktivierung ist, ist der biochemische Mechanismus der Interaktion noch nicht gut verstanden. Hier haben wir die SOS1-GRB2-Interaktion unter die Lupe genommen und eine allosterische Regulation der GRB2-SOS1-Interaktion vorgeschlagen, die durch die GRB2-Interaktion mit dem aktivierten Rezeptor an der Plasmamembran gesteuert wird. GRB2 ist nicht das einzige SH3-haltige Protein, das mit SOS1 interagiert. SOS1 umfasst mehr als 10 Prolin-reiche Motive. Daher stellten wir die Hypothese auf, dass es weitere SH3-haltige Proteine geben muss, die mit SOS1 interagieren und es regulieren. Die Charakterisierung der Interaktion von SH3-Domänen im menschlichen Genom mit den Prolin-reichen Motiven von SOS1 bestätigte die Interaktion von nicht nur bereits berichteten, sondern auch neuen Bindungspartner von SOS1, darunter SPD2A, ARHGAP12, OBSCN, RIMBP3 und SORBS1.

Der RHO-spezifische GDP-Dissoziationsinhibitor 1 (GDI1), ein anderer Typ eines kleinen GTPase-Regulators, bindet an isoprenylierte RHO-GTPasen und extrahiert sie aus der Membran. Der Mechanismus und die strukturelle Spezifität von GDI1 blieben unklar. Diese Studie lieferte neue mechanistische Details über die Funktion von GDI1 gegenüber RHO GTPasen, insbesondere RAC1. Demnach unterliegt die Membranextraktion von RHO GTPasen durch GDI einem 3-Schritt-Mechanismus: (1) Eine unspezifische Assoziation von GDI mit der „Switch region“ der RHO-GTPasen; (2) ein elektrostatischer Schalter, der die Interaktionsspezifität zwischen der C-terminalen polybasischen Region der RHO-GTPasen und zwei unterschiedlichen negativ geladenen Regionen von GDI1 bestimmt; (3) eine unspezifische Verdrängung der Geranylgeranyl-Einheit von der Membran und ihre Sequestrierung in einen hydrophoben Spalt, der sie effektiv vom wässrigen Milieu abschirmt. Diese Studie stellt das Paradigma der RAC1-Regulation durch GDI1 eindeutig in Frage. Neben dem Verständnis der GDI-Interaktion identifizierten und charakterisierten wir den ersten niedermolekularen RHO-GDI1-Inhibitor als Pseudo-Naturprodukt (NP) mit dem Namen Rhonin. Unsere Daten zeigten, dass Rhonin die Bindung von GDI1 an RHO GTPasen hemmt und somit auch die Signaltransduktion über den nicht-kanonischen Hedgehog-Signalweg hemmt.

Aktive, GTP-gebundene RAS-Proteine interagieren selektiv mit nachgeschalteten Effektoren und leiten Signale über mehrere Signalwege weiter, um verschiedene zelluläre Prozesse wie Proliferation, Differenzierung und Apoptose zu steuern. RAS-Effektoren sind hauptsächlich RAS-Assoziations- (RA) oder RAS-Bindungsdomäne (RB) enthaltende Proteine. Hier untersuchten wir eingehend die Spezifität der Interaktion verschiedener RAS-Proteine mit der RA-Domänen-Familie, die sogenannten RASSFs. Wir fanden neuartige Interaktionen zwischen RRAS1, RIT1 und RALA und RASSF7, RASSF9 bzw. RASSF1, die systematisch in ihrer Sequenz, Struktur und Bindung untersucht und durch Mutationsanalysen validiert wurden. Diese Daten lieferten eine Reihe von unterschiedlichen funktionellen Eigenschaften und mutmaßlichen biologischen Rollen, die nun im zellulären Kontext untersucht werden sollten. Mutationen in RAS-Genen wurden nicht nur bei Krebserkrankungen, sondern auch bei Entwicklungsstörungen, einschließlich des Noonan-Syndroms (NS), gefunden. Wir konnten zeigen, dass die NS-verursachenden Mutationen in den RRAS2-Varianten hochkonservierte Aminosäuren betreffen, die um die Nukleotid-Bindungstasche der GTPase herum lokalisiert sind. Es wurde vorhergesagt, dass sie verschiedene Aspekte des biochemischen Verhaltens von RRAS2 beeinflussen, einschließlich der Nukleotidbindung, der GTP-Hydrolyse und der Interaktion mit Effektoren. Zusätzlich erhöhen alle pathogenen Varianten die Aktivierung der MAPK-Kaskade und wirken sich unterschiedlich auf die Zellmorphologie und die Reorganisation des Zytoskeletts aus.

Abbreviation

aa	amino acid
ERK	extracellular regulated kinase
FTase	farnesyltransferase
FMRP	Fragile x mental retardation protein
GAP	GTPase-activating protein
GDP	guanosine diphosphate
GEF	guanine nucleotide exchange factor
GGTase I	geranylgeranyltransferase type I
GTP	guanosine triphosphate
GTPases	guanosine triphosphatase
GRB2	growth factor receptor-bound protein 2
HRAS	Harvey rat sarcoma
HVR	hypervariable region
KRAS	Kirsten rat sarcoma
MEK	MAP/ERK kinase
MRAS	muscle rat sarcoma
NRAS	neuroblastoma rat sarcoma
PH	pleckstrin homology
PIP3	phosphoinositide 3,4,5-trisphosphate
PI3K	phosphoinositide 3-kinase
PTM	post-translational modification
RAF	rapidly accelerated fibrosarcoma
RAL	RAS like
RAP2A	RAS related protein 2A
RAS	rat sarcoma
RASD	RAS, dexamethasone-induced
RASSF	RAS-association domain family
RHO	RAS homolog
RHEB	RAS homolog enriched in brain
RRAS	related RAS
SH2	SRC homology 2
SH3	SRC homology 3
SOS	Son of sevenless

Amino acid abbreviations

Name	Letter code	Name	Letter code	Name	Letter code	Name	Letter code
Alanine	Ala (A)	Glutamic acid	Glu (E)	Leucine	Leu (L)	Serine	Ser (S)
Arginine	Arg (R)	Glutamine	Gln (Q)	Lysine	Lys (K)	Threonine	Thr (T)
Asparagine	Asn (N)	Glycine	Gly (G)	Methionine	Met (M)	Trypthophan	Trp (W)
Aspartic acid	Asp (D)	Histidine	His (H)	Phenylalanine	Phe (F)	Tyrosine	Try (Y)
Cysteine	Cys (C)	Isoleucine	Ile (I)	Proline	Pro (P)	Valine	Val (V)

Chapter I
Introduction

1.1 RAS Superfamily

The onset of RAS research dates back to 1964 when Harvey discovered HRAS (*1*) and Kirsten discovered KRAS a few years later (*2*). In 1980 RAS was introduced as an oncogene in bladder cancer and later in other cancer cell lines (*3-5*). RAS superfamily members are small guanosine triphosphatases (GTPases; 21-25 kDa) which act as binary molecular switches cycling between an active GTP bound and an inactive GDP bound form. The RAS GTPases comprise over 150 members in the human genome which are divided into five major groups based on their sequence and functional similarities, including, RAS, RHO, RAB, RAN, and ARF (Figure 1) (*6, 7*). The RHO family members play a role in the control of actin dynamic activities including cell division, migration and vesicle transportation. RHOA, RAC1, and CDC42 are the best studied RHO family members (*8-10*). The RAS family controls cellular proliferation, differentiation, and apoptosis, comprising three classical RAS paralogs (H-, K-, and N-RAS), RAP (RAP1A, RAP1B, RAP2A, and RAP2B), ARF, and RAL proteins (RALA and RALB) (*11*). The RAB and ARF families regulate vesicle trafficking (*12-14*). The RAB family is the largest GTPases family with 61 members (*15*). The RAN family regulates nuclear transportation(*16, 17*). Therefore, small GTPases play a central role in various signaling pathways and cellular functions (*18*). They interact with their effectors once they are located at the membrane in GTP bound form. Posttranslational modifications of RAS GTPases are required for their membrane association (*19*).The specific subcellular localization of RAS GTPases where they are able to interact with different effector proteins allow them to work as modulators of a remarkably complex and diverse range of cellular processes (*18*).

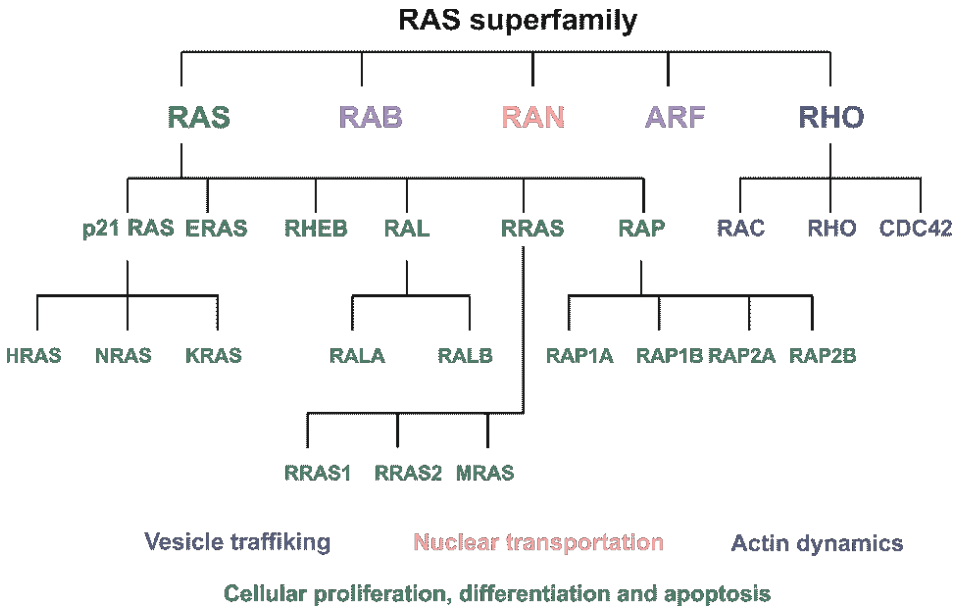

Figure 1. RAS superfamily. The RAS superfamily comprises more than 150 family members and is divided into five major groups by comparing their sequence and functional similarities. The RAS paralogs (H-, K-, and N-RAS), RAP (RAP1A, RAP 1B, RAP 2A, and RAP 2B), ARF and RAL proteins (RALA and RALB) are involved in various cellular behaviors, such as proliferation, differentiation, and apoptosis. The RHO paralogs, including RAC, RHO and CDC42, control among other processes actin dynamics.

1.2 RAS structure

RAS structure consists of six beta-strands and five alpha-helices creating two functional domains: Guanosine nucleotide binding domain (G domain) and a C-terminal membrane binding region (known as CAAX box), which is a farnesylation recognition site and enables membrane binding upon lipid modification. The G domain is a GDP/GTP binding domain containing five G motifs. The G1 motif or the P-loop binds to the beta phosphate of GDP and GTP. The G2 motif or Switch I binds to the γ-phosphate of GTP with its threonine 35 residues (H-RAS numbering). The G3 motif or Switch II contains aspartate 57 and glutamine 61. Aspartate 57 is specific for guanine versus adenine binding and glutamine 61 activates a catalytic water molecule for hydrolysis of GTP to GDP. The G4 motif interacts with guanine. The G5 motif contains alanine 146, which provides specificity for guanine rather than adenine (*6, 20*). RAS proteins include an additional C-terminal hypervariable (HV) sequence, which is located in front of the CAAX box. The hypervariable region of N-RAS, H-RAS and KRAS4A, but not KRAS4B, has a cysteine that can get modified by a palmitate fatty acid which also contributes to membrane association (Figure 2) (*21*).

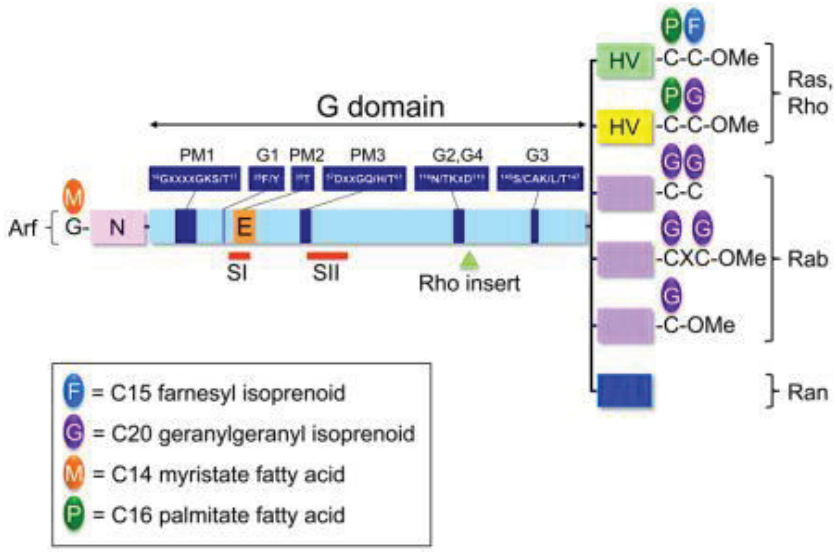

Figure 2.RAS GTPase structure. RAS GTPases have a guanosine nucleotide binding domain (G domain) containing five G motifs, a hypervariable region (HVR) and a C-terminal site (known as CAAX box) (*21*).

1.3 RAS effectors

RAS in the GTP-bound state undergoes conformational rearrangements of switch I and switch II regions that is suitable for the interaction with their effectors (*6*). Structural analysis of different RAS effectors in complexes with RAS GTPases have revealed a common domain to all RAS effectors which are responsible for the interaction with the RAS proteins. RAS effectors are characterized by presenting a domain with a ubiquitin (UB-) like topology that can be further subdivided into the RAS association (RA) domains, the RAS binding (RB) domains, and the PI3K-RB domain subfamilies (*22*). RBD and RA domains consists of about 80–100 amino acids (*23*). RAS effectors were

defined as enzymes or scaffold proteins that trigger the intracellular signaling leading to cell growth and proliferation (*24*). Conversely, a class of RAS effectors has been discovered that participate rather in growth and tumor suppressive pathways (*25, 26*). This type of RAS effectors is termed RAS association domain family (RASSF). RASSFs interact with RAS by means of a putative RA domain of all RASSF members (*26, 27*). A sequence based data analysis has shown that the largest number of UB-like domains belong to the RA family (65%), followed by the RBD (15%) and PI3K-RBD (12%) domains (Figure 3). Three UB-like domains cannot be classified due to their sequence similarity to RA and RB domains (Figure 3) (*22*).

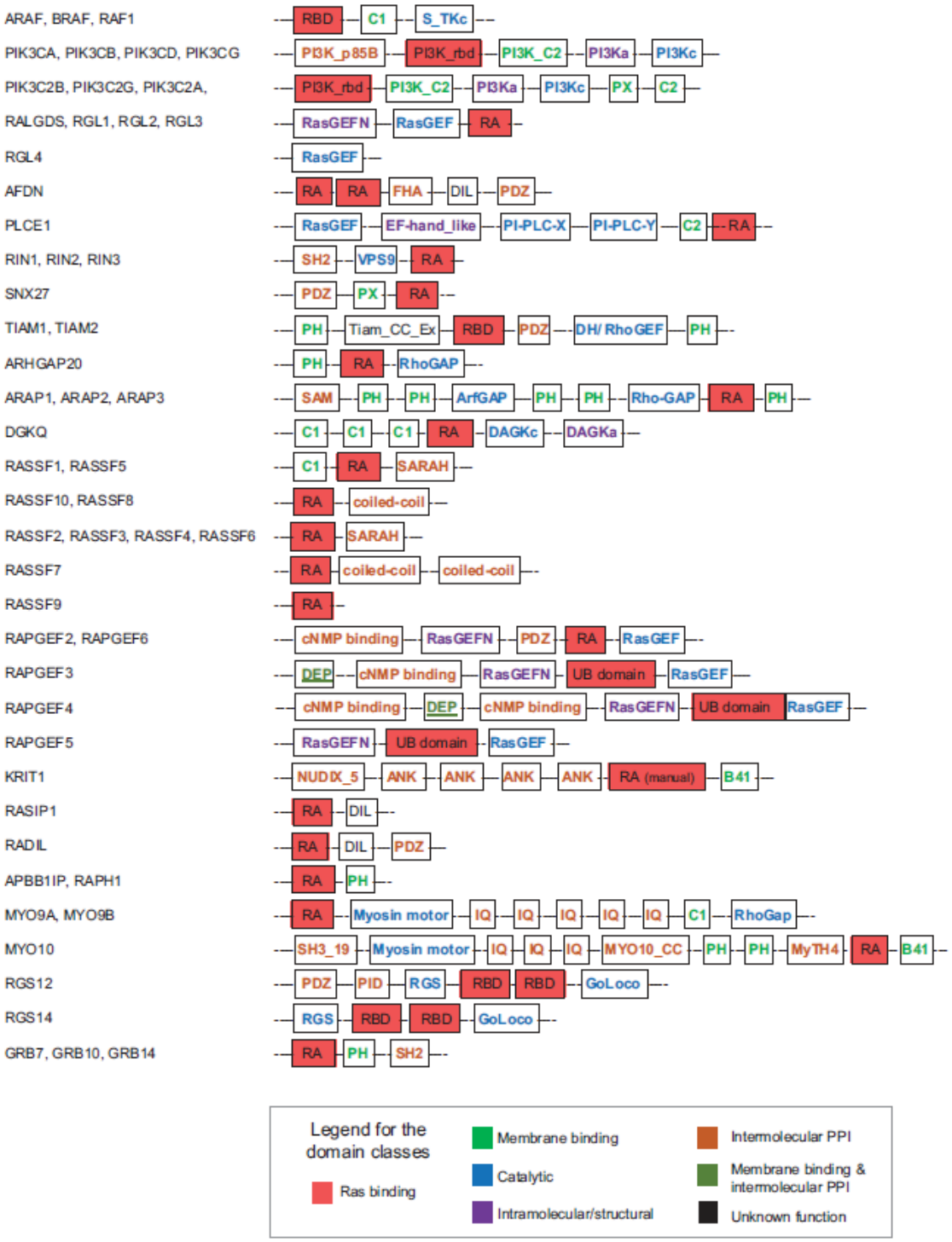

Figure 3. Domain composition of putative human RAS effectors. RAS effectors contain mainly RA, RB, PI3K-RBD and UB domains (in red) (*28*).

1.4 RAS GTPase regulation

The RAS signaling is dependent on conformational changes of RAS between GTP-bound and GDP-bound form (Figure 4). GTP-bound RAS GTPases represent the active state, which interacts with various effectors. The GppNHp-bound and GDP-bound

structures of RAS were predicted by molecular dynamics simulation in 1997 and later the crystal structure of the transient state of GTP and GDP RAS GTPases was solved in 1990, which was similar to the predicted structure (*29, 30*). The activation of RAS GTPases is catalyzed by guanine nucleotide exchange factors (GEFs), while the inactivation through GTP hydrolysis is stimulated by GTPase-activating proteins (GAPs) (*31*). The rates of GEF and GAP stimulated reactions are accelerated by several orders of magnitude (10^5) in comparison with the intrinsic nucleotide exchange and GTP hydrolysis reactions (*6, 32*). Furthermore, there are two levels of RAS GTPase regulation at the membrane. RHOGDI (RHO GDP-dissociation inhibitor) was reported to be a specific regulator for RHO GTPase family members and PDE-delta is a specific KRAS regulator. RHO GTPases are displaced from the membrane and solubilized in the cytosol by the action of RHOGDIs. There are three RHOGDI isoforms, RHOGDI1, RHOGDI2 and RHOGDI3. RHOGDI1 is ubiquitously expressed. RHOGDI2 is expressed in hematopoietic tissue, particularly in B- and T-lymphocytes, and RHOGDI3 is preferentially expressed in the brain, pancreas, lung, kidney, and testis (*33-35*). Phosphodiesterase-δ (PDEδ; also known as PDE6δ, PrBP/δ, andPDE6D) sequesters KRAS4b from the membrane to the cytoplasm and consequently enhancing its diffusion throughout the cell (*36-38*).

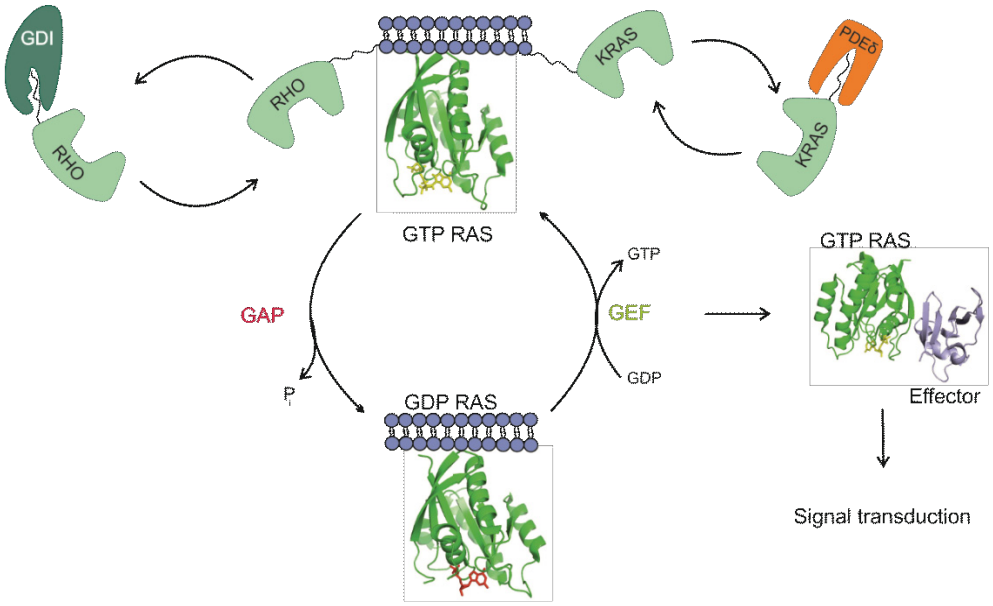

Figure 4.Schematic view of the RAS and RHO cycles. RAS and RHO cycles between GDP- and GTP-bound forms, which are regulated *via* two regulatory proteins, GEFs and GAPs, which catalyze the otherwise slow intrinsic reactions by several orders of magnitude. GTP-bound RAS proteins interact with downstream effectors and thus control various cellular functions. Two regulators PDEδ and GDI specifically and sequesters KRAS and RHO GTPases from the membrane to the cytoplasm, respectively.

1.5 Mechanism of GEF stimulated reaction

GEFs interact with the switch regions and the phosphate-binding loop of the RAS GTPases. The activation of RAS proteins starts with the dissociation of the Mg^{2+} ion, which generates a low-affinity RAS-GDP-GEF complex followed up by rapid GDP release. The catalyzed GEF reaction is dependent on the concentration of free nucleotides, such as GTP, that is required for GDP displacement (*39-41*). There were two proposed models for the GEF-catalyzed GTP/GDP exchange, substitution and displacement of GDP by GTP. In the substituted mechanism, GEF directly leads to a conformational change in RAS GTPases resulting in GDP release and GTP binding. In the displacement mechanism, GEF binds to RAS and makes a tertiary complex of RAS-GDP-GEF and GTP. The GDP is released and GTP binds to RAS (Figure 5) (*40*). Zhong Gue et al. clearly rejected this model and proposed a simple allosteric model. The displacement of the nucleotide by GEF is not the key step in the nucleotide exchange reaction. Instead, the complex of GTPase with GEF interact with guanine nucleotides that are present in cells. The excess amount of the displacing nucleotide is needed to be present over the displaced nucleotide. Usually, under cellular conditions, GTP exists in an excess amount over GDP, therefore; GTPase-GEF complex bind to GTP resulting in the release of GDP and consequently dissociation of the GEF (Fig. 5) (*42*).

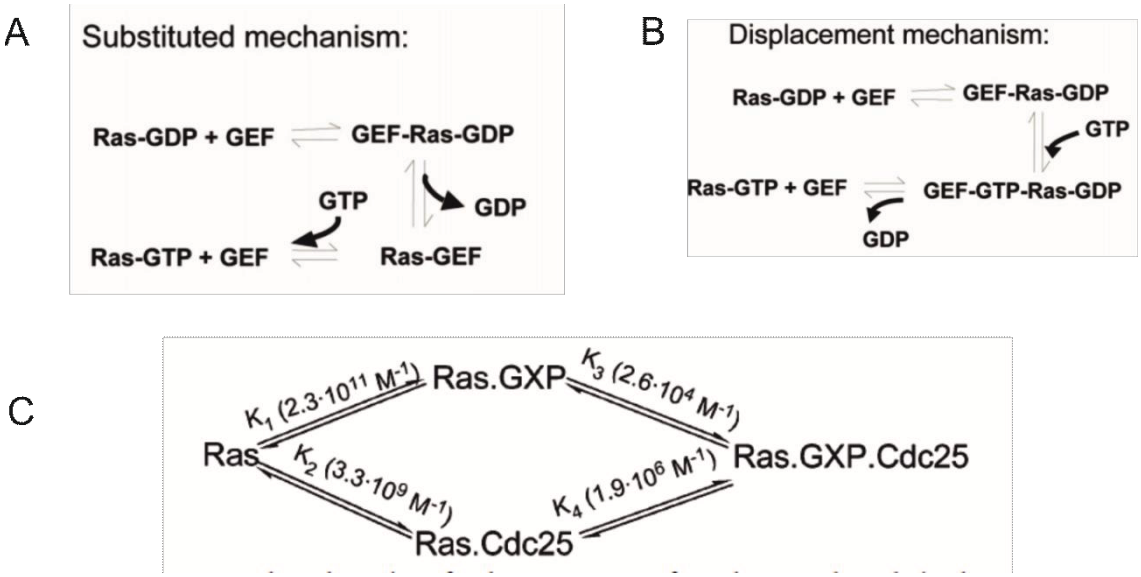

Figure 5. The mechanism of GEF stimulated nucleotide displacement in RAS GTPases. The substituted mechanism for GEF-catalyzed GDP/GTP exchange on RAS (A). The nucleotide displacement mechanism for GEF-catalyzed GDP/GTP exchange on RAS (B). The proposed nucleotide displacement mechanism by the formation of the quaternary intermediate GEF−(GDP−RAS-GTP) complex. GEF binds to RAS-GDP and GTP attacks by its phosphate moiety to the RAS nucleotide binding site. A quaternary intermediate GEF−(GDP−RAS-GTP) complex undergoes a conformation change that is suitable for the GDP binding dissociation (C). Zhong Guo et al rejected part A and B and proposed a simple allosteric model. Accordingly, the nucleotide is exchanged in the present of an excess amount of the displacing nucleotide over the displaced nucleotide (*40, 42*).

1.6 RASGEFs in human proteome

GEFs regulate activation of RAS signaling through the exchange of GDP to GTP which enables the interaction of RAS with downstream effectors. RAS GEFs are usually multidomain proteins containing a CDC25 domain that acts in combination with a RAS exchange motif (REM) domain as the catalytic machinery. Most of the human GEFs consist of a REM domain as a catalytic domain, while other domains are involved in protein-lipid and protein-protein interactions which behave as localization signals or as scaffold protein complexes. RHO GEFs contain a Dbl homology (DH) domain, playing the part in combination with a Pleckstrin homology (PH) (*43*). Some of RASGEFs also contain a DH-PH domain and are reported to serve also as RHO GEFs, such as SOS1, SOS2, RASGRF1, and RASGRF2. The most important and distributed human RAS GEFs are listed up below (Figure 6) (*44, 45*).

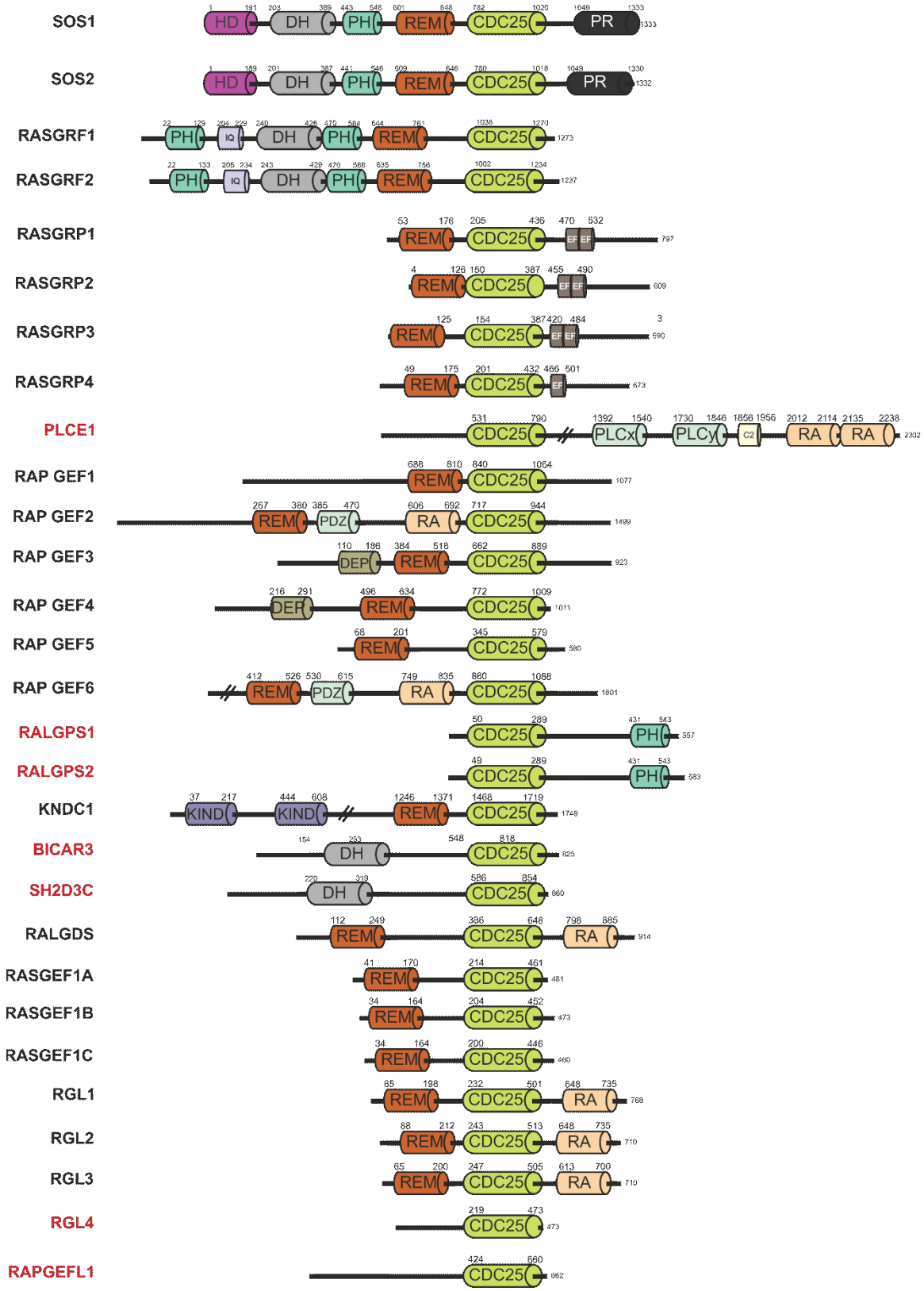

Figure 6.The most distributed RAS GEFS in the human genome. The domain organization of RASGEFs demonstrates that they mostly share a REM-CDC25 tandem as a catalytic machine. In a few cases, CDC25 alone is responsible for the catalytic activity of the nucleotide exchange reaction (in red).

1.7 Son of sevenless

Son of Sevenless (SOS) was discovered in *Drosophila melanogaster* as a key factor for normal eye development (*46*). The development of the Drosophila eye is controlled by intercellular signaling mechanisms similar to other developmental processes. Activation of the Sevenless receptor tyrosine kinase is required for the specification of the R7 photoreceptor cell in each of the 800 single eye units (ommatidia) of the developing Drosophila eye (*46*). Activation of RAS by SOS is a fundamental step in normal eye development in Drosophila. SOS1 mutation was reported to disrupt the normal eye development in this specie. SOS has two human homologs, SOS1 and SOS2. SOS1 protein is a widely distributed RASGEF in human compassing 1333 amino acids (aa). SOS1 also has been found to be a key player in T-cell development (*47-52*).

1.8 SOS1 domain organization

SOS1 is a multidomain protein and every single domain has a distinct function. The regulation of SOS1 activity is governed by the operations of its intra-domain interactions (*53-56*). SOS1 holds several domains, for instance, the Histone domain (HD), the Dbl homology (DH) and the Pleckstrin homology (PH), REM, CDC25, and the proline-rich domain (Figure 7).

HD accommodates two tandem histone folds. It negatively adjusts SOS1 activity by stabilizing an auto inhibitory structure of SOS1 (*57-59*).

DH domains share about ~200 aa and have been proposed to act as RHOGEFs in different studies (*60*). Dbl was experimentally identified as an oncogene in the NIHT3T cell line (*61, 62*). Later it was reported to be a GEF for CDC42 (*63*). SOS1 DH domain has been described to be a specific GEF for RAC1 (*45*).

DH domain is mostly followed by the PH domain (*43*), which is well known as a phosphoinositide recognition domain (*64, 65*). It was exhibited that DH activity was not altered by the binding of the PH domain to the liposome (*66*). The N-terminal domains of SOS1 including HD, DH, and PH negatively administer the CDC25 activity. Their interaction with the C-terminus of SOS1 modifies its conformation into an autoinhibited structure. SOS1 recruitment to the plasma membrane and interaction of its PH domain with the membrane has been introduced to be a standout step in the SOS1 activation (*57, 67, 68*).

SOS1 carries a helical hairpin containing helices αH and αI between its PH and REM domains that displace the switch I region of RAS from the nucleotide binding site (*69*). CDC25 is the core region of SOS1 catalytic activity sharing high sequence similarities to CDC25, a RASGEF in Saccharomyces cerevisiae (*70*). The catalytic center of SOS1, CAT, composes of REM and CDC25 domains. The crystal structure of CAT clearly exhibits two RAS binding sites, with REM as an allosteric binding site and CDC25 as a catalytic RAS binding site (*71*). Cooperation of activated RAS to the allosteric binding site commands a conformational change of CDC25, which in turn catalyzes the nucleotide exchange of RAS (*69*).

The proline-rich domain (PRD) is placed at the C-terminus of SOS1 and exposes binding sites for SH3 domain-containing proteins, such as GRB2. SH3 domains usually comprise about 60 aa and commit protein-protein interaction in different signaling pathways (*72, 73*). Interaction of GRB2 SH3 domains with SOS1 PRD is engaged in the recruitment of SOS1 to the plasma membrane where RAS GTPases are localized. SOS1 recruitment to the plasma membrane facilitates the unleash of SOS1 autoinhibition (*67, 74, 75*).

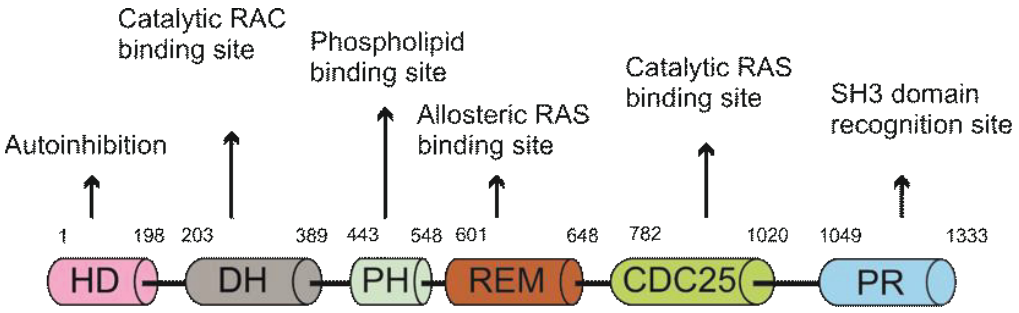

Figure 7. SOS1 domain organization. SOS1 is a multidomain protein and each domain has a distinct function in the control of SOS1 activity.

1.9 SOS1 Regulation

SOS1 exists in an autoinhibited structure in the cytoplasm in which DH binds to REM and conceals the allosteric site of REM (*76, 77*). HD interacts with the DH PH SOS1 domains and stabilizes the autoinhibited structure of SOS1 (*57*). Interaction of PH domain with phosphatidylinositol 4,5-bisphosphate (PIP2), relieves the autoinhibition (Figure 8) (*56, 78*). SOS1 recruitment to the plasma membrane is a milestone for its activation. The GRB2 adaptor protein engages with SOS1 PRD *via* its SH3 domains and recruits SOS1 to the plasma membrane.

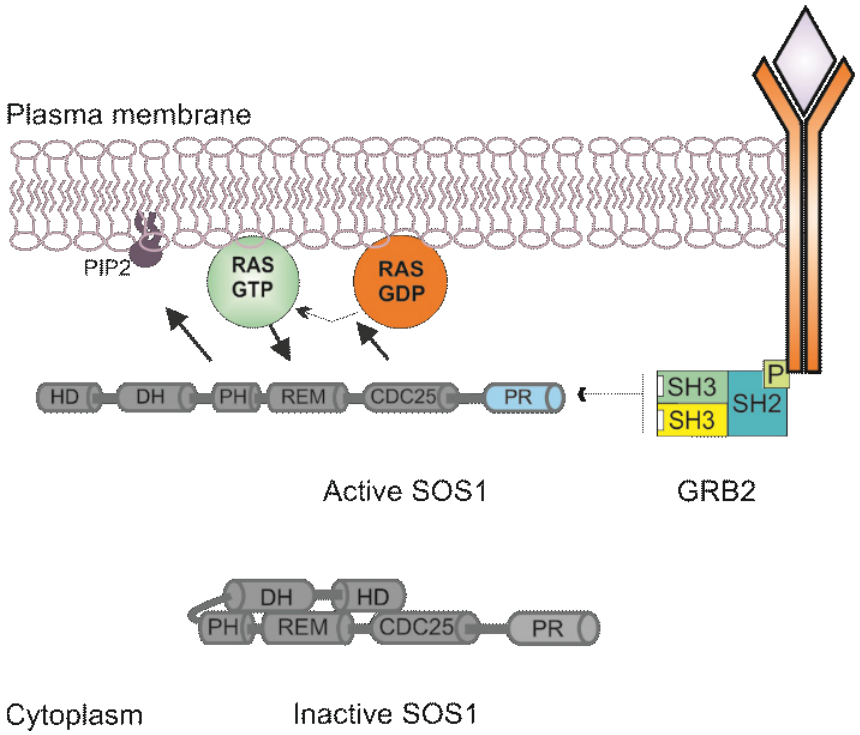

Figure 8.The mechanism of SOS1 activation at the membrane. SOS1 activation is a multistep process, mainly regulated *via* intra-domain interactions. Interaction of SOS1 domains in cytoplasm results in an autoinhibited structure of SOS1. DH domain interacts with the REM domain and blocks the allosteric binding site of RAS proteins. HD stabilizes the inhibited structure of SOS1. Upon receptor activation, SOS1 is recruited to the plasma membrane *via* adaptor protein GRB2. SOS1 binds to the membrane *via* its PH domain which in turn releases its autoinhibited state. The allosteric RAS binding site consequently is free for association with active RAS leading to activation of CDC25 and RAS activation.

1.10 Mechanism of SOS1-catalyzed RAS activation

The activity of the CAT domain is supervised by the allosteric effect of activated RAS. It is disclosed that SOS1 can get activated by its product in a positive feedback regulation (*79*). The crystal structure of human HRAS in complex with the CAT domain of SOS1 uncovered HRAS activation by SOS1. SOS1 disrupts the tight interaction of nucleotides with RAS by the insertion of an α-helix from SOS1 into RAS and altering the chemical environment of the binding site for the phosphate groups of the nucleotide and magnesium ion. Insertion of an α-helix from SOS1 into RAS results in a conformational change in the switch I region of RAS and opening up the nucleotide binding site of RAS. The side chains of the inserted α-helix also affect the conformation of the switch II region of RAS resulting in a change of the binding site for the phosphate groups of the nucleotide and the magnesium ion. Consequently, SOS1 stimulates the nucleotide exchange of RAS GTPases by altering the RAS conformation into the active conformation which allows the release of GDP and rebinding of GTP (*71*).

1.11 SOS1 role in various diseases

SOS1 dysregulation, overexpression and mutations have been reported in various diseases, such as ovarian cancer, prostate cancer, Noonan syndrome, hereditary fibromatosis type one, and uveal melanoma.

SOS1 overexpression correlates with ovarian cancer metastasis where it was found that RAC activation was facilitated by SOS1/EPS8/ABI1 complex in metastatic cells. It was also proven that the integrity of this tri-complex is essential for metastatic cell migration. coexpression of SOS1, EPS8, and ABI1, but not of any individual member of SOS1/EPS8/ABI1 complex, leads to advanced stages of ovarian cancer patients (*80*). Overexpression of SOS1 was detected in prostate cancer epithelial cells from African-American men and it was shown that depletion of SOS1 in prostate cancer cells (PC3 and DU145) correlates with a decrease in cell proliferation, migration, and invasion (*81*). SOS1 mutations also have been associated with Noonan syndrome (NS) which is a developmental disorder associated with learning problems, facial dysmorphic, and cardiac defects. *SOS1* was identified as the second major gene underlying NS and 26 mutations in SOS1 were reported to be associated with NS (*79, 82-84*). Hereditary gingival fibromatosis type one is an autosomal dominant disease in which patients suffer from overgrowth of gum. The responsible mutation for HGF1 in *SOS1* gene is due to an insertion of a cytosine between nucleotides 126,142 and 126,143 in codon 1083 (Figure 9) (*85, 86*). Recently SOS1 overexpression was introduced as a cause of uveal melanoma, a malignant tumor of the eye (*87, 88*).

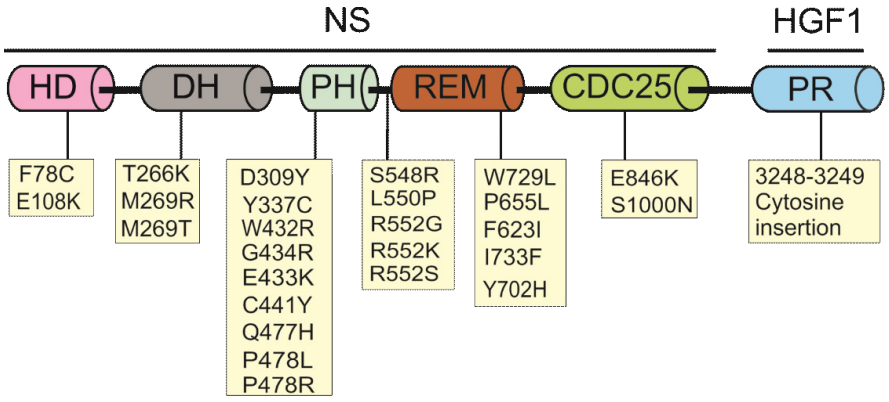

Figure 9. Human SOS1 mutations. Reported human SOS1 mutations in Noonan syndrome (NS) and Hereditary gingival fibromatosis type one (HGF1).

1.12 SH3 domains

SH3 domains are small domains containing about 60 amino acids. It was first identified as a 50 amino acid similar sequences in CTIO transforming protein (p47gag-ak), phospholipase C, and the c-SRC and c-ABL gene products (*89*). The solution structure of the SH3 domain of SRC was solved in 1992 (*90*). The binding site of SH3 domains was defined when the 3BP-1 protein was found to bind to the SH3 domain of ABL *via* a nine- or ten-amino acid stretch poly proline region (*91, 92*). SH3 domain containing

proteins carry various cellular functions but they can be mostly found in adaptor and scaffold proteins which facilitates protein complex formation (Figure 10). SH3 domains manly interact with proline-rich motifs (PRMs). Three major sites of SH3 domains are important for the interaction with PRMs involving the hydrophobic patch with conserved aromatic residues, flanked by the RT loop with conserved arginine and threonine residues and the n-SRC loop of the SH3 domain (*93, 94*). The residues located at the variable loops define the specificity and affinity of the SH3-PRMs interactions (*95*). The specificity of the SH3-PRMs interaction is generally modest, with a low micromolar range affinity (*93, 94, 96, 97*).

SH3 domain mutation was reported in a variety of human diseases, for an instance, mutation in α-spectrin, MYO7A, SH3TC2, and CASK SH3 domains respectively cause neurodegenerative diseases (*98, 99*), deafness (*100, 101*), peripheral nerve inflammation (*102, 103*), and microcephaly and cerebellar hypoplasia (*104*). Mutation of the STAMBP SH3-binding motif causes microcephaly-capillary malformation syndrome (*105*).

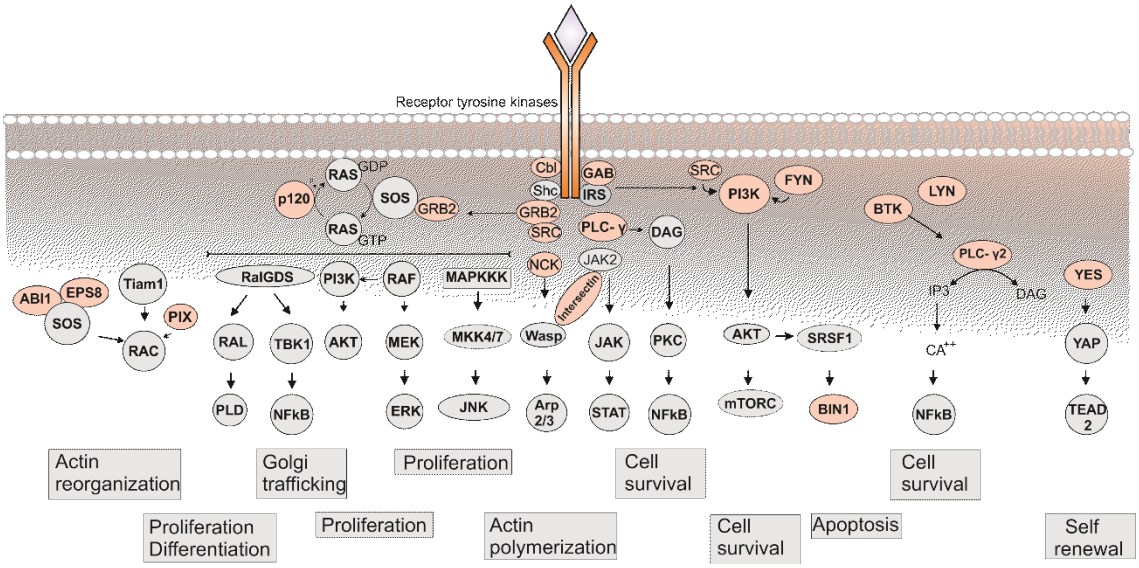

Figure 10.SH3 domain containing proteins in signaling pathways. The critical role of SH3 containing proteins is highlighted in different signalling pathways. SH3 domains are marked in light orange. The presence of SH3 domains in various proteins, especially as adaptor and scaffold proteins facilitate complex formation resulting in signal transduction.

1.13 GRB2

The adaptor protein GRB2 play a prominent role in intracellular signal transduction linking activated receptors to various signaling pathways (*106*). GRB2 has three functional domains, an SH2 domain flanked between two SH3 domains. It binds to the specific phosphotyrosine of activated receptors *via* its SH2 domain and to the proline-rich motifs *via* its SH3 domains (*107*). SOS1, guanine nucleotide exchange factor, and the GAB1, docker, are the best characterized proline-rich motif containing partners of GRB2 (*108*). GAB1 comprises an N-terminal PH domain and a C-terminal proline-rich

domain. It mediates signaling between receptor tyrosine kinases (RTKs) and downstream molecules, like RAS and Akt (*109*).

Recruitment of SOS1 *via* GRB2 to the membrane surface facilitates RAS activation (*108, 110*). But the recruitment of GAB1 *via* GRB2 to the membrane provides docking platforms for the PI3K lipid kinase (*108*), which respectively activate Akt, a key player in cell growth and survival (*111*).

Direct and indirect interaction of GRB2, SHC or FRS2 dependent, to the activated receptor tyrosine kinases recruit SOS1 to the plasma membrane and consequently activate RAS GTPases. GRB2 directly, SHC and FRS2 independent, interacts with TRKA(*112*). It indirectly, FRS2 dependent, interacts with FGF receptor (*113*). GRB2 could directly or indirectly, SHC dependent, interact with EGF receptor

(*114*). SHC interaction with GRB2 SH2 domain enhances GRB2-SOS1 association. Inhibition of SHC-GRB2 interaction abolishes the enhanced association between Grb2 and SOS1. SHC regulates GRB2-SOS1 interaction and is controlling the extend of RAS activation (*115*). GRB2 interaction with receptor, scaffold or adaptor proteins has a specific pattern for various receptors and regulate GRB2-SOS1 interaction and finally RAS activation.

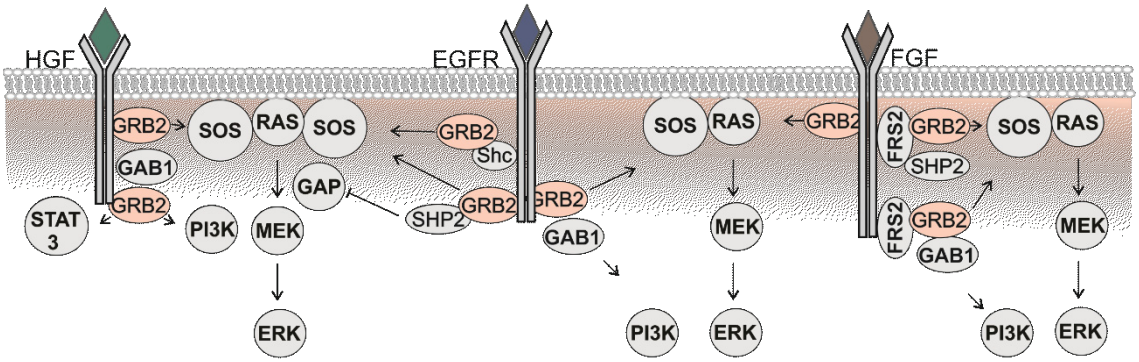

Figure 11. GRB2 role in signaling pathways. Adaptor protein GRB2 links activated receptors to the downstream signaling pathways and facilitates protein complex activation in signal transductions. It mostly takes part as an adaptor protein for MAPK and AKT pathways.

Aims and objectives

The RAS family GTPases play a decisive role in diverse cellular processes and their dysregulation is linked to the progression of different diseases, such as developmental disorders, and cancers. The active GTP-bound state of RAS GTPases goes along with a conformational change in switch I and II regions, which is controlled by the GDP/GTP exchange reaction and accelerated by the interaction with GEFs. Although their crucial role associated with human diseases have been analysed still there is no effective drugs on the market over 35 years of research on RAS GTPases. Here, we aimed to investigate the regulatory processes and the interaction selectivity towards downstream effectors, which may provide insights as potential therapeutic drug targets.

SOS1 is a ubiquitously expressed RAS activator. It has been implicated as a drug target although the molecular mechanism of its regulation is still unclear. The aim of this thesis was to investigate SOS1 activation and activity under different conditions. Therefore, we intended to investigate the RASGEF activity of different SOS1 protein fragments towards RAS GTPases.

GRB2 is an adaptor protein that directly binds SOS1 and recruits it to the plasma membrane where RAS GTPases are localized, although the significance of this interaction is still not clear. This thesis aimed to better understand the molecular mechanism of GRB2-SOS1 interaction, determine and characterize SOS1 binding regions of GRB2, and study the role of SOS1-GRB2 interaction on RAS activation.

SOS1 appears to interact, beside GRB2, with other SH3-containing proteins by obviously using ten different proline-rich motifs at its C-terminus. In the context of this thesis, we focused on the characterization of the 212 SH3-containing proteins in the human proteome, comprising of 298 different SH3 domains based on their interaction with proline-rich motifs of SOS1.

Another study should shed light on the selectivity of different RAS paralogs towards 10 members of the RAS domain-containing RASSF family. Therefore, this thesis tried to define the RAS and RAS effector binding sites and possible RAS binding partners. We attempted to Intelligibly study the sequence-structure-property relationship of RAS-RAS effector interaction.

RHO-specific GDP-dissociation inhibitor 1 (GDI1) is a regulator of RHO GTPases which binds to the isoprenylated RHO GTPases and extracts them from the membrane. The mechanism and structural specificity of GDI1 remained unclear. Another aim of this study was to provide insight into the mechanistic details about the GDI1 function towards RHO GTPases.

Chapter II

Structural fingerprints, interactions, and signaling networks of RAS family proteins beyond RAS isoforms

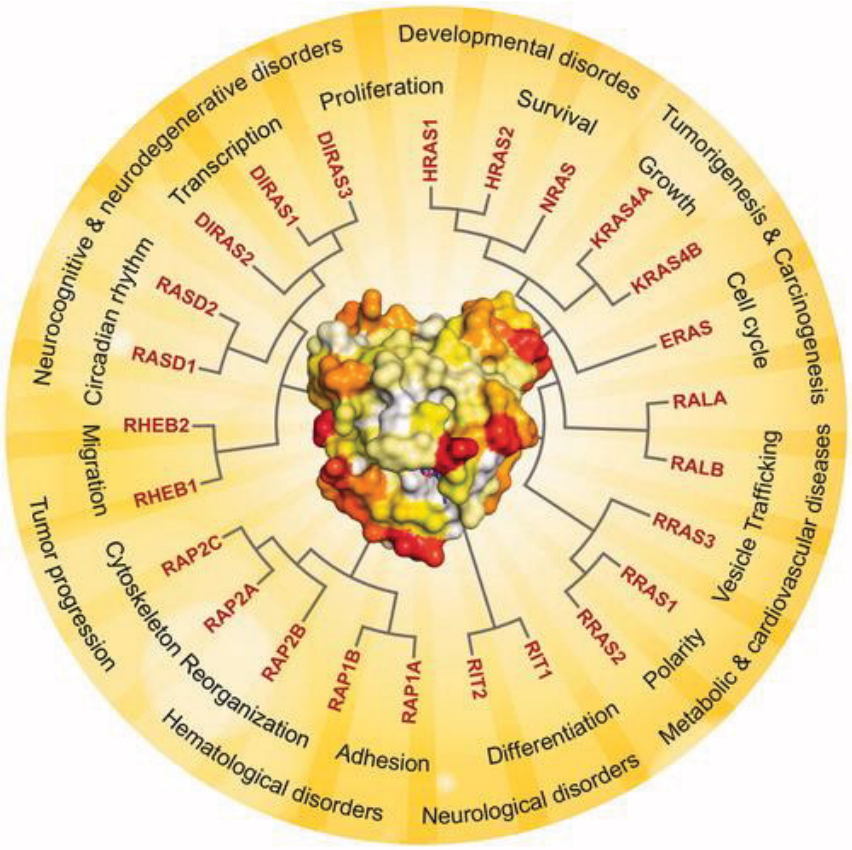

Published in:	Critical Reviews in Biochemistry and Molecular Biology
Impact factor:	6.069 (2019)
Own Proportion to this work:	10%
	Compilation of the literature about structures, diseases, and signal transduction of RAP GTPases, writing the manuscript

Taylor & Francis
Taylor & Francis Group

Critical Reviews in Biochemistry and Molecular Biology

ISSN: 1040-9238 (Print) 1549-7798 (Online) Journal homepage: https://www.tandfonline.com/loi/ibmg20

Structural fingerprints, interactions, and signaling networks of RAS family proteins beyond RAS isoforms

Saeideh Nakhaei-Rad, Fereshteh Haghighi, Parivash Nouri, Soheila Rezaei Adariani, Jana Lissy, Neda S. Kazemein Jasemi, Radovan Dvorsky & Mohammad Reza Ahmadian

To cite this article: Saeideh Nakhaei-Rad, Fereshteh Haghighi, Parivash Nouri, Soheila Rezaei Adariani, Jana Lissy, Neda S. Kazemein Jasemi, Radovan Dvorsky & Mohammad Reza Ahmadian (2018) Structural fingerprints, interactions, and signaling networks of RAS family proteins beyond RAS isoforms, Critical Reviews in Biochemistry and Molecular Biology, 53:2, 130-156, DOI: 10.1080/10409238.2018.1431605

To link to this article: https://doi.org/10.1080/10409238.2018.1431605

Published online: 19 Feb 2018.

CRITICAL REVIEWS IN BIOCHEMISTRY AND MOLECULAR BIOLOGY, 2018
VOL. 53, NO. 2, 130–156
https://doi.org/10.1080/10409238.2018.1431605

Taylor & Francis
Taylor & Francis Group

REVIEW ARTICLE

Check for updates

Structural fingerprints, interactions, and signaling networks of RAS family proteins beyond RAS isoforms

Saeideh Nakhaei-Rad, Fereshteh Haghighi, Parivash Nouri, Soheila Rezaei Adariani, Jana Lissy, Neda S. Kazemein Jasemi, Radovan Dvorsky and Mohammad Reza Ahmadian

Institute of Biochemistry and Molecular Biology II, Medical Faculty, Heinrich-Heine University, Düsseldorf, Germany

ABSTRACT

Among the signaling molecules indirectly linked to many different cell surface receptors, RAS proteins essentially respond to a diverse range of extracellular cues. They control activities of multiple signaling pathways and consequently a wide array of cellular processes, including survival, growth, adhesion, migration, and differentiation. Any dysregulation of these pathway leads, thus, to cancer, developmental disorders, metabolic, and cardiovascular diseases. The biochemistry of RAS family proteins has become multifaceted since the discovery of the first members, more than 40 years ago. Substantial knowledge has been attained about molecular mechanisms underlying post-translational modification, membrane localization, regulation, and signal transduction through diverse effector molecules. However, the increasing complexity of the underlying signaling mechanisms is considerable, in part due to multiple effector pathways, crosstalks between them and eventually feedback mechanisms. Here, we take a broad view of regulatory and signaling networks of all RAS family proteins that extends beyond RAS paralogs. As described in this review, a lot is known but a lot has to be discovered yet.

Graphical abstract: The RAS paralogs, KRAS4B, NRAS, and HRAS, are the best investigated members of the RAS family, not only because of their oncogenic capacity. This protein family, however, contains 22 additional isoforms and paralogs, most of which are distantly related, with typically 20–30% amino acid identity, although they share a conserved GTP-binding domain [the color spectrum goes from white (for identical) through yellow and orange (for partially conserved) to red (for highly variable amino acids). RAS family proteins control a wide array of signaling pathways and cellular processes distinct from those controlled by RAS paralogs. This review focuses on common features and differences of RAS family proteins regarding their structure, function, regulation, signaling, and involvement in diseases.

ARTICLE HISTORY
Received 9 October 2017
Revised 18 January 2018
Accepted 19 January 2018

KEYWORDS
Effectors; GAPs; GEFs; protein family; RAS; scaffold proteins; signal transduction

Historical background

The history of the RAS protein family dates back in 1960s, when the highly oncogenic Harvey and Kirsten murine sarcoma viruses (Ha-MSV and Ki-MSV) were discovered by Jennifer Harvey and later Werner Kirsten to cause rapid tumor formation in rats (Malumbres and Barbacid 2003) (Figure 1). These viral oncogenes, named Harvey and Kirsten RAS (HRAS and KRAS), along with their neuroblastoma RAS (NRAS) viral oncogene homolog, are activated versions of genes encoding 21-kDa phospho-protein (p21) with guanine nucleotide (GDP and GTP) binding and GTP hydrolyzing activities (Malumbres and Barbacid 2003). Later studies have provided evidences for the existence of specific regulators (guanine nucleotide exchange factors or GEFs and GTPase activating proteins or GAPs) and effector proteins activating individual pathways (Cherfils and Zeghouf 2013; Hennig et al. 2015; Upadhyaya et al. 2016; Keeton et al. 2017). As the founding members and prototypes of the RAS superfamily proteins (Wennerberg 2005; Wittinghofer and Vetter 2011; Rojas et al. 2012), HRAS, KRAS, and NRAS have become the subject of intense investigations due to their central involvements in signal transduction and their critical contribution to human diseases and disorders (Hobbs et al. 2016; Simanshu et al. 2017).

In this review, we describe current understanding of the regulatory mechanisms of individual RAS proteins and their signaling networks beyond the RAS paralogs. Phylogenic analysis identified 25 members of the RAS family out of 35 sequences (van Dam et al. 2011) (Figure 2). RASL, RERG, and NKIRAS proteins exhibit strong sequence deviations and thus, excluded from the list. The RAD family proteins, which are also excluded, make up together with RAS, RHO, RAB, ARF, RAN, and RAG the RAS superfamily (Rojas et al. 2012).

By the time passing, new evidences indicate tissue- and cell-specific function of RAS proteins. The sequence similarity between RAS proteins, especially in effector

CONTACT Mohammad Reza Ahmadian reza.ahmadian@hhu.de Institute of Biochemistry and Molecular Biology II, Medical Faculty, Heinrich-Heine University, Universitätsstrasse. 1, Building 22.03.06, Düsseldorf 40255, Germany

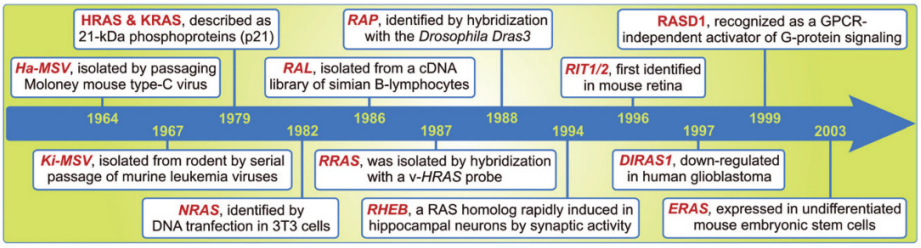

Figure 1. Historical timeline of the discovery of various members of the RAS family.

binding regions (see next section) was tempting to speculate overlapping functions for related RAS proteins. However, we need to consider the timing, subcellular localization and external stimuli that selectively regulate individual RAS proteins. This complexity comes in part because of their hypervariable region at C-terminus and sequence deviations in the full-length proteins, which provide additional binding sites for various scaffolding and adaptors proteins. Therefore, we discuss unique aspects of each RAS subfamily in term of tissue expression, upstream stimuli, receptor activation, interactions with regulators and effector that collectively fine-tune individual cellular functions under normal and pathological conditions. A large number of data, which will not be considered in detail, are summarized in Table 1.

RAS isoforms versus paralogs

The RAS family includes 23 genes coding for at least 25 proteins. Based on sequence identity, structure and function, the RAS proteins were divided into eight paralog groups: RAS, RAL, RRAS, RIT, RAP, RHEB, RASD, and DIRAS (Figure 2). Average sequence homology among paralogs vary between 30% and 60% while exceeds 90% within individual paralog groups. We introduced, for more clarity, names of some members, for example RRAS2 for TC21, RRAS3 for MRAS, RIT2 for RIN, RASD1 for DEXRAS, RASD2 for RHES, and DIRAS1 for RIG.

While majority of RAS proteins corresponds to one unique gene, some RAS family members are transcribed by the same genes. These isoforms, thus, originate from different mRNA transcripts, produced by alternative splicing and mostly differ in their subcellular localization. One example is HRAS with three isoforms p21, p19, and HRAS variant, which are designated HRAS1–3. HRAS1 (generally known as HRAS) has a stop codon in exon 4A and is translated to yield a p21-kDa protein with the canonical sequence with 189 amino acids. An in-frame stop codon in exon IDX leads to a transcript translated to produce a novel 170-amino acid protein called HRAS2 (known as p19HRAS or HRASIDX) (Cohen et al. 1989). HRAS3, a RASopathy-associated gene with a *de novo* 10-nucleotide-long deletion promoting constitutive retention of exon IDX in *HRAS1* gene (Pantaleoni et al. 2017). These three HRAS isoforms share an identical G domain and considerably different amino acids from 152 to 189 (Figure 2). HRAS3 contains an insertion of 24 amino acids between the residues 151 and 152 of HRAS1 (Pantaleoni et al. 2017). The other example is the *KRAS* gene, which encodes two transcripts, KRAS4A and KRAS4B, which are processed by alternative splicing of fourth coding exons 4A and 4B (McGrath et al. 1983). Also in this case, yielded proteins of 189 and 188 residues that significantly differ in their very C-terminal end (Figure 2), which take different ways of membrane trafficking (see below). HRAS and KRAS isoforms are co-expressed widely in human tissues (Guil et al. 2003; Plowman et al. 2006). Until now, no isoform of NRAS has been reported.

Structural fingerprints

The G domain and its molecular switch function

The RAS family proteins are usually known as molecular switches, cycling between an active GTP-bound state and an inactive GDP-bound state (Vetter and Wittinghofer 2001). Accordingly, they share a conserved GDP/GTP-binding domain (or G domain), which is responsible for nucleotide-dependent conformational changes. The structural differences between the two states are primarily confined to two highly mobile regions, designated as switch I (residues 28–39) and switch II (residues 59–74) (Figure 2). In the active state Tyr-32 and Thr-35 in switch I and Gly-60 in switch II form a hydrogen bonding network with the γ-phosphate of GTP. GTP hydrolysis triggers drastic rearrangements of the switch regions, resulting in the reorientation of these three critical residues away from the active site. Although the G domain uses a universally conserved switching mechanism (Wittinghofer and

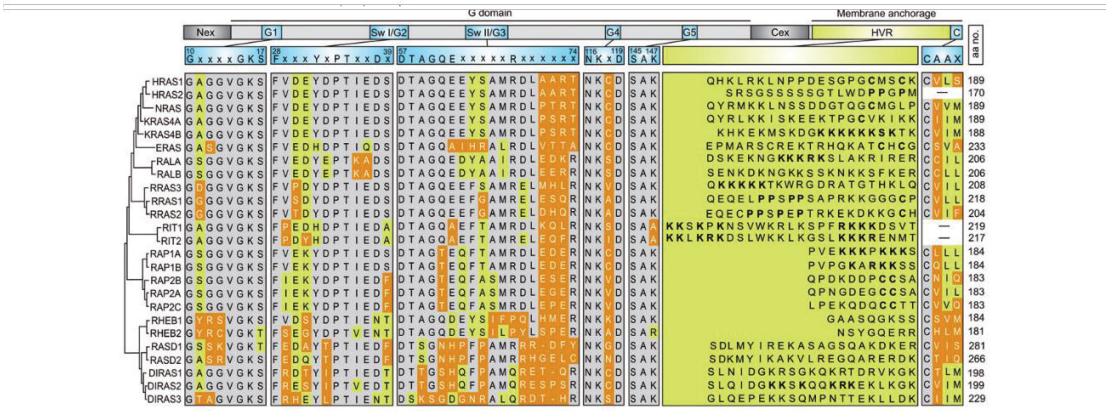

Figure 2. Evolutionary conservation of RAS family members. Signature motifs of 25 RAS-related proteins are presented according to their phylogenetic categorization. These proteins consist of a G domain with the five conserved motifs and a variable C-terminal membrane anchorage region, divided in hypervariable region (HVR) and the CAAX motif[©]. HVR contains several cysteines and serines for post-translational modifications, positively charged residues and other putative motifs, for example PXXP motifs as binding sites for SH3 domain-containing proteins. Certain members exhibit extensions at their N-terminal (Nex) and C-terminal (Cex) ends, which are summarized in Table 2. Conserved residues are shown in gray, homologous residues in orange and variable residues in olive.

Vetter 2011), its structure, function and GTP hydrolysis (or GTPase) reaction are adapted to many different signaling pathways and processes (see below).

The G domain consists of five conserved motifs, termed G1-G5 (Bourne et al. 1991) (Figure 2), which are central in nucleotide and magnesium binding. G1 is also known as the phosphate-binding loop or P-loop, as it is responsible for the binding of the phosphate groups of GDP and GTP. P-loop exists not only in GTP-binding proteins but also in ATP-binding proteins (Saraste et al. 1990) and typically contains several critical residues followed by a conserved lysine and a serine or threonine. Gly-12 and Gly-13 (HRAS numbering) are frequently mutated codons in human tumors (Malumbres and Barbacid 2003) leading to impairment of the GTPase reaction (Ahmadian et al. 1999). The majority of RAS family members contain a glycine at position 12 except ERAS, RASD1/2, and DIRAS3. These GTP-binding proteins do not act as molecular switches as they are GAP insensitive and thus persist in a constitutive active state (Kontani et al. 2002; Nakhaei-Rad et al. 2015). RHEB1 and RHEB2 have an extremely slow GTPase reaction due to an arginine and a serine or a cysteine instead of Gly-12 and Gly-13, respectively, but is interestingly switched off by RHEBGAPs, such as tuberin (also called TSC2) (Scrima et al. 2008). In the case of ERAS and RASD1/2, there is Ser-12 instead of glycine, and DIRAS3 harbors alanine in this position. In contrast to Gly-12 mutation, Ser-17 mutation to asparagine is used as dominant negative RAS mutant. Overexpressed RAS (S17N) tightly binds to endogenous RASGEFs and sequesters them from endogenous RAS proteins, and thus, interferes with RAS activation (Feig 1999). G2 (also called effector loop) is an integral part of effector-binding site and contains the highly conserved Tyr-32 and an invariant Thr-35 (HRAS numbering), which are critical for the conformational rearrangement of switch I. RIT1/2 contain histidine at the corresponding position of Tyr-32, which may be the reason for an accelerated nucleotide dissociation (Shao et al. 1999). G3 is a part of switch II and contains the critical catalytic Gln-61 position. Similarly to Gly-12 mutations, replacement of Gln-61 by virtually any other amino acid significantly reduces the intrinsic hydrolysis rate, prevents the GAP-mediated inactivation and, thus, induces oncogenic transformation by constitutive activation of RAS (Malumbres and Barbacid 2003). There is a threonine in RAP paralogs instead of Gln-61, asparagine in RASD1/2, glycine in DIRAS3 and serine in DIRAS1/2. In contrast to RASD1/2 and DIRAS3, which seem to have an impaired GTPase activity (Kontani et al. 2002), Thr-61 in RAP paralogs and most interesting Ser-65 in DIRAS1 and DIRAS2 (Gln-61 in HRAS1), do not compromise the GTPase reaction especially in the presence of RASGAPs (Scrima et al. 2008) (see "Regulatory proteins" section for more detail). GTPase deficiency of RASD and DIRAS

Table 1. Data summary for the RAS family proteins.

Proteins	Synonyme	Expression pattern	Upstream signals	GEFs	GAPs	Downstream target	Post-translational modifications
HRAS1	p21HRAS	Ubiquitous	Growth factors, phorbol esters	RASGRF, SOS1/2, RASGRP1–4, PLCε	p120RASGAP, NF1, RASA1–3, SynGAP1	C/BRAF, PI3K, RalGDS, PLCε, RASSF, RGL3, FAK	Far, Cm, Palm, Ub, S-Nit
HRAS2	p19HRAS	n. d.	n. d.	n. d.	n. d.	RACK1	n. d.
HRAS3	HRAS^{1x0X}	RASopathy gene	n. d.	n. d.	n. d.	n. d.	Far, Cm, Palm, Ub
NRAS		Ubiquitous	Growth factors, phorbol esters, LI3, CSF1	SOS1/2, RASGRP1–4	p120RASGAP, NF1, RASA1–3, SynGAP1	C/BRAF, PI3K, RALGDS, PLCε, RASSF, Calmodulin (KRAS4B)	Far, Cm, Palm
KRAS4A							
KRAS4B	HRAS2, RASK2						Far, Cm, P, Ac, Ub
ERAS	KRAS2, HRASP	Embryonic stem cells, hepatic stellate cells	n. d.	n. d.	n. d.	PI3Kα/δ, RASSF5	Far, Cm, Palm
RALA		Ubiquitous	Aurora-A, PKA, alpha-thrombin	RALGDS, RALGPS1/2 RGL1–4	RALGAP1/2	RalBP1, SEC5, EXO84, PLD1, PLCδ, ZONAB, TBK1	Ger, Cm Palm, P, Ub
RALB			PKCα, thrombin				
RRAS1	RRAS	Ubiquitous	Sema4D/3E-plexin B1/D1, EphB2; SRC, TCF8, NOTCH1, IL9, ORP3/VAP-A	RASGRF, C3G, CalDAG-GEFI/II/III	p120RASGAP,GAP1, NF1	PLCε, Gridin, FLNa, PI3K, RAP1, RAF, RIN2, VEGF	Ger, Cm, P
RRAS2	TC21	Heart, placenta, kidney, ovaries, skeletal muscle	IL9/IL3			CRAF	
RRAS3	MRAS	Brain		SOS1, RASGRF		SHOC2/PP1C, CRAF, RGL3	Ger, Cm
RIT1	RIBB, RIT, ROC1	Ubiquitous	NGF/EGF, injury, stress, PACAP38, Gαi/s/o	SOS1, GRF	SynGAP, GAP1	PAR6, RALGDS, RGL2/3, MKK3/6, SIN1, BRAF	P
RIT2	RIN, ROC2	Adult brain	NGF/EGF, PACAP38, Gαi/s/o, Forskolin/KCl			PAR6	n. d.
RAP1A	KREV1	Ubiquitous	cAMP, PLC, E-cadherin, ERM, Glucose, FGF2, GLP1, PAR4, integrins	EPAC1/2, Repac, CALDAG-GEF, PDZGEF1/22, C3G, DOCK4, PLCε1	RapGAP-I/II, SIPA1, E6TP1/SPAR, SPA-Ls, CAPR I	B/CRAF, AF6, KRIT1, RAPL, PI3K, ARAP3, RIAM, RGS14, RPIP9	Ger, Cm, P
RAP1B	OK/SW-cl.11	B/T cells					
RAP2A		B/T cells, excitatory synapses	PLC, cAMP	C3G, EPAC, CalDAGGEFI, PDZGEF1		JNK, MAP4K4, PARG1, TNIK, RPIP9, MINK, PLCε	Ger, Cm, Plam, P
RAP2B		Platelet, neutrophils	Thrombin, convulxin				Ger, Far, Cm, Palm
RAP2C		Circulating mononuclear leukocytes, liver, skeletal muscle, prostate, uterus, rectum, stomach, and bladder		PDZGEF1	n. d.	TNIK	
RHEB1		Ubiquitous	EGF, NGF, hypoxia, amino acids, forskolin, Low glocuse, BDNF, insulin, FGF	TCTP	TSC1/2, RGS10	mTOR, FKBP38, PLD1, PERK, BACE1, CRAF, NIX/LC3-II, Dynein, NOTCH1, RASSF1	Far, Cm, P
RHEB2		Ubiquitous, brain	NGF, SPC	n. d.	TSC1/2	mTOR, AKT1, CAD	
RASD1	AGS1, DEXRAS1	Brain, heart, liver, kidney, skeletal muscle, pancreas, placenta	Corticosteroids, estrogen, T3, nNOS	CAPON	n. d.	Gαi/o, PAP7, FE65, PLCδ	F, Cm
RASD2	RHES, TEM2	Corpus striatum, olfactory tubercle				PAP7	
DIRAS1	RIG, GBTS1	Brain, heart	n. d.	n. d.	RAPGAP1/2	CRAF, RAC1, EPAC1, smgGDS	Far, Ger
DIRAS2		Brain			RAPGAP1/2	smgGDS	
DIRAS3	ARHI, NOEY2, RHOI	Ovary, breast epithelial cells			n. d.	STAT3, CRAF	Myr

Ac: acetylation; Cm: carboxymethylation; Far: farnesylataion; Ger: geranylgeranylation; n. d.: not determind; Palm: palmitoylation; P: phosphorylation; Ub: ubiquitination; Myr: N-myristoylation; S-nit: S-nitrosylation.

paralogs may even be strengthened by an additional amino acid deviation at position 59 (Figure 2). G4 and G5 contain invariant residues and are responsible for the guanine base recognition. Mutation of Asp-119 in RAS changes the nucleotide specificity from guanosine to xanthosine nucleotides (Schmidt et al. 1996) and acts as dominant negative in a dose dependent manner (Tuder et al. 1999). G5 provides Ser-145 that stabilizes Asp-119 of G4. Ala-146 binds the guanine base and is another determinant for the guanine-binding ability of the RAS proteins. Lys-147 is replaced in RIT1/2 by alanine and may affect, together with the deviation in G2, the nucleotide binding affinity (Shao et al. 1999).

Membrane anchorage and subcellular distribution

Interactions between signaling proteins and cellular membranes are emerging as important modulators of

cellular signaling. The spatiotemporal organization in cells is largely dependent on both the nature and the dynamics of the association of proteins with specific sites of the cell membranes (Herrero et al. 2016). Association of RAS proteins with cellular membranes is mediated through a series of post-translational modifications and distinct motifs at their very C-terminal end (Wright and Philips 2006; Omerovic and Prior 2009; Cox et al. 2015; Nussinov et al. 2016; Wang and Casey 2016). RAS proteins, except for RIT1/2, serve as substrates for isoprenyl-transferring enzymes, which covalently and irreversibly attach a 15-carbon farnesyl or a 20-carbon geranylgeranyl moiety to the cysteine residue of the very C-terminal CAAX (C is cysteine, A is any aliphatic amino acid and X is any amino acid) motif (Figure 2). This motif is present in more than 100 proteins and necessary for diverse cellular processes (Lane and Beese 2006).

If the amino acid in the X position of CAAX is a leucine, as in the case of RALA/B, RRAS1/3, RAP1A/B, RAP2A (Figure 2), then geranylgeranyl transferase modifies the protein with a geranylgeranyl moiety (Benetka et al. 2006), otherwise the protein is modified with a farnesyl moiety by farnesyl transferase (Ahearn et al. 2011; Berndt et al. 2011). Two post-prenylation enzymatic steps are critical for proper localization, including proteolytic cleavage of the AAX residues by the endopeptidase RCE1 and methylation of the terminal isoprenylcysteine by the methyltransferase ICMT (Winter-Vann and Casey 2005; Ahearn et al. 2011; Berndt et al. 2011).

Due to a relatively weak affinity of isoprenylated proteins for cellular membranes (Silvius and l'Heureux 1994), additional motifs in the hypervariable region (HVR) are engaged in fine-tuning membrane association with RAS proteins (Figure 2) and their functions (Abankwa et al. 2007; Hanzal-Bayer and Hancock 2007; Omerovic and Prior 2009). Some RAS proteins, e.g. KRAS4B, RALA, RRAS3, and RIT1/2 (Figure 2), contain a stretch of positively charged amino acids (called polybasic region or PBR; Figure 2), which has been implicated to contact negatively charged phospholipids of the cell membrane (Banerjee et al. 2016; Nussinov et al. 2016). Membrane association of KRAS4B is modulated in different ways (Ashery et al. 2006; Bhagatji et al. 2010; Alvarez-Moya et al. 2011). PDEδ binds to farnesylated KRAS4B (Dharmaiah et al. 2016) and transport it from perinuclear membranes to plasma membrane (Chandra et al. 2011; Schmick et al. 2014). ERK1/2 phosphorylates RRAS1/2 at Ser-186 and Ser-201, but not RRAS3, and does not affect their subcellular localization but rather stimulates their activation (Fremin et al. 2016).

A further way of increasing the affinity of isoprenylated proteins for cellular membranes is an addition of one or more lipid anchors. KRAS4A, NRAS, HRAS1, ERAS, RRAS1, RAP2A/B, and RALA/B are palmitoylated by acyl protein transferases at cysteines prior to the CAAX motif (Figure 2) (Hancock et al. 1989; Beranger et al. 1991; Schroeder et al. 1997; Takahashi et al. 2005; Uechi et al. 2009; Gentry et al. 2015; Tabaczar et al. 2017). In contrast to HRAS1, HRAS2 does not have any C-terminal sites for post-translational modifications (Figure 2), and appears to be distributed between cytosol and nucleus (Guil et al. 2003). Another emerging concept in the field is based on physical interaction of the G domain itself with lipid membrane. A membrane-based, nucleotide-dependent conformational switch operates through distinct regions on the surface of RAS proteins, including the HVR, which reorient with respect to the plasma membrane (Abankwa et al. 2010; Cirstea et al. 2010). G domain-membrane interaction may contribute to the specificity of signal transduction and may underlay additional control elements. A critical aspect in this context is the organization of RAS proteins into protein–lipid complexes. These so-called nanoclusters concentrate RAS at the plasma membrane. They are the sites of effector recruitment and activation, and are essential for signal transmission (Abankwa et al. 2007; Zhou and Hancock 2015). It is not entirely clear how RAS nanoclustering is regulated (see "Modulatory scaffold proteins" section).

Modulatory post-translational modifications

Trafficking of RAS proteins (Wurtzel et al. 2015) have recently been shown to be highly specific for respective RAS proteins and dependent on specific post-translational modifications beyond prenylation and acylation (Oertli et al. 2000; Berzat et al. 2006; Calvo and Crespo 2009; Jang et al. 2015; Lynch et al. 2015; Schmick et al. 2015), namely, phosphorylation (Bivona et al. 2006; Sung et al. 2013), ubiquitination (Jura et al. 2006; Rodriguez-Viciana and McCormick 2006; de la Vega et al. 2010; Wang et al. 2015), and S-nitrosylation (Shanshiashvili et al. 2011; Chen et al. 2015). The molecular basis of these modifications is mostly still unclear.

Acetylation of KRAS at Lys-104 interferes with GEF-induced nucleotide exchange (Yang et al. 2012, 2013; Knyphausen et al. 2016). S-nitrosylation of Cys-118 of HRAS promotes nucleotide exchange (Lander et al. 1995; Williams et al. 2003; Heo and Campbell 2004). Ubiquitination of HRAS at Lys-117 accelerates intrinsic nucleotide exchange, thereby promoting GTP loading, while KRAS monoubiquitination at Lys-147 leads to an impaired regulator-mediated GTP hydrolysis (Baker et al.

2013a, 2013b; Sasaki et al. 2011). RRAS1 phosphorylation at Tyr-66 by EphB2 receptor and Src blocks its effector interaction, for example with CRAF (Zou et al. 1999, 2002). In contrast, ERK1/2 phosphorylates RRAS1 and RRAS2 at the C-terminal HVR at Ser-186 and Ser-201, respectively and promotes cell adhesion and migration (Fremin et al. 2016). In addition, phosphorylation of RAS proteins also modulates their subcellular localization. KRAS phosphorylation by PKC at the C-terminal Ser-181 promotes its dissociation from the plasma membrane and translocation to intracellular membranes, including the outer membrane of mitochondria (Bivona et al. 2006). A similar scenario is RALA phosphorylation at Ser-194 by Aurora-A, which promotes RALA relocalization from the plasma membrane to mitochondria leading to mitochondrial fission (Kashatus et al. 2011).

The concept of family member selectivity

In spite of sharing a conserved G domain, each RAS family member has specific deviation within and additional features outside the G domain that make them unique in regulation and function. In the following, we compare individual members in the frame of 11 subfamilies with HRAS as a prototype of the family. Many members of the RAS family exhibit unique amino acid extensions at their N-terminal (N_{ex}) and C-terminal (C_{ex}) ends (Figure 2 and Table 2). The N-terminus of ERAS, which appears to undergo multiple interaction with other proteins (H. Nakhaeizadeh, J. Lissy, S. Rezaei Adariani, S. Nakhaei-Rad, M.R. Ahmadian, unpublished) and contains putative SH3-binding motifs, like RRAS1 and HRAS2/3 (Table 2). RRAS1 N-terminus, interestingly is critical for protein targeting and function (Wang et al. 2000). These motifs may provide additional mechanisms for sorting and trafficking to specific subcellular sites, as proposed for ERAS (Nakhaei-Rad et al. 2015). RRAS paralogs contain extended N-termini that seems to be critical for cell migration (Holly et al. 2005). RALA N-terminal extension is involved in SRC-induced PLD activation (Jiang et al. 1995). Signal-induced recruitment of DIRAS3 to the plasma membrane appears to be regulated by its N-terminal extension (Klingauf et al. 2013), which is essential for its interaction with STAT3 and importin (Nishimoto et al. 2005; Huang et al. 2009). Notably, DIRAS3 contains a glycine at position 2, which usually is used as a site for myristoylation (Resh 2004).

Protein interaction networks

RAS proteins are known to undergo interactions with diverse types of proteins, some of which are summarized as follows.

Regulatory proteins

RAS is believed to persist in its inactive form in resting cells. This scenario is based on the assumption that its intrinsic GTPase reaction is faster than its intrinsic GDP/GTP exchange reaction. A further issue is that these very slow reactions require catalysis by GEFs and GAPs, respectively, which are controlled by upstream signals and locally regulate RAS activity. There are, however, several RAS family members, including ERAS, DIRAS3, and RASD1/2, which exhibit distinct amino acid deviations in G1 and G3 motifs (Figure 2). These proteins accumulate themselves in GTP-bound form due to their impaired GTP hydrolysis and GAP insensitivity (Kontani et al. 2002; Nakhaei-Rad et al. 2015; Ogita et al. 2015), and may underlay a different mechanism of regulation. Unlike classical RAS proteins, these GTP binding proteins are not ubiquitously expressed (Table 1) and may be regulated at the level of transcription as recently shown for ERAS (Nakhaeizadeh et al. 2016). All other members of the RAS family appear to act as intracellular switches and to be controlled by GEFs and GAPs (Table 1). However, no RHEBGEF has been identified so far.

Table 2. Amino acid extensions beyond the G domain and HVR (see text for more detail).

N-terminal extensions	
ERAS	[1]MELPTKPGTFDLGLATWSPSFQGETHRAQARRRDVGRQ
RRAS1	[1]MSSGAASGTGRGRPRGGGPGPGDPPP
RRAS2	[1]MAAAGWRDGSG
RRAS3	[1]MATSAVPSDN
RALA	[1]MAANKPKGQNS
RALB	[1]MAANKSKGQSS
RIT1	[1]MDSGTRPVGSCCSSPAGL
RIT2	[1]MEVENEASCSPGSASGG
RASD1	[1]MKLAAMIKKMCPSDSELSIP
RASD2	[1]MMKTLSSGNCTLSVPA
DIRAS3	[1]MGNASFGSKEQKLLKRLRLLPALLILRAFKPHRK
C-terminal extensions	
HRAS2	[152]SRSGSSSSSGTLWDPPGPM
HRAS3	[152]SRSGSSSSSGTPRDPCDPAAPRAG
RASD1	[197]LPSEMSPDLHRKVSVQYCDVLHKKALRNKKLLRAGSGGGGGDPGDAFGIVAPFARR
RASD2	[192]LPHEMSPALHRKISVQYGDAFHPRPFCMRRVKEMDAYGMVSPFARR

Postulated GEF activity of TCTP towards RHEB1 has been disproved (Rehmann et al. 2008b). There are no specific GEFs and GAPs described for RIT1/2 yet (Shi et al. 2013).

There are 30 RASGEFs known in human genome (van Dam et al. 2009) sharing a common catalytic domain, called CDC25 (Crechet et al. 1990; Quilliam et al. 2002; Mitin et al. 2005; van Dam et al. 2011). Consistent with the RHOGEF family (Jaiswal et al. 2013), RASGEFs also exhibit selectivity profile towards distinct groups of the RAS family (Popovic et al. 2013), which is a pivotal step in establishing specific activation of the downstream signaling pathways (Figure 3). The CDC25 domains of SOS1, EPAC2 and RALGDS specifically bind HRAS, RAP2B, dRal, the *Drosophila* ortholog of RALA, respectively and structurally rearrange critical regions of the nucleotide-binding site, including P-loop and switch I/II and consequently catalyze the GDP/GTP exchange (Boriack-Sjodin et al. 1998; Rehmann et al. 2008a; Popovic et al. 2016). They apparently operate by a simple allosteric competitive mechanism (Guo et al. 2005). In the cell, the specificity of the RASGEFs is obviously determined by other domains of the respective proteins, for example SOS1 (Gureasko et al. 2008).

Unlike GEFs, GAPs for different groups of the RAS family are mechanistically rather heterogeneous (Scheffzek and Ahmadian 2005). RASGAPs provide common structural fingerprints (Ahmadian et al. 2003), especially a catalytic arginine, which stabilizes Gln-61 of RAS and RRAS paralogs and stimulate the very slow GTPase reaction (Ahmadian et al. 1997; Scheffzek et al. 1997). RAPGAPs as well as the RHEBGAP, tuberin or TSC2, utilize a catalytic asparagine that substitute for the non-functional threonine of RAP paralogs and glutamine of RHEB1 in the switch II regions (Daumke et al. 2004; Yu et al. 2005; Scrima et al. 2008; Marshall et al. 2009). Tuberin requires for its GAP activity a heterodimerization with non-catalytic hamartin (also called TSC1) (Li et al. 2004). GAP1^{IP4BP}, however, utilizes a catalytic arginine to inactivate RAP1 (Kupzig et al. 2009). RALGAPs share a similar catalytic mechanism as RHEBGAPs. They undergo a complex with a non-catalytic subunit and stimulate the GTPase reaction of RALA/B, most likely by supplying a catalytic asparagine, too (Shirakawa et al. 2009). DIRAS1/2 share GAPs with RAP paralogs, which also have a serine instead of a catalytic glutamine (Figure 2) and can be inactivated by RAPGAPs (Gasper et al. 2010).

Effector selectivity

Signal transduction implies physical association of RAS proteins with and activation of a spectrum of functionally diverse downstream effectors. Effectors specifically interact with the active, GTP-bound form of the RAS proteins, usually, in response to extracellular signals, and link them to downstream signaling pathways in all eukaryotes (Karnoub and Weinberg 2008; Gutierrez-Erlandsson et al. 2013). They act as protein or lipid kinases, phospholipase, GEFs, GAPs and scaffold proteins (Table 1) (Herrmann 2003; Rajalingam et al. 2007; Castellano and Downward 2010; Ferro and Trabalzini 2010; Bunney and Katan 2011; Chan and Katan 2013; Nakhaei-Rad et al. 2016; Nakhaeizadeh et al. 2016). Two major groups of effectors contain RAS binding (RB) and RAS association (RA) domains, respectively (Repasky et al. 2004; Wohlgemuth et al. 2005; Nakhaeizadeh et al. 2016). Mining in the UniProt database led to the identification of 118 distinct human proteins containing RB and RA domains (Rezaei Adariani, Dvorsky et al., unpublished). Notably, both types of domains utilize critical determinants for the interaction with different RAS proteins, particularly the intermolecular β-sheets (Nakhaeizadeh et al. 2016). Structural studies have provided deep insights into the binding modes and interaction specificities (Mott and Owen 2015) and yet, the precise mechanism, through which effector association with activated RAS proteins results in effector activation, is still unclear. It is, however, generally accepted that RAS proteins participate directly in the activation of their downstream effectors and do not simply mediate recruitment to specific sites of the membrane.

The RAS paralogs share a similar effector binding regions with other members of the RAS family but also show distinct deviations (residues 30 and 31 in switch I, and 64, 65, 71, 72, and 73 in switch II) suggesting that they may share downstream effectors with different affinities (Wittinghofer and Nassar 1996). ERAS preferentially interacts with PI3K rather than CRAF as compared to HRAS. Trp-79 of ERAS (Arg-41 in HRAS) turned out to be critical for ERAS binding to PI3K, RALGDS, and PLCε (Nakhaei-Rad et al. 2015). Ser-34 of RHEB1, and Lys-31 in RAP1A (Glu-31 in HRAS1) have been discussed as specificity determining for their effectors (Wittinghofer and Nassar 1996). Notably, residues 70–72 (67–69 in HRAS1) in the switch II region appear to undergo contacts with Arg-15 and Ser-16 (Gly-12 and Gly-13 in HRAS1) in P-loop and may contribute to an alternative mechanism of intrinsic GTP hydrolysis (Karassek et al. 2010).

Modulatory scaffold proteins

Signal transduction of RAS family proteins are maintained by at least three classes of interacting partners. These include regulators (GEFs and GAPs) that control

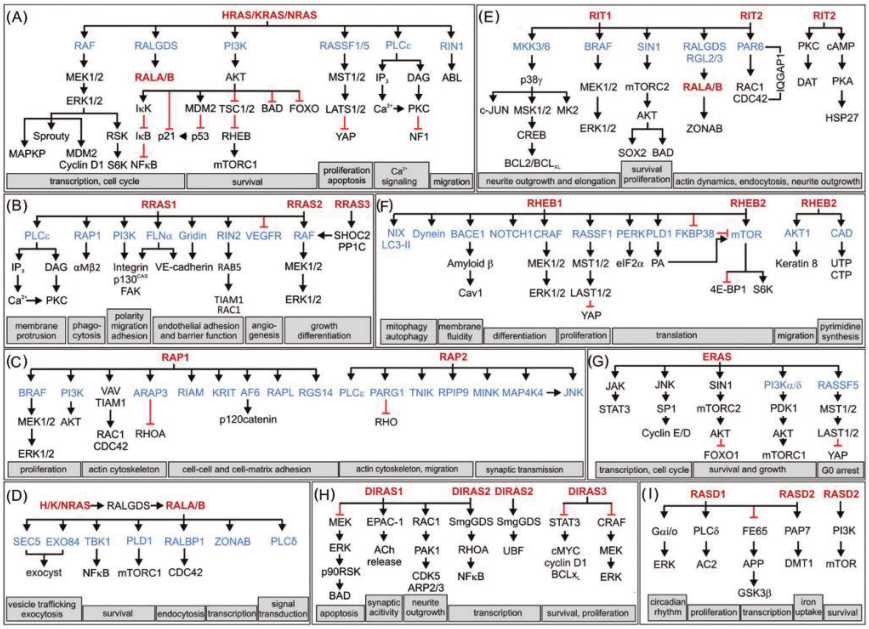

Figure 3. Signal transduction pathways downstream of the RAS family proteins. Signaling schemes are divided in different paralog in red colors (A–I). Reviewed effectors are shown in blue. Other downstream interacting proteins are shown in black. Black arrows indicate activating events and red lines inhibiting events in pathways. See D for missing RALA/B signaling in A.

the GTPase cycle and a wide spectrum of effectors that initiate signaling cascades downstream of the RAS proteins. It has become evident that an increasing number of additional RAS scaffold proteins, including CAM, GAL1, GAL3, IQGAP1, NCL, NPM1, SHOC2, SHP2, SPRY, SPRED1, and GAB1, are critical in modulating and integrating RAS proteins in various signaling networks at the biological membranes. CAM binds to KRAS4B PBR (Wu et al. 2011; Sperlich et al. 2016) and determines activation of distinct downstream pathways (Nussinov et al. 2015; Jang et al. 2017). KRAS4B interaction with CAM leads to the suppression of the non-canonical Wnt/Ca^{2+} pathway that strongly contributes to its tumorigenic properties (Wang et al. 2015). Similarly, CAM binds to RALA and PLCδ and modulates RALA-mediated PLCδ activity (Grujic and Bhullar 2009). RIT2 PBR acting as a docking site for CAM is essential for the EGF dependent RIT2 signal transduction (Lee et al. 1996). A CAM interaction of *Drosophila* Ric, a RIT1/2 ortholog, has been shown, however, to negatively regulate Ric crosstalk to the RAS-MAPK pathway (Harrison et al. 2005). SHOC2 (also called SUR-8) in complex with PP1c links RRAS3 with the inactive CRAF and stimulates CRAF activity by dephosphorylating of SHOC2, thus, promotes the RAS-RAF-controlled MAPK activation to control proliferation and neurite outgrowth (Cordeddu et al. 2009; Motta et al. 2016). SHOC2 also binds p110α subunit of PI3K and regulates cell motility, invasion, and metastasis (Kaduwal et al. 2015). IQGAP1, which contains an inactive RASGAP domain (Kurella et al. 2009; Nouri et al. 2017), binds BRAF and ERK1/2, and potentiates their activity in response to EGF (Ren et al. 2007). An ERK1/2-binding IQGAP1 peptide has been reported to disrupt IQGAP1-ERK1/2 interactions and inhibit RAS- and RAF-driven tumorigenesis (Jameson et al. 2013). GAL1, GAL3, NPM1, and NCL has been suggested to modulate RAS nanocluster formation and activate the MAPK pathway but the molecular nature remains to be determined (Plowman et al. 2008; Inder et al. 2009). GAL1 has recently been shown to form a complex with CRAF and potentiate HRAS nanoclustering (Blazevits et al. 2016). Other scaffold proteins, such as SPRY,

SPRED1, and GAB1 act differently. SPRY2, for example, interrupts signal transduction from FGFR to RAS by binding to GRB2 and disrupting the GRB2-SOS complex if phosphorylated by CK1 (Yim et al. 2015). SPRY2 appears to regulate the specific activation of RAC1 by HRAS, which probably would be mediated by TIAM1 and PI3K (Lito et al. 2009). SPRED1 interferes with the membrane anchorage and signaling of KRAS but not HRAS (Siljamaki and Abankwa 2016) and modulate the activity of NF1, a RASGAP, by binding and recruiting it to the plasma membrane (Dunzendorfer-Matt et al. 2016). GAB1 modulates, together with the tyrosine phosphatase SHP2, p120RASGAP activity by recruiting it to activated EGFR at the plasma membrane (Montagner et al. 2005). Future studies will shed light on the underlying mechanisms of these groups of modulatory proteins, the total number of which may increase.

Signal integration and transduction

RAS family proteins link the extracellular signals, transduced through their receptors, with multiple signaling pathways and consequently control a wide array of cellular processes. Different RAS paralogs have unique roles in modulating the cellular processes. The specificity comes from several levels: Subcellular localization, upstream stimuli, interactions with scaffolds, regulators and target proteins, and downstream signaling. In this part, we describe more precisely the conditions under which individual RAS proteins are activated and how they transduce the signal.

Upstream signals

The convergence of multiple upstream cascades on the RAS proteins mostly underlay a similar mechanism. Different types of extracellular signals, transmitted across the plasma membrane by diverse cell surface receptors are linked with RAS proteins through different, specific GEFs and GAPs (Table 1) (Quilliam et al. 2002; Hennig et al. 2015). Interestingly, activation of different transmembrane receptors, including receptor tyrosine kinases (RTKs), G-protein coupled receptors (GPCRs), ion channel receptors (e.g. mGluR or NMDAR), cytokine receptors and adhesion receptors, lead to the activation of distinct RAS proteins in distinct cell types. For example, IL3, CSF1, and EGF preferentially activate KRAS4B and RRAS3 over HRAS or NRAS in B and T lymphocytes (Ehrhardt et al. 2004), GLP1 and PAR4 peptide activate RAP1 in islet cells and platelets, respectively (Trumper et al. 2005), FGF2 activates RAP1A/B in endothelial cells (Yan et al. 2008), IL9/IL3 activate RRAS3 in T-helper cells (Louahed et al. 1999), EGF, and NGF activate RIT1 in non-neuronal and neuronal tissues (Shi and Andres 2005), EGF, NGF, and PACAP38 neuropeptide activate RIT2 in neuronal tissues (Spencer et al. 2002b; Shi et al. 2008), EGF and forskolin activate RHEB in rat pheochromocytoma PC12 cells (Yee and Worley 1997), while insulin, FGF and BDNF activate the RHEB1 in neuronal cells (Yamagata et al. 1994; Zhang et al. 2003; Takei 2004), and glucocorticoid dexamethasone induces a RASD1-mediated adipogenesis in adipocytes (Cha et al. 2013). nNOS activation via NMDR stimulation results in S-nitrosylation and CAPON adaptor acts as a GEF to activate RASD1 (Fang et al. 2000; Cheah et al. 2006). L-DOPA, thyroid hormone and Estrogen regulate RASD2 in striatal tissue (Subramaniam et al. 2011; Ghiglieri et al. 2015).

The upstream signals specifically activate distinct GEFs, which in turn selectively activate distinct members of the RAS family and ultimately control distinct cellular processes (Buday and Downward 2008). A nice example is RAP1-mediated formation of cell-cell junction regulated by five different RAP1GEFs (Kooistra et al. 2007). Prominent examples are EPAC1/2, which is directly activated by cAMP (de Rooij et al. 1998), controls cellular processes ranging from insulin secretion to cardiac contraction and vascular permeability (Gloerich and Bos 2010). A different scenario is CalDAG-GEFIII (also called RASGRP3) that operates on multiple RAS proteins (Rebhun et al. 2000; Yamashita et al. 2000). In endothelial cells, CalDAG-GEFIII activates RRAS1 and interferes with transendothelial permeability and angiogenesis, respectively (Ichimiya et al. 2015), while it affects inflammatory response in macrophages by activating RAP1 (Tang et al. 2014). Other well-studied GEFs are SOS1/2, RASGRP1–4, and RASGRF1/2 (Hennig et al. 2015). Collective binding of multiple SOS1 and GRB2 domains to their protein and phospholipid ligands are finely tuned in order to cooperatively control cellular processes, including pluripotency and differentiation factors (Findlay et al. 2013). RASGRP1 opposes EGFR-SOS1 signals and suppresses proliferation in normal intestinal epithelial cells (Depeille et al. 2015). RASGRF1/2 carry out specific roles in three forms of synaptic plasticity in the CA1 region of the hippocampus (Jin et al. 2014). RALGDS, an effector of different RAS proteins (Ferro and Trabalzini 2010; Yoshizawa et al. 2017), activates RALA to regulate insulin-secretory process in pancreatic β-cells in response to intracellular Ca^{2+} and cAMP (Ljubicic et al. 2009) and to promote exocytosis of endothelial Weibel-Palade bodies (Rondaij et al. 2008). The latter, which are also regulated by cAMP-EPAC-RAP1 (van Hooren et al. 2012), are critical elements of hemostasis, inflammation or angiogenesis (Mourik and Eikenboom 2017).

Contrary to GEFs, only a few reports are known about the signaling cascades, which control recruitment and activation of GAPs. In the thymus, p120RASGAP, the GAP prototype (Trahey and McCormick 1987), acts for example as a negative regulator of the RAS-MAPK pathway during positive selection and survival of naive T cells (Lapinski et al. 2011). The activity of p120 is regulated by ANXA6O, which binds p120 and recruit it to the membrane in a Ca^{2+}-dependent manner (Grewal et al. 2005; Grewal and Enrich 2006). The much larger NF1 regulates for example RAS inactivation in dendritic spines of pyramidal neurons in the CA1 region of the rat hippocampus (Oliveira and Yasuda 2014). Dual-specificity RASGAP paralogs, $GAP1^{IP4BP}$ and CAPRI, coordinate RAS and RAP signaling pathways (Kupzig et al. 2006; Sot et al. 2010). Inhibition of $GAP1^{IP4BP}$ by an integrin $\alpha_{IIb}\beta_3$ outside-in signaling via PI3K leads to sustained RAP1 activation and platelet spreading (Battram et al. 2017). Ca^{2+}-dependent dimerization of CAPRI, a $GAP1^{IP4BP}$ paralog, switches its specificity from RASGAP to RAPGAP (Dai et al. 2011). SynGAP is another dual-specificity GAP, which is a negative regulator of RAS and RAP proteins in dendritic spines (Jeyabalan and Clement 2016). It is one of the most abundant post-synaptic density proteins, where it binds as a homo-trimer to multiple copies of PSD95 (Zeng et al. 2016). SynGAP requires its C2 domain to catalyze RAP inactivation (Pena et al. 2008). Spine-associated, classical RAPGAPs, SPAR1–3, are recruited through their interactions with Fezzin proteins to the post-synaptic SHANK scaffold and regulate dendritic spine morphology (Dolnik et al. 2016).

Semaphorins, the plexin family of semaphorin receptors, exhibit GAP activities towards RRAS paralogs (Hota and Buck 2012). Sema3E-PLXND1 counteracts angiogenesis through RRAS inactivation (Sakurai et al. 2010). However, SEMA4D–PLXNB1–RND1 complex inactivates RRAS in order to induce growth cone collapse in hippocampal neurons (Oinuma et al. 2004), while SEMA4D-PLXNB1 acts on RRAS3 to regulate actin-based dendrite remodeling (Tasaka et al. 2012). As the GAP activities of PLXNs is a matter of debate, a structural, and biochemical study has shown that PLXNs apparently use a non-canonical catalytic mechanism to act as GAPs on RAP but not on RRAS paralogs (Wang et al. 2012). In this study, SEMA3A stimulated the RAPGAP activity of PLXNA1 to induce neuronal growth cone collapse.

TSC1/TSC2 heterodimerization facilitates TSC2 RHEBGAP activity leading to RHEB inactivation and inhibition of the RHEB-induces mTORC1 activation (Tee et al. 2003; Long et al. 2005). VPS34, a class III PI3K, upregulates RHEB and mTOR activities via production of PIP_3 and recruits PIKFYVE to the plasma membrane, where VPS34 forms a complex with PIKFYVE and TSC1 (Mohan et al. 2016). This in turn disengages TSC2 from the TSC1/TSC2 heterodimer, leading to TSC2 ubiquitination and degradation. Arginine, a key activator of mTORC1, cooperates with growth factor signaling, which suppresses lysosomal localization of the TSC complex and interaction with RHEB (Carroll et al. 2016). MCRS1 regulates the lysosome localization of RHEB1 in an amino acid-dependent manner and inhibits TSC2 binding to RHEB1 (Fawal et al. 2015). In myoblasts, however, TSC2 phosphorylation and inactivation by ERK results in activation of the RHEB-mTORC1 axis and regulation of protein synthesis (Miyazaki and Takemasa 2017).

Downstream targets and pathways

Classical RAS signaling

Specific regulation of cellular functions by the members of the RAS family depends on selective interaction with downstream targets, the effectors (Mott and Owen 2015; Nakhaeizadeh et al. 2016), which transduce the signal to distinct pathways (Cox and Der 2003; Bos 2005; Rajalingam et al. 2007; Braun and Shannon 2008; Karnoub and Weinberg 2008; Castellano and Downward 2010; Dodd and Tee 2012; Gentry et al. 2014). More than 60 effectors reported for the RAS family proteins (Table 1) can activate about 49 pathways (Figure 3). RAF kinases (ARAF, BRAF, and CRAF) are the major and best-studied effectors for RAS family. These kinases are critical elements of the MAPK pathway, which control gene expression and thus, different cellular processes including proliferation, apoptosis, and differentiation (Desideri et al. 2015). RAF kinases phosphorylate MEK, which in turn phosphorylates ERK kinases and triggers their translocation into the nucleus, where they activate transcription factors, such as ELK1, ETS1, MYC, FOS, and DUSP1 (Unal et al. 2017). Rarely analyzed are, however, a large number of other CRAF substrates, which are involved in different processes, including adenylyl cycle, vimentin kinase, Rb, CDC25, troponin T, DMPK, and MYPT (Galaktionov et al. 1995; Janosch et al. 2000; Shimizu et al. 2000; Broustas et al. 2001; Hindley and Kolch 2002; Ehrenreiter et al. 2005; Kaliman and Llagostera 2008; Davis and Chellappan 2008; Niault and Baccarini 2010). CRAF directly associates with MST2, ASK1, ROCK, and calcineurin, and controls proliferation, apoptosis, contraction, and motility, respectively (Chen et al. 2001; Niault and Baccarini 2010; Romano et al. 2014; Desideri et al. 2015; Varga et al. 2017).

CRAF and BRAF are apparently downstream of many different members of the RAS family, including HRAS,

KRAS4B, NRAS, RAP1A, RRAS1, RRAS2, RRAS3, RHEB1, RIT1, and DIRAS3 (Figure 3) (Self et al. 2001; Wellbrock et al. 2004; Jin et al. 2006; Karbowniczek et al. 2006; Baljuls et al. 2012; Mott and Owen 2015; Yaoita et al. 2016). CRAF activity is known to be directly dependent on its heterodimer formation with BRAF, which appears to be stabilized by ARAF as a scaffold protein (Rebocho and Marais 2013). Also ARAF homodimer seems to promote MAPK pathway activation (Mooz et al. 2014). However, due to a lower binding affinity for ARAF, HRAS seems to preferentially activate CRAF (Weber et al. 2000). In contrast to HRAS1, HRAS2 does not interact with two known HRAS effectors, CRAF and RIN1 (Guil et al. 2003). HRAS2 interacts with RACK1, a scaffolding protein that forms multiprotein complexes with p120RASGAP, MAP kinases, PKCs, and SRC proteins (Guil et al. 2003). It also regulates telomerase activity through its interaction with p73 and arrest cell cycle at G1/S phase (Camats et al. 2009). The RASopathy-associated HRAS3, which has a 24-amino acid insertion at Gly-151 and Val-152 with partial similarity to the C-terminus of HRAS2 (Table 2), is a weak hyperactive RAS protein with constitutive plasma membrane localization in comparison to HRAS1. It has been suggested that it may, due to its insertion, interact with signaling platforms located at different subcellular compartments (Pantaleoni et al. 2017).

The second best-characterized RAS effector family, PI3K (class I PI3K), phosphorylates phosphoinositide (4,5) bisphosphate (PIP_2) and generates the second messenger phosphoinositide (3,4,5) trisphosphate (PIP_3) that recruits the wide range of protein effectors through their pleckstrin homology (PH) domain to the membrane. Target proteins could be kinases (e.g. AKT and PDK1), adaptor proteins, GEFs, or GAPs that regulate different cellular processes (Vanhaesebroeck et al. 2001). PI3K-AKT pathway is very well known in controlling cell cycle entry, cell growth, survival, and metabolism (Castellano and Downward 2011). HRAS1, NRAS, KRAS4B, ERAS, RRAS, and RAP1A activate PI3Ks. AKT or protein kinase B (PKB) belongs to AGC subfamily of protein kinases. AKT is one of the key proteins downstream of PI3K-PIP3 involved in a wide range of the cellular processes, such as cell proliferation, metabolism, growth, autophagy inhibition, and survival (Andjelkovic et al. 1997; Pearce et al. 2010; Hers et al. 2011). Upon extracellular stimuli and the tyrosine receptor activation, class I PI3K generates the PIP3 that engages both PDK1 and AKT through PH domain to the plasma membrane. PDK1 phosphorylates AKT at position Thr-308 that is located on the catalytic domain of AKT (Alessi et al. 1997). This phosphorylation triggers the inhibitory phosphorylation of TSC1/2 that is a well-known GAP for RHEB protein. Phosphorylation of TSC1/2 suppresses its inhibitory effect on mTORC1 (Inoki et al. 2002, 2003). Second key phosphorylation site for AKT is on the hydrophobic motifs of AKT Ser-473 that will be phosphorylated through the second mTOR complex (mTORC2).

Other RAS effectors are RALGDS, PLCε, and RASSF. RALGDS links RAS with RALA/B, and regulates cellular processes such as vesicular trafficking, endocytosis and migration (Ferro and Trabalzini 2010). RPM/RGL3, another member of the RALGDS family, is an effector for both HRAS and RRAS3, which has inhibitory effects on the MAPK pathway (Ehrhardt et al. 2001). Dual functions of PLCε, activated by RAS proteins (Kelley et al. 2001; Song et al. 2001; Ada-Nguema et al. 2006; Bunney et al. 2006, 2009), include RAPGEF and PIP_2 lipase C activities, which controls endocytosis, exocytosis, and cytoskeletal reorganization (Bunney and Katan 2006). RASSF5 (also called NORE1) forms a complex with MST1/2 kinases, human orthologs of Hippo, and promotes apoptosis and cell cycle arrest (Stieglitz et al. 2008; Chan and Katan 2013). RASSF1 is also potential tumor suppressor and is required for death receptor-dependent apoptosis and mediates activation of STK3/MST2 and STK4/MST1 during FAS-induced apoptosis by preventing their dephosphorylation (Praskova et al. 2004). Notably, there are many more RAS effectors reported, e.g. TIAM1, p120RASGAP, RIN, AF6, IMP, GRB7, and SIN1 (Pamonsinlapatham et al. 2009; Berndt et al. 2011; Stephen et al. 2014; McCormick 2015, 2016).

It is believed that different RAS isoforms can generate specific biological functions. HRAS has a critical role in mediating different cellular effects. Focal adhesion kinase (FAK) is a widely expressed non-receptor tyrosine kinase and is stimulated by PDGF. HRAS plays as an intermediate protein regulating PDGF-induced FAK tyrosine phosphorylation in human hepatic stellate cells (HSCs) (Carloni et al. 2000). Oncogenic HRAS preferentially activates endogenous CRAF compared to ARAF, which is due to the reduced binding affinity of HRAS for ARAF (Weber et al. 2000). In primary hepatocytes, HRAS is the major mediator of ERK induced proliferation and survival, while HRAS and KRAS both mediate PI3K-induced survival (Rosseland et al. 2008). KRAS4A and KRAS4B share the same effectors but some proteins are specific for KRAS4B, such as CAM (Villalonga et al. 2001), which facilitates KRAS4B interaction with CRAF, RASGAP, and plasma membrane. Moreover, it has been shown that KRAS4B binding to CAM will lead to the suppression of non-canonical WNT signaling that strongly contributes to its tumorigenic properties (Wang et al. 2015).

RRAS signaling

RRAS binds FLNa and promotes endothelial barrier function, which is loss if interfering with the RRAS-FLNA interaction (Griffiths et al. 2011). Another RRAS effector is gridin that is associated with VE-cadherin and controls transendothelial permeability (Griffiths et al. 2011; Ichimiya et al. 2015). In response to a wide variety of inflammatory mediators, RRAS also activates, together with RAP1, αMβ2 integrin in macrophages via a pathway involving RAP1 (Caron et al. 2000), stimulates the formation of focal adhesion through FAK and p130CAS (Kwong et al. 2003), activates PLCε and controls the actin cytoskeleton arrangement (Ada-Nguema et al. 2006). The RRAS-RIN2-RAB5 axis recruits the RACGEF TIAM1 to control RAC1-dependent endothelial cell adhesion (Sandri et al. 2012).

RAP signaling

RAP proteins contribute to several biological processes which are often related to the cytoskeleton, adhesion receptors, and cellular trafficking (Frische and Zwartkruis 2010). RAP1 regulates adhesion to ECM via activation of RGS14, PKD1, and RAPL (Nonaka et al. 2008; Plak et al. 2016; Zhang et al. 2017), controls cell–cell junction via interaction with AF6 and KRIT1 (Glading et al. 2007; Kooistra et al. 2007). RAP2 interacts with MAP4K4, MINK, TNIK, RPIP9, PARG1, and PLCε and, thus, participates in different pathways (Rebhun et al. 2000; Ohba et al. 2001; Stork 2003; Stope et al. 2004). In neurons, RAP2 regulates JNK activity leading to depotentiation by mediating synaptic internalization of AMPA receptors (Zhu et al. 2005). The RAP2 effector MAP4K4, but obviously not TNIK, mediates activation of JNK pathway (Machida et al. 2004). RAP2 interaction with TNIK increases the kinase activity and interferes with the cell spreading. TNIK is a specific RAP2 effector and is involved in actin cytoskeleton regulation (Taira et al. 2004). PLCε is activated via RAP2B and its activation increases intracellular level of Ca^{2+}. RAP2B is involved in Lung cancer development through its interaction with PLCε (Nonaka et al. 2008; Tyutyunnykova et al. 2017). PARG1 is a specific effector of RAP2 which induces typical cytoskeletal changes for RHO inactivation in fibroblasts. RAP2 interacts with ZPH region of PARG1 which mediates suppression of PARG1 action (Myagmar et al. 2005). RPIP9 is a RAP2 effector and its activation happens during the malignant breast epithelial transformation and is related to metastatic lymph node invasion (Raguz et al. 2005). Misshapen/NIKs-related kinase (MINK) is a RAP2 interacting protein whose interaction with RAP2 is GTP dependent. MINK is enriched in the brain and activated MINK phosphorylates the postsynaptic scaffold protein TANC1 (Nonaka et al. 2008).

RAL signaling

A well-studied function of RAL proteins is the regulation and assembly of the multiprotein exocyst complex and, therefore, regulation of exocytosis. Activated RALA, but none of the other RAS proteins, interacts with SEC5 and EXO84 in a competitive manner (Moskalenko et al. 2002; Sugihara et al. 2002; Jin et al. 2005). RALA-SEC5 and RALA-EXO84 interactions are critical regulators of vesicle trafficking and exocytosis of adhesion molecules, transporters, and receptors in many cell types and organisms (de Leeuw et al. 2001; Shipitsin and Feig 2004; Kawato et al. 2008; Lopez et al. 2008; Sanchez-Ruiz et al. 2011; Teodoro et al. 2013). RAL-exocyst complex regulates the actin cytoskeletal organization by mediating filopodia formation (Sugihara et al. 2002), cellular motility (Spiczka and Yeaman 2008), autophagosome formation (Bodemann et al. 2011), protein sorting (Shipitsin and Feig 2004), neurite branching (Lalli and Hall 2005), and cytokinesis (Cascone et al. 2008; Shirakawa and Horiuchi 2015). RALBP1 (also called RLIP76), the first RAL effector that have been described, regulates mitotic progression of cytokinesis (Cascone et al. 2008), and endocytosis of EGF and insulin receptors through the interaction with active RALA and RALB (Nakashima et al. 1999; Jullien-Flores et al. 2000). RALA interaction with PLD1 stimulates together with ARF6 mTORC1 signaling (Xu et al. 2011) and modulates localization of the cell cycle inhibitor, p27 (Tazat et al. 2013). This interaction, however, appears to be nucleotide-independent and mediated via the 11 amino acid extension of RALA (Jiang et al. 1995).

RIT signaling

RIT1/2 interact, among known RAS effectors, with AF6 and RALGDS family proteins, which consists of RALGDS, RGL, RGL2/Rlf, and RGL3 (Ferro and Trabalzini 2010), that directly link RIT1 to RAL signaling pathways (Shao et al. 1999; Shao and Andres 2000). RIT2 targets the RAC/CDC42 activation via PAR6 and regulates neurite outgrowth in PC12 cells (Hoshino and Nakamura 2003; Hoshino et al. 2005). RIT1 binds SIN1 and may regulate AKT phosphorylation by mTORC2 (Cai and Andres 2014). This and other studies confirmed the unique role of RIT1 but no other RAS proteins in protection against cellular stress (Shi et al. 2011; Cai et al. 2012). In this context, RIT1 also activates the second survival cascade, p38-MSK1-CREB, which results in expression of anti-apoptotic proteins, such as BCL-2 and BLC-XL (Shi et al. 2012). Activation of the RIT1-MKK3/MKK6-p38γ axis

promotes c-JUN transcriptional activity (Sakabe et al. 2002). RIT1 regulates the p38-MK2-HSP27 axis and by subsequent AKT activation and BAD phosphorylation, leads to the inhibition of apoptosis induced by ROS (Cai et al. 2011).

RIT1/2 are also involved in neuron differentiation, neurogenesis, neurite growth, and branching. RIT1 links NGF signaling to the MEK-ERK signal pathway (Spencer et al. 2002a) and regulates neurite elongation and branching *via* BRAF and p38 but not the AKT pathway (Hynds et al. 2003; Shi and Andres 2005). RIT1, however, modulates the proliferation and differentiation of neuronal progenitor cells *via* SIN1-mTORC2-AKT axis in adult brain, which results, among others, in phosphorylation of SOX2, a stem cell-specific transcriptional factor (Mir et al. 2017). RIT2 has been found in different protein complexes. Downstream of PACAP38-Gαs-SRC axis, RIT2 controls neuronal differentiation via HSP27, which stabilizes the actin cytoskeleton (Shi et al. 2008). In addition, RIT2 participates in regulated, PKC-dependent, endocytosis and internalization of DAT1, and terminates dopamine signaling in the brain (Navaroli et al. 2011).

RHEB signaling

RHEB1 plays an essential role in different organs and regulates various cellular processes ranging from cell growth to apoptosis (Ehrkamp et al. 2013). A well-studied pathway is RHEB1-mTORC1 that regulates translation, autophagy, and cell growth (Heard et al. 2014; Armijo et al. 2016; Potheraveedu et al. 2017). RHEB1 directly binds and activates mTOR (Long et al. 2005). This activity is obviously modulated by different proteins. PLD1 binds RHEB1 and potentiates mTOR activation and presumably leads to cell size regulation (Sun et al. 2008). PLD1-produced phosphatidic acid directly interacts with the mTOR domain that is targeted by rapamycin (Fang et al. 2001). In contrast, PDE4D and GAPDH bind to RHEB1 and sequester it from mTOR activation (Lee et al. 2009; Kim et al. 2010). The latter is regulated by cAMP and Gly-3-P, which binds PDE4D and GAPDH, respectively, and release RHEB1 to bind mTOR and activates mTORC1 (Lee et al. 2009; Kim et al. 2010). Due to its high similarity to HRAS within the switch I region, RHEB1 has been shown to interact with CRAF and BRAF although with a different binding affinity (Karassek et al. 2010). While RHEB1 binding to BRAF inhibits its kinase activity and prevents BRAF-dependent activation of the MAPK pathway (Im et al. 2002; Karbowniczek et al. 2004), it appears to bind CRAF and activates cell transformation and neurite outgrowth (Yee and Worley 1997). In addition, RHEB1 binds dynein and blocks aggresome formation and autophagy (Zhou et al. 2009), interacts with FKBP38 and interferes with the BCL2 family protein association with the pro-apoptotic BAX/BAK proteins (Ma et al. 2010), and RHEB1-NOTCH association is involved in cell-fate decision (Karbowniczek et al. 2010). In addition, RHEB interaction with β-site amyloid precursor protein (APP)-cleaving enzyme1 (β-secretase, BACE1) results in its instability and lower level of amyloid β generation (Shahani et al. 2014). Protein kinase-like ER kinase (PERK) is known as a novel RHEB1 effector and its activation results in an eIF2α phosphorylation and inhibition of protein synthesis again in a mTORC-independent manner (Tyagi et al. 2015). In addition, there is a crosstalk between RHEB1 and Hippo pathway, where RHEB1 stimulates Hippo signaling via binding to RASSF1. However, the RASSF1 binding to RHEB has an adverse effect on mTORC activity (Nelson and Clark 2016).

ERAS signaling

Our knowledge about effector interaction and signal transduction of ERAS as well as DIRAS and RASD paralogs is very limited. The constitutive active ERAS controls growth of mouse embryonic stem cells and maintains quiescence in rat hepatic stellate cells via the PI3K-PDK1-AKT-mTORC1 axis (Takahashi et al. 2003; Nakhaei-Rad et al. 2016). ERAS may also regulate other pathways, including MST1/2-LATS1/2-YAP and SIN1-mTORC2 (Nakhaei-Rad et al. 2016), which remains to be proved.

DIRAS signaling

DIRAS proteins antagonizes RAS signaling (Bergom et al. 2016) leading to decreased levels of phosphorylation of CRAF, MEK, ERK, p90RSK, and BAD (Zhu et al. 2013). In *Caenorhabditis elegans*, DIRas-1 ortholog binds to Epac-1 and modulates the synaptic plasticity in neurons (Tada et al. 2012). Zebrafish DIRas increases the protein levels and activity of Rac1 and regulates via Rac1-Pak1-Cdk5-ARP2/3 axis neurite outgrowth (Yeh and Hsu 2016). DIRAS3 interferes with IL6-induced STAT3 phosphorylation and transcriptional activity towards cMYC, Cyclin D1, and Bcl-xL (Nishimoto et al. 2005). Moreover, DIRAS3 directly binds CRAF probably via its N-terminal extension and interferes with MEK-ERK1/2 activation (Klingauf et al. 2013).

RASD signaling

RASD1 (also called AGS1 or DEXRAS) is a non-receptor activator of $G_{\alpha i}$ and $G_{\alpha o}$ proteins (Cismowski et al. 1999;

Cismowski et al. 2000; Blumer and Lanier 2014). It blocks receptor-mediated sensitization of AC1 in a Gβγ-dependent manner (Nguyen and Watts 2005) and inhibits PMA-induced activation stimulation of AC2 by interfering with PKCδ autophosphorylation (Nguyen and Watts 2006). RASD2 (also called RHES) binds to PAP7 in a PKA-dependent manner and activates DMT1 and iron uptake in the striatum (Choi et al. 2013).

Dysfunctions and diseases

As RAS family proteins essentially control a wide variety of cellular processes, it is obvious that any dysregulation or dysfunction of the respective signaling pathways results in the development of human diseases, including developmental, hematological, neurocognitive and neurodegenerative disorders, metabolic and cardiovascular diseases, and cancer.

Somatic mutations, frequently identified for example in *KRAS4B*, *HRAS*, *NRAS*, and *RIT1* (COSMIC), contribute to robust gain-of-function (GoF) effects and to various types of cancers as well as leukemia and lymphoma tumors (The Cancer Genome Atlas Research Network 2014; Simanshu et al. 2017). Such oncogenes are constitutive active and thus, strongly contribute to neoplastic signal transduction (Hobbs et al. 2016). Similarly, GoF mutations of genes frequently related to *BRAF* and *PI3K*, cause constitutive activation of the MAPK and PDK1-AKT/PKB pathways (Santarpia et al. 2012; Mandal et al. 2016). In contrast, loss-of-function (LoF) mutations of tumor-suppressive DIRAS genes is associated with progression of various cancers, including esophageal, ovarian, breast, and colon cancers and particularly also glioblastoma (Ligon et al. 1997; Ellis et al. 2002; Reif et al. 2011; Zhu et al. 2013; Zheng et al. 2017). A proposed mechanism for the tumor suppressive functions of DIRAS1 is sequestration of SmgGDS from activation of KRAS4B, RAP1A, and RHOA (Bergom et al. 2016). Negative regulation of ERK and p38 by DIRAS1 appears to induce apoptosis and inhibit invasion and metastasis (Zhu et al. 2013). DIRAS3 downregulation may underlay transcriptional mechanisms, involving E2F1 and E2F4, and also loss of DIRAS3 mRNA binding proteins (Guénard and Durocher 2010). LoF somatic mutations in the *NF1* gene, encoding a RASGAP protein, result in dysregulation of the RAS/MAPK pathway and thus, cause neurofibromatosis, a multisystem disorder, and tumor predisposition syndrome (Philpott et al. 2017; Postema et al. 2018). Somatic *NF1* mutations are associated with the development of sporadic tumors in children (Brems et al. 2009; Ratner and Miller 2015; Varan et al. 2016; Philpott et al. 2017).

Mild GoF effects by germline mutations of *KRAS4B*, *HRAS1/2*, *NRAS*, *RIT1*, and *RRAS1/3* genes (NSEuroNet database) cause a class of developmental syndromes. These phenotypically overlapping genetic disorders collectively known as RASopathies are mainly caused by dysregulation of the RAS-MAPK pathway. RASopathies include Noonan syndrome (genes encoding KRAS4B, NRAS, RRAS1/3, RIT1, SOS1, SOS2, RASGAP1M, BRAF, CRAF), cardio-facio-cutaneous syndrome (KRAS4B, BRAF, ERK1/2), Costello syndrome (HRAS1, HRAS2), neurofibromatosis type 1 (neurofibromin), Legius syndrome (SPRED1), Noonan syndrome with multiple lentigines (BRAF, CRAF), and capillary malformation/arteriovenous malformation syndrome (p120RASGAP) (Rauen 2013; Flex et al. 2014; Korf et al. 2015; Lissewski et al. 2015; Aoki et al. 2016; Tidyman and Rauen 2016; Cao et al. 2017; Higgins et al. 2017; Pantaleoni et al. 2017; Simanshu et al. 2017; Ueda et al. 2017). RASopathies have pleiomorphic features, including in part facial anomalies, cognitive impairment, and congenital heart defects (Gelb et al. 2015; Lissewski et al. 2015; Aoki et al. 2016; Cave et al. 2016; Mainberger et al. 2016; Simanshu et al. 2017). Inactivating germline mutations in *NF1* gene are associated with impaired activation of the RAS pathways and increase risk of neoplasms (Alkindy et al. 2012; Ratner and Miller 2015).

RAS proteins are also involved in neuropsychiatric and neurodegenerative disorders, e.g. RIT2 in schizophrenia and autism (Glessner et al. 2010; Navaroli et al. 2011; Liu et al. 2016), RIT2 and DIRAS1 in Parkinson's disease (Latourelle et al. 2012; Pankratz et al. 2012; Nalls et al. 2014), RASD2 and RRAS1 in Huntington's disease (Miller et al. 2012; Ray et al. 2014; Vahatupa et al. 2016). Alterations in the expressional control of DIRAS2 also contribute to the ADHD phenotype of the attention deficit-hyperactivity disorder (Reif et al. 2011; Grunewald et al. 2016). RASD1 plays a role in synchronizing circadian rhythms, as its deletion impairs circadian entrainment to light cycles and alters phase shifts to light (Cheng et al. 2004). The molecular nature of these (dys)functions are not well understood. However, several biochemical studies have provided valuable molecular insights into the roles of RAS protein in these disorders. The RASD2 activity as a SUMO-E3 ligase (Subramaniam et al. 2010) on the polyglutamine-expanded mutant huntingtin protein leading to augmented neurotoxicity and likely to Huntington's disease (Harrison 2012; Thapliyal et al. 2014). S-nitrosylation and activation of RASD1 by NMDA-nNOS pathway induces physiological iron uptake through interaction with PAP7 and activation of DMT1, and may be critical for NMDA neurotoxicity (Cheah et al. 2006; Chen et al. 2013; Choi

et al. 2013). The role of RIT2 in neuropsychiatric disorders may be based on its role in the internalization and downregulation of biogenic amine transporters, which are discussed to be central to autism (Navaroli et al. 2011).

Conclusions and perspectives

More than 30 years intensive research and tens of thousands of published studies have provided valuable insights into biology, biochemistry, and biophysics of the RAS family proteins. We have gained deep knowledge about their membrane trafficking, structure–function relationship, mechanisms of GDP/GTP binding, and accelerated nucleotide exchange by GEFs, intrinsic and GAP-stimulated GTP hydrolysis, interaction with effectors, and activation of diverse signaling pathways. However, these studies have their eligible confinement: Cell-free investigations have been predominantly carried out in the absence of lipid membrane using defined domains rather than full-length proteins, and cell-based studies have been mostly performed using heterologous expression of tagged genes and their variants in a methodologically congenial cell lines. As the omics era is coming to an end and the research becomes decelerated, many new movements are emerged, especially due to the accessibility of new technologies. Several novel mechanisms have been uncovered that have extended our understanding the role of protein–protein/protein–lipid interactions, and various types of post-translational modifications in the modulation of the RAS protein activity. Another issue is the activation mechanism of regulators and effectors. Notably, identification of additional components of the RAS interaction networks is a critical step towards understanding both the relationship between the RAS proteins and the selective activation of respective effectors, and the molecular signatures required for spatiotemporal integration and activation of the GEFs and GAPs. Identification and functional reconstitution of specific interaction networks by using appropriate liposomes and full-length regulators and effector proteins may eventually provide fundamental insights into the functional characterization of multiprotein complexes of RAS and the complete identification of regulatory mechanisms. In this context, an interesting issue, which is increasingly appreciated, is a RAS-membrane interaction that appears to generate RAS isoform specificity with respect to regulator and effector interactions. This is likely achieved by scaffold proteins which may modulate isoform specificity at specific site of the cell. Hence, elucidation of the RAS signal transduction requires not only RAS-effector interactions but also additional structures and interplay of multiprotein complexes. Keeping this in mind, accumulating evidence support a role for cell type-dependent RAS paralog functions that should prompt future efforts to examine the respective pathways in a more context-specific manner. Such efforts could lead to the identification of disease-specific therapeutic opportunities.

Acknowledgements

We thank Dr Balal Sadeghi for critical reading of the manuscript. We are grateful to our colleagues from the Institute of Biochemistry and Molecular Biology II of the Heinrich-Heine University Düsseldorf for their support. We apologize to the many scientists and colleagues whose original studies could not be included in this Review owing to space constraints.

Disclosure statement

The authors declare no conflict of interest.

Funding

This study was supported by the Research committee of the Medical Faculty of the Heinrich-Heine University Düsseldorf (FoKo; grant number 9772617); the German Research Foundation (Deutsche Forschungsgemeinschaft or DFG) through the Collaborative Research Center 974 [SFB 974; project A03]; the German Federal Ministry of Education and Research (BMBF) – German Network of RASopathy Research (GeNeRARe); the European Network on Noonan Syndrome and Related Disorders (NSEuroNet).

References

Abankwa D, Gorfe AA, Hancock JF. 2007. Ras nanoclusters: molecular structure and assembly. Semin Cell Dev Biol. 18:599–607.

Abankwa D, Gorfe AA, Inder K, Hancock JF. 2010. Ras membrane orientation and nanodomain localization generate isoform diversity. Proc Natl Acad Sci USA. 107:1130–1135.

Ada-Nguema AS, Xenias H, Hofman JM, Wiggins CH, Sheetz MP, Keely PJ. 2006. The small GTPase R-Ras regulates organization of actin and drives membrane protrusions through the activity of PLCepsilon. J Cell Sci. 119:1307–1319.

Ahearn IM, Haigis K, Bar-Sagi D, Philips MR. 2011. Regulating the regulator: post-translational modification of RAS. Nat Rev Mol Cell Biol. 13:39–51.

Ahmadian MR, Kiel C, Stege P, Scheffzek K. 2003. Structural fingerprints of the Ras-GTPase activating proteins neurofibromin and p120GAP. J Mol Biol. 329:699–710.

Ahmadian MR, Stege P, Scheffzek K, Wittinghofer A. 1997. Confirmation of the arginine-finger hypothesis for the GAP-stimulated GTP-hydrolysis reaction of Ras. Nat Struct Mol Biol. 4:686–689.

Ahmadian MR, Zor T, Vogt D, Kabsch W, Selinger Z, Wittinghofer A, Scheffzek K. 1999. Guanosine triphosphatase stimulation of oncogenic Ras mutants. Proc Natl Acad Sci USA. 96:7065–7070.

Alessi DR, James SR, Downes CP, Holmes AB, Gaffney PR, Reese CB, Cohen P. 1997. Characterization of a 3-phosphoinositide-dependent protein kinase which phosphorylates and activates protein kinase Balpha. Curr Biol. 7:261–269.

Alkindy A, Chuzhanova N, Kini U, Cooper DN, Upadhyaya M. 2012. Genotype-phenotype associations in neurofibromatosis type 1 (NF1): an increased risk of tumor complications in patients with NF1 splice-site mutations? Hum Genomics. 6:12.

Alvarez-Moya B, Barcelo C, Tebar F, Jaumot M, Agell N. 2011. CaM interaction and Ser181 phosphorylation as new K-Ras signaling modulators. Small GTPases. 2:99–103.

Andjelkovic M, Alessi DR, Meier R, Fernandez A, Lamb NJ, Frech M, Cron P, Cohen P, Lucocq JM, Hemmings BA. 1997. Role of translocation in the activation and function of protein kinase B. J Biol Chem. 272:31515–31524.

Aoki Y, Niihori T, Inoue S, Matsubara Y. 2016. Recent advances in RASopathies. J Hum Genet. 61:33–39.

Armijo ME, Campos T, Fuentes-Villalobos F, Palma ME, Pincheira R, Castro AF. 2016. Rheb signaling and tumorigenesis: mTORC1 and new horizons. Int J Cancer. 138:1815–1823.

Ashery U, Yizhar O, Rotblat B, Kloog Y. 2006. Nonconventional trafficking of Ras associated with Ras signal organization. Traffic. 7:119–126.

Baker R, Lewis SM, Sasaki AT, Wilkerson EM, Locasale JW, Cantley LC, Kuhlman B, Dohlman HG, Campbell SL. 2013a. Site-specific monoubiquitination activates Ras by impeding GTPase-activating protein function. Nat Struct Mol Biol. 20:46–52.

Baker R, Wilkerson EM, Sumita K, Isom DG, Sasaki AT, Dohlman HG, Campbell SL. 2013b. Differences in the regulation of K-Ras and H-Ras isoforms by monoubiquitination. J Biol Chem. 288:36856–36862.

Baljuls A, Beck M, Oenel A, Robubi A, Kroschewski R, Hekman M, Rudel T, Rapp UR. 2012. The tumor suppressor DiRas3 forms a complex with H-Ras and C-RAF proteins and regulates localization, dimerization, and kinase activity of C-RAF. J Biol Chem. 287:23128–23140.

Banerjee A, Jang H, Nussinov R, Gaponenko V. 2016. The disordered hypervariable region and the folded catalytic domain of oncogenic K-Ras4B partner in phospholipid binding. Curr Opin Struct Biol. 36:10–17.

Battram AM, Durrant TN, Agbani EO, Heesom KJ, Paul DS, Piatt R, Poole AW, Cullen PJ, Bergmeier W, Moore SF, Hers I. 2017. The phosphatidylinositol 3,4,5-trisphosphate (PI(3,4,5)P3) binder Rasa3 regulates phosphoinositide 3-kinase (PI3K)-dependent Integrin alphallbbeta3 outside-in signaling. J Biol Chem. 292:1691–1704.

Benetka W, Koranda M, Maurer-Stroh S, Pittner F, Eisenhaber F. 2006. Farnesylation or geranylgeranylation? Efficient assays for testing protein prenylation in vitro and in vivo. BMC Biochem. 7:6.

Beranger F, Tavitian A, de Gunzburg J. 1991. Post-translational processing and subcellular localization of the Ras-related Rap2 protein. Oncogene. 6:1835–1842.

Bergom C, Hauser AD, Rymaszewski A, Gonyo P, Prokop JW, Jennings BC, Lawton AJ, Frei A, Lorimer EL, Aguilera-Barrantes I, et al. 2016. The tumor-suppressive small GTPase DiRas1 binds the noncanonical guanine nucleotide exchange factor SmgGDS and antagonizes SmgGDS interactions with oncogenic small GTPases. J Biol Chem. 291:6534–6545.

Berndt N, Hamilton AD, Sebti SM. 2011. Targeting protein prenylation for cancer therapy. Nat Rev Cancer. 11:775.

Berzat AC, Brady DC, Fiordalisi JJ, Cox AD. 2006. Using inhibitors of prenylation to block localization and transforming activity. Methods Enzymol. 407:575–597.

Bhagatji P, Leventis R, Rich R, Lin CJ, Silvius JR. 2010. Multiple cellular proteins modulate the dynamics of K-ras association with the plasma membrane. Biophys J. 99:3327–3335.

Bivona TG, Quatela SE, Bodemann BO, Ahearn IM, Soskis MJ, Mor A, Miura J, Wiener HH, Wright L, Saba SG, et al. 2006. PKC regulates a farnesyl-electrostatic switch on K-Ras that promotes its association with Bcl-XL on mitochondria and induces apoptosis. Mol Cell. 21:481–493.

Blazevits O, Mideksa YG, Solman M, Ligabue A, Ariotti N, Nakhaeizadeh H, Fansa EK, Papageorgiou AC, Wittinghofer A, Ahmadian MR, Abankwa D. 2016. Galectin-1 dimers can scaffold Raf-effectors to increase H-ras nanoclustering. Sci Rep. 6:24165.

Blumer JB, Lanier SM. 2014. Activators of G protein signaling exhibit broad functionality and define a distinct core signaling triad. Mol Pharmacol. 85:388–396.

Bodemann BO, Orvedahl A, Cheng T, Ram RR, Ou YH, Formstecher E, Maiti M, Hazelett CC, Wauson EM, Balakireva M, et al. 2011. RalB and the exocyst mediate the cellular starvation response by direct activation of autophagosome assembly. Cell. 144:253–267.

Boriack-Sjodin PA, Margarit SM, Bar-Sagi D, Kuriyan J. 1998. The structural basis of the activation of Ras by Sos. Nature. 394:337–343.

Bos JL. 2005. Linking Rap to cell adhesion. Curr Opin Cell Biol. 17:123–128.

Bourne HR, Sanders DA, McCormick F. 1991. The GTPase superfamily: conserved structure and molecular mechanism. Nature. 349:117.

Braun BS, Shannon K. 2008. Targeting Ras in myeloid leukemias. Clin Cancer Res. 14:2249–2252.

Brems H, Beert E, de Ravel T, Legius E. 2009. Mechanisms in the pathogenesis of malignant tumours in neurofibromatosis type 1. Lancet Oncol. 10:508–515.

Broustas CG, Grammatikakis N, Eto M, Dent P, Brautigan DL, Kasid U. 2001. Phosphorylation of the myosin-binding subunit of myosin phosphatase by Raf-1 and inhibition of phosphatase activity. J Biol Chem. 277:3053–3059.

Buday L, Downward J. 2008. Many faces of Ras activation. Biochim Biophys Acta. 1786:178–187.

Bunney TD, Baxendale RW, Katan M. 2009. Regulatory links between PLC enzymes and Ras superfamily GTPases: signalling via PLCepsilon. Adv Enzyme Regul. 49:54–58.

Bunney TD, Harris R, Gandarillas NL, Josephs MB, Roe SM, Sorli SC, Paterson HF, Rodrigues-Lima F, Esposito D, Ponting CP, et al. 2006. Structural and mechanistic insights into ras association domains of phospholipase C epsilon. Mol Cell. 21:495–507.

Bunney TD, Katan M. 2006. Phospholipase C epsilon: linking second messengers and small GTPases. Trends Cell Biol.16:640–648.

Bunney TD, Katan M. 2011. PLC regulation: emerging pictures for molecular mechanisms. Trends Biochem Sci. 36:88–96.
Cai W, Andres DA. 2014. mTORC2 is required for rit-mediated oxidative stress resistance. PLoS One. 9:e115602
Cai W, Rudolph JL, Harrison SM, Jin L, Frantz AL, Harrison DA, Andres DA. 2011. An evolutionarily conserved Rit GTPase-p38 MAPK signaling pathway mediates oxidative stress resistance. Mol Biol Cell. 22:3231–3241.
Cai W, Rudolph JL, Sengoku T, Andres DA. 2012. Rit GTPase regulates a p38 MAPK-dependent neuronal survival pathway. Neurosci Lett. 531:125–130.
Calvo F, Crespo P. 2009. Structural and spatial determinants regulating TC21 activation by RasGRF family nucleotide exchange factors. Mol Biol Cell. 20:4289–4302.
Camats M, Kokolo M, Heesom KJ, Ladomery M, Bach-Elias M. 2009. P19 H-ras induces G1/S phase delay maintaining cells in a reversible quiescence state. PLoS One. 4:e8513.
Cao H, Alrejaye N, Klein OD, Goodwin AF, Oberoi S. 2017. A review of craniofacial and dental findings of the RASopathies. Orthod Craniofac Res. 20 Suppl 1:32–38.
Carloni V, Pinzani M, Giusti S, Romanelli RG, Parola M, Bellomo G, Failli P, Hamilton AD, Sebti SM, Laffi G, Gentilini P. 2000. Tyrosine phosphorylation of focal adhesion kinase by PDGF is dependent on ras in human hepatic stellate cells. Hepatology 31:131–140.
Caron E, Self AJ, Hall A. 2000. The GTPase Rap1 controls functional activation of macrophage integrin alphaMbeta2 by LPS and other inflammatory mediators. Curr Biol. 10:974–978.
Carroll B, Maetzel D, Maddocks OD, Otten G, Ratcliff M, Smith GR, Dunlop EA, Passos JF, Davies OR, Jaenisch R, et al. 2016. Control of TSC2-Rheb signaling axis by arginine regulates mTORC1 activity. Elife. 5:e11058.
Cascone I, Selimoglu R, Ozdemir C, Del Nery E, Yeaman C, White M, Camonis J. 2008. Distinct roles of RalA and RalB in the progression of cytokinesis are supported by distinct RalGEFs. EMBO J. 27:2375–2387.
Castellano E, Downward J. 2010. Role of RAS in the regulation of PI 3-kinase. Curr Top Microbiol Immunol. 346:143–169.
Castellano E, Downward J. 2011. RAS interaction with PI3K: more than just another effector pathway. Genes Cancer. 2:261–274.
Cave H, Caye A, Strullu M, Aladjidi N, Vignal C, Ferster A, Mechinaud F, Domenech C, Pierri F, Contet A, et al. 2016. Acute lymphoblastic leukemia in the context of RASopathies. Eur J Med Genet. 59:173–178.
Cha JY, Kim HJ, Yu JH, Xu J, Kim D, Paul BD, Choi H, Kim S, Lee YJ, Ho GP, et al. 2013. Dexras1 mediates glucocorticoid-associated adipogenesis and diet-induced obesity. Proc Natl Acad Sci USA. 110:20575–20580.
Chan JJ, Katan M. 2013. PLCε and the RASSF family in tumour suppression and other functions. Adv Biol Regul. 53:258–279.
Chandra A, Grecco HE, Pisupati V, Perera D, Cassidy L, Skoulidis F, Ismail SA, Hedberg C, Hanzal-Bayer M, Venkitaraman AR, et al. 2011. The GDI-like solubilizing factor PDEdelta sustains the spatial organization and signalling of Ras family proteins. Nat Cell Biol. 14:148–158.
Cheah JH, Kim SF, Hester LD, Clancy KW, Patterson SE, Papadopoulos V, Snyder SH. 2006. NMDA receptor-nitric oxide transmission mediates neuronal iron homeostasis via the GTPase Dexras1. Neuron 51:431–440.
Chen J, Fujii K, Zhang L, Roberts T, Fu H. 2001. Raf-1 promotes cell survival by antagonizing apoptosis signal-regulating kinase 1 through a MEK-ERK independent mechanism. Proc Natl Acad Sci USA. 98:7783–7788.
Chen Y, Khan RS, Cwanger A, Song Y, Steenstra C, Bang S, Cheah JH, Dunaief J, Shindler KS, Snyder SH. 2013. Dexras1, a small GTPase, is required for glutamate-NMDA neurotoxicity. J Neurosci. 33:3582–3587.
Chen Y, Mathias L, Falero-Perez JM, Kim SF. 2015. PKA-mediated phosphorylation of Dexras1 suppresses iron trafficking by inhibiting S-nitrosylation. FEBS Lett. 589:3212–3219.
Cheng H-YM, Obrietan K, Cain SW, Lee BY, Agostino PV, Joza NA, Harrington ME, Ralph MR, Penninger JM. 2004. Dexras1 potentiates photic and suppresses nonphotic responses of the circadian clock. Neuron. 43:715–728.
Cherfils J, Zeghouf M. 2013. Regulation of small GTPases by GEFs, GAPs, and GDIs. Physiol Rev. 93:269–309.
Choi BR, Bang S, Chen Y, Cheah JH, Kim SF. 2013. PKA modulates iron trafficking in the striatum via small GTPase, Rhes. Neuroscience. 253:214–220.
Cirstea IC, Kutsche K, Dvorsky R, Gremer L, Carta C, Horn D, Roberts AE, Lepri F, Merbitz-Zahradnik T, Konig R, et al. 2010. A restricted spectrum of NRAS mutations causes Noonan syndrome. Nat Genet. 42:27–29.
Cismowski MJ, Ma C, Ribas C, Xie X, Spruyt M, Lizano JS, Lanier SM, Duzic E. 2000. Activation of heterotrimeric G-protein signaling by a Ras-related protein implications for signal integration. J Biol Chem. 275:23421–23424.
Cismowski MJ, Takesono A, Ma C, Lizano JS, Xie X, Fuernkranz H, Lanier SM, Duzic E. 1999. Genetic screens in yeast to identify mammalian nonreceptor modulators of G-protein signaling. Nat Biotechnol. 17:878–883.
Cohen JB, Broz SD, Levinson AD. 1989. Expression of the H-ras proto-oncogene is controlled by alternative splicing. Cell. 58:461–472.
Cordeddu V, Di Schiavi E, Pennacchio LA, Ma'ayan A, Sarkozy A, Fodale V, Cecchetti S, Cardinale A, Martin J, Schackwitz W, et al. 2009. Mutation of SHOC2 promotes aberrant protein N-myristoylation and causes Noonan-like syndrome with loose anagen hair. Nat Genet. 41:1022–1026.
Cox AD, Der CJ. 2003. The dark side of Ras: regulation of apoptosis. Oncogene. 22:8999–9006.
Cox AD, Der CJ, Philips MR. 2015. Targeting RAS membrane association: back to the future for anti-RAS drug discovery? Clin Cancer Res. 21:1819–1827.
Crechet JB, Poullet P, Mistou MY, Parmeggiani A, Camonis J, Boy-Marcotte E, Damak F, Jacquet M. 1990. Enhancement of the GDP-GTP exchange of RAS proteins by the carboxyl-terminal domain of SCD25. Science. 248:866–868.
Dai Y, Walker SA, de Vet E, Cook S, Welch HC, Lockyer PJ. 2011. Ca^{2+}-dependent monomer and dimer formation switches CAPRI Protein between Ras GTPase-activating protein (GAP) and RapGAP activities. J Biol Chem. 286:19905–19916.
Daumke O, Weyand M, Chakrabarti PP, Vetter IR, Wittinghofer A. 2004. The GTPase-activating protein Rap1GAP uses a catalytic asparagine. Nature. 429:197–201.
Davis RK, Chellappan S. 2008. Disrupting the Rb-Raf-1 interaction: a potential therapeutic target for cancer. Drug News Perspect. 21:331–335.

de la Vega M, Burrows JF, McFarlane C, Govender U, Scott CJ, Johnston JA. 2010. The deubiquitinating enzyme USP17 blocks N-Ras membrane trafficking and activation but leaves K-Ras unaffected. J Biol Chem. 285:12028–12036.

de Leeuw HP, Fernandez-Borja M, Reits EA, Romani de Wit T, Wijers-Koster PM, Hordijk PL, Neefjes J, van Mourik JA, Voorberg J. 2001. Small GTP-binding protein Ral modulates regulated exocytosis of von Willebrand factor by endothelial cells. Arterioscler Thromb Vasc Biol. 21:899–904.

de Rooij J, Zwartkruis FJ, Verheijen MH, Cool RH, Nijman SM, Wittinghofer A, Bos JL. 1998. Epac is a Rap1 guanine-nucleotide-exchange factor directly activated by cyclic AMP. Nature. 396:474–477.

Depeille P, Henricks LM, van de Ven RA, Lemmens E, Wang CY, Matli M, Werb Z, Haigis KM, Donner D, Warren R, Roose JP. 2015. RasGRP1 opposes proliferative EGFR-SOS1-Ras signals and restricts intestinal epithelial cell growth. Nat Cell Biol. 17:804–815.

Desideri E, Cavallo AL, Baccarini M. 2015. Alike but different: RAF paralogs and their signaling outputs. Cell. 161:967–970.

Dharmaiah S, Bindu L, Tran TH, Gillette WK, Frank PH, Ghirlando R, Nissley DV, Esposito D, McCormick F, Stephen AG, Simanshu DK. 2016. Structural basis of recognition of farnesylated and methylated KRAS4b by PDEdelta. Proc Natl Acad Sci USA. 113:E6766–E6775.

Dodd KM, Tee AR. 2012. Leucine and mTORC1: a complex relationship. Am J Physiol Endocrinol Metab. 302:E1329–E1342.

Dolnik A, Kanwal N, Mackert S, Halbedl S, Proepper C, Bockmann J, Schoen M, Boeckers TM, Kuhl SJ, Schmeisser MJ. 2016. Sipa1l3/SPAR3 is targeted to postsynaptic specializations and interacts with the Fezzin ProSAPiP1/Lzts3. J Neurochem. 136:28–35.

Dunzendorfer-Matt T, Mercado EL, Maly K, McCormick F, Scheffzek K. 2016. The neurofibromin recruitment factor Spred1 binds to the GAP related domain without affecting Ras inactivation. Proc Natl Acad Sci USA. 113:7497–7502.

Ehrenreiter K, Piazzolla D, Velamoor V, Sobczak I, Small JV, Takeda J, Leung T, Baccarini M. 2005. Raf-1 regulates Rho signaling and cell migration. J Cell Biol. 168:955–964.

Ehrhardt A, David MD, Ehrhardt GR, Schrader JW. 2004. Distinct mechanisms determine the patterns of differential activation of H-Ras, N-Ras, K-Ras 4B, and M-Ras by receptors for growth factors or antigen. Mol Cell Biol. 24:6311–6323.

Ehrhardt GR, Korherr C, Wieler JS, Knaus M, Schrader JW. 2001. A novel potential effector of M-Ras and p21 Ras negatively regulates p21 Ras-mediated gene induction and cell growth. Oncogene. 20:188–197.

Ehrkamp A, Herrmann C, Stoll R, Heumann R. 2013. Ras and rheb signaling in survival and cell death. Cancers (Basel). 5:639–661.

Ellis CA, Vos MD, Howell H, Vallecorsa T, Fults DW, Clark GJ. 2002. Rig is a novel Ras-related protein and potential neural tumor suppressor. Proc Natl Acad Sci USA. 99:9876–9881.

Fang M, Jaffrey SR, Sawa A, Ye K, Luo X, Snyder SH. 2000. Dexras1: a G protein specifically coupled to neuronal nitric oxide synthase via CAPON. Neuron 28:183–193.

Fang Y, Vilella-Bach M, Bachmann R, Flanigan A, Chen J. 2001. Phosphatidic acid-mediated mitogenic activation of mTOR signaling. Science. 294:1942–1945.

Fawal MA, Brandt M, Djouder N. 2015. MCRS1 binds and couples Rheb to amino acid-dependent mTORC1 activation. Dev Cell. 33:67–81.

Feig LA. 1999. Tools of the trade: use of dominant-inhibitory mutants of Ras-family GTPases. Nat Cell Biol. 1:E25–E27.

Ferro E, Trabalzini L. 2010. RalGDS family members couple Ras to Ral signalling and that's not all. Cell Signal. 22:1804–1810.

Findlay GM, Smith MJ, Lanner F, Hsiung MS, Gish GD, Petsalaki E, Cockburn K, Kaneko T, Huang H, Bagshaw RD, et al. 2013. Interaction domains of Sos1/Grb2 are finely tuned for cooperative control of embryonic stem cell fate. Cell. 152:1008–1020.

Flex E, Jaiswal M, Pantaleoni F, Martinelli S, Strullu M, Fansa EK, Caye A, De Luca A, Lepri F, Dvorsky R, et al. 2014. Activating mutations in RRAS underlie a phenotype within the RASopathy spectrum and contribute to leukaemogenesis. Hum Mol Genet. 23:4315–4327.

Fremin C, Guegan JP, Plutoni C, Mahaffey J, Philips MR, Emery G, Meloche S. 2016. ERK1/2-induced phosphorylation of R-Ras GTPases stimulates their oncogenic potential. Oncogene. 35:5692–5698.

Frische EW, Zwartkruis FJ. 2010. Rap1, a mercenary among the Ras-like GTPases. Dev Biol. 340:1–9.

Galaktionov K, Jessus C, Beach D. 1995. Raf1 interaction with Cdc25 phosphatase ties mitogenic signal transduction to cell cycle activation. Genes Dev. 9:1046–1058.

Gasper R, Sot B, Wittinghofer A. 2010. GTPase activity of Di-Ras proteins is stimulated by Rap1GAP proteins. Small GTPases. 1:133–141.

Gelb BD, Roberts AE, Tartaglia M. 2015. Cardiomyopathies in Noonan syndrome and the other RASopathies. Prog Pediatr Cardiol. 39:13–19.

Gentry LR, Martin TD, Reiner DJ, Der CJ. 2014. Ral small GTPase signaling and oncogenesis: More than just 15 minutes of fame. Biochim Biophys Acta. 1843:2976–2988.

Gentry LR, Nishimura A, Cox AD, Martin TD, Tsygankov D, Nishida M, Elston TC, Der CJ. 2015. Divergent roles of CAAX motif-signaled posttranslational modifications in the regulation and subcellular localization of Ral GTPases. J Biol Chem. 290:22851–22861.

Ghiglieri V, Napolitano F, Pelosi B, Schepisi C, Migliarini S, Di Maio A, Pendolino V, Mancini M, Sciamanna G, Vitucci D, et al. 2015. Rhes influences striatal cAMP/PKA-dependent signaling and synaptic plasticity in a gender-sensitive fashion. Sci Rep. 5:10933.

Glading A, Han J, Stockton RA, Ginsberg MH. 2007. KRIT-1/CCM1 is a Rap1 effector that regulates endothelial cell cell junctions. J Cell Biol. 179:247–254.

Glessner JT, Reilly MP, Kim CE, Takahashi N, Albano A, Hou C, Bradfield JP, Zhang H, Sleiman PM, Flory JH, et al. 2010. Strong synaptic transmission impact by copy number variations in schizophrenia. Proc Natl Acad Sci USA. 107:10584–10589.

Gloerich M, Bos JL. 2010. Epac: defining a new mechanism for cAMP action. Annu Rev Pharmacol Toxicol. 50:355–375.

Grewal T, Enrich C. 2006. Molecular mechanisms involved in Ras inactivation: the annexin A6-p120GAP complex. Bioessays. 28:1211–1220.

Grewal T, Evans R, Rentero C, Tebar F, Cubells L, de Diego I, Kirchhoff MF, Hughes WE, Heeren J, Rye KA, et al. 2005. Annexin A6 stimulates the membrane recruitment of

p120GAP to modulate Ras and Raf-1 activity. Oncogene. 24:5809–5820.
Griffiths GS, Grundl M, Allen JS, III, Matter ML. 2011. R-Ras interacts with filamin a to maintain endothelial barrier function. J Cell Physiol. 226:2287–2296.
Grujic O, Bhullar RP. 2009. Ral GTPase interacts with the N-terminal in addition to the C-terminal region of PLC-delta1. Biochem Biophys Res Commun. 383:401–405.
Grunewald L, Landaas ET, Geissler J, Weber H, Quast C, Roh S, Schartner C, Lesch KP, Romanos M, Kittel-Schneider S, et al. 2016. Functional impact of an ADHD-associated DIRAS2 promoter polymorphism. Neuropsychopharmacology. 41:3025–3031.
Guénard F, Durocher F. (2010). DHX9 (DEAH (Asp-Glu-Ala-His) box polypeptide 9). Atlas Genet Cytogenet Oncol Haematol. 14:548.
Guil S, de La Iglesia N, Fernandez-Larrea J, Cifuentes D, Ferrer JC, Guinovart JJ, Bach-Elias M. 2003. Alternative splicing of the human proto-oncogene c-H-ras renders a new Ras family protein that trafficks to cytoplasm and nucleus. Cancer Res. 63:5178–5187.
Guo Z, Ahmadian MR, Goody RS. 2005. Guanine nucleotide exchange factors operate by a simple allosteric competitive mechanism. Biochemistry. 44:15423–15429.
Gureasko J, Galush WJ, Boykevisch S, Sondermann H, Bar-Sagi D, Groves JT, Kuriyan J. 2008. Membrane-dependent signal integration by the Ras activator Son of sevenless. Nat Struct Mol Biol. 15:452–461.
Gutierrez-Erlandsson S, Herrero-Vidal P, Fernandez-Alfara M, Hernandez-Garcia S, Gonzalo-Flores S, Mudarra-Rubio A, Fresno M, Cubelos B. 2013. R-RAS2 overexpression in tumors of the human central nervous system. Mol Cancer. 12:127.
Hancock JF, Magee AI, Childs JE, Marshall CJ. 1989. All ras proteins are polyisoprenylated but only some are palmitoylated. Cell. 57:1167–1177.
Hanzal-Bayer MF, Hancock JF. 2007. Lipid rafts and membrane traffic. FEBS Lett. 581:2098–2104.
Harrison LM. 2012. Rhes: a GTP-binding protein integral to striatal physiology and pathology. Cell Mol Neurobiol. 32:907–918.
Harrison SM, Rudolph JL, Spencer ML, Wes PD, Montell C, Andres DA, Harrison DA. 2005. Activated RIC, a small GTPase, genetically interacts with the Ras pathway and calmodulin during Drosophila development. Dev Dyn. 232:817–826.
Heard JJ, Fong V, Bathaie SZ, Tamanoi F. 2014. Recent progress in the study of the Rheb family GTPases. Cell Signal. 26:1950–1957.
Hennig A, Markwart R, Esparza-Franco MA, Ladds G, Rubio I. 2015. Ras activation revisited: role of GEF and GAP systems. Biol Chem. 396:831–848.
Heo J, Campbell SL. 2004. Mechanism of p21Ras S-nitrosylation and kinetics of nitric oxide-mediated guanine nucleotide exchange. Biochemistry. 43:2314–2322.
Herrero A, Matallanas D, Kolch W. 2016. The spatiotemporal regulation of RAS signalling. Biochem Soc Trans. 44:1517–1522.
Herrmann C. 2003. Ras-effector interactions: after one decade. Curr Opin Struct Biol. 13:122–129.
Hers I, Vincent EE, Tavaré JM. 2011. Akt signalling in health and disease. Cell Signal. 23:1515–1527.
Higgins EM, Bos JM, Mason-Suares H, Tester DJ, Ackerman JP, MacRae CA, Sol-Church K, Gripp KW, Urrutia R, Ackerman MJ. 2017. Elucidation of MRAS-mediated Noonan syndrome with cardiac hypertrophy. JCI Insight. 2:e91225.
Hindley A, Kolch W. 2002. Extracellular signal regulated kinase (ERK)/mitogen activated protein kinase (MAPK)-independent functions of Raf kinases. J Cell Sci. 115:1575–1581.
Hobbs GA, Der CJ, Rossman KL. 2016. RAS isoforms and mutations in cancer at a glance. J Cell Sci. 129:1287–1292.
Holly SP, Larson MK, Parise LV. 2005. The unique N-terminus of R-ras is required for Rac activation and precise regulation of cell migration. Mol Biol Cell. 16:2458–2469.
Hoshino M, Nakamura S. 2003. Small GTPase Rin induces neurite outgrowth through Rac/Cdc42 and calmodulin in PC12 cells. J Cell Biol. 163:1067–1076.
Hoshino M, Yoshimori T, Nakamura S. 2005. Small GTPase proteins Rin and Rit bind to PAR6 GTP-dependently and regulate cell transformation. J Biol Chem. 280:22868–22874.
Hota PK, Buck M. 2012. Plexin structures are coming: opportunities for multilevel investigations of semaphorin guidance receptors, their cell signaling mechanisms, and functions. Cell Mol Life Sci. 69:3765–3805.
Huang S, Chang IS, Lin W, Ye W, Luo RZ, Lu Z, Lu Y, Zhang K, Liao WS, Tao T, et al. 2009. ARHI (DIRAS3), an imprinted tumour suppressor gene, binds to importins and blocks nuclear import of cargo proteins. Biosci Rep. 30:159–168.
Hynds DL, Spencer ML, Andres DA, Snow DM. 2003. Rit promotes MEK-independent neurite branching in human neuroblastoma cells. J Cell Sci. 116:1925–1935.
Ichimiya H, Maeda K, Enomoto A, Weng L, Takahashi M, Murohara T. 2015. Girdin/GIV regulates transendothelial permeability by controlling VE-cadherin trafficking through the small GTPase, R-Ras. Biochem Biophys Res Commun. 461:260–267.
Im E, von Lintig FC, Chen J, Zhuang S, Qui W, Chowdhury S, Worley PF, Boss GR, Pilz RB. 2002. Rheb is in a high activation state and inhibits B-Raf kinase in mammalian cells. Oncogene. 21:6356–6365.
Inder KL, Lau C, Loo D, Chaudhary N, Goodall A, Martin S, Jones A, van der Hoeven D, Parton RG, Hill MM, Hancock JF. 2009. Nucleophosmin and nucleolin regulate K-Ras plasma membrane interactions and MAPK signal transduction. J Biol Chem. 284:28410–28419.
Inoki K, Li Y, Xu T, Guan KL. 2003. Rheb GTPase is a direct target of TSC2 GAP activity and regulates mTOR signaling. Genes Dev. 17:1829–1834.
Inoki K, Li Y, Zhu T, Wu J, Guan KL. 2002. TSC2 is phosphorylated and inhibited by Akt and suppresses mTOR signalling. Nat Cell Biol. 4:648–657.
Jaiswal M, Dvorsky R, Ahmadian MR. 2013. Deciphering the molecular and functional basis of Dbl family proteins: a novel systematic approach toward classification of selective activation of the Rho family proteins. J Biol Chem. 288:4486–4500.
Jameson KL, Mazur PK, Zehnder AM, Zhang J, Zarnegar B, Sage J, Khavari PA. 2013. IQGAP1 scaffold-kinase interaction blockade selectively targets RAS-MAP kinase-driven tumors. Nat Med. 19:626–630.
Jang H, Abraham SJ, Chavan TS, Hitchinson B, Khavrutskii L, Tarasova NI, Nussinov R, Gaponenko V. 2015. Mechanisms

of membrane binding of small GTPase K-Ras4B farnesylated hypervariable region. J Biol Chem. 290:9465–9477.
Jang H, Banerjee A, Chavan T, Gaponenko V, Nussinov R. 2017. Flexible-body motions of calmodulin and the farnesylated hypervariable region yield a high-affinity interaction enabling K-Ras4B membrane extraction. J Biol Chem. 292:12544–12559.
Janosch P, Kieser A, Eulitz M, Lovric J, Sauer G, Reichert M, Gounari F, Buscher D, Baccarini M, Mischak H, Kolch W. 2000. The Raf-1 kinase associates with vimentin kinases and regulates the structure of vimentin filaments. FASEB J. 14:2008–2021.
Jeyabalan N, Clement JP. 2016. SYNGAP1: mind the gap. Front Cell Neurosci. 10:32.
Jiang H, Luo JQ, Urano T, Frankel P, Lu Z, Foster DA, Feig LA. 1995. Involvement of Ral GTPase in v-Src-induced phospholipase D activation. Nature. 378:409–412.
Jin A, Kurosu T, Tsuji K, Mizuchi D, Arai A, Fujita H, Hattori M, Minato N, Miura O. 2006. BCR/ABL and IL-3 activate Rap1 to stimulate the B-Raf/MEK/Erk and Akt signaling pathways and to regulate proliferation, apoptosis, and adhesion. Oncogene. 25:4332–4340.
Jin R, Junutula JR, Matern HT, Ervin KE, Scheller RH, Brunger AT. 2005. Exo84 and Sec5 are competitive regulatory Sec6/8 effectors to the RalA GTPase. EMBO J. 24:2064–2074.
Jin SX, Bartolome C, Arai JA, Hoffman L, Uzturk BG, Kumar-Singh R, Waxham MN, Feig LA. 2014. Domain contributions to signaling specificity differences between Ras-guanine nucleotide releasing factor (Ras-GRF) 1 and Ras-GRF2. J Biol Chem. 289:16551–16564.
Jullien-Flores V, Mahe Y, Mirey G, Leprince C, Meunier-Bisceuil B, Sorkin A, Camonis JH. 2000. RLIP76, an effector of the GTPase Ral, interacts with the AP2 complex: involvement of the Ral pathway in receptor endocytosis. J Cell Sci. 113: 2837–2844.
Jura N, Scotto-Lavino E, Sobczyk A, Bar-Sagi D. 2006. Differential modification of Ras proteins by ubiquitination. Mol Cell. 21:679–687.
Kaduwal S, Jeong WJ, Park JC, Lee KH, Lee YM, Jeon SH, Lim YB, Min do S, Choi KY. 2015. Sur8/Shoc2 promotes cell motility and metastasis through activation of Ras-PI3K signaling. Oncotarget. 6:33091–33105.
Kaliman P, Llagostera E. 2008. Myotonic dystrophy protein kinase (DMPK) and its role in the pathogenesis of myotonic dystrophy 1. Cell Signal. 20:1935–1941.
Karassek S, Berghaus C, Schwarten M, Goemans CG, Ohse N, Kock G, Jockers K, Neumann S, Gottfried S, Herrmann C, et al. 2010. Ras homolog enriched in brain (Rheb) enhances apoptotic signaling. J Biol Chem. 285:33979–33991.
Karbowniczek M, Cash T, Cheung M, Robertson GP, Astrinidis A, Henske EP. 2004. Regulation of B-Raf kinase activity by tuberin and Rheb is mammalian target of rapamycin (mTOR)-independent. J Biol Chem. 279:29930–29937.
Karbowniczek M, Robertson GP, Henske EP. 2006. Rheb inhibits C-raf activity and B-raf/C-raf heterodimerization. J Biol Chem. 281:25447–25456.
Karbowniczek M, Zitserman D, Khabibullin D, Hartman T, Yu J, Morrison T, Nicolas E, Squillace R, Roegiers F, Henske EP. 2010. The evolutionarily conserved TSC/Rheb pathway activates Notch in tuberous sclerosis complex and Drosophila external sensory organ development. J Clin Invest. 120:93–102.
Karnoub AE, Weinberg RA. 2008. Ras oncogenes: split personalities. Nat Rev Mol Cell Biol. 9:517–531.
Kashatus DF, Lim KH, Brady DC, Pershing NL, Cox AD, Counter CM. 2011. RALA and RALBP1 regulate mitochondrial fission at mitosis. Nat Cell Biol. 13:1108–1115.
Kawato M, Shirakawa R, Kondo H, Higashi T, Ikeda T, Okawa K, Fukai S, Nureki O, Kita T, Horiuchi H. 2008. Regulation of platelet dense granule secretion by the Ral GTPase-exocyst pathway. J Biol Chem. 283:166–174.
Keeton AB, Salter EA, Piazza GA. 2017. The RAS-effector interaction as a drug target. Cancer Res. 77:221–226.
Kelley GG, Reks SE, Ondrako JM, Smrcka AV. 2001. Phospholipase C(epsilon): a novel Ras effector. EMBO J. 20:743–754.
Kim HW, Ha SH, Lee MN, Huston E, Kim DH, Jang SK, Suh PG, Houslay MD, Ryu SH. 2010. Cyclic AMP controls mTOR through regulation of the dynamic interaction between Rheb and phosphodiesterase 4D. Mol Cell Biol. 30:5406–5420.
Klingauf M, Beck M, Berge U, Turgay Y, Heinzer S, Horvath P, Kroschewski R. 2013. The tumour suppressor DiRas3 interacts with C-RAF and downregulates MEK activity to restrict cell migration. Biol Cell. 105:91–107.
Knyphausen P, Lang F, Baldus L, Extra A, Lammers M. 2016. Insights into K-Ras 4B regulation by post-translational lysine acetylation. Biol Chem. 397:1071–1085.
Kontani K, Tada M, Ogawa T, Okai T, Saito K, Araki Y, Katada T. 2002. Di-Ras, a distinct subgroup of ras family GTPases with unique biochemical properties. J Biol Chem. 277:41070–41078.
Kooistra MR, Dube N, Bos JL. 2007. Rap1: a key regulator in cell-cell junction formation. J Cell Sci. 120:17–22.
Korf B, Ahmadian R, Allanson J, Aoki Y, Bakker A, Wright EB, Denger B, Elgersma Y, Gelb BD, Gripp KW, et al. 2015. The third international meeting on genetic disorders in the RAS/MAPK pathway: towards a therapeutic approach. Am J Med Genet. 167A:1741–1746.
Kupzig S, Bouyoucef-Cherchalli D, Yarwood S, Sessions R, Cullen PJ. 2009. The ability of GAP1IP4BP to function as a Rap1 GTPase-activating protein (GAP) requires its Ras GAP-related domain and an arginine finger rather than an asparagine thumb. Mol Cell Biol. 29:3929–3940.
Kupzig S, Deaconescu D, Bouyoucef D, Walker SA, Liu Q, Polte CL, Daumke O, Ishizaki T, Lockyer PJ, Wittinghofer A, Cullen PJ. 2006. GAP1 family members constitute bifunctional Ras and Rap GTPase-activating proteins. J Biol Chem. 281:9891–9900.
Kurella VB, Richard JM, Parke CL, Lecour LF, Jr., Bellamy HD, Worthylake DK. 2009. Crystal structure of the GTPase-activating protein-related domain from IQGAP1. J Biol Chem. 284:14857–14865.
Kwong L, Wozniak MA, Collins AS, Wilson SD, Keely PJ. 2003. R-Ras promotes focal adhesion formation through focal adhesion kinase and p130(Cas) by a novel mechanism that differs from integrins. Mol Cell Biol. 23:933–949.
Lalli G, Hall A. 2005. Ral GTPases regulate neurite branching through GAP-43 and the exocyst complex. J Cell Biol. 171:857–869.
Lander HM, Ogiste JS, Pearce SF, Levi R, Novogrodsky A. 1995. Nitric oxide-stimulated guanine nucleotide exchange on p21ras. J Biol Chem. 270:7017–7020.

Lane KT, Beese LS. 2006. Thematic review series: lipid post-translational modifications. Structural biology of protein farnesyltransferase and geranylgeranyltransferase type I. J Lipid Res. 47:681–699.
Lapinski PE, Qiao Y, Chang CH, King PD. 2011. A role for p120 RasGAP in thymocyte positive selection and survival of naive T cells. J Immunol. 187:151–163.
Latourelle JC, Dumitriu A, Hadzi TC, Beach TG, Myers RH. 2012. Evaluation of Parkinson disease risk variants as expression-QTLs. PLoS One. 7:e46199.
Lee CH, Della NG, Chew CE, Zack DJ. 1996. Rin, a neuron-specific and calmodulin-binding small G-protein, and Rit define a novel subfamily of ras proteins. J Neurosci. 16:6784–6794.
Lee MN, Ha SH, Kim J, Koh A, Lee CS, Kim JH, Jeon H, Kim DH, Suh PG, Ryu SH. 2009. Glycolytic flux signals to mTOR through glyceraldehyde-3-phosphate dehydrogenase-mediated regulation of Rheb. Mol Cell Biol. 29:3991–4001.
Li Y, Corradetti MN, Inoki K, Guan KL. 2004. TSC2: filling the GAP in the mTOR signaling pathway. Trends Biochem Sci. 29:32–38.
Ligon AH, Pershouse MA, Jasser SA, Yung WK, Steck PA. 1997. Identification of a novel gene product, RIG, that is down-regulated in human glioblastoma. Oncogene. 14:1075–1081.
Lissewski C, Kant SG, Stark Z, Schanze I, Zenker M. 2015. Copy number variants including RAS pathway genes - How much RASopathy is in the phenotype?. Am J Med Genet. 167A:2685–2690.
Lito P, Mets BD, Appledorn DM, Maher VM, McCormick JJ. 2009. Sprouty 2 regulates DNA damage-induced apoptosis in Ras-transformed human fibroblasts. J Biol Chem. 284:848–854.
Liu X, Shimada T, Otowa T, Wu YY, Kawamura Y, Tochigi M, Iwata Y, Umekage T, Toyota T, Maekawa M, et al. 2016. Genome-wide association study of Autism spectrum disorder in the east Asian populations. Autism Res. 9:340–349.
Ljubicic S, Bezzi P, Vitale N, Regazzi R. 2009. The GTPase RalA regulates different steps of the secretory process in pancreatic beta-cells. PLoS One. 4:e7770.
Long X, Lin Y, Ortiz-Vega S, Yonezawa K, Avruch J. 2005. Rheb binds and regulates the mTOR kinase. Curr Biol. 15:702–713.
Lopez JA, Kwan EP, Xie L, He Y, James DE, Gaisano HY. 2008. The RalA GTPase is a central regulator of insulin exocytosis from pancreatic islet beta cells. J Biol Chem. 283:17939–17945.
Louahed J, Grasso L, De Smet C, Van Roost E, Wildmann C, Nicolaides NC, Levitt RC, Renauld JC. 1999. Interleukin-9-induced expression of M-Ras/R-Ras3 oncogene in T-helper clones. Blood. 94:1701–1710.
Lynch SJ, Snitkin H, Gumper I, Philips MR, Sabatini D, Pellicer A. 2015. The differential palmitoylation states of N-Ras and H-Ras determine their distinct Golgi subcompartment localizations. J Cell Physiol. 230:610–619.
Ma D, Bai X, Zou H, Lai Y, Jiang Y. 2010. Rheb GTPase controls apoptosis by regulating interaction of FKBP38 with Bcl-2 and Bcl-XL. J Biol Chem. 285:8621–8627.
Machida N, Umikawa M, Takei K, Sakima N, Myagmar BE, Taira K, Uezato H, Ogawa Y, Kariya K. 2004. Mitogen-activated protein kinase kinase kinase kinase 4 as a putative effector of Rap2 to activate the c-Jun N-terminal kinase. J Biol Chem. 279:15711–15714.
Mainberger F, Langer S, Mall V, Jung NH. 2016. Impaired synaptic plasticity in RASopathies: a mini-review. J Neural Transm. 123:1133–1138.
Malumbres M, Barbacid M. 2003. RAS oncogenes: the first 30 years. Nat Rev Cancer. 3:459.
Mandal R, Becker S, Strebhardt K. 2016. Stamping out RAF and MEK1/2 to inhibit the ERK1/2 pathway: an emerging threat to anticancer therapy. Oncogene. 35:2547–2561.
Marshall CB, Ho J, Buerger C, Plevin MJ, Li GY, Li Z, Ikura M, Stambolic V. 2009. Characterization of the intrinsic and TSC2-GAP-regulated GTPase activity of Rheb by real-time NMR. Sci Signal. 2:ra3.
McCormick F. 2015. KRAS as a therapeutic target. Clin Cancer Res. 21:1797–1801.
McCormick F. 2016. K-Ras protein as a drug target. J Mol Med. 94:253–258.
McGrath JP, Capon DJ, Smith DH, Chen EY, Seeburg PH, Goeddel DV, Levinson AD. 1983. Structure and organization of the human Ki-ras proto-oncogene and a related processed pseudogene. Nature. 304:501–506.
Miller JP, Yates BE, Al-Ramahi I, Berman AE, Sanhueza M, Kim E, de Haro M, DeGiacomo F, Torcassi C, Holcomb J, et al. 2012. A genome-scale RNA-interference screen identifies RRAS signaling as a pathologic feature of Huntington's disease. PLoS Genet. 8:e1003042.
Mir S, Cai W, Andres DA. 2017. RIT1 GTPase regulates Sox2 transcriptional activity and hippocampal neurogenesis. J Biol Chem. 292:2054–2064.
Mitin N, Rossman KL, Der CJ. 2005. Signaling interplay in Ras superfamily function. Curr Biol. 15:R563–R574.
Miyazaki M, Takemasa T. 2017. TSC2/Rheb signaling mediates ERK-dependent regulation of mTORC1 activity in C2C12 myoblasts. FEBS Open Biol. 7:424–433.
Mohan N, Shen Y, Dokmanovic M, Endo Y, Hirsch DS, Wu WJ. 2016. VPS34 regulates TSC1/TSC2 heterodimer to mediate RheB and mTORC1/S6K1 activation and cellular transformation. Oncotarget. 7:52239–52254.
Montagner A, Yart A, Dance M, Perret B, Salles JP, Raynal P. 2005. A novel role for Gab1 and SHP2 in epidermal growth factor-induced Ras activation. J Biol Chem. 280:5350–5360.
Mooz J, Oberoi-Khanuja TK, Harms GS, Wang W, Jaiswal BS, Seshagiri S, Tikkanen R, Rajalingam K. 2014. Dimerization of the kinase ARAF promotes MAPK pathway activation and cell migration. Sci Signal. 7:ra73.
Moskalenko S, Henry DO, Rosse C, Mirey G, Camonis JH, White MA. 2002. The exocyst is a Ral effector complex. Nat Cell Biol. 4:66–72.
Mott HR, Owen D. 2015. Structures of Ras superfamily effector complexes: what have we learnt in two decades?. Crit Rev Biochem Mol Biol. 50:85–133.
Motta M, Chillemi G, Fodale V, Cecchetti S, Coppola S, Stipo S, Cordeddu V, Macioce P, Gelb BD, Tartaglia M. 2016. SHOC2 subcellular shuttling requires the KEKE motif-rich region and N-terminal leucine-rich repeat domain and impacts on ERK signalling. Hum Mol Genet. 25:3824–3835.
Mourik M, Eikenboom J. 2017. Lifecycle of Weibel-Palade bodies. Hamostaseologie. 37:13–24.
Myagmar BE, Umikawa M, Asato T, Taira K, Oshiro M, Hino A, Takei K, Uezato H, Kariya K. 2005. PARG1, a protein-

tyrosine phosphatase-associated RhoGAP, as a putative Rap2 effector. Biochem Biophys Res Commun. 329:1046–1052.
Nakashima S, Morinaka K, Koyama S, Ikeda M, Kishida M, Okawa K, Iwamatsu A, Kishida S, Kikuchi A. 1999. Small G protein Ral and its downstream molecules regulate endocytosis of EGF and insulin receptors. EMBO J. 18:3629–3642.
Nakhaei-Rad S, Nakhaeizadeh H, Gotze S, Kordes C, Sawitza I, Hoffmann MJ, Franke M, Schulz WA, Scheller J, Piekorz RP, et al. 2016. The role of embryonic stem cell-expressed RAS (ERAS) in the maintenance of quiescent hepatic stellate cells. J Biol Chem. 291:8399–8413.
Nakhaei-Rad S, Nakhaeizadeh H, Kordes C, Cirstea IC, Schmick M, Dvorsky R, Bastiaens PI, Häussinger D, Ahmadian MR. 2015. The function of embryonic stem cell-expressed Ras (E-Ras), a unique Ras family member, correlates with its additional motifs and its structural properties. J Biol Chem. 290:15892–15903.
Nakhaeizadeh H, Amin E, Nakhaei-Rad S, Dvorsky R, Ahmadian MR. 2016. The RAS-effector interface: isoform-specific differences in the effector binding regions. PLoS One. 11:e0167145.
Nalls MA, Pankratz N, Lill CM, Do CB, Hernandez DG, Saad M, DeStefano AL, Kara E, Bras J, Sharma M, et al. 2014. Large-scale meta-analysis of genome-wide association data identifies six new risk loci for Parkinson's disease. Nat Genet. 46:989–993.
Navaroli DM, Stevens ZH, Uzelac Z, Gabriel L, King MJ, Lifshitz LM, Sitte HH, Melikian HE. 2011. The plasma membrane-associated GTPase Rin interacts with the dopamine transporter and is required for protein kinase C-regulated dopamine transporter trafficking. J Neurosci. 31:13758–13770.
Nelson N, Clark GJ. 2016. Rheb may complex with RASSF1A to coordinate Hippo and TOR signaling. Oncotarget. 7:33821–33831.
Nguyen CH, Watts VJ. 2005. Dexras1 blocks receptor-mediated heterologous sensitization of adenylyl cyclase 1. Biochem Biophys Res Commun. 332:913–920.
Nguyen CH, Watts VJ. 2006. Dexamethasone-induced Ras protein 1 negatively regulates protein kinase C δ: implications for adenylyl cyclase 2 signaling. Mol Pharmacol. 69:1763–1771.
Niault TS, Baccarini M. 2010. Targets of Raf in tumorigenesis. Carcinogenesis. 31:1165–1174.
Nishimoto A, Yu Y, Lu Z, Mao X, Ren Z, Watowich SS, Mills GB, Liao WS, Chen X, Bast RC Jr, Luo RZ. 2005. A Ras homologue member I directly inhibits signal transducers and activators of transcription 3 translocation and activity in human breast and ovarian cancer cells. Cancer Res. 65:6701–6710.
Nonaka H, Takei K, Umikawa M, Oshiro M, Kuninaka K, Bayarjargal M, Asato T, Yamashiro Y, Uechi Y, Endo S, et al. 2008. MINK is a Rap2 effector for phosphorylation of the postsynaptic scaffold protein TANC1. Biochem Biophys Res Commun. 377:573–578.
Nouri K, Timson DJ, Ahmadian MR. 2017. New model for the interaction of IQGAP1 with CDC42 and RAC1. Small GTPases. [2017 Jun 19];[1–7]. [Epub ahead of print]. doi: 10.1080/21541248.2017.1321169
Nussinov R, Muratcioglu S, Tsai CJ, Jang H, Gursoy A, Keskin O. 2015. The key role of calmodulin in KRAS-driven adenocarcinomas. Mol Cancer Res. 13:1265–1273.
Nussinov R, Tsai CJ, Chakrabarti M, Jang H. 2016. A new view of ras isoforms in cancers. Cancer Res. 76:18–23.
Oertli B, Han J, Marte BM, Sethi T, Downward J, Ginsberg M, Hughes PE. 2000. The effector loop and prenylation site of R-Ras are involved in the regulation of integrin function. Oncogene. 19:4961–4969.
Ogita Y, Egami S, Ebihara A, Ueda N, Katada T, Kontani K. 2015. Di-Ras2 protein forms a complex with SmgGDS protein in brain cytosol in order to be in a low affinity state for guanine nucleotides. J Biol Chem. 290:20245–20256.
Ohba Y, Ikuta K, Ogura A, Matsuda J, Mochizuki N, Nagashima K, Kurokawa K, Mayer BJ, Maki K, Miyazaki J, Matsuda M. 2001. Requirement for C3G-dependent Rap1 activation for cell adhesion and embryogenesis. EMBO J. 20:3333–3341.
Oinuma I, Ishikawa Y, Katoh H, Negishi M. 2004. The Semaphorin 4D receptor Plexin-B1 is a GTPase activating protein for R-Ras. Science. 305:862–865.
Oliveira AF, Yasuda R. 2014. Neurofibromin is the major ras inactivator in dendritic spines. J Neurosci. 34:776–783.
Omerovic J, Prior IA. 2009. Compartmentalized signalling: Ras proteins and signalling nanoclusters. FEBS J. 276:1817–1825.
Pamonsinlapatham P, Hadj-Slimane R, Lepelletier Y, Allain B, Toccafondi M, Garbay C, Raynaud F. 2009. p120-Ras GTPase activating protein (RasGAP): a multi-interacting protein in downstream signaling. Biochimie. 91:320–328.
Pankratz N, Beecham GW, DeStefano AL, Dawson TM, Doheny KF, Factor SA, Hamza TH, Hung AY, Hyman BT, Ivinson AJ, et al. 2012. Meta-analysis of Parkinson's disease: identification of a novel locus, RIT2. Ann Neurol. 71:370–384.
Pantaleoni F, Lev D, Cirstea IC, Motta M, Lepri FR, Bottero L, Cecchetti S, Linger I, Paolacci S, Flex E, et al. 2017. Aberrant HRAS transcript processing underlies a distinctive phenotype within the RASopathy clinical spectrum. Hum Mutat. 38:798–804.
Pearce LR, Komander D, Alessi DR. 2010. The nuts and bolts of AGC protein kinases. Nat Rev Mol Cell Biol. 11:9–22.
Pena V, Hothorn M, Eberth A, Kaschau N, Parret A, Gremer L, Bonneau F, Ahmadian MR, Scheffzek K. 2008. The C2 domain of SynGAP is essential for stimulation of the Rap GTPase reaction. EMBO Rep. 9:350–355.
Philpott C, Tovell H, Frayling IM, Cooper DN, Upadhyaya M. 2017. The NF1 somatic mutational landscape in sporadic human cancers. Hum Genomics. 11:13.
Plak K, Pots H, Van Haastert PJ, Kortholt A. 2016. Direct Interaction between TalinB and Rap1 is necessary for adhesion of Dictyostelium cells. BMC Cell Biol. 17:1.
Plowman SJ, Ariotti N, Goodall A, Parton RG, Hancock JF. 2008. Electrostatic interactions positively regulate K-Ras nanocluster formation and function. Mol Cell Biol. 28:4377–4385.
Plowman SJ, Berry RL, Bader SA, Luo F, Arends MJ, Harrison DJ, Hooper ML, Patek CE. 2006. K-ras 4A and 4B are co-expressed widely in human tissues, and their ratio is altered in sporadic colorectal cancer. J Exp Clin Cancer Res. 25:259–267.

Popovic M, Rensen-de Leeuw M, Rehmann H. 2013. Selectivity of CDC25 homology domain-containing guanine nucleotide exchange factors. J Mol Biol. 425:2782–2794.

Popovic M, Schouten A, Rensen-de Leeuw M, Rehmann H. 2016. The structure of the Guanine Nucleotide Exchange Factor Rlf in complex with the small G-protein Ral identifies conformational intermediates of the exchange reaction and the basis for the selectivity. J Struct Biol. 193:106–114.

Postema FAM, Hopman SMJ, Hennekam RC, Merks JHM. 2018. Consequences of diagnosing a tumor predisposition syndrome in children with cancer: a literature review. Pediatr Blood Cancer. 65:e26718.

Potheraveedu VN, Schopel M, Stoll R, Heumann R. 2017. Rheb in neuronal degeneration, regeneration, and connectivity. Biol Chem. 398:589–606.

Praskova M, Khoklatchev A, Ortiz-Vega S, Avruch J. 2004. Regulation of the MST1 kinase by autophosphorylation, by the growth inhibitory proteins, RASSF1 and NORE1, and by Ras. Biochem J. 381:453–462.

Quilliam LA, Rebhun JF, Castro AF. 2002. A growing family of guanine nucleotide exchange factors is responsible for activation of Ras-family GTPases. Prog Nucleic Acid Res Mol Biol. 71:391–444.

Raguz S, De Bella MT, Slade MJ, Higgins CF, Coombes RC, Yague E. 2005. Expression of RPIP9 (Rap2 interacting protein 9) is activated in breast carcinoma and correlates with a poor prognosis. Int J Cancer. 117:934–941.

Rajalingam K, Schreck R, Rapp UR, Albert S. 2007. Ras oncogenes and their downstream targets. Biochim Biophys Acta. 1773:1177–1195.

Ratner N, Miller SJ. 2015. A RASopathy gene commonly mutated in cancer: the neurofibromatosis type 1 tumour suppressor. Nat Rev Cancer. 15:290–301.

Rauen KA. 2013. The RASopathies. Annu Rev Genomics Hum Genet. 14:355–369.

Ray A, Basu S, Miller NM, Chan AM, Dittel BN. 2014. An increase in tolerogenic dendritic cell and natural regulatory T cell numbers during experimental autoimmune encephalomyelitis in Rras-/- mice results in attenuated disease. J Immunol. 192:5109–5117.

Rebhun JF, Castro AF, Quilliam LA. 2000. Identification of guanine nucleotide exchange factors (GEFs) for the Rap1 GTPase. Regulation of MR-GEF by M-Ras-GTP interaction. J Biol Chem. 275:34901–34908.

Rebocho AP, Marais R. 2013. ARAF acts as a scaffold to stabilize BRAF:CRAF heterodimers. Oncogene. 32:3207–3212.

Rehmann H, Arias-Palomo E, Hadders MA, Schwede F, Llorca O, Bos JL. 2008a. Structure of Epac2 in complex with a cyclic AMP analogue and RAP1B. Nature. 455:124–127.

Rehmann H, Bruning M, Berghaus C, Schwarten M, Kohler K, Stocker H, Stoll R, Zwartkruis FJ, Wittinghofer A. 2008b. Biochemical characterisation of TCTP questions its function as a guanine nucleotide exchange factor for Rheb. FEBS Lett 582:3005–3010.

Reif A, Nguyen TT, Weissflog L, Jacob CP, Romanos M, Renner TJ, Buttenschon HN, Kittel-Schneider S, Gessner A, Weber H, et al. 2011. DIRAS2 is associated with adult ADHD, related traits, and co-morbid disorders. Neuropsychopharmacology. 36:2318–2327.

Ren JG, Li Z, Sacks DB. 2007. IQGAP1 modulates activation of B-Raf. Proc Natl Acad Sci USA. 104:10465–10469.

Repasky GA, Chenette EJ, Der CJ. 2004. Renewing the conspiracy theory debate: does Raf function alone to mediate Ras oncogenesis?. Trends Cell Biol. 14:639–647.

Resh MD. 2004. Membrane targeting of lipid modified signal transduction proteins. Subcell Biochem. 37:217–232.

Rodriguez-Viciana P, McCormick F. 2006. Ras ubiquitination: coupling spatial sorting and signal transmission. Cancer Cell. 9:243–244.

Rojas AM, Fuentes G, Rausell A, Valencia A. 2012. The Ras protein superfamily: evolutionary tree and role of conserved amino acids. J Cell Biol. 196:189–201.

Romano D, Nguyen LK, Matallanas D, Halasz M, Doherty C, Kholodenko BN, Kolch W. 2014. Protein interaction switches coordinate Raf-1 and MST2/Hippo signalling. Nat Cell Biol. 16:673–684.

Rondaij MG, Bierings R, van Agtmaal EL, Gijzen KA, Sellink E, Kragt A, Ferguson SS, Mertens K, Hannah MJ, van Mourik JA, et al. 2008. Guanine exchange factor RalGDS mediates exocytosis of Weibel-Palade bodies from endothelial cells. Blood 112:56–63.

Rosseland CM, Wierod L, Flinder LI, Oksvold MP, Skarpen E, Huitfeldt HS. 2008. Distinct functions of H-Ras and K-Ras in proliferation and survival of primary hepatocytes due to selective activation of ERK and PI3K. J Cell Physiol. 215:818–826.

Sakabe K, Teramoto H, Zohar M, Behbahani B, Miyazaki H, Chikumi H, Gutkind JS. 2002. Potent transforming activity of the small GTP-binding protein Rit in NIH 3T3 cells: evidence for a role of a p38gamma-dependent signaling pathway. FEBS Lett. 511:15–20.

Sakurai A, Gavard J, Annas-Linhares Y, Basile JR, Amornphimoltham P, Palmby TR, Yagi H, Zhang F, Randazzo PA, Li X, et al. 2010. Semaphorin 3E initiates antiangiogenic signaling through plexin D1 by regulating Arf6 and R-Ras. Mol Cell Biol. 30:3086–3098.

Sanchez-Ruiz J, Mejias R, Garcia-Belando M, Barber DF, Gonzalez-Garcia A. 2011. Ral GTPases regulate cell-mediated cytotoxicity in NK cells. J Immunol. 187:2433–2441.

Sandri C, Caccavari F, Valdembri D, Camillo C, Veltel S, Santambrogio M, Lanzetti L, Bussolino F, Ivaska J, Serini G. 2012. The R-Ras/RIN2/Rab5 complex controls endothelial cell adhesion and morphogenesis via active integrin endocytosis and Rac signaling. Cell Res. 22:1479–1501.

Santarpia L, Lippman SM, El-Naggar AK. 2012. Targeting the MAPK-RAS-RAF signaling pathway in cancer therapy. Expert Opin Ther Targets. 16:103–119.

Saraste M, Sibbald PR, Wittinghofer A. 1990. The P-loop – a common motif in ATP-and GTP-binding proteins. Trends Biochem Sci. 15:430–434.

Sasaki AT, Carracedo A, Locasale JW, Anastasiou D, Takeuchi K, Kahoud ER, Haviv S, Asara JM, Pandolfi PP, Cantley LC. 2011. Ubiquitination of K-Ras enhances activation and facilitates binding to select downstream effectors. Sci Signal. 4:ra13.

Scheffzek K, Ahmadian MR. 2005. GTPase activating proteins: structural and functional insights 18 years after discovery. Cell Mol Life Sci. 62:3014–3038.

Scheffzek K, Ahmadian MR, Kabsch W, Wiesmuller L, Lautwein A, Schmitz F, Wittinghofer A. 1997. The Ras-RasGAP complex: structural basis for GTPase activation and its loss in oncogenic Ras mutants. Science. 277:333–338.

Schmick M, Kraemer A, Bastiaens PI. 2015. Ras moves to stay in place. Trends Cell Biol. 25:190–197.
Schmick M, Vartak N, Papke B, Kovacevic M, Truxius DC, Rossmannek L, Bastiaens PIH. 2014. KRas localizes to the plasma membrane by spatial cycles of solubilization, trapping and vesicular transport. Cell. 157:459–471.
Schmidt M, Bienek C, Rümenapp U, Zhang C, Lümmen G, Jakobs KH, Just I, Aktories K, Moos M, von Eichel-Streiber C. 1996. A role for Rho in receptor-and G protein-stimulated phospholipase C Reduction in phosphatidylinositol 4, 5-bisphosphate by *Clostridium difficile* toxin B. Naunyn-Schmiedeberg's Arch Pharmacol. 354:87–94.
Schroeder H, Leventis R, Rex S, Schelhaas M, Nagele E, Waldmann H, Silvius JR. 1997. S-Acylation and plasma membrane targeting of the farnesylated carboxyl-terminal peptide of N-ras in mammalian fibroblasts. Biochemistry. 36:13102–13109.
Scrima A, Thomas C, Deaconescu D, Wittinghofer A. 2008. The Rap-RapGAP complex: GTP hydrolysis without catalytic glutamine and arginine residues. EMBO J. 27:1145–1153.
Self AJ, Caron E, Paterson HF, Hall A. 2001. Analysis of R-Ras signalling pathways. J Cell Sci. 114:1357–1366.
Shahani N, Pryor W, Swarnkar S, Kholodilov N, Thinakaran G, Burke RE, Subramaniam S. 2014. Rheb GTPase regulates beta-secretase levels and amyloid beta generation. J Biol Chem. 289:5799–5808.
Shanshiashvili L, Narmania N, Barbakadze T, Zhuravliova E, Natsvlishvili N, Ramsden J, Mikeladze DG. 2011. S-nitrosylation decreases the adsorption of H-Ras in lipid bilayer and changes intrinsic catalytic activity. Cell Biochem Biophys. 59:191–199.
Shao H, Andres DA. 2000. A novel RalGEF-like protein, RGL3, as a candidate effector for rit and Ras. J Biol Chem. 275:26914–26924.
Shao H, Kadono-Okuda K, Finlin BS, Andres DA. 1999. Biochemical characterization of the Ras-related GTPases Rit and Rin. Arch Biochem Biophys. 371:207–219.
Shi GX, Andres DA. 2005. Rit contributes to nerve growth factor-induced neuronal differentiation via activation of B-Raf-extracellular signal-regulated kinase and p38 mitogen-activated protein kinase cascades. Mol Cell Biol. 25:830–846.
Shi GX, Cai W, Andres DA. 2012. Rit-mediated stress resistance involves a p38-mitogen- and stress-activated protein kinase 1 (MSK1)-dependent cAMP response element-binding protein (CREB) activation cascade. J Biol Chem. 287:39859–39868.
Shi GX, Cai W, Andres DA. 2013. Rit subfamily small GTPases: regulators in neuronal differentiation and survival. Cell Signal. 25:2060–2068.
Shi GX, Jin L, Andres DA. 2008. Pituitary adenylate cyclase-activating polypeptide 38-mediated Rin activation requires Src and contributes to the regulation of HSP27 signaling during neuronal differentiation. Mol Cell Biol. 28:4940–4951.
Shi GX, Jin L, Andres DA. 2011. A rit GTPase-p38 mitogen-activated protein kinase survival pathway confers resistance to cellular stress. Mol Cell Biol. 31:1938–1948.
Shimizu M, Wang W, Walch ET, Dunne PW, Epstein HF. 2000. Rac-1 and Raf-1 kinases, components of distinct signaling pathways, activate myotonic dystrophy protein kinase. FEBS Lett. 475:273–277.
Shipitsin M, Feig LA. 2004. RalA but not RalB enhances polarized delivery of membrane proteins to the basolateral surface of epithelial cells. Mol Cell Biol. 24:5746–5756.
Shirakawa R, Fukai S, Kawato M, Higashi T, Kondo H, Ikeda T, Nakayama E, Okawa K, Nureki O, Kimura T, et al. 2009. Tuberous sclerosis tumor suppressor complex-like complexes act as GTPase-activating proteins for Ral GTPases. J Biol Chem. 284:21580–21588.
Shirakawa R, Horiuchi H. 2015. Ral GTPases: crucial mediators of exocytosis and tumourigenesis. J Biochem. 157:285–299.
Siljamaki E, Abankwa D. 2016. SPRED1 Interferes with K-ras but Not H-ras Membrane Anchorage and Signaling. Mol Cell Biol. 36:2612–2625.
Silvius JR, l'Heureux F. 1994. Fluorometric evaluation of the affinities of isoprenylated peptides for lipid bilayers. Biochemistry. 33:3014–3022.
Simanshu DK, Nissley DV, McCormick F. 2017. RAS proteins and their regulators in human disease. Cell. 170:17–33.
Song C, Hu CD, Masago M, Kariyai K, Yamawaki-Kataoka Y, Shibatohge M, Wu D, Satoh T, Kataoka T. 2001. Regulation of a novel human phospholipase C, PLCepsilon, through membrane targeting by Ras. J Biol Chem. 276:2752–2757.
Sot B, Kotting C, Deaconescu D, Suveyzdis Y, Gerwert K, Wittinghofer A. 2010. Unravelling the mechanism of dual-specificity GAPs. EMBO J. 29:1205–1214.
Spencer ML, Shao H, Andres DA. 2002a. Induction of neurite extension and survival in pheochromocytoma cells by the Rit GTPase. J Biol Chem. 277:20160–20168.
Spencer ML, Shao H, Tucker HM, Andres DA. 2002b. Nerve growth factor-dependent activation of the small GTPase Rin. J Biol Chem. 277:17605–17615.
Sperlich B, Kapoor S, Waldmann H, Winter R, Weise K. 2016. Regulation of K-Ras4B membrane binding by calmodulin. Biophys J. 111:113–122.
Spiczka KS, Yeaman C. 2008. Ral-regulated interaction between Sec5 and paxillin targets Exocyst to focal complexes during cell migration. J Cell Sci. 121:2880–2891.
Stephen AG, Esposito D, Bagni RK, McCormick F. 2014. Dragging ras back in the ring. Cancer Cell. 25:272–281.
Stieglitz B, Bee C, Schwarz D, Yildiz O, Moshnikova A, Khokhlatchev A, Herrmann C. 2008. Novel type of Ras effector interaction established between tumour suppressor NORE1A and Ras switch II. EMBO J. 27:1995–2005.
Stope MB, Vom Dorp F, Szatkowski D, Bohm A, Keiper M, Nolte J, Oude Weernink PA, Rosskopf D, Evellin S, Jakobs KH, Schmidt M. 2004. Rap2B-dependent stimulation of phospholipase C-epsilon by epidermal growth factor receptor mediated by c-Src phosphorylation of RasGRP3. Mol Cell Biol. 24:4664–4676.
Stork PJ. 2003. Does Rap1 deserve a bad Rap?. Trends Biochem Sci. 28:267–275.
Subramaniam S, Mealer RG, Sixt KM, Barrow RK, Usiello A, Snyder SH. 2010. Rhes, a physiologic regulator of sumoylation, enhances cross-sumoylation between the basic sumoylation enzymes E1 and Ubc9. J Biol Chem. 285:20428–20432.
Subramaniam S, Napolitano F, Mealer RG, Kim S, Errico F, Barrow R, Shahani N, Tyagi R, Snyder SH, Usiello A. 2011. Rhes, a striatal-enriched small G protein, mediates mTOR signaling and L-DOPA-induced dyskinesia. Nat Neurosci. 15:191–193.

Sugihara K, Asano S, Tanaka K, Iwamatsu A, Okawa K, Ohta Y. 2002. The exocyst complex binds the small GTPase RalA to mediate filopodia formation. Nat Cell Biol. 4:73–78.

Sun Y, Fang Y, Yoon MS, Zhang C, Roccio M, Zwartkruis FJ, Armstrong M, Brown HA, Chen J. 2008. Phospholipase D1 is an effector of Rheb in the mTOR pathway. Proc Natl Acad Sci USA. 105:8286–8291.

Sung PJ, Tsai FD, Vais H, Court H, Yang J, Fehrenbacher N, Foskett JK, Philips MR. 2013. Phosphorylated K-Ras limits cell survival by blocking Bcl-xL sensitization of inositol trisphosphate receptors. Proc Natl Acad Sci USA. 110:20593–20598.

Tabaczar S, Czogalla A, Podkalicka J, Biernatowska A, Sikorski AF. 2017. Protein palmitoylation: Palmitoyltransferases and their specificity. Exp Biol Med (Maywood). 242:1150–1157.

Tada M, Gengyo-Ando K, Kobayashi T, Fukuyama M, Mitani S, Kontani K, Katada T. 2012. Neuronally expressed Ras-family GTPase Di-Ras modulates synaptic activity in *Caenorhabditis elegans*. Genes Cells. 17:778–789.

Taira K, Umikawa M, Takei K, Myagmar BE, Shinzato M, Machida N, Uezato H, Nonaka S, Kariya K. 2004. The Traf2- and Nck-interacting kinase as a putative effector of Rap2 to regulate actin cytoskeleton. J Biol Chem. 279:49488–49496.

Takahashi K, Mitsui K, Yamanaka S. 2003. Role of ERas in promoting tumour-like properties in mouse embryonic stem cells. Nature. 423:541–545.

Takahashi K, Nakagawa M, Young SG, Yamanaka S. 2005. Differential membrane localization of ERas and Rheb, two Ras-related proteins involved in the phosphatidylinositol 3-kinase/mTOR pathway. J Biol Chem. 280:32768–32774.

Takei N. 2004. Brain-derived neurotrophic factor induces mammalian target of rapamycin-dependent local activation of translation machinery and protein synthesis in neuronal dendrites. J Neurosci. 24:9760–9769.

Tang S, Chen T, Yu Z, Zhu X, Yang M, Xie B, Li N, Cao X, Wang J. 2014. RasGRP3 limits Toll-like receptor-triggered inflammatory response in macrophages by activating Rap1 small GTPase. Nat Commun. 5:4657.

Tasaka G, Negishi M, Oinuma I. 2012. Semaphorin 4D/Plexin-B1-mediated M-Ras GAP activity regulates actin-based dendrite remodeling through Lamellipodin. J Neurosci. 32:8293–8305.

Tazat K, Harsat M, Goldshmid-Shagal A, Ehrlich M, Henis YI. 2013. Dual effects of Ral-activated pathways on p27 localization and TGF-beta signaling. Mol Biol Cell. 24:1812–1824.

Tee AR, Manning BD, Roux PP, Cantley LC, Blenis J. 2003. Tuberous sclerosis complex gene products, Tuberin and Hamartin, control mTOR signaling by acting as a GTPase-activating protein complex toward Rheb. Curr Biol. 13:1259–1268.

Teodoro RO, Pekkurnaz G, Nasser A, Higashi-Kovtun ME, Balakireva M, McLachlan IG, Camonis J, Schwarz TL. 2013. Ral mediates activity-dependent growth of postsynaptic membranes via recruitment of the exocyst. EMBO J. 32:2039–2055.

Thapliyal A, Verma R, Kumar N. 2014. Small G proteins Dexras1 and RHES and their role in pathophysiological processes. Int J Cell Biol. 2014:308535.

The Cancer Genome Atlas Research Network. 2014. Comprehensive molecular profiling of lung adenocarcinoma. Nature 511:543–550.

Tidyman WE, Rauen KA. 2016. Expansion of the RASopathies. Curr Genet Med Rep. 4:57–64.

Trahey M, McCormick F. 1987. A cytoplasmic protein stimulates normal N-ras p21 GTPase, but does not affect oncogenic mutants. Science. 238:542–545.

Trumper J, Ross D, Jahr H, Brendel MD, Goke R, Horsch D. 2005. The Rap-B-Raf signalling pathway is activated by glucose and glucagon-like peptide-1 in human islet cells. Diabetologia. 48:1534–1540.

Tuder RM, Cool CD, Geraci MW, Wang J, Abman SH, Wright L, Badesch D, Voelkel NF. 1999. Prostacyclin synthase expression is decreased in lungs from patients with severe pulmonary hypertension. Am J Respir Crit Care Med. 159:1925–1932.

Tyagi R, Shahani N, Gorgen L, Ferretti M, Pryor W, Chen PY, Swarnkar S, Worley PF, Karbstein K, Snyder SH, Subramaniam S. 2015. Rheb inhibits protein synthesis by activating the PERK-eIF2alpha signaling cascade. Cell Rep. 10:684–693.

Tyutyunnykova A, Telegeev G, Dubrovska A. 2017. The controversial role of phospholipase C epsilon (PLCε) in cancer development and progression. J Cancer. 8:716–729.

Uechi Y, Bayarjargal M, Umikawa M, Oshiro M, Takei K, Yamashiro Y, Asato T, Endo S, Misaki R, Taguchi T, Kariya K. 2009. Rap2 function requires palmitoylation and recycling endosome localization. Biochem Biophys Res Commun. 378:732–737.

Ueda K, Yaoita M, Niihori T, Aoki Y, Okamoto N. 2017. Craniosynostosis in patients with RASopathies: accumulating clinical evidence for expanding the phenotype. Am J Med Genet. 173:2346–2352.

Unal EB, Uhlitz F, Bluthgen N. 2017. A compendium of ERK targets. FEBS Lett. 591:2607–2615.

Upadhyaya P, Bedewy W, Pei D. 2016. Direct Inhibitors of Ras-Effector Protein Interactions. Mini Rev Med Chem. 16:376–382.

Vahatupa M, Prince S, Vataja S, Mertimo T, Kataja M, Kinnunen K, Marjomaki V, Uusitalo H, Komatsu M, Jarvinen TA, Uusitalo-Jarvinen H. 2016. Lack of R-Ras leads to increased vascular permeability in ischemic retinopathy. Invest Ophthalmol Vis Sci. 57:4898–4909.

van Dam TJ, Bos JL, Snel B. 2011. Evolution of the Ras-like small GTPases and their regulators. Small GTPases. 2:4–16.

van Dam TJ, Rehmann H, Bos JL, Snel B. 2009. Phylogeny of the CDC25 homology domain reveals rapid differentiation of Ras pathways between early animals and fungi. Cell Signal. 21:1579–1585.

van Hooren KW, van Agtmaal EL, Fernandez-Borja M, van Mourik JA, Voorberg J, Bierings R. 2012. The Epac-Rap1 signaling pathway controls cAMP-mediated exocytosis of Weibel-Palade bodies in endothelial cells. J Biol Chem. 287:24713–24720.

Vanhaesebroeck B, Leevers SJ, Ahmadi K, Timms J, Katso R, Driscoll PC, Woscholski R, Parker PJ, Waterfield MD. 2001. Synthesis and function of 3-phosphorylated inositol lipids. Annu Rev Biochem. 70:535–602.

Varan A, Sen H, Aydin B, Yalcin B, Kutluk T, Akyuz C. 2016. Neurofibromatosis type 1 and malignancy in childhood. Clin Genet. 89:341–345.

Varga A, Ehrenreiter K, Aschenbrenner B, Kocieniewski P, Kochanczyk M, Lipniacki T, Baccarini M. 2017. RAF1/BRAF

Sugihara K, Asano S, Tanaka K, Iwamatsu A, Okawa K, Ohta Y. 2002. The exocyst complex binds the small GTPase RalA to mediate filopodia formation. Nat Cell Biol. 4:73–78.

Sun Y, Fang Y, Yoon MS, Zhang C, Roccio M, Zwartkruis FJ, Armstrong M, Brown HA, Chen J. 2008. Phospholipase D1 is an effector of Rheb in the mTOR pathway. Proc Natl Acad Sci USA. 105:8286–8291.

Sung PJ, Tsai FD, Vais H, Court H, Yang J, Fehrenbacher N, Foskett JK, Philips MR. 2013. Phosphorylated K-Ras limits cell survival by blocking Bcl-xL sensitization of inositol trisphosphate receptors. Proc Natl Acad Sci USA. 110:20593–20598.

Tabaczar S, Czogalla A, Podkalicka J, Biernatowska A, Sikorski AF. 2017. Protein palmitoylation: Palmitoyltransferases and their specificity. Exp Biol Med (Maywood). 242:1150–1157.

Tada M, Gengyo-Ando K, Kobayashi T, Fukuyama M, Mitani S, Kontani K, Katada T. 2012. Neuronally expressed Ras-family GTPase Di-Ras modulates synaptic activity in *Caenorhabditis elegans*. Genes Cells. 17:778–789.

Taira K, Umikawa M, Takei K, Myagmar BE, Shinzato M, Machida N, Uezato H, Nonaka S, Kariya K. 2004. The Traf2- and Nck-interacting kinase as a putative effector of Rap2 to regulate actin cytoskeleton. J Biol Chem. 279:49488–49496.

Takahashi K, Mitsui K, Yamanaka S. 2003. Role of ERas in promoting tumour-like properties in mouse embryonic stem cells. Nature. 423:541–545.

Takahashi K, Nakagawa M, Young SG, Yamanaka S. 2005. Differential membrane localization of ERas and Rheb, two Ras-related proteins involved in the phosphatidylinositol 3-kinase/mTOR pathway. J Biol Chem. 280:32768–32774.

Takei N. 2004. Brain-derived neurotrophic factor induces mammalian target of rapamycin-dependent local activation of translation machinery and protein synthesis in neuronal dendrites. J Neurosci. 24:9760–9769.

Tang S, Chen T, Yu Z, Zhu X, Yang M, Xie B, Li N, Cao X, Wang J. 2014. RasGRP3 limits Toll-like receptor-triggered inflammatory response in macrophages by activating Rap1 small GTPase. Nat Commun. 5:4657.

Tasaka G, Negishi M, Oinuma I. 2012. Semaphorin 4D/Plexin-B1-mediated M-Ras GAP activity regulates actin-based dendrite remodeling through Lamellipodin. J Neurosci. 32:8293–8305.

Tazat K, Harsat M, Goldshmid-Shagal A, Ehrlich M, Henis YI. 2013. Dual effects of Ral-activated pathways on p27 localization and TGF-beta signaling. Mol Biol Cell. 24:1812–1824.

Tee AR, Manning BD, Roux PP, Cantley LC, Blenis J. 2003. Tuberous sclerosis complex gene products, Tuberin and Hamartin, control mTOR signaling by acting as a GTPase-activating protein complex toward Rheb. Curr Biol. 13:1259–1268.

Teodoro RO, Pekkurnaz G, Nasser A, Higashi-Kovtun ME, Balakireva M, McLachlan IG, Camonis J, Schwarz TL. 2013. Ral mediates activity-dependent growth of postsynaptic membranes via recruitment of the exocyst. EMBO J. 32:2039–2055.

Thapliyal A, Verma R, Kumar N. 2014. Small G proteins Dexras1 and RHES and their role in pathophysiological processes. Int J Cell Biol. 2014:308535.

The Cancer Genome Atlas Research Network. 2014. Comprehensive molecular profiling of lung adenocarcinoma. Nature 511:543–550.

Tidyman WE, Rauen KA. 2016. Expansion of the RASopathies. Curr Genet Med Rep. 4:57–64.

Trahey M, McCormick F. 1987. A cytoplasmic protein stimulates normal N-ras p21 GTPase, but does not affect oncogenic mutants. Science. 238:542–545.

Trumper J, Ross D, Jahr H, Brendel MD, Goke R, Horsch D. 2005. The Rap-B-Raf signalling pathway is activated by glucose and glucagon-like peptide-1 in human islet cells. Diabetologia. 48:1534–1540.

Tuder RM, Cool CD, Geraci MW, Wang J, Abman SH, Wright L, Badesch D, Voelkel NF. 1999. Prostacyclin synthase expression is decreased in lungs from patients with severe pulmonary hypertension. Am J Respir Crit Care Med. 159:1925–1932.

Tyagi R, Shahani N, Gorgen L, Ferretti M, Pryor W, Chen PY, Swarnkar S, Worley PF, Karbstein K, Snyder SH, Subramaniam S. 2015. Rheb inhibits protein synthesis by activating the PERK-eIF2alpha signaling cascade. Cell Rep. 10:684–693.

Tyutyunnykova A, Telegeev G, Dubrovska A. 2017. The controversial role of phospholipase C epsilon (PLCε) in cancer development and progression. J Cancer. 8:716–729.

Uechi Y, Bayarjargal M, Umikawa M, Oshiro M, Takei K, Yamashiro Y, Asato T, Endo S, Misaki R, Taguchi T, Kariya K. 2009. Rap2 function requires palmitoylation and recycling endosome localization. Biochem Biophys Res Commun. 378:732–737.

Ueda K, Yaoita M, Niihori T, Aoki Y, Okamoto N. 2017. Craniosynostosis in patients with RASopathies: accumulating clinical evidence for expanding the phenotype. Am J Med Genet. 173:2346–2352.

Unal EB, Uhlitz F, Bluthgen N. 2017. A compendium of ERK targets. FEBS Lett. 591:2607–2615.

Upadhyaya P, Bedewy W, Pei D. 2016. Direct Inhibitors of Ras-Effector Protein Interactions. Mini Rev Med Chem. 16:376–382.

Vahatupa M, Prince S, Vataja S, Mertimo T, Kataja M, Kinnunen K, Marjomaki V, Uusitalo H, Komatsu M, Jarvinen TA, Uusitalo-Jarvinen H. 2016. Lack of R-Ras leads to increased vascular permeability in ischemic retinopathy. Invest Ophthalmol Vis Sci. 57:4898–4909.

van Dam TJ, Bos JL, Snel B. 2011. Evolution of the Ras-like small GTPases and their regulators. Small GTPases. 2:4–16.

van Dam TJ, Rehmann H, Bos JL, Snel B. 2009. Phylogeny of the CDC25 homology domain reveals rapid differentiation of Ras pathways between early animals and fungi. Cell Signal. 21:1579–1585.

van Hooren KW, van Agtmaal EL, Fernandez-Borja M, van Mourik JA, Voorberg J, Bierings R. 2012. The Epac-Rap1 signaling pathway controls cAMP-mediated exocytosis of Weibel-Palade bodies in endothelial cells. J Biol Chem. 287:24713–24720.

Vanhaesebroeck B, Leevers SJ, Ahmadi K, Timms J, Katso R, Driscoll PC, Woscholski R, Parker PJ, Waterfield MD. 2001. Synthesis and function of 3-phosphorylated inositol lipids. Annu Rev Biochem. 70:535–602.

Varan A, Sen H, Aydin B, Yalcin B, Kutluk T, Akyuz C. 2016. Neurofibromatosis type 1 and malignancy in childhood. Clin Genet. 89:341–345.

Varga A, Ehrenreiter K, Aschenbrenner B, Kocieniewski P, Kochanczyk M, Lipniacki T, Baccarini M. 2017. RAF1/BRAF

Zhou Y, Hancock JF. 2015. Ras nanoclusters: Versatile lipid-based signaling platforms. Biochim Biophys Acta. 1853:841–849.

Zhu Y, Pak D, Qin Y, McCormack SG, Kim MJ, Baumgart JP, Velamoor V, Auberson YP, Osten P, van Aelst L, et al. 2005. Rap2-JNK removes synaptic AMPA receptors during depotentiation. Neuron. 46:905–916.

Zhu YH, Fu L, Chen L, Qin YR, Liu H, Xie F, Zeng T, Dong SS, Li J, Li Y, et al. 2013. Downregulation of the novel tumor suppressor DIRAS1 predicts poor prognosis in esophageal squamous cell carcinoma. Cancer Res. 73:2298–2309.

Zou JX, Liu Y, Pasquale EB, Ruoslahti E. 2002. Activated SRC oncogene phosphorylates R-ras and suppresses integrin activity. J Biol Chem. 277:1824–1827.

Zou JX, Wang B, Kalo MS, Zisch AH, Pasquale EB, Ruoslahti E. 1999. An Eph receptor regulates integrin activity through R-Ras. Proc Natl Acad Sci USA. 96:13813–13818.

Chapter III

Activating mutations of *RRAS2* are a rare cause of Noonan syndrome

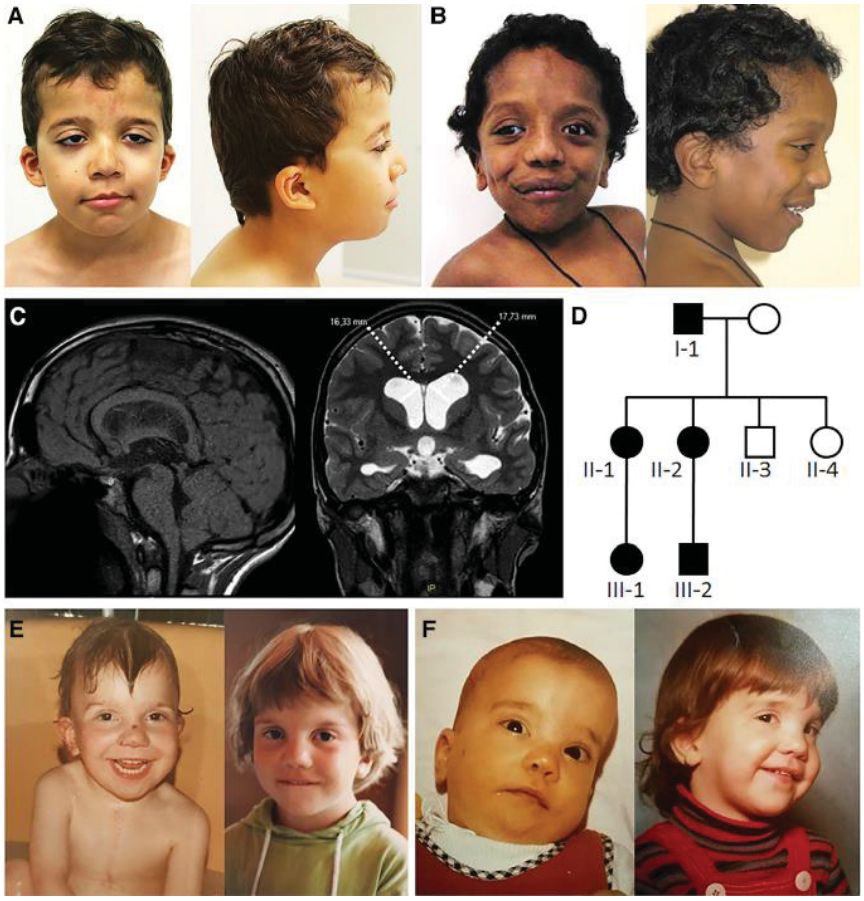

Published in:	American journal of human genetics
Impact factor:	5.96 (2019)
Own Proportion to this work:	5%
	Biochemical analysis of RRAS2 WT and different variants regarding the ntrinsic and GEF-catalyzednucleotide exchange reaction

REPORT

Activating Mutations of *RRAS2* Are a Rare Cause of Noonan Syndrome

Yline Capri,[1,20] Elisabetta Flex,[2,20] Oliver H.F. Krumbach,[3,20] Giovanna Carpentieri,[2,4] Serena Cecchetti,[5] Christina Lißewski,[6] Soheila Rezaei Adariani,[3] Denny Schanze,[6] Julia Brinkmann,[6] Juliette Piard,[7] Francesca Pantaleoni,[4] Francesca R. Lepri,[4] Elaine Suk-Ying Goh,[8] Karen Chong,[9] Elliot Stieglitz,[10] Julia Meyer,[10] Alma Kuechler,[11] Nuria C. Bramswig,[11] Stephanie Sacharow,[12] Marion Strullu,[1,13] Yoann Vial,[1,13] Cédric Vignal,[1] George Kensah,[14] Goran Cuturilo,[15,16] Neda S. Kazemein Jasemi,[3] Radovan Dvorsky,[3] Kristin G. Monaghan,[17] Lisa M. Vincent,[17,18] Hélène Cavé,[1,13] Alain Verloes,[1,19] Mohammad R. Ahmadian,[3,21] Marco Tartaglia,[4,21,*] and Martin Zenker[6,21,*]

Aberrant signaling through pathways controlling cell response to extracellular stimuli constitutes a central theme in disorders affecting development. Signaling through RAS and the MAPK cascade controls a variety of cell decisions in response to cytokines, hormones, and growth factors, and its upregulation causes Noonan syndrome (NS), a developmental disorder whose major features include a distinctive facies, a wide spectrum of cardiac defects, short stature, variable cognitive impairment, and predisposition to malignancies. NS is genetically heterogeneous, and mutations in more than ten genes have been reported to underlie this disorder. Despite the large number of genes implicated, about 10%–20% of affected individuals with a clinical diagnosis of NS do not have mutations in known RASopathy-associated genes, indicating that additional unidentified genes contribute to the disease, when mutated. By using a mixed strategy of functional candidacy and exome sequencing, we identify *RRAS2* as a gene implicated in NS in six unrelated subjects/families. We show that the NS-causing *RRAS2* variants affect highly conserved residues localized around the nucleotide binding pocket of the GTPase and are predicted to variably affect diverse aspects of RRAS2 biochemical behavior, including nucleotide binding, GTP hydrolysis, and interaction with effectors. Additionally, all pathogenic variants increase activation of the MAPK cascade and variably impact cell morphology and cytoskeletal rearrangement. Finally, we provide a characterization of the clinical phenotype associated with *RRAS2* mutations.

Noonan syndrome (NS [MIM: PS163950]) is one of the most common monogenic disorders affecting development and growth.[1] The phenotype of NS comprises a distinctive facies (e.g., hypertelorism, downslanting palpebral fissures, ptosis, and low-set/posteriorly rotated ears), cardiac abnormalities (a wide spectrum of congenital heart defects and cardiomyopathy), postnatally reduced growth, skeletal defects (chest and spine), cryptorchidism, bleeding diathesis, as well as variable neurocognitive impairment and predisposition to malignancies,[1,2] most commonly juvenile myelomonocytic leukemia (JMML [MIM: 607785]).[3] NS is generally transmitted as an autosomal-dominant trait and is genetically heterogeneous. So far, pathogenic variants in more than ten genes have been reported as causative events underlying this disorder.[4] While mutations in *PTPN11* (MIM: 176876), *SOS1* (MIM: 182530), *RAF1* (MIM: 164760), and *RIT1* (MIM: 609591) have been documented to occur most frequently,[5–11] a smaller proportion of cases has been ascribed to mutations in other functionally related genes, including *NRAS* (MIM: 164790), *KRAS* (MIM: 190070), *BRAF* (MIM: 164757), *MAP2K1* (MIM: 176872), *SOS2* (MIM: 601247), *LZTR1* (MIM: 600574), *MRAS* (MIM: 608435), and *RASA2* (MIM: 601589).[12–20] Although the causal link between mutations in a subset of these genes and the disorder still remains to be confirmed,[4] the accumulated molecular evidence strongly supports the view that NS is caused by upregulated intracellular traffic through the RAS-mitogen-activated protein kinase (MAPK) signaling pathway.[21,22] Other disorders clinically related to NS (e.g., cardio-facio-cutaneous syndrome [MIM: PS115150], Costello syndrome [MIM: 218040], neurofibromatosis type 1 [MIM: 162200], Legius syndrome [MIM: 611431], Mazzanti syndrome [MIM: 607721], and Noonan syndrome with multiple lentigines

[1]Département de Génétique, Assistance Publique des Hôpitaux de Paris (AP-HP) Hôpital Robert Debré, 75019 Paris, France; [2]Department of Oncology and Molecular Medicine, Istituto Superiore di Sanità, 00161 Rome, Italy; [3]Institute of Biochemistry and Molecular Biology II, Medical Faculty of the Heinrich Heine University, 40225 Düsseldorf, Germany; [4]Genetics and Rare Diseases Research Division, Ospedale Pediatrico Bambino Gesù, IRCCS, 00146 Rome, Italy; [5]Microscopy Area, Core Facilities, Istituto Superiore di Sanità, 00161 Rome, Italy; [6]Institute of Human Genetics, University Hospital Magdeburg, 39120 Magdeburg, Germany; [7]Human Genetic Center – CHU St Jacques, 25000 Besancon, France; [8]Laboratory Medicine and Genetics, Trillium Health Partners, Mississauga, ON L5M 2N1, Canada; [9]Department of Obstetrics and Gynecology, The Prenatal Diagnosis and Medical Genetics Program, Mount Sinai Hospital, Toronto, ON M5G 1Z5, Canada; [10]Department of Pediatrics, Benioff Children's Hospital, University of California, San Francisco, San Francisco, CA 94107, USA; [11]Institut für Humangenetik, Universitätsklinikum Essen, Universität Duisburg-Essen, 45147 Essen, Germany; [12]Boston Children's Hospital and Harvard Medical School, Boston, MA 02115, USA; [13]INSERM UMR 1131, Institut de Recherche Saint-Louis, Université de Paris, 75010 Paris, France; [14]Department of Thoracic and Cardiovascular Surgery, University Medical Center Göttingen, 37075 Göttingen, Germany; [15]Faculty of Medicine, University of Belgrade, 11000 Belgrade, Serbia; [16]University Children's Hospital, 11000 Belgrade, Serbia; [17]GeneDx, Gaithersburg, MD 20877, USA; [18]Center for Cancer of Blood Disorders, Children's National Health System, Washington, DC 20010, USA; [19]INSERM UMR 1141 - Université de Paris, 75019 Paris, France
[20]These authors contributed equally to this work
[21]These authors contributed equally to this work
*Correspondence: marco.tartaglia@opbg.net (M.T.), martin.zenker@med.ovgu.de (M.Z.)
https://doi.org/10.1016/j.ajhg.2019.04.013.

[MIM: PS151100]) are also caused by mutations in genes encoding key proteins of the RAS-MAPK signaling backbone or upstream regulators (i.e., *CBL*, *HRAS*, *KRAS*, *NF1*, *SPRED1*, *SHOC2*, *BRAF*, *MAP2K1*, and *MAP2K2*).[21,22] In all these related conditions, termed RASopathies, increased signaling through RAS and the MAPK cascade can result from upregulated activity of RAS proteins, enhanced function of upstream signal transducers (e.g., proteins positively controlling RAS function) or downstream RAS effectors, as well as from the inefficient signaling switch-off by feedback mechanisms (e.g., neurofibromin and CBL loss of function). More recently, the use of whole-exome sequencing (WES) has allowed the discovery of RASopathy-associated genes encoding signal transducers or modulators that do not belong to the canonical RAS-MAPK pathway, but when functionally perturbed, are predicted to impact RAS signaling by still poorly characterized circuits.[20,23–29]

A remarkable finding of the molecular genetics of NS and other RASopathies is the occurrence of conserved themes in the mechanism of disease. This applies in particular to mutations affecting genes encoding the various members of the RAS superfamily of GTPases that have been implicated in these disorders, including *KRAS*, *HRAS*, *NRAS*, *RRAS*, *MRAS*, and *CDC42*.[11–14,20,23–26,30] Missense mutations in these genes affect a small number of highly conserved amino acid residues that lead to overactivation of these proteins by decreasing/impairing their GTPase activity in response to GTPase-activating proteins (GAPs), increasing guanine nucleotide exchange factor (GEF)-independent GDP release, altering binding properties to effectors, or a combination of these mechanisms.[31] Notably, while these germline mutations may affect the same residues that are generally mutated in cancer, multiple lines of evidence indicate that RASopathy-causing changes are generally less activating than their respective cancer-associated somatic lesions.[21]

Despite the large number of genes implicated in NS and related phenotypes, about 10%–20% of affected individuals with a convincing clinical diagnosis of NS do not have mutations in currently known RASopathy-associated genes, indicating that other unidentified genes contribute to this disorder. Through the use of complementary approaches based on "functional candidacy" (parallel sequencing of selected gene panels containing functionally related candidate genes) or WES, we identified *RRAS2* (MIM: 600098; GenBank: NM_012250.5) as a gene implicated in NS. We provide structural, biochemical, and functional data to support the causal link between *RRAS2* mutations and NS, outline the mechanisms by which mutations perturb RRAS2 function, and characterize the clinical phenotype associated with these gene lesions.

Subjects from six unrelated families were included in the study. Clinical data and DNA samples were collected from the participating families after written informed consent was obtained. DNA samples were stored and used under research projects approved by the Review Boards of the participating institutions. Because of a suspected RASopathy, subjects 1, 2, 3-III-1, and 5 were referred for diagnostic genetic testing by sequencing of an "extended" panel of RASopathy-associated genes designed to include a set of candidate disease genes selected in the frame of the NSEuroNet Consortium, while subjects 4 and 6 were analyzed by WES (Supplemental Subjects and Methods). In five cases, the *RRAS2* variant (c.68G>T [p.Gly23Val], c.65_73dup [p.Gly22_Gly24dup], c.70_78dup [p.Gly24_Gly26dup], c.208G>A [p.Ala70Thr], c.215A>T [p.Gln72Leu]) arose *de novo* (i.e., it was not identified in parental blood DNA samples). In family 3, mutation scan in one affected family member (3-III-1) identified the heterozygous c.208G>A missense change, and subsequent co-segregation analysis confirmed the occurrence of the variant in three similarly affected relatives. All variants were validated by Sanger sequencing. In all cases, no other candidate variant was identified, further supporting the clinical relevance of this finding. In subject 4, the *RRAS2* variant was detected in both amniocyte and peripheral blood DNA, at 44% and 46% of reads, respectively, indicating the heterozygous mutation was present in the germline of the subject. The clinical data of the affected subjects from the six families are shown in Table 1, facial features of four affected individuals as well as the pedigree of family 3 are presented in Figure 1, and a detailed clinical history is provided in the Supplemental Note. Taken together, the identified *RRAS2* variants included three different nucleotide substitutions predicting missense changes of highly conserved amino acid residues (Gly23, Ala70, and Gln72) among RRAS2 orthologs and paralogs (Figure S1). Alterations to the corresponding positions in other GTPases of the RAS superfamily have already been reported to cause RASopathies or to contribute to oncogenesis (Table S1). In the remaining cases, we identified two small in-frame duplications (p.Gly22_Gly24dup, p.Gly24_Gly26dup) affecting the well-established mutational hotspot of RAS proteins (Figure 2A). Of note, p.Gly22_Gly24dup had previously been reported as somatic event in an uterine leiomyosarcoma specimen,[32] and other similar, but not identical, small in-frame duplications affecting these residues have also been reported in association with different cancers in the Catalogue of Somatic Mutations in Cancer (COSMIC database). The two small in-frame duplications and c.68G>T (p.Gly23Val) and c.215A>T (p.Gln72Leu) substitutions were absent from general population databases, while the c.208G>A (p.Ala70Thr) change had previously been reported in two subjects in gnomAD (heterozygous state, frequency < 0.00001) (Table S2). Multiple *in silico* prediction algorithms uniformly rated these changes as deleterious/pathogenic (Table S2).

RRAS2 (RAS related 2, also known as TC21, teratocarcinoma 21) is a member of the RAS superfamily of GTPases, originally described in 1990.[33] The protein shares the same four conserved functional domains with HRAS, KRAS, and NRAS, and about 55% amino acid sequence homology with HRAS (Figure 2A), which reaches 80%

Table 1. Clinical Features and Genotype of Individuals with *RRAS2* Variants

			Family 3						
	Subject 1	**Subject 2**	**3-II-1**	**3-II-2**	**3-III-1**	**3-III-2**	**Subject 4**	**Subject 5**	**Subject 6**
Origin	Algerian	Sri Lanka	German				Indian	Serbian	South American/ Ashkenazi
Gender	M	M	F	F	F	M	M	F	M
Age at last visit	7 y 11 m	12 y 2 m	32 y	40 y	7 y 1 m	1 y 7 m	2 weeks	8 y 10 m	22 m (last measurement 18 m)
RRAS2 variant	c.65_73dup (p.Gly22_Gly24dup)	c.68G>T (p.Gly23Val)	c.208G>A (p.Ala70Thr)	c.208G>A (p.Ala70Thr)	c.208G>A (p.Ala70Thr)	c.208G>A (p.Ala70Thr)	c.215A>T (p.Gln72Leu)	c.208G>A (p.Ala70Thr)	c.70_78dup (p.Gly24_ Gly26dup)
Inheritance	*de novo*	*de novo*	presumed paternal	presumed paternal	maternal	maternal	*de novo*	*de novo*	*de novo*
Prenatal features	NF, PH	PH	NA	NA	NA	N	NF, fetal ventriculo-megaly and cardiac abnormalities	NF	PH, LGA
Birth measurements: weight, length, OFC (weeks GA)	3,730 g, 50.5 cm, 37 cm (35)	3,180 g, 46.5 cm, 35 cm (35)	NA	3,740 g, 51 cm, 36 cm	3,110 g, 48 cm, 36 cm (39)	2,440 g, 48 cm, 32 cm (35)	2,400 g (33)	NA	3,600 g, 51 cm, 38 cm (35)
Feeding difficulties	PF	PF, TF	NA	NA	PF	N	NA	N	N
Height at last examination	125.5 cm (+0.3 SD)	139.5 (−1.5 SD) 85 cm (−3.3 SD)[a]	160 cm (−1.3 SD)	170 cm (+0.3 SD)	108 cm (−3.0 SD)	78 cm (−1.8 SD)	NA	122 cm (−2.1 SD)	84.5 cm (+0.5 SD)
Weight	27.5 kg (−0.5 SD)	32.5 kg (−1.4 SD)	NA	59 kg (↓0.1 SD)	18.6 kg (↓1.8 SD)	11 kg (↓0.4 SD)	NA	22 kg (−1.9 SD)	12.5 kg (−0.7 SD)
OFC	54 cm (↓1.2 SD)	57 cm (↓2.5 SD)	52.5 cm (−2.2 SD)	55.5 cm (+0.2 SD)	52 cm (+0.4 SD)	49 cm (−0.2 SD)	NA	52.5 cm (↓0.2 SD)	54.5 cm (↓5.0 SD)
Cryptorchidism	N	N	NA	NA	NA	N	hypoplastic scrotum	NA	N
Congenital heart defect	SVAoS	VSD	VSD	N	N	N	TOF	AVSD, multiple VSDs	N
Lymphatic anomalies	N	N	N	N	N	N	N	N	N
Facial anomalies	typical NS	typical NS	suggestive NS	very mild in adulthood	typical NS	typical NS	multiple anomalies	suggestive NS	typical NS
Development	N	mild MD, mild LD	N	N	mild MD, mild LD	N	NA	N	mild global delay
Neurology	N	Chiari malformation	N	N	N	N	non-obstructive hydrocephalus	N	mild ventriculomegaly, hypotonia
Skeletal	N	N	N	N	N	N	11 rib pairs, proximally placed thumb, spinal canal stenosis	pectus excavatum	N

(*Continued on next page*)

Table 1. *Continued*

	Subject 1	Subject 2	Family 3				Subject 4	Subject 5	Subject 6
			3-II-1	3-II-2	3-III-1	3-III-2			
Hematology & oncology	N	lymphopenia	N	N	N	N	thrombocytopenia	N	N
Skin and hair	glabellar heamangioma	N	N	N	atopic dermatitis,	N	N	N	glabellar hemangioma
Ocular	N	strabismus	N	strabismus	hyperopia, bilateral ptosis	N	NA	N	strabismic amblyopia, esotropia
Other malformations/ anomalies	N	GH deficiency, GH treatment from age 4 y	unilateral duplex kidney	N	multiple allergies, bronchitis	N	labyrinth dysplasia, anteriorly placed anus	minor hippocampal malformation on brain MRI	N

Abbreviations: AVSD, atrioventricular septal defect; F, female; GA, gestational age; GD, global delay; GH, growth hormone; LD, learning difficulties; LGA, large for gestational age; M, male; m, months; MD, motor delay; N, none/normal; NA, not applicable/not available; NE, nuchal edema; OFC, occipitofrontal head circumference; PF, poor feeding reported; PH, polyhydramnios; SVAoS, supravalvular aortic stenosis; TF, tube feeding (>4 weeks); TOF, Tetralogy of Fallot; y, years.
[a]Before onset of growth hormone treatment at age 3 y 6 m.

when considering the region between residues 5 to 120 (i.e., excluding the hypervariable tail at the C terminus).[34,35] RRAS2 controls multiple cellular processes, including proliferation, survival, and migration, and its functional dysregulation has been documented to contribute to oncogenesis.[34,36,37] Indeed, a number of oncogenic RRAS2 variants have been reported, including the p.Gly23Val, p.Ala70Thr, and p.Gln72Leu changes, in a variety of solid tumors (Table S1). More recently, the p.Gln72Leu change in RRAS2 has been identified in subjects with isolated JMML,[38] which represents the archetypal somatic RASopathy. Notably, germline mutations in other *RAS* genes affecting analogous codons to those observed in the present cases have also been identified (Table S1), including the missense mutation p.Gln87Leu in RRAS (homologous to p.Gln72Leu in RRAS2), previously reported in individuals having features reminiscent of NS.[23]

In order to decipher the consequences of the observed amino acid changes and the small in-frame duplications on the molecular structure of RRAS2, we performed structural modeling. A closer view into the active site of RRAS2 structure in its active form (Figure 2B, left) revealed that the identified *RRAS2* mutations affect residues localized around the nucleotide binding pocket of the GTPase. The corresponding amino acids, including Gly22-Gly26, Ala70, and Gln72, do not only play a critical role in GDP/GTP exchange and GTP hydrolysis but also are involved in stabilization of the switch regions (Figure 2B, right), which are the binding sites for both RRAS2 regulators (GEFs and GAPs) and effectors.[39] Specifically, the amino acid stretch encompassing Gly22 to Gly26 constitutes part of the phosphate-binding loop (P loop; residues Gly21 to Ser28) that is responsible for binding to the phosphate groups of either GTP or GDP. These residues play a critical role in nucleotide binding and hydrolysis by contacting both the β-γ phosphates of GTP (shown as GppNHp, a non-hydrolyzable GTP analog in Figure 2B) and residues 67 to 69 of the switch II region (SwII; Asp68 to Arg84). Val25 stabilizes the P loop by contacting Val92, Ser94, and Ser100. The Gly22-to-Gly24 and Gly24-to-Gly26 duplications were predicted to destabilize the P loop and result in increased nucleotide exchange and decreased GTP hydrolysis reactions. Differently, Ala70 and Gln72 are located in the switch II region of the GTPase and are directly involved in Mg^{2+} coordination and GTP hydrolysis reaction. Additionally, Ala70 and Gln72 stabilize the switch I region (SwI; Phe39-Ser50) by contacting Ile47 and Glu48, respectively. Based on these considerations, the NS-associated amino acid changes were expected to affect various aspects of RRAS2 biochemical behavior, including a faster nucleotide exchange, an impaired GTP hydrolysis, and a decrease in GEF, GAP, and effector interactions. Subsequent biochemical analysis of $RRAS2^{p.Ala70Thr}$ clearly confirmed these structural predictions, as assessment of the intrinsic and stimulated nucleotide exchange demonstrated a significantly increased

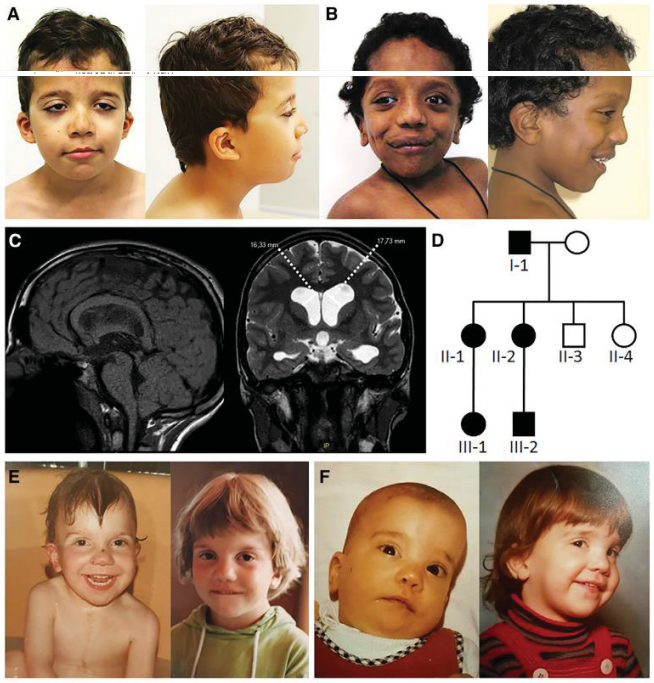

Figure 1. Clinical Features of Individuals with Heterozygous Noonan Syndrome-Causing *RRAS2* Variants
(A) Clinical appearance of subject 1 at 7 years and 11 months. Note the distinctive NS features, including bitemporal narrowing, downslanting palpebral fissures, ptosis, low-set ears, and low posterior hairline.
(B) Facial features of subject 2 at 2 years and 6 months. Facial features overlap those characterizing subject 1, even though a "coarse" face is also observed.
(C) Subject 2 brain MRI at 11 years and 9 months showing Chiari type 1 malformation and bilateral ventricular dilatation.
(D) Pedigree of family 3.
(E) Clinical appearance of subject 3-II-1 at the age of 11 months and 4.5 years.
(F) Facial features of subject 3-II-2 at 9 months and 5 years. The NS facial gestalt of subjects 3-II-1 and 3-II-2 became less obvious in adulthood.

response of the RRAS2$^{p.Ala70Thr}$ protein to GEF as compared to wild-type RRAS2 (Figure 2C). In contrast, the GTP hydrolysis reactions of the mutant were reduced compared to the wild-type protein. Particularly, the GAP-stimulated GTPase activity of RRAS2$^{p.Ala70Thr}$ was significantly decreased (9-fold) (Figure 2C). Finally, the binding properties to two RRAS2 effectors, RAF1 (CRAF) and RASSF5, were assessed. While the affinity of the interaction with CRAF was comparable to that of wild-type RRAS2, binding to RASSF5 was abolished (Figure 2C). This suggests the p.Ala70Thr change leads to a structural rearrangement of RRAS2 switch II, which is a key binding site for RASSF5 but not for CRAF. Overall, these data support that the p.Ala70Thr change leads to an accumulation of RRAS2 in its GTP-bound active state, which predicts an increase in signaling activity. The impaired binding to RASSF5, however, suggest a possible differential impact of the missense change on downstream signaling pathways.

RRAS2 shares downstream effectors with the other members of the RAS subfamily;[35] however, little information exists about the function of this protein in cellular processes and development. Similarly, scant data exist on the specific role of this protein in intracellular signaling as well as on the extent of functional overlap with the other RAS proteins implicated in RASopathies. To explore the consequences of NS-associated *RRAS2* mutations on the intracellular signaling pathways affected in NS, the signaling flows through the MAPK and phosphatidylinostiol-3 kinase (PI3K)-AKT cascades were evaluated using transient expression in HEK293T cells. Expression of all mutants resulted in variably enhanced ERK phosphorylation compared to cells overexpressing the wild-type protein (Figure 3A). Notably, RRAS2$^{p.Ala70Thr}$ and RRAS2$^{p.Gln72Leu}$ were observed to constitutively promote increased ERK phosphorylation, while only a slight increase was observed basally in cells expressing the RRAS2$^{p.Gly22_Gly24dup}$ and RRAS2$^{p.Gly23Val}$ mutants. However, this slight increase substantially strengthened after stimulation with EGF. This activating role of p.Gly22_Gly24dup is in line with previous evidence supporting the gain-of-function role of short insertional mutations in the P loop of other members of the RAS family.[40] Based on previous data indicating that upregulated RRAS2 promotes tumorigenesis in a PI3K-dependent manner,[41] the impact of NS-associated mutants on PI3K-AKT signaling was also assessed. No significant difference in the extent of AKT phosphorylation was documented, indicating a specific functional link between RRAS2 and the MAPK signaling cascade, at least in the present experimental conditions. In line with these findings, *Rras2* KO mice showed a downmodulation of Erk activation and unaltered levels of phosphorylated Akt.[42]

RAS proteins interact with multiple signaling platforms, which allow these proteins to differentially control multiple signaling pathways.[43] Such complex behavior is attained by their dynamic interaction with the plasma membrane and other intracellular membranes (i.e., endosomes, endoplasmic reticulum, and Golgi). To explore any perturbing effect of mutations on the subcellular

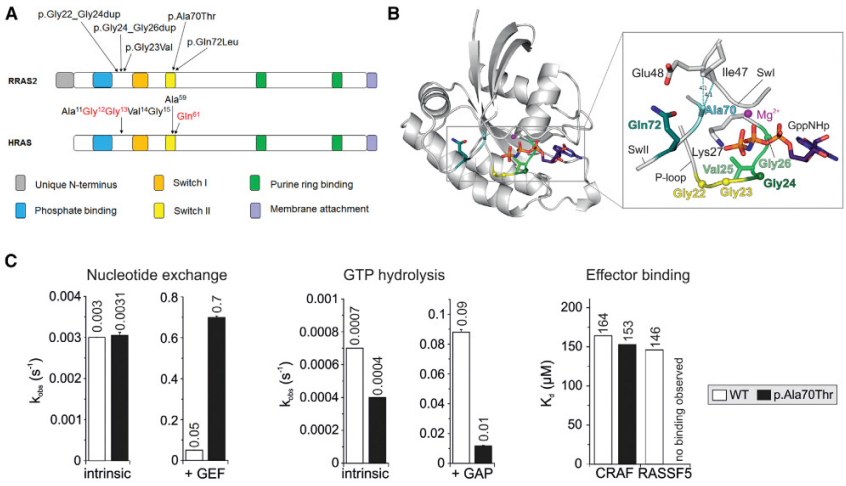

Figure 2. RRAS2 Structure and Location and Functional Impact of Noonan Syndrome-Causing Variants
(A) Schematic representation of RRAS2 and HRAS proteins. Conserved motifs critical for tight guanine nucleotide binding and hydrolysis, and position of the disease-causing RRAS2 variants are illustrated together with the homologous residues of HRAS. The three residues representing the mutational hotspots of oncogenic *HRAS* mutations are shown in red.
(B) Structural modeling of RRAS2 variants. A structural model of the active GTP-bound RRAS2 protein highlights the relative position of the disease-causing missense or insertion mutations. All *RRAS2* mutations affect residues that are located in the nucleotide binding active site region, which contains integral elements involved in GDP/GTP binding, GTP hydrolysis, and interactions with regulators (GEFs and GAPs) and effectors.
(C) Biochemical assessment of $RRAS2^{p.Ala70Thr}$. $RRAS2^{WT}$ and $RRAS2^{p.Ala70Thr}$ proteins were biochemically characterized regarding their nucleotide exchange (left), GTP hydrolysis (middle), and effector binding (right) properties. The nucleotide exchange reaction was measured in the absence (intrinsic) and in the presence of the catalytic RASGEF domain of mouse RASGRF1, while the catalytic activity of the GTPase was assessed in the absence (intrinsic) and in the presence of the p120 RASGAP GAP domain. The RAS-binding and RAS association domains of CRAF and RASSF5 were used to evaluate the binding behavior of the $RRAS2^{p.Ala70Thr}$ mutant to RAS effectors. Overall, the data indicate that the p.Ala70Thr change leads to an accumulation of the protein in its GTP-bound active state, resulting to an increased signaling activity. The missense change, however, is predicted to differentially impact on the diverse downstream signaling pathways.

localization and distribution of RRAS2, including possible preferential targeting to specific intracellular domains, confocal laser scanning microscopy analysis was performed in HEK293T cells transiently expressing Myc-tagged RRAS2 constructs under starved condition. Similarly to the wild-type protein, a fraction of all RRAS2 mutant proteins co-localized with GM130, indicating their targeting to the Golgi apparatus, and the remainder were largely found at the plasma membrane (Figure 3B, left), indicating that mutations do not cause any overt subcellular redistribution of the GTPase. Notably, transient expression of all mutants was found to variably impact cell morphology and cytoskeletal rearrangement, with all mutant proteins promoting spreading and adhesion (Figure 3B, right). Taken together, these experimental data suggest that NS-associated *RRAS2* mutations variably upregulate MAPK signaling and are likely to affect cellular processes depending on cytoskeleton rearrangement similar to observations of RASopathy-causing KRAS mutants.[44]

Our findings establish *RRAS2* germline mutations as a cause of NS. Although previous screening of a cohort of 116 subjects with a clinical diagnosis of NS without a genetic explanation did not identify germline pathogenic *RRAS2* variants,[45] the present collaborative effort allowed to identify six unrelated affected individuals. Of the case subjects reported here, two individuals carrying *de novo* germline NS-causing *RRAS2* variants (subjects 1 and 2) were identified among 1,220 samples addressed to Robert Debré Hospital, Paris, for diagnostic testing for NS, between February 2016 and September 2018. Within the same period, 181 of these subjects were found to carry a *PTPN11* mutation. At the University Hospital of Magdeburg, screening of a multigene panel including *RRAS2* in a cohort of 280 subjects with a tentative diagnosis of NS and negative results for mutations in previously known genes yielded two *RRAS2* mutation-positive cases. Finally, no putative *RRAS2* mutation was identified among 150 case subjects with a clinical diagnosis of NS from Ospedale Pediatrico Bambino Gesù, Rome. Overall, these findings indicate that *RRAS2* mutations are rare events in NS.

The phenotypes associated with the two *RRAS2* mutation hotspots were found to fit well within the clinical spectrum of NS even though they appeared variable in terms of

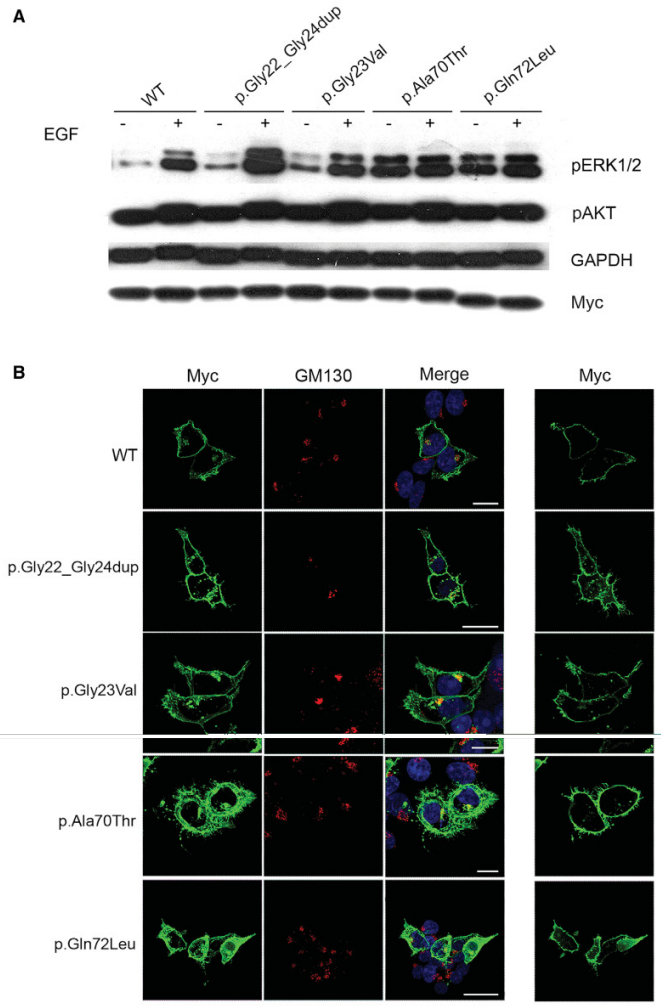

Figure 3. Biochemical and Functional Characterization of Noonan Syndrome-Causing *RRAS2* Variants

(A) ERK and AKT phosphorylation assays. HEK293T cells were transfected with the indicated Myc-tagged RRAS2 constructs. Following starvation (18 h) and EGF stimulation (30 ng/mL for 15 min), ERK and AKT phosphorylation levels were evaluated using a mouse monoclonal anti-phospho-p44/42 ERK (Thr202/Tyr204) antibody and a rabbit polyclonal anti-phospho-AKT (Ser473) antibody, respectively. To assess myc-RRAS2 protein levels, 20 μg of total lysates were immunoblotted with a mouse monoclonal anti-Myc antibody. Membranes were re-probed with mouse monoclonal anti-GAPDH antibody for protein normalization. Representative blot of three performed experiments are shown.

(B) RRAS2 subcellular localization showed by confocal laser scanning microscopy (CLSM) observations (left). Assays were performed on HEK293T cells starved overnight and stained with an anti-Myc mouse monoclonal antibody, followed by goat anti-mouse Alexa Fluor-488 (green), and an anti-GM130 (Golgi marker) rabbit polyclonal antibody, followed by goat anti-rabbit Alexa Fluor-594 (red). Nuclei are visualized by DAPI staining (blue). Co-localization areas were detected in yellow. CLSM observation were also performed at the basal level of cells to show the distinctive pattern of adhesion-like structures and cytoskeletal rearrangement in cells expressing the RRAS2 mutants (right). In all panels, bars correspond to 21 μm.

severity. While individuals 1, 2, 5, and 6 had features fitting typical NS, the phenotype in some affected members of family 3 was relatively mild. On the other hand, subject 4 showed a complex and particularly severe phenotype with multiple congenital anomalies and neonatal lethality. Of note, prenatal features (nuchal edema, polyhydramnios, and/or cardiomyopathy) were reported in five of six subjects, and none showed pulmonary valve stenosis or hypertrophic cardiomyopathy. While the small size of the studied cohort does not allow us to outline specific genotype-phenotype correlations, we hypothesize that such variable expressivity likely reflects the differential strength of individual variants to perturb RRAS2 function and intracellular signaling. Consistent with the collected functional data, p.Gln72Leu (analogous to p.Gln61Leu in HRAS, NRAS, and KRAS) is a strong activating mutation and has not been observed to occur as a germline event in *HRAS*, *KRAS*, or *NRAS*. Similar differences in the biological and phenotypic consequences have previously been reported for *HRAS*, *NRAS*, and *KRAS*,[12–14,30,31,46–53] including the positions corresponding to the presently identified *RRAS2* mutations. The genotype-phenotype correlations in *HRAS* are illustrative and correlate well with the present findings: while p.Ala59Thr has been associated with Costello syndrome and p.Gly12Val has been reported with severe expression of Costello syndrome,[46] p.Gln61Leu and other changes at this codon have only been reported as somatic events in cancer (Table S1).

A noticeable finding of this study is the observation of a diverse impact of the p.Ala70Thr on RRAS2 binding to CRAF/RAF1 and RASSF5. These data suggest the possibility that multiple signaling pathways downstream of RRAS2 may contribute to dysregulation of cellular processes

(e.g., cell proliferation). As expected, a variable hyperactivation of the MAPK pathway resulting from the hyperactive state of the GTPase and unaltered binding to CRAF was observed for the NS-causing RRAS2^{Ala70Thr} protein. Remarkably, impaired binding of this mutant to RASSF5, a known tumor suppressor protein negatively modulating YAP1 levels through activation of the Hippo pathway, was also observed. YAP1 is a transcriptional cofactor promoting cell proliferation, which undergoes RASSF5-mediated phosphorylation and degradation.[54] The impaired binding of RRAS2 to RASSF5 raises the possibility that a less effective Hippo-mediated control of YAP1 levels may contribute to disease pathogenesis in NS.

Among RAS GTPases, RRAS2 exhibits the highest amino acid identity to HRAS, KRAS, and NRAS.[35] Somatic mutations in *RRAS2* have been established to contribute to oncogenesis, even though in a substantially restricted tumor type and less frequently compared to *HRAS*, *KRAS*, and *NRAS*. Consistently, it was originally demonstrated that RRAS2 proteins containing amino acid substitutions analogous to those with oncogenic role in HRAS, KRAS, and NRAS have transforming properties comparable to the strong transforming activity of RAS oncoproteins and similarly promote constitutive activation of the MAPK cascade.[55] Our findings, which are in line with the data presented in an accompanying report by Niihori et al. published in this issue,[56] further extend these observations by demonstrating the clinical relevance of a narrow spectrum of germline pathogenic variants in *RRAS2* as the event underlying a small fraction of NS cases via upregulation of MAPK signaling. Further studies are required to more accurately define the precise mechanisms and circuits linking upregulated RRAS2 function and RAS-MAPK signaling dysregulation.

Accession Numbers

The accession numbers for the five *RRAS2* variants reported in this paper are ClinVar: SCV000902249–SCV000902253.

Supplemental Data

Supplemental Data can be found online at https://doi.org/10.1016/j.ajhg.2019.04.013.

Acknowledgments

The authors thank the subjects and their families for participating in this study. This work was supported by the ERN-ITHACA networking (A.V. and M.T.) and grants from E-Rare (NSEuroNet, ERARE15-pp-063) to H.C., M.R.A. (01GM1602B), M.T., and M.Z. (01GM1602A), AIRC (IG21614) and Ministero della Salute (Ricerca Corrente 2017, 2018) to M.T., German Federal Ministry of Education and Research - BMBF (German Network for RASopathy Research "GeNeRARe") to M.R.A. (01GM1519D and 01GM1902C) and M.Z. (01GM1519A), and the German Research Foundation through the Collaborative Research Center 974 (SFB 974) "Communication and Systems Relevance during Liver Injury and Regeneration" to M.R.A and grant number ZE 524-10/1 to M.Z.

Declaration of Interests

K.G.M. declares no additional conflicts of interest beyond her employment affiliation. L.M.V. is a former employee of GeneDx. All the other authors declare no competing interests.

Received: March 6, 2019
Accepted: April 18, 2019
Published: May 23, 2019

Web Resources

CADD, https://cadd.gs.washington.edu/
ClinVar, https://www.ncbi.nlm.nih.gov/clinvar/
COSMIC, https://cancer.sanger.ac.uk/cosmic
dbSNP, https://www.ncbi.nlm.nih.gov/snp
Exome Aggregation Consortium (ExAC) Browser, http://exac.broadinstitute.org/
GenBank, https://www.ncbi.nlm.nih.gov/genbank
GeneMatcher, https://genematcher.org
gnomAD, https://gnomad.broadinstitute.org/
Muscle, https://www.ebi.ac.uk/Tools/msa/muscle/
MutationAssessor, http://mutationassessor.org/r3/
MutationTaster, http://mutationtaster.org
MutPred2, http://mutpred.mutdb.org/
OMIM, http://www.omim.org/
PolyPhen-2, http://genetics.bwh.harvard.edu/pph2/
PROVEAN, http://provean.jcvi.org/index.php

References

1. Roberts, A.E., Allanson, J.E., Tartaglia, M., and Gelb, B.D. (2013). Noonan syndrome. Lancet *381*, 333–342.
2. Tartaglia, M., Gelb, B.D., and Zenker, M. (2011). Noonan syndrome and clinically related disorders. Best Pract. Res. Clin. Endocrinol. Metab. *25*, 161–179.
3. Strullu, M., Caye, A., Lachenaud, J., Cassinat, B., Gazal, S., Fenneteau, O., Pouvreau, N., Pereira, S., Baumann, C., Contet, A., et al. (2014). Juvenile myelomonocytic leukaemia and Noonan syndrome. J. Med. Genet. *51*, 689–697.
4. Grant, A.R., Cushman, B.J., Cavé, H., Dillon, M.W., Gelb, B.D., Gripp, K.W., Lee, J.A., Mason-Suares, H., Rauen, K.A., Tartaglia, M., et al. (2018). Assessing the gene-disease association of 19 genes with the RASopathies using the ClinGen gene curation framework. Hum. Mutat. *39*, 1485–1493.
5. Tartaglia, M., Mehler, E.L., Goldberg, R., Zampino, G., Brunner, H.G., Kremer, H., van der Burgt, I., Crosby, A.H., Ion, A., Jeffery, S., et al. (2001). Mutations in PTPN11, encoding the protein tyrosine phosphatase SHP-2, cause Noonan syndrome. Nat. Genet. *29*, 465–468.
6. Tartaglia, M., Pennacchio, L.A., Zhao, C., Yadav, K.K., Fodale, V., Sarkozy, A., Pandit, B., Oishi, K., Martinelli, S., Schackwitz, W., et al. (2007). Gain-of-function *SOS1* mutations cause a distinctive form of Noonan syndrome. Nat. Genet. *39*, 75–79.
7. Roberts, A.E., Araki, T., Swanson, K.D., Montgomery, K.T., Schiripo, T.A., Joshi, V.A., Li, L., Yassin, Y., Tamburino, A.M., Neel, B.G., and Kucherlapati, R.S. (2007). Germline gain-of-function mutations in *SOS1* cause Noonan syndrome. Nat. Genet. *39*, 70–74.
8. Zenker, M., Horn, D., Wieczorek, D., Allanson, J., Pauli, S., van der Burgt, I., Doerr, H.-G., Gaspar, H., Hofbeck, M., Gillessen-Kaesbach, G., et al. (2007). SOS1 is the second most common

Noonan gene but plays no major role in cardio-facio-cutaneous syndrome. J. Med. Genet. *44*, 651–656.

9. Pandit, B., Sarkozy, A., Pennacchio, L.A., Carta, C., Oishi, K., Martinelli, S., Pogna, E.A., Schackwitz, W., Ustaszewska, A., Landstrom, A., et al. (2007). Gain-of-function RAF1 mutations cause Noonan and LEOPARD syndromes with hypertrophic cardiomyopathy. Nat. Genet. *39*, 1007–1012.
10. Razzaque, M.A., Nishizawa, T., Komoike, Y., Yagi, H., Furutani, M., Amo, R., Kamisago, M., Momma, K., Katayama, H., Nakagawa, M., et al. (2007). Germline gain-of-function mutations in *RAF1* cause Noonan syndrome. Nat. Genet. *39*, 1013–1017.
11. Kouz, K., Lissewski, C., Spranger, S., Mitter, D., Riess, A., Lopez-Gonzalez, V., Lüttgen, S., Aydin, H., von Deimling, F., Evers, C., et al. (2016). Genotype and phenotype in patients with Noonan syndrome and a *RIT1* mutation. Genet. Med. *18*, 1226–1234.
12. Cirstea, I.C., Kutsche, K., Dvorsky, R., Gremer, L., Carta, C., Horn, D., Roberts, A.E., Lepri, F., Merbitz-Zahradnik, T., König, R., et al. (2010). A restricted spectrum of NRAS mutations causes Noonan syndrome. Nat. Genet. *42*, 27–29.
13. Schubbert, S., Zenker, M., Rowe, S.L., Böll, S., Klein, C., Bollag, G., van der Burgt, I., Musante, L., Kalscheuer, V., Wehner, L.-E., et al. (2006). Germline *KRAS* mutations cause Noonan syndrome. Nat. Genet. *38*, 331–336.
14. Zenker, M., Lehmann, K., Schulz, A.L., Barth, H., Hansmann, D., Koenig, R., Korinthenberg, R., Kreiss-Nachtsheim, M., Meinecke, P., Morlot, S., et al. (2007). Expansion of the genotypic and phenotypic spectrum in patients with KRAS germline mutations. J. Med. Genet. *44*, 131–135.
15. Sarkozy, A., Carta, C., Moretti, S., Zampino, G., Digilio, M.C., Pantaleoni, F., Scioletti, A.P., Esposito, G., Cordeddu, V., Lepri, F., et al. (2009). Germline *BRAF* mutations in Noonan, LEOPARD, and cardiofaciocutaneous syndromes: molecular diversity and associated phenotypic spectrum. Hum. Mutat. *30*, 695–702.
16. Nava, C., Hanna, N., Michot, C., Pereira, S., Pouvreau, N., Niihori, T., Aoki, Y., Matsubara, Y., Arveiler, B., Lacombe, D., et al. (2007). Cardio-facio-cutaneous and Noonan syndromes due to mutations in the RAS/MAPK signalling pathway: genotype-phenotype relationships and overlap with Costello syndrome. J. Med. Genet. *44*, 763–771.
17. Yamamoto, G.L., Aguena, M., Gos, M., Hung, C., Pilch, J., Fahiminiya, S., Abramowicz, A., Cristian, I., Buscarilli, M., Naslavsky, M.S., et al. (2015). Rare variants in *SOS2* and *LZTR1* are associated with Noonan syndrome. J. Med. Genet. *52*, 413–421.
18. Cordeddu, V., Yin, J.C., Gunnarsson, C., Virtanen, C., Drunat, S., Lepri, F., De Luca, A., Rossi, C., Ciolfi, A., Pugh, T.J., et al. (2015). Activating Mutations Affecting the Dbl Homology Domain of SOS2 Cause Noonan Syndrome. Hum. Mutat. *36*, 1080–1087.
19. Chen, P.-C., Yin, J., Yu, H.-W., Yuan, T., Fernandez, M., Yung, C.K., Trinh, Q.M., Peltekova, V.D., Reid, J.G., Tworog-Dube, E., et al. (2014). Next-generation sequencing identifies rare variants associated with Noonan syndrome. Proc. Natl. Acad. Sci. USA *111*, 11473–11478.
20. Higgins, E.M., Bos, J.M., Mason-Suares, H., Tester, D.J., Ackerman, J.P., MacRae, C.A., Sol-Church, K., Gripp, K.W., Urrutia, R., and Ackerman, M.J. (2017). Elucidation of *MRAS*-mediated Noonan syndrome with cardiac hypertrophy. JCI Insight *2*, e91225.
21. Tartaglia, M., and Gelb, B.D. (2010). Disorders of dysregulated signal traffic through the RAS-MAPK pathway: phenotypic spectrum and molecular mechanisms. Ann. N Y Acad. Sci. *1214*, 99–121.
22. Rauen, K.A. (2013). The RASopathies. Annu. Rev. Genomics Hum. Genet. *14*, 355–369.
23. Flex, E., Jaiswal, M., Pantaleoni, F., Martinelli, S., Strullu, M., Fansa, E.K., Caye, A., De Luca, A., Lepri, F., Dvorsky, R., et al. (2014). Activating mutations in RRAS underlie a phenotype within the RASopathy spectrum and contribute to leukaemogenesis. Hum. Mol. Genet. *23*, 4315–4327.
24. Gripp, K.W., Aldinger, K.A., Bennett, J.T., Baker, L., Tusi, J., Powell-Hamilton, N., Stabley, D., Sol-Church, K., Timms, A.E., and Dobyns, W.B. (2016). A novel rasopathy caused by recurrent de novo missense mutations in *PPP1CB* closely resembles Noonan syndrome with loose anagen hair. Am. J. Med. Genet. A. *170*, 2237–2247.
25. Martinelli, S., Krumbach, O.H.F., Pantaleoni, F., Coppola, S., Amin, E., Pannone, L., Nouri, K., Farina, L., Dvorsky, R., Lepri, F., et al.; University of Washington Center for Mendelian Genomics (2018). Functional Dysregulation of CDC42 Causes Diverse Developmental Phenotypes. Am. J. Hum. Genet. *102*, 309–320.
26. Young, L.C., Hartig, N., Boned Del Río, I., Sari, S., Ringham-Terry, B., Wainwright, J.R., Jones, G.G., McCormick, F., and Rodriguez-Viciana, P. (2018). SHOC2-MRAS-PP1 complex positively regulates RAF activity and contributes to Noonan syndrome pathogenesis. Proc. Natl. Acad. Sci. USA *115*, E10576–E10585.
27. Motta, M., Fidan, M., Bellacchio, E., Pantaleoni, F., Schneider-Heieck, K., Coppola, S., Borck, G., Salviati, L., Zenker, M., Cirstea, I.C., and Tartaglia, M. (2018). Dominant Noonan syndrome-causing LZTR1 mutations specifically affect the kelch domain substrate-recognition surface and enhance RAS-MAPK signaling. Hum. Mol. Genet. *28*, 1007–1022.
28. Bigenzahn, J.W., Collu, G.M., Kartnig, F., Pieraks, M., Vladimer, G.I., Heinz, L.X., Sedlyarov, V., Schischlik, F., Fauster, A., Rebsamen, M., et al. (2018). LZTR1 is a regulator of RAS ubiquitination and signaling. Science *362*, 1171–1177.
29. Steklov, M., Pandolfi, S., Baietti, M.F., Batiuk, A., Carai, P., Najm, P., Zhang, M., Jang, H., Renzi, F., Cai, Y., et al. (2018). Mutations in LZTR1 drive human disease by dysregulating RAS ubiquitination. Science *362*, 1177–1182.
30. Aoki, Y., Niihori, T., Kawame, H., Kurosawa, K., Ohashi, H., Tanaka, Y., Filocamo, M., Kato, K., Suzuki, Y., Kure, S., and Matsubara, Y. (2005). Germline mutations in *HRAS* proto-oncogene cause Costello syndrome. Nat. Genet. *37*, 1038–1040.
31. Gremer, L., Gilsbach, B., Ahmadian, M.R., and Wittinghofer, A. (2008). Fluoride complexes of oncogenic Ras mutants to study the Ras-RasGap interaction. Biol. Chem. *389*, 1163–1171.
32. Huang, Y., Saez, R., Chao, L., Santos, E., Aaronson, S.A., and Chan, A.M. (1995). A novel insertional mutation in the TC21 gene activates its transforming activity in a human leiomyosarcoma cell line. Oncogene *11*, 1255–1260.
33. Drivas, G.T., Shih, A., Coutavas, E., Rush, M.G., and D'Eustachio, P. (1990). Characterization of four novel ras-like genes expressed in a human teratocarcinoma cell line. Mol. Cell. Biol. *10*, 1793–1798.
34. Bos, J.L. (1997). Ras-like GTPases. Biochim. Biophys. Acta *1333*, M19–M31.
35. Nakhaei-Rad, S., Haghighi, F., Nouri, P., Rezaei Adariani, S., Lissy, J., Kazemein Jasemi, N.S., Dvorsky, R., and Ahmadian, M.R. (2018). Structural fingerprints, interactions, and

signaling networks of RAS family proteins beyond RAS isoforms. Crit. Rev. Biochem. Mol. Biol. *53*, 130–156.

36. Graham, S.M., Oldham, S.M., Martin, C.B., Drugan, J.K., Zohn, I.E., Campbell, S., and Der, C.J. (1999). TC21 and Ras share indistinguishable transforming and differentiating activities. Oncogene *18*, 2107–2116.
37. Erdogan, M., Pozzi, A., Bhowmick, N., Moses, H.L., and Zent, R. (2007). Signaling pathways regulating TC21-induced tumorigenesis. J. Biol. Chem. *282*, 27713–27720.
38. Stieglitz, E., Taylor-Weiner, A.N., Chang, T.Y., Gelston, L.C., Wang, Y.-D., Mazor, T., Esquivel, E., Yu, A., Seepo, S., Olsen, S., et al. (2015). The genomic landscape of juvenile myelomonocytic leukemia. Nat. Genet. *47*, 1326–1333.
39. Vetter, I.R., and Wittinghofer, A. (2001). The guanine nucleotide-binding switch in three dimensions. Science *294*, 1299–1304.
40. Klockow, B., Ahmadian, M.R., Block, C., and Wittinghofer, A. (2000). Oncogenic insertional mutations in the P-loop of Ras are overactive in MAP kinase signaling. Oncogene *19*, 5367–5376.
41. Larive, R.M., Moriggi, G., Menacho-Márquez, M., Cañamero, M., de Álava, E., Alarcón, B., Dosil, M., and Bustelo, X.R. (2014). Contribution of the R-Ras2 GTP-binding protein to primary breast tumorigenesis and late-stage metastatic disease. Nat. Commun. *5*, 3881.
42. Larive, R.M., Abad, A., Cardaba, C.M., Hernández, T., Cañamero, M., de Álava, E., Santos, E., Alarcón, B., and Bustelo, X.R. (2012). The Ras-like protein R-Ras2/TC21 is important for proper mammary gland development. Mol. Biol. Cell *23*, 2373–2387.
43. Hancock, J.F. (2003). Ras proteins: different signals from different locations. Nat. Rev. Mol. Cell Biol. *4*, 373–384.
44. Gremer, L., Merbitz-Zahradnik, T., Dvorsky, R., Cirstea, I.C., Kratz, C.P., Zenker, M., Wittinghofer, A., and Ahmadian, M.R. (2011). Germline KRAS mutations cause aberrant biochemical and physical properties leading to developmental disorders. Hum. Mutat. *32*, 33–43.
45. Ceremsak, J.J., Yu, A., Esquivel, E., Lissewski, C., Zenker, M., Loh, M.L., and Stieglitz, E. (2016). Germline *RRAS2* mutations are not associated with Noonan syndrome. J. Med. Genet. *53*, 728.
46. Quélin, C., Loget, P., Rozel, C., D'Hervé, D., Fradin, M., Demurger, F., Odent, S., Pasquier, L., Cavé, H., and Marcorelles, P. (2017). Fetal costello syndrome with neuromuscular spindles excess and p.Gly12Val HRAS mutation. Eur. J. Med. Genet. *60*, 395–398.
47. Carta, C., Pantaleoni, F., Bocchinfuso, G., Stella, L., Vasta, I., Sarkozy, A., Digilio, C., Palleschi, A., Pizzuti, A., Grammatico, P., et al. (2006). Germline missense mutations affecting KRAS Isoform B are associated with a severe Noonan syndrome phenotype. Am. J. Hum. Genet. *79*, 129–135.
48. Gripp, K.W., Hopkins, E., Sol-Church, K., Stabley, D.L., Axelrad, M.E., Doyle, D., Dobyns, W.B., Hudson, C., Johnson, J., Tenconi, R., et al. (2011). Phenotypic analysis of individuals with Costello syndrome due to HRAS p.G13C. Am. J. Med. Genet. A. *155A*, 706–716.
49. Gripp, K.W., Sol-Church, K., Smpokou, P., Graham, G.E., Stevenson, D.A., Hanson, H., Viskochil, D.H., Baker, L.C., Russo, B., Gardner, N., et al. (2015). An attenuated phenotype of Costello syndrome in three unrelated individuals with a *HRAS* c.179G>A (p.Gly60Asp) mutation correlates with uncommon functional consequences. Am. J. Med. Genet. A. *167A*, 2085–2097.
50. Bertola, D., Buscarilli, M., Stabley, D.L., Baker, L., Doyle, D., Bartholomew, D.W., Sol-Church, K., and Gripp, K.W. (2017). Phenotypic spectrum of Costello syndrome individuals harboring the rare *HRAS* mutation p.Gly13Asp. Am. J. Med. Genet. A. *173*, 1309–1318.
51. Pantaleoni, F., Lev, D., Cirstea, I.C., Motta, M., Lepri, F.R., Bottero, L., Cecchetti, S., Linger, I., Paolacci, S., Flex, E., et al. (2017). Aberrant HRAS transcript processing underlies a distinctive phenotype within the RASopathy clinical spectrum. Hum. Mutat. *38*, 798–804.
52. Altmüller, F., Lissewski, C., Bertola, D., Flex, E., Stark, Z., Spranger, S., Baynam, G., Buscarilli, M., Dyack, S., Gillis, J., et al. (2017). Genotype and phenotype spectrum of NRAS germline variants. Eur. J. Hum. Genet. *25*, 823–831.
53. Stark, Z., Gillessen-Kaesbach, G., Ryan, M.M., Cirstea, I.C., Gremer, L., Ahmadian, M.R., Savarirayan, R., and Zenker, M. (2012). Two novel germline KRAS mutations: expanding the molecular and clinical phenotype. Clin. Genet. *81*, 590–594.
54. Nussinov, R., Zhang, M., Tsai, C.J., Liao, T.J., Fushman, D., and Jang, H. (2018). Autoinhibition in Ras effectors Raf, PI3Kα, and RASSF5: a comprehensive review underscoring the challenges in pharmacological intervention. Biophys. Rev. *10*, 1263–1282.
55. Graham, S.M., Cox, A.D., Drivas, G., Rush, M.G., D'Eustachio, P., and Der, C.J. (1994). Aberrant function of the Ras-related protein TC21/R-Ras2 triggers malignant transformation. Mol. Cell. Biol. *14*, 4108–4115.
56. Niihori, T., Nagai, K., Fujita, A., Ohashi, H., Okamoto, N., Okada, S., Harada, A., Kihara, H., Arbogast, T., Funayama, R., et al. (2019). Germline activating *RRAS2* mutations cause Noonan syndrome. Am. J. Hum. Genet. *104*, this issue, 1233–1240.

Chapter IV

Novel FMRP interaction networks linked to *cellular* stress

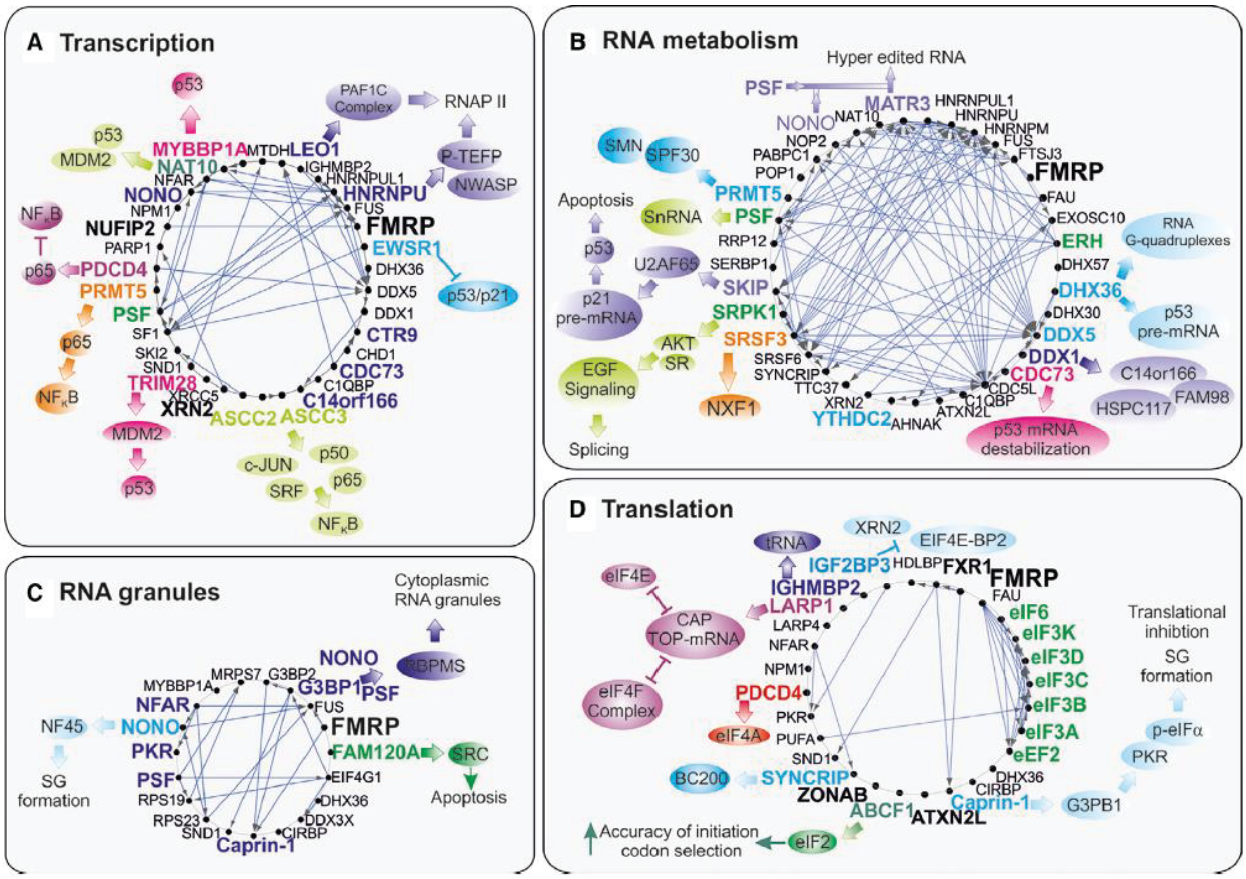

Published in:	FEBS journal
Impact factor:	4.739 (2020)
Own Proportion to this work:	15%
	Prurification of G3BP1 protein and the analysis of its Interaction with FMRP using pulldown assay and immunoprecipitation, writing the manuscript

The FEBS Journal

FEBS PRESS science publishing by scientists

Novel FMRP interaction networks linked to cellular stress

Mohamed S. Taha[1,2], Fereshteh Haghighi[1,*], Anja Stefanski[3], Saeideh Nakhaei-Rad[1,†], Neda S. Kazemein Jasemi[1], Mohamed Aghyad Al Kabbani[1], Boris Görg[4], Masahiro Fujii[5], Phillip A. Lang[6], Dieter Häussinger[4], Roland P. Piekorz[1], Kai Stühler[3] and Mohammad R. Ahmadian[1]

1 Institute of Biochemistry and Molecular Biology II, Medical Faculty of the Heinrich Heine University, Düsseldorf, Germany
2 Research on Children with Special Needs Department, Medical Research Branch, National Research Centre, Cairo, Egypt
3 Molecular Proteomics Laboratory, Heinrich Heine-University, Düsseldorf, Germany
4 Clinic of Gastroenterology, Hepatology and Infectious Diseases, Medical Faculty of the Heinrich Heine-University, Düsseldorf, Germany
5 Division of Virology, Niigata University Graduate School of Medical and Dental Sciences, Niigata, Japan
6 Department of Molecular Medicine II, Medical Faculty, Heinrich Heine-University, Düsseldorf, Germany

Keywords
FMRP; fragile X mental retardation protein; protein interaction network; RNA-binding; stress granule

Correspondence
M. R. Ahmadian, Institute of Biochemistry and Molecular Biology II, Medical Faculty of the Heinrich Heine University, Universitätsstrasse 1, Building 22.03.06, 40255 Düsseldorf, Germany
Tel: +49 (0)211 81 12384
E-mail: reza.ahmadian@hhu.de

Present address
*Department of Thoracic and Cardiovascular Surgery, University Medical Center Göttingen, Göttingen, Germany
†Stem Cell Biology and Regenerative Medicine Research Group, Institute of Biotechnology, Ferdowsi University of Mashhad, Mashhad, Iran

Mohamed S. Taha and Fereshteh Haghighi contributed equally to this work

(Received 30 September 2019, revised 9 April 2020, accepted 3 June 2020)

doi:10.1111/febs.15443

Silencing of the fragile X mental retardation 1 (*FMR1*) gene and consequently lack of synthesis of FMR protein (FMRP) are associated with fragile X syndrome, which is one of the most prevalent inherited intellectual disabilities, with additional roles in increased viral infection, liver disease, and reduced cancer risk. FMRP plays critical roles in chromatin dynamics, RNA binding, mRNA transport, and mRNA translation. However, the underlying molecular mechanisms, including the (sub)cellular FMRP protein networks, remain elusive. Here, we employed affinity pull-down and quantitative LC-MS/MS analyses with FMRP. We identified known and novel candidate FMRP-binding proteins as well as protein complexes. FMRP interacted with 180 proteins, 28 of which interacted with its N terminus. Interaction with the C terminus of FMRP was observed for 102 proteins, and 48 proteins interacted with both termini. This FMRP interactome comprises known FMRP-binding proteins, including the ribosomal proteins FXR1P, NUFIP2, Caprin-1, and numerous novel FMRP candidate interacting proteins that localize to different subcellular compartments, including CARF, LARP1, LEO1, NOG2, G3BP1, NONO, NPM1, SKIP, SND1, SQSTM1, and TRIM28. Our data considerably expand the protein and RNA interaction networks of FMRP, which thereby suggest that, in addition to its known functions, FMRP participates in transcription, RNA metabolism, ribonucleoprotein stress granule formation, translation, DNA damage response, chromatin dynamics, cell cycle regulation, ribosome biogenesis, miRNA biogenesis, and mitochondrial organization. Thus, FMRP seems associated with multiple cellular processes both under normal and cell stress conditions in neuronal as well as non-neuronal cell types, as exemplified by its role in the formation of stress granules.

Abbreviations
CNS, central nervous system; DDR, DNA damage response; DSBs, DNA double-strand breaks; FMRP, fragile X mental retardation protein; FXR1P, fragile X mental retardation syndrome-related protein 1; FXS, fragile X syndrome; G3BP1, RAS GTPase-activating protein SH3 domain-binding protein 1; HDF, human dermal fibroblast; iPSC, induced pluripotent stem cells; KH0, K homology 0 domain; ncRNA, noncoding RNA; NES, nuclear export signal; NLS, nuclear localization signal; NoLS, nucleolar localization signal; NPM1, nucleophosmin; PKR, protein kinase R; RBP, RNA-binding protein; RGG, arginine–glycine–glycine-rich; RNP, ribonucleoprotein; SGs, stress granules; snRNP, small nuclear RNP; Tud, tudor domain.

Introduction

Genetic deficiency of the fragile X mental retardation protein (FMRP; also known as FRAXA, MGC87458, POF, and POF1) results in the most common inherited form of intellectual disability, fragile X syndrome (FXS; also known as Escalante's syndrome or Martin–Bell syndrome) [1]. FMRP plays critical roles in germline development during oogenesis [2], spermatogenesis [3], regulation of heart rate during development [4], endothelial cell proliferation, angiogenesis [5], stem cell maintenance, differentiation [6], and tumor progression. FXS patients seem to have a lower risk of developing cancer [7]. In view of these numerous and different, seemingly fundamental functions, it is appropriate to appreciate common roles of FMRP throughout the body, that is, beyond the brain and spinal cord. However, how FMRP functions are linked to these cellular processes and outputs in different cellular contexts remains as an open question.

FMRP is a well-studied RNA-binding protein (RBP) that regulates local translation [8–14] and is involved in the control of calcium channels [15], actin cytoskeletal dynamics [16–18], chromatin dynamics [19], DNA damage response (DDR) [19,20], and replication stress response [21]. These cellular functions presume physical properties for FMRP, which are required for both the recognition and localization of messenger RNA (mRNA) targets and direct association with a multitude of proteins moreover protein complexes [22,23]. FMRP consists of an N-terminal domain comprising two Tudor (Tud) domains, and one K homology 0 (KH0) domain, a central region comprising two KH1 and KH2 domains, while a C-terminal domain comprising a phosphorylation site [24] in addition to an arginine–glycine–glycine (RGG) region [25]. FMRP displays a nuclear localization signal (NLS), a nuclear export signal (NES), and two nucleolar localization signals (NoLSs) [23,26–29], consequently localizing FMRP to different subcellular compartments in the cytosol and nucleus [23]. Nuclear FMRP has been suggested to regulate the DDR and genomic stability as a chromatin-binding protein [19].

The most prominent and studied function of FMRP is translational regulation. Moreover, FMRP is a member of the FXR protein family that includes fragile X-related protein 1 (FXR1P) and fragile X-related protein 2 (FXR2P). They share high sequence conservation with their N-terminal and central regions, as well as form heteromeric complexes [30–33]. All three FMRP family members are RNA-binding proteins that regulate translation of their cargo mRNAs and associate physically also functionally with the microRNA pathway [34]. FMRP has been shown to suppress the translation of its target mRNAs via association with either stalled nontranslating polyribosomes or microRNA [35–38]. This can lead to the formation of cytoplasmic ribonucleoprotein (RNP) granules, which control the expression, repression, or decay of specific mRNAs [39]. There are many types of cytoplasmic RNA granules, which differ markedly in size, composition, and mode of biogenesis [40]. Some granules, such as processing bodies (P-bodies) and stress granules (SGs), which are assembled by many cell types, transport, store, or degrade mRNAs, thereby indirectly regulating protein synthesis [39,41–43]. Accordingly, they contribute to various aspects of cellular homeostasis. There is increasing evidence suggesting that such RNP granules are associated with several age-related neurodegenerative diseases [44]. However, the molecular networks that regulate and guide FMRP toward these cellular processes need further investigations.

We hypothesize that FMRP is involved in numerous cellular functions in various subcellular compartments. Therefore, in this study, we addressed novel FMRP-interacting proteins using a proteomic approach. We described known and numerous novel potential FMRP interactors and networks that are involved in diverse subcellular processes, in both neuronal and non-neuronal cells.

Results

Ubiquitous expression of FMRP in human cells

In a previous study, we observed large amounts of FMRP in different cell lines, that is, COS7, HEK293, HeLa, MDCKII, MEF, and NIH3T3 [23]. To examine the existence of FMRP in various types of non-neuronal human cells, we investigated different types of cells. As depicted in Fig. 1A, FMRP was expressed in many types of non-neuronal cells, consistent with findings in thrombocytes [45] and human embryonic stem cells [46]. Mouse brain lysate was used as neuronal tissue control. This suggests that FMRP likely represents a protein with important and conserved functions across human tissues.

Identification of novel FMRP-interacting proteins

To identify proteins associated with different regions of FMRP in a proteomic approach, we used HeLa cells as a cellular model. We conducted affinity pull-down experiments using total HeLa cell lysates and

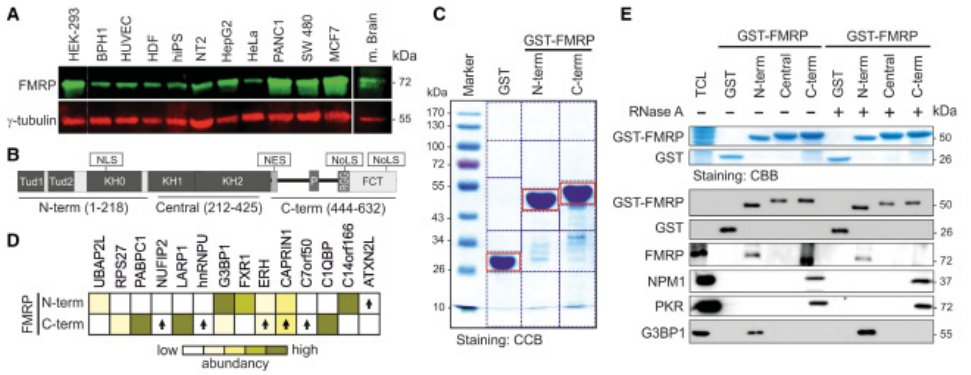

Fig. 1. FMRP protein interaction networks linked to the N- and C-terminal regions of FMRP. (A) Immunoblot analysis depicting the expression pattern of FMRP in different human cell lines, including epithelial HEK293 cells, benign prostatic hyperplasia epithelial cell line (BPH1), primary endothelial HUVECs, human dermal fibroblasts (HDF), human induced pluripotent stem cells (hiPSCs), embryonal carcinoma cells (NT2), and cancerous cell lines from different tissues (HeLa, HepG2, MCF7, PANC1, and SW480), and total mouse brain lysate as neuronal tissue control ($n = 3$). γ-Tubulin served as loading controls. All lysates were adjusted to 50 $\mu g \cdot \mu L^{-1}$, and 20 μg of each lysate was used for immunoblotting. Dashed lines indicate that one lane has been removed. (B) Schematic diagram highlighting major domains and motifs of FMRP. FCT, FMRP C terminus; KH0, KH1, and KH2, tandem K homology domain (first described for hnRNPK); NES, nuclear export signal; NLS, nuclear localization signal; NoLS, nucleolar localization signal; RGG, arginine–glycine–glycine region; P, phosphorylation sites; Tud1 and Tud2, tandem tudor domains. The FMRP fragments used in this study are the N-terminal (N-term), the central, and the C-terminal (C-term) fragments. (C) Proteins from total HeLa cell lysates were affinity-purified using GST or GST-FMRP beads and analyzed by SDS/PAGE. Blue boxes indicate gel fragments excised for mass spectrometric (MS) analysis. Red boxes indicate GST, GST-$FMRP^{N\text{-}term}$, and GST-$FMRP^{C\text{-}term}$, which were excluded from MS analysis. Samples from three independent experiments were used for MS analysis. (D) Proteins identified to bind to both N- and C-terminal domains of FMRP (Table 3) revealed different abundances, which were determined based on the normalized values of the label-free quantification intensity values. The abundance is sorted from 'high or 1' to 'low or 0' based on color codes. The arrows are indicators for slightly higher levels of the proteins with the same color codes. (E) Immunoblot analysis of newly identified FMRP-interacting proteins. GST pull-down experiments were conducted by mixing purified GST fusion proteins of $FMRP^{N\text{-}term}$, $FMRP^{central}$, and $FMRP^{C\text{-}term}$ as well as GST (negative control) immobilized on GSH agarose beads with total cell lysates (TCL) from HeLa cells in the presence (+) and in the absence (–) of RNase A ($n = 2$). Proteins retained on the beads were resolved by CBB-stained SDS/PAGE (upper panel) and processed for western blotting using monoclonal antibodies against GST and various FMRP-interacting proteins (lower panels).

purified GST fusion protein fragments consisting of the N-terminal (N-term: aa 1–218), central (aa 212–425), and C-terminal (C-term: aa 444–632) domains of human FMRP (Fig. 1B).

Since most FMRP protein–protein interactions were exclusively achieved via the N or C termini and rarely via the central RNA-binding fragments [47–50], we excluded the latter from further analysis. Pull-down samples were separated on SDS gels, which were cut in different fractions, excluding the bands related to GST-$FMRP^{N\text{-}term}$, GST-$FMRP^{C\text{-}term}$, and the GST control (Fig. 1C, red boxes). The gel fractions were reduced, alkylated, and digested with trypsin. The resulting peptide mixtures were analyzed by mass spectrometry as described in the Materials and methods.

All proteins interacting with GST-$FMRP^{N\text{-}term}$ and/or GST-$FMRP^{C\text{-}term}$ were detected, individually validated with a high degree of confidence based on the peptide sequences using specific databases and programs as described in the Materials and methods. The criteria for considering proteins as significant interactors of FMRP included their presence in all three independent pull-down experiments, their absence in the GST pull-down controls, and P-values of < 0.05.

Collectively, we short-listed a set of 102 FMRP-interacting proteins, 22 of which were associated with $FMRP^{N\text{-}term}$, 67 were associated with $FMRP^{C\text{-}term}$, and 13 were found to bind to both termini (Tables 1–3). Table 4 summarizes 78 isoforms and paralogs, including the array of ribosomal proteins that were excluded from the major lists of binding partners. In our proteomic approach, we found nine previously reported FMRP interactors, that is, ATXN2L, Caprin-1, DDX5, FMRP, FXR1P, MOV10, NUFIP2, PABP1, and PARP1 [22,38,51–53]. Known FMRP-interacting partners, such as nucleolin and CYFIP [23],

Table 1. Proteins interacting with the N terminus of FMRP ($FMRP^{N\text{-}term}$). Underlined proteins were previously described as direct or indirect interacting partners of FMRP. Proteins highlighted in bold are RNA-binding proteins, and proteins in italic are components of the SGs. Some proteins have more than one name (http://www.genecards.org), and some alternative names or synonyms are therefore included in parentheses.

Protein name	Function	MW, kDa	*P*-value	Unique pep	Seq. cove-rage (%)	Acc. ID
Actin-depolymerizing factor (ADF, Destrin)	Actin dynamics	18.5	0.005	3	22.4	P60981
AHNAK nucleoprotein 2 (AHNAK2)*	Calcium signaling	616.2	0.004	66	34	Q8IVF2
Anterior gradient protein 2 homolog (AGR2, AG2)	Differentiation	20.0	0.016	3	20	O95994
Cold-inducible RNA-binding protein (CIRBP, A18hnRNP)	mRNA stabilization, translation, SGs	18.6	0.009	6	37.8	Q14011
Collaborator of ARF (CARF, CDKN2AIP)	DDR, cell growth	61.1	0.004	7	21.9	Q9NXV6
DEAD box protein 5 (DDX5, p68) *	Transcription, mRNA processing	69.1	0.005	20	47.6	P17844
DEAH box protein 36 (DHX36, RHAU) *	Transcription, mRNA processing, translation, SGs	114.7	0.003	9	11.4	Q9H2U1
Eukaryotic translation initiation factor 3 subunit K (eIF3K)	Translation	25.043	0.020	7	38.5	Q9UBQ5
Ewing sarcoma breakpoint region 1 protein (EWSR1)	Transcription	68.4	0.003	4	10.3	Q01844
Fragile X mental retardation protein (FMRP, FRAXA, POF1)	DDR, transcription, RNA processing, transport, translation, SGs	71.1	0.007	42	54	Q06787
Fused in sarcoma (FUS, TLS)	mRNA splicing, transcription	53.4	0.001	2	26.6	P35637
MAP7 domain-containing protein 2 (MAP7D2)	Microtubule cytoskeleton organization	82.0	0.007	3	6.9	Q96T17
Melanoma inhibitory activity protein 3 (MIA3, TANGO)	Transport, ER-Golgi transport, exocytosis	213.6	0.001	24	16.5	Q5JRA6
Non-POU domain-containing octamer-binding protein (NONO)	DDR, transcription, mRNA splicing, RNA granule, innate immune response	54.2	0.007	9	27.8	Q15233
Polypyrimidine tract-binding protein-associated splicing factor (SFPQ, PSF)*	DDR, transcription, mRNA splicing, RNA granules, innate immune response	76.1	0.002	2	19.6	P23246
Protein FAM98A	Lysosome localization, proliferation	55.4	0.005	7	20.4	Q8NCA5
Protein LSM12 homolog (LSM12)	Posttranscriptional regulation, circadian clocks	21.7	0.006	5	33.5	Q3MHD2
Ski-interacting protein (SKIP, SNW1)	mRNA processing, splicing, apoptotic pathway	61.5	0.002	4	9.6	Q13573
Transketolase (TKT)	Pentose phosphate pathway, growth regulation	67.9	0.019	9	26.6	P29401
Tropomyosin-receptor kinase-fused gene protein (TFG)	Protein transport, secretory pathways	43.4	0.011	12	41.5	Q92734
40S ribosomal protein S23 (RPS23)*	Translation, SGs	15.8	0.003	8	49.7	P62266
60S ribosomal protein L36 (RPL36)*	Translation	12.2	0.000	5	30.5	Q9Y3U8

*Paralogs or related proteins identified are listed in Table 4.

were excluded in this study as they were also present in the GST pull-down controls. Other FMRP-interacting proteins, including EIF4E [54], AGO1 [55], and β-catenin [56], were absent in our lists, which may be based on expression levels in different cell types and/or on experimental pull-down conditions.

A group of 13 proteins was found to be associated with both N-terminal and C-terminal fragments of FMRP (Table 3). One obvious explanation is that FMRP may interact with two proteins within the same protein complex. In this case, components of a protein complex that do not directly bind to FMRP will be pulled down. For these candidates, we calculated the values of the exponentially modified protein abundance index (emPAI) [57] by comparing the number of identified MS/MS spectra from the same protein in each of the multiple LC-MS/MS datasets. Therefore, the term 'abundance' was used to suggest one possible interacting domain. Based on the label-free quantification intensity value, we measured the abundance of each candidate in the $FMRP^{N\text{-}term}$ and $FMRP^{C\text{-}term}$ pull-down experiments (Fig. 1D). As exemplified for

Table 2. Proteins interacting with the C terminus of FMRP ($FMRP^{C\text{-}term}$). Underlined proteins were previously described as direct or indirect interacting partners of FMRP. Proteins highlighted in bold are RNA-binding proteins, and proteins in italic are components of the SGs. Some proteins have more than one name (http://www.genecards.org), and some alternative names or synonyms are therefore included in parentheses.

Protein name	Function	MW, kDa	*P*-value	Unique pep	Seq. cove-rage (%)	Acc. ID
Activating signal cointegrator 1 complex 2 subunit 2 (ASCC2)*	Transcription	86.3	0.001	7	12.5	Q9H1I8
ATPase family AAA domain-containing protein 3A (ATAD3A)*	Cell growth, apoptosis	71.3	0.010	8	13.7	Q9NVI7
ATP-binding cassette subfamily F member 1 (ABCF1)	Translation, transport	96.0	0.002	10	12.8	Q8NE71
Bcl-2-associated transcription factor 1 (BCLAF1, BTF)	DDR, transcription, apoptosis	106.1	0.000	7	10.4	Q9NYF8
Cell division cycle 5-like protein (CDC5L)	DDR, cell cycle, mRNA splicing, differentiation	92.2	0.003	11	21.3	Q99459
Cell division cycle protein 73 (CDC73, parafibromin)	Transcription, mRNA processing, apoptosis	60.5	0.019	16	29.9	Q6P1J9
Chromo-domain helicase DNA-binding protein 1 (CHD1)	Chromatin remodeling, DDR, transcription	196.6	0.007	6	5.8	O14646
Elongation factor 2 (eEF2)	Translation	95.3	0.020	27	43.1	P13639
Eukaryotic translation initiation factor 4 gamma 1 (EIF4G1)*	Translation, SGs, mitochondrial organization, autophagy cell death, cell growth	175.4	0.001	19	15.5	Q04637
Eukaryotic translation initiation factor 6 (eIF6, p27BBP)*	Ribosome biogenesis, transport, translation	26.6	0.000	7	52.2	P56537
Exosome component 10 (EXOSC10, RRP6)	RNA processing	100.8	0.005	8	10.8	Q01780
Glypican-1 (GPC1)	Endosome localization, differentiation	61.7	0.006	9	21	P35052
Helicase-like protein (HLP, Ski2, SKIV2L)	Transcription, ribosome biogenesis	137.7	0.000	10	10.9	Q15477
Immunoglobulin mu binding protein 2 (IGHMBP2, SMUBP2)	Transcription, translation	109.1	0.008	4	6.2	P38935
Insulin-like growth factor 2 mRNA-binding protein 3 (IGF2BP3)	mRNA transport, translation	63.7	0.003	12	27.5	O00425
Karyopherin subunit α2 (KPNA2, SRP1-α)	Nuclear import	57.8	0.006	7	22.1	P52292
Large subunit GTPase 1 homolog GTPase 1 (hLSG1)	Ribosome biogenesis, transport	75.2	0.017	9	19.1	Q9H089
Long-chain 3 hydroxyacyl-CoA dehydrogenase (HADHA)	RNA silencing, miRNA biogenesis	83.0	0.002	24	42.5	P40939
Matrin-3 (MATR3)	Innate immune response	94.6	0.006	5	8.9	P43243
Metadherin (MTDH, AEG1, LYRIC)	Transcription, NFκB pathway	63.8	0.001	5	10.8	Q86UE4
Mitochondrial ribosomal protein S28 (MRP-S28, S28mt)*	Mitochondrial translation	20.8	0.000	6	33.7	Q9Y2Q9
Myb-binding protein 1A (MYBBP1A, p160)	Transcription, stress response, cell cycle	148.8	0.005	9	8.7	Q9BQG0
N-acetyltransferase 10 (NAT10, ALP)	RNA processing	115.7	0.000	8	10.9	Q9H0A0
Nuclear factors associated with dsRNA (NFAR, NF90, ILF3)	Transcription, translation, antiviral response	95.3	0.001	9	11.8	Q12906
Nucleolar GTP-binding protein 2 (GNL2, NOG2)*	Ribosome biogenesis	83.6	0.001	6	10.8	Q13823
Nucleolar protein 2 homolog (NOP2, NOL1, NSUN6)	RNA processing, ribosome biogenesis	89.2	0.001	7	10.9	P46087
Nucleophosmin (NPM1, B23, Numartin)	Ribosome assembly, biogenesis, mRNA stability, translation, transcription	32.6	0.010	8	44.2	P06748
Oxidative stress-associated Src activator (FAM120A, C9orf10)	Oxidative stress	121.8	0.000	10	12.4	Q9NZB2
Poly [ADP-ribose] polymerase 1 (PARP1, ADPRT1)	DDR, transcription, mitochondrial organization	113.0	0.001	18	24.4	P09874

Table 2. (Continued).

Protein name	Function	MW, kDa	*P*-value	Unique pep	Seq. cove-rage (%)	Acc. ID
Pre-rRNA-processing protein (TSR1)	Ribosome biogenesis, RNA processing	91.8	0.008	8	13.2	Q2NL82
Programmed cell death protein 4 (PDCD4, H731)	Transcription, cell cycle, apoptosis	51.7	0.002	9	24.3	Q53EL6
Protein arginine N-methyltransferase 5 (PRMT5, JBP1, SKB1)	Transcription, spliceosome assembly	72.6	0.010	9	20.6	O14744
Protein FtsJ homolog 3 (FTSJ3, SB92)	RNA processing, ribosome biogenesis	96.6	0.000	6	9.7	Q8IY81
Protein kinase RNA-activated (PKR, EIF2AK2)	Transcription, mRNA processing, translation	62.1	0.019	11	21.6	P19525
Protein LTV1 homolog (LTV1)	RNA processing, 40S ribosome biogenesis	54.8	0.005	5	11.4	Q96GA3
Protein PRRC2C	Translation, differentiation	316.7	0.002	15	6.8	Q9Y520
Pumilio homolog 3 (PUFA)	Translation	73.5	0.013	8	16.5	Q15397
Putative helicase MOV-10 (MOV10)	Transcription, miRNA biogenesis, RNA interference, RNA granules	113.6	0.005	5	7.3	Q9HCE1
Ribonuclease P/MRP protein subunit (POP1)	RNA processing	114.6	0.002	9	11.8	Q99575
RNA polymerase-associated protein (LEO1)	Transcription, RNA metabolism	75.4	0.001	6	10.5	Q8WVC0
RNA polymerase-associated protein CTR9 homologous (CTR9)	Transcription	133.4	0.011	9	7.3	Q6PD62
RRP12-like protein (RRP12)	rRNA processing, ribosome biogenesis	143.6	0.003	7	8.1	Q5JTH9
SDA1 domain-containing protein 1 (SDAD1, hSDA)	Ribosome biogenesis, transport, actin cytoskeleton organization	79.8	0.013	3	4.7	Q9NVU7
Sequestosome-1 (SQSTM1, p62)	Mitophagy, stress response, differentiation	47.7	0.011	8	31.8	Q13501
Serine/arginine-rich protein-specific kinase 1 (SRPK1)	RNA splicing, chromosome segregation	74.3	0.000	4	9.4	Q96SB4
Serine/arginine-rich splicing factor 3 (SRSF3, SRP20) *	RNA splicing, transport	19.3	0.000	7	42.7	P84103
SERPINE1 mRNA-binding protein 1 (SERBP1, PAIRBP1)	mRNA stability, apoptosis	44.9	0.012	13	33.6	Q8NC51
Single-stranded DNA-binding protein (SSBP1, SOSS)	Replication, mitochondrion organization	17.2	0.006	5	33.8	Q04837
Staphylococcal nuclease domain-containing protein 1 (SND1, TDRD11)	Transcription, RNA interference, SGs	101.9	0.010	11	18.7	Q7KZF4
Synaptotagmin-binding cytoplasmic RNA-interacting protein (SYNCRIP, hnRNPQ) *	RNA processing, splicing, translation	69.6	0.005	11	26.9	O60506
Targeting protein for Xklp2 (TPX2, DIL-2)	Microtubule organization, cell cycle, apoptosis	85.6	0.020	12	20.2	Q9ULW0
Tetratricopeptide repeat protein 37 (TTC37, Ski3)	RNA processing	175.4	0.000	16	13	Q6PGP7
Transcription intermediary factor 1β (TRIM28, KAP1)	DDR, transcription	88.5	0.003	6	11.7	Q13263
Transglutaminase-3 TGase-3 (TGM3, TGE)	Proliferation, migration, NF-κB pathway	76.6	0.010	3	7.5	Q08188
Ubiquitin carboxyl-terminal hydrolase 10 (USP10)	DDR, autophagy	87.1	0.003	6	9.8	Q14694
Unconventional myosin-IC (MYO1C, MMIb)	Cytoskeletal rearrangements, motility	121.6	0.012	5	7.1	O00159
Valosin-containing protein (VCP)	DDR, lysosome transport, autophagy	89.3	0.019	5	9.4	P55072
Vigilin (VGL, HDLBP)	Lipid transport	141.4	0.001	9	10.2	Q00341
X-ray repair cross-complementing protein 6 (XRCC6, Ku70) *	DDR, transcription, innate immune response	69.8	0.001	38	61.7	P12956
Y-box-binding protein 3 (YBX3, CSDA, ZONAB)	Transcription, translation, RNA binding	40.1	0.006	7	47	P16989
YTH domain-containing 2 (YTHDC2)	RNA processing	160.1	0.005	5	4.9	Q9H6S0

Table 2. (Continued).

Protein name	Function	MW, kDa	*P*-value	Unique pep	Seq. cove-rage (%)	Acc. ID
Zinc finger CCCH-type antiviral protein 1 (ZC3HAV1, ZAP)	Innate immune response	101.4	0.003	5	8.7	Q7Z2W4
Zinc finger protein 622 (ZNF622, ZPR9)	Ribosome biogenesis, apoptosis	54.2	0.007	11	30	Q969S3
40S ribosomal protein S19 (RPS19)*	Ribosome biogenesis, translation	16.1	0.011	12	26	P39019
40S ribosomal protein S30 (FAU)	RNA processing, translation, apoptosis	6.6	0.002	3	12.2	P62861
5′–3′ exoribonuclease 2 (XRN2)	Transcription, RNA processing	108.5	0.007	5	8	Q9H0D6
60S ribosomal protein L6 (RPL6, TXREB1)*	RNA processing, ribosome assembly, translation	32.7	0.004	1	49.7	Q02878

*Paralogs or related proteins identified are listed in Table 4.

C16orf166, C1QBP, and PABP1, some FMRP-interacting proteins were clearly more capable of interacting with one FMRP terminus than the other, while other interacting partners (e.g., Caprin-1 and NUFIP2) were found at nearly the same protein levels in both $FMRP^{N\text{-}term}$ and $FMRP^{C\text{-}term}$ pull-down experiments (Fig. 1D, arrows). In that case, the arrows were used to indicate slightly higher levels of these proteins with the same color codes. This differentiation method was prominent for some proteins, for example, the highly abundant protein G3BP1, which was shown by immunoblotting analysis to interact only with $FMRP^{N\text{-}term}$ (Fig. 1E).

Another critical aspect is the oligomerization properties of FMRP through its N terminus [29]. In this scenario, GST-$FMRP^{N\text{-}term}$ binds endogenous, oligomeric FMRP and, in this way, proteins interacting with its C terminus. Moreover, FXR1P and FXR2P are structural and functional paralogs of FMRP that undergo heterotypic interactions with FMRP [32]. Accordingly, we found FXR1P in our analysis associated with GST-$FMRP^{N\text{-}term}$. FXR1P and FXR2P have been shown to increase the connectivity of FMRP with a large number of proteins among them also ATXN2L, Caprin-1, EIF3A, EWSR1, NONO, and SFPQ [31], which were also detected in our study.

Interestingly, the vast majority of interactions involve the C terminus of FMRP (Table 2) and not its N terminus, as we and others previously proposed [23,48]. A striking characteristic of $FMRP^{C\text{-}term}$ is the presence of unstructured regions, including arginine–glycine–glycine-rich (RGG) motifs, phosphorylation sites, a nuclear export signal (NES), and two newly identified NoLSs [23,58]. It has also been reported that many FMRP-binding proteins contain RGG motifs [59], which may interact not only with proteins but also with RNAs [59–61]. A large number of the identified FMRP interaction partners were RNA-binding proteins, processing, and/or transporting proteins, including components of the translation machinery, different helicases, and transcription factors (Tables 1–4; highlighted in bold). Thus, we tested three different FMRP-interacting proteins such as nucleophosmin-1 (NPM1), protein kinase R (PKR), and RAS GTPase-activating protein SH3 domain-binding protein 1 (G3BP1) for their RNA dependency on interacting with purified FMRP in the presence and absence of RNase A. As shown in Fig. 1E, FMRP interacts with endogenous FMRP and G3BP1 via its N-terminal region, while it interacts with NPM1 as well as PKR via its C-terminal region. None of these interactors bind to the central region of FMRP. RNase A treatment of the lysates for 45 min at 4 °C did not affect the interaction of $FMRP^{C\text{-}term}$ with NPM1 and PKR. In contrast, G3BP1 binding to $FMRP^{N\text{-}term}$ appears to be facilitated.

Functional categorization of the FMRP interactome

The FMRP-interacting proteins identified in this study were classified into three ontologies: biological process, molecular function, and subcellular component (Fig. 2). These functions imply an intracellular shuttling of FMRP into/between different subcellular compartments of the cell. FMRP has been previously described to be predominantly cytoplasmic [62].

Biological processes

FMRP-interacting RNA helicases comprise DDX5, DHX9, and CHD1 (which are involved in the DNA damage response) as well as DDX1, DDX3X, DHX15, DDX17, DHX36, IGHMBP2, MOV10, HLP/SKI2, YTHDC2, and YBX3 (Fig. 3B). The FMRP-associated proteins AGR2 and ATAD3A are

Table 3. Proteins (directly or indirectly) interacting with both $FMRP^{N\text{-}term}$ and $FMRP^{C\text{-}term}$. Underlined proteins were previously described as direct or indirect interacting partners of FMRP. Proteins highlighted in bold are RNA-binding proteins, and proteins in *italic* are components of the SGs. Some proteins have more than one name (http://www.genecards.org), and some alternative names or synonyms are therefore included in parentheses.

Protein name	Function	MW, kDa	*P*-value	Unique pep.	Seq. coverage (%)	Acc. ID
Ataxin-2-like protein (ATXN2L)	RNA metabolism, processing, SGs, p-body	113.3	0.006/0.004	13	16.2	Q8WWM7
Complement component 1 Q subcomponent-binding protein (C1QBP, HABP1)	Transcription, mRNA processing, ribosome assembly, mitochondrial translation apoptosis, innate immune response	31.3	0.012/0.000	9	42.9	Q07021
Cytoplasmic activation/ proliferation-associated protein 1 (Caprin-1, GPIAP1, RNG105)	Translation, differentiation	78.3	0.000/0.000	17	34.1	Q14444
Enhancer of rudimentary homolog (ERH)	Cell cycle	12.3	0.000/0.000	3	37.5	P84090
Fragile X mental retardation syndrome-related protein 1 (FXR1, hFXR1P)	RNA binding, translation, apoptosis, differentiation	69.7	0.000/0.003	23	52.7	P51114
Heterogeneous nuclear ribonucleoprotein U, hnRNPU (HNRNPU, SAF-A) *	Transcription, DDR, RNA processing, granules, mitotic spindle assembly	90.5	0.000/0.000	8	14.4	Q00839
La-related protein 1 (LARP1)*	Translation, cell proliferation	123.4	0.000/0.000	23	25.5	Q6PKG0
Nuclear fragile X mental retardation-interacting protein 2 (NUFIP2, 82-FIP)	RNA binding, transport, SGs	76.1	0.016/0.005	5	14.4	Q7Z417
Polyadenylate-binding protein 1 (PABPC1, PAB1) *	RNA splicing, mRNA silencing, translation	70.6	0.002/0.006	16	34.3	P11940
RAS GTPase-activating protein SH3 domain-binding protein 1 (G3BP1)*	SGs, innate immune response	52.1	0.000/0.000	14	47.2	Q13283
RNA transcription, translation, and transport factor protein (C14orf166, CGI-99, hCLE)	RNA metabolism, transport	28.1	0.001/0.000	21	75.4	Q9Y224
Ubiquitin-associated protein 2-like (UBAP2L, NICE4)*	RNA binding	114.5	0.000/0.001	8	12	Q14157
Uncharacterized protein C7orf50	Uncharacterized	22.1	0.014/0.001	5	41.8	Q9BRJ6

*Paralogs or related proteins identified are listed in Table 4.

involved in differentiation, cell growth, and apoptosis. Several FMRP-interacting proteins are well-studied splicing factors, such as ERH, NONO, PRMT5, PSF, SKIP, SRSF3, and SRPK1 (Fig. 3B).

Molecular function

The vast majority of FMRP-interacting proteins are involved in binding nucleic acids, especially mRNA, rRNA, and miRNA (Tables 1–4; bold), and thereby participate in transcription, RNA metabolism, SG formation, and translation (Fig. 3). FMRP was found in complex with several RNAP II-associated factors, including C14orf166, CTR9, CDC73, and LEO1 (Fig. 3A). FMRP interacts with transcription and chromatin remodeling components, such as its interaction with PSF, NONO, and hnRNPU. Various FMRP-associated proteins modulate NFκB-, Rb-, and p53-controlled transcription (Fig. 3A). Major FMRP-interacting proteins involved in translation include initiation factors eEF2, eIF3A, eIF4G1, and eIF6, eIF4-interacting PDCD4, ribosome-associated helicases IGHMBP2 and YBX3, and the SG proteins ATXN2L, Caprin-1, SYNCRIP, and VGL (Fig. 3D; Tables 1–4).

FMRP is associated with multiple cellular processes

The FMRP-interacting proteins identified in this study were classified into three ontologies: biological process, molecular function, and cellular component (Fig. 2).

Table 4. Isoforms and paralogs of FMRP-interacting proteins depicted in Tables 1–3. Gene names (accession numbers) of different paralogs or related proteins, including ribosomal proteins (RPs) associated with $FMRP^{N\text{-term}}$ and $FMRP^{C\text{-term}}$, are collected; one example each is highlighted with asterisks (*) in Tables 1–3. Proteins highlighted in bold are RNA-binding proteins.

Interaction with $FMRP^{N\text{-term}}$
AHNAK1 (Q09666), **RPL13A** (P40429), **RPL18A** (Q02543), **RPS12** (P25398), **SF1** (Q15637), **UBAP2** (Q5T6F2)
Interaction with $FMRP^{C\text{-term}}$
ASCC3 (Q8N3C0), ATAD3B (Q5T9A4), **DHX9** (Q08211), **DHX15** (O43143), **DHX30** (Q7L2E3), **DHX57** (Q6P158), **eIF3A** (Q14152), **eIF3B** (P55884), **eIF3C** (Q99613), **eIF3D** (O15371), **GNL3** (Q9BVP2), **hnRNPM** (P52272), **hnRNPUL1** (Q9BUJ2), **LARP4** (Q71RC2), **MRPL12** (P52815), **MRPS2** (Q9Y399), **MRPS7** (Q9Y2R9), **NOG1** (Q9BZE4), **RPLP1** (P05386), **RPLP2** (P05387), **RPL4** (P36578), **RPL8** (P62917), **RPL9** (P32969), **RPL10** (P27635), **RPL10A** (P62906), **RPL13** (P26373), **RPL13A** (P40429), **RPL14** (P50914), **RPL19** (P84098), **RPL23A** (P62750), **RPL29** (P47914), **RPL35A** (P18077), **RPL37A** (P61513), **RPS5** (P46782), **RPS27L** (Q71UM5), **SRSF6** (Q13247), **XRCC5** (P13010)
Interaction with both $FMRP^{N\text{-term}}$ and $FMRP^{C\text{-term}}$
DDX1 (Q92499), **DDX17** (Q92841), **DDX3X** (O00571), **DDX3Y** (O15523), **DHX36** (Q9H2U1), G3BP2 (Q9UN86), **PABP3** (Q3ZCS4), **RPL9** (P32969), **RPL10** (P27635), **RPL10A** (P62906), **RPL15** (P61313), **RPL17** (P18621), **RPL18** (Q07020), **RPL21** (P46778), **RPL23** (P62829), **RPL24** (P83731), **RPL26** (P61254), **RPL26L1** (P61254), **RPL27A** (P46776), **RPL28** (P46779), **RPL30** (P62888), **RPL38** (P63173), **RPS8** (P62241), **RPS9** (P46781), **RPS14** (P62263), **RPS16** (P62249), **RPS17** (P08708), **RPS17L** (P0CW22), **RPS18** (P62269), **RPS20** (P60866), **RPS21** (P63220), **RPS24** (P62847), **RPS26** (P62854), **RPS27** (P42677), **RPS28** (P62857)

The vast majority of these proteins are involved in binding nucleic acids, especially mRNA, rRNA, and miRNA (Tables 1–4; bold), and thereby participate in transcription, RNA metabolism, SG formation, and translation (Fig. 3). These functions imply a continuous intracellular transport of FMRP into/between different subcellular compartments of the cell. Notably, LTV1 and KPNA2, which were found in our proteomic analysis (Table 2), may be involved in the nucleocytoplasmic shuttling of FMRP.

FMRP colocalization and interaction with stress granule components

FMRP regulates as RNA-binding protein translation that results from the formation of cytoplasmic ribonucleoprotein (RNP) granules, that is, P-bodies and SGs [28]. Therefore, to obtain mechanistic insights into FMRP function in this process, we selected NONO and G3BP1 two interacting partners of FMRP for further analysis. We performed co-immunoprecipitation of endogenous FMRP interactors from HeLa cell lysates. Consistent with Fig. 1E, we observed NONO and G3BP1 as interacting proteins in immunoblot analysis (Fig. 4A). Notably, NONO and G3BP1 have been previously described as components of neuronal cytoplasmic RNP granules [63].

A different type of cytoplasmic RNA granules represents stress granules (SGs), which have been shown to contain FMRP [64] and G3BP1 [65]. However, a direct interaction between FMRP and G3BP1 has not yet been reported. Thus, we performed pull-down experiments employing different G3BP1 fragments (Fig. 4B) that were overexpressed in HeLa cells using purified GST-$FMRP^{N\text{-term}}$. As depicted in Fig. 4C, G3BP1 full-length (FL) and the fragment M3, but not M1, M2, or M4, bound to $FMRP^{N\text{-term}}$, indicating that the proline-rich region (PXXP) of G3BP1, which is located between the acidic region and the RRM/RGG, may be involved in interaction with $FMRP^{N\text{-term}}$. The acidic

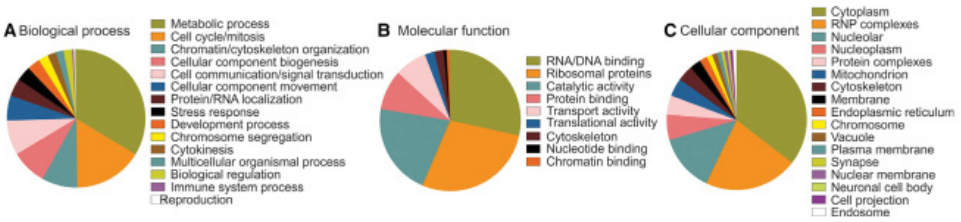

Fig. 2. Gene Ontology analysis of the identified FMRP-interacting proteins categorized according to biological process, molecular function, and subcellular localization. (A) FMRP-associated partners were sorted into 15 biological processes with a predominance of metabolic pathways (31% of all interactors). (B) From the molecular functions, nucleic acid (RNA/DNA)-binding proteins (35%) and ribosomal assembly factors (30%) are the major groups of FMRP interactors. (C) Cellular component classification revealed that FMRP is localized in different subcellular compartments, predominantly in the cytosol (35%).

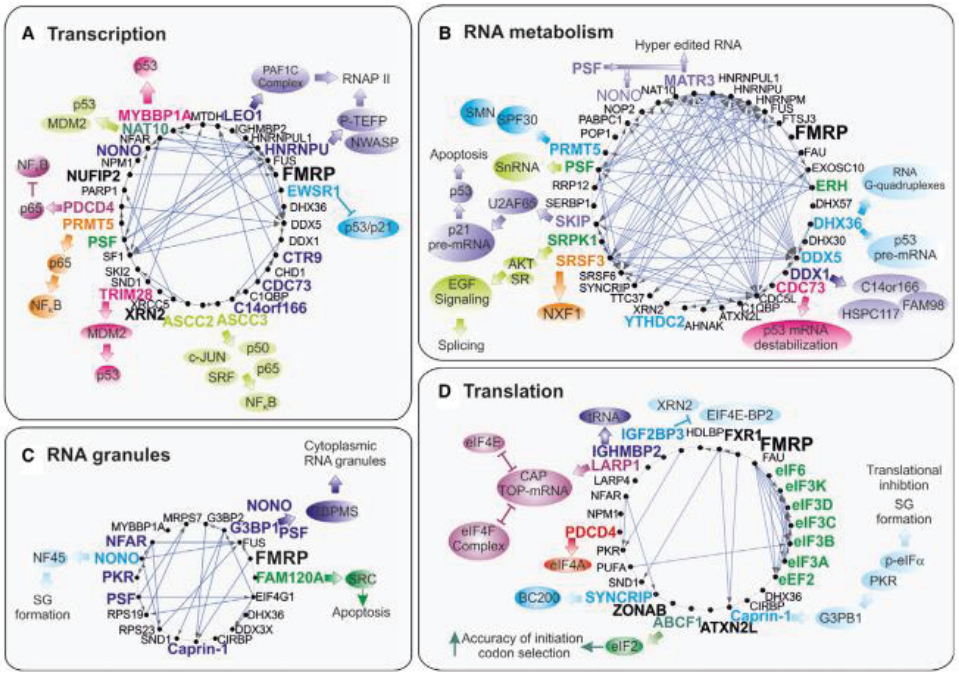

Fig. 3. Functional interaction map for FMRP. Interaction networks of FMRP-interacting proteins involved in transcription (A), RNA metabolism (B), RNA granules (C), and translation (D) were visualized by STRING. Black circle nodes indicate proteins identified in this study. Blue line edges indicate protein–protein interaction networks. The functions of the proteins highlighted in larger font were described in more detail in this study.

region of G3BP1 has been shown to have an inhibitory effect on G3BP1/2 protein interactions [65,66]. Therefore, we assume that G3BP1 has a similar effect when expressed without the NTF-like domain. Consequently, it may counteract the binding of G3BP1 M2 to $FMRP^{N\text{-}term}$, but not G3BP1 FL.

To examine whether FMRP directly binds to G3BP1, we have expressed three fragments of G3BP1 (M1, PXXP, and M3; Fig. 4B) and FMRP (N-term, central, and C-term) and combined them in cell-free affinity pull-down experiments. Virtually, no binding was observed using reciprocal GST-FMRP and GST-G3BP1 fragments, respectively, to GST control protein under similar conditions (data not shown). Notably, $FMRP^{N\text{-}term}$ was pulled down not only by GST-M1 protein but also by GST control protein under similar conditions (data not shown).

To investigate the functional relevance of this interaction, we next analyzed the relative levels of FMRP and G3BP1 as well as their association and localization in different cell lines treated with the oxidative stress agent sodium arsenite. The expression levels of FMRP and particularly G3BP1 increased in cells under stress conditions, as indicated especially for HEK293 cells and human dermal fibroblasts (Fig. 4D), which further suggest that these two proteins have critical functions under stress conditions.

We next analyzed the interaction of G3BP1 with the N-terminal, central, and C-terminal fragments of FMRP purified as GST fusion proteins and mixed with lysates of HeLa cells which were subjected to treatment with sodium arsenite. As shown in Fig. 4E, G3BP1 was equally associated with $FMRP^{N\text{-}term}$ independent of sodium arsenite treatment even so the amounts of $FMRP^{N\text{-}term}$-bound FMRP were increased under stress conditions. It is important to note that FMRP was strongly associated with the RNA-binding central fragment, but not the C-terminal fragment. This prompted us to examine the subcellular distributions of FMRP and G3BP1 in different cell lines in

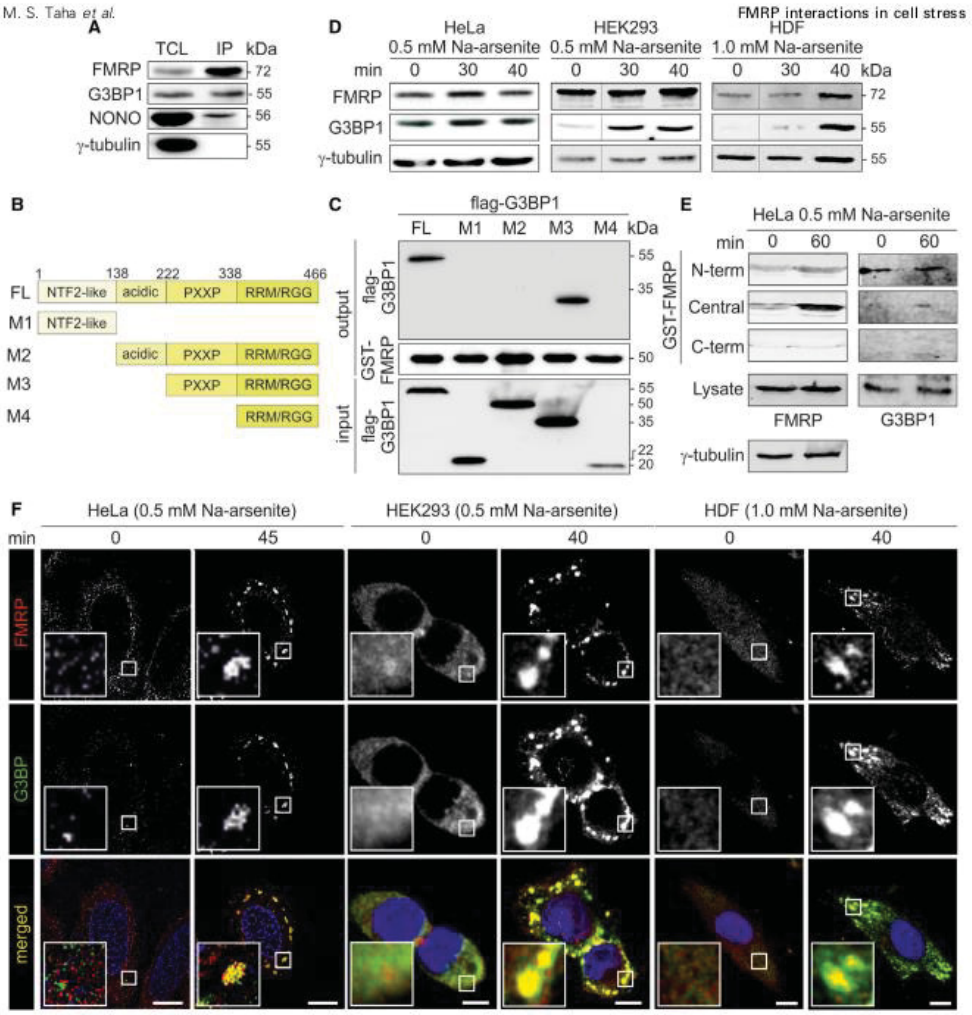

Fig. 4. FMRP indirectly interacts and colocalizes with G3BP1 in stress granules. (A) Co-immunoprecipitation of G3BP1 and NONO with FMRP. Endogenous FMRP was immunoprecipitated (IP) from HeLa total cell lysates (TCL) using an anti-FMRP antibody. Immunoprecipitated endogenous proteins were probed with anti-G3BP and anti-NONO antibodies ($n = 2$). γ-Tubulin was used as a negative control. (B) Domain organization of G3BP1 and the fragments used in this study. G3BP1 consists of four domains, an N-terminal nuclear transport factor 2-like domain (NTF2-like), an acidic region, a proline-rich region (PXXP), and a C-terminal region encompassing both an RNA recognition (RRM) and an arginine–glycine–glycine (RGG) domain. (C) Pull-down experiments were conducted by mixing GST-FMRP$^{N\text{-term}}$ immobilized on glutathione–agarose beads with HeLa cell lysates overexpressing Flag-tagged G3BP1 wild-type protein or deletion mutants. Proteins retained on the beads were resolved by SDS/PAGE and processed by western blot analysis using anti-Flag and anti-GST antibodies to visualize G3BP1 and FMRP$^{N\text{-term}}$ proteins, respectively ($n = 2$). (D) Increasing cellular FMRP and G3BP1 protein levels upon sodium arsenite treatment ($n = 3$). Dashed lines indicate that two lanes have been removed. (E) Endogenous FMRP and G3BP1 were pulled down from HeLa cell lysates before and after treatment with sodium arsenite using purified FMRP fragments as GST fusion proteins ($n = 2$). γ-Tubulin is the loading control for both FMRP and G3BP1 panels. The molecular weights are the same indicated in A. (F) Colocalization of endogenous FMRP (red) and G3BP1 (green) in SGs was visualized by structured illumination super-resolution microscopy (SR-SIM) in HeLa cells or using an LSM510 Meta confocal microscope in HEK293 and HDF cells treated with sodium arsenite as indicated ($n = 3$). DNA was stained using DAPI (blue). The boxes depict magnified areas. Scale bar: 10 μm.

the presence and absence of sodium arsenite. Confocal and super-resolution microscopy imaging revealed that both FMRP and G3BP1 are recruited to and accumulated in SGs (Fig. 4F), presumably in large protein complexes [67]. In contract, G3BP1 and FMRP hardly colocalized subcellularly in untreated cells (Fig. 4F, magnified images). Taken together, our findings rather favor an indirect interaction between FMRP and G3BP1.

Discussion

This comprehensive study was based on several factors such as reproducible culture conditions, available subcellular fractionation and subcellular localization data [23], possible roles of FMRP in cancer progression [68], and the fact that FMRP, as a multifunctional protein, is expressed in many types of non-neuronal cells (Fig. 1A).

FMRP has been previously linked to different biological functions, for example, RNA transport, protein translation, actin cytoskeleton remodeling, and SG formation [1,12,14,19,35,36,69–76]. Most of these functions have been linked to the ability of FMRP to control the translation of numerous different mRNAs [77], potentially explaining why FMRP is expressed in several tissues and cell lines, including iPSCs (Fig. 1A) [6]. Moreover, FMRP has been reported to be predominantly cytoplasmic [62]. However, in recent years, it has become increasingly evident that FMRP translocates into the nucleus due to sequence motifs responsible for its nuclear import and export as well as nucleolar localization [19,21,23,28,78–84].

In the following section, we discuss selected functional relationships of newly identified proteins that potentially interact with FMRP in selected cellular processes (Fig. 3 and Tables 1–4).

Transcription

Eukaryotic gene transcription is evolutionarily highly conserved between budding yeast and humans. This is based on deep structural and functional homologies among promoter factors, regulatory proteins, and RNA polymerases [85]. The latter are divided into three different enzyme systems: RNA polymerase I (RNAP I) synthesizes ribosomal RNA (rRNA); RNAP II synthesizes mRNAs and different types of noncoding RNA (ncRNA); and RNAP III synthesizes tRNA and some types of ncRNA. The fact that more than 400 different mRNAs are associated with FMRP [9,68,86] strongly indicates that FMRP may be involved in diverse processes, including mRNA synthesis by RNAP II, processing by the spliceosome, and transport. These proteins, together with PAF1 and RTF1, belong to the highly conserved and broadly utilized PAF1 complex (PAF1C), which regulates a variety of processes, such as transcription-coupled histone modifications; initiation, elongation, and termination of transcription by RNAP II; and RNA processing [87]. Another possible role of FMRP is in transcription and chromatin remodeling. Some of its interacting proteins are together with RNAP II, p-TEFb, NWASP, and nuclear actin key elements in cell reprogramming and differentiation [88]. P-TEFb also regulates transcription termination by promoting chromatin recruitment and activating the FMRP-associating cotranscriptional RNA processing enzyme XRN2 [67]. SKIP potentiates the activity of various transcription factors, including the vitamin D receptor, CBF1, SMAD2/3, and MYOD, and synergizes with SKI in overcoming pRb-mediated cell cycle arrest [89].

BCLAF1, which also binds FXR1P [90], controls p53 expression in a PKCδ-dependent manner [91]. MYBBP1A has been reported to enhance p53 tetramerization and acetylation in response to nucleolar disruption [92]. NAT10 regulates p53 activation through p53 acetylation and MDM2 ubiquitination [93]. In contrast, EWSR1 induces acute myeloid leukemia by inhibiting the p53/p21 pathway [94]. The interaction of the nuclear corepressor TRIM28 with MDM2 contributes to p53 inactivation [95,96]. ASCC2 and ASCC3 are components of the ASC-1 complex that stimulate transactivation by NFκB, SRF, and AP1 through direct binding to SRF, c-JUN, p50, and p65 [97]. PRMT5 dimethylates the p65 subunit to activate NFκB [98], whereas the tumor suppressor PDCD4 inhibits NFκB-dependent transcription, for example, in human glioblastoma cells by direct interaction with p65 [99]. XRN2 interacts with the NFκB-repressing factor and regulates transcription elongation [100]. MYBBP1A appears to be an NFκB corepressor of transcription by competing with p300 [101]. In this context, TGM3, a candidate tumor suppressor [102], appears to interfere with the NFκB signaling pathway and promote proliferation [103].

The FMRP-associated proteins AGR2, ATAD3A, DHX15, and RPL17 were identified in a proteome-wide analysis of hepatocellular carcinoma as binding partners of AGR2 [104]. Their FMRP-associated roles in transcriptional control remain to be investigated. Thus, FMRP appears to contribute the RNAP II-associated synchronization of biosynthesis, processing, transport, stability, and translational control of mRNAs through protein binding and RNA binding.

RNA metabolism

The majority of FMRP-interacting proteins are RBPs and are involved in RNA metabolism, which refers to any event in the life cycle of RNA molecules, including their synthesis, folding/unfolding, splicing, modification, processing, nuclear export, transport, storage, translation activation or inhibition, and degradation. RNA helicases are RBPs, which represent a large family of proteins that play central roles in almost all biological processes in living cells [105]. The majority of FMRP-associated proteins are involved in RNA metabolism and include RNA helicases and splicing factors.

DDX1 has been found together with the FMRP-associating proteins PSF, Caprin-1, and PQBP1 in a protein complex that interacts in an RNA-dependent manner [106]. PQBP1 has been shown to colocalize with FMRP at SGs [106]. DDX3X has been shown to stimulate the translation of a subset of mRNAs with long and structured 5′ UTRs, such as RAC1 [107]. On the other hand, DDX3X promotes cell migration and spreading by physically interacting with PABP1 and Caprin-1 [108], two other FMRP-associated proteins.

The FMRP-associated proteins AGR2, ATAD3A, DHX15, and RPL17 were identified in a proteome-wide analysis of hepatocellular carcinoma as binding partners of AGR2 [104]. A common function of FMRP and DHX36 is binding to RNA G-quadruplexes, which are stable secondary structures that play key roles in RNA metabolism [109]. In this way, DHX36 regulates p53 pre-mRNA 3′-end processing following UV-induced DNA damage [110], while CDC73 targets and destabilizes p53 mRNA [111]. IGHMBP2 was suggested to be a component of the translational machinery by physically associating with tRNAs [112]. Among other functions, DDX1, DDX3X, DHX9, and MOV10 are involved in nuclear RNA export [105]. Similar to FMRP, SKIP localizes in both the nucleolus and cytoplasm. It may be involved in ribosome biogenesis and translation [113]. The functional relation of the RNA helicase YTHDC2 to FMRP remains unclear.

The removal of introns from pre-mRNA transcripts is a critical intermediate step in the expression of protein-coding genes. This process takes place in the nucleoplasm and is catalyzed by a large and dynamic small nuclear RNP (snRNP) complex called the spliceosome [114,115]. PSF and NONO form heterodimers and participate in various aspects of RNA metabolism, including transcription, pre-mRNA splicing, 3′ polyadenylation of mRNA, and nuclear retention of mRNA [116,117]. The splicing of mRNA requires a group of essential factors known as SR proteins, which undergo cytoplasmic–nuclear shuttling upon phosphorylation by SRPK1 [116,117]. Interestingly, the AKT-SRPK1-SR axis constitutes a major pathway in transducing EGF signaling to regulate alternative splicing in the nucleus. SRPK1-mediated phosphorylation of SRSF1 has been shown to regulate alternative splicing of RAC1B [118], which is a hyperactive form of RAC1 [119]. Moreover, ERH appears to regulate SRPK1-mediated phosphorylation of the lamin B receptor and SR proteins [120]. ERH is also associated with RNA processing complexes. It binds to the spliceosomal Sm complex and is required for splicing various mRNAs, including the mitotic motor protein CENP-E [121] and the DDR protein ATM [122]. PSF interacts with snRNA components of the spliceosome, is a component of the 3′ polyadenylation complexes SF-A, and binds together with MATR3 and NONO to hyper-edited RNA [117]. SKIP counteracts p53-induced apoptosis by recruiting the 3′ splice site recognition factor U2AF65 to the p21 pre-mRNA [123]. The methylation of arginines, for example, by PRMT5, enhance interactions with the tudor domains of the splicing factors SMN and SPF30 [124]. SRSF3 links pre-mRNA processing to mRNA export by recruiting the nuclear export factor NXF1 [125]. The FMRP-interacting proteins C14orf166 and DDX1 form a complex with both HSPC117 and FAM98B, underlay a nucleocytoplasmic shuttling in response to transcriptional activity, and may play a role in nuclear and cytoplasmic RNA fate [126]. Notably, C14orf166 interacts with RNAP II, modulates nuclear RNA metabolism, participates in RNA splicing, and is present in cytoplasmic RNA granules involved in localized translation [126].

RNA granules

Cytoplasmic RNP granules in germ cells (polar and germinal granules), somatic cells (SGs and processing bodies), and neurons (neuronal granules) have emerged as important players in the posttranscriptional regulation of gene expression. RNA granules contain various ribosomal subunits, translation factors, decay enzymes, helicases, scaffold proteins, and RNA-binding proteins, and they control the localization, stability, and translation of their RNA cargo (Fig. 3C) [127,128]. A very recent report has demonstrated a central role of FMRP in granule biology by monitoring the transport and fusion of RNA granules throughout neuronal processes [43]. Most interestingly, RNA granules, isolated and purified from mouse brain homogenates [43], contain more than 20 FMRP-interacting proteins. Three

FMRP-associated proteins, G3BP1, NONO, and PSF, have been detected in RNA granules [63]. FMRP immunoprecipitation revealed that G3BP1 and NONO co-immunoprecipitated with FMRP in HeLa total cell lysates (Fig. 4A), suggesting their critical interrelated roles in the formation, integrity, and/or transport of cytoplasmic RNP granules. This and the fact that FMRP exists in almost every cell type (Fig. 1A) strongly indicate the existence of such RNA granules as the regulatory machinery for local translation in the cell.

The activation of stress response pathways often promotes SG formation throughout the cytoplasm of stressed cells [129]. SGs are dynamic aggregates of untranslated mRNAs that are sorted between decay, storage, or polysome assembly [129,130]. SGs also contain many signaling proteins [130]. The association of FMRP with the translation machinery and polysomes in SGs has been described frequently in several laboratories [11,64,131–134]. Thus, it was not surprising that FMRP itself and many FMRP-interacting proteins have been shown to localize in SGs [135–142], the vast majority of which are RBPs (Tables 1–4). Inhibition of translation initiation, achieved by the phosphorylation of eIF2α or by blocking assembly of the eIF4F complex (see below), results in the formation of SGs [130,143]. NFAR, a double-stranded RNA-binding nuclear protein, that is, similar to eIF2α, a PKR substrate [144], undergoes a heterodimeric complex with NF45 and thereby modulates RNA granule assembly and disassembly [145]. NFAR was identified in this proteomic study as one of many Caprin-1- and G3BP1-associated proteins, which we also found to be associated with FMRP [145]. SGs regulate double-stranded RNA-dependent PKR activation through a complex containing G3BP1 and Caprin-1 [146], and probably also FMRP. It has been reported that PKR recruitment to SGs requires the PXXP region of G3BP1 [147], which appears to be essential for the interaction with FMRP (Fig. 4B,C). The role of FMRP in SG formation has been discussed in several studies [64,131,148], but the molecular mechanism of FMRP function awaits further investigation.

Translation

Translational control has an impact on many cellular and developmental processes, and most steps of translation are subjected to specific regulation. The role of FMRP as a regulator of local translation has been best investigated for neurons [10,38]. FMRP transports coding and noncoding RNAs to the synapse and participates in local protein synthesis in dendrites. Thus, FMRP potentially influences signaling pathways involved in spine morphogenesis [10,76,149]. Increasing evidence suggests that FMRP interferes with the translation of its target mRNAs in two different ways: suppression of translational initiation and translocation and/or activation of miRNA pathways [1,34,71–73,149].

In neurons, the vast majority of FMRP is associated with both its target mRNAs [11] and stalled, nontranslating polyribosomes [134,150]. This process appears to be regulated by FMRP phosphorylation [24,151]. eIF4G plays a key functional role in the initiation of cap-dependent translation by acting as an adapter to nucleate the assembly of the heterotrimeric eIF4F complex [152]. The latter consists of eIF4G, eIF4E, and eIF4A. Together with poly(A)-binding protein and eIF3, eIF4F subsequently triggers the recruitment of the 43S ribosomal preinitiation complex to the messenger RNA template [143]. PDCD4 suppresses cap-dependent translation initiation. PDCD4 tightly binds eIF4A in its inactive conformation and blocks its incorporation into the eIF4F complex, which consists of eIF4A, eIF4E, and eIF4G1/eIF4G3 [153], that then recruits the 40S ribosomal subunit to start translation initiation [154]. Analogous to PDCD4, LARP1 is also an FMRP-interacting protein and directly binds the cap and region adjacent to the 5′-TOP motif of TOP mRNAs, thereby effectively impeding access of eIF4E to the cap and preventing eIF4F assembly [155]. Interestingly, IGF2BP3 in complex with the ribonuclease XRN2 (two FMRP-interacting proteins) destabilizes eIF4E-BP2, a negative regulator of eIF4E [156]. Caprin-1 binds G3BP1 and induces phosphorylation of eIF2α most likely through the activation of PKR, the inhibition of translation, and the formation of cytoplasmic SG [157].

Several other FMRP-associated proteins act on translation at different levels and in different ways. The multi-KH protein VGL associates with free and membrane-bound ribosomes and is generally necessary for the localization of mRNAs to actively translating ribosomes [158]. IGHMBP2 is a component of the translational machinery, which physically associates with tRNAs [159]. Brain cytoplasmic RNA of 200 nucleotides (BC200 RNA) is a brain-specific, small noncoding RNA with a somato-dendritic distribution in primate neurons. SYNCRIP interacts specifically with BC200 RNA and may recruit it to mRNA transport complexes involved in the regulation of localized translation in dendrites [43,160]. Remarkably, several other known translational regulators, including FMRP and PABP1, are components of the BC200 RNP complex [160]. FMRP promotes the translation of specific

mRNAs in a complex with NAT1, eIF2, and PRRC2C [161]. In this context, we identified PRRC2C and NAT10, but not NAT1, as FMRP-interacting proteins (Fig. 3D). Another FMRP-associated protein is ABCF1, which influences the accuracy of initiation codon selection by binding eIF2 and efficiently initiates translation [162].

Domain-dependent interactions of FMRP

The N terminus of FMRP harbors different protein-binding characteristics due to various subdomains (Fig. 1B). Two conserved Tud1/2 domains (also called the N-terminal domain of FMRP 1 and FMRP 2 or NDF1 and NDF2, respectively) [23,48] are within the 'Royal Family' of proteins, which includes Agenet, MBT, PWWP, and chromo-domains [163]. FMRP and Tud1/2 have been shown to selectively associate with trimethyl-lysine peptides derived from histones H3K9 and H4K20 [48,78] together with chromatin [19]. The N terminus of FMRP has been proposed to be a platform for multiple protein–protein interactions [48]. However, we detected only a relatively small number of binding proteins for $FMRP^{N\text{-}term}$ compared with $FMRP^{C\text{-}term}$. A recent structure of the flexible $FMRP^{N\text{-}term}$ has revealed that this domain resembles a K homology (KH) domain [164] that is directly linked to the tandem KH domains of $FMRP^{central}$ (Fig. 1B). KH domains are typically RNA and single-stranded DNA-binding modules; these molecules were first described for the heterogeneous nuclear RNA-binding protein (hnRNPK) [165,166]. A similar scenario as discussed above for $FMRP^{C\text{-}term}$ may apply for $FMRP^{N\text{-}term}$, that is, its interactions may not all be direct protein–protein interactions but rather mediated via RNAs. G3BP1 belongs to the evolutionarily conserved hnRNP family. It is involved in an array of biological activities, ranging from cell cycle regulation to mRNA metabolism and SG assembly [65,167]. However, our data indicate that G3BP1 associates with $FMRP^{N\text{-}term}$ in an RNA-independent manner but most likely dependent on other proteins.

At this stage, it is important to note that the identification of protein–protein interactions by a combination of affinity purification and mass spectrometry has one drawback: Direct (physical) interactions are mixed with indirect interactions. The same is also true for co-IP experiments. There are strikingly a number of mathematical modeling and algorithmic efforts for prediction and assessment of direct interactions [168]. These approaches will, however, not displace direct biophysical measurements of two proteins or protein domains purified from heterologous systems. This study opens the door to further explore the involvement of FMRP in unknown and new cellular functions.

Conclusions

The data presented in this work considerably expand the physical and functional candidate protein and RNA interaction networks of FMRP and suggest its participation in various fundamental cellular processes throughout the body beyond the central and peripheral nervous systems. Accordingly, FMRP functions may start in the nucleolus following cytoplasmic–nuclear translocation, where it may be involved in the biogenesis of ribosomal subunits and most likely their nuclear export. FMRP may be part of the transcriptional factory by regulating gene expression via interaction and orchestration of RNA polymerase II, where it directly binds to a large set of mRNAs and transports them to sites of local translation. Upon any kind of cellular stress, FMRP accumulates at sites of stress responses and facilitates, for example, the stabilization of double-stranded RNA binding and the activation of PKR, leading to SG formation. Moreover, our novel FMRP interactome analysis indicates that FMRP may play central roles in the DNA damage response, cell cycle regulation, intracellular transport, and actin dynamics, and that FMRP virally triggers innate immune responses. Of note, FMRP may also be involved in mitochondrial quality control and mitophagy, functions that are directly related to neurodegenerative and cognitive disorders, including FXS, Huntington's disease, Alzheimer's disease, Down syndrome, and progressive supranuclear palsy. Our work provides valuable insights and constitutes a useful starting point for future studies of the cellular functions of FMRP in both non-neuronal and neuronal cells.

Materials and methods

Constructs and proteins

Amino-terminal (N-term: aa 1–218), central (aa 212–425), and carboxy-terminal (C-term: aa 444–632) fragments of human FMRP, as well as NTF2-like/acidic (or M1; aa 1–122), PXXP (aa 123–338), and PXXP-RRM/RGG (or M3; aa 123–466) fragments of human G3BP1, were amplified by standard PCR and cloned into pGEX-4T1. *Escherichia coli* BL21 Rosetta was transformed with the respective FMRP and G3BP1 plasmids. The expression and purification of the proteins were performed as previously described [169,170]. pFLAG-CMV2 was used for G3BP1 constructs comprising full-length (FL), NTF2-like/acidic or M1

(1–138), acidic-PXXP-RRM/RGG or M2 (139–466), PXXP-RRM/RGG or M3 (222–466), and RRM/RGG or M4 (338–466), as reported previously [65].

Antibodies and other reagents

The antibodies used in this study were as follows: Anti-Caprin-1 (ab241071), anti-FMRP (ab17722), and anti-nucleophosmin (ab10530) (purchased from Abcam, Boston, MA, USA); anti-FMRP (F6072), anti-G3BP (611126), and anti-PKR (Sc-6282), (purchased from BD Biosciences, San Jose, CA, USA); and anti-γ-tubulin (T5326) (purchased from Sigma-Aldrich, Taufkirchen, Germany). The anti-GST antibody was made in our laboratory. 4′,6-Diamidino-2-phenylindole (DAPI) was purchased from Thermo Fisher (Waltham, MA, USA), and sodium arsenite was purchased from Merck. Anti-FLAG (F3165) antibody, and secondary antibodies (IgG) Alexa Fluor 488 and 564 were obtained from Thermo Fisher. RNase treatment was performed using RNase A (Qiagen, Hilden, Germany) as described previously [23].

Cell culture

HEK293 (human embryonic kidney cells), HDF (human dermal fibroblasts), and cancer cell lines such as HepG2, HeLa, PANC1, and MCF7 were cultured in DMEM (Thermo Fisher, 11965092), whereas NT2, BPH1, and SW480 cells were cultured in RPMI (Thermo Fisher, 11875093); all media were supplemented with 10% FBS (Thermo Fisher, 10270-106). Human iPSCs were cultured as previously described [171]; briefly, cells were cultured in irradiated mouse embryonic fibroblast (iMEF) conditioned medium supplemented with 100 $ng \cdot mL^{-1}$ bFGF (PeproTech, 100-18B; Cranbury, NJ, USA). HUVECs were cultured in endothelial cell growth medium (PromoCell, GmbH, Heidelberg, Germany) containing 100 $U \cdot mL^{-1}$ penicillin and streptomycin (Genaxxon bioscience, M3140.0100; GmbH, Ulm, Germany).

Immunofluorescence microscopy

Confocal imaging of HeLa cells was performed as described previously [23]. Images were obtained as single optical slides using an LSM510 Meta confocal (ZEISS, Jena, Germany) microscope equipped with a 40×/1.3 immersion objective and excitation wavelengths of 364, 488, and 546 nm. Super-resolution structured illumination microscopy (SR-SIM) was performed as described recently [172] using the ELYRA microscope (ZEISS, Jena, Germany) with an alpha Plan-Fluor 100×/1.45 M27 oil-immersion objective and immersion oil type 518 F/30 °C (ZEISS, Jena, Germany). Images were acquired using ZEN 2.0 software (ZEISS, Oberkochen, Germany).

Transfection and pull-down assay

GST pull-down experiments were conducted as described previously [23]. GST-$FMRP^{N\text{-}term}$, GST-$FMRP^{C\text{-}term}$, and GST as a negative control were immobilized on GSH agarose beads, subsequently mixed with HeLa total cell lysate and incubated for 1 h, at 4 °C to pull-down associating proteins and protein complexes. The beads from three independent experiments were washed four times, boiled in 1× SDS loading buffer for 5 min, and separated on 10% tricine sodium dodecyl sulfate (SDS)/polyacrylamide gels. Lanes of Coomassie Brilliant Blue (CBB)-stained SDS gels were cut in different sections, excluding the bands related to GST-$FMRP^{N\text{-}term}$, GST-$FMRP^{C\text{-}term}$, and the GST control. Gel sections were subjected to mass spectrometry. The pull-down of flag-tagged G3BP1 protein fragments that were overexpressed in HeLa cells was performed using purified GST-$FMRP^{N\text{-}term}$ and visualized by immunoblotting using anti-Flag and anti-GST antibodies. HeLa cells were transfected using TurboFect Transfection Reagent (Thermo Scientific) as previously described [23].

Immunoprecipitation

For co-immunoprecipitation, HeLa cells were lysed in immunoprecipitation buffer (20 mM Tris/HCl pH 7.4, 150 mM NaCl, 5 mM $MgCl_2$, 0.5% NP-40, 10 mM β-glycerophosphate, 0.5 mM Na_3VO_4, 10% glycerol, and EDTA-free protease inhibitor). IP from total cell lysates was carried out for 2 h at 4 °C with an anti-FMRP antibody (ab17722; Abcam). The beads were washed five times with IP buffer lacking NP-40, and eluted proteins were heated in SDS/Laemmli buffer at 95 °C and analyzed by immunoblotting.

Immunoblotting

Cell lysates were prepared using lysis buffer [50 mM Tris/HCl pH 7.5, 100 mM NaCl, 2 mM $MgCl_2$, 1% IGEPAL CA-630, 10% glycerol, 20 mM β-glycerophosphate, 1 mM Na_3VO_4, EDTA-free protease inhibitor (Roche, Basel, Switzerland)], and protein concentrations were measured by Bradford assay (Bio-Rad, Irvine, CA, USA). Equal amounts of total cell lysates (40 µg) were loaded on SDS/PAGE gels. After electrophoresis, proteins were transferred to nitrocellulose membranes and blocked for 1 h in 5% nonfat dry milk (Merck, Taufkirchen, Germany)/TBST (Tris-buffered saline, 0.05% Tween 20). Membranes were probed with primary antibodies at 4 °C overnight and later stained for 1 h at room temperature with both horseradish peroxidase (HRP)-conjugated secondary antibodies (1 : 5000 dilution) and fluorescent secondary antibodies (1 : 10 000 dilution) (Agilent, Santa Clara, CA, USA). Signals were visualized using ECL (enhanced chemiluminescence) reagent (GE Healthcare, Menlo Park, CA, USA)

5 Zhao X, Wang Y, Meng C & Fang N (2018) FMRP regulates endothelial cell proliferation and angiogenesis via the miR-181a-CaM-CaMKII pathway. *Cell Biol Int* **42**, 1432–1444.

6 Li Y & Zhao X (2014) Concise review: Fragile X proteins in stem cell maintenance and differentiation. *Stem Cells* **32**, 1724–1733.

7 Schultz-Pedersen S, Hasle H, Olsen JH & Friedrich U (2001) Evidence of decreased risk of cancer in individuals with fragile X. *Am J Med Genet* **103**, 226–230.

8 Ascano M Jr, Mukherjee N, Bandaru P, Miller JB, Nusbaum JD, Corcoran DL, Langlois C, Munschauer M, Dewell S, Hafner M *et al*. (2012) FMRP targets distinct mRNA sequence elements to regulate protein expression. *Nature* **492**, 382–386.

9 Brown V, Jin P, Ceman S, Darnell JC, O'Donnell WT, Tenenbaum SA, Jin X, Feng Y, Wilkinson KD, Keene JD *et al*. (2001) Microarray identification of FMRP-associated brain mRNAs and altered mRNA translational profiles in fragile X syndrome. *Cell* **107**, 477–487.

10 Darnell JC & Klann E (2013) The translation of translational control by FMRP: therapeutic targets for FXS. *Nat Neurosci* **16**, 1530–1536.

11 Darnell JC, Van Driesche SJ, Zhang C, Hung KY, Mele A, Fraser CE, Stone EF, Chen C, Fak JJ, Chi SW *et al*. (2011) FMRP stalls ribosomal translocation on mRNAs linked to synaptic function and autism. *Cell* **146**, 247–261.

12 Fernandez E, Rajan N & Bagni C (2013) The FMRP regulon: from targets to disease convergence. *Front Neurosci* **7**, 191.

13 Sakano H, Zorio DAR, Wang X, Ting YS, Noble WS, MacCoss MJ, Rubel EW & Wang Y (2017) Proteomic analyses of nucleus laminaris identified candidate targets of the fragile X mental retardation protein. *J Comp Neurol* **525**, 3341–3359.

14 Santoro MR, Bray SM & Warren ST (2012) Molecular mechanisms of fragile X syndrome: a twenty-year perspective. *Annu Rev Pathol* **7**, 219–245.

15 Ferron L, Nieto-Rostro M, Cassidy JS & Dolphin AC (2014) Fragile X mental retardation protein controls synaptic vesicle exocytosis by modulating N-type calcium channel density. *Nat Commun* **5**, 3628.

16 Billuart P & Chelly J (2003) From fragile X mental retardation protein to Rac1 GTPase: new insights from Fly CYFIP. *Neuron* **38**, 843–845.

17 Nolze A, Schneider J, Keil R, Lederer M, Huttelmaier S, Kessels MM, Qualmann B & Hatzfeld M (2013) FMRP regulates actin filament organization via the armadillo protein p0071. *RNA* **19**, 1483–1496.

18 Schenck A, Bardoni B, Langmann C, Harden N, Mandel JL & Giangrande A (2003) CYFIP/Sra-1 controls neuronal connectivity in *Drosophila* and links the Rac1 GTPase pathway to the fragile X protein. *Neuron* **38**, 887–898.

19 Alpatov R, Lesch BJ, Nakamoto-Kinoshita M, Blanco A, Chen S, Stutzer A, Armache KJ, Simon MD, Xu C, Ali M *et al*. (2014) A chromatin-dependent role of the fragile X mental retardation protein FMRP in the DNA damage response. *Cell* **157**, 869–881.

20 Liu J, Koscielska KA, Cao Z, Hulsizer S, Grace N, Mitchell G, Nacey C, Githinji J, McGee J, Garcia-Arocena D *et al*. (2012) Signaling defects in iPSC-derived fragile X premutation neurons. *Hum Mol Genet* **21**, 3795–3805.

21 Zhang W, Cheng Y, Li Y, Chen Z, Jin P & Chen D (2014) A feed-forward mechanism involving *Drosophila* fragile X mental retardation protein triggers a replication stress-induced DNA damage response. *Hum Mol Genet* **23**, 5188–5196.

22 Pasciuto E & Bagni C (2014) SnapShot: FMRP interacting proteins. *Cell* **159**, 218 e211.

23 Taha MS, Nouri K, Milroy LG, Moll JM, Herrmann C, Brunsveld L, Piekorz RP & Ahmadian MR (2014) Subcellular fractionation and localization studies reveal a direct interaction of the fragile X mental retardation protein (FMRP) with nucleolin. *PLoS One* **9**, e91465.

24 Bartley CM, O'Keefe RA & Bordey A (2014) FMRP S499 is phosphorylated independent of mTORC1-S6K1 activity. *PLoS One* **9**, e96956.

25 Myrick LK, Hashimoto H, Cheng X & Warren ST (2015) Human FMRP contains an integral tandem Agenet (Tudor) and KH motif in the amino terminal domain. *Hum Mol Genet* **24**, 1733–1740.

26 Bardoni B, Sittler A, Shen Y & Mandel JL (1997) Analysis of domains affecting intracellular localization of the FMRP protein. *Neurobiol Dis* **4**, 329–336.

27 Feng Y, Gutekunst CA, Eberhart DE, Yi H, Warren ST & Hersch SM (1997) Fragile X mental retardation protein: nucleocytoplasmic shuttling and association with somatodendritic ribosomes. *J Neurosci* **17**, 1539–1547.

28 Kim M, Bellini M & Ceman S (2009) Fragile X mental retardation protein FMRP binds mRNAs in the nucleus. *Mol Cell Biol* **29**, 214–228.

29 Tamanini F, Bontekoe C, Bakker CE, van Unen L, Anar B, Willemsen R, Yoshida M, Galjaard H, Oostra BA & Hoogeveen AT (1999) Different targets for the fragile X-related proteins revealed by their distinct nuclear localizations. *Hum Mol Genet* **8**, 863–869.

30 Hoogeveen AT, Willemsen R & Oostra BA (2002) Fragile X syndrome, the fragile X related proteins, and animal models. *Microsc Res Tech* **57**, 148–155.

31 Sakai Y, Shaw CA, Dawson BC, Dugas DV, Al-Mohtaseb Z, Hill DE & Zoghbi HY (2011) Protein interactome reveals converging molecular pathways among autism disorders. *Sci Transl Med* **3**, 86ra49.

32 Schenck A, Bardoni B, Moro A, Bagni C & Mandel J-L (2001) A highly conserved protein family interacting with the fragile X mental retardation protein (FMRP) and displaying selective interactions with FMRP-related proteins FXR1P and FXR2P. *Proc Natl Acad Sci USA* **98**, 8844–8849.

33 Winograd C & Ceman S (2011) Fragile X family members have important and non-overlapping functions. *Biomol Concepts* **2**, 343–352.

34 Cheever A & Ceman S (2009) Translation regulation of mRNAs by the fragile X family of proteins through the microRNA pathway. *RNA Biol* **6**, 175–178.

35 Wang T, Bray SM & Warren ST (2012) New perspectives on the biology of fragile X syndrome. *Curr Opin Genet Dev* **22**, 256–263.

36 Chen E & Joseph S (2015) Fragile X mental retardation protein: a paradigm for translational control by RNA-binding proteins. *Biochimie* **114**, 147–154.

37 Irwin SA, Galvez R & Greenough WT (2000) Dendritic spine structural anomalies in fragile-X mental retardation syndrome. *Cereb Cortex* **10**, 1038–1044.

38 Kenny PJ, Zhou H, Kim M, Skariah G, Khetani RS, Drnevich J, Arcila ML, Kosik KS & Ceman S (2014) MOV10 and FMRP regulate AGO2 association with microRNA recognition elements. *Cell Rep* **9**, 1729–1741.

39 Alberti S, Mateju D, Mediani L & Carra S (2017) Granulostasis: protein quality control of RNP Granules. *Front Mol Neurosci* **10**, 84.

40 Moujaber O & Stochaj U (2018) Cytoplasmic RNA granules in somatic maintenance. *Gerontology* **64**, 485–494.

41 Sfakianos AP, Whitmarsh AJ & Ashe MP (2016) Ribonucleoprotein bodies are phased in. *Biochem Soc Trans* **44**, 1411–1416.

42 Chyung E, LeBlanc HF, Fallon JR & Akins MR (2018) Fragile X granules are a family of axonal ribonucleoprotein particles with circuit-dependent protein composition and mRNA cargos. *J Comp Neurol* **526**, 96–108.

43 El Fatimy R, Davidovic L, Tremblay S, Jaglin X, Dury A, Robert C, De Koninck P & Khandjian EW (2016) Tracking the fragile X mental retardation protein in a highly ordered neuronal ribonucleoparticles population: a link between stalled polyribosomes and RNA granules. *PLoS Genet* **12**, e1006192.

44 Maziuk B, Ballance HI & Wolozin B (2017) Dysregulation of RNA binding protein aggregation in neurodegenerative disorders. *Front Mol Neurosci* **10**, 89.

45 McCoy M, Poliquin-Duchesneau D & Corbin F (2016) Molecular dynamics of FMRP and other RNA-binding proteins in MEG-01 differentiation: the role of mRNP complexes in non-neuronal development. *Biochem Cell Biol* **94**, 597–608.

46 D'Souza MN, Gowda NKC, Tiwari V, Babu RO, Anand P, Dastidar SG, Singh R, Selvaraja B, Pal R, Ramesh A *et al.* (2018) FMRP interacts with C/D box snoRNA in the nucleus and regulates ribosomal RNA methylation. *iScience* **9**, 399–411.

47 Menon RP, Gibson TJ & Pastore A (2004) The C terminus of fragile X mental retardation protein interacts with the multi-domain Ran-binding protein in the microtubule-organising centre. *J Mol Biol* **343**, 43–53.

48 Ramos A, Hollingworth D, Adinolfi S, Castets M, Kelly G, Frenkiel TA, Bardoni B & Pastore A (2006) The structure of the N-terminal domain of the fragile X mental retardation protein: a platform for protein-protein interaction. *Structure* **14**, 21–31.

49 Siomi H, Choi M, Siomi MC, Nussbaum RL & Dreyfuss G (1994) Essential role for KH domains in RNA binding: impaired RNA binding by a mutation in the KH domain of FMR1 that causes fragile X syndrome. *Cell* **77**, 33–39.

50 Zalfa F & Bagni C (2004) Molecular insights into mental retardation: multiple functions for the fragile X mental retardation protein? *Curr Issues Mol Biol* **6**, 73–88.

51 El Fatimy R, Tremblay S, Dury AY, Solomon S, De Koninck P, Schrader JW & Khandjian EW (2012) Fragile X mental retardation protein interacts with the RNA-binding protein Caprin1 in neuronal RiboNucleoProtein complexes [corrected]. *PLoS One* **7**, e39338.

52 Tamanini F, Van Unen L, Bakker C, Sacchi N, Galjaard H, Oostra BA & Hoogeveen AT (1999) Oligomerization properties of fragile-X mental-retardation protein (FMRP) and the fragile-X-related proteins FXR1P and FXR2P. *Biochem J* **343** (Pt 3), 517–523.

53 Bardoni B, Schenck A & Mandel JL (1999) A novel RNA-binding nuclear protein that interacts with the fragile X mental retardation (FMR1) protein. *Hum Mol Genet* **8**, 2557–2566.

54 Beggs JE, Tian S, Jones GG, Xie J, Iadevaia V, Jenei V, Thomas G & Proud CG (2015) The MAP kinase-interacting kinases regulate cell migration, vimentin expression and eIF4E/CYFIP1 binding. *Biochem J* **467**, 63–76.

55 Yang L, Duan R, Chen D, Wang J & Jin P (2007) Fragile X mental retardation protein modulates the fate of germline stem cells in *Drosophila*. *Hum Mol Genet* **16**, 1814–1820.

56 Ehyai S, Miyake T, Williams D, Vinayak J, Bayfield MA & McDermott JC (2018) FMRP recruitment of beta-catenin to the translation pre-initiation complex represses translation. *EMBO Rep* **19**, e45536.

57 Ishihama Y, Oda Y, Tabata T, Sato T, Nagasu T, Rappsilber J & Mann M (2005) Exponentially modified protein abundance index (emPAI) for estimation of absolute protein amount in proteomics by the number of sequenced peptides per protein. *Mol Cell Proteomics* **4**, 1265–1272.

58 Ramos A, Hollingworth D & Pastore A (2003) G-quartet-dependent recognition between the FMRP RGG box and RNA. *RNA* **9**, 1198–1207.

59 Thandapani P, O'Connor TR, Bailey TL & Richard S (2013) Defining the RGG/RG motif. *Mol Cell* **50**, 613–623.

60 Phan AT, Kuryavyi V, Darnell JC, Serganov A, Majumdar A, Ilin S, Raslin T, Polonskaia A, Chen C, Clain D *et al.* (2011) Structure-function studies of FMRP RGG peptide recognition of an RNA duplex-quadruplex junction. *Nat Struct Mol Biol* **18**, 796–804.

61 Takahama K, Kino K, Arai S, Kurokawa R & Oyoshi T (2011) Identification of Ewing's sarcoma protein as a G-quadruplex DNA- and RNA-binding protein. *FEBS J* **278**, 988–998.

62 Tamanini F, Willemsen R, van Unen L, Bontekoe C, Galjaard H, Oostra BA & Hoogeveen AT (1997) Differential expression of FMR1, FXR1 and FXR2 proteins in human brain and testis. *Hum Mol Genet* **6**, 1315–1322.

63 Furukawa MT, Sakamoto H & Inoue K (2015) Interaction and colocalization of HERMES/RBPMS with NonO, PSF, and G3BP1 in neuronal cytoplasmic RNP granules in mouse retinal line cells. *Genes Cells* **20**, 257–266.

64 Kim SH, Dong WK, Weiler IJ & Greenough WT (2006) Fragile X mental retardation protein shifts between polyribosomes and stress granules after neuronal injury by arsenite stress or in vivo hippocampal electrode insertion. *J Neurosci* **26**, 2413–2418.

65 Matsuki H, Takahashi M, Higuchi M, Makokha GN, Oie M & Fujii M (2013) Both G3BP1 and G3BP2 contribute to stress granule formation. *Genes Cells* **18**, 135–146.

66 Tourriere H, Chebli K, Zekri L, Courselaud B, Blanchard JM, Bertrand E & Tazi J (2003) The RasGAP-associated endoribonuclease G3BP assembles stress granules. *J Cell Biol* **160**, 823–831.

67 Sanso M, Levin RS, Lipp JJ, Wang VY, Greifenberg AK, Quezada EM, Ali A, Ghosh A, Larochelle S, Rana TM *et al.* (2016) P-TEFb regulation of transcription termination factor Xrn2 revealed by a chemical genetic screen for Cdk9 substrates. *Genes Dev* **30**, 117–131.

68 Luca R, Averna M, Zalfa F, Vecchi M, Bianchi F, La Fata G, Del Nonno F, Nardacci R, Bianchi M, Nuciforo P *et al.* (2013) The fragile X protein binds mRNAs involved in cancer progression and modulates metastasis formation. *EMBO Mol Med* **5**, 1523–1536.

69 Sethna F, Moon C & Wang H (2014) From FMRP function to potential therapies for fragile X syndrome. *Neurochem Res* **39**, 1016–1031.

70 Bardoni B, Davidovic L, Bensaid M & Khandjian EW (2006) The fragile X syndrome: exploring its molecular basis and seeking a treatment. *Expert Rev Mol Med* **8**, 1–16.

71 Sidorov MS, Auerbach BD & Bear MF (2013) Fragile X mental retardation protein and synaptic plasticity. *Mol Brain* **6**, 15.

72 Kenny P & Ceman S (2016) RNA secondary structure modulates FMRP's bi-functional role in the microRNA pathway. *Int J Mol Sci* **17**, 985.

73 Kim M & Ceman S (2012) Fragile X mental retardation protein: past, present and future. *Curr Protein Pept Sci* **13**, 358–371.

74 Zalfa F, Achsel T & Bagni C (2006) mRNPs, polysomes or granules: FMRP in neuronal protein synthesis. *Curr Opin Neurobiol* **16**, 265–269.

75 Garber K, Smith KT, Reines D & Warren ST (2006) Transcription, translation and fragile X syndrome. *Curr Opin Genet Dev* **16**, 270–275.

76 Santos AR, Kanellopoulos AK & Bagni C (2014) Learning and behavioral deficits associated with the absence of the fragile X mental retardation protein: what a fly and mouse model can teach us. *Learn Mem* **21**, 543–555.

77 Pasciuto E & Bagni C (2014) SnapShot: FMRP mRNA targets and diseases. *Cell* **158**, 1446 e1441.

78 Adams-Cioaba MA, Guo Y, Bian C, Amaya MF, Lam R, Wasney GA, Vedadi M, Xu C & Min J (2010) Structural studies of the tandem Tudor domains of fragile X mental retardation related proteins FXR1 and FXR2. *PLoS One* **5**, e13559.

79 Dube M, Huot ME & Khandjian EW (2000) Muscle specific fragile X related protein 1 isoforms are sequestered in the nucleus of undifferentiated myoblast. *BMC Genet* **1**, 4.

80 Bardoni B, Castets M, Huot ME, Schenck A, Adinolfi S, Corbin F, Pastore A, Khandjian EW & Mandel JL (2003) 82-FIP, a novel FMRP (fragile X mental retardation protein) interacting protein, shows a cell cycle-dependent intracellular localization. *Hum Mol Genet* **12**, 1689–1698.

81 Lai D, Sakkas D & Huang Y (2006) The fragile X mental retardation protein interacts with a distinct mRNA nuclear export factor NXF2. *RNA* **12**, 1446–1449.

82 Dury AY, El Fatimy R, Tremblay S, Rose TM, Cote J, De Koninck P & Khandjian EW (2013) Nuclear fragile X mental retardation protein is localized to Cajal bodies. *PLoS Genet* **9**, e1003890.

83 Okray Z, de Esch CE, Van Esch H, Devriendt K, Claeys A, Yan J, Verbeeck J, Froyen G, Willemsen R, de Vrij FM *et al.* (2015) A novel fragile X syndrome mutation reveals a conserved role for the carboxy-terminus in FMRP localization and function. *EMBO Mol Med* **7**, 423–437.

84 Tan W, Schauder C, Naryshkina T, Minakhina S & Steward R (2016) Zfrp8 forms a complex with fragile-X mental retardation protein and regulates its localization and function. *Dev Biol* **410**, 202–212.

85 Vannini A & Cramer P (2012) Conservation between the RNA polymerase I, II, and III transcription initiation machineries. *Mol Cell* **45**, 439–446.

86 Miyashiro KY, Beckel-Mitchener A, Purk TP, Becker KG, Barret T, Liu L, Carbonetto S, Weiler IJ, Greenough WT & Eberwine J (2003) RNA cargoes associating with FMRP reveal deficits in cellular functioning in Fmr1 null mice. *Neuron* **37**, 417–431.

87 Tomson BN & Arndt KM (2013) The many roles of the conserved eukaryotic Paf1 complex in regulating transcription, histone modifications, and disease states. *Biochim Biophys Acta* **1829**, 116–126.

88 Miyamoto K & Gurdon JB (2013) Transcriptional regulation and nuclear reprogramming: roles of nuclear actin and actin-binding proteins. *Cell Mol Life Sci* **70**, 3289–3302.

89 Folk P, Puta F & Skruzny M (2004) Transcriptional coregulator SNW/SKIP: the concealed tie of dissimilar pathways. *Cell Mol Life Sci* **61**, 629–640.

90 Ma Y, Wang C, Li B, Qin L, Su J, Yang M & He S (2014) Bcl-2-associated transcription factor 1 interacts with fragile X-related protein 1. *Acta Biochim Biophys Sin (Shanghai)* **46**, 119–127.

91 Liu H, Lu ZG, Miki Y & Yoshida K (2007) Protein kinase C delta induces transcription of the TP53 tumor suppressor gene by controlling death-promoting factor Btf in the apoptotic response to DNA damage. *Mol Cell Biol* **27**, 8480–8491.

92 Ono W, Hayashi Y, Yokoyama W, Kuroda T, Kishimoto H, Ito I, Kimura K, Akaogi K, Waku T & Yanagisawa J (2014) The nucleolar protein Myb-binding protein 1A (MYBBP1A) enhances p53 tetramerization and acetylation in response to nucleolar disruption. *J Biol Chem* **289**, 4928–4940.

93 Liu X, Tan Y, Zhang C, Zhang Y, Zhang L, Ren P, Deng H, Luo J, Ke Y & Du X (2016) NAT10 regulates p53 activation through acetylating p53 at K120 and ubiquitinating Mdm2. *EMBO Rep* **17**, 349–366.

94 Endo A, Tomizawa D, Aoki Y, Morio T, Mizutani S & Takagi M (2016) EWSR1/ELF5 induces acute myeloid leukemia by inhibiting p53/p21 pathway. *Cancer Sci* **107**, 1745–1754.

95 Wang C, Ivanov A, Chen L, Fredericks WJ, Seto E, Rauscher FJ III & Chen J (2005) MDM2 interaction with nuclear corepressor KAP1 contributes to p53 inactivation. *EMBO J* **24**, 3279–3290.

96 Okamoto K, Kitabayashi I & Taya Y (2006) KAP1 dictates p53 response induced by chemotherapeutic agents via Mdm2 interaction. *Biochem Biophys Res Commun* **351**, 216–222.

97 Jung DJ, Sung HS, Goo YW, Lee HM, Park OK, Jung SY, Lim J, Kim HJ, Lee SK, Kim TS *et al.* (2002) Novel transcription coactivator complex containing activating signal cointegrator 1. *Mol Cell Biol* **22**, 5203–5211.

98 Wei H, Wang B, Miyagi M, She Y, Gopalan B, Huang DB, Ghosh G, Stark GR & Lu T (2013) PRMT5 dimethylates R30 of the p65 subunit to activate NF-kappaB. *Proc Natl Acad Sci USA* **110**, 13516–13521.

99 Hwang SK, Baker AR, Young MR & Colburn NH (2014) Tumor suppressor PDCD4 inhibits NF-kappaB-dependent transcription in human glioblastoma cells by direct interaction with p65. *Carcinogenesis* **35**, 1469–1480.

100 Rother S, Bartels M, Schweda AT, Resch K, Pallua N & Nourbakhsh M (2016) NF-kappaB-repressing factor phosphorylation regulates transcription elongation via its interactions with 5'–>3' exoribonuclease 2 and negative elongation factor. *FASEB J* **30**, 174–185.

101 Owen HR, Elser M, Cheung E, Gersbach M, Kraus WL & Hottiger MO (2007) MYBBP1a is a novel repressor of NF-kappaB. *J Mol Biol* **366**, 725–736.

102 Ormsbee Golden BD, Wuebben EL & Rizzino A (2013) Sox2 expression is regulated by a negative feedback loop in embryonic stem cells that involves AKT signaling and FoxO1. *PLoS One* **8**, e76345.

103 Li W, Zhang Z, Zhao W & Han N (2016) Transglutaminase 3 protein modulates human esophageal cancer cell growth by targeting the NF-kappaB signaling pathway. *Oncol Rep* **36**, 1723–1730.

104 Yu H, Zhao J, Lin L, Zhang Y, Zhong F, Liu Y, Yu Y, Shen H, Han M, He F *et al.* (2012) Proteomic study explores AGR2 as pro-metastatic protein in HCC. *Mol Biosyst* **8**, 2710–2718.

105 Bourgeois CF, Mortreux F & Auboeuf D (2016) The multiple functions of RNA helicases as drivers and regulators of gene expression. *Nat Rev Mol Cell Biol* **17**, 426–438.

106 Kunde SA, Musante L, Grimme A, Fischer U, Muller E, Wanker EE & Kalscheuer VM (2011) The X-chromosome-linked intellectual disability protein PQBP1 is a component of neuronal RNA granules and regulates the appearance of stress granules. *Hum Mol Genet* **20**, 4916–4931.

107 Chen HH, Yu HI, Cho WC & Tarn WY (2015) DDX3 modulates cell adhesion and motility and cancer cell metastasis via Rac1-mediated signaling pathway. *Oncogene* **34**, 2790–2800.

108 Copsey AC, Cooper S, Parker R, Lineham E, Lapworth C, Jallad D, Sweet S & Morley SJ (2017) DDX3X interacts with PABP1 and caprin-1 at the leading edge of migrating fibroblasts and is required for efficient cell spreading. *Biochem J* **474**, 3109–3120. https://doi.org/10.1042/bcj20170354

109 Song J, Perreault JP, Topisirovic I & Richard S (2016) RNA G-quadruplexes and their potential regulatory roles in translation. *Translation (Austin)* **4**, e1244031.

110 Newman M, Sfaxi R, Saha A, Monchaud D, Teulade-Fichou MP & Vagner S (2016) The G-quadruplex-specific RNA helicase DHX36 regulates p53 pre-mRNA 3'-end processing following UV-induced DNA damage. *J Mol Biol* **429**, 3121–3131.

111 Jo JH, Chung TM, Youn H & Yoo JY (2014) Cytoplasmic parafibromin/hCdc73 targets and destabilizes p53 mRNA to control p53-mediated apoptosis. *Nat Commun* **5**, 5433.

112 de Planell-Saguer M, Schroeder DG, Rodicio MC, Cox GA & Mourelatos Z (2009) Biochemical and genetic evidence for a role of IGHMBP2 in the translational machinery. *Hum Mol Genet* **18**, 2115–2126.

113 Qu X, Yang Z, Zhang S, Shen L, Dangel AW, Hughes JH, Redman KL, Wu LC & Yu CY (1998) The human DEVH-box protein Ski2w from the HLA is localized in nucleoli and ribosomes. *Nucleic Acids Res* **26**, 4068–4077.

114 Matera AG & Wang Z (2014) A day in the life of the spliceosome. *Nat Rev Mol Cell Biol* **15**, 108–121.

115 Will CL & Luhrmann R (2011) Spliceosome structure and function. *Cold Spring Harb Perspect Biol* **3**, a003707.

116 Passon DM, Lee M, Rackham O, Stanley WA, Sadowska A, Filipovska A, Fox AH & Bond CS (2012) Structure of the heterodimer of human NONO and paraspeckle protein component 1 and analysis of its role in subnuclear body formation. *Proc Natl Acad Sci USA* **109**, 4846–4850.

117 Yarosh CA, Iacona JR, Lutz CS & Lynch KW (2015) PSF: nuclear busy-body or nuclear facilitator? *Wiley Interdiscip Rev RNA* **6**, 351–367.

118 Goncalves V, Henriques AF, Pereira JF, Neves Costa A, Moyer MP, Moita LF, Gama-Carvalho M, Matos P & Jordan P (2014) Phosphorylation of SRSF1 by SRPK1 regulates alternative splicing of tumor-related Rac1b in colorectal cells. *RNA* **20**, 474–482.

119 Fiegen D, Haeusler LC, Blumenstein L, Herbrand U, Dvorsky R, Vetter IR & Ahmadian MR (2004) Alternative splicing of Rac1 generates Rac1b, a self-activating GTPase. *J Biol Chem* **279**, 4743–4749.

120 Drakouli S, Lyberopoulou A, Papathanassiou M, Mylonis I & Georgatsou E (2017) Enhancer of rudimentary homologue interacts with scaffold attachment factor B at the nuclear matrix to regulate SR protein phosphorylation. *FEBS J* **284**, 2482–2500.

121 Weng MT, Lee JH, Wei SC, Li Q, Shahamatdar S, Hsu D, Schetter AJ, Swatkoski S, Mannan P, Garfield S *et al*. (2012) Evolutionarily conserved protein ERH controls CENP-E mRNA splicing and is required for the survival of KRAS mutant cancer cells. *Proc Natl Acad Sci USA* **109**, E3659–E3667.

122 Weng MT, Tung TH, Lee JH, Wei SC, Lin HL, Huang YJ, Wong JM, Luo J & Sheu JC (2015) Enhancer of rudimentary homolog regulates DNA damage response in hepatocellular carcinoma. *Sci Rep* **5**, 9357.

123 Chen Y, Zhang L & Jones KA (2011) SKIP counteracts p53-mediated apoptosis via selective regulation of p21Cip1 mRNA splicing. *Genes Dev* **25**, 701–716.

124 Gayatri S & Bedford MT (2014) Readers of histone methylarginine marks. *Biochim Biophys Acta* **1839**, 702–710.

125 Muller-McNicoll M, Botti V, de Jesus Domingues AM, Brandl H, Schwich OD, Steiner MC, Curk T, Poser I, Zarnack K & Neugebauer KM (2016) SR proteins are NXF1 adaptors that link alternative RNA processing to mRNA export. *Genes Dev* **30**, 553–566.

126 Perez-Gonzalez A, Pazo A, Navajas R, Ciordia S, Rodriguez-Frandsen A & Nieto A (2014) hCLE/C14orf166 associates with DDX1-HSPC117-FAM98B in a novel transcription-dependent shuttling RNA-transporting complex. *PLoS One* **9**, e90957.

127 Anderson P & Kedersha N (2006) RNA granules. *J Cell Biol* **172**, 803–808.

128 Stoecklin G & Kedersha N (2013) Relationship of GW/P-bodies with stress granules. *Adv Exp Med Biol* **768**, 197–211.

129 Kedersha N & Anderson P (2009) Regulation of translation by stress granules and processing bodies. *Prog Mol Biol Transl Sci* **90**, 155–185.

130 Kedersha N, Ivanov P & Anderson P (2013) Stress granules and cell signaling: more than just a passing phase? *Trends Biochem Sci* **38**, 494–506.

131 Gareau C, Houssin E, Martel D, Coudert L, Mellaoui S, Huot ME, Laprise P & Mazroui R (2013) Characterization of fragile X mental retardation protein recruitment and dynamics in *Drosophila* stress granules. *PLoS One* **8**, e55342.

132 Pascual ML, Luchelli L, Habif M & Boccaccio GL (2012) Synaptic activity regulated mRNA-silencing foci for the fine tuning of local protein synthesis at the synapse. *Commun Integr Biol* **5**, 388–392.

133 Mazroui R, Huot ME, Tremblay S, Filion C, Labelle Y & Khandjian EW (2002) Trapping of messenger RNA by fragile X mental retardation protein into cytoplasmic granules induces translation repression. *Hum Mol Genet* **11**, 3007–3017.

134 Stefani G, Fraser CE, Darnell JC & Darnell RB (2004) Fragile X mental retardation protein is

108 Copsey AC, Cooper S, Parker R, Lineham E, Lapworth C, Jallad D, Sweet S & Morley SJ (2017) DDX3X interacts with PABP1 and caprin-1 at the leading edge of migrating fibroblasts and is required for efficient cell spreading. *Biochem J* **474**, 3109–3120. https://doi.org/10.1042/bcj20170354

109 Song J, Perreault JP, Topisirovic I & Richard S (2016) RNA G-quadruplexes and their potential regulatory roles in translation. *Translation (Austin)* **4**, e1244031.

110 Newman M, Sfaxi R, Saha A, Monchaud D, Teulade-Fichou MP & Vagner S (2016) The G-quadruplex-specific RNA helicase DHX36 regulates p53 pre-mRNA 3'-end processing following UV-induced DNA damage. *J Mol Biol* **429**, 3121–3131.

111 Jo JH, Chung TM, Youn H & Yoo JY (2014) Cytoplasmic parafibromin/hCdc73 targets and destabilizes p53 mRNA to control p53-mediated apoptosis. *Nat Commun* **5**, 5433.

112 de Planell-Saguer M, Schroeder DG, Rodicio MC, Cox GA & Mourelatos Z (2009) Biochemical and genetic evidence for a role of IGHMBP2 in the translational machinery. *Hum Mol Genet* **18**, 2115–2126.

113 Qu X, Yang Z, Zhang S, Shen L, Dangel AW, Hughes JH, Redman KL, Wu LC & Yu CY (1998) The human DEVH-box protein Ski2w from the HLA is localized in nucleoli and ribosomes. *Nucleic Acids Res* **26**, 4068–4077.

114 Matera AG & Wang Z (2014) A day in the life of the spliceosome. *Nat Rev Mol Cell Biol* **15**, 108–121.

115 Will CL & Luhrmann R (2011) Spliceosome structure and function. *Cold Spring Harb Perspect Biol* **3**, a003707.

116 Passon DM, Lee M, Rackham O, Stanley WA, Sadowska A, Filipovska A, Fox AH & Bond CS (2012) Structure of the heterodimer of human NONO and paraspeckle protein component 1 and analysis of its role in subnuclear body formation. *Proc Natl Acad Sci USA* **109**, 4846–4850.

117 Yarosh CA, Iacona JR, Lutz CS & Lynch KW (2015) PSF: nuclear busy-body or nuclear facilitator? *Wiley Interdiscip Rev RNA* **6**, 351–367.

118 Goncalves V, Henriques AF, Pereira JF, Neves Costa A, Moyer MP, Moita LF, Gama-Carvalho M, Matos P & Jordan P (2014) Phosphorylation of SRSF1 by SRPK1 regulates alternative splicing of tumor-related Rac1b in colorectal cells. *RNA* **20**, 474–482.

119 Fiegen D, Haeusler LC, Blumenstein L, Herbrand U, Dvorsky R, Vetter IR & Ahmadian MR (2004) Alternative splicing of Rac1 generates Rac1b, a self-activating GTPase. *J Biol Chem* **279**, 4743–4749.

120 Drakouli S, Lyberopoulou A, Papathanassiou M, Mylonis I & Georgatsou E (2017) Enhancer of rudimentary homologue interacts with scaffold attachment factor B at the nuclear matrix to regulate SR protein phosphorylation. *FEBS J* **284**, 2482–2500.

121 Weng MT, Lee JH, Wei SC, Li Q, Shahamatdar S, Hsu D, Schetter AJ, Swatkoski S, Mannan P, Garfield S *et al*. (2012) Evolutionarily conserved protein ERH controls CENP-E mRNA splicing and is required for the survival of KRAS mutant cancer cells. *Proc Natl Acad Sci USA* **109**, E3659–E3667.

122 Weng MT, Tung TH, Lee JH, Wei SC, Lin HL, Huang YJ, Wong JM, Luo J & Sheu JC (2015) Enhancer of rudimentary homolog regulates DNA damage response in hepatocellular carcinoma. *Sci Rep* **5**, 9357.

123 Chen Y, Zhang L & Jones KA (2011) SKIP counteracts p53-mediated apoptosis via selective regulation of p21Cip1 mRNA splicing. *Genes Dev* **25**, 701–716.

124 Gayatri S & Bedford MT (2014) Readers of histone methylarginine marks. *Biochim Biophys Acta* **1839**, 702–710.

125 Muller-McNicoll M, Botti V, de Jesus Domingues AM, Brandl H, Schwich OD, Steiner MC, Curk T, Poser I, Zarnack K & Neugebauer KM (2016) SR proteins are NXF1 adaptors that link alternative RNA processing to mRNA export. *Genes Dev* **30**, 553–566.

126 Perez-Gonzalez A, Pazo A, Navajas R, Ciordia S, Rodriguez-Frandsen A & Nieto A (2014) hCLE/C14orf166 associates with DDX1-HSPC117-FAM98B in a novel transcription-dependent shuttling RNA-transporting complex. *PLoS One* **9**, e90957.

127 Anderson P & Kedersha N (2006) RNA granules. *J Cell Biol* **172**, 803–808.

128 Stoecklin G & Kedersha N (2013) Relationship of GW/P-bodies with stress granules. *Adv Exp Med Biol* **768**, 197–211.

129 Kedersha N & Anderson P (2009) Regulation of translation by stress granules and processing bodies. *Prog Mol Biol Transl Sci* **90**, 155–185.

130 Kedersha N, Ivanov P & Anderson P (2013) Stress granules and cell signaling: more than just a passing phase? *Trends Biochem Sci* **38**, 494–506.

131 Gareau C, Houssin E, Martel D, Coudert L, Mellaoui S, Huot ME, Laprise P & Mazroui R (2013) Characterization of fragile X mental retardation protein recruitment and dynamics in *Drosophila* stress granules. *PLoS One* **8**, e55342.

132 Pascual ML, Luchelli L, Habif M & Boccaccio GL (2012) Synaptic activity regulated mRNA-silencing foci for the fine tuning of local protein synthesis at the synapse. *Commun Integr Biol* **5**, 388–392.

133 Mazroui R, Huot ME, Tremblay S, Filion C, Labelle Y & Khandjian EW (2002) Trapping of messenger RNA by fragile X mental retardation protein into cytoplasmic granules induces translation repression. *Hum Mol Genet* **11**, 3007–3017.

134 Stefani G, Fraser CE, Darnell JC & Darnell RB (2004) Fragile X mental retardation protein is

associated with translating polyribosomes in neuronal cells. *J Neurosci* **24**, 7272–7276.
135 Lee YJ, Wei HM, Chen LY & Li C (2014) Localization of SERBP1 in stress granules and nucleoli. *FEBS J* **281**, 352–364.
136 Bish R, Cuevas-Polo N, Cheng Z, Hambardzumyan D, Munschauer M, Landthaler M & Vogel C (2015) Comprehensive protein interactome analysis of a key RNA helicase: detection of novel stress granule proteins. *Biomolecules* **5**, 1441–1466.
137 Yuan L, Xiao Y, Zhou Q, Yuan D, Wu B, Chen G & Zhou J (2014) Proteomic analysis reveals that MAEL, a component of nuage, interacts with stress granule proteins in cancer cells. *Oncol Rep* **31**, 342–350.
138 Bai Y, Dong Z, Shang Q, Zhao H, Wang L, Guo C, Gao F, Zhang L & Wang Q (2016) Pdcd4 is involved in the formation of stress granule in response to oxidized low-density lipoprotein or high-fat diet. *PLoS One* **11**, e0159568.
139 Kedersha N, Panas MD, Achorn CA, Lyons S, Tisdale S, Hickman T, Thomas M, Lieberman J, McInerney GM, Ivanov P *et al*. (2016) G3BP-Caprin1-USP10 complexes mediate stress granule condensation and associate with 40S subunits. *J Cell Biol* **212**, 845–860.
140 Tosar LJ, Thomas MG, Baez MV, Ibanez I, Chernomoretz A & Boccaccio GL (2012) Staufen: from embryo polarity to cellular stress and neurodegeneration. *Front Biosci (Schol Ed)* **4**, 432–452.
141 Kobayashi T, Winslow S, Sunesson L, Hellman U & Larsson C (2012) PKCalpha binds G3BP2 and regulates stress granule formation following cellular stress. *PLoS One* **7**, e35820.
142 Moser JJ, Eystathioy T, Chan EK & Fritzler MJ (2007) Markers of mRNA stabilization and degradation, and RNAi within astrocytoma GW bodies. *J Neurosci Res* **85**, 3619–3631.
143 Panas MD, Ivanov P & Anderson P (2016) Mechanistic insights into mammalian stress granule dynamics. *J Cell Biol* **215**, 313–323.
144 Saunders LR, Perkins DJ, Balachandran S, Michaels R, Ford R, Mayeda A & Barber GN (2001) Characterization of two evolutionarily conserved, alternatively spliced nuclear phosphoproteins, NFAR-1 and -2, that function in mRNA processing and interact with the double-stranded RNA-dependent protein kinase, PKR. *J Biol Chem* **276**, 32300–32312.
145 Shiina N & Nakayama K (2014) RNA granule assembly and disassembly modulated by nuclear factor associated with double-stranded RNA 2 and nuclear factor 45. *J Biol Chem* **289**, 21163–21180.
146 Reineke LC, Kedersha N, Langereis MA, van Kuppeveld FJ & Lloyd RE (2015) Stress granules regulate double-stranded RNA-dependent protein kinase activation through a complex containing G3BP1 and Caprin1. *MBio* **6**, e02486.
147 Reineke LC & Lloyd RE (2015) The stress granule protein G3BP1 recruits protein kinase R to promote multiple innate immune antiviral responses. *J Virol* **89**, 2575–2589.
148 Didiot MC, Subramanian M, Flatter E, Mandel JL & Moine H (2009) Cells lacking the fragile X mental retardation protein (FMRP) have normal RISC activity but exhibit altered stress granule assembly. *Mol Biol Cell* **20**, 428–437.
149 Richter JD, Bassell GJ & Klann E (2015) Dysregulation and restoration of translational homeostasis in fragile X syndrome. *Nat Rev Neurosci* **16**, 595–605.
150 Khandjian EW, Huot ME, Tremblay S, Davidovic L, Mazroui R & Bardoni B (2004) Biochemical evidence for the association of fragile X mental retardation protein with brain polyribosomal ribonucleoparticles. *Proc Natl Acad Sci USA* **101**, 13357–13362.
151 Ceman S, O'Donnell WT, Reed M, Patton S, Pohl J & Warren ST (2003) Phosphorylation influences the translation state of FMRP-associated polyribosomes. *Hum Mol Genet* **12**, 3295–3305.
152 Das S & Das B (2016) eIF4G-an integrator of mRNA metabolism? *FEMS Yeast Res* **16**, fow087.
153 Loh PG, Yang HS, Walsh MA, Wang Q, Wang X, Cheng Z, Liu D & Song H (2009) Structural basis for translational inhibition by the tumour suppressor Pdcd4. *EMBO J* **28**, 274–285.
154 Yang HS, Jansen AP, Komar AA, Zheng X, Merrick WC, Costes S, Lockett SJ, Sonenberg N & Colburn NH (2003) The transformation suppressor Pdcd4 is a novel eukaryotic translation initiation factor 4A binding protein that inhibits translation. *Mol Cell Biol* **23**, 26–37.
155 Lahr RM, Fonseca BD, Ciotti GE, Al-Ashtal HA, Jia JJ, Niklaus MR, Blagden SP, Alain T & Berman AJ (2017) La-related protein 1 (LARP1) binds the mRNA cap, blocking eIF4F assembly on TOP mRNAs. *Elife* **6**, e24146.
156 Mizutani R, Imamachi N, Suzuki Y, Yoshida H, Tochigi N, Oonishi T, Suzuki Y & Akimitsu N (2016) Oncofetal protein IGF2BP3 facilitates the activity of proto-oncogene protein eIF4E through the destabilization of EIF4E-BP2 mRNA. *Oncogene* **35**, 3495–3502.
157 Solomon S, Xu Y, Wang B, David MD, Schubert P, Kennedy D & Schrader JW (2007) Distinct structural features of caprin-1 mediate its interaction with G3BP-1 and its induction of phosphorylation of eukaryotic translation initiation factor 2alpha, entry to cytoplasmic stress granules, and selective interaction with a subset of mRNAs. *Mol Cell Biol* **27**, 2324–2342.

158 Kruse C, Willkomm D, Gebken J, Schuh A, Stossberg H, Vollbrandt T & Muller PK (2003) The multi-KH protein vigilin associates with free and membrane-bound ribosomes. *Cell Mol Life Sci* **60**, 2219–2227.
159 Guenther UP, Handoko L, Laggerbauer B, Jablonka S, Chari A, Alzheimer M, Ohmer J, Plottner O, Gehring N, Sickmann A *et al.* (2009) IGHMBP2 is a ribosome-associated helicase inactive in the neuromuscular disorder distal SMA type 1 (DSMA1). *Hum Mol Genet* **18**, 1288–1300.
160 Duning K, Buck F, Barnekow A & Kremerskothen J (2008) SYNCRIP, a component of dendritically localized mRNPs, binds to the translation regulator BC200 RNA. *J Neurochem* **105**, 351–359.
161 Sugiyama H, Takahashi K, Yamamoto T, Iwasaki M, Narita M, Nakamura M, Rand TA, Nakagawa M, Watanabe A & Yamanaka S (2017) Nat1 promotes translation of specific proteins that induce differentiation of mouse embryonic stem cells. *Proc Natl Acad Sci USA* **114**, 340–345.
162 Stewart JD, Cowan JL, Perry LS, Coldwell MJ & Proud CG (2015) ABC50 mutants modify translation start codon selection. *Biochem J* **467**, 217–229.
163 Maurer-Stroh S, Dickens NJ, Hughes-Davies L, Kouzarides T, Eisenhaber F & Ponting CP (2003) The Tudor domain 'Royal Family': Tudor, plant Agenet, Chromo, PWWP and MBT domains. *Trends Biochem Sci* **28**, 69–74.
164 Hu Y, Chen Z, Fu Y, He Q, Jiang L, Zheng J, Gao Y, Mei P & Ren X (2015) The amino-terminal structure of human fragile X mental retardation protein obtained using precipitant-immobilized imprinted polymers. *Nat Commun* **6**, 6634.
165 Valverde R, Edwards L & Regan L (2008) Structure and function of KH domains. *FEBS J* **275**, 2712–2726.
166 Nicastro G, Taylor IA & Ramos A (2015) KH-RNA interactions: back in the groove. *Curr Opin Struct Biol* **30**, 63–70.
167 Oi N, Yuan J, Malakhova M, Luo K, Li Y, Ryu J, Zhang L, Bode AM, Xu Z, Lou Z *et al.* (2015) Resveratrol induces apoptosis by directly targeting Ras-GTPase-activating protein SH3 domain-binding protein 1. *Oncogene* **34**, 2660–2671.
168 Kim ED, Sabharwal A, Vetta AR & Blanchette M (2010) Predicting direct protein interactions from affinity purification mass spectrometry data. *Algorithms Mol Biol* **5**, 34.
169 Eberth A & Ahmadian MR (2009) In vitro GEF and GAP assays. *Curr Protoc Cell Biol* **Chapter 14**, Unit 14.9.
170 Jaiswal M, Gremer L, Dvorsky R, Haeusler LC, Cirstea IC, Uhlenbrock K & Ahmadian MR (2011) Mechanistic insights into specificity, activity, and regulatory elements of the regulator of G-protein signaling (RGS)-containing Rho-specific guanine nucleotide exchange factors (GEFs) p115, PDZ-RhoGEF (PRG), and leukemia-associated RhoGEF (LARG). *J Biol Chem* **286**, 18202–18212.
171 Haghighi F, Dahlmann J, Nakhaei-Rad S, Lang A, Kutschka I, Zenker M, Kensah G, Piekorz RP & Ahmadian MR (2018) bFGF-mediated pluripotency maintenance in human induced pluripotent stem cells is associated with NRAS-MAPK signaling. *Cell Commun Signal* **16**, 96.
172 Gorg B, Karababa A, Shafigullina A, Bidmon HJ & Haussinger D (2015) Ammonia-induced senescence in cultured rat astrocytes and in human cerebral cortex in hepatic encephalopathy. *Glia* **63**, 37–50.
173 Poschmann G, Seyfarth K, Besong Agbo D, Klafki HW, Rozman J, Wurst W, Wiltfang J, Meyer HE, Klingenspor M & Stuhler K (2014) High-fat diet induced isoform changes of the Parkinson's disease protein DJ-1. *J Proteome Res* **13**, 2339–2351.
174 Tusher VG, Tibshirani R & Chu G (2001) Significance analysis of microarrays applied to the ionizing radiation response. *Proc Natl Acad Sci USA* **98**, 5116–5121.
175 Mi H, Huang X, Muruganujan A, Tang H, Mills C, Kang D & Thomas PD (2017) PANTHER version 11: expanded annotation data from Gene Ontology and Reactome pathways, and data analysis tool enhancements. *Nucleic Acids Res* **45**, D183–D189.
176 Shannon P, Markiel A, Ozier O, Baliga NS, Wang JT, Ramage D, Amin N, Schwikowski B & Ideker T (2003) Cytoscape: a software environment for integrated models of biomolecular interaction networks. *Genome Res* **13**, 2498–2504.

Chapter V

The binding selectivity of effectors for RAS proteins

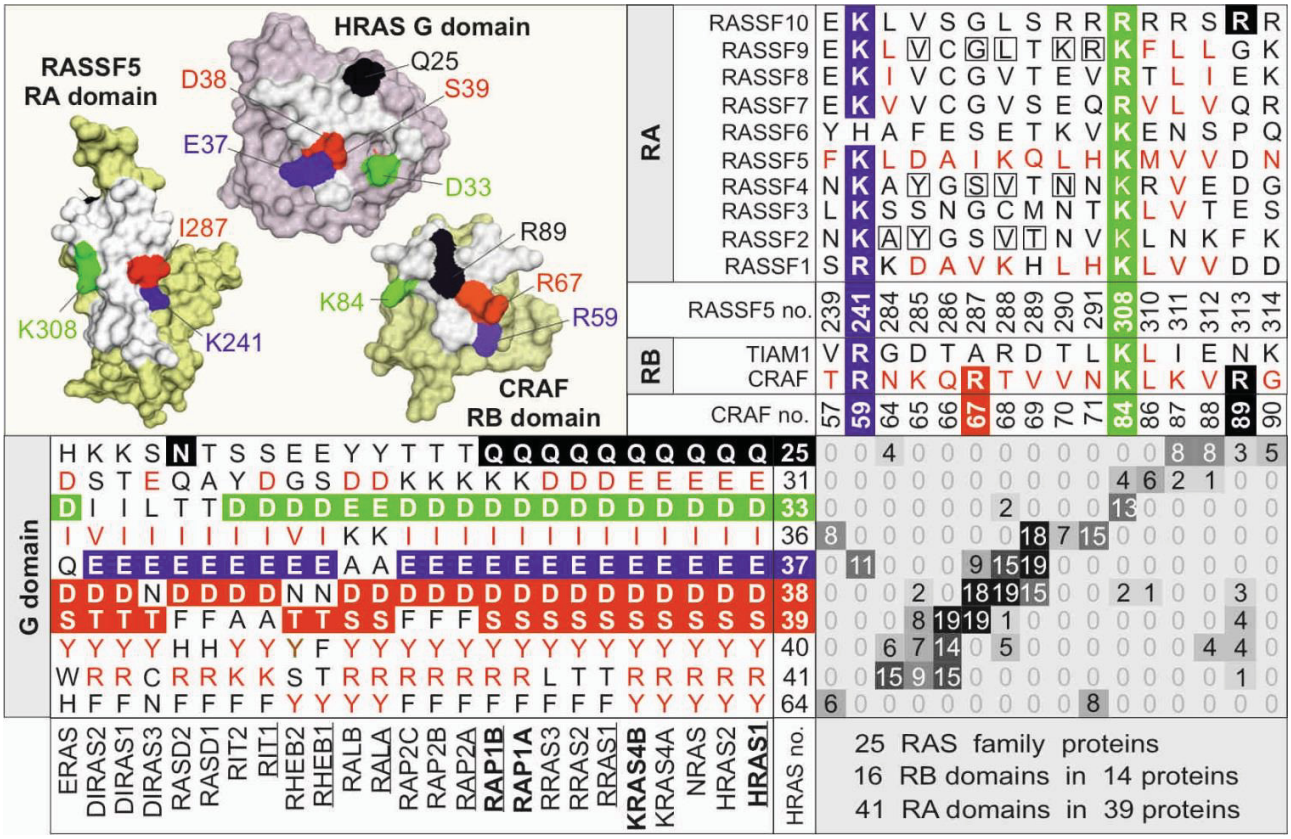

Published in:	Journal of Molecular Biology
Impact factor:	4.238 (2020)
Own Proportion to this work:	40%

Purification of RAS GTPases, RASSFs, mutational and interaction analysis of RAS GTPases with RAS effectors using Fluorescence polarization, and Pulldown assay of RASSF5,7 and 9 with RIT1 and

HRAS using HEK293 cell line, writing and revising the manuscript

The RAS binding selectivity of the RAS-association domain family proteins*

Soheila Rezaei Adariani[1#], Neda S. Kazemein Jasemi[1#], Farhad Bazgir[1], Christoph Wittich[1], Ehsan Amin[1,2], Claus A. M. Seidel[3], Radovan Dvorsky[1], Mohammad R. Ahmadian[1@]

[1] Institute of Biochemistry and Molecular Biology II, Heinrich Heine University, Medical Faculty, 40225 Düsseldorf, Germany

[2] Institute of Neural and Sensory Physiology, Heinrich Heine University, Medical Faculty, 40225 Düsseldorf, Germany

[3] Chair of Molecular Physical Chemistry, Heinrich Heine University, 40225 Düsseldorf, Germany

*Running title: RAS-RASSF selectivity

[#]These authors equally contributed to this study

@Corresponding author: reza.ahmadian@hhu.de

Key words: Effectors; GTPase; NORE-1; protein interactions; RAS; RA domain; RAF kinase; RASSF; RASSF1; RASSF5; RAS association domain; RAS binding domain; RB domain

RAS effectors specifically interact with the GTP-bound RAS proteins to link extracellular signals to downstream signaling pathways. Physical interactions of the effectors are achieved by two types of domains, called RAS binding (RB) and RAS association (RA) domains, which share common structural characteristics. Searching through the human proteome databases, we extracted 41 RA domains in 39 proteins and 16 RB domains in 14 proteins in the human proteome, each of which can specifically select one of the 25 members in the RAS family. Most of the RA/RB domain containing proteins have remained largely uncharacterized, although the molecular nature of RAS-effector interactions is well-studied for

some proteins. Here, we comprehensively investigated the sequence-structure-function relationship between different representatives of the RAS family, including HRAS, RRAS, RALA, RAP1B, RAP2A, RHEB1, and RIT1, with all members of RA domain family proteins (RASSFs) and the RB domain-containing CRAF. The binding affinity for RAS-effector interactions, determined using fluorescence polarization, broadly ranges between high (0.3 μM) and very low (500 μM) affinities, which raised a central question about the relevance of variable binding affinities in the regulation of signaling events. Our study determined mainly two hotspots throughout the RA/RB domains from an average of 19 RAS-binding residues. Moreover, we found novel interactions of RRAS1, RIT1, and RALA for RASSF7, RASSF9, and RASSF1, respectively, which were systematically explored in sequence-structure-property relationship analysis, and validated by mutational analysis. Distinct functional properties and possible biological roles of these interactions remain to be investigated in the cellular context.

Introduction

RAS family proteins control activities of multiple signaling pathways and consequently a wide array of cellular processes, including survival, growth, adhesion, migration, and differentiation (*116*). Any dysregulation of these pathways leads, thus, to cancer, developmental disorders, metabolic, and cardiovascular diseases (*117*). Signal transduction implies a physical association of RAS proteins with and activation of a spectrum of functionally diverse downstream effectors, *e.g.*, CRAF, PI3Kα, TIAM1, RALGDS, PLCε, and RASSF5 (*23, 118-125*). RAS-effector interaction essentially requires RAS association with membranes (*126*), and its activation by specific regulatory proteins (*e.g.*, guanine nucleotide exchange factors or GEFs), leading to the formation of GTP-bound, active RAS (*127-129*). Notably, RAS proteins change their conformation mainly at two mobile regions, designated as a switch I (residues 30-40) and switch II (residues 60-68) (*6, 130, 131*). Only in GTP-bound form, the switch regions of the RAS proteins provide a platform for the association of the effector proteins (*132, 133*).

To date, two types of domains, the RAS binding (RB) and RAS association (RA) domains, have been defined for various effectors. They are comprised of 80-100 amino acids and have a similar ubiquitin-like topology (*122, 134-137*). Considering different RAS effectors, RB, and RA domain interactions with RAS proteins do not exhibit the same mode of interaction between different RAS effectors. However, CRAF RB and RALGDS RA domains share a similar structure and contact the switch I region *via* a similar binding mode (*138, 139*). In contrast, PI3Kα RB, RASSF5 RA, and PLCε RA domains do not share sequence and structural similarity but commonly associate with the switch regions, particularly switch I (*140-142*). RAS-effector interaction strikingly shares a similar binding mode adopted by three components: Two antiparallel β-sheets of the RA/RB domains and the RAS switch I region, respectively, and the first α-helix of the RA/RB domains (*143*).

In this study, we conducted an in-depth database search in the human proteome and extracted 57 RA/RB domains. We used 10 RASSF RA domains to analyze their interactions with 7 representatives of the RAS proteins family, including HRAS, RRAS1, RAP1B, RAP2A, RALA, RIT1, and RHEB1.

CRAF RB domain was used as control. The binding analysis was performed under the same conditions using fluorescence polarization. Obtained dissociation constants (K_d) with a broad range (0.3 – 500 μM) along with a matrix for a potential interaction of 25 RAS proteins and 57 RA/RB domains provide us a detailed view of the sequence-structure-property relationships of RAS-effector binding capabilities.

Results

Human proteome contains 39 RA and 14 RB domain-containing proteins

Mining in the UniProt database led to the extraction of 130 RB and 145 RA domain-containing proteins, respectively. In a parallel search using HMMER, 127 RB and 164 RA domain-containing proteins were extracted. These numbers were reduced to 46 RB and 97 RA domain-containing proteins by excluding proteins containing RHO binding domains, mitochondrial proton/calcium antiporter domain, and receptors. In the last step, all isoforms with identical sequences of the RB and RA domains were excluded using multiple sequence alignments generated with the ClustalW algorithm. This approach identified a total number of 16 RB domains in 14 RB domain-containing proteins and 41 RA domains in 39 RA domain-containing proteins, (Fig. S1; Tables S1, S2). Both types of RAS effector domains share sequence identity 10.5% and 9.2% and sequence similarity of 25.5% and 20.2% (Fig. S2 and S3).

The direct interaction of different RA domain-containing proteins with RAS proteins has been comprehensively analyzed (*136, 144*). However, the majority of proteins with a RA domain, remain uncharacterized (Table S1). The RAS association domain family (RASSF), which controls a broad range of signaling pathways (*122, 145*), is the largest RA domain-containing protein family (Fig. 1). Their RA domains differently interact with classical RAS proteins (*122, 137*). Among them, only the interaction of RASSF1 and RASSF5/NORE1 RA domains have been characterized quantitatively so far (*136, 144*). Other characterized RA domain-containing proteins, including RALGDS-like proteins, PLCε, AF6, RIN1/2, and PDZGEF1/2, regulate diverse cellular processes. They share high structural similarity and exhibit differential selectivity for HRAS and RAP1B (*136, 144*).

RB domain-containing proteins are mostly kinases (Table S2). The serine/threonine RAF kinase family proteins (A/B/CRAF; (*146*)) activate the MEK-ERK axis and controls cell proliferation and differentiation (*147, 148*). PI3Kα generates phosphatidylinositol (3,4,5)-trisphosphate (PIP_3) and regulates cell growth, cell survival, cytoskeleton reorganization, and metabolism (*149*). RGS12/14, which usually act as inactivators of Gα proteins (*150*), physically interact with various members of the RAS family. They appear to facilitate the assembly of the components of the MAPK pathway through direct association with activated HRAS (*151*). TIAM1/2, which act as specific GEFs for the RHO family proteins and control cell migration (*152, 153*), have been suggested to recognize activated RAS proteins (*154*). However, their direct interaction with RAS proteins has not been shown to date (*136*). Moreover, a few proteins, reported as RAS effectors, do not apparently contain a RA/RB domain (Table S3).

Variable affinities for the RAS-effector interactions

To determine the binding capability between the effector domains and diverse

proteins of the RAS family, the following proteins were selected for this study: (i) All 10 RASSF family proteins as representative RA domain-containing effector proteins; (ii) CRAF RB domain (Fig. 1) was used as a representative of the RB domain-containing proteins; and (iii) The RAS family includes 23 genes coding for at least 25 proteins, which share, considering their G domains, sequence identity of 48.6% and sequence similarity of 61.5% (Fig. S4). Based on sequence identity, structure and function of their G domains, the RAS proteins were divided into eight paralog groups: RAS, RRAS, RAP, RAL, RIT, RHEB, RASD and DIRAS (*155*). RAS-related proteins RASLs, RERG, RERGL, NKIRAS1/2 were excluded from this list and study due to their major sequence deviations.

To monitor binding we applied a fluorescence polarization assay (*134*) to determine the dissociation constants (K_d) for the RAS-effector interactions. For this, we prepared HRAS, RRAS, RAP1B, RAP2A, RALA, RIT1 and RHEB1 in complex with a non-hydrolysable, fluorescent analog of GTP, called mGppNHp. Representatives of RASD and DIRAS groups were not applied due to their physical instability *in vitro*. Small-sized RB and RA domains were fused to maltose-binding protein (MBP, 42 kDa) to increase their overall molecular weight, and to ensure a homogeneous monomeric form of the fusion proteins. Figure 1 shows an SDS gels for all purified proteins used in this study.

Increasing concentrations of MBP-fused effector proteins were titrated to RAS•mGppNHp proteins to assess the binding capability of the respective interaction pairs. We observed a significant change in fluorescence polarization for the majority of the measurements (Fig. S5 and S6A). However, evaluated K_d values ranged from 0.3 to more than 500 µM. These data are summarized in Table S5 and illustrated in Figure 2. Under these experimental conditions, the CRAF RB domain revealed the highest affinity for HRAS and RRAS1 while RASSF5 RA domain exhibited a relatively high affinity for HRAS, RAP1B and RAP2A (Fig. 2A, B, green bars). The intermediate affinities were obtained for the interaction of CRAF RB domain with RAP1B as well as RASSF1 with RAP1B, RAP2A and RALA, RASSF9 with RIT1 and RASSF7 with RRAS1 (Fig. 2A, B; blue bars). The majority of the interaction pairs showed, however, low and very low affinities (Fig. 2B, red and black bars, respectively). Among them, RHEB notably revealed the majority of low affinity interactions. No binding was observed for twelve pairwise interactions.

Purified MBP, which was titrated to HRAS•mGppNHp as a negative control, exhibited no interaction (Fig. S7A). The reproducibility of the fluorescence polarization measurements was assessed by determining the K_d value for the interaction between HRAS•mGppNHp with RASSF1-RA in three different experiments

Identification of common RAS binding site pattern in RA/RB domains

To understand the atomic interactions between RAS and effector proteins, and explain observed variable affinities, we analyzed various structures of RAS-effector protein complexes. To date, 13 structures of RAS-effector protein complexes exist in the PDB (Table S6). As some of them contain more than one complex in the unit cell, there were altogether 19 complexes available for the analysis. In order to map atomic interactions responsible for observed variable affinities, we

have extracted information about interacting interface from all of the above mentioned complex structures (Fig. S8 and S9) and combined them with their sequence alignments (Fig. S2-S4). It is important to note that some amino acids, aligned according to the sequence, were quite distant in the space. Therefore, we edited the sequence alignment to synchronize it with the structural alignment. Our python code finally took sequence alignments with PDB files of complex structures as inputs and calculated all interaction pairs in analyzed complex structures in the form of an interaction matrix. The resultant matrix comprehensively relates the interacting residues on both sides of the complexes, with RAS paralogs as rows and the RA/RB domains as columns (Fig. 3). All numbering in this study is based on HRAS on the one side and CRAF and RASSF5, for RB and RA domains respectively, on the other side.

Each element of the matrix that can be accounted for a `hotspot´, relates one homologous residue from RAS proteins to one homologous residue from the RA/RB domains. The number value of this element, ranging from 0 to 19, represents the number of complex structures in which these residues interact (Fig. 3). Thus, zero means that these two residues do not contact each other in any structure while a maximal value 19 means that this particular interaction exists in all analyzed complex structures of the RAS-RA/RB domains. We have sorted the residues at both sides of the matrix according to their conservation *vs.* variability. As can be seen in Figures S4 and S9, the majority of the residues (14 out of 20) on the side of 25 RAS proteins are conserved, nine of which (Q/N25, D/E33, I/V36, E37, D38, S/T39, Y40, R/K41 in switch I, and Y64 in the switch II; HRAS numbering) account for major hotspots (Fig. 3). On the other side, and in contrast, the majority of 19 RAS interacting residues in RA/RB domains are variable and only 2 distant residues are conserved (R/K59 and K/R84; CRAF numbering; R/K241 and K/R308; RASSF5 numbering) (Fig. 3 and S9).

However, what is striking is the middle cluster of the matrix with the most frequent interactions between the conserved residues in the switch I region of the RAS proteins (β2-strand residues 36-41; HRAS numbering) and the variable residues of the RA/RB domains (β2-strand residues 64-71; CRAF numbering; residues 284-291; RASSF5 numbering) (Fig. 3 and S9). This cluster adopts an arrangement of intermolecular β-sheet interactions in an anti-parallel fashion (Fig. S8). A substantial number of the contacts in this cluster are mediated by main-chain/main-chain interactions, which typically involve hydrogen bonds between the N-H group and the carbonyl oxygen of the amino acids 37-39 from the RAS side and positions 66-69 (CRAF numbering) and 286-289 (RASSF5 numbering) from the side of the RA/RB domains.

Switched RASSF binding selectivity by hotspots residue-swapping

To prove the impact of the hotspot residues on the selectivity of the RASSF RA domain interactions with RAS family proteins, we selected the weak and strong RAS-RASSF interactions, and substituted 4-5 amino acids in the hotspot region (Fig 3, boxed residues) RASSF2 to RASSF1 as well as RASSF4 and RASSF9 to RASSF5. The variants, RASSF2-to-1, RASSF4-to-5, and RASSF9-to-5 (Fig. 1), were successfully expressed and purified. Their binding affinities for HRAS, RIT1, RALA, RAP2A and RRAS1 were measured using fluorescence polarization (Fig. S10).

Remarkable differences in binding affinities of the analyzed RASSF variants are summarized in Figure 4 for comparison. RASSF2-to-1 variant revealed a significant increase of RALA (*p<.006*) and RRAS1 (*p<0.014*) binding affinity compared to RASSF2 but declined compared to RASSF1. In contrast, RIT1, which did not show any binding to RASSF2 and a very low affinity to RASSF1, now exhibited a reasonable K_d value of 65 µM for RASSF2-to-1. The RASSF4-to-5 variant, on the one hand, showed a tremendous increase in affinity for HRAS of about 20-fold (*p<.0118*), and on the other hand, diminished RIT1 property to bind RASSF4 by 3-fold (*p<.0351*). These data suggest that the hotspot residues favor RASSF4 binding to RIT1 whereas those residues of RASSF5 counteract RIT1 binding. Similarly, the RASSF4-to-5 affinity for RAP2A was increased by 2.5-fold (n.s., *p<.087*), which emphasizes the high affinity RAP2A-RASSF5 interaction. The RASSF9-to-5 variant showed a 4.5-fold increase in HRAS binding affinity as compared to RASSF9 (*p<.008*) that can be attributed to the high affinity interaction of HRAS with RASSF5. The intermediate affinity of RASSF9 for RIT1 of 27 µM is validated by the RASSF9-to-5 variant, which revealed a 5.5-fold higher K_d value (*p<.005*). The interaction of the RASSF9-to-5 variant with RALA was drastically enhanced (K_d = 35 µM) considering the lack of RASSF9 binding to RALA.

Our data on residue-swapping in RASSF proteins successfully validated the key role of hotspot residues in the RAS-RASSF interaction, particularly RASSF1-RALA, RASSF5-HRAS, and RASSF9-RIT1.

RIT1 pull-down from cell lysates by RASSF7 and RASSF9

To prove physiological relevance of identified RIT1 interactions with RASSF7 and RASSF9, we transfect Human Embryonic Kidney (HEK) 293T cells with human RIT1 and used His-tagged RA domains of RASSF7 and RASSF9 to pull down HA-tagged RIT1 from the cell lysates. As control, we used lysates of HRAS-transfected cells and His-tagged RASSF5 RA domain to pull down FLAG-HRAS. As shown in Figure 5A, RIT1 bound to RASSF7 and RASSF9 but not to RASSF5, which was, in contrast, able to pull down HRAS. Data of three independent experiments, were quantified by a Li-Cor Odyssey imaging system and expressed as signal intensity (Fig. 5B), confirmed the significance of the RIT1 interaction with RASSF7 and RASSF9 ($p < 0.01$).

Discussion

Effector selection and activation by a RAS protein in a proper cellular context and appropriate protein network are known to initiate a cascade of biochemical reactions and thus controls defined cellular functions in all types of cells. It is also increasingly clear that functionalization of the effectors with various modular building blocks, mainly the RA/RB domains, is a prerequisite for successful orchestration of a series of spatiotemporal events, including recruitment, subcellular localization, assembly of proactive protein complexes, and ultimately association with and activation *via* the RAS protein. An issue that is investigated in-depth in this study is how many effectors for RAS proteins exist in the human proteome and how they achieve the desired affinity and selectivity for their cognate RAS protein.

The total numbers of RAS effectors differ from study to study. A SMART database search has provided 108 RA and 20 RB domain-containing proteins in one of the early and first comprehensive studies on RAS-effector interactions (*136*). These numbers have been slightly reduced to 100 RA domains and only a few members of RB domain-

containing proteins, including A/B/CRAF, TIAM1/2 and RGS12/14 proteins (*144*). In the next studies, Kiel *et al*. has come to around 70 human proteins, containing RA and RB domains (*156*). Ibáñez Gaspar *et al*. have analyzed in their very recent, comprehensive study 56 established and predicted RAS effectors with the potential ability to bind to RAS oncoproteins (*28*). Our search, using the UniProt database and the program HMMER, alongside with a cross-check of each individual sequence, ended up with 41 RA in 39 RA domain-containing proteins and 16 RB in 14 RB domain-containing proteins (Fig. S1). Thus, our lists contain 53 proteins, also including RALGDSL2 and SNX17 (Tables S1 and S2). SNX17 along with SNX27 and SNX31, which possess a FERM-like domain, have been shown to directly bind to GTP-bound HRAS (*157*), and may thus be involved in endosomal RAS signaling processes (*158*). However, we exclude RASGEF3-5, KRIT1, and RGL4. Sequences, related to RA or RB domains, were not found in other proteins (Table S3), such as SIN1, SNX31, HK1 (Hexokinase 1), and SHANK2-3, which have been recently described as new RAS effector proteins (*157, 159-162*).

In order to refine a comprehensive list of RAS proteins and their effectors regarding their capabilities of mutual binding, we have investigated pairwise interaction between selected proteins (Fig. 2), related them to available structural data (Fig. 3), and combined them with data described in previous studies (Fig. S9).

The RASSF family contains 10 members and is divided into two groups; RASSF1-6 typically have C-terminal RA and SARAH domains and RASSF7-10 an N-terminal RA domain (Fig. 1) (*163*). However, RAS-binding residues are not conserved in group two of the RASSF family and overall, the RA domains of these two RASSF groups are about 25% identical. Our data showed a much lower binding affinity between RAS family members and RA domains of group two (Fig. 2).

In a very recent study, Dhanaraman *et al*. have performed RASSF pull-down experiments under similar conditions as previously published by Chan *et al*. (*122, 137*). As already stated by the reviewer, this approach has limitations to detect affinities lower than 10-30 µM, which is dependent on several variables like the buffer and centrifugation speed. Chan *et al*. have observed HRAS interactions with RASSF6 and RASSF7 as well, which were determined in the present study, although with very high K_d values (Fig. 2). RASSF5 binding to KRAS and HRAS, as reported by Dhanaraman *et al*., also confirms a previous study by Nakhaeizadeh *et al*., which has shown similar binding affinities of the effector domains, including RASSF5-RA, towards the RAS paralogs, HRAS, KRAS and NRAS (*134*). In contrast, Dhanaraman *et al*. have examined RAP1A and RASSF5, consistent with our study with RAP1B and RAP2A (Fig. 2), but did not consider them as interactions, again due to the approach limitation of 10 µM (see below).

RASSF1 and RASSF5 RA domains share the highest sequence homology and several residues, including L282, D285, A286, I/V287, K288, H291, K308, V311, V312, and D313 (RASSF5 numbering), involved in RAS interaction (Fig. 3), are almost identical. These RASSFs have been described in many studies as effectors for H/K/NRAS, RRAS1, and RAP1A (*25, 132, 145, 164*). Accordingly, we have determined high and intermediate affinities for their association with RAS family members in this study (Fig. 2) and in part also in a previous report (*134*). Interestingly,

RASSF proteins turned out to interact with several other RAS-related proteins, beyond the classical RAS paralogs. Shifman and colleagues have recently shown by immunoprecipitation experiments that RASSF1 also interacts with ERAS and DIRAS3 (*165*), which are atypical members of the RAS family (*155*). Similarly, Dhanaraman *et al*. have very recently demonstrated the interaction of RASSF1 with GEM, REM1, REM2 and RASL12 GTPase proteins (*137*). These GTPases, which belong to the RGK GTPase family, regulate voltage-dependent calcium channels and cell shape (*137*). The present study showed that RIT1 interacts RASSF7 and RASSF9, and RALA with RASSF1. These interactions, which successfully validated the key role of hotspot residues in the RAS-RASSF interaction (Fig. 4), confirmed our predicted interaction model (Fig. 3). The RALA-RASSF1 interaction seems rather relevant since the presence of four RASSF1 hotspot residues in RASSF2 considerably enhanced RALA binding (Fig. 4). RALA, as well as RALB, contain lysine and alanine at positions 36 and 37, respectively (HRAS numbering), rather different residues than isoleucine and glutamate in other RAS proteins, which are known to be critical for the RAS-effector interactions (*166*). RALA-RASSF1 interaction has not been reported to date and awaits further cell-based investigations, especially because the RASSF2-to-1 variant gained binding affinity towards RALA (Fig. 4). Similarly, RALA-RASSF5 interaction appears rather relevant as the RASSF9-to-5 variant affected the binding of RALA. This has been also demonstrated by hotspots residue-swapping of RASSF9 to RASSF5. While RALA showed a K_d value of 35 μM for RASSF9-to-5 while it did not show any binding to RASSF9, suggesting that very few key residues are sufficient to generate the appropriate binding surface. This notion presumes that analyzed RA domains share a conserved mode of RAS recognition based on the formation of an intermolecular, antiparallel β sheet (*134, 137*).

Among all RASSF family members, only RASSF1 and RASSF5 interact in high or intermediate affinities with all investigated RAS family members, with an exception of RIT1 (Fig. 2). RASSF7-9 RA domains share high sequence similarity and are different from RASSF10 (Fig. S2). A common signature of the RASSF members is the existence of the K/R241 and K/R308 hotspots (Fig. 3). They revealed, with a few exceptions, comparable K_d values for different representatives of the RAS family (Fig. 2). RIT1-RASSF7 and RIT1-RASSF9 interactions with affinities of 34 and 27 μM are quite remarkable, especially because these proteins have not been reported yet as RAS effectors. RIT1 contains an alanine instead of the conserved S/T39 (HRAS numbering) and RASSF9 contains two negatively charged glutamic acids instead of the positively charged lysine residues at 307 and 308 (RASSF5 numbering; Fig. S2). These two drastic deviations may be responsible for the very low affinity of RASSF9 for HRAS due to electrostatic repulsion with D33. However, RIT1 contains also an aspartic acid at the corresponding position and yet shows an intermediate affinity for RASSF9. The relevance of RIT1-RASSF9 interaction was successfully validated by residue-swapping. Substitution of five RASSF9 to RASSF5 residues, which did not bind RIT1, significantly impaired the interaction (Fig. 4). Moreover, cell-based pulldown experiments confirmed the relevance of RASSF7 and RASSF9 as potential RIT1 effectors, and support the notion that K_d values of about 30 μM can be considered physiologically relevant. It is important to note that GTPase-effector interactions in the cell take

place in a context of multivalent platform very different from the isolated domains and bimolecular interaction under cell-free conditions. Effectors are full-length, associated with accessory proteins, and eventually the cell membrane, and are subjected to distinct control mechanisms, including posttranslational modifications. Validated antibodies against these proteins will enable us in near future to take the next step namely determining the appropriate cell type that endogenously expresses the desired proteins and to unambiguously verify RIT1-RASSF interaction.

RHEB broadly exhibited low-affinity interaction with RASSF1-7, particularly RASSF1 (Fig. 2), which may be based on a large number of amino acid deviations in both switch regions (Fig. 3 and S4). It has been proposed that RHEB may complex with RASSF1 to coordinate signaling pathways, after processing by MST/LATS and TOR kinases (*167*). In the presence of RASSF1, RHEB has been shown to stimulate the MST/LATS/YAP pathways but is suppressed in its ability to activate the TOR pathway. The physical interaction of RHEB with RASSFs remains to be shown in cells, like it has been shown for other RAS and RAS-like proteins (*165*).

CRAF RB domain is one of the most and best-studied RAS effectors with the highest selectivity for the H/K/NRAS paralogs and to a certain extent also for the RRAS proteins (*134*). CRAF RB domain revealed an intermediate affinity for RAP1B and RHEB1 but not for RIT1 or RAP2A (Fig. 2). The RAP1 and RAP2 subgroups differ at positions 25 and 39 (HRAS numbering), which are in the case of RAP1 proteins occupied by favorable glutamine and serine (Fig. 3). The two orders of magnitude lower affinity of RAP1B for CRAF RB domain stems from the drastic deviation at position 31 (HRAS numbering). K31 in RAP proteins obviously collides with the K84 in CRAF and disfavors a RAP-CRAF interaction (Fig. S9); this was the reason why RAP1A mutated at this site was used for successful determination of the complex structure between RAP1A and the CRAF RB domain (*139*). Phosphorylation of RAP1A at S11 has been recently proposed to promote RAP1A-CRAF RB domain interaction (*168*). Devanand and colleagues have proposed that phosphorylation of S11 allosterically modulates the dynamics of RAP1A switch regions, which consequently promotes the RAP1A-CRAF complex formation and downstream signaling (*169*).

An intermediate affinity for CRAF RB domain interaction with RHEB G domain (Fig. 2) points to previous reports of a direct relationship between these two crucial signaling molecules. PKA-dependent phosphorylation of CRAF at S43 has been shown to reciprocally potentiate RHEB-CRAF interaction and to decrease CRAF interaction with HRAS (*170*). An asparagine instead of D38 (HRAS numbering) in the switch I region seems to be critical for the unique CRAF binding properties of RHEB. In a different study, Henske and coworkers have shown that RHEB interacts with and inhibits BRAF (*171*). In this context, RHEB not only hinders the BRAF association with HRAS but also interferes with BRAF activation and its heterodimerization with CRAF. As the RB domains of the RAF paralogs are conserved (*146*), mainly regarding their RAS binding residues (Fig. S3), differences between BRAF and CRAF interactions with RHEB may stem from deviations outside the RB domains or from different phosphorylation states. Heard *et al*. have recently reported a strong interaction between RHEB-GTP and BRAF (but not with CRAF) and that RHEB overexpression

decreases and RHEB knockdown increases RAF/MEK/ERK activation (*172*). They have shown that a variant of RHEB (Y35 to asparagine; Y32 in HRAS) impedes RHEB interaction with BRAF leading to an increased BRAF/CRAF heterodimerization and thus activation of the MAPK pathway. Accordingly, they have proposed a dual function for RHEB, suppression of the MAPK pathway and mTORC1 activation (*172*).

RIT1-CRAF interaction has been frequently proposed due to their critical roles in developmental disorders, collectively called RASopathy (*173*), but not directly shown. We observed a very low affinity for these two proteins (Fig. 2), which may stem from the sequence deviation between RIT1 and HRAS in their switch I region (Fig. 3). In an early study on biochemical characterization of RIT, Andres and coworkers have shown that RIT1 interacts with RA domains of RALGDS and AF6 but not with the CRAF RB domain (*174*). In a different study, they have shown that RIT1 binds and activates BRAF but not CRAF (*175*). This may again implicate those additional regions may exist outside the conserved RB domains of the RAF paralogs, which differently facilitate the interaction with the RAS proteins, like RIT1 or RHEB.

An ever-present central concern in the biophysical investigation of protein-protein interactions is the relevance of low (10-30 μM) to very low (>> 30 μM) affinity interactions in the regulation of signaling events. These protein complexes rely on weak, transient interactions that are emerging as important components of large signaling complexes at the plasma membrane that are required to respond to external stimuli. Cellular membranes play a critical role in the localization and orientation of protein complexes and in fine-tuning of protein functions (*176*). The activity of RAS and RAF paralogs is regulated through different parameters, including membrane association. Analysis of dynamic interactions between KRAS4B and lipid bilayer membrane has revealed that association of ARAF RB domain with active KRAS4B not only reorients KRAS4B at the membrane surface but also facilitates membrane binding of ARAF RBD itself (*177*). Four basic residues, K28, K66, R68, and K69, are engaged in lipid binding. Another emerging concept is based on the physical interaction of the G domain itself with a lipid membrane. A membrane-based, nucleotide-dependent conformational switch operates through distinct regions on the surface of RAS proteins, including the hypervariable region (HVR), which reorients with respect to the plasma membrane (*178-192*). Mazhab-Jafari and colleagues have proposed two different orientations of KRAS4B facing toward the membrane (*177, 193*). KRAS4B in an exposed GDP-bound form favors α4/α5 helices, which considerably reorients upon activation, and favors β1-β3 sheets and α2/α3 helices from the G domain, and K167/K172 from HVR, in an occluded GTP-bound form. G domain-membrane interaction may not only stabilize protein complexes but may also contribute to the specificity of signal transduction. A critical aspect in this context is the organization of RAS proteins into protein-lipid complexes. These so-called nanoclusters concentrate RAS at the plasma membrane. They are the sites of effector recruitment and activation and are essential for signal transmission (*178, 181, 194, 195*).

A frequently encountered issue in the enhancement of RAS-effector interaction is posttranslational modification. Thurman *et al*. have recently demonstrated that the ubiquitylation of KRAS at L147 impairs RAS-RASGAP interaction and facilitates RAS-CRAF association and MAPK signaling (*196*). Barceló et al. have shown that PKC-catalyzed phosphorylation of KRAS at S181 results in an

increased interaction of KRAS with CRAF and PI3Kα (*197*). Several studies have previously shown that the CRAF CR domain undergoes direct interaction with HRAS, which appears to be enhanced by the farnesyl moiety if using farnesylated RAS (*129, 198-203*). A possible HRAS-CRAF CR domain interaction has been proposed to be, contrary to the CRAF RB domain, outside of the switch regions of HRAS and thus independent of its nucleotide-bound state. In contrast, Y32 and Y64 phosphorylation by SRC alters the conformation of switch I and II regions, markedly reduces RAS binding to CRAF and concomitantly increases binding to RASGAPs and the rate of GTP hydrolysis (*204, 205*)

Another aspect related to very low affinity interactions involves a secondary RAS binding site, in addition to the RA/RB domain, in terms of a two-step, two-domain binding model. The two-domain model accommodates at least two different enhancer mechanisms. One is the direct enhancement of a selective RAS-effector interaction required for effector activation, proposed for the interactions of yeast RAS2 with two sites in adenylyl cyclase (*206*), HRAS with RB and CR domains of CRAF (*146*), and HRAS with two RA domains of PLCε (*207*). The latter may involve a high-affinity, GTP-dependent binding of the RA2 domain accompanied by low-affinity, GTP-independent binding of the RA1 domain. The deletion of one of the RA domains inhibits HRAS-induced PLCε activation (*207*). Notably, AF6 also possesses two RA domains and RGS12/14 two RB domains, respectively (*28*). Such a tandem arrangement of RA respective RB domains may enhance their affinity towards RAS, increase effector occupancy by additional endogenous events and thus the signaling output. An emerging concept, therefore, is the action of membrane binding CR domain that stabilizes RAS-CRAF RB domain interaction accompanied by S621 phosphorylation, and 14-3-3 binding that collectively facilitates RAF activation (*199, 200, 208-211*).

The formation of multiprotein complexes underlies a multistep assembly mechanism that follows a defined and probably short path from the cytoplasm, just underneath the membrane, to the membrane where membrane-associated proteins, for example, RAS proteins, are anchored. The first step, which has been designated as the piggyback mechanism (*212*), most likely increases local concentrations of protein components in a small volume and may drive cytoplasmic phase separations (*213-215*). The second step is the site-specific association of assembled protein complex with membrane-associated components, such as RAS proteins, which in turn are connected to receptors and co-receptors (*28, 214, 215*). In this way, a machinery of signaling molecules is orchestrated before the ligand activates the receptor. This is fine-tuned and prepared for an efficient signal transduction. Of course, it remains to be figured out why some interactions are in the nanomolar range (*e.g.,* 20 nM) and some in the micromolar range (*e.g.,* 20 μM or more). Given that the latter is involved in the initiation of multivalent macromolecular interactions, the final complex formation comes along after multivalent interactions have proceeded (*216*). This obviously increases significantly both the number of interacting complexes and overall binding affinity by orders of magnitude (*28*). The nanomolar affinity, however, may determine the selectivity for a sequential formation of two complexes. These interactions are often characterized by fast association and slow dissociation rates,

indicating the formation of stable complexes (*217-219*).

Experimental procedures

Constructs

Gene fragments encoding RAs of RASSF1 (accession number Q9NS23; amino acids or aa 194-288), RASSF2 (P50749; aa 176-264), RASSF3 (Q86WH2; aa 79-187), RASSF4 (Q9H2L5; aa 174-262), RASSF5 (Q5EBH1; aa 200–358), RASSF6 (Q6ZTQ3; aa 218-306), RASSF7 (Q02833; aa 6-89), RASSF8 (Q8NHQ8, aa 1-82), RASSF9 (O75901, aa 25-119), and RASSF10 (A6NK89; aa 4-133) as well as CRAF RB domain (P04049, aa 51–131) were cloned into pMal-c5X-His vector. The variants RASSF2-to-1 (A186K/Y187D/V190K/T191H), RASSF4-to-5 (Y185D/S187I/V188K/N188L) and RASSF9-to-5 (V40D/G42I/L43K/K45L/R46H) were generated by BioCat Gene Synthesis (BioCat GmbH) in pMal-c5X-His vector. Constructs for the prokaryotic expression of human HRAS, RRAS, RALA, RHEB1, RIT1, RAP2A and RAP1B isoforms were described previously (*120*). For mammalian expression, human HRAS and RIT1 were cloned in pcDNA3.1-Flag and pMT2-HA vectors, respectively.

Proteins

All RASSF and RAS proteins were expressed in Escherichia coli using the pMal-His and pGEX expression systems and purified using Ni-NTA and glutathione based affinity chromatography as described previously (*220*). RAS•mGppNHp was prepared as described (*220*). mGppNHp is a fluorescent, non-hydrolysable analog of GTP; m stands for the methylanthraniloyl (m) and GppNHp for Guanosine-5'-[(β,γ)-imido]triphosphate.

Fluorescence polarization

Increasing concentrations of RA/RB domains (0.002-300 μM) were added to the solution of mGppNHp-bound RAS family proteins (1 μM) in a buffer, containing 30 mM Tris-HCl, pH 7.4, 100 mM NaCl, 5 mM $MgCl_2$, 3 mM DTT) using fluorescence polarization on a Fluoromax 4 fluorimeter as described previously (*189*). The excitation wavelength was 360 nm and the emission wavelength 450 nm. The dissociation constants (K_d) for the RAS-effector interaction were evaluated using a quadratic ligand binding equation.

Bioinformatics

Information about RB and RA domains were obtained either from annotations in the UniProt database or in parallel using the program suite HMMER [http://hmmer.org/]. HMMER uses a Hidden Markov Model to compare sequences. Unlike CLUSTAL, which directly compares corresponding amino acids in the alignment, HMMER also takes adjacent amino acids into account. To do so, it calculates a Profile HMM before sequence comparison. It determines which amino acids are suitable at a given position. In the context of some protein domain, Profile can be viewed as a mapping of its characteristic features required for the domain structure, function or interaction. Sequence alignments were performed in the Bioedit program using the ClustalW algorithm (*221*). By using Chimera, the sequence alignments were adjust with superimposed structures (*138*). An interaction matrix is based on intermolecular contacts in complex structures (*134*). A python code was written to match sequence alignments with complex structures (Table S7) and calculated intermolecular contacts were put in the form of the interaction matrix. The intermolecular contacts were defined as pair residues with a distance of 4.0 Å between effectors and RAS proteins in available complex structures in the protein

data bank (http://www.pdb.org). Biopython modules (*222*) were also used to elucidate corresponding residues in all available complex structures. The structural representation was generated using Pymol viewer (*223*).

Cell-based assays

3.2 millions of HEK 293T cells were seeded in 10 cm plates in DMEM supplemented with 10 % fetal bovine serum (FBS) 14 h prior to transfection. The cells were transfected at 80% to 90% confluency using TurboFect transfection reagent (R0532, Thermo Scientific), with Flag-tagged HRAS and HA-tagged RIT1 constructs, or no plasmid as a negative control. At 24 h post-transfection, cells were washed in ice-cold Phosphate-buffered saline (PBS) and lysed in ice-cold lysis buffer, containing 50mM Tris/HCl pH 7.5, 5 mM $MgCl_2$, 100 mM NaCl, 1% Igepal CA-630, 10% glycerol, 20 mM ß-glycerolphosphate, 1 mM Na-orthovanadate, EDTA-free inhibitor cocktail 1 tablet/50 ml. 200 µg cell lysate were added to 20 µg His-tagged MBP-RASSF proteins coupled with 100 µl Ni-NTA beads. The samples were incubated for 30 min on the rotator at 4°C. After 3 washing with the lysis buffer and centrifugation steps (30 sec at 300xg), the samples were subjected to SDS-PAGE (12.5% polyacrylamide). HRAS and RIT1 were detected by immunoblotting using a rabbit anti-His (RM146) antibody (Thermo Fisher), a rabbit polyclonal anti-FLAG (F7425) antibody (Sigma), and a rabbit polyclonal anti-HA (SC-805) antibody (Santa Cruz), respectively. The immunoblots were evaluated using an Odyssey Fc Imaging System (LI-CORE Biosciences).

Data availability statement

All the data are in the manuscript.

Acknowledgements. We thank C. Herrmann and Mathilda Katan and Alfred Wittinghofer for sharing plasmids, and Kotsene Loumonvi for technical assistance.

Authors´ contributions. M.R.A. conceived and coordinated the study; S.R.A., N.S.K.J., and M.R.A. designed and wrote the paper; S.R.A., N.S.K.J., C.W., and F.B. designed, performed, and analyzed the experiments; S.R.A., R.D., and E.A. performed structural analysis; C.A.M.S. contributed to the conception of this work and provided critical feedback on data interpretation; all authors reviewed the results and approved the final version of the manuscript.

Funding. This study was supported by the European Network on Noonan Syndrome and Related Disorders (NSEuroNet, grant number: 01GM1621B); the German Research Foundation (Deutsche Forschungsgemeinschaft or DFG) through the International Research Training Group “Intra- and interorgan communication of the cardiovascular system” (grant number: IRTG 1902-p6); the German Federal Ministry of Education and Research (BMBF) – German Network of RASopathy Research (GeNeRARe, grant numbers: 01GM1902C).

Competing interests. The authors declare no competing financial interest.

References

1. Jaiswal, M., Dvorsky, R., Amin, E., Risse, S. L., Fansa, E. K., Zhang, S. C., Taha, M. S., Gauhar, A. R., Nakhaei-Rad, S., Kordes, C., Koessmeier, K. T., Cirstea, I. C., Olayioye, M. A., Haussinger, D., and Ahmadian, M. R. (2014) Functional cross-talk between ras and rho pathways: a Ras-specific GTPase-activating protein (p120RasGAP) competitively inhibits the RhoGAP activity of deleted in liver cancer (DLC) tumor suppressor by masking the catalytic arginine finger. *J Biol Chem* **289**, 6839-6849

2. Simanshu, D. K., Nissley, D. V., and McCormick, F. (2017) RAS proteins and their regulators in human disease. *Cell* **170**, 17-33

3. Gutierrez-Erlandsson, S., Herrero-Vidal, P., Fernandez-Alfara, M., Hernandez-Garcia, S., Gonzalo-Flores, S., Mudarra-Rubio, A., Fresno, M., and Cubelos, B. (2013) R-RAS2 overexpression in tumors of the human central nervous system. *Molecular cancer* **12**, 127

4. Karnoub, A. E., and Weinberg, R. A. (2008) Ras oncogenes: split personalities. *Nature reviews Molecular cell biology* **9**, 517-531

5. Herrmann, C. (2003) Ras–effector interactions: after one decade. *Current opinion in structural biology* **13**, 122-129

6. Nakhaei-Rad, S., Nakhaeizadeh, H., Götze, S., Kordes, C., Sawitza, I., Hoffmann, M. J., Franke, M., Schulz, W. A., Scheller, J., and Piekorz, R. P. (2016) The role of embryonic stem cell-expressed RAS (ERAS) in the maintenance of quiescent hepatic stellate cells. *Journal of Biological Chemistry*, jbc. M115. 700088

7. Castellano, E., and Downward, J. (2010) Role of RAS in the regulation of PI 3-kinase. in *Phosphoinositide 3-kinase in Health and Disease*, Springer. pp 143-169

8. Chan, J. J., Flatters, D., Rodrigues-Lima, F., Yan, J., Thalassinos, K., and Katan, M. (2013) Comparative analysis of interactions of RASSF1-10. *Advances in biological regulation* **53**, 190-201

9. Bunney, T. D., and Katan, M. (2011) PLC regulation: emerging pictures for molecular mechanisms. *Trends in biochemical sciences* **36**, 88-96

10. Ferro, E., and Trabalzini, L. (2010) RalGDS family members couple Ras to Ral signalling and that's not all. *Cellular signalling* **22**, 1804-1810

11. Rajalingam, K., Schreck, R., Rapp, U. R., and Albert, Š. (2007) Ras oncogenes and their downstream targets. *Biochimica et Biophysica Acta (BBA)-Molecular Cell Research* **1773**, 1177-1195

12. Nussinov, R., Tsai, C.-J., Muratcioglu, S., Jang, H., Gursoy, A., and Keskin, O. (2015) Principles of K-Ras effector organization and the role of oncogenic K-Ras in cancer initiation through G1 cell cycle deregulation. *Expert review of proteomics* **12**, 669-682

13. Ahearn, I. M., Haigis, K., Bar-Sagi, D., and Philips, M. R. (2012) Regulating the regulator: post-translational modification of RAS. *Nature reviews Molecular cell biology* **13**, 39

14. Hennig, A., Markwart, R., Esparza-Franco, M. A., Ladds, G., and Rubio, I. (2015) Ras activation revisited: role of GEF and GAP systems. *Biological chemistry* **396**, 831-848

15. Fischer, A., Hekman, M., Kuhlmann, J., Rubio, I., Wiese, S., and Rapp, U. R. (2007) B-and C-RAF Display Essential Differences in Their Binding to Ras THE ISOTYPE-SPECIFIC N TERMINUS OF B-RAF FACILITATES RAS BINDING. *Journal of Biological Chemistry* **282**, 26503-26516

16. Mott, H. R., and Owen, D. (2015) Structures of Ras superfamily effector complexes: What have we learnt in two decades? *Critical reviews in biochemistry and molecular biology* **50**, 85-133

17. Vetter, I. R., and Wittinghofer, A. (2001) The guanine nucleotide-binding switch in three dimensions. *Science* **294**, 1299-1304

18. Filchtinski, D., Sharabi, O., Rüppel, A., Vetter, I. R., Herrmann, C., and Shifman, J. M. (2010) What makes Ras an efficient molecular switch: a computational, biophysical, and structural study of Ras-GDP interactions with mutants of Raf. *Journal of molecular biology* **399**, 422-435

19. Erijman, A., and M Shifman, J. (2016) RAS/effector interactions from structural and biophysical perspective. *Mini reviews in medicinal chemistry* **16**, 370-375

20. Nassar, N., Horn, G., Herrmann, C., Block, C., Janknecht, R., and Wittinghofer, A. (1996) Ras/Rap effector specificity determined by charge reversal. *Nature structural biology* **3**, 723-729

21. Nakhaeizadeh, H., Amin, E., Nakhaei-Rad, S., Dvorsky, R., and Ahmadian, M. R. (2016) The RAS-effector interface: isoform-specific differences in the effector binding regions. *PLoS One* **11**, e0167145

22. Repasky, G. A., Chenette, E. J., and Der, C. J. (2004) Renewing the conspiracy theory debate: does Raf function alone to mediate Ras oncogenesis? *Trends in cell biology* **14**, 639-647

23. Wohlgemuth, S., Kiel, C., Krämer, A., Serrano, L., Wittinghofer, F., and Herrmann, C. (2005) Recognizing and defining true Ras binding domains I: biochemical analysis. *Journal of molecular biology* **348**, 741-758

24. Dhanaraman, T., Singh, S., Killoran, R. C., Singh, A., Xu, X., Shifman, J. M., and Smith, M. J. (2020) RASSF effectors couple diverse RAS subfamily GTPases to the Hippo pathway. *Science Signaling* **13**

25. Goddard, T. D., Huang, C. C., Meng, E. C., Pettersen, E. F., Couch, G. S., Morris, J. H., and Ferrin, T. E. (2018) UCSF ChimeraX: Meeting modern challenges in visualization and analysis. *Protein Science* **27**, 14-25

26. Nassar, N., Horn, G., Herrmann, C. A., Scherer, A., McCormick, F., and Wittinghofer, A. (1995) The 2.2 Å crystal structure of the Ras-binding domain of the serine/threonine kinase c-Raf1 in complex with RaplA and a GTP analogue. *Nature* **375**, 554

27. Bunney, T. D., Harris, R., Gandarillas, N. L., Josephs, M. B., Roe, S. M., Sorli, S. C., Paterson, H. F., Rodrigues-Lima, F., Esposito, D., and Ponting, C. P. (2006) Structural and mechanistic insights into ras association domains of phospholipase C epsilon. *Molecular cell* **21**, 495-507

28. Stieglitz, B., Bee, C., Schwarz, D., Yildiz, Ö., Moshnikova, A., Khokhlatchev, A., and Herrmann, C. (2008) Novel type of Ras effector interaction established between tumour suppressor NORE1A and Ras switch II. *The EMBO journal* **27**, 1995-2005

29. Pacold, M. E., Suire, S., Perisic, O., Lara-Gonzalez, S., Davis, C. T., Walker, E. H., Hawkins, P. T., Stephens, L., Eccleston, J. F., and Williams, R. L. (2000) Crystal structure and functional analysis of Ras binding to its effector phosphoinositide 3-kinase γ. *Cell* **103**, 931-944

30. Smith, M. J., Ottoni, E., Ishiyama, N., Goudreault, M., Haman, A., Meyer, C., Tucholska, M., Gasmi-Seabrook, G., Menezes, S., and Laister, R. C. (2017) Evolution of AF6-RAS association and its implications in mixed-lineage leukemia. *Nature communications* **8**, 1-13

31. Kiel, C., Wohlgemuth, S., Rousseau, F., Schymkowitz, J., Ferkinghoff-Borg, J., Wittinghofer, F., and Serrano, L. (2005) Recognizing and defining true Ras binding domains II: in silico prediction based on homology modelling and energy calculations. *Journal of molecular biology* **348**, 759-775

32. Donninger, H., Schmidt, M. L., Mezzanotte, J., Barnoud, T., and Clark, G. J. (2016) Ras signaling through RASSF proteins. in *Seminars in cell & developmental biology*, Elsevier

33. Rezaei Adariani, S., Buchholzer, M., Akbarzadeh, M., Nakhaei-Rad, S., Dvorsky, R., and Ahmadian, M. R. (2018) Structural snapshots of RAF kinase interactions. *Biochemical Society Transactions* **46**, 1393-1406

34. Haghighi, F., Dahlmann, J., Nakhaei-Rad, S., Lang, A., Kutschka, I., Zenker, M., Kensah, G., Piekorz, R. P., and Ahmadian, M. R. (2018) bFGF-mediated pluripotency maintenance in human induced pluripotent stem cells is associated with NRAS-MAPK signaling. *Cell Communication and Signaling* **16**, 96

35. Desideri, E., Cavallo, A. L., and Baccarini, M. (2015) Alike but different: RAF paralogs and their signaling outputs. *Cell* **161**, 967-970

36. Castellano, E., and Downward, J. (2011) RAS interaction with PI3K: more than just another effector pathway. *Genes & cancer* **2**, 261-274

37. Ross, E. M., and Wilkie, T. M. (2000) GTPase-activating proteins for heterotrimeric G proteins: regulators of G protein signaling (RGS) and RGS-like proteins. *Annual review of biochemistry* **69**, 795-827

38. Willard, F. S., Willard, M. D., Kimple, A. J., Soundararajan, M., Oestreich, E. A., Li, X., Sowa, N. A., Kimple, R. J., Doyle, D. A., and Der, C. J. (2009) Regulator of G-protein signaling 14 (RGS14) is a selective H-Ras effector. *PloS one* **4**

39. Malliri, A., and Collard, J. G. (2003) Role of Rho-family proteins in cell adhesion and cancer. *Current opinion in cell biology* **15**, 583-589

40. Rooney, C., White, G., Nazgiewicz, A., Woodcock, S. A., Anderson, K. I., Ballestrem, C., and Malliri, A. (2010) The Rac activator STEF (Tiam2) regulates cell migration by microtubule-mediated focal adhesion disassembly. *EMBO reports* **11**, 292-298

41. Yamauchi, J., Miyamoto, Y., Tanoue, A., Shooter, E. M., and Chan, J. R. (2005) Ras activation of a Rac1 exchange factor, Tiam1, mediates neurotrophin-3-induced Schwann cell migration. *Proceedings of the National Academy of Sciences* **102**, 14889-14894

42. Nakhaei-Rad, S., Haghighi, F., Nouri, P., Rezaei Adariani, S., Lissy, J., Kazemein Jasemi, N. S., Dvorsky, R., and Ahmadian, M. R. (2018) Structural fingerprints, interactions, and signaling networks of RAS family proteins beyond RAS isoforms. *Critical reviews in biochemistry and molecular biology* **53**, 130-156

43. Kiel, C., Foglierini, M., Kuemmerer, N., Beltrao, P., and Serrano, L. (2007) A genome-wide Ras-effector interaction network. *Journal of molecular biology* **370**, 1020-1032

44. Ibáñez Gaspar, V., Catozzi, S., Ternet, C., Luthert, P. J., and Kiel, C. (2020) Analysis of Ras-effector interaction competition in large intestine and colorectal cancer context. *Small GTPases*, 1-17

45. Ghai, R., Mobli, M., Norwood, S. J., Bugarcic, A., Teasdale, R. D., King, G. F., and Collins, B. M. (2011) Phox homology band 4.1/ezrin/radixin/moesin-like proteins function as molecular scaffolds that interact with cargo receptors and Ras GTPases. *Proceedings of the National Academy of Sciences* **108**, 7763-7768

46. Ghai, R., and Collins, B. (2011) PX-FERM proteins: A link between endosomal trafficking and signaling? *Small GTPases* **2**, 7763-7768

47. Amendola, C. R., Mahaffey, J. P., Parker, S. J., Ahearn, I. M., Chen, W.-C., Zhou, M., Court, H., Shi, J., Mendoza, S. L., and Morten, M. J. (2019) KRAS4A directly regulates hexokinase 1. *Nature* **576**, 482-486

48. Chowdhury, D., and Hell, J. W. (2020) How CBP/Shank3 Guards Rap and H-Ras. *Structure* **28**, 274-276

49. Cai, Q., Hosokawa, T., Zeng, M., Hayashi, Y., and Zhang, M. (2020) Shank3 Binds to and Stabilizes the Active Form of Rap1 and HRas GTPases via Its NTD-ANK Tandem with Distinct Mechanisms. *Structure* **28**, 290-300. e294

50. Miyan, J., Asif, M., Malik, S. A., Dubey, P., Singh, V., Singh, K., Mitra, K., Pandey, D., Haq, W., and Amita, H. (2019) Direct physical interaction of active Ras with mSIN1 regulates mTORC2 signaling. *BMC cancer* **19**, 1-16

51. Iwasa, H., Hossain, S., and Hata, Y. (2018) Tumor suppressor C-RASSF proteins. *Cellular and Molecular Life Sciences* **75**, 1773-1787

52. Gordon, M., and Baksh, S. (2011) RASSF1A: not a prototypical Ras effector. *Small GTPases* **2**, 5729-5740

53. van der Weyden, L., and Adams, D. J. (2007) The Ras-association domain family (RASSF) members and their role in human tumourigenesis. *Biochimica et Biophysica Acta (BBA)-Reviews on Cancer* **1776**, 58-85

54. Thillaivillalan, D., Singh, S., Killoran, R. C., Singh, A., Xu, X., Shifman, J., and Smith, M. J. (2020) RASSF effectors couple diverse RAS subfamily GTPases to the Hippo pathway. *bioRxiv*

55. Bauer, B., Mirey, G., Vetter, I. R., García-Ranea, J. A., Valencia, A., Wittinghofer, A., Camonis, J. H., and Cool, R. H. (1999) Effector recognition by the small GTP-binding proteins Ras and Ral. *Journal of Biological Chemistry* **274**, 17763-17770

56. Nelson, N., and Clark, G. J. (2016) Rheb may complex with RASSF1A to coordinate Hippo and TOR signaling. *Oncotarget* **7**, 33821

57. Devanand, T., Venkatraman, P., and Vemparala, S. (2018) Phosphorylation promotes binding affinity of Rap-Raf complex by allosteric modulation of switch loop dynamics. *Scientific reports* **8**, 1-15

58. Devanand, T., Krishnaswamy, S., and Vemparala, S. (2019) Interdigitation of Lipids Induced by Membrane–Active Proteins. *The Journal of membrane biology* **252**, 331-342

59. Yee, W. M., and Worley, P. F. (1997) Rheb interacts with Raf-1 kinase and may function to integrate growth factor-and protein kinase A-dependent signals. *Molecular and cellular biology* **17**, 921-933

60. Karbowniczek, M., Robertson, G. P., and Henske, E. P. (2006) Rheb inhibits C-raf activity and B-raf/C-raf heterodimerization. *Journal of Biological Chemistry* **281**, 25447-25456

61. Heard, J. J., Phung, I., Potes, M. I., and Tamanoi, F. (2018) An oncogenic mutant of RHEB, RHEB Y35N, exhibits an altered interaction with BRAF resulting in cancer transformation. *BMC cancer* **18**, 69

62. Yaoita, M., Niihori, T., Mizuno, S., Okamoto, N., Hayashi, S., Watanabe, A., Yokozawa, M., Suzumura, H., Nakahara, A., and Nakano, Y. (2016) Spectrum of mutations and genotype–phenotype analysis in Noonan syndrome patients with RIT1 mutations. *Human genetics* **135**, 209-222

63. Shao, H., Kadono-Okuda, K., Finlin, B. S., and Andres, D. A. (1999) Biochemical characterization of the Ras-related GTPases Rit and Rin. *Archives of biochemistry and biophysics* **371**, 207-219

64. Shi, G.-X., and Andres, D. A. (2005) Rit contributes to nerve growth factor-induced neuronal differentiation via activation of B-Raf-extracellular signal-regulated kinase and p38 mitogen-activated protein kinase cascades. *Molecular and cellular biology* **25**, 830-846

65. Chavan, T. S., Muratcioglu, S., Marszalek, R., Jang, H., Keskin, O., Gursoy, A., Nussinov, R., and Gaponenko, V. (2015) Plasma membrane regulates Ras signaling networks. *Cellular logistics* **5**, e1136374

66. Mazhab-Jafari, M. T., Marshall, C. B., Smith, M. J., Gasmi-Seabrook, G. M., Stathopulos, P. B., Inagaki, F., Kay, L. E., Neel, B. G., and Ikura, M. (2015) Oncogenic and RASopathy-associated K-RAS mutations relieve membrane-dependent occlusion of the effector-binding site. *Proceedings of the National Academy of Sciences* **112**, 6625-6630

67. Abankwa, D., Gorfe, A. A., and Hancock, J. F. (2007) Ras nanoclusters: molecular structure and assembly. *Semin Cell Dev Biol* **18**, 599-607

68. Abankwa, D., Gorfe, A. A., Inder, K., and Hancock, J. F. (2010) Ras membrane orientation and nanodomain localization generate isoform diversity. *Proc Natl Acad Sci U S A* **107**, 1130-1135

69. Cirstea, I. C., Kutsche, K., Dvorsky, R., Gremer, L., Carta, C., Horn, D., Roberts, A. E., Lepri, F., Merbitz-Zahradnik, T., Konig, R., Kratz, C. P., Pantaleoni, F., Dentici, M. L., Joshi, V. A., Kucherlapati, R. S., Mazzanti, L., Mundlos, S., Patton, M. A., Silengo, M. C., Rossi, C., Zampino, G., Digilio, C., Stuppia, L., Seemanova, E., Pennacchio, L. A., Gelb, B. D., Dallapiccola, B., Wittinghofer, A., Ahmadian, M. R., Tartaglia, M., and Zenker, M. (2010) A restricted spectrum of NRAS mutations causes Noonan syndrome. *Nat Genet* **42**, 27-29

70. Zhou, Y., and Hancock, J. F. (2018) Deciphering lipid codes: K-Ras as a paradigm. *Traffic* **19**, 157-165

71. Kapoor, S., Triola, G., Vetter, I. R., Erlkamp, M., Waldmann, H., and Winter, R. (2012) Revealing conformational substates of lipidated N-Ras protein by pressure modulation. *Proc Natl Acad Sci U S A* **109**, 460-465

72. Vogel, A., Nikolaus, J., Weise, K., Triola, G., Waldmann, H., Winter, R., Herrmann, A., and Huster, D. (2014) Interaction of the human N-Ras protein with lipid raft model membranes of varying degrees of complexity. *Biol Chem* **395**, 779-789

73. Sperlich, B., Kapoor, S., Waldmann, H., Winter, R., and Weise, K. (2016) Regulation of K-Ras4B Membrane Binding by Calmodulin. *Biophys J* **111**, 113-122

74. Erwin, N., Patra, S., Dwivedi, M., Weise, K., and Winter, R. (2017) Influence of isoform-specific Ras lipidation motifs on protein partitioning and dynamics in model membrane systems of various complexity. *Biol Chem* **398**, 547-563

75. Abankwa, D., Gorfe, A. A., Inder, K., and Hancock, J. F. (2010) Ras membrane orientation and nanodomain localization generate isoform diversity. *Proceedings of the National Academy of Sciences* **107**, 1130-1135

76. Cirstea, I. C., Kutsche, K., Dvorsky, R., Gremer, L., Carta, C., Horn, D., Roberts, A. E., Lepri, F., Merbitz-Zahradnik, T., and König, R. (2010) A restricted spectrum of NRAS mutations causes Noonan syndrome. *Nature genetics* **42**, 27-29

77. Abankwa, D., Gorfe, A. A., and Hancock, J. F. (2007) Ras nanoclusters: molecular structure and assembly. in *Seminars in cell & developmental biology*, Elsevier

78. Nouri, K., Fansa, E. K., Amin, E., Dvorsky, R., Gremer, L., Willbold, D., Schmitt, L., Timson, D. J., and Ahmadian, M. R. (2016) IQGAP1 interaction with RHO family proteins revisited kinetic and equilibrium evidence for multiple distinct binding sites. *Journal of Biological Chemistry* **291**, 26364-26376

79. Yoon, S. Y., Tefferi, A., and Li, C. Y. (2000) Cellular distribution of platelet-derived growth factor, transforming growth factor-beta, basic fibroblast growth factor, and their receptors in normal bone marrow. *Acta Haematol* **104**, 151-157

80. Zhou, Y., and Hancock, J. F. (2018) Deciphering lipid codes: K-Ras as a paradigm. *Traffic* **19**, 157-165

81. Kapoor, S., Triola, G., Vetter, I. R., Erlkamp, M., Waldmann, H., and Winter, R. (2012) Revealing conformational substates of lipidated N-Ras protein by pressure modulation. *Proceedings of the National Academy of Sciences* **109**, 460-465

82. Mazhab-Jafari, M. T., Marshall, C. B., Smith, M. J., Gasmi-Seabrook, G. M., Stathopulos, P. B., Inagaki, F., Kay, L. E., Neel, B. G., and Ikura, M. (2015) Oncogenic and RASopathy-associated K-RAS mutations relieve membrane-dependent occlusion of the effector-binding site. *Proc Natl Acad Sci U S A* **112**, 6625-6630

83. Nussinov, R., Tsai, C. J., and Jang, H. (2018) Is Nanoclustering essential for all oncogenic KRas pathways? Can it explain why wild-type KRas can inhibit its oncogenic variant? *Semin Cancer Biol*

84. Nussinov, R., Tsai, C.-J., and Jang, H. (2020) Ras assemblies and signaling at the membrane. *Current Opinion in Structural Biology* **62**, 140-148

85. Thurman, R., Siraliev-Perez, E., and Campbell, S. L. (2017) RAS ubiquitylation modulates effector interactions. *Small GTPases*, 1-6

86. Barceló, C., Paco, N., Morell, M., Alvarez-Moya, B., Bota-Rabassedas, N., Jaumot, M., Vilardell, F., Capella, G., and Agell, N. (2014) Phosphorylation at Ser-181 of oncogenic KRAS is required for tumor growth. *Cancer research* **74**, 1190-1199

87. Thapar, R., Williams, J. G., and Campbell, S. L. (2004) NMR characterization of full-length farnesylated and non-farnesylated H-Ras and its implications for Raf activation. *Journal of molecular biology* **343**, 1391-1408

88. Li, Z.-L., Prakash, P., and Buck, M. (2018) A "tug of war" maintains a dynamic protein–membrane complex: molecular dynamics simulations of C-Raf RBD-CRD bound to K-Ras4B at an anionic membrane. *ACS central science* **4**, 298-305

89. Li, S., Jang, H., Zhang, J., and Nussinov, R. (2018) Raf-1 cysteine-rich domain increases the affinity of K-Ras/Raf at the membrane, promoting MAPK signaling. *Structure* **26**, 513-525. e512

90. Hu, C.-D., Kariya, K.-i., Tamada, M., Akasaka, K., Shirouzu, M., Yokoyama, S., and Kataoka, T. (1995) Cysteine-rich region of Raf-1 interacts with activator domain of post-translationally modified Ha-Ras. *Journal of Biological Chemistry* **270**, 30274-30277

91. Williams, J. G., Drugan, J. K., Yi, G.-S., Clark, G. J., Der, C. J., and Campbell, S. L. (2000) Elucidation of binding determinants and functional consequences of Ras/Raf-cysteine-rich domain interactions. *Journal of Biological Chemistry* **275**, 22172-22179

92. Ke, H., Matsumoto, S., Murashima, Y., Taniguchi-Tamura, H., Miyamoto, R., Yoshikawa, Y., Tsuda, C., Kumasaka, T., Mizohata, E., and Edamatsu, H. (2017) Structural basis for intramolecular interaction of post-translationally modified H-Ras• GTP prepared by protein ligation. *FEBS letters* **591**, 2470-2481

93. Bunda, S., Heir, P., Srikumar, T., Cook, J. D., Burrell, K., Kano, Y., Lee, J. E., Zadeh, G., Raught, B., and Ohh, M. (2014) Src promotes GTPase activity of Ras via tyrosine 32 phosphorylation. *Proceedings of the National Academy of Sciences* **111**, E3785-E3794

94. Kano, Y., Gebregiworgis, T., Marshall, C. B., Radulovich, N., Poon, B. P., St-Germain, J., Cook, J. D., Valencia-Sama, I., Grant, B. M., and Herrera, S. G. (2019) Tyrosyl phosphorylation of KRAS stalls GTPase cycle via alteration of switch I and II conformation. *Nature communications* **10**, 1-14

95. Shima, F., Okada, T., Kido, M., Sen, H., Tanaka, Y., Tamada, M., Hu, C.-D., Yamawaki-Kataoka, Y., Kariya, K.-i., and Kataoka, T. (2000) Association of yeast adenylyl cyclase with cyclase-associated protein CAP forms a second Ras-binding site which mediates its Ras-dependent activation. *Molecular and cellular biology* **20**, 26-33

96. Kelley, G. G., Reks, S. E., Ondrako, J. M., and Smrcka, A. V. (2001) Phospholipase Cϵ: a novel Ras effector. *The EMBO journal* **20**, 743-754

97. Travers, T., López, C. A., Van, Q. N., Neale, C., Tonelli, M., Stephen, A. G., and Gnanakaran, S. (2018) Molecular recognition of RAS/RAF complex at the membrane: Role of RAF cysteine-rich domain. *Scientific reports* **8**, 1-15

98. Lakshman, B., Messing, S., Schmid, E. M., Clogston, J. D., Gillette, W. K., Esposito, D., Kessing, B., Fletcher, D. A., Nissley, D. V., and McCormick, F. (2019) Quantitative biophysical analysis defines key components modulating recruitment of the GTPase KRAS to the plasma membrane. *Journal of Biological Chemistry* **294**, 2193-2207

99. Park, E., Rawson, S., Li, K., Kim, B.-W., Ficarro, S. B., Gonzalez-Del Pino, G., Sharif, H., Marto, J. A., Jeon, H., and Eck, M. J. (2019) Architecture of autoinhibited and active BRAF–MEK1–14-3-3 complexes. *Nature* **575**, 545-550

100. Jang, H., Zhang, M., and Nussinov, R. (2020) The quaternary assembly of KRas4B with Raf-1 at the membrane. *Computational and Structural Biotechnology Journal*

101. Kholodenko, B. N., Hoek, J. B., and Westerhoff, H. V. (2000) Why cytoplasmic signalling proteins should be recruited to cell membranes. *Trends in cell biology* **10**, 173-178

102. Sukenik, S., Ren, P., and Gruebele, M. (2017) Weak protein–protein interactions in live cells are quantified by cell-volume modulation. *Proceedings of the National Academy of Sciences* **114**, 6776-6781

103. Case, L. B., Ditlev, J. A., and Rosen, M. K. (2019) Regulation of transmembrane signaling by phase separation. *Annual Review of Biophysics* **48**, 465-494

104. Bratek-Skicki, A., Pancsa, R., Meszaros, B., Van Lindt, J., and Tompa, P. (2020) A guide to regulation of the formation of biomolecular condensates. *The FEBS Journal*

105. Banani, S. F., Lee, H. O., Hyman, A. A., and Rosen, M. K. (2017) Biomolecular condensates: organizers of cellular biochemistry. *Nature reviews Molecular cell biology* **18**, 285-298

106. Kiel, C., Selzer, T., Shaul, Y., Schreiber, G., and Herrmann, C. (2004) Electrostatically optimized Ras-binding Ral guanine dissociation stimulator mutants increase the rate of

association by stabilizing the encounter complex. *Proceedings of the National Academy of Sciences* **101**, 9223-9228

107. Kiel, C., Filchtinski, D., Spoerner, M., Schreiber, G., Kalbitzer, H. R., and Herrmann, C. (2009) Improved binding of Raf to Ras· GDP is correlated with biological activity. *Journal of Biological Chemistry* **284**, 31893-31902

108. Schreiber, G., Haran, G., and Zhou, H.-X. (2009) Fundamental aspects of protein− protein association kinetics. *Chemical reviews* **109**, 839-860

109. Gremer, L., Merbitz-Zahradnik, T., Dvorsky, R., Cirstea, I. C., Kratz, C. P., Zenker, M., Wittinghofer, A., and Ahmadian, M. R. (2011) Germline KRAS mutations cause aberrant biochemical and physical properties leading to developmental disorders. *Human mutation* **32**, 33-43

110. Hall, T. A. (1999) BioEdit: a user-friendly biological sequence alignment editor and analysis program for Windows 95/98/NT. in *Nucleic acids symposium series*, [London]: Information Retrieval Ltd., c1979-c2000.

111. Cock, P. J., Antao, T., Chang, J. T., Chapman, B. A., Cox, C. J., Dalke, A., Friedberg, I., Hamelryck, T., Kauff, F., and Wilczynski, B. (2009) Biopython: freely available Python tools for computational molecular biology and bioinformatics. *Bioinformatics* **25**, 1422-1423

112. DeLano, W. L. (2002) The PyMOL molecular graphics system. *http://www. pymol. org*

Abbreviations and nomenclature

AF6, ALL1-fused gene from chromosome 6; CR domain, cysteine-rich domain; ERK, extracellular signal-regulated kinase; GAP, GTPase-activating protein; GEF, guanine nucleotide exchange factor; GTP, guanosine triphosphate; GTPase, guanosine triphosphatase; HK1, hexokinase-1; HRAS, Harvey rat sarcoma; KRAS, Kristen rat sarcoma; MAPK, mitogen-activated protein kinase; MBP, maltose binding protein; MEK, MAPK/ERK kinase; NKIRAS, NF-kappa-B inhibitor-interacting RAS-like protein; NORE1, novel RAS effector; NRAS, neuroblastoma RAS; PDZGEF, PDZ domain-containing guanine nucleotide exchange factor; PI3K, phosphoinositide 3-kinase; PKC, protein kinase C; PLCε, phospholipase C epsilon; RA, RAS association domain; RAF, rapidly accelerated fibrosarcoma; RALA, RAS-like protein A; RALGDS, RAL guanine nucleotide dissociation stimulator; RAP, RAS proximate; RAS, rat sarcoma; RASD, Dexamethasone-induced RAS-related; RASSF, RAS association domain family; RB, RAS binding domain; RERG, RAS-related and estrogen-regulated growth inhibitor; RERGL, RAS-related and estrogen-regulated growth inhibitor-like protein; RGL, RAL guanine nucleotide dissociation stimulator-like;

RGS, regulator of G protein signaling; RHEB, RAS homologous enriched in brain; RHO, RAS homologous; RIN, RAS and RAB interactor; RIT, RAS-like protein expressed in many tissues; RRAS, RAS-related protein; SARAH, Salvador-RASSF-Hippo domain; SHANK, SH3 and multiple ankyrin repeat domain; SIN1, stress-activated protein kinase-interacting protein 1; SNX17, sorting nexin-17; TIAM, T-lymphoma invasion and metastasis protein.

Figure legends

Figure 1. Domain organization of effector proteins. Schematic representation of RASSF1-10 proteins, and CRAF. Different domains are highlighted, including RAS Association domain (RA) in red, RAS Binding domain (RB) in yellow, and other domains in blue. Based on their domain organization, the RASSF family proteins are divided in group 1 (RASSF1-6) and group 2 with N-terminal RA domains (RASSF7-10). Coomasssie brilliant blue stained SDS-gels show purified RAS proteins as well as the RA/RB domains purified as MBP fusion proteins.

Figure 2. Differential binding affinities for the RA/RB domain interactions with various RAS subfamily members. The interactions between 7 RAS subfamily members with 12 effector proteins (10 RA domains of the RASSF protein family and CRAF RB domain) were determined by titrating mGppNHp-bound, active forms of RAS proteins (1 μM, respectively) with increasing concentrations of the respective effector domains as MBP fusion proteins (Fig. S5 and S6). (A) Data of four representative experiments are shown for the interaction of RALA, RAP2A, RRAS1and RIT1 with RASSF1, 5, 7 and 9, respectively. (B) Evaluated K_d values (above the bars; Table S5) were divided in high affinity (0.1 – 5 μM; green), intermediate affinity (6 – 30μM; blue), low affinity (31 – 90 μM; red) and very low affinity (91-510 μM; black). No binding (n.b.) stands for K_d values higher than 500 μM. The error bars were derived from the fitting errors.

Figure 3. Interaction matrix adapted for the structures of RAS complexes with effector domains. Interaction matrix of RAS family proteins with the RA/RB proteins used in this study is generated to demonstrate interacting residues in respective structures (see Table S6). It comprises the amino acid sequence alignments of the RAS proteins (lower left panel) and the effector domains (upper right panel), respectively, extracted from the complete alignments in Fig. S2-S4. Each element corresponds to a possible interaction of RAS residues (row; HRAS numbering) and effector (column; CRAF and RASSF5 numbering, respectively). The number of actual contact sites between RAS and the effector domains (with distances of 4 Å or less) were calculated and are indicated with positive numbers for matrix elements. Extracted structures of HRAS (in orchid) and the RA domain of RASSF5 and RB domain of CRAF (in olive) from their surface complexes are presented (top left panel). Key interaction hotspots with the same color codes are highlighted on the surface structures as well as in the interaction matrix and the secondary structures, respectively. Boxed residues in RASSF2, 4 and 9 were replaces to RASSF1 and 5, respectively, to validate the impact of these hotspot residues on the interaction with RAS family proteins (Fig. 4).

Revised Figure 4. Validation of RAS-RASSF selectivity by hotspots residue-swapping in RASSF RA domains. The interactions of the RASSF hotspot variants (RASSF2-to-1: A186K/Y187D/V190K/T191H, RASSF4-to-5: Y185D/S187I/V188K/N188L and RASSF9-to-5:

V40D/G42I/L43K/K45L/R46H; see Fig. 3, boxed residues) with various RAS family proteins (RIT1, RALA, RRAS1, HRAS, and RAP2A) were determined by fluorescence polarization (see Fig. S10), and evaluated K_d values were plotted as bar charts together with K_d values of wild type RASSF1, 2, 4, 5 and 9. (* $p < 0.05$; ** $p < 0.01$). Color codes highlight RASSF wild types (red and black) and RASSF variants (green). The error bars were derived from the fitting errors.

Figure 5. Binding analysis of RIT1 and HRAS with RASSF1-RA, RASSF7-RA and RASSF9-RA using pulldown assay. (A) HA-RIT1 and FLAG-HRAS, overexpressed in HEK 293T cells, were pulled down using the His-tagged MBP-RA domains of RASSF5, RASSF7 and RASSF9, respectively, and immunoblotted (IB) using anti-HA and anti-FLAG antibodies. Immunoblots of total cell lysates (TCL) were served as loading control to detect HA-RIT1 and FLAG-HRAS. An anti-His antibody was used for detection of the His-tagged MBP-RA domains of RASSF5, RASSF7 and RASSF9 as an input loading control (more detail in Fig. S11). (B) The graphs represent densitometric analysis of three independent experiments under the same conditions as shown in (A). All values were normalized to the loading control. All data are expressed as the mean of triplicate experiments ± standard deviation (unpaired t-test, *p < 0.05, **p < 0.01 and ***p < 0.001).

Figure 1

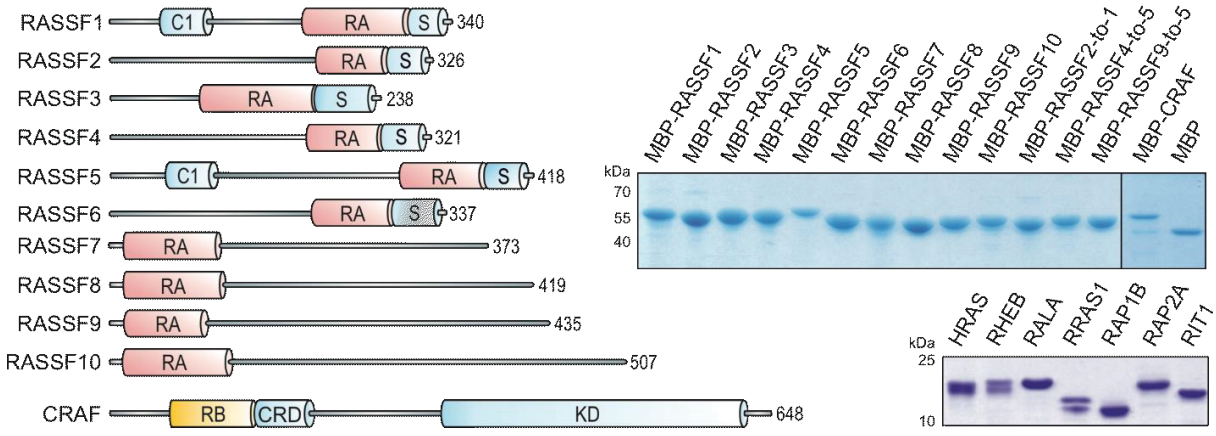

Figure 2

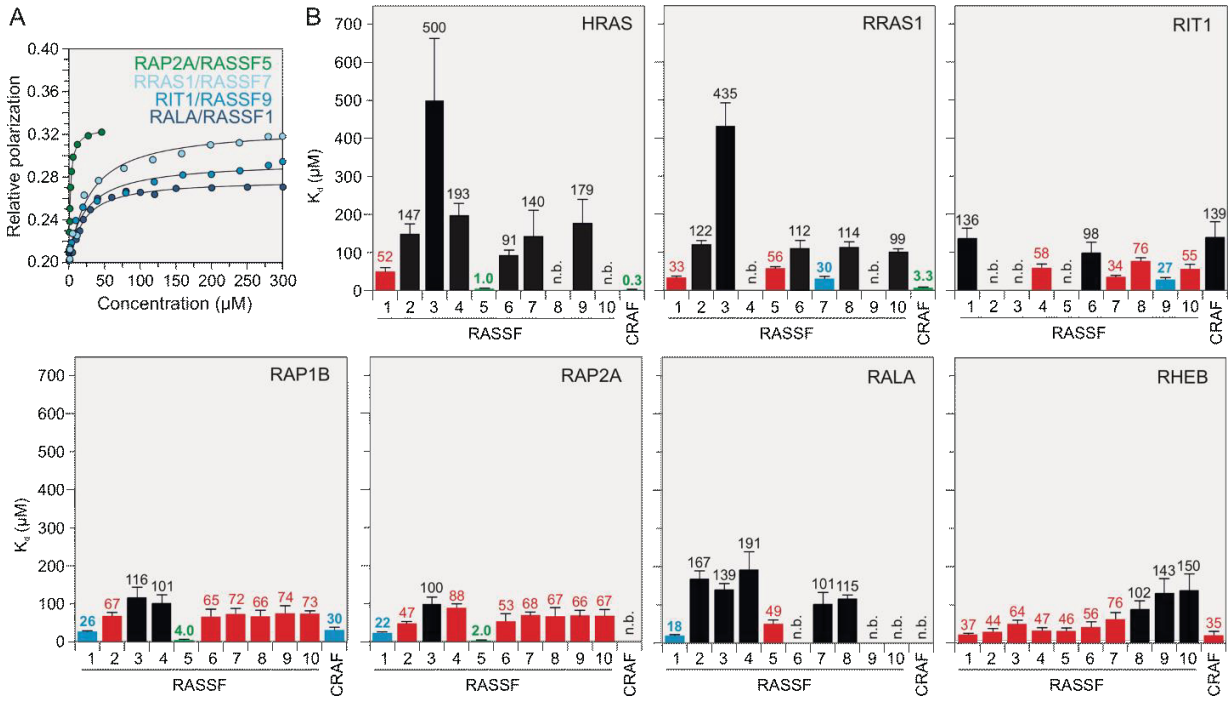

Figure 3

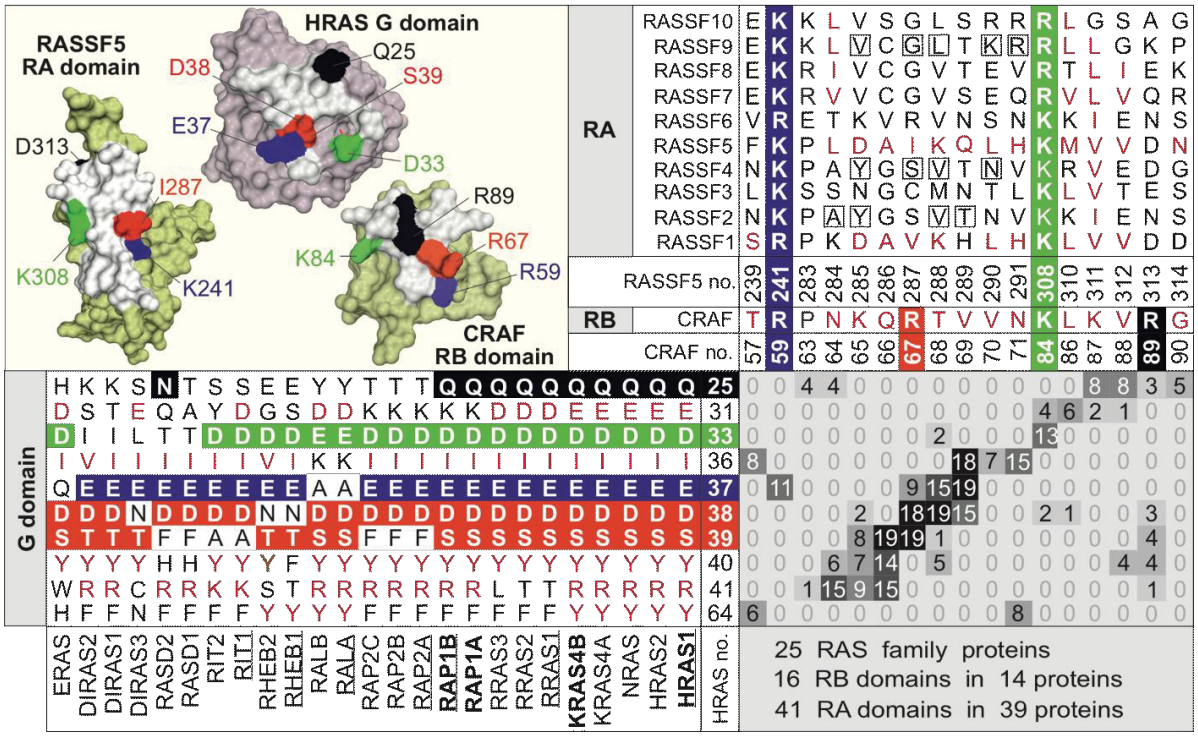

Figure 4

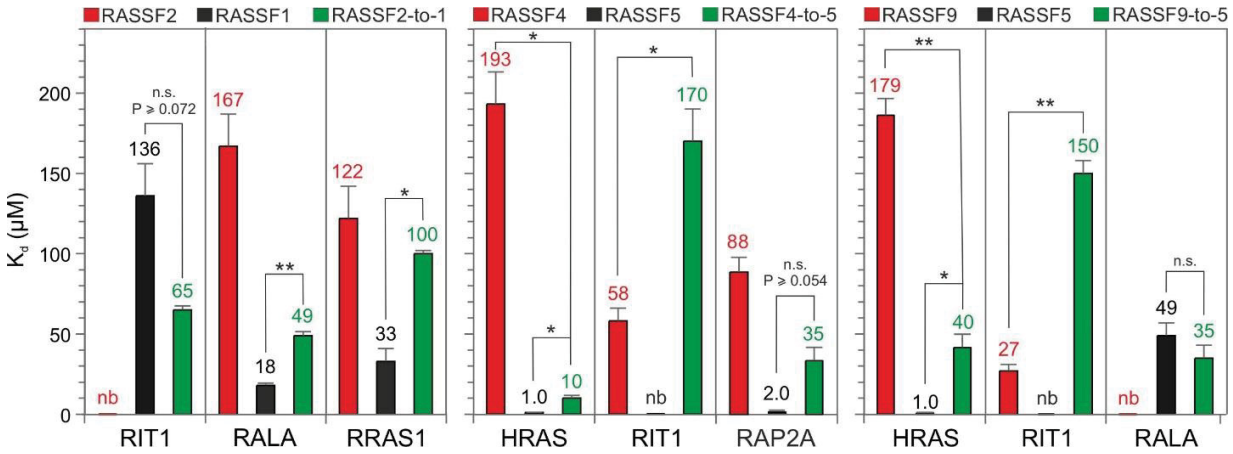
RASSF2
RASSF1
RASSF2-to-1
RASSF4
RASSF5
RASSF4-to-5
RASSF9
RASSF5
RASSF9-to-5
K_d (µM)
200
150
100
50
0
n.s.
P ≥ 0.072
136
65
nb
167
18
49
122
33
100
193
1.0
10
58
nb
170
88
2.0
n.s.
P ≥ 0.054
35
179
1.0
40
27
nb
150
49
35
RIT1
RALA
RRAS1
HRAS
RIT1
RAP2A
HRAS
RIT1
RALA

Chapter VI

The Pseudo Natural Product Rhonin Targets RHOGDI1

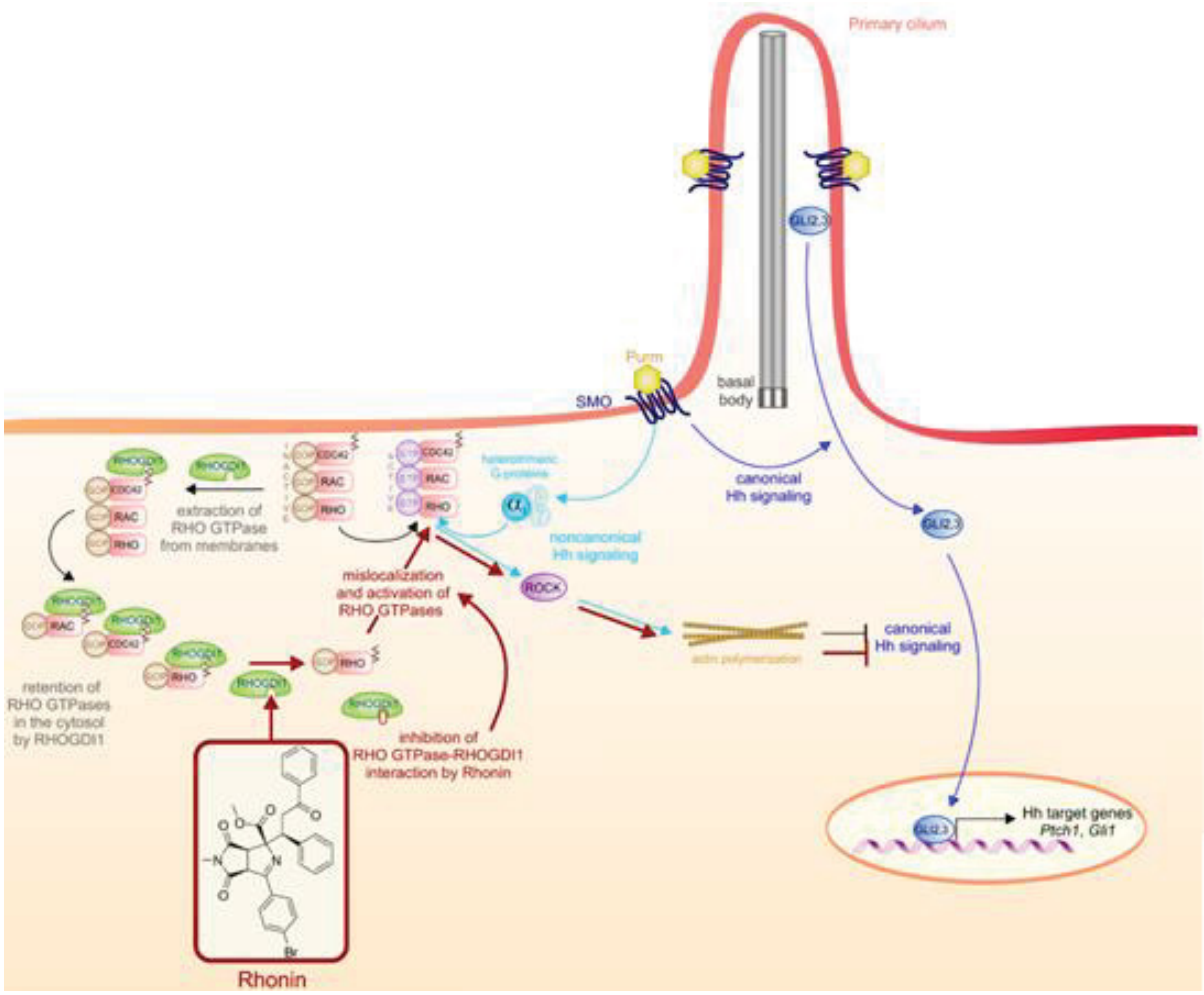

Revised in:	Nature chemical biology
Impact factor:	12.587 (2020)
Own Proportion to this work:	10%
	Transfection of siRNA and RHO GTPases in cells treated with Rohnin and analysis by subcellular fractionation

The Pseudo Natural Product Rhonin Targets RHOGDI1

Sumersing Patil,[1] Erchang Shang,[1] Rishikesh Narayan,[1,2] Mohammad Akbarzadeh,[3] Marcel Buchholzer,[3] Neda S. Kazemein Jasemi,[3] Marco Potowski,[4] Hacer Karatas,[1] George Karageorgis,[1,5] Christian Merten,[6] Christopher Golz,[4] Carsten Strohmann,[4] Andrey P. Antonchick,[1] Petra Janning,[1] Roger Goody,[1] Mohammad Reza Ahmadian,[3] Slava Ziegler,[1] Herbert Waldmann,[1,4*]

Affiliations

[1] Department of Chemical Biology, Max-Planck-Institute of Molecular Physiology, Otto-Hahn-Straße 11, 44227 Dortmund, Germany

[2] School of Chemical and Biological Sciences (SCBS), IIT Goa, Farmagudi, Ponda, Goa-403401, India

[3] Institute of Biochemistry and Molecular Biology II, Medical Faculty, Heinrich-Heine-University, Düsseldorf 40225, Germany

[4] Faculty of Chemistry and Chemical Biology, Technical University Dortmund, Otto-Hahn-Straße 6, 44221 Dortmund, Germany

[5] School of Chemistry, University of Leeds, LS2 9JT, Leeds, U.K

[6] Faculty of Chemistry and Biochemistry, Organic Chemistry II, Ruhr-University Bochum Universitätsstrasse 150, 44780 Bochum, Germany

*Correspondence: herbert.waldmann@mpi-dortmund.mpg.de

Abstract

For the discovery of novel chemical matter, *in general* endowed with bioactivity strategies may be particularly efficient that combine previous insight about biological relevance, *e.g.* natural product (NP) structure, with methods that enable efficient coverage of chemical space, such as fragment based design. We describe the *de novo* combination of different 5-membered NP-derived N-heteroatom fragments to structurally unprecedented "*pseudo natural products"* in an efficient complexity-generating and enantioselective one-pot synthesis sequence. The pseudo NPs inherit characteristic elements of NP structure but occupy areas of chemical space not covered by NP-derived chemotypes, and may have novel biological targets. Investigation of the pseudo-NPs in unbiased phenotypic assays and target identification led to the discovery of the first small-molecule ligand of the RHO GDP-dissociation inhibitor1 (RHOGDI1), termed Rhonin. Rhonin inhibits binding of the RHOGDI1 chaperone to GDP-bound Rho GTPases, induces activation of the GTPases and inhibits signal transduction through a non-canonical Hedgehog (Hh) pathway.

Introduction

The discovery of novel chemical matter, *in general* endowed with bioactivity and biological relevance is at the heart of chemical biology. Such compound classes may have new biological targets and modes of action, and, therefore, their bioactivity will best be evaluated in unbiased target-agnostic phenotypic assays, followed by target identification and validation.(*224-226*)

Strategies for the design of such novel compound classes can draw from previous insight about biological relevance of compound classes as for instance gained by Biology Oriented Synthesis (BIOS). In BIOS, complex natural product (NP) scaffolds are reduced to less complex, synthetically better accessible structures retaining the characteristic properties of the guiding NPs.(*227*) However, BIOS covers only a small fraction of natural product-like chemical space and arrives at compound classes that may retain the kind of bioactivity of the guiding NPs. These limitations can be overcome by the design and synthesis of "pseudo-natural products".(*228*) In pseudo-NPs natural product fragments that represent NP structure and properties(*229*) are combined *de novo* to unprecedented NP-inspired compound classes not accessible by known biosynthesis pathways. Pseudo-NPs inherit characteristic NP structures and properties but go beyond the chemical space explored by nature and, therefore, promise to have unexpected bioactivity and targets.

Five-membered N-heterocycles are defining structural units of numerous natural products with diverse bioactivity. Thus, succinimides occur for instance in the haterumaimides, which have antitumor activity(*230*), and the fungal metabolite hirsutellone, which is active against *Mycobacterium tuberculosis* (Figure 1a).(*231*) Pyrrolines are characteristic structural elements of eudistomin alkaloids with calmodulin antagonist activity (Figure 1a)(*232*) and the tobacco alkaloid myosmine(*233*) (Figure 1a). Pyrrolidines occur as isolated scaffolds in various structurally simple alkaloids like nicotine or fused to other scaffolds in structurally more complex alkaloids, such as

dendrobine (Figure 1a). In addition, in the nicotin receptor agonist epibatidine two pyrrolidines are fused in a bicyclic [2.2.1] arrangement (Figure 1a).

In light of this diverse occurrence of five-membered N-heterocycles in NPs, we designed and synthesized a pseudo-NP collection which combines these fragments in different connectivities. Phenotypic investigation of bioactivity and target identification led to the discovery of the novel Hedgehog pathway inhibitor Rhonin. Rhonin is the first small-molecule ligand of the RHO GDP-dissociation inhibitor1 (RHOGDI1), and inhibits binding of this chaperone to GDP-bound Rho GTPases. Its discovery establishes a link between RHOGDI1 and Hh signaling through a non-canonical pathway.

Results

Establishment of a tandem catalysis sequence

For the synthesis of a pseudo-NP collection we considered to combine 5-membered N-heterocycle fragments in a complexity-generating manner and by different connectivities (Figure 1b), i.e. such that (i) the fragments do not share atoms and are linked via one bond (monopodal connection; green bonds, Figure 1b), (ii) they share two atoms linked via a common bond (edge fusion; red bonds, Figure 1b) or they may be linked in a bicyclic arrangement sharing three atoms and two bonds (bridge fusion; magenta bonds, Figure 1b). Thereby related but different pseudo-NPs could be synthesized based on a limited set of fragments.

It was planned to initially construct pyrrolidines by means of an enantioselective dipolar cycloaddition of azomethine ylides with maleimides. This would yield an edge-fused pyrrolidine-succinimide pseudo-NP class, i. e. **3**. Subsequent oxidation of the pyrrolidine to an imine would give rise to a succinimide-pyrroline combination **4** which can undergo further transformations. The imine could be converted to a new azomethine ylide which might react with maleimides in a second 1,3-dipolar cycloaddition to yield a double fused pseudo-NP class **5** combining two succinimides with a bicyclic azabicyclo[2.2.1] scaffold characteristic for epibatidine. Nucleophilic addition to maleimides will generate a pseudo-NP class **6** containing two fragments linked by an edge fusion to a second succinimide fragment via a monopodal connection. Finally, conjugate addition to different □□□-unsaturated electrophiles would yield pseudo-NPs **7** in which a succinimide and a pyrrolidine are combined. The side chain may contain additional natural product fragments.

By means of this divergent synthesis approach several different pseudo-NP types would be accessible efficiently making use of a unified strategy. This synthesis strategy offers several attractive features. The metal-catalyzed 1,3-dipolar cycloaddition and the subsequent regio- and

chemoselective oxidation could potentially be coupled in a novel tandem catalytic approach in which the metal catalyst used for the cycloaddition could be employed in combination with an oxidizing agent. Such tandem catalysis sequences combining two or more mechanistically distinct chemical reactions are considered to be particularly attractive, since they enable expedient generation of molecular complexity and efficiency of the reaction sequence.(*234*) Hitherto Δ^1-pyrrolines have been synthesized by means of cycloaddition of Münchnones to electron-deficient alkenes.(*235, 236*) Thus, the tandem catalysis strategy outlined in Figure 1b also represents a novel method for the synthesis of this compound class.

In order to identify suitable reaction conditions for the tandem catalysis sequence, azomethine ylide **2a** (Figure 2a; R^2 = 4-Br) was reacted with *N*-methylmaleimide **1a** (R^1 = Me) in CH_2Cl_2 in the presence of $Cu(CH_3CN)_4PF_6$ as catalyst and (*R*)-Fesulphos [(R_p)-2-(*tert*-butylthio)-1-(diphenylphosphino)ferrocene)] as chiral ligand for the 1,3-dipolar cycloaddition.(*237*),(*238*) Subsequent addition of TBHP as terminal oxidant for the Cu(I) catalyzed oxidation gratifyingly yielded the desired pyrroline **4a** (Figure 1b; R^1 = Me, R^2 = 4-Br) in good yield (82%) and with complete regio- and chemoselectivity. Combination of these two steps with the envisaged additional cycloaddition and conjugate addition required careful optimization of the reaction conditions (see the Supplementary Information for details). After substantial experimentation, use of 1.5 equivalents of each Et_3N and maleimide in CH_2Cl_2 was found to be best for the formation of Michael addition products **6**. The double cycloaddition to tricyclic products **5** proceeded best in the presence of 0.5 equiv of DBU in THF. In CH_2Cl_2 and in the presence of DBU, instead nucleophilic addition to acyclic Michael acceptors occurred and products **7** were obtained (see the Supplementary Information for details).

Synthesis of a pseudo-NP collection.

The successful identification of conditions for the selective formation of the three envisaged compound classes enabled the assembly of a pseudo-NP collection. In the synthesis of double cycloadducts **5** (Figure 2a, conditions A) the aromatic ring of the azomethine ylides **2** can be varied (Figure 2a, **5a**-**5d**). Electron-donating and -accepting substituents on the phenyl ring were well tolerated and gave the cycloadducts **5a-d** in good yields and with generally excellent enantioselectivity (see Figure 2a). In addition, both aryl and alkyl maleimides could be successfully employed in the reaction in different order and combination (Figure 2a, **5e**, **5f**).

Under the conditions identified for the Michael addition to unsaturated cyclic electrophiles a variety of azomethine ylide precursors embodying electron-donating or –withdrawing substituents gave the corresponding products **6** in excellent yield and with high diastereo- and enantioselectivity (Figure 2a, **6a**-**6e**) and independent of the electronic nature and the position of the substituents on the phenyl ring in the dipole. Acyclic electrophiles like chalcone and different vinyl- and ethynyl ketones gave the corresponding products **7** in good yields and with high *ee* (Figure 2a, **7a**-**7i**). Notably, in the case of styryl-vinyl ketone, a single regioisomer **7e** was obtained in 72% yield. Ethynyl-phenyl ketone yielded the *E*-isomer **7g** in 71% yield.

The relative configuration of the cycloadducts was unambiguouly assigned by means of a crystal structure obtained for *rac*-**6a**. By means of VCD spectroscopy, the absolute configuration of the major diastereomer of **7a** was determined as (*S*)-**7a**. For **7h** a crystal structure analysis established the *E*-configuration (see the Supplementary Information for details). Since the diastereoselectivity of the last functionalization is determined by the two stereocenters established in the first cycloaddition, the absolute configuration of all other compounds was assigned by analogy. For a mechanistic proposal to rationalize the observed direction and level of stereochemical induction see Supplementary Scheme S1.

These results demonstrate that the synthesis strategy efficiently yields a pseudo NP collection including the formation of three stereocenters and a tetrasubstituted carbon atom, in a highly efficient one pot reaction.

Cheminformatic analysis

The chemical space occupied by the new pseudo-NPs was analyzed by employing the natural-product score (NP-score) distribution(*239*) as measure. Since the majority of the collection is defined by pyrrolines fused to succinimides, the NP-score was calculated for the sub-library defined by this scaffold and compared with both the score calculated for NPs in ChEMBL(*240*) and the score calculated for marketed and experimental drugs listed in DrugBank.(*241*) The pyrroline-derived pseudo-NPs display a narrow distribution in a region of the NP-Score graph which is sparsely covered by NPs (Figure 2b). The fact that the combination of NP-derived fragments yields compounds with properties diverging from NPs may be counterintuitive. However, the fragment combination generated here is not encountered in nature, such that the NP-score distribution of these pseudo-NPs should be different to NPs themselves. Comparison to the set of compounds in DrugBank which represent approved and experimental drugs, demonstrates that the pseudo-NPs display NP-scores in an area populated by synthetically accessible biologically relevant molecules. However, an additional analysis of the principal moments of inertia (PMI)(*242*), used as a measure of molecular shape, revealed that the pseudo-NPs described here have a high degree of three-dimensionality (Figure 2c) compared to typical synthetically accessible compound collections.(*243*) Further analysis using Lipinski-rule-of-5 (Lipinski-Ro5) criteria showed that only 42 % of the newly synthesized collection is included within the limits of drug-like space (Figure 2d), indicating that *de novo* combinations of NP-derived fragments may result in compound collections with enhanced biological relevance even when deviating from established metrics.

The analysis indicates that the succinimide-pyrroline pseudo-NPs may occupy a previously not accessible fraction of NP-inspired chemical space, reflecting the fact that they are not obtainable via current biosynthetic pathways. This novel scaffold may be endowed by design with advantageous physiochemical properties, as the pseudo-NP collection displays a NP-score distribution closer to the region occupied by approved drugs, even if the majority of the collection falls outside the limits of Lipinski-Ro5 space.

Biological evaluation of the pseudo NP collection

Investigation of biological activity of the pseudo NP collection in several cell-based assays monitoring modulation of autophagy, Wnt signaling, reactive oxygen species (ROS) induction, Notch signaling, and Hedgehog (Hh) signaling revealed that the pyrroline-derived compounds are potent and selective inhibitors of Hh pathway-dependent osteogenesis in pluripotent mouse mesenchymal C3H/10T1/2 cells (see Supplementary Table S6). Despite the limited number of compounds, trends for structure-activity correlation became apparent. Thus, extension of the ketone part of the most potent hit **7a,** e.g. by introduction of a *para*-Br substituent into the aryl ketone part (to yield **7b**), or by a *para*-F into the phenyl ring (Figure 2a, compare **7a** and **7d**) abolished activity. The configuration of the stereocenter generated in the final conjugate addition to yield e.g. **7a** has only minor impact on the bioactivity (Supplementary Table S6, compare **7a** and its epimer **7a-epi**). A phenyl group is not strictly required in the electrophile for activity, since methyl-vinyl ketone yielded active compound **7c** (Figure 2a and Supplementary Table S6, **7c**). However, in the presence of a phenyl group derived either from the aryl ketone part or the aryl-vinyl part of the electrophile, activity is higher (compare **7c** to **7a**, **7g** and **7e**). All active cycloadducts were derived from N-methyl maleimide. If the methyl group was replaced by a phenyl substituent, activity was lost (compare **7c** and **7f**). The most potent compound **7a** (Figure 3a; ultimately termed Rhonin, see below) showed an IC_{50} value of 1.60 ± 0.15 µM in the orthogonal GLI-dependent reporter gene assay in Sonic hedgehog (Shh)-LIGHT2 cells (see Supplementary

Table S6 and Figure 3b) and was selected for in-depth biological characterization. Rhonin dose dependently suppressed the expression of the Hh target genes *Ptch1* and *Gli1* to approx. 20 % (Figure 3c), thus confirming Hh pathway inhibition.

Most Hh pathway inhibitors target the seven pass transmembrane protein Smoothened (SMO) and often affect SMO ciliary localization(*244*). However, Rhonin did not displace the SMO binder BODIPY-cyclopamine from SMO (Figure 3d and Supplementary Figure S1). In addition, Rhonin did not affect localization of SMO to cilia as indicated by the co-localization of acetylated tubulin (as a ciliary marker) and SMO (Figure 3e). These findings indicate that Rhonin acts downstream of SMO.

Rhonin targets RHOGDI1

For target identification, affinity probes **8** and **9** (Figure 4a) were synthesized based on the structure-activity relationship. The corresponding Boc protected analogue of **8** retained significant Hh pathway inhibiting activity (**S10a**, IC_{50} = 12.0 ± 1.2 µM, Supplementary Table S6), whereas the Boc-protected analogue of **9** was inactive (**S10b**, Supplementary Table S6). After immobilization of the probes and affinity-based target enrichment (pulldown), label-free quantification of proteins that selectively bound to the active probe **8** as compared to the control probe **9** indicated RHO GDP-dissociation inhibitor 1 (RHOGDI1), Filamin-B and Filamin-C as potential targets (Supplementary Table S7). Subsequent immunoblotting after the pulldown confirmed the selective enrichment of RHOGDI1 but not of Filamin-B and Filamin-C (Figures 4b and 4c and Supplementary Figure S2) such that RHOGDI1 was further evaluated as target.

RHOGDI1 is a chaperone for geranylgeranylated (GerGer) proteins, in particular the RHO GTPases.(*245*) The major fraction (90 - 95%) of prenylated RHO GTPases are maintained in stable soluble state in the cytosol by RHOGDI1.(*246*) Rhonin directly binds to RHOGDI1 as

demonstrated for the fluorescent Rhonin derivative **10** which displays a dissociation constant (K_d) of 7.2 µM (Figures 4d and 4e). RHOGDI1 can extract GDP-bound inactive RHO GTPases from membranes and sequesters them in the cytosol. In an *in vitro* liposome sedimentation assay,(*247*) addition of RHOGDI1 to liposomes loaded with prenylated GDP-bound RAC1 resulted in extraction of RAC1, i.e., RAC1 was detected in the soluble fraction (Figure 4f). However, in the presence of Rhonin and RHOGDI1, RAC1 remained bound to the liposomes, i.e., RAC1 was detected in the insoluble fraction. This finding indicates that Rhonin inhibits the extraction of RAC1 by RHOGDI1. The structurally similar Rhonin analog **7d** (Figure 2a), which did not inhibit Hh signaling, also did not inhibit extraction of RAC1 from liposomes (Figure 4f). Similar results were obtained in a liposome flotation assay(*248*) (Supplementary Figures S3a and S3b). In addition to RAC1, Rhonin also inhibited the RHOGDI1-mediated extraction of RHOA and CDC42 (Supplementary Figure S3c and S3d). Rhonin slowed down the kinetics of geranylgeranylated RAC1 extraction mediated by RHOGDI1 in an surface plasmon resonance (SPR) setup using immobilized synthetic $PI(4,5)P_2$-rich liposomes loaded with geranylgeranylated GDP-bound RAC1, whereas the inactive derivative **7d** did not (Supplementary Figures S4a-c). These results suggest that Rhonin may directly modulate the RHOGDI1-RAC1 interaction. Whereas non-prenylated TAMRA-GDP-RAC1 bound to RHOGDI1 with a K_d of 14 µM, which is in agreement with previous reports,(*249*) in the presence of Rhonin the K_d value for the RHOGDI1-RAC1 interaction increased to 134 µM, which indicates that Rhonin does interfere with RHOGDI1-RAC1-GDP complex formation (Supplementary Figures S4d and S4e).

To gain insight into the binding site for Rhonin on RHOGDI1, competition between fluorescent derivative **10** and prenylated RAC1 was monitored. Addition of prenylated RAC1 to a pre-formed **10**-RHOGDI1 complex reduced fluorescence polarization, indicating displacement of **10** from RHOGDI1 (Figure 4g). However, non-prenylated RAC1 was able to bind RHOGDI1 but could not displace the ligand. Moreover, increasing concentration of Rhonin competed with the binding of

RHOGDI1 to a GerGer-RAB1 peptide, which was previously shown to bind to the prenyl binding pocket of RHOGDI1 (Figure 4h).(*250*) Based on the obtained results, the measured affinity between Rhonin and RHOGDI1 (K_d = 7.2 µM from Fig. 4e, 6 µM from Figures S4d and S4e) might initially appear to be too low to interfere with the extremely high affinity GerGer-RAC1/RHOGDI1 interaction (K_d = ca. 10^{-11} M (*251*)), and this would be true if Rhonin and GerGer-RAC1 were competing directly for binding to RHOGDI1 in the absence of other factors. However, as shown in Figure 4f, there is clear displacement of RAC1 from its complex with RHOGDI1 in the presence of liposomes. The reason for this is that there is already substantial competition for RAC1 binding to RHOGDI1 from the high concentration of lipids that are able to bind RAC1 with relatively high affinity, and this competition can be modified by Rhonin. We have simulated the effect of Rhonin on the distribution of RAC1 between RHOGDI1 and the liposome surface under the conditions of Figure 4f in the form of a titration with increasing Rhonin concentration using the values of the affinities already mentioned and an effective K_d for binding of a geranylgeranyl group to liposomes of 0.2 µM (defined with respect to the total exposed lipid concentration(*252*)). As shown in Supplementary Figure 4f, there is a predicted displacement of RAC1 from RHOGDI1 in the micromolar to hundreds of micromolar range of Rhonin concentration, and at 50 µM Rhonin, the concentration used for the experiment of Figure 4f, ca. 40% of RAC1 is bound to liposomes, in approximate agreement with the results of Figure 4f. Effectively, Rhonin acts as a buffer that reduces the free concentration of RHOGDI1 and this leads to the effects seen. These results show that Hh-pathway inhibitor **7a** targets RHOGDI1 and inhibits its RHO GTPase binding activity most likely by binding to the geranylgeranyl binding site of RHOGDI1. Hence, the compound was termed Rhonin. In order to determine selectivity for binding to RHOGDI1, displacement of fluorescein-labelled atorvastatin K_D = 58 nM from the prenyl-binding pocket of the lipoprotein chaperone PDE□□was investigated.(*253*) PDE□□binds preferably binds farnesylated lipoproteins like the Ras- and Rheb GTPases. Rhonin does not compete with fluorescein-labelled

atorvastatin for binding to PDE□□ indicating selectivity for RHOGDI1 (Supplementary Figure S4g).

RHOGDI is a negative regulator of Hh signaling

To examine the role of RHOGDI1 in Hh signaling we depleted RHOGDI1 using two different small interfering RNAs with a knockdown efficiency of 88 % for siRNA-1 and 64 % for siRNA-2 (Figure 5a). siRNA-1-mediated knockdown of RHOGDI1 along with simultaneous activation of the Hh pathway increased the levels of the Hh target genes *Ptch1* and *Gli1* (Figure 5b). By analogy, purmorphamine-mediated osteoblast differentiation was increased upon RHOGDI1 depletion (Figure 5c). Conversely, RHOGDI1 overexpression decreased Hh pathway activity (Figure 5d and Supplementary Figure S5b). These results indicate that, in principle, RHOGDI1 is a negative regulator of Hh signaling.

The different RHOGDI1 knockdown efficiencies achieved with siRNA-1 and siRNA-2 allow to explore the activity of Rhonin under graded depletion of RHOGDI1. Decreasing RHOGDI1 levels correlated with a decrease in Rhonin's ability to suppress Hh signaling, i.e., the compound had no (for siRNA-1, 88% knockdown) or only a weaker (for siRNA-2, 64% knockdown) influence on Hh target gene expression upon stimulation with purmorphamine (Figure 5b and Supplementary Figure S6). This result provides strong evidence that Rhonin inhibits Hh signaling by targeting RHOGDI1, as depletion of the entire target protein pool, e.g., by knockout or efficient knockdown, is expected to lead to full inactivity of the compound.

Rhonin activates RHO GTPases by inhibiting RHOGDI1

Since RHOGDI1 is a negative regulator of RHO GTPases, it is to be expected that an inhibitor of RHOGDI1 should positively affect the activity of RHO GTPases. Depletion of RHOGDI1 lowered the total level of RHOA and increased the level of RHOA-GTP by two fold (Figure 6a and 6b), which is in agreement with previous reports.(*246*) Stimulation of Hh signaling with purmorphamine

slightly increased the RHOA-GTP level. Notably, in the presence or absence of purmorphamine, treatment with Rhonin led to increased levels of GTP-bound RHOA. This finding indicates that RHOGDI1 inhibition by Rhonin phenocopies RHOGDI1 depletion. A similar but weaker trend was observed for RAC1 and CDC42 (Figure 6b).

RHO GTPases regulate formation of the actin cytoskeleton in fibroblasts and endothelial cells.(*254*) Serum starvation inhibits RHO GTPases and leads to disruption of the actin cytoskeleton (Figure 6c).(*255, 256*) Treatment of serum-starved cells with Rhonin for 24 h resulted in a dense network of actin stress fibers. The onset of stress fiber formation was observed as early as 2 h after treatment with Rhonin, indicating activation of RHOA (and most likely RHO associated kinase, ROCK). Interference with RHOGDI1 function should alter the subcellular localization of RHO GTPases.(*246*) Indeed, treatment with Rhonin led to a shift of the three RHO GTPases from the cytosolic to the heavy membrane fraction with the strongest influence on RHOA (Figure 6d and 6e and Supplementary Figure S7). The heavy membrane fraction contains the plasma membrane and the rough endoplasmic reticulum (rER). Thus, upon treatment with Rhonin the amount of RHO GTPases at the plasma membrane increases, i.e. the site of RHO-GTPase activation. Alternatively, the GTPases are mislocalized and trapped at the rER, thus preventing their activation. These findings show that Rhonin leads to activation and change in the subcellular localization of RHO GTPases.

Discussion

Efficient strategies for the discovery of new bioactive compounds with novel chemotypes may best build on established biological relevance of compound classes and their underlying scaffolds. In particular, natural product (NP) structure and activity have provided inspiration (*227*) for strategies like Biology Oriented Synthesis (*257, 258*) and natural product ring-distortion and modification (*259, 260*). However, NP-related compound collections usually represent only

focused areas of chemical space, and also of biological target space. Thus, strategies that enable efficient and wider coverage of biologically relevant, NP-related chemical space, like fragment based design, are highly desirable and in high demand.

Application of fragment-based design to the synthesis of NP-inspired compound collections, calls for *de novo* combinations of NP fragments.(*229*) The resulting novel compound classes will inherit characteristic NP-structures, properties and relevance but go beyond the chemical space explored by nature because they will not be accessible by known biosynthesis pathways. Thus, they may be regarded as “pseudo natural products”.(*228*) This term has been previously used by Suga *et al*., (*261, 262*) to describe cyclopeptides synthesized *in vitro,* as well as by Oshima *et al*. (*263, 264*) to characterize hybrid compounds obtained by biosynthetic pathway interception. Due to the unprecedented combination of NP fragments pseudo-NPs may have unexpected and novel targets which may not be related to the bioactivity of the guiding NPs. Hence their bioactivity should be analyzed in unbiased, target-agnostic phenotypic assays to widely cover biological target space.

We validate the “pseudo natural product” concept by the design, synthesis and evaluation of a compound collection that combines five-membered N-heterocycles (i.e. pyrrolidines, pyrrolines and succinimides) characteristic for NP classes with different structure and different biosynthetic origin, in novel arrangements and with different connectivities.

Cheminformatic analysis, employing the NP-score as measure for NP-likeness, indicated that the pyrroline-derived pseudo-NPs occupy an area of chemical space previously not accessible to and, therefore, only sparsely covered by NPs. Rather the pseudo-NPs display NP scores characteristic for drug-like compound classes, such that they may be endowed by design with advantageous physiochemical properties.

The novel pseudo-NP Rhonin proved to be an inhibitor of Hh signaling. The Hh signaling pathway is vital for organ development and body patterning during embryogenesis and its inappropriate activation is linked to several types of cancers. SMO is the most druggable target in Hh signaling, however, there is a need to impinge the pathway downstream of SMO due to recently discovered drug-resistant mutations in SMO.(*265*) In addition, there are SMO-dependent and –independent non-canonical Hh-pathways for which small molecule modulators have rarely been developed.(*266, 267*) We demonstrate that Rhonin binds to RHOGDI1, which translates to displacement of RHOGDI1-bound RHO GTPases, results in enrichment of GTP-bound RHO GTPases in membranes and establishes a link between RHOGDI1 and Hh signalling. The compound most likely directly binds into the prenyl binding pocket. Efficient depletion of RHOGDI1 completely abolished the pathway inhibitory activity of Rhonin and validates RHOGDI1 as the target protein with regard to Hh pathway inhibition. To the best of our knowledge, no direct RHOGDI1 inhibitor has been described to date. The only reported small molecule related to RHOGDI1 function is secramine A, which inhibits CDC42-mediated actin polymerization in a RHOGDI1-dependent manner.(*268*) However, a direct interaction between secramine A and RHOGDI1has not been shown.

RHOGDI1 is a chaperone and negative regulator of the geranylgeranylated RHO GTPases RHOA, RAC1 and CDC42(*269*) which regulate the actin cytoskeleton and, thus, processes like cell adhesion, establishment of cell polarity and cell migration.(*269*) RHOGDI1 binds and buries the membrane-anchoring geranylgeranyl moiety of the GTPases in a hydrophobic pocket and, thereby, increases their solubility in the cytosol.(*245*) It extracts RHO GTPases from membranes and sequesters them in the cytosol, thus preventing their activation at the target membrane.(*245*) In the absence of RHOGDI, the cytosolic pool of the geranylgeranylated RHO GTPases, constituting 90-95% of total RHO GTPases, is rapidly degraded by the proteasome, while the levels of membrane-bound GTP-bound RHO GTPases increase.(*270, 271*) However, these

activated RHO GTPases may fail to properly localize to their target membranes and accumulate at the endoplasmic reticulum , thus effectors may not be activated.(*246*) As opposed to activation of all GTPases, in *RHOGDI1*$^{-/-}$ mice activation of only RHOA but not RAC1 and CDC42 was observed along with hyper-phosphorylation of myosin light chain.(*272*) Activation of only RHOA was also evident in the detection of stress fiber formation upon RHOGDI knockdown in HUVEC cells.(*272*) Interestingly, Rhonin increases the level of GTP-bound RHOA and induces stress fiber formation, which is in line with increased activity of RHOA.(*273*)

Direct involvement of RHOGDI1 in Hh pathway regulation has not been reported before. However, RHO GTPases have been linked to Smo-dependent, non-canonical Hh signaling(*266, 267*) (Supplementary Figure S8a). SMO can signal through $G\alpha_i$ to activate RHOA and RAC1 and modulate the actin cytoskeleton in a non-canonical fashion.(*274-277*) In addition, RHOA has been linked to GLI-mediated transcription. However, the signal to RHOA was transmitted via by $G\alpha_{12}$ or $G\alpha_{13}$ and did not include SMO or SHH.(*278, 279*) In hematopoietic stem cells, a constitutively active mutant of RAC1 induced higher expression of GLI-2 and SHH. Conversely, dominant negative RAC1 decreased the expression of GLI-2 and SHH, therefore suggesting a GLI-dependent regulation of Hh signaling by RHO GTPases.(*280*) Furthermore, *IFT80* (Intraflagellar transport protein 80) deletion causes cilia defects and leads to suppression of Hh-GLI signaling and osteoblast differentiation while increasing Hh-SMO-$G\alpha_i$-RHOA-stress fiber signaling.(*281*) The resulting RHOA activation and its suppressive influence on Hh-induced osteogenesis was partially or fully reverted by RHOA or ROCK inhibition or by disrupting the actin cytoskeleton.(*281*) Inhibition of actin assembly positively influences ciliogenesis,(*281, 282*) and RHO GTPases have also been linked to ciliogenesis, i.e. CDC42 restricts the frequency of ciliated cells and axoneme length by recruiting the regulators of actin dynamics.(*283*) However, although depletion of CDC42 increases axoneme length and ciliation, it suppresses canonical Hh signaling.(*283*) Thus, an intricate interplay between RHO GTPases and GLI-mediated transcription exists and genetic or

pharmacological modulation of RHOGDI1 is expected to have a pleiotropic influence with not readily predictable outcome with regard to osteogenesis and Hh-SMO-GLI signaling.

The non-canonical SMO-RHOA pathway suppresses the SMO-GLI pathway(*281*), and RHOGDI1 knockdown should positively modulate the SMO-GLI axis because the amount of GTP-bound RHO GTPases will increase but downstream effectors may not be activated. Indeed, we observed increased Hh-mediated osteogenesis upon depletion of RHOGDI1. However, knockdown of RHOGDI1 should also impair CDC42-controlled ciliation that may negatively influence Hh-GLI-related processes. The $G\alpha_{12}/G\alpha_{13}$-RHOA-GLI axis, if active during osteogenesis in the employed cell line, would likewise be inhibited by RHOGDI1 depletion. We observe, most likely as net sum of all effects on RHO GTPases, an increase in osteogenesis upon RHOGDI1 knockdown. Pathway perturbation and RHOGDI1 inhibition by Rhonin have effects on Hh signaling opposite to RHOGDI1 depletion. Such divergence between chemical and genetic perturbations has been observed before and, actually, may differentiate a chemical-biological analysis form a genetic investigation.(*284, 285*) Genetic knockout or knockdown remove or reduce the target protein, whereas small molecules modulate individual binding sites or functions. RHOGDI1 recognizes its target GTPases via two binding sites. While Rhonin affects binding to the prenyl binding pocket, RHOGDI1 knockdown abolishes binding to both sites.

Our findings suggest that Rhonin influences canonical Hh signaling via a non-canonical route. They are in agreement with a mode of action in which Rhonin binds to RHOGDI1, prevents the extraction of RHO GTPases from membranes and, thereby, leads to increased pools of active, GTP-bound RHO GTPases. Whether all three GTPases are activated or not, would depend on the employed system since activity of RHO GTPases will depend on different factors, i.e. phosphorylation, ubiquitination, GEFs and GAPs etc.(*269*). Our data indicate that, in contrast to RHOGDI1 depletion, inhibition of RHOGDI1 with Rhonin increases RHOA activity, thus causing

stress fiber formation. Increased actin polymerization has been linked to impaired cilia-related function(*281, 286*) and may be the causal link between RHOA activity and Hh-GLI pathway inhibition (Supplementary Figure S8b).

Acknowledgments

This work was supported by the Max Planck Society and the European Research Council under the European Union's Seventh Framework Programme (FP7/2007–2013, ERC Grant agreement no. 268309), as well as the German Research Foundation (DFG, AH 92/8-1), the Cluster of Excellence RESOLV ("Ruhr Explores Solvation") (EXC-2033, project 390677874; formerly EXC 1069), the International Research Training Group (IRTG 1902, SP6), the European Network on Noonan Syndrome and Related Disorders (NSEuroNet, 01GM1602B), the German Federal Ministry of Education and Research – German Network of RASopathy Research (GeNeRARe, 01GM1519D). We thank Dr. Sonja Sievers and the Compound Management and Screening Center (COMAS), Dortmund, Germany for screening the compounds. We thank Lena Knauer and Kathrin Louven (Technical University Dortmund) for performing X-ray crystallographic analysis. We are grateful towards Dr. Peter Bieling (Max Planck Institute of Molecular Physiology, Dortmund), Dr. Leif Dehmelt (Technical University Dortmund) and Dr. Oliver Rocks (Max Delbrück Center for Molecular Medicine, Berlin) for valuable discussions.

Author contributions

S.P. carried out biological experiments, affinity probe synthesis, target identification and genetic validations. E.S. and R.N. synthesized the pseudo-NP compound library. M.A., M.B. and N.J. performed biological experiments, M.P. and H.K. synthesized chemical probes. G.K. performed chemoinformatic analysis. C.G. and C.S. analyzed crystallography data and C. M. conducted the VCD measurements and subsequent calculations. P.J. carried out the MS-proteomics analysis.

R.G. performed the simulations. H.W., S.Z. and M.R.A. designed research. S.P., E.S., S.Z, and H.W. wrote the manuscript. All authors discussed the results and commented on the manuscript.

References

1. Ursu, A. & Waldmann, H. Hide and seek: Identification and confirmation of small molecule protein targets. *Bioorg Med Chem Lett* **25**, 3079-86 (2015).
2. Wagner, B.K. & Schreiber, S.L. The Power of Sophisticated Phenotypic Screening and Modern Mechanism-of-Action Methods. *Cell Chem Biol* **23**, 3-9 (2016).
3. Vincent, F. et al. Developing predictive assays: the phenotypic screening "rule of 3". *Sci Transl Med* **7**, 293ps15 (2015).
4. van Hattum, H. & Waldmann, H. Biology-oriented synthesis: harnessing the power of evolution. *J Am Chem Soc* **136**, 11853-9 (2014).
5. Karageorgis, G. et al. Chromopynones are pseudo natural product glucose uptake inhibitors targeting glucose transporters GLUT-1 and -3. *Nature Chemistry* (2018).
6. Over, B. et al. Natural-product-derived fragments for fragment-based ligand discovery. *Nat Chem* **5**, 21-8 (2013).
7. Uddin, M.J., Kokubo, S., Ueda, K., Suenaga, K. & Uemura, D. Haterumaimides F−I, Four New Cytotoxic Diterpene Alkaloids from an Ascidian Lissoclinum Species. *Journal of Natural Products* **64**, 1169-1173 (2001).
8. Isaka, M. et al. Hirsutellones A–E, antimycobacterial alkaloids from the insect pathogenic fungus Hirsutella nivea BCC 2594. *Tetrahedron* **61**, 5577-5583 (2005).
9. Kobayashi, J.i., Nakamura, H., Ohizumi, Y. & Hirata, Y. Eudistomidin-A, a novel calmodulin antagonist from the okinawan tunicate eudistoma glaucus. *Tetrahedron Letters* **27**, 1191-1194 (1986).
10. Tyroller, S., Zwickenpflug, W. & Richter, E. New Sources of Dietary Myosmine Uptake from Cereals, Fruits, Vegetables, and Milk. *Journal of Agricultural and Food Chemistry* **50**, 4909-4915 (2002).
11. Lohr, T.L. & Marks, T.J. Orthogonal tandem catalysis. *Nat Chem* **7**, 477-82 (2015).
12. Melhado, A.D., Amarante, G.W., Wang, Z.J., Luparia, M. & Toste, F.D. Gold(I)-Catalyzed Diastereo- and Enantioselective 1,3-Dipolar Cycloaddition and Mannich Reactions of Azlactones. *Journal of the American Chemical Society* **133**, 3517-3527 (2011).
13. Sun, W. et al. Organocatalytic Diastereo- and Enantioselective 1,3-Dipolar Cycloaddition of Azlactones and Methyleneindolinones. **52**, 8633-8637 (2013).
14. Antonchick, A.P. et al. Highly enantioselective synthesis and cellular evaluation of spirooxindoles inspired by natural products. *Nature Chemistry* **2**, 735 (2010).
15. Narayan, R., Potowski, M., Jia, Z.-J., Antonchick, A.P. & Waldmann, H. Catalytic Enantioselective 1,3-Dipolar Cycloadditions of Azomethine Ylides for Biology-Oriented Synthesis. *Accounts of Chemical Research* **47**, 1296-1310 (2014).
16. Ertl, P., Roggo, S. & Schuffenhauer, A. Natural Product-likeness Score and Its Application for Prioritization of Compound Libraries. *Journal of Chemical Information and Modeling* **48**, 68-74 (2008).
17. Bento, A.P. et al. The ChEMBL bioactivity database: an update. *Nucleic Acids Research* **42**, D1083-D1090 (2014).
18. Law, V. et al. DrugBank 4.0: shedding new light on drug metabolism. *Nucleic Acids Research* **42**, D1091-D1097 (2014).

19. Sauer, W.H.B. & Schwarz, M.K. Molecular Shape Diversity of Combinatorial Libraries: A Prerequisite for Broad Bioactivity. *Journal of Chemical Information and Computer Sciences* **43**, 987-1003 (2003).
20. Colomer, I. et al. A divergent synthetic approach to diverse molecular scaffolds: assessment of lead-likeness using LLAMA, an open-access computational tool. *Chemical Communications* **52**, 7209-7212 (2016).
21. Lin, T.L. & Matsui, W. Hedgehog pathway as a drug target: Smoothened inhibitors in development. *OncoTargets and therapy* **5**, 47-58 (2012).
22. Garcia-Mata, R., Boulter, E. & Burridge, K. The 'invisible hand': regulation of RHO GTPases by RHOGDIs. *Nat Rev Mol Cell Biol* **12**, 493-504 (2011).
23. Boulter, E. et al. Regulation of Rho GTPase crosstalk, degradation and activity by RhoGDI1. *Nat Cell Biol* **12**, 477-83 (2010).
24. Zhang, S.-C. et al. Liposome Reconstitution and Modulation of Recombinant Prenylated Human Rac1 by GEFs, GDI1 and Pak1. *PLOS ONE* **9**, e102425 (2014).
25. Bigay, J., Casella, J.F., Drin, G., Mesmin, B. & Antonny, B. ArfGAP1 responds to membrane curvature through the folding of a lipid packing sensor motif. *Embo j* **24**, 2244-53 (2005).
26. Newcombe, A.R., Stockley, R.W., Hunter, J.L. & Webb, M.R. The Interaction between Rac1 and Its Guanine Nucleotide Dissociation Inhibitor (GDI), Monitored by a Single Fluorescent Coumarin Attached to GDI. *Biochemistry* **38**, 6879-6886 (1999).
27. Mejuch, T. et al. Small-Molecule Inhibition of the UNC119-Cargo Interaction. *Angew Chem Int Ed Engl* **56**, 6181-6186 (2017).
28. Tnimov, Z. et al. Quantitative analysis of prenylated RhoA interaction with its chaperone, RhoGDI. *J Biol Chem* **287**, 26549-62 (2012).
29. Silvius, J.R. & l'Heureux, F. Fluorimetric evaluation of the affinities of isoprenylated peptides for lipid bilayers. *Biochemistry* **33**, 3014-22 (1994).
30. Shepard, A.R. et al. Identification of PDE6D as a molecular target of anecortave acetate via a methotrexate-anchored yeast three-hybrid screen. *ACS Chem Biol* **8**, 549-58 (2013).
31. Guilluy, C., Garcia-Mata, R. & Burridge, K. Rho protein crosstalk: another social network? *Trends Cell Biol* **21**, 718-26 (2011).
32. Ridley, A.J. & Hall, A. The small GTP-binding protein rho regulates the assembly of focal adhesions and actin stress fibers in response to growth factors. *Cell* **70**, 389-99 (1992).
33. Ridley, A.J., Paterson, H.F., Johnston, C.L., Diekmann, D. & Hall, A. The small GTP-binding protein rac regulates growth factor-induced membrane ruffling. *Cell* **70**, 401-10 (1992).
34. Bon, R.S. & Waldmann, H. Bioactivity-guided navigation of chemical space. *Acc Chem Res* **43**, 1103-14 (2010).
35. Wetzel, S., Bon, R.S., Kumar, K. & Waldmann, H. Biology-oriented synthesis. *Angew Chem Int Ed Engl* **50**, 10800-26 (2011).
36. Huigens, R.W. et al. A ring-distortion strategy to construct stereochemically complex and structurally diverse compounds from natural products. *Nature Chemistry* **5**, 195-202 (2013).
37. Rafferty, R.J., Hicklin, R.W., Maloof, K.A. & Hergenrother, P.J. Synthesis of Complex and Diverse Compounds through Ring Distortion of Abietic Acid. *Angewandte Chemie-International Edition* **53**, 220-224 (2014).
38. Goto, Y., Ito, Y., Kato, Y., Tsunoda, S. & Suga, H. One-Pot Synthesis of Azoline-Containing Peptides in a Cell-free Translation System Integrated with a Posttranslational Cyclodehydratase. *Chemistry & Biology* **21**, 766-774 (2014).

39. Ozaki, T. et al. Dissection of goadsporin biosynthesis by in vitro reconstitution leading to designer analogues expressed in vivo. *Nature Communications* **8**: 14207 (2017), DOI: 10.1038/ncomms14207 |
40. Asai, T. et al. Use of a biosynthetic intermediate to explore the chemical diversity of pseudo-natural fungal polyketides. *Nature Chemistry* **7**, 737-743 (2015).
41. Kikuchi, H. et al. Monoterpene Indole Alkaloid-Like Compounds Based on Diversity-Enhanced Extracts of Iridoid-Containing Plants and Their Immune Checkpoint Inhibitory Activity. *Organic Letters* **18**, 5948-5951 (2016).
42. Cook, D.R., Rossman, K.L. & Der, C.J. Rho guanine nucleotide exchange factors: regulators of Rho GTPase activity in development and disease. *Oncogene* **33**, 4021-35 (2014).
43. Teperino, R., Aberger, F., Esterbauer, H., Riobo, N. & Pospisilik, J.A. Canonical and non-canonical Hedgehog signalling and the control of metabolism. *Semin Cell Dev Biol* **33**, 81-92 (2014).
44. Robbins, D.J., Fei, D.L. & Riobo, N.A. The Hedgehog signal transduction network. *Sci Signal* **5**, re6 (2012).
45. Pelish, H.E. et al. Secramine inhibits Cdc42-dependent functions in cells and Cdc42 activation in vitro. *Nature Chemical Biology* **2**, 39 (2005).
46. Hodge, R.G. & Ridley, A.J. Regulating Rho GTPases and their regulators. *Nature Reviews Molecular Cell Biology* **17**, 496-510 (2016).
47. Arnst, J.L. et al. Discovery and characterization of small molecule Rac1 inhibitors. *Oncotarget* **8**, 34586-34600 (2017).
48. Hong, L. et al. Characterization of a Cdc42 protein inhibitor and its use as a molecular probe. *J Biol Chem* **288**, 8531-43 (2013).
49. Gorovoy, M. et al. RhoGDI-1 modulation of the activity of monomeric RhoGTPase RhoA regulates endothelial barrier function in mouse lungs. *Circulation Research* **101**, 50-58 (2007).
50. Schaefer, A., Reinhard, N.R. & Hordijk, P.L. Toward understanding RhoGTPase specificity: structure, function and local activation. *Small GTPases* **5**, 6 (2014).
51. Carballo, G.B., Honorato, J.R., de Lopes, G.P.F. & Spohr, T.C.L.D.E. A highlight on Sonic hedgehog pathway. *Cell Communication and Signaling* **16**(2018).
52. Pandit, T. & Ogden, S.K. Contributions of Noncanonical Smoothened Signaling During Embryonic Development. *Journal of Developmental Biology* **5**(2017).
53. Chinchilla, P., Xiao, L., Kazanietz, M.G. & Riobo, N.A. Hedgehog proteins activate pro-angiogenic responses in endothelial cells through non-canonical signaling pathways. *Cell Cycle* **9**, 570-79 (2010).
54. Polizio, A.H. et al. Heterotrimeric G(i) Proteins Link Hedgehog Signaling to Activation of Rho Small GTPases to Promote Fibroblast Migration. *Journal of Biological Chemistry* **286**, 19589-19596 (2011).
55. Kasai, K. et al. The G12 family of heterotrimeric G proteins and Rho GTPase mediate Sonic hedgehog signalling. *Genes Cells* **9**, 49-58 (2004).
56. Douglas, A.E. et al. The alpha Subunit of the G Protein G(13) Regulates Activity of One or More Gli Transcription Factors Independently of Smoothened. *Journal of Biological Chemistry* **286**, 30714-30722 (2011).
57. Choi, S.S. et al. Activation of Rac1 promotes hedgehog-mediated acquisition of the myofibroblastic phenotype in rat and human hepatic stellate cells. *Hepatology* **52**, 278-90 (2010).
58. Yuan, X. et al. Ciliary IFT80 balances canonical versus non-canonical hedgehog signalling for osteoblast differentiation. *Nature Communications* **7**(2016).

59. Kim, J. et al. Functional genomic screen for modulators of ciliogenesis and cilium length. *Nature* **464**, 1048-U114 (2010).
60. Drummond, M.L. et al. Actin polymerization controls cilia-mediated signaling. *Journal of Cell Biology* **217**, 3255-3266 (2018).
61. Knight, Z.A. & Shokat, K.M. Chemical genetics: Where genetics and pharmacology meet. *Cell* **128**, 425-430 (2007).
62. Weiss, W.A., Taylor, S.S. & Shokat, K.M. Recognizing and exploiting differences between RNAi and small-molecule inhibitors. *Nature Chemical Biology* **3**, 739-744 (2007).
63. Mirvis, M., Stearns, T. & Nelson, W.J. Cilium structure, assembly, and disassembly regulated by the cytoskeleton. *Biochemical Journal* **475**, 2329-2353 (2018).

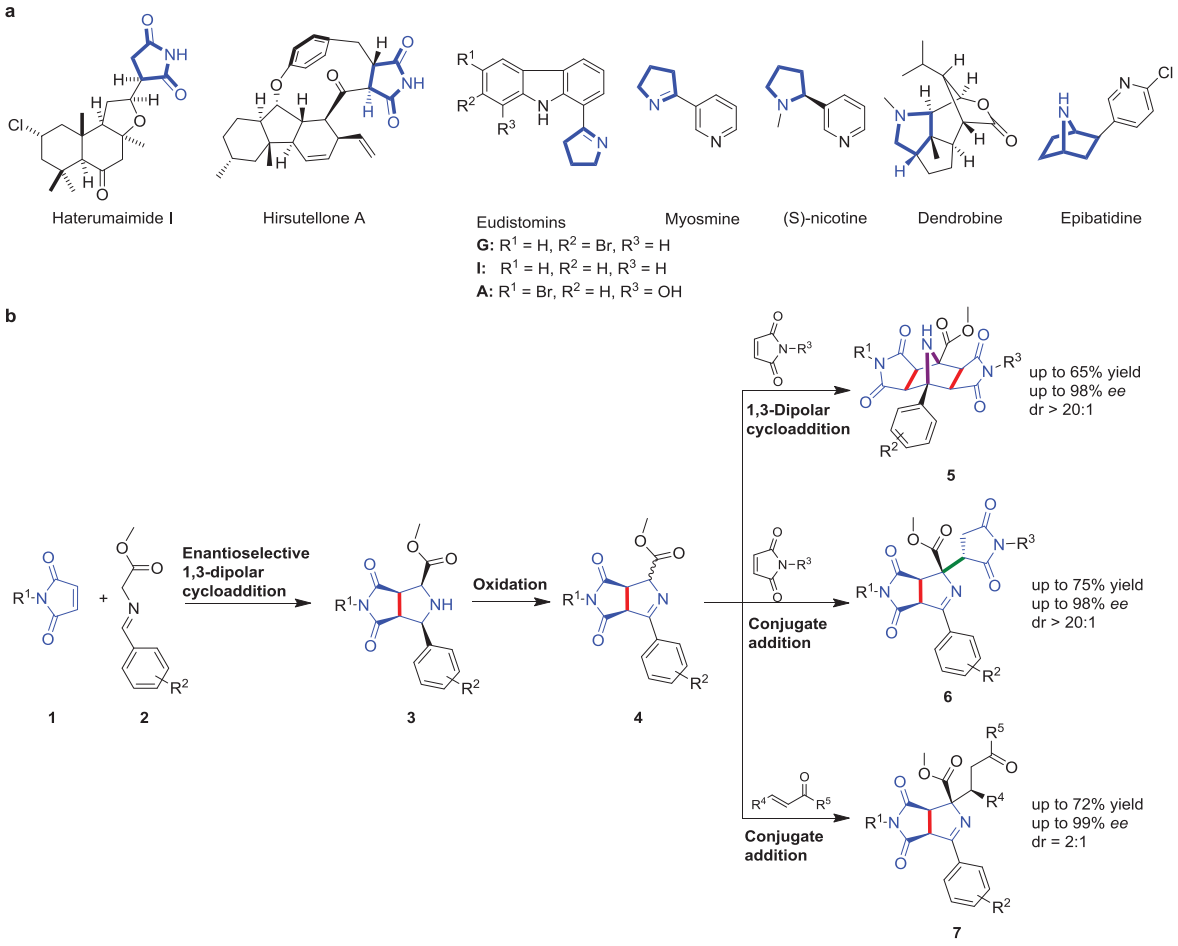

Figure 1. Design of a pseudo-NP collection (**a**) Representative natural products embodying 5-membered N-heterocycles; (**b**) Tandem catalysis sequence for the synthesis of a pseudo-NP collection containing 5-membered N-heterocycles in different connectivities.

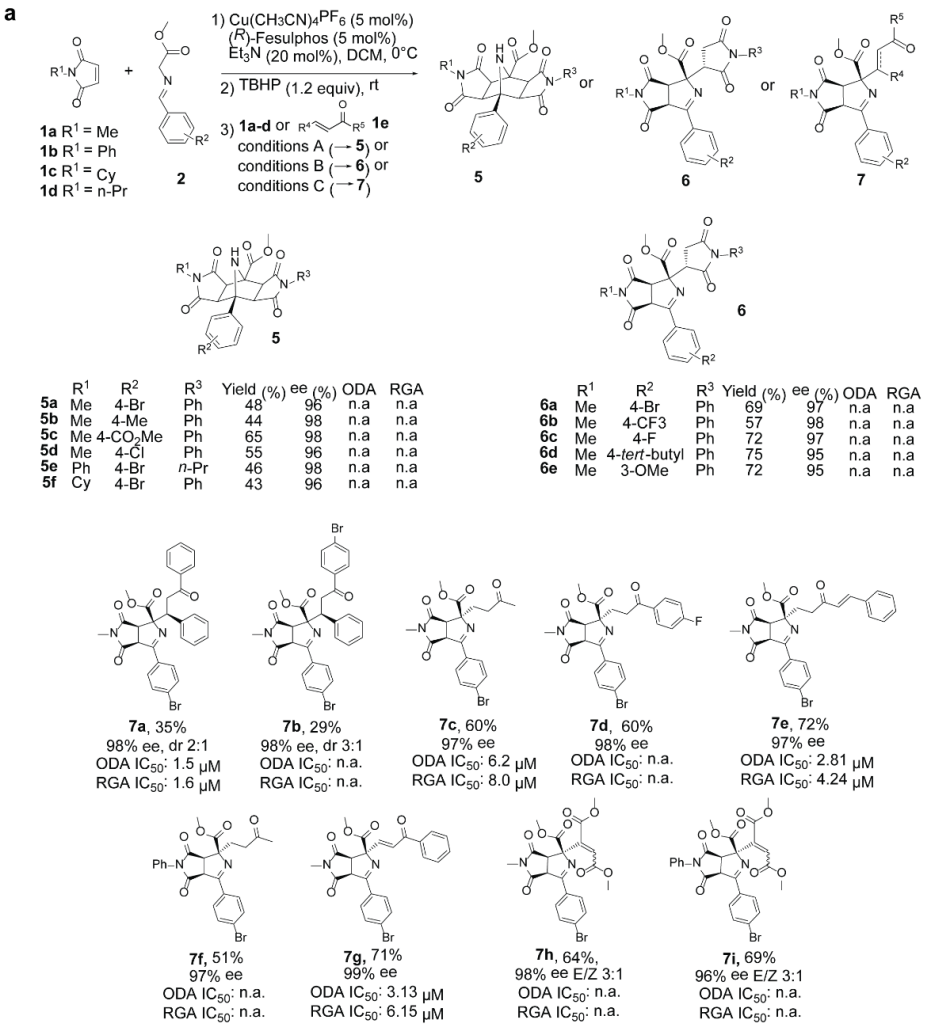

	R^1	R^2	R^3	Yield (%)	ee (%)	ODA	RGA
5a	Me	4-Br	Ph	48	96	n.a	n.a
5b	Me	4-Me	Ph	44	98	n.a	n.a
5c	Me	4-CO_2Me	Ph	65	98	n.a	n.a
5d	Me	4-Cl	Ph	55	96	n.a	n.a
5e	Ph	4-Br	*n*-Pr	46	98	n.a	n.a
5f	Cy	4-Br	Ph	43	96	n.a	n.a

	R^1	R^2	R^3	Yield (%)	ee (%)	ODA	RGA
6a	Me	4-Br	Ph	69	97	n.a	n.a
6b	Me	4-CF3	Ph	57	98	n.a	n.a
6c	Me	4-F	Ph	72	97	n.a	n.a
6d	Me	4-*tert*-butyl	Ph	75	95	n.a	n.a
6e	Me	3-OMe	Ph	72	95	n.a	n.a

7a, 35%
98% ee, dr 2:1
ODA IC_{50}: 1.5 µM
RGA IC_{50}: 1.6 µM

7b, 29%
98% ee, dr 3:1
ODA IC_{50}: n.a.
RGA IC_{50}: n.a.

7c, 60%
97% ee
ODA IC_{50}: 6.2 µM
RGA IC_{50}: 8.0 µM

7d, 60%
98% ee
ODA IC_{50}: n.a.
RGA IC_{50}: n.a.

7e, 72%
97% ee
ODA IC_{50}: 2.81 µM
RGA IC_{50}: 4.24 µM

7f, 51%
97% ee
ODA IC_{50}: n.a.
RGA IC_{50}: n.a.

7g, 71%
99% ee
ODA IC_{50}: 3.13 µM
RGA IC_{50}: 6.15 µM

7h, 64%,
98% ee E/Z 3:1
ODA IC_{50}: n.a.
RGA IC_{50}: n.a.

7i, 69%
96% ee E/Z 3:1
ODA IC_{50}: n.a.
RGA IC_{50}: n.a.

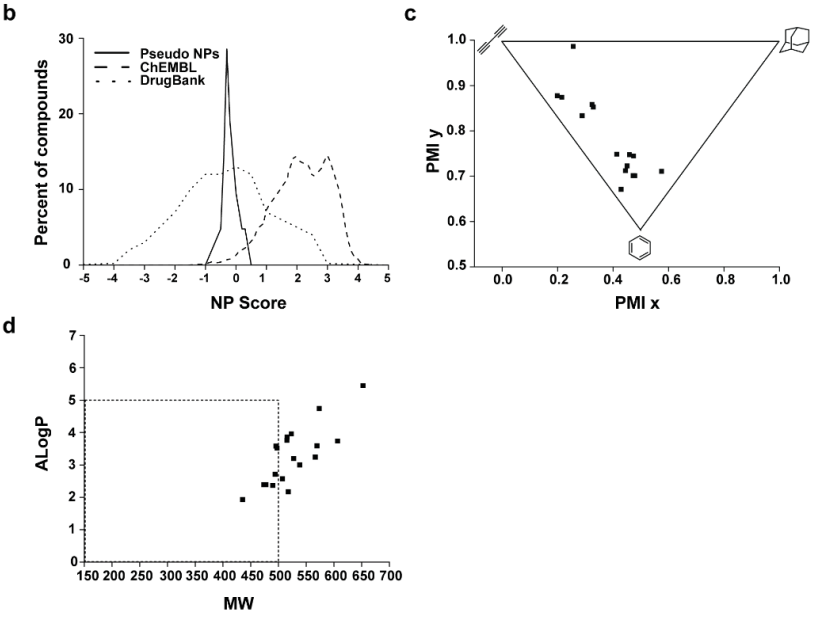

Figure 2. Synthesis of a pseudo-NPs that occupy a distinct portion of chemical space. (a) Reaction conditions: A) **1a-d** (3 equiv), DBU (0.5 equiv), THF, rt; B) **1a-d** (1.5 equiv), Et_3N (1.5 equiv), DCM, rt; C) **1e** (1.5 equiv), DBU (0.5 equiv), DCM, rt. For **7a** the yield represents the epimeric mixture of the phenylethyl ketone. ODA: Osteoblast differentiation assay. RGA: Reporter gene assay. All ODA and RGA data are mean values of three independent experiments (n = 3) ± s.d. **(b)** NP-likeness score comparison of NPs represented in ChEMBL (dashed curve), Drugbank (dotted curve) and succinimide-pyrroline pseudo NPs (solid curve). **(c)** PMI plot for succinimide-pyrroline pseudo-NPs. **(d)** ALogP vs MW plot of succinimide-pyrroline pseudo NPs.

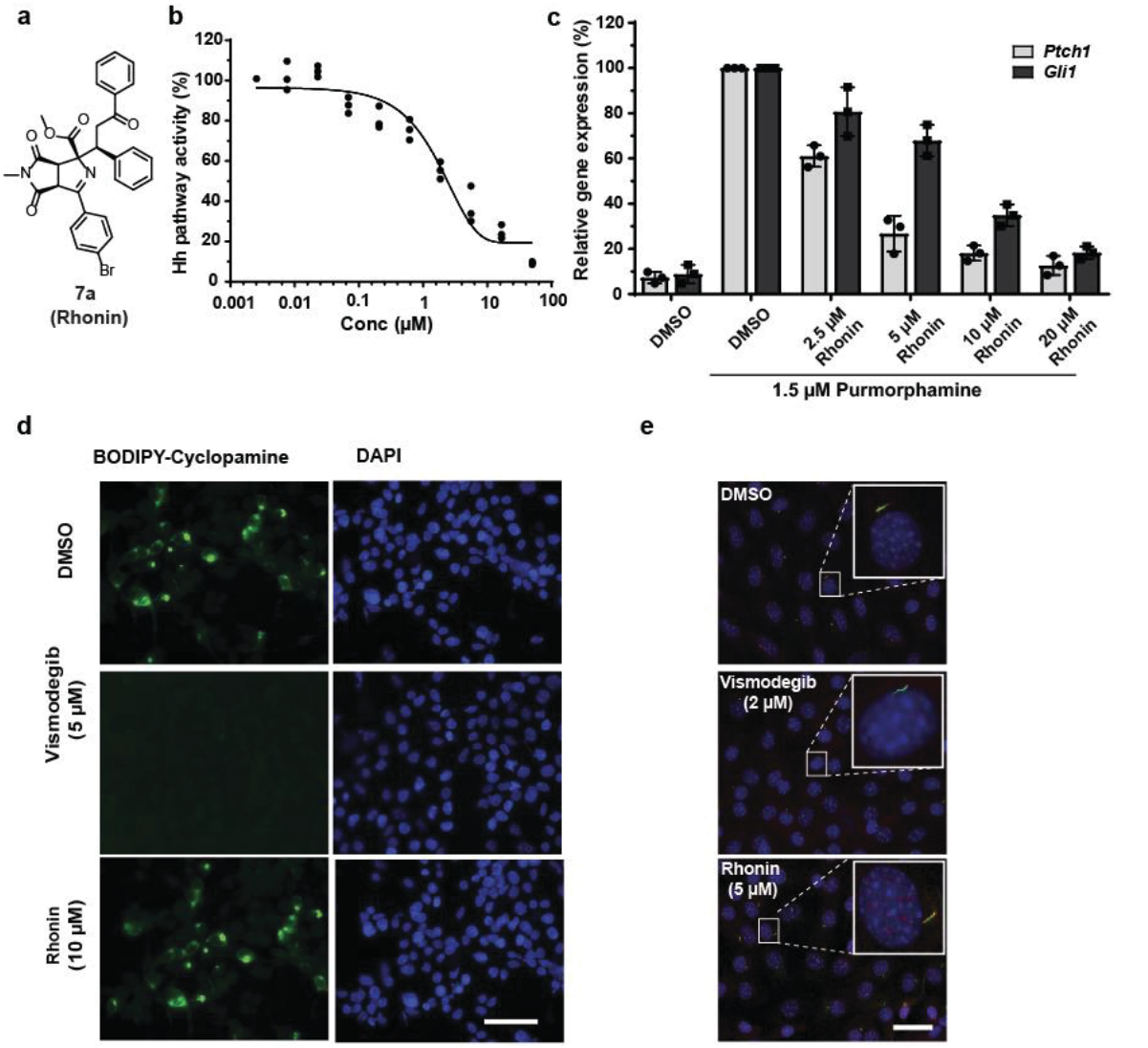

Figure 3. Rhonin inhibits GLI-dependent Hh signaling and acts downstream of SMO. (a) Structure of Rhonin (**7a**). **(b)** Rhonin inhibits GLI-dependent reporter gene expression in Shh-LIGHT2 cells. Cells were treated with 1.5 μM purmorphamine and different concentrations of the compound for 48 h. Firefly (fluc) and *Renilla* luciferase (rluc) activities were determined and ratios of fluc/rluc signals were calculated as a measure of Hh pathway activity. Nonlinear regression analysis was performed using a four parameter fit. Data of three independent experiments (n = 3) are shown. **(c)** C3H/10T1/2 cells were treated with purmorphamine (1.5 μM) and different

concentrations of Rhonin or DMSO as a control for 48 h prior to isolation of total RNA. Following cDNA preparation, the relative expression levels of *Ptch1*, *Gli1* and *Gapdh* were determined by means of RT-qPCR. Expression levels of *Ptch1* and *Gli1* were normalized to the levels of *Gapdh* and were related to the value of purmorphamine-treated cells (set to 100 %). Data are mean values of three independent experiments (n = 3) ± s.d. (**d**) HEK293T cells were transiently transfected with SMO expressing plasmid or empty vector. 48 h later cells were treated with BODIPY-cyclopamine (5 nM, green) followed by addition of 10 µM of Rhonin or 5 µM vismodegib and DMSO as controls and incubation for 1 h. Cells were then fixed and stained with DAPI to visualize the nuclei (blue). Scale bar: 20 µm. (**e**) NIH/3T3 cells were serum starved to induce ciliation and treated with 1.5 µM purmorphamine for 2 h followed by addition of 2 µM vismodegib or 5 µM Rhonin, and further incubation for 12 h. Cells were then fixed and stained with DAPI to visualize the nuclei (blue), SMO was stained with an anti-SMO antibody (red) and cilia stained with an antibody against acetylated tubulin (Ac-tubulin, green). Insets: representative single cilia. Scale bar: 10 µm.

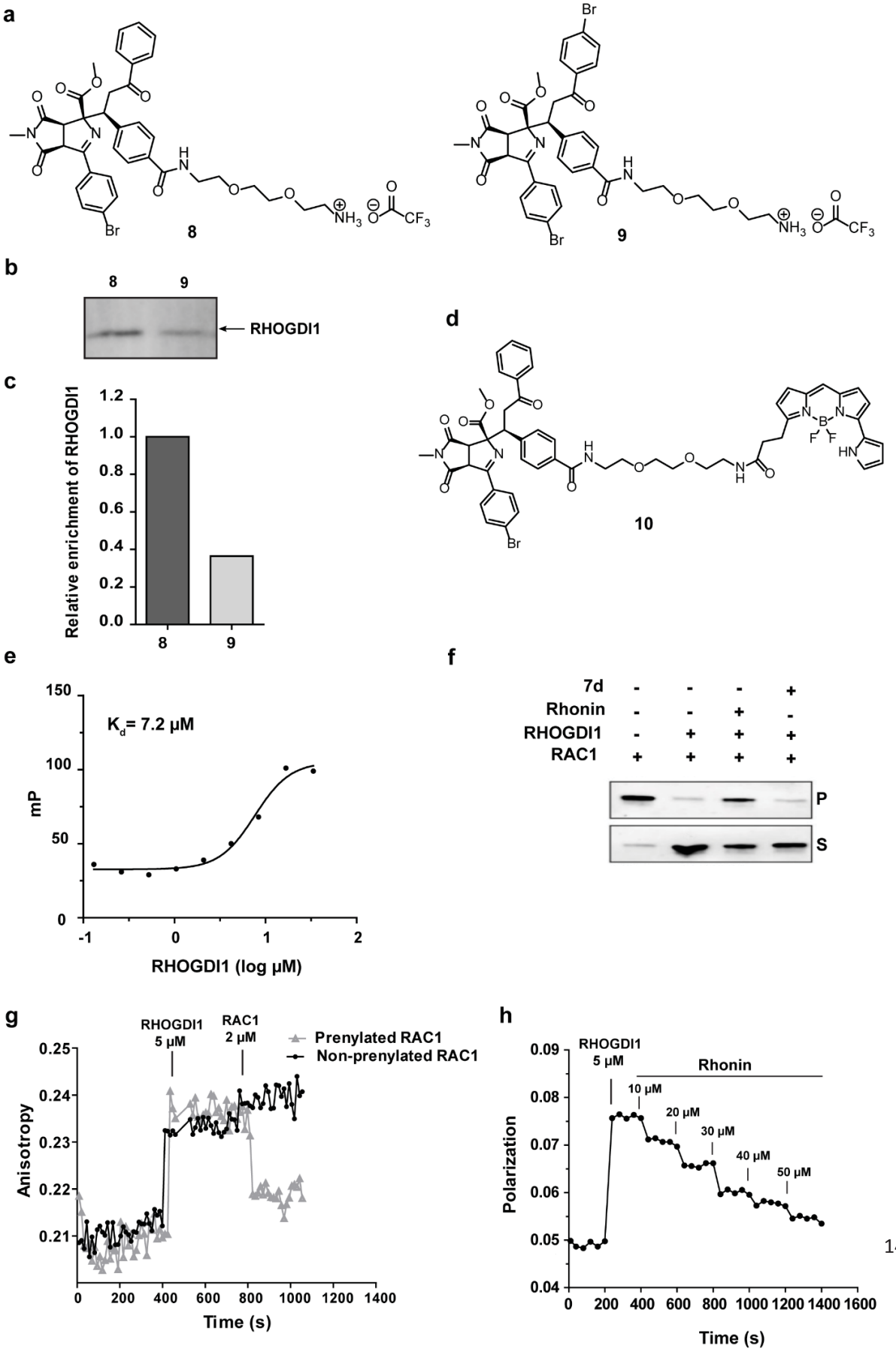
a
8
9
b
8
9
RHOGDI1
c
Relative enrichment of RHOGDI1
d
10
e
K_d= 7.2 µM
mP
RHOGDI1 (log µM)
f
7d
Rhonin
RHOGDI1
RAC1
P
S
g
RHOGDI1 5 µM
RAC1 2 µM
Prenylated RAC1
Non-prenylated RAC1
Anisotropy
Time (s)
h
RHOGDI1 5 µM
Rhonin
10 µM
20 µM
30 µM
40 µM
50 µM
Polarization
Time (s)

Figure 4. Rhonin is a RHOGDI1 inhibitor. (a) Structure of the affinity probes **8** and **9**. **(b)** Affinity-based enrichment of RHOGDI1 by probe **8** as compared to probe **9**. Active probe **8** and inactive probe **9** were immobilized on NHS ester magnetic beads and exposed to NIH/3T3 lysates. Bound proteins were eluted and analyzed by immunoblotting using a RHOGDI1-specific antibody. **(c)** Densitometric analysis of (**b**) for quantification of RHOGDI1 enrichment. Data is representative for three biological replicates. (**d**) Structure of the fluorescent Rhonin derivative **10**. (**e**) Binding of the Rhonin derivative **10** to RHOGDI1. Fluorescence polarization measurements were performed using **10** and titrating increasing concentrations of RHOGDI1. Data is representative of three independent experiments. **(f)** Displacement of prenylated GDP-bound RAC1 (1 μM) from synthetic liposomes (2.7 mM lipids) by GST-RHOGDI1 (1.5 μM) in the presence or absence of 50 μM Rhonin or inactive derivative **7d** was determined using a liposome sedimentation assay. Data is representative of three independent experiments. P: pellet; S: supernatant. (**g**) Competition of the Rhonin derivative **10** with RAC1. Fluorescence polarization measurements were performed by adding 2 μM prenylated RAC1 or non-prenylated RAC1 into a mixture of 2 μM compound **10** and 5 μM RHOGDI1. Data is representative of three independent experiments. (**h**) Interference of Rhonin with the binding of RHOGDI1 to a GerGer-RAB1 peptide. Fluorescence polarization measurements were performed by titrating Rhonin into a mixture of 5 μM FITC-labelled GerGer-Rab1 peptide and 50 μM RHOGDI1.

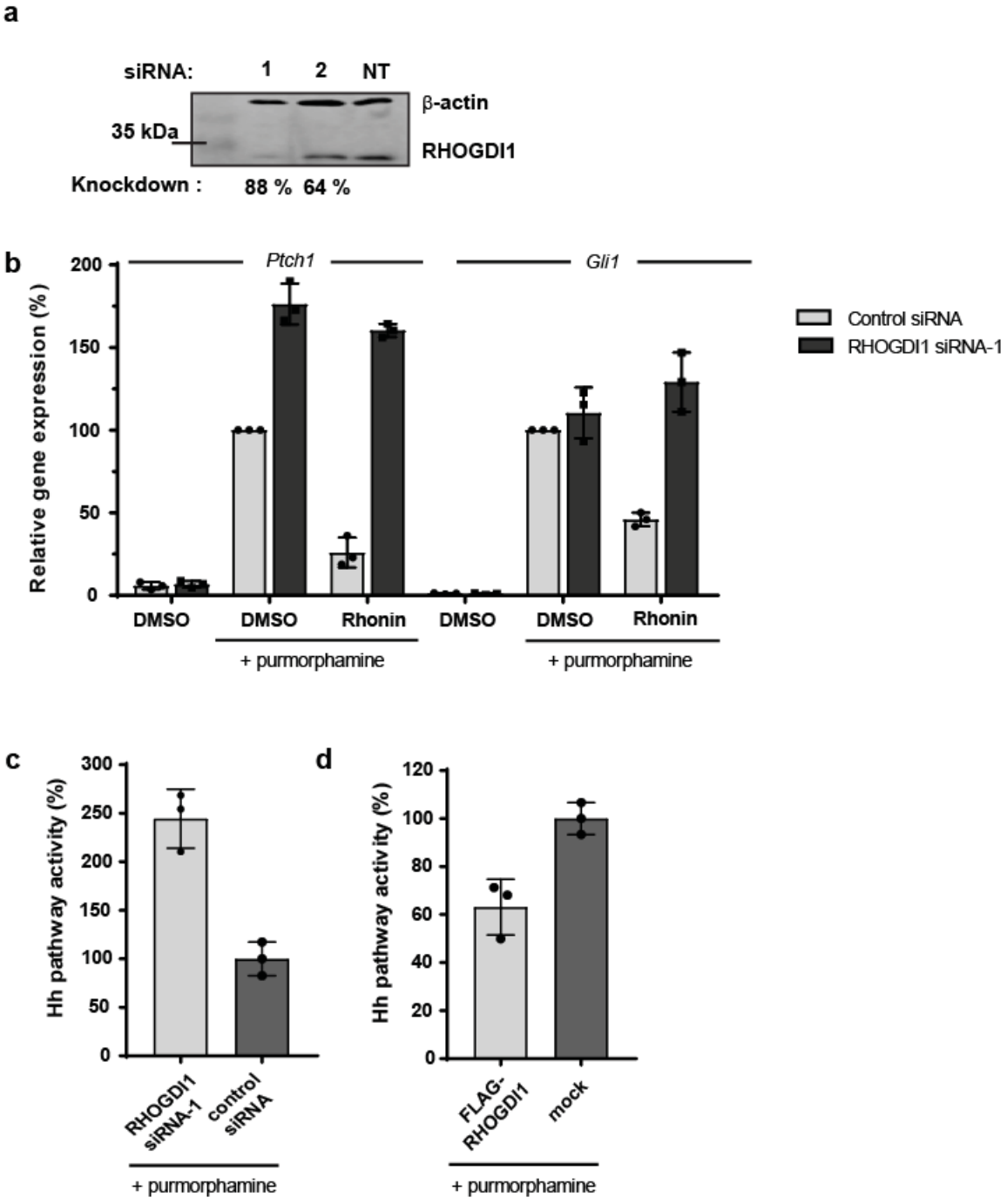

Figure 5. RHOGDI1 is a negative regulator of Hh signaling. (a) RHOGDI1 knockdown efficiency for siRNA-1 and siRNA-2 as used in **b** and Supplementary Figure S5**. (b)** NIH/3T3 cells were transfected with RHOGDI1 siRNA-1 or control siRNA. After 48 h cells

were treated with purmorphamine (1.5 µM) and 20 µM of Rhonin or DMSO as a control for 48 h before isolation of total RNA. Following cDNA preparation, the relative expression levels of *Ptch1*, *Gli1* and *Gapdh* were determined by means of RT-qPCR. Expression levels of *Ptch1* and *Gli1* were normalized to the levels of *Gapdh* and are depicted as percentage of gene expression in cells activated with purmorphamine (100 %). All data are mean values of three independent experiments (n = 3) ± s.d. **(c)** C3H/10T1/2 cells were transfected with RHOGDI1 siRNA-1 and control siRNA. After 48 h the cells were treated with 1.5 µM purmorphamine and DMSO and osteoblast differentiation was monitored after 96 h. The Hh pathway activity in cells treated with purmorphamine and control siRNA was set to 100%. All data are mean values of three independent experiments (n = 3) ± s.d. See also Supplementary Figure 5a. **(d)** C3H/10T1/2 cells were transfected with 800 ng FLAG-RHOGDI1 plasmid or empty vector. After 24 h the cells were treated with 1.5 µM purmorphamine and DMSO and osteoblast differentiation was monitored after 72 h. The Hh pathway activity in cells that were transfected with the empty vector and treated with purmorphamine was set to 100%. All data are mean values of three independent experiments (n = 3) ± s.d. See also Supplementary Figure 5b.

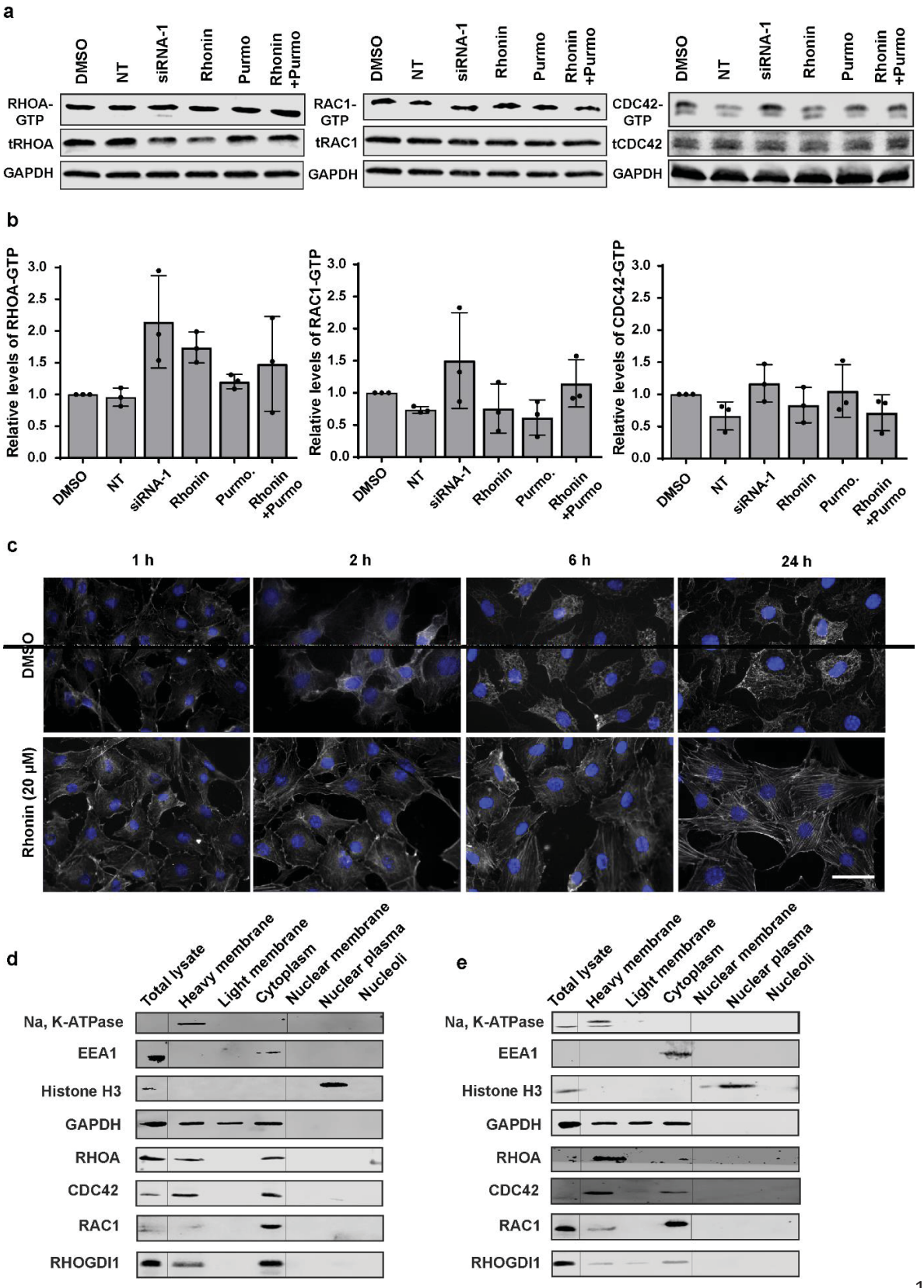
a
DMSO
NT
siRNA-1
Rhonin
Purmo
Rhonin +Purmo
RHOA-GTP
tRHOA
GAPDH
RAC1-GTP
tRAC1
CDC42-GTP
tCDC42
b
Relative levels of RHOA-GTP
Relative levels of RAC1-GTP
Relative levels of CDC42-GTP
c
1 h
2 h
6 h
24 h
DMSO
Rhonin (20 µM)
d
e
Total lysate
Heavy membrane
Light membrane
Cytoplasm
Nuclear membrane
Nuclear plasma
Nucleoli
Na, K-ATPase
EEA1
Histone H3
GAPDH
RHOA
CDC42
RAC1
RHOGDI1

Figure 6. Influence of Rhonin on RHO GTPases in cells. (a) GST pull-down of GTP-bound RHOA, RAC1 and CDC42 by GST-fused effector proteins. GST-fused effector proteins of RHOA (Rhotekin) or RAC1 and CDC42 (PAK) were employed to enrich the GTP-bound GTPases in NIH/3T3 cells after RHOGDI1 knockdown by siRNA-1 and non-targeting siRNA (NT) or treatment with DMSO, Rhonin or purmorphamine. Proteins were detected by means of immunoblotting using specific antibodies for RHOA, RAC1 and CDC42. Data is representative of three independent experiments. (**b)** Densitometric quantification of the relative levels of RHOA-GTP, RAC1-GTP and CDC42-GTP after normalization to the total levels (t) of each GTPase and as compared to DMSO (set to 1). Data are mean values of three independent experiments (n = 3) ± s.d. **(c)** NIH/3T3 cells were serum starved for 48 h to inactivate RHO GTPases. Cells were then treated with DMSO or Rhonin for 24 h. Cells were fixed and stained with DAPI and phalloidin-rhodamine to visualize the nuclei (blue) and actin filaments (grey), respectively. Images are representative of three biological replicates. Scale bar: 10 µm. **(d** and **e)** NIH/3T3 cells were treated with DMSO (**d**) or 10 µM Rhonin (**e**) and fractionated into six distinct fractions using ultracentrifugation. The fractions were analyzed using antibodies for RHOA, RAC1, CDC42 and for specific markers of each fraction including Na+/K+-ATPase (plasma membrane), EEA1 (endosomes), GAPDH (cytoplasm) and histone H3 (nuclear fraction). Data are representative of three independent experiments.

Online Methods

Chemistry

General information

Unless otherwise noted, all commercially available compounds were used as provided without further purifications. Dry solvents (THF, toluene) were used as commercially available; CH_2Cl_2 was purified by the Solvent Purification System *M-BRAUN Glovebox Technology SPS-800*. Solvents for chromatography were technical grade.
Analytical thin-layer chromatography (TLC) was performed on *Merck silica gel aluminium plates* with F-254 indicator. Compounds were visualized by irradiation with UV light or potassium permanganate staining. Column chromatography was performed using *silica gel Merck 60* (particle size 0.040-0.063 mm). Solvent mixtures are understood as volume/volume.
^{1}H-NMR and ^{13}C-NMR were recorded on a *Bruker DRX400* (400 MHz), *Bruker DRX500* (500 MHz) and *INOVA500* (500 MHz) using $CDCl_3$ or $(CD_3)_2SO$ as solvent. Data are reported in the following order: chemical shift (δ) values are reported in ppm with the solvent resonance as internal standard (CDCl3: δ = 7.26 ppm for ^{1}H, δ = 77.16 ppm for ^{13}C; $(CD_3)_2SO$: δ = 3.30 ppm for ^{1}H, δ = 39.52 ppm for ^{13}C); multiplicities are indicated br s (broadened singlet), s (singlet), d (doublet), t (triplet), q (quartet) m (multiplet); coupling constants (*J*) are given in Hertz (Hz).
High resolution mass spectra were recorded on a *LTQ Orbitrap* mass spectrometer coupled to an *Acceka HPLC*-System (HPLC column: *Hypersyl GOLD*, 50 mm x 1 mm, particle size 1.9 µm, ionization method: electron spray ionization). Fourier transform infrared spectroscopy (FT-IR) spectra were obtained with a *Bruker Tensor 27* spectrometer (ATR, neat) and are reported in terms of frequency of absorption (cm^{-1}). Optical rotations were measured in a *Schmidt + Haensch Polartronic HH8* polarimeter. The enantiomeric excesses were determined by HPLC analysis using a chiral stationary phase column (column: CHIRALCEL IC, eluent: (DCM/EtOH = 100/2) / *iso*-hexane). The chiral HPLC methods were calibrated with the corresponding racemic mixtures. The ratio of diastereomers was determined by 1H-NMR analysis. Chemical yields refer to pure isolated substances. Yields, enantiomeric excesses, and diastereoselectivity are given in the tables.
The chemicals and solvents were purchased from the companies Sigma-Aldrich, Acros Organics, ABCR and Alfa Aesar. (*Rp*)-2-(*tert*-Butylthio)-1-(diphenyl-phosphino)ferrocene (purity: 98%), Tetrakis(acetonitrile)copper(I) hexafluorophosphate (purity; 97%) and Tetrakis(acetonitrile)copper(I) tetrafluoroborate (purity: 97%) were purchased from Sigma-Aldrich.
General procedures

GP-1: General Optimized Procedure for the formation for double cycloaddition product 5:

$Cu(CH_3CN)_4PF_6$ (5 mol%) and (*R*)-Fesulphos (5 mol%) was transferred to a dry reaction vial with a stir bar and 0.5 mL of dry CH_2Cl_2 was added and stirred for 10 mins at rt. Then, first maleimide **1** (1 equiv) and azomethine ylide **2** (1.05 equiv) was successively added followed by the addition of Et_3N (20 mol%). The reaction mixture was left to stir at 0°C till the completion (0.5 – 1h) as monitored by TLC. After the completion of the cycloaddition, TBHP (70% aq. soln) (1.2 equiv) was

added to the reaction mixture and left to stir at rt till completion (monitored by TLC). Then, all the volatiles were removed in vacuo and THF (1mL/0.1 mmol) was added to the reaction vial. To this solution, DBU (0.5 equiv) was added and finally, *N*-phenylmaleimide (3 equiv as solution in 0.5 mL THF) was added dropwise and stirred at rt till completion. The crude reaction mixture was directly put on the column and separated using EA/PE (40-80%) mixture. The products **5** are very weakly UV active but can be visualized using $KMnO_4$ stain.

GP-2: General Optimized Procedure for the formation for Michael Addition product 6 and 7:

$Cu(CH_3CN)_4PF_6$ (5 mol%) and (*R*)-Fesulphos (5 mol%) was transferred to a dry reaction vial with a stir bar and 0.5 mL of dry CH_2Cl_2 was added and stirred for 10 mins at rt. Then, maleimide **1** (1 equiv) and azomethine ylide **2** (1.05 equiv) was successively added followed by the addition of Et_3N (20 mol%). The reaction mixture was left to stir at 0°C till the completion (0.5 – 1h) as monitored by TLC. After the completion of the cycloaddition, TBHP (70% aq. soln) (1.2 equiv) was added to the reaction mixture and left to stir at rt until completion (monitored by TLC). Finally to this solution, base and electrophile was added and the mixture was stirred at rt until completion. The crude reaction mixture was directly put on the column and separated using EA/PE (30-60%) mixture. The products **6/7** are UV active and can be visualized under standard UV lamp.

Biology

Materials

Dulbecco's Modified Eagle's medium (DMEM), **L**-glutamine, sodium pyruvate, penicillin/streptomycin, fetal bovine serum (FBS) and fetal calf serum (FCS) were obtained from PAN Biotech, Germany. The chemiluminescent substrate CDP-Star was purchased from Roche, Switzerland. Dual-Luciferase Reporter Assay System was obtained from Promega, USA. Anti-SMO rabbit Ab (#ab38686) and anti-β-actin rabbit polyclonal Ab (#ab8227) were purchased from Abcam, USA. Anti-N-acetylated tubulin mouse Ab (#T6793) was purchased from Sigma Aldrich, Germany. Anti-RHOGDI-1 mouse Ab (#sc-373724) was purchased from Santa Cruz Biotechnology, USA. Anti-Filamin-B polyclonal Ab (# PA5-21345) and anti-Filamin-C polyclonal Ab (# PA5-45573) were purchased from Thermo Fisher Scientific, Germany. Phalloidin coupled to TRITC was obtained from Sigma, Germany. Anti-rabbit-Alexa594 goat Ab (#A11012) and anti-mouse-Alexa488 donkey (#A21202) were purchased from Invitrogen, Germany. Anti-mouse-IR800 donkey Ab (#926-32212) and anti-rabbit-IR680 donkey (#926-68072) antibodies were obtained from LI-COR, Biosciences, USA. Anti-Histone H3 rabbit Ab (#9715), anti RhoA (67B9) Rabbit Ab (#2117), EEA1 rabbit Ab (#2411), and Anti GAPDH (14C10) Rabbit Ab (#2118 S) were purchased from Cell Signaling Technologies. Anti-CDC42 Clone 44/CDC42 (RUO) mouse (# 610929) was purchased from Bioscience. Anti-Rac1 mouse Ab, clone 23A8 (# 05-389), and Anti-Na+/K+ ATPase (α Subunit) mouse Ab (#A276) was purchased from Merck.

pGEN-mSMO, was a gift from Philip Beachy, Addgene plasmid # 37673, Addgene, USA.[1]

pCMV3-N-FLAG-mArhgdia (MG52485-NF) and pCMV3-N-Flag-NCV (CV016) were

purchased from Sino Biologicals, Beijing, China. pGEX-4T1-Rhotekin-HR1 (aa. 1-89) and pGEX-2TK-PAK1-RBD (aa 57-141) were used as previously described.[2] siRNA duplexes (mouse Arhgdia (192662) siRNA 1 – CGACUGACCUUGGUAUGCA, J-064240-05-0002; mouse Arhgdia (192662) siRNA 2 – UCAAGUCGCGCUUCACAGA, J-064240-06-0002; non-targeting siRNA - UGGUUUACAUGUCGACUAA, D-001810-01-05) were purchased from GE Healthcare Europe GmbH, Germany.

Cell lines

NIH/3T3 cells were obtained from DSMZ, Germany (DSMZ ACC 59) and were cultured in DMEM (high glucose) supplemented with 10% heat-inactivated FCS, 2 mM L-glutamine and 1 mM sodium pyruvate. Shh-LIGHT2 cells (NIH/3T3 cells stably transfected with a Gli-responsive firefly luciferase reporter plasmid and a pRL-TK constituitive Renilla luciferase expression vector)[1] were cultured in the same culturing medium supplemented with 400 µg ml^{-1} G418 and 150 µg ml^{-1} Zeocin as selecting agents. The murine osteoblasts C3H/10T1/2 (ATCC CCL-226) were obtained from ATCC, USA and were cultured in DMEM (high glucose) supplemented with 10% heat-inactivated FCS, 6 mM L-glutamine, 1 mM sodium pyruvate. HEK293T cells (ATCC, England) were grown in DMEM containing 10% FBS, 100 U ml^{-1} penicillin and 0.1 mg ml^{-1} streptomycin. All cell lines were maintained at 37 °C and 5% CO_2 in a humidified atmosphere. All the cell lines were regularly assayed for mycoplasma and were confirmed to be mycoplasma-free. Transfection of DNA constructs and siRNAs were performed using Fugene HD (Promega), Lipofectamine® LTX (Invitrogen) and DharmaFECT™ (GE Healthcare) transfection reagent according to the manufacturer's directions.

Osteoblast differentiation assay

The osteoblast differentiation assay was performed by the Compound Management and Screening Center (COMAS) in Dortmund, Germany. C3H/10T1/2 cells were seeded (800 per well) in white 384-well plates. After incubation for 16 h, compounds or DMSO were added to a final concentration of 10 µM using the acoustic nanoliter dispenser ECHO 520 (Labcyte). One hour later, osteogenesis was induced with 1.5 µM purmorphamine. Plates were incubated for 96 h at 37 °C and 5% CO_2. Alkaline phosphatase activity was measured by replacing the medium with 35 µL osteogenesis-lysis buffer (lysis buffer: 100 mM Tris pH 9.5, 250 mM NaCl, 25 mM $MgCl_2$, 1% Triton X-100, sterile filtered) containing 1:100 chemiluminescent substrate CDP-Star® (Promega) for one hour in the dark at 25 °C. The luminescence was monitored using the Paradigm plate reader (Molecular Devices, USA). Dose-response analyses were performed for all hit compounds using a three-fold dilution series starting from a concentration of 30 µM. Half-maximal inhibitory concentrations (IC_{50}) were calculated using the Quattro software suite (Quattro Research, Planegg, Germany).

The effect of test compounds on the viability of C3H/10T1/2 cells was determined by CellTiter-Glo Luminescence cell viability assay (Promega). Cells were treated as described for the osteogenesis assay prior to addition of the CellTiter-Glo® reagent according to manufacturer's

protocol. Compounds causing at least a 50% reduction in the osteogenesis assay and retaining cell viability of at least 80% were considered as hits. Dose-response analyses were performed for all hit compounds using a three-fold dilution series starting from a concentration of 30 µM. Half-maximal inhibitory concentrations (IC_{50}) were calculated using the Quattro software suite (Quattro Research GmbH).

GLI-dependent reporter gene assay

Shh-LIGHT2 cells were seeded (2.5×10^4 per well) in 96-well plates. After incubation for 16 h, medium was replaced by low serum-containing medium (0.5% FCS) supplemented with 1.5 µM purmorphamine. One hour later, various concentrations of the compounds or DMSO as a control were added and cells were further incubated for 48 h. Firefly and *Renilla* luciferase activities were determined by means of the Dual-Luciferase® Reporter Assay System (Promega) according to the manufacturer's protocol and luminescence was measured using the Infinite® M200 plate reader (Tecan, Austria).

SMO binding assay

HEK293T cells were seeded (1.5×10^4 per well) on poly-D-lysine-coated coverslips placed in a 24-well plate. 16 h later cells were transfected with the SMO expressing plasmid (pGEN-mSMO) using Fugene HD (Promega) according to the manufacturer's protocol. After 48 h of incubation at 37 °C, cells were washed once with PBS and incubated further in fresh DMEM medium containing 0.5% FBS, 5 nM BODIPY-cyclopamine and various concentrations of the test compounds or DMSO as a control. One hour later cells were washed twice with PBS and fixed with 3% paraformaldehyde for 10 min at room temperature and subsequently permeabilized with 0.1% (v/v) triton X-100 in PBS for 5 min at room temperature. Cells were then stained with 1 µg/ml DAPI for 10 min and were mounted on glass slides using Aqua Polymount (Polysciences Inc). Images were acquired on an Axiovert Observer Z1 microscope (Carl Zeiss, Germany) using a Plan-Apochromat 63x/1.40 Oil DIC M27 objective.

Additionally, SMO binding was confirmed by flow cytometry. HEK293T cells were seeded (3×10^5 per well) in 6-well plate and transfected with the SMO expressing plasmid pGEN-mSMO as described above. After 48 h of incubation the medium was replaced by DMEM containing 0.5% FBS, 5 nM BODIPY-cyclopamine and various concentrations of the test compounds or DMSO as a control. Following incubation for 5 h cells were washed once with PBS, detached using trypsin/EDTA (0.05/0.02% (v/v) in PBS), and collected by centrifugation at 250 x g for 5 min at room temperature. Cells were washed twice and then suspended in ice-cold PBS. Cell suspensions were subjected to flow cytometry analysis employing the BD LSR II Flow Cytometer (laser line: 488 nm, emission filter: 530/30) to detect the presence of BODIPY. Data analysis was performed using the Flowing software, version 2.5.1 (Perttu Terho, Centre for Biotechnology, Turku, Finland, http://flowingsoftware.btk.fi).

Immunofluorescence

To detect ciliary localization of SMO, NIH/3T3 cells (3×10^4 per well) were seeded on coverslis in 24-well plates and cultured for 16 h. Cells were then incubated for 12 h in DMEM containing 0.5% FCS to induce ciliation followed by treatment with 1.5 µM purmorphamine and various concentrations of the test compounds or DMSO as a control. 12 h later cells were washed with PBS followed by fixation in 4% ice-cold paraformaldehyde for 10 min. Permeabilization and blocking was performed with a solution containing 0.1% Triton X-100 and 1% heat-inactivated horse serum in PBS for 30 min at room temperature. Samples were then incubated with mouse anti-N-acetylated tubulin antibody (dilution 1:5000) as a marker for cilia and rabbit anti-SMO antibody (dilution 1:200) overnight at 4 °C followed by washing and subsequent incubation with Alexa Fluor 594-conjugated goat anti-rabbit and Alexa Fluor 488-conjugated donkey anti-mouse antibodies (1:500 dilutions) and DAPI (0.1 µg/mL) for 45 min at room temperature. Coverslips were washed and mounted using Aqua Polymount (Polysciences Inc). Images were acquired with Axiovert Observer microscope Z1 (Carl Zeiss, Germany) using a Plan-Apochromat 63x/1.40 Oil DIC M27 objective.

For stress fiber staining, NIH/3T3 cells were cultivated in medium containing 0.5 % FCS for 24 h. Cells were then serum-starved for 24 h in serum-free medium to inactivate RHO GTPases. Cells were then treated with DMSO or 20 µM Rhonin for 24 h and incubated at 37 °C. Cells were washed and fixed with 3% paraformaldehyde for 10 min at room temperature and subsequently permeabilized with 0.1% (v/v) triton X-100 in PBS in 1x PBS for 5 min at room temperature. Cells were stained with 0.5µg/mL Phalloidin-TRITC and 1 µg/mL DAPI for 30 min and were mounted on glass slides using Aqua Polymount (Polysciences Inc). Images were acquired on an Axiovert Observer Z1 microscope (Carl Zeiss, Germany) using a Plan-Apochromat 63x/1.40 Oil DIC M27 objective.

Reverse transcription- quantitative PCR (RT-qPCR)

C3H10T1/2 cells were seeded (2×10^4 per well) in 24-well plates. 16 h later cells were treated with 1.5 µM purmorphamine and the test compounds or DMSO for 48 h. Total RNA was isolated using the RNeasy mini kit (Qiagen) according to the manufacturer's protocol. The concentration of purified RNA was determined by means of the Nanodrop 2000. 500 ng total RNA was used to prepare complementary DNA (cDNA) using QuantiTect Reverse Transcription Kit (Qiagen) according to the manufacturer's protocol. The expression of Hh target genes *Ptch1* and *Gli1* and the reference gene *Gapdh* was determined by means of quantitative PCR using the QuantiFast SYBR Green PCR Kit (Qiagen) and iQ 5 Real-Time PCR Detection System (Bio-Rad) and the following oligonucleotides: *Ptch1*: 5′-CTCTGGAGCAGATTTCCAAGG-3′ and 5′-TGCCGCAGTTCTTTTGAATG-3′, *Gli1*: 5′-GGAAGTCCTATTCACGCCTTGA-3′ and 5′-CAACCTTCTTGCTCACACATGTAAG-3′, *Gapdh*: 5′-AGCCTCGTCCCGTAGACAAAAT-3′ and 5′-CCGTGAGTGGAGTCATACTGGA-3′. The expression levels of *Ptch1* and *Gli1* were determined using the $2^{-\Delta\Delta}$Ct method.[3]

Knockdown of RHOGDI1

Which cells were transiently transfected with RHOGDI1 siRNA-1 or siRNA-2 and non-targeting siRNA using DharmaFECT™ reagent by employing the manufacturer's protocol. Briefly, NIH/3T3 cells were seeded in T25 cell culture flask. Upon reaching ca. 70 % confluence, cells were transiently transfected with DharmaFECT™ transfection reagent. For the transfection, siRNAs and DharmaFECT™ transfection reagent were independently mixed with Opti-MEM® serum-free media in low-binding tubes and incubated for 5 min at room temperature. Subsequently, the lipid solution was added to the siRNA solution in the ratio 1:1 and incubated for 20 min at room temperature. The corresponding lipid:siRNA solution was diluted 1:5 with the respective cell culture medium and was added to cells , which were seeded on the previous day, by replacing the old medium and incubated for 48 h at 37 °C. Cells were detached and reseeded at 20,000 cells per well in 24-well plate for determining the target gene expression upon RHOGDI1 knockdown. Knockdown efficiency was determined by immunoblotting using anti-RHOGDI1 specific antibodies.

Immunoblotting

Unless otherwise mentioned, the cells were lysed in 1X SDS buffer without bromophenol blue. The resulting lysates were analyzed by DC Assay (Bio-Rad) for protein concentrations determination. The cell lysates were then supplemented with bromophenol blue and boiled at 95 °C for 10 min. The cooked proteins were loaded on 10% polyacrylamide gels and run at a constant voltage of 80 V for 15 min followed by 120 V for approximately 1.5 h. Protein were transferred on PVDF membrane using semi-dry transfer at 25 V for 45 min alternatively by using tank blotting at 100 V for 60 min. Membrane were washed and blocked in LI-COR blocking buffer for 1 h at room temperature. The blocking buffer was replaced with fresh LI-COR blocking buffer containing primary antibodies and incubated overnight at 4 °C. Membranes were washed with TBS-T (3 x 5 min) and incubated with the secondary antibody in blocking buffer for one hour at room temperature. Signals were visualized using Odyssey Fc imaging system (LI-COR Biosciences). Quantification of band intensities was performed by densitometry of scanned signals with the aid of image studio software (Version 4.0.21, LI-COR Biosciences, ©2014).

RHOGDI1 overexpression

C3H10T1/2 cells were transiently transfected with pCMV3-N-FLAG-mArhgdia or pCMV3-N-Flag-NCV using Lipofectamine® LTX & PLUS ™ reagent according to manufacturer's protocol. Briefly, C3H10T1/2 cells were seeded in a T25 cell culture flask and incubated overnight at 37 °C and 5% CO_2. For the transfection, plasmid DNA and PLUS reagent were diluted in Opti-MEM® medium and incubated for 5 min at room temperature. Lipofectamine® LTX reagent was directly added to this mixture and incubated for 30 min at room temperature. The DNA-lipid complex was added dropwise to the cells in the flask and incubated for 24 h. Cell were then detached and reseeded at 5,000 cells per well in 96-well plate for determining the effect of RHOGDI1 overexpression on osteoblast differentiation as described above.

Cell lysate preparation for chemical proteomics

NIH/3T3 cells were grown to 90-95% confluence and were then detached using cell dissociation solution for 5 min at 37 °C and 5% CO_2. Cells were suspended in cell culture medium and pelleted by centrifugation at 250 x g, 5 min at 4 °C. Cell pellets were then washed thrice with ice-cold PBS and lysed in lysis buffer containing 50 mM PIPES, 50 mM NaCl, 5 mM $MgCl_2$, 5 mM EGTA, 0.1 % NP40, 0.1 % Triton X-100, 0.1 % Tween®20, with freshly added 1 mM DTT, EDTA-free protease inhibitors (Complete EDTA-free, Roche) and phosphatase inhibitors (PhosphoSTOP, Roche). To assure complete cell lysis, the suspension was passed through 0.9 µm and 0.45 µm cannula 10 times each and incubated on ice for 40 min with intermittent vortexing every five minutes until a homogeneous mixture was obtained. The resulting homogenate was centrifuged at 18,000 x g for 30 min at 4 °C and the supernatant was subsequently snap frozen in liquid nitrogen and stored at -80 °C. Total protein content was determined by DC protein assay (Bio-Rad, Germany).

Affinity chromatography enrichment of compound-bound proteins

25 µL N-hydroxysuccinimide magnetic beads (GE Healthcare) were activated with 500 µL 1 mM HCl for 1 min. HCl was replaced by 500 µL coupling buffer (0.15 M triethanolamine, 0.5 M NaCl, pH 8.3) containing 10 µM of free amine affinity probes (S11a and S11b) and incubated for 2 h at room temperature with overhead rotation. The residual active groups of N-hydroxysuccinimide magnetic were quenched by alternating incubation with 500 µL block A buffer (0.5 M ethanolamine, 0.5 M NaCl, pH 8.3) and block B buffer (0.1 M sodium aceate, 0.5 M NaCl, pH 4.0) for 5 min three times each. For protein binding, the magnetic beads were equilibrated with 500 µL lysis buffer followed by incubation with 500 µL lysate (protein concentration: 2 mg/mL) 2 h at 4 °C with overhead rotation. In order to wash out non-specifically bound proteins, the beads were first washed with 500 µL lysis buffer containing 25 mM $MgCl_2$ followed by three times washing with 500 µL PBS. Tryptic digestion of bead-bound proteins was carried out in two stages. First, bound proteins were reduced by incubating the beads with 50 µL reducing buffer (1 mM DTT, 8 M urea in 50 mM Tris (pH 7.5)) at 30 °C for 30 min with shaking. Later, the reduced proteins were alkylated by addition of 5.5 µL alkylating solution (1 mM DTT, 50 mM chloroacetamide, 8 M urea in 50 mM Tris pH 7.5) and further incubation in the dark at 30 °C for 30 min while shaking at 350 rpm. The reduced and alkylated proteins were digested by adding 1 µg LysC at 37 °C for 1 h while shaking at 350 rpm. The supernatant was transferred to a new tube and the beads were further incubated with 50 mM Tris-HCl (pH 7.5) containing 1 µg trypsin at 37 °C for 1 h while shaking at 350 rpm. Both supernatants were combined together and further digested by adding 2 µg trypsin for 16 h at 37 °C with continuous shaking. The enzymatic digestion was stopped by addition of 2 µL proteomics grade trifluoroacetic acid (TFA). In order to purify the resulting peptides, STAGE tips were prepared by loading the 200 µL microtips with two layers of C18 (octadecyl) disks. The tips with C18 disks were activated by addition of 100 µL methanol. Furthermore, the tips were calibrated by washing with 100 µL Buffer B (20% H_2O / 80% acetonitrile with 0.1% formic acid) and 100 µL Buffer A (H_2O with 0.1% formic acid). The peptide purification was achieved by

passing the digestion solution over the activated STAGE tips. Bound peptides were eluted twice using 20 µL Buffer B and the solvent was evaporated by means of rotary speed vacuum evaporator.

Mass spectrometry and data evaluation

In order to analyse the tryptic peptides, the samples were purified by UltiMateTM 3000 RSLC nano system (Dionex, Germany) and MS/MS analysis was carried out using Q Exactive™ HF Hybrid Quadrupole-Orbitrap Mass Spectrometer equipped with a nano-spray source (Nanospray Flex Ion Source, Thermo Scientific). Briefly, the tryptic peptides were solubilized in 20 µL 0.1% (v/v) TFA in water and 3 µL were injected onto a pre-column cartridge (5 µm, 100 Å, 300 µm ID * 5 mm, Dionex, Germany) using 0.1% (v/v) TFA in water as eluent with a flow rate of 30 µL/min. Desalting was performed for 5 min with eluent flow through followed by back-flushing of the sample during the whole analysis from the pre-column to the PepMap100 RSLC C18 nano-HPLC column (2 µm, 100 Å, 75 µm ID × 50 cm, nanoViper, Dionex, Germany) using a linear gradient starting with 95% water containing 0.1% (v/v) formic acid / 5% (v/v) acetonitrile containing 0.1% (v/v) formic acid and increasing to 70% water containing 0.1% (v/v) formic acid / 30% (v/v) acetonitrile containing 0.1% (v/v) formic acid after 95 min using a flow rate of 300 nL/min. The nano-HPLC was coupled to the Quadrupole-Orbitrap Mass Spectrometer using a standard coated SilicaTip (ID 20 µm, Tip-ID 10 µM, New Objective, Woburn, MA, USA), mass range of m/z 300 to 1650 was acquired with a resolution of 60000 for a full scan, followed by up to ten high energy collision dissociation (HCD) MS/MS scans of the most intense at least doubly charged ions with a resolution of 15000.

Data evaluation was performed using MaxQuant software[4] (v.1.5.3.30) including the Andromeda search algorithm and searching the mouse reference proteome of the Uniprot database. Briefly, the search was performed for full enzymatic trypsin cleavages allowing two miscleavages. For protein modifications carbamidomethylation was chosen as fixed and oxidation of methionine and acetylation of the N-terminus as variable modifications. The mass accuracy for full mass spectra was set to 20 ppm for the first and 4.5 ppm for the second search. The mass accuracy for MS/MS spectra was set to 20 ppm. The false discovery rates for peptide and protein identification were set to 1%. Relative quantification of proteins was carried out using the label-free quantification algorithm implemented in MaxQuant. Further data evaluation was performed using Perseus software[5] (v. 1.5.2.6). Proteins not identified with at least two peptides in at least one of the samples and known contamination were filtered off. Samples resulting from pulldown using the active probe were grouped together and those from the pulldown using the inactive one as well. Label-free quantification (LFQ) intensities were logarithmized (log2) and proteins, which were not three times quantified in at least one of the groups, were filtered off. Missing values were imputed using small normal distributed values (width 0.3, down shift 1.8) and a two sided t-test (s0 = 1, FDR 0.05) was performed. Proteins which were statistically significant enriched by the active probe compared to the inactive one were considered as hits.

Fluorescence polarization

The binding of Rhonin to RHOGDI1 was confirmed by fluorescence polarization experiments. RHOGDI1 was titrated against 1 µM of the fluorescent Rhonin derivative **10** in buffer containing 20 mM Hepes, pH 7.4, 150 mM NaCl, 5 mM $MgCl_2$, 3 mM DTT and incubated for 30 min. The change in fluorescence polarization was monitored at an excitation / emission wavelengths of 540 nm and 590 nm, respectively. To understand the impact of geranylgeranyl moiety on the interaction of RHOGDI and RAC1, 5 µM RHOGDI was added to 2 µM fluorescent Rhonin in buffer containing 20 mM HEPES, pH 7.4, 150 mM NaCl, 5 mM $MgCl_2$, 3 mM DTT, led to increase in anisotropy signal. 2 µM of prenylated/ or non-prenylated RAC1 were added in two independent experiments. Geranygeranylated RAC1 (GerGer-RAC1) was dissolved in a buffer containing 1% CHAPS and 0.5% sodium cholate in order to remain stable.

To determine the effect of Rhonin on the binding of RHOGDI1 to non-prenylated RAC1-GDP, fluorescence polarization measurements were performed by titrating 1 µM TAMRA-GDP-bound RAC1 with increasing concentrations of RHOGDI1 in the presence and absence of 50 µM Rhonin in buffer containing 30 mM Tris-HCl, pH 7.5, 150 mM NaCl, 5 mM $MgCl_2$, 1% DMSO. The change in the fluorescence polarization was monitored at an excitation and emission wavelengths of 557 nm and 583 nm, respectively.

Competition-based fluorescence polarization were performed by titrating Rhonin with 30 nM fluorescein-labelled atorvastatin and 60 nM GST-PDE6D in PBS buffer containing 0.05% CHAPS,1% DMSO.

Liposome sedimentation assay

Liposomes were prepared by self-assembly of the lipids (500 µg) containing 20% (w/w) phosphatidylethanolamine, 45% (w/w) phosphatidylcholine, 20% (w/w) phosphatidylserine, 10% (w/w) cholesterol, and 5% (w/w) phosphatidylinositol 4,5-bisphosphate. Liposome assays were performed by mixing, sonicating (20 s with minimal power, 50% off and 50% on) and extruding (0.2 µM filter) the lipids in 300 µl of a buffer, containing 20 mM HEPES-NaOH pH 7.4, 50 mM NaCl, 3 mM DTT, 5 mM $MgCl_2$. 1 µM GerGer-RAC1-GDP was added to the liposomes and incubated for 20 min on ice. 1.5 µM GST-RHOGDI-1 and the compounds or DMSO were added to the liposome-GerGer-RAC1-GDP complex prior to incubation on ice for 30 min. The samples were centrifuged at 20,000 x g for 30 min at 4 °C. The resulting pellet and supernatant fractions were collected and analyzed by immunoblotting. 10 µl of each sample were loaded on a SDS-PAGE gel for Western blotting. Specific antibodies were used to visualize RAC1, CDC42 and RHOA.

Liposome flotation assay

10 µM of GerGer-RAC1-GDP was added to liposomes suspended in flotation assay buffer containing 20 mM HEPES-NaOH pH 7.4, 50 mM NaCl, 3 mM DTT, 5 mM $MgCl_2$, and incubated for 20 min on ice. The liposomes were prepared by using self-assembling the lipids (500 µg lipids in 300 µl buffer), containing 15% (w/w) phosphatidylethanolamine, 0.5% (w/w) NBD-PE (N-(7-nitrobenz-2-oxa-1,3-diazol-4-yl)-1,2-dihexadecanoyl-sn-glycero-3-phosphoethanolamine, triethylammonium salt), 45% (w/w) phosphatidylcholine, 20% (w/w) phosphatidylserine, 10% (w/w)cholesterol, and 5% (w/w) phosphatidylinositol 4,5-bisphosphate. 15 µM of GST-RHOGDI-1 and compounds or DMSO was added to liposome-GerGer-RAC1-GDP complex and samples were further incubated on ice for 30 min. The samples were added to 30% (w/v) sucrose solution. The resulting suspension was overlaid with protein buffer containing 25% (w/v) sucrose and finally with 50 µl of buffer without sucrose. The resulting samples were centrifuged at 140000 x g for 1 h at 4 °C. The upper liposome-containing phase (detected by fluorescent NDB-PE) was collected and analyzed by immunoblotting.

Surface plasmon resonance (SPR)

Biacore® X100 instrument (Biacore, now GE Healthcare) was used to analyze the effect of Rhonin on the GerGer-RAC1-GDP and RHOGDI-1 interaction. Liposomes suspended in SPR buffer (20 mM HEPES, pH 7.4, 50 mM NaCl, 5 mM MgCl2, 3 mM DTT) were immobilized by injecting 0.5 mM liposomes with flowrate of 5 µL/min on the surface of a Pioneer® L1 sensor chip (GE Healthcare) for the period of 900 s, as indicated by a constant signal. Unbound liposomes were removed by passing the buffer and 10 mM NaOH with flowrate of 5 µL/min for 30 s over the sensor chip. Buffer containing 15 µM GerGer-RAC1-GDP was passed with flowrate of 5 µL/min over the immobilized liposomes to facilitate the loading of GerGer-RAC1-GDP on to the liposomes. The effect of compounds on the association of GerGer-RAC1-GDP with liposomes and the resulting dissociation of GerGer-RAC1 upon passing 25 µM of RHOGDI-1 was monitored by the change in the response unit signal.

Protein expression and purification

Human Rhotekin HR1 (aa. 1-89) and human PAK1-RBD (aa. 57-141) encoded on pGEX vectors were expressed over night as GST fusion proteins in E. coli BL21 (DE) after induction of 0.2 mM IPTG. These RHO effectors were extracted by cell lysis performed by sonication of the cells. After centrifugation of the cellular debris the supernatant was used to attach the GST-fused effector proteins to the GSH Sepharose beads.[2]

Insect cell purification system was used for expression and purification of prenylated proteins based on an established protocol.[6] *Sf*9/or *TNAO*38 insect cells (*Sf*9 used only for virus geeration and amplification) were grown to the level of 1.5×10^6 cells/ml before they were transduced with Baculoviruses encoding genes related to the RHO GTPases. Cells were resuspended in lysis buffer, containing 20 mM HEPES-NaOH pH 7.4, 150 mM NaCl, 2 mM β-mercaptoethanol, 5 mM $MgCl_2$, 0.1 mM GDP, 10 mM imidazole and the optimized detergents including 1% CHAPS and 0.5% sodium cholate.[6] Cells were lysed by sonication in ice. After centrifugation for 20 min in 20000 x g, supernatants were collected and loaded on a Ni-NTA column (Qiagen, Hilden, Germany). The protein was eluted by passing a buffer containing 300 mM imidazole into the Ni-NTA column. The eluted solution was further purified on an analytical Superdex 75 column (10/300 GL, GE-Healthcare, Uppsala, Sweden) using 20 mM HEPES-NaOH pH 7.4, 150 mM NaCl, 3 mM DTT, 5 mM $MgCl_2$ and 0.5% (w/v) Na-cholate as buffer system. Non-prenylated RAC1 and human RHOGDI1 were prepared from *E. coli as a GST recombinant protein as described previously.*[6]

For expression of GST-PDEδ, *E. coli* RosettaTM2 cells transformed with PDE6D expression plasmid (pGex4T5) were inoculated in TB medium containing 100 µg/ml ampicillin and 30 µg/ml chloramphenicol to a total volume of 10 L. The protein expression in *E. coli* was induced with 0.2 mM IPTG at OD600 = 1.33. Cells were cultivated overnight at 18 ° C with shaking. Cells then were pelleted by centrifugation at 4000xg for 20 min at 4 ° C and stored at -20 ° C. To purify the proteins, the pellet

was resuspended in lysis buffer (30 mM TRIS-HCl pH 7.5, 100 mM NaCl, 1 mM 2-mercaptoethanol and 1 mM PMSF. DNaseI (10 µg / ml) was added to the cell suspension and the sample was sonicated three times for 1 min on ice and disrupted three times with Microfluidizer. To separate the cell debris, the lysate was centrifuged for 35 min at 20000xg. GST-PDEδ was purified by affinity chromatography via binding to GSH-Sepharose using FPLC. The lysate purified from cell debris was slowly pumped onto a GSH column using a peristaltic pump (the column was previously washed with 3 column volume lysis buffer) and washed with 5 column volume lysis buffer (until absorption at 280 nm was constant). The elution occurred with 4 column volume elution buffer (30 mM TRIS-HCl pH 7.5, 100 mM NaCl, 1 mM 2-mercaptoethanol, 200 mM glutathione). The GST-PDEδ containing fractions were concentrated by ultrafiltration and then slowly using a 5 ml Superloops on a gel filtration column (HiLoad Superdex 26/60 Superdex 75 prep grade, GE Healthcare) equilibrated with 1 column volume gel filtration buffer (20 mM TRIS-HCl pH 7.5, 300 mM NaCl, 1 mM 2-mercaptoethanol).

Pull down of active RHO GTPases

Pull-down of active (i.e., GTP-bound) RHO GTPases was performed by using GSH sepharose beads (GE Healthcare, UK) from NIH/3T3 total cell lysates. NIH/3T3 cells were treated with DMSO, purmorphamine and/or, Rhonin for 24 h or transfected with RHOGDI1 siRNA-1 or non-targeting siRNA. RHO GTPases were obtained by lysis of 15 cm cell dishes with 500 µl Fish buffer (50 mM Tris/HCl pH 7.4, 100 mM NaCl, 2 mM $MgCl_2$, 1% Igepal Ca-630, 10% glycerol, 20 mM beta-glyceolphosphate, 1 mM sodium orthovanadate, cOmplete™, EDTA-free Protease Inhibitor Cocktail (Roche, Basel, Switzerland)). GSH Sepharose beads were washed three times with 1 ml Fish buffer. Equal amounts of bacterial lysates containing GST (negative control) or GST-fused effector proteins were added to the GSH Sepharose beads and incubated at 4°C for 1 h followed by another three times washing with 1 ml of Fish buffer. Thereafter, the total cell lysate obtained from one 15-cm dish was added to the GST beads and incubated for 30 min at 4°C. Samples were washed three times with 1 ml Fish buffer. Laemmli buffer was added into the samples before heat denaturation for 10 min at 95°C. The protein-protein interaction was analyzed by SDS-PAGE and immunoblotting.

Sub-cellular fractionation

NIH/3T3 cells were treated with 10 µM Rhonin or DMSO for 24 h. The cells were collected by trypsinization and scraping out the cells. After centrifugation step, the pellet was washed three times with PBS and was resuspended in a detergent-free lysis buffer containing 10 mM Tris/HCl (pH 7.4), 10 mM NaCl, 0.5 mM $MgCl_2$, and EDTA-free protease inhibitor. The total cell lysate was centrifuged at 1200 x g for 5 min at 4 °C after homogenization by using an insulin syringe. The supernatant was collected and further subjected to a 16,000 x g centrifugation to isolate the heavy membrane pellet and cytoplasm and light membrane in the supernatant. The cytosolic supernatant was divided into light membrane and cytoplasm by applying 130,000 x g centrifugation for 90 minutes. The nuclear pellet was resuspended in 250 mM sucrose solution containing 10 mM $MgCl_2$ which were layered on top of an 880 mM sucrose cushion containing 0.5 mM MgCl2. Nuclear fraction was centrifuged at 1,200 x g for 10 minutes to obtain the intact nuclear. The intact nuclear was homogenized using a Balch homogenizer (clearance of 8 mm) and 8-10 up-and-down strokes and later were separated to nucleoli and nucleoplasm fractions.[7] The nucleoplasm and nuclear membrane were separated by centrifugation of nuclear fraction at 130,000 x g for 90 minutes. The resulting pellet contained the nuclear membrane and the supernatant contained the nucleoplasm fraction. All subcellular fractionation steps were carried out at 4°C. Protein concentrations of all fractions were determined by the Bradford assay and all fractions were mixed with 5x SDS-PAGE loading buffer. The separated fractions were analyzed by specific marker for each fraction and the protein localization was analyzed by applying immunoblotting.

Data availability

All data generated or analyzed during this study are included in this published article (and its supplementary information).

References (Method section)

1. Taipale, J. et al. Effects of oncogenic mutations in Smoothened and Patched can be reversed by cyclopamine. *Nature* **406**, 1005 (2000).
2. Herbrand, U. & Ahmadian, M.R. p190-RhoGAP as an integral component of the Tiam1/Rac1-induced downregulation of Rho. *Biol Chem* **387**, 311-7 (2006).
3. Pfaffl, M.W. A new mathematical model for relative quantification in real-time RT-PCR. *Nucleic Acids Res* **29**, e45 (2001).
4. Cox, J. & Mann, M. MaxQuant enables high peptide identification rates, individualized p.p.b.-range mass accuracies and proteome-wide protein quantification. *Nat Biotechnol* **26**, 1367-72 (2008).
5. Tyanova, S. & Cox, J. Perseus: A Bioinformatics Platform for Integrative Analysis of Proteomics Data in Cancer Research. *Methods Mol Biol* **1711**, 133-148 (2018).
6. Zhang, S.C. et al. Liposome reconstitution and modulation of recombinant prenylated human Rac1 by GEFs, GDI1 and Pak1. *PLoS One* **9**, e102425 (2014).
7. Taha, M.S. et al. Subcellular Fractionation and Localization Studies Reveal a Direct Interaction of the Fragile X Mental Retardation Protein (FMRP) with Nucleolin. *PLOS ONE* **9**, e91465 (2014).

Chapter VII

Novel insights into the regulation of the RAC1-membrane interaction by RHOGDI1: An electrostatic force mechanism

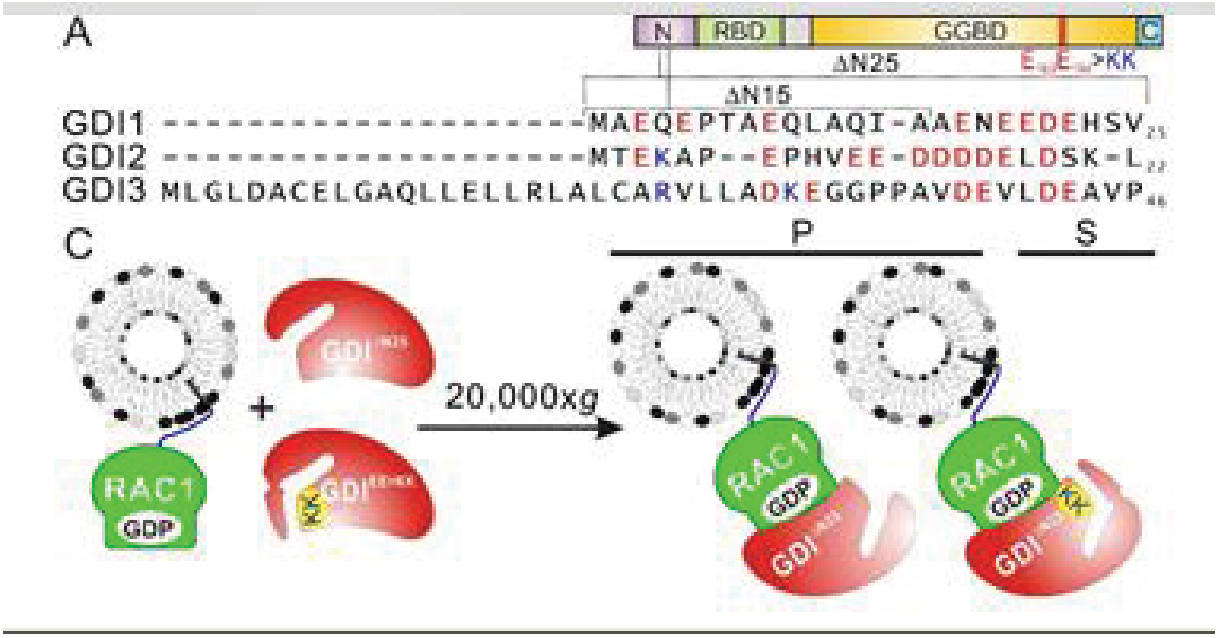

Status:	In preparation
Own Proportion to this work:	30% Purification of GDI1 WT and variants and analysis of their interactions with RHO GTPases using fluorescence polarization and liposome sedimentationassay

Novel molecular and functional insights into the regulation of the RAC1-membrane interaction by GDI1: An electrostatic force mechanism*

Niloufar Mossadeghzadeh[1§], Neda Sadat Kazemein Jasemi[1§], Mohammad Akbarzadeh[1#§], Jisca Majolée[2], Si-Cai Zhang[1#], Peter L Hordijk[2], Radovan Dvorsky[1], Mohammad Reza Ahmadian[1]

[1]Institute of Biochemistry and Molecular Biology II, Heinrich-Heine University, Düsseldorf, Germany; [22]Dept. of Physiology, Amsterdam UMC, location VUmc, De Boelelaan, 1108, Amsterdam, The Netherlands

[§]These authors equally contributed to this study

[#]Current addresses: M. Akbarzadeh (PhD), Department of Chemical Biology, Max Planck Institute of Molecular Physiology, Otto-Hahn-Strasse 11, 44227 Dortmund, Germany; S.C. Zhang (PhD), Department of Microbiology and Immunobiology and Department of Surgery, Harvard Medical School, Boston, MA, 02115, USA.

[*]Running title: Electrostatic Force-driven RAC1-GDI interaction

Corresponding author:
Reza Ahmadian (PhD)
Institute of Biochemistry and Molecular Biology II
Medical faculty of the Heinrich Heine University
Universitaetsstrasse 1, building 22.03.05
40255 Düsseldorf, Germany

Tel.: +49-211-811 2384
Fax: +49-211-811 2726
E-mail: reza.ahmadian@hhu.de

Key words: CDC42; Geranylgeranyl; guanine nucleotide dissociation inhibitors; *hypervariable region;* lipid bilayer; liposomes; membrane cycling; RAC1; RAC2; RHOA; RHO-GDI

Three decades of research document the spatiotemporal dynamics of RHO family GTPases regulated by guanine nucleotide dissociation inhibitors (GDIs). To address the yet unresolved interplay of the kinetic mechanism and structural specificity, the GDI-controlled spatial segregation of geranylgeranylated RAC1 was reconstituted *in vitro*. Various biochemical and biophysical measurements, including on and off rate from biomimetic liposomes immobilized on the sensor surface of a surface plasmon resonance instrument, provided unprecedented mechanistic details for GDI function over RHO proteins. Accordingly, membrane release of RHO GTPases by GDI underlies a 3-step mechanism: (1) A non-specific association of GDI with switch regions of the RHO GTPases; (2) an electrostatic switch determining the interaction specificity between the C-terminal polybasic region of RHO GTPases and two distinct negatively charged clusters of GDI1; (3) a non-specific displacement of geranylgeranyl moiety from membrane and its sequestration into a hydrophobic cleft, effectively shielding it from the aqueous milieu. This study unambiguously challenges the paradigm of RAC1 regulation by GDI1.

The RHO family GTPases, most prominently RAC1, CDC42, and RHOA, share two common functional characteristics, membrane anchorage and an on/off switch cycle(1). They typically contain a conserved GDP/GTP binding domain, called G domain, and a C-terminal hypervariable region (HVR) ending with a consensus sequence known as CAAX (C is cysteine, A is any aliphatic amino acid, and X is any amino acid). Subcellular localization, that is known to be critical for biological activity of Rho GTPases, is achieved by a series of posttranslational modifications at a cysteine residue in the CAAX motif, including isoprenylation (geranylgeranyl or farnesyl), endoproteolysis and carboxyl methylation (2). Thus, membrane-associated RHO GTPases act, with some exceptions(3), as molecular switches by cycling between an inactive GDP-bound state and an active GTP-bound state. This cycle underlies two critical intrinsic functions, GDP-GTP exchange and GTP hydrolysis, which induce structural rearrangements of two regions of the protein, called switch I and Switch II (3), and is controlled by two classes of regulatory proteins, including guanine nucleotide exchange factors (GEFs), and GTPase activating proteins (GAPs) (4). The formation of the active GTP-bound state of RHO GTPases is accompanied by a conformational change in two regions, known as switch I and II (encompassing amino acids or aa 29–42 and 62–68, respectively) (4). Thus, RHO GTPases act as dynamic switches in many developmental and cellular contexts (5) by selectively binding to and activating structurally and functionally diverse effectors. This class of proteins activates a wide variety of downstream signaling cascades (6–9)thereby regulating many important physiological and pathophysiological processes in eukaryotic cells (10–12)

The spatial and temporal activation of RHO GTPases inside a cell is fundamental, for example, to the regulation of local movements and cell-cell contacts that are required for morphogenesis (12). They are commonly found to cycle between two pools, a membrane-associated and a cytosolic pool. Given the fact that membrane attachment is a prerequisite for the signaling roles of this protein family, it is clear that reversible membrane translocation offers cells a means to regulate the location of the activation event.

However, there is a serious handicap to such physical cycling for RHO GTPases. The highly hydrophobic geranylgeranyl moiety of RHO proteins renders them energetically unfavorable to partition into the cytosol as individual monomers. Posttranslationally modified RHO proteins can only detach from membranes if they are assisted by a chaperone that shields the bulky lipid moieties from the aqueous environment of the cytosol. The chaperone role is played by a RHO-specific, ubiquitous guanine nucleotide dissociation Inhibitor (GDI) proteins, RHOGDI (4, 13).

In contrast to the tremendous number of the other regulatory proteins of the RHO family (74 GEFs and 66 GAPs) (14, 15) only 3 GDIs exists in the human genome. The RHOGDI family includes the ubiquitously expressed GDI1 (or RhoGDIα)(16), GDI2 (GDIβ, LY-GDI or D4-GDI) mainly in hematopoietic tissue(17), and GDI3 (or GDIγ) that is usually expressed in human cerebral, lung and pancreatic tissue (18). Unlike the other two GDIs, GDI3 contains an N-terminal extension that confers anchorage into the membranes of Golgi vesicles (19). GDI1 and GDI2 contain at their very N-terminus are a large number of acidic residues, which have been proposed to be essential for their function in cell (20). In addition to their physiological expression, GDIs are also expressed in several human cancers, including breast, liver, ovarian, pancreatic cancers, and myeloid leukemia(13, 17, 21, 22). Changes in GDI expression levels have shown pro- or anti-tumorigenic effects that depend on the cell type and tissue. One reason for this debate is most probably due to the lack of our understanding of the basic mechanism of the GDI function and their binding specificities to the different Rho proteins.

Understanding the mechanisms by which signaling events are localized and the physiological consequences of spatial restriction are major questions in cell biology. Comprehensive studies in the last three decades have provided insight into structure and function of these regulators acting as a shuttle for the RHO GTPases(13, 23–25) . The shuttling process, which considerably differs from the KRAS4B^{Far}-PDEδ (26–29), involves release of RHO GTPases from donor membranes, formation of inhibitory cytosolic GDI-RHO GTPases complexes, and delivery of RHO GTPases to target membranes(13, 25). Accordingly, it has been proposed that GDI regulates the isoprenylation process in the cell(30). GDI is known to release RHO GTPases from the membrane, maintains them in an inactivated state, and protects against both degradation and unspecific activation by Rho-specific GEFs(13, 31, 32). Structural studies by different groups have revealed two sites of interaction between GDI and RHO GTPases(33–37). First, an N-terminal regulatory arm of the GDI binds to the switch regions of RHO GTPases leading to the inhibition of both GDP dissociation and GTP hydrolysis. Second, the geranylgeranyl moiety of RHO GTPases inserts into a hydrophobic pocket of the GDI molecule leading to membrane release. Collectively, these studies have clearly demonstrated how GDIs interact with and serve as negative regulators of RHO GTPases but the basic mechanisms of how they pull the isoprenoid moiety from the membrane.

In this study, we propose a molecular interaction model for RHO GTPase membrane release by GDI supported by structure-function correlation and kinetic analysis of RHO GTPase interaction with and release from biomimetic liposomes in the presence and absence of GDI SPR sensors.

RESULTS AND DISCUSSION

Geranylgeranyl moiety is dispensable for RAC1-GDI1 interaction. To understand the impact of isoprenyl moiety of RAC1 on GDI binding, we determined the rates of GDI association with both geranylgeranylated RAC1 ($RAC1^{GG}$) from insect cells and non-isoprenylated RAC1 full-length ($RAC1^{FL}$) from *Escherichia coli* using stopped-flow fluorometric assay. Figure 1A shows a rapid decrease in fluorescence after mixing GDI1 with the RAC1 proteins, which is directly related to the association reaction between the RAC1-GDI1 pairs. Observed rate constants (k_{obs}) obtained by a single exponential fitting increased in a linear fashion as a function of the GDI1 concentrations (Fig. 1B), yielded similar association rate constants (k_{on}) for both $RAC1^{GG}$ and $RAC1^{FL}$. The dissociation of the GDI1 from mdGDP-bound RAC1 proteins was measured in a displacement experiment. Observed single exponential fluorescence increase yielded respective dissociation rate constants (k_{off}), which differ only 3-fold (Fig. 1C). Calculated dissociation constants (K_d) from the ratio of the k_{off} and k_{on} values (Fig. 1D) unexpectedly revealed only a 7-fold higher affinity for $RAC1^{GG}$ *versus* $RAC1^{FL}$. This result clearly contradicts existing models which have suggested that the isoprenyl moiety of the RHO GTPases contributes to orders of magnitude higher binding affinity for GDI as compared to non-isoprenylated RHO GTPases(38–41).

To confirm the kinetic data obtained with the stopped-flow fluorimetry, we next used two other methods, fluorescence polarization and surface plasmon resonance (SPR), to further investigate the impact of geranylgeranyl moiety on the RAC-GDI1 interaction. Equilibrium K_d values of 0.96 and 0.38 µM, determined in fluorescence polarization mode by titrating increasing concentrations of GST-GDI1 to $RAC1^{GG}$•mdGDP and $RAC1^{FL}$•mdGDP, respectively (Fig. 1E). These affinities are in good agreement with the values determined by stopped-flow fluorimetric analysis shown in Figure 1D. To extend above experiments with a label-free real-time assay, we employed SPR Biacore to study the RAC1-GDI1 interaction. Therefore, we injected different concentrations of GDP-bound $RAC1^{GG}$ and $RAC1^{FL}$ to immobilized GST-GDI1 (Fig. 1F and 1G). The evaluated K_d of 0.065 and 0.3 µM, respectively, revealed again a slightly higher binding affinity of GDI1 for isoprenylated RAC1 vs. non-isoprenylated RAC1.

Kinetic and equilibrium data clearly revealed that the RAC1-GDI1 interaction is not really dependent on the presence of the geranylgeranyl moiety. The binding affinities determined for the RAC1-GDI1 interaction by three different methods clearly indicate that GDI1 binds to non-isoprenylated RAC1 as efficiently as it does to isoprenylated RAC1; $RAC1^{GG}$ exhibited only 2.5 to 4.6-fold lower K_d values as compared to that of $RAC1^{FL}$. Collectively, these data clearly challenge the current regulatory model that the isoprenyl moiety at the C-terminus of RHO GTPases contributes to several orders higher binding affinity of GDI1.

Conserved G domain is not rate-limiting for the GDI1 binding. The above findings prompted us to unambiguously challenge the paradigm of RAC1 regulation by GDI1. To this end, we investigated the interactions of the three GDI paralogs, GDI1, GDI2 and GDI3, with various non-isoprenylated members of the RHO GTPase family (Table S1). GDI3 was purified as an N-terminal truncated variant lacking the amphipathic helix (amino acids or aa 1-20). Kinetics of association of the GDIs (2 µM) with 0.2 µM mdGDP-bound RHO GTPase was monitored under the same conditions as

described above for RAC1. Calculated k_{obs} values for each measurement (Fig. S1) was plotted as bar charts in Figure 2A, which clearly shows that all three GDIs associated with RAC1, RAC3, RHOG and RHOA under the experimental conditions but apparently not with RAC2, CDC42, TC10, TCL, RHOB, RHOC, RHOD and RIF. GDI2 and GDI3 showed significantly faster association with RAC3 as compared to GDI1. Most remarkably, GDI2 was able, unlike GDI1 and GDI3, to bind RAC2. This result clearly indicate for the very first time that GDIs can discriminate between the RHO GTPases by interacting with some but not all Rho proteins.

To examine binding properties, the respective association rate constants (k_{on}) and the dissociation rate constants (k_{off}) were determined for the interaction of GDI1 with RAC1, RAC3, RHOG and RHOA, and GDI2 with RAC2 under conditions described above (Fig. 1A-D, and S2). All kinetic parameters along with calculated dissociation constants (K_d) are summarized in Figure 2B. The data are very similar for the GDI1 interaction with RAC1, RAC3, RHOG and RHOA with K_d values between 0.9 and 3.2 µM. RAC2-GDI2 interaction, however, exhibited a binding affinity that is 19-fold lower as compared to RAC1-GDI1 interaction, which stems from a 10-fold faster dissociation rate of GDI2 from RAC2 (Fig. 2B).

The biochemical characterization described previously together with structural studies have shown that the RAC paralogs exhibit different properties concerning ligand– and protein–protein interactions (42). Whereas RAC1 and RAC3 behave almost identically, RAC2 revealed a 25-fold lower nucleotide affinity because of a decreased nucleotide association rate, a slightly higher PAK binding affinity, and a significant increase in GEF-catalyzed nucleotide dissociation. These aberrant properties most likely are the consequence of different conformational flexibilities in the switch I region (43).

To understand this result, integrated sequence-structure analysis extracted from all available GDI structures in complex with RHO GTPases (Table S2) and depicted in an interaction matrix (Fig. 2C) revealed that almost all amino acids of the G domain (aa 1-176) involved in RHO GTPase-GDI interactions are the same in different RHO GTPases. GDIs appear to mainly contact RHO GTPases through the switch I and II regions, and the α-helix 3 (shown in grey). Same is true also for the GDIs, which apply identical residues, with a few exceptions, to contact RHO GTPases. Major part of the contacts stem from the N-terminal switch bind domain (SWBD in green) and some from the C-terminal geranylgeranyl binding domain (GGBD in orange; Fig. 2D and 2E). So, identical contact sites do not explain observed differences of kinetic measurements and rather suggests a GDI1 modulatory region outside the G domain, namely HVR.

A comparison of available structures of the RAC1-GDI1 and RAC2-GDI2 complexes revealed a rather high sequence identity (33, 34). An inspection of the interaction matrix revealed very few amino acid deviations within the RAC G domains (Y/F89) and GDI paralogs (A/P/G31, E/K/R53, A/T/V54; Fig. S3). However, Y89 in RAC1 and RAC3 undergoes contacts with H23 and V25 of GDI1 which may not be achieved by F89 in RAC2 that may only contact V25 but not with S23. Among the deviations in GDIs, the loop containing A/G31 in GDI1 and GDI3 is in close vicinity of D65/R66 of RAC paralogs, which may, in the case of P31 in RAC2, adopt a different orientation and thereby influence RAC2-GDI2 binding. Residues in SWBD, such as E53 and A54 (GDI1 numbering) appear to be critical for

RHO-GTPase-GDI interaction. The double mutation L55/L56 to serines in GDI1 has been shown to drastically decrease its affinity for RAC1 (44).

The interaction matrix showed a conserved interface between RHO GTPases and GDIs but the missing parts of most structures are, on the one hand, t the C-terminal HVR (178-190 aa in RAC1; Fig. 2E) (45), and on the other hand, the N-terminal of the GDIs (1-25 aa in GDI1; Fig. 2D)(20). The crystal structure of the $RAC1^{GG}$•GDP•GDI1 complex (PDB code: 1HH4) has remarkably provided the first revealed evidence for the existence of a network of electrostatic interactions between these otherwise highly flexible regions (33). Accordingly, GDI1 obviously supplies two sets of negatively charged residues to grasp the polybasic motif of RAC1 HVR. These are E109, D140, D143, E163 and E164 of GDI1 GGBD across from E17, E19, E20, D21 and E22 at the flexible NTA of GDI1 (Fig. 2E). Thus, it seems that GDI1 applies an electrostatic pincer towards the polybasic motif of RAC1 and extract it from the membrane. This mechanistic model is now investigated in-depth.

RAC1 polybasic motif dictates GDI1 binding. A sequence analysis of HVRs of GDI1 associating RHO GTPases (`binders´) versus those with no observed GDI1 association (`non-binders´) showed clear differences in both numbers and relative positions of positively charged residues (Fig. 3A). To examine the impact of HVR on the RHO GTPase-GDI1 interaction we measured the kinetics of GDI1 association with different HVR variants of RAC1 and RAC2. Remarkably, a loss of RAC1 association was observed with a C-terminal truncated variant lacking HVR-CAAX ($RAC1^{\Delta C10}$) as well as KRKRK-to-EEEEE ($RAC1^{5xE}$; charge-reversal variant) and KRKRK-to-QQKRA (RAC1-to-RAC2 or $RAC1^{RAC2}$ variant). In contrast, a gain of GDI association with RAC2 was observed with QQKRA-to-KRKRK (RAC2-to-RAC1 or $RAC2^{RAC1}$ variant; Fig. 3B). These findings were verified by using fluorescence polarization experiments (Fig. S2). These data are summarized in Figure 3C and revealed that (i) $RAC1^{\Delta C10}$ yet bound GDI1 with a 26-fold lower affinity as compared to $RAC1^{WT}$, (ii) $RAC1^{5xE}$, binding to GDI1 was yet observed with a very low affinity while this was not possible for $RAC1^{RAC2}$, and (iii) $RAC2^{RAC1}$ did, in contrast to $RAC2^{WT}$, bind GDI1 with an almost similar affinity as determined for $RAC1^{WT}$. HVR alteration completely abolished GDI1 association with RAC1 but achieved GDI1 association with RAC2.

Result clearly demonstrates that the critical role of polybasic motif of RAC1 in dictating GDI1 binding. It seems that both an increase of overall positive charge in HVRs of RAC2 and the distance of the basic residues from the geranylgeranyl site strongly reinforce GDI1 binding affinity. We hypothesize that RAC1 polybasic motif enables GDI1 to pull the GG moiety from the plasma membrane and direct it into the hydrophobic cavity of its GG binding domains (GGBD).

The relative position and the order of the basic residues in HVR seem to contribute to the formation of an electrostatic network (Fig. 2E) that may significantly stabilize GDI1 interaction with for example RAC1 and RAC3 but not RAC2. Synthetic peptides containing the polybasic motifs of RAC1 (aa 178-188), but not RAC2 (178-188), has been shown to inhibit NADPH oxidase activity in a RAC1-dependent system, and interfere with the translocation of RAC1 proteins to the plasma membrane (46) While the geranylgeranyl moiety mediates membrane anchorage, polybasic motif of RAC1 interacts with plasma membrane

phosphoinositides and stabilizes its proper orientation (47).

Electrostatic pincer residues of GDI1 grasp RAC1 HVR. GDI1 function appears to be driven by a mechanism that generates electrostatic force, attracting the polybasic motif of RAC1. To examine this mechanism, we generated different deletion and change reversal variants of GDI1and measured both their binding capabilities to $RAC1^{GG}$ and $RAC1^{FL}$, and their functional properties to displace $RAC1^{GG}$ from PIP-enriched synthetic liposomes. $GDI1^{E121K}$, which does not contact RAC1 HVR but switch 2 region (Fig. 2E), was used as a control. Kinetic analysis showed that the GDI most variants are disabled in associating with RAC1 (Fig. 4A). Substitutions of D140, E163 and E164 for lysines or deletion of the N-terminal and very C-terminal amino acids significantly impaired GDI1 binding to isoprenylated and non-isoprenylated RAC1, as compared to $GDI1^{WT}$. Most drastic effects were observed with the N-terminal deletion variants with 25 and 58 amino acids (ΔN25 and ΔN58), on the one hand, and double (E163K and E164K or 2E>2K) and triple (E140K, E163K and E164K or 3E>3K) mutations, on the other, which did not bind the RAC proteins under the experimental conditions. Fluorescence polarization measurements verified most GDI1 variants were yet able to bind $RAC1^{FL}$, but with up to three orders of magnitude lower binding affinities (Figure 4B). RAC1 binding was completely abolished in the case of ΔN58 and 3E>3K variants. $GDI1^{\Delta N58}$ not only lacks the very N-terminal acidic resides, that are integral element of the electrostatic pincer function, but also the switch binding domain (SWBD), which undergoes multiple contacts to RAC1 switch regions (Fig. 2C-D). $GDI1^{3E>3K}$ mostly likely creating intermolecular charge repulsion towards positively changed HVR.

To analyse the function of the GDI variants in extracting $RAC1^{GG}$ from the liposomes, we performed a liposome sedimentation assay, as established previously (32). Therefore, we mixed PIP-enriched liposomes (200 μm in diameter) with GDP-bound $RAC1^{GG}$, sedimented, and isolated liposome-bound $RAC1^{GG}$ from the pellet fraction (Fig. 4C, first lane). Next, 1 μM $RAC1^{GG}$•GDP bound to liposomes was mixed 2 μM GDI1 WT and variants (2 μM, respectively) to measure their ability to displace $RAC1^{GG}$ from the liposomes. Figure 4C shows that $GDI1^{WT}$ quantitatively displaced $RAC1^{GG}$ from the liposomes. In contrast, the majority of the GDI1 variants revealed significant reduction in their activities that is consistent with the kinetic and equilibrium measurements (Fig. 4A and 4B). Particularly, $GDI1^{\Delta N58}$ and $GDI1^{3E>3K}$ were completely disabled in binding and extracting $RAC1^{GG}$ from the liposomes, strongly supporting the notion that GDI1 supplies an electrostatic pincer to grasp RAC1 and pull it out from the plasma membrane. Moreover, $GDI1^{E121K}$ and $GDI1^{2E>2K}$ remained partially associated with liposomes and were sedimented in the pellet fraction (Fig. 4A and 4B). In fact, these mutants were able to bind to the $RAC1^{GG}$ on the liposomes but could not extract from the liposomes.

YFP-RAC1 and FLAG-GDI1 variants were ectopically expressed in HUVECs to analyze the molecular basis of their interactions using immunofluorescence (Fig. 4D and S8). In the absence of FLAG-GDI1, $YFP\text{-}RAC1^{WT}$ was both localized in the cytoplasm and at the plasma membrane (arrow head). When either $GDI1^{WT}$ or $GDI^{\Delta N15}$ were co-expressed, $RAC1^{WT}$ was displaced from the plasma membrane and resided in the cytoplasm. In contrast, $GDI^{\Delta N25}$ and $GDI^{2E>2K}$ interestingly co-localized with $RAC1^{WT}$ at the plasma membrane (arrow head), supporting above

data that they still bind RAC1^{WT} but were disabled in displacing it from the membrane (Fig. 4C). The RAC1^{WT} localization pattern in co-expression with GDI$^{\Delta N25}$ and GDI$^{2E>2K}$ was similar to the RAC1^{WT} localization in the absence of GDI. In contrast, RAC1^{5xE} was exclusively cytosolic both in the absence of GDI1^{WT} and in the presence of ~~RAC1~~^{WT}, GDI$^{\Delta N15}$, GDI$^{\Delta N25}$, and GDI$^{2E>2K}$. Co-expression of GDI1^{WT} and RAC1^{5xE} seemed to result in localization of RAC1^{5xE} in perinuclear structure. ~~to endosomes~~. Similar to RAC1^{WT}, co-expression of RAC1^{5xE} without GDI or with GDI$^{\Delta N25}$ and GDI$^{2E>2K}$ resulted in similar RAC1 localization. Furthermore, GDI$^{\Delta N25}$ was stronger in comparison with RAC1^{WT}, which is due to the reduction of repulsion between exist between 25 N-terminal of GDI and HVR of RAC1^{5xE}.

The results above are consistent with previous findings, and support the concept of an electrostatic pincer mechanism on a subset of RHO family GTPases. An early NMR study has shown that deletion of the highly flexible N-terminal region of GDI1 impairs its activity to displace RAC1 from the plasma membrane in HeLa cell (48). Mutations of R186 to cysteine in CDC42 HVR of CDC42 has been very recently shown to disrupt its interaction with GDI1 in patients with a novel autoimmune hematological disorder (49). Thus, electrostatic complementarity between GGBD with the corresponding negative potentials, as shown in this study, and the polybasic region of RAC1, on the one side, and the negative potentials of the N-terminal, rather flexible NTA moving towards the the polybasic region from the other side, obviously provide the required forces to facilitate RAC1 displacement from the membrane(33, 34, 48, 50).

GDI1 buckles RAC1 into its site. A closed look into the RAC1^{GG}-GDP-GDI1 complex (PDB code: 1HH4) revealed that the very terminal regions of GDI1 may undergo electrostatic interaction and thus tighten the complex and avoid dissociation. To examine this hypothesis, we functionally analyzed two flanking deletion variants of GDI1 regarding RAC1 binding and membrane extraction. Kinetic analysis showed that the association rate of GDI1$^{\Delta N15}$ and GDI1$^{\Delta C6}$ were drastically slowed down up to 24-fold especially for mGDP-bound RAC1^{GG} (Fig. 4A). Equilibrium measurements of these terminally deleted variants revealed massive reduction in the K_d values of 440- and 140-fold, respectively, as compared to GDI1^{WT} (Fig. 4B). These GDI1 variants, also exhibited a reduced activity in RAC1GG displacement form the liposomes (Fig. 4B).

These data about the roles of the terminal regions of GDI1, which may hold true for GDI2 and GDI3 due to sequence similarities (Fig. 2D), strongly suggest that these regions may act as a `buckle´ that connects them and safeguards RAC1-bound state of the GDI.

CONCLUSIONS

This study elucidated a distinct and specific mode of GDI interaction that holds for only a subset of RHO GTPases. Our data uncovered a latent set of interactions between RAC1 and GDI1, which add additional insight into the multi-step process that facilitates membrane extraction and inhibition of RAC1 activation, by for example TIAM1(32). Thereby, GDI1 binds with its SWBD to the highly conserved switch regions (ref) of RAC1^{GG} on the membrane, followed by the GGBD binding that attracts RAC1 HVR associated with the negatively charged phospholipids(47) . This step may initiate an electrostatic steering mechanism, which, resulting from long-range charge-

charge interactions, dictates selective recognition of the HVR positive potentials by the GDI1 NTA negative potentials. This process may generate the required force to pull the geranylgeranyl moiety from membrane and place it into GGBD hydrophobic cleft. A last step may be locking $RAC1^{GG}$-GDI1 interaction through the very terminal residues od GDI1 NTA and CT.

Electrostatic steering mechanism has been previously demonstrated for the interaction between CDC42 and WASP(51, 52), VWF and GPIbα(53). It results from long-range charge-charge interactions, and dictates selective bimolecular recognition. Notably, electrostatic steering forces control the accelerated association reaction of two molecules but not the association reaction (51). This small list of interactions may now be extended to interactions between GDIs and RHO GTPases, such as RAC1.

Spatiotemporal activation of RHO proteins needs that various regulators communicate together. GDI as a membrane cycling factor regulates the state of activation of RHO proteins by displacing them from different membranes and masking them from their activation by GEFs or proteasomal degradation (13). Specific binding of the GDI proteins toward RAC1 in the term of fast-kinetic elucidate a new mechanism through electrostatic switched between HVR of RAC and N-terminal negatively charged motif of GDI. Nevertheless, HVR determines the kinetic of membrane localization of RHO GTPases(47). In this context, high affinity of RAC1 membrane binding calls for a tighter interaction with GDI in order to displace it from membranes.

The molecular mechanisms that control the formation of the RAC1-GDI1 complex and the dissociation of RAC1 from GDI1 and its (re)association with the cell membrane still remain unclear. Various factors and activities have been implicated to modulate these mechanisms. These are proteins, including $p75^{NTR}$, ezrin, radixin and merlin of the ERM family, coronin-1A, synectin, and also phospholipids, such PIP_3, or posttranslational modifications, phosphorylation, acetylation, and sumoylation.

While RAC1 G domain mediates regulation and signaling(4), its HVR, modulated various posttranslational modifications, finetunes intracellular trafficking, compartmentalization, subcellular localization, interactions, and membrane association by interacting with a variety of proteins(45). Given this and the results presented in this study, it seems crucial and an interesting area for future research to examine modulatory mechanisms, controlling RAC1 function, impinge on its C-terminal region. And last but not least because of understanding the molecular basis of RAC1 deregulation and dysfunction, implicated in a variety of diseases, such as atherosclerosis, diabetes and cancer (54).

Materials and methods

Constructs

For bacterial expression, RHO GTPase and GDI1 variants, and different GDI variants were cloned into pGEX vectors. For baculovirus-insect cell expression, human RAC1 was subcloned into pFastBacHTB vector (Invitrogen, Carlsbad, CA). For expression in human cells RAC1 and GDI1 variants were cloned in pEYFP and pcDNA-FLAG vectors.

Proteins

All proteins produced using *Escherichia coli* and baculovirus-insect cell expression system as described. (32)

Liposome assays

The liposomes were freshly prepared to perform Liposome sedimentation as described.(32)

Surface plasmon resonance

Surface plasmon resonance (SPR) (Biacore X100 system) was carried out as described(55) .

Fluorescence measurements

Kinetics and equilibrium measurements were performed as described. (56)

Sequence and Structural Analysis

Sequence alignments were performed with BioEdit program using ClustalW algorithm (57). The intermolecular contacts were determined (<4.0 Å) between the GDIs and RHO GTPases using available RHO GTPase-GDI complex structures in the Protein Data Bank. A python code has been written including BioPython modules (pairwise2 and SubsMat.MatrixInfo) (58) to get PDB and alignment files and returns corresponding interaction pairs in a matrix form. All structural representations were generated using PyMOL viewer(59) .

Nucleofection

pEGFP-RAC1 and pcDNA3-FLAG-GDI1 plasmids were microporated into HUVECs to perform confocal imaging according to standard protocol as described(60).

Data availability statement

All the data are in the manuscript.

ACKNOWLEDGEMENTS

We are grateful to E. Amin, B. Anthony, K. Nouri, K. Sandhoff and Christoph Wittig for helpful advice and stimulating discussion.

AUTHORS´ CONTRIBUTIONS

M.R.A. conceived and coordinated the study; N.M. N.S.K.J., M.A. and J.M. designed, performed, and analyzed the experiments; R.D. performed structural analysis; N.M. N.S.K.J., M.A. and M.R.A. designed and wrote the paper; all authors reviewed the results and approved the final version of the manuscript.

FUNDING

This study was supported by the German Research Foundation (Deutsche Forschungsgemeinschaft or DFG; AH 92/8-1), the German Research Foundation (Deutsche Forschungsgemeinschaft or DFG) through the International Research Training Group “Intra- and interorgan communication of the cardiovascular system” (grant number: IRTG 1902-p6), the European Network on Noonan Syndrome and Related Disorders (NSEuroNet, grant number: 01GM1621B); the German Federal Ministry of Education and Research (BMBF) – German Network of RASopathy Research (GeNeRARe, grant numbers: 01GM1902C).

COMPETING INTERESTS

The authors declare no competing financial interest.

REFERENCES

1. Wennerberg, K., and Der, C. J. (2004) Rho-family GTPases: It's not only Rac and Rho (and i like it). *J. Cell Sci.* **117**, 1301–1312

2. Roberts, P. J., Mitin, N., Keller, P. J., Chenette, E. J., Madigan, J. P., Currin, R. O., Cox, A. D., Wilson, O., Kirschmeier, P., and Der, C. J. (2008) Rho family GTPase modification and dependence on CAAX motif-signaled posttranslational modification. *J. Biol. Chem.* **283**, 25150–25163

3. Ahmadian, M. R., Jaiswal, M., Fansa, E. K., and Dvorsky, R. (2013) New insight into the molecular switch mechanism of human Rho family proteins: Shifting a paradigm. *Biol. Chem.* **394**, 89–95

4. Dvorsky, R., and Ahmadian, M. R. (2004) Always look on the bright site of Rho: Structural implications for a conserved intermolecular interface. *EMBO Rep.* **5**, 1130–1136

5. Cherfils, J., and Zeghouf, M. (2013) Regulation of small GTPases by GEFs, GAPs, and GDIs. *Physiol. Rev.* **93**, 269–309

6. Bishop, A. L., and Hall, A. (2000) Rho GTPases and their effector proteins. *Biochem. J.* **348**, 241–255

7. White, C. D., Erdemir, H. H., and Sacks, D. B. (2012) IQGAP1 and its binding proteins control diverse biological functions. *Cell. Signal.* **24**, 826–834

8. Watanabe, T., Wang, S., and Kaibuchi, K. (2015) IQGAPs as Key Regulators of Actin-cytoskeleton Dynamics Mini-review and Review. *Cell Struct. Funct.* **40**, 69–77

9. Abel, A. M., Schuldt, K. M., Rajasekaran, K., Hwang, D., Riese, M. J., Rao, S., Thakar, M. S., and Malarkannan, S. (2015) IQGAP1: Insights into the function of a molecular puppeteer. *Mol. Immunol.* **65**, 336–349

10. Heasman, S. J., and Ridley, A. J. (2008) Mammalian Rho GTPases: New insights into their functions from in vivo studies. *Nat. Rev. Mol. Cell Biol.* **9**, 690–701

11. Hedman, A. C., Smith, J. M., and Sacks, D. B. (2015) The biology of IQGAP proteins: beyond the cytoskeleton . *EMBO Rep.* **16**, 427–446

12. Hall, A. (2012) Rho family GTPases. in *Biochemical Society Transactions*, pp. 1378–1382, Portland Press, **40**, 1378–1382

13. Garcia-Mata, R., Boulter, E., and Burridge, K. (2011) The "invisible hand": Regulation of RHO GTPases by RHOGDIs. *Nat. Rev. Mol. Cell Biol.* **12**, 493–504

14. Jaiswal, M., Dvorsky, R., and Ahmadian, M. R. (2013) Deciphering the molecular and functional basis of Dbl family proteins: A novel systematic approach toward classification of selective activation of the Rho family proteins. *J. Biol. Chem.* **288**, 4486–4500

15. Amin, E., Jaiswal, M., Derewenda, U., Reis, K., Nouri, K., Koessmeier, K. T., Aspenström, P., Somlyo, A. V., Dvorsky, R., and Ahmadian, M. R. (2016) Deciphering the molecular and

functional basis of RHOGAP family proteins: A systematic approach toward selective inactivation of RHO family proteins. *J. Biol. Chem.* **291**, 20353–20371

16. Xie, F., Shao, S., Aziz, A. ur R., Zhang, B., Wang, H., and Liu, B. (2017) Role of Rho-specific guanine nucleotide dissociation inhibitor α regulation in cell migration. *Acta Histochem.* **119**, 183–189

17. Griner, E. M., and Theodorescu, D. (2012) The faces and friends of RhoGDI2. *Cancer Metastasis Rev.* **31**, 519–528

18. De León-Bautista, M. P., Del Carmen Cardenas-Aguayo, M., Casique-Aguirre, D., Almaraz-Salinas, M., Parraguirre-Martinez, S., Olivo-Diaz, A., Del Rocío Thompson-Bonilla, M., and Vargas, M. (2016) Immunological and functional characterization of RhoGDI3 and its molecular targets RhoG and RhoB in human pancreatic cancerous and normal cells. *PLoS One*. **11**, e0166370–e0166370

19. Brunet, N., Morin, A., and Olofsson, B. (2002) RhoGDI-3 regulates RhoG and targets this protein to the Golgi complex through its unique N-terminal domain. *Traffic*. **3**, 342–358

20. Ueyama, T., Son, J., Kobayashi, T., Hamada, T., Nakamura, T., Sakaguchi, H., Shirafuji, T., and Saito, N. (2013) Negative Charges in the Flexible N-Terminal Domain of Rho GDP-Dissociation Inhibitors (RhoGDIs) Regulate the Targeting of the RhoGDI–Rac1 Complex to Membranes. *J. Immunol.* **191**, 2560–2569

21. Xiao, Y., Lin, V. Y., Ke, S., Lin, G. E., Lin, F.-T., and Lin, W.-C. (2014) 14-3-3 Promotes Breast Cancer Invasion and Metastasis by Inhibiting RhoGDI . *Mol. Cell. Biol.* **34**, 2635–2649

22. Harding, M. A., and Theodorescu, D. (2010) RhoGDI signaling provides targets for cancer therapy. *Eur. J. Cancer*. **46**, 1252–1259

23. Moissoglu, K., and Schwartz, M. A. (2014) Spatial and temporal control of Rho GTPase functions. *Cell. Logist.* **4**, e943618

24. Hodge, R. G., and Ridley, A. J. (2016) Regulating Rho GTPases and their regulators. *Nat. Rev. Mol. Cell Biol.* **17**, 496–510

25. DerMardirossian, C., and Bokoch, G. M. (2005) GDIs: Central regulatory molecules in Rho GTPase activation. *Trends Cell Biol.* **15**, 356–363

26. Dharmaiah, S., Bindu, L., Tran, T. H., Gillette, W. K., Frank, P. H., Ghirlando, R., Nissley, D. V., Esposito, D., McCormick, F., Stephen, A. G., and Simanshu, D. K. (2016) Structural basis of recognition of farnesylated and methylated KRAS4b by PDEd. *Proc. Natl. Acad. Sci. U. S. A.* **113**, E6766–E6775

27. Weise, K., Kapoor, S., Werkmüller, A., Möbitz, S., Zimmermann, G., Triola, G., Waldmann, H., and Winter, R. (2012) Dissociation of the K-Ras4B/PDEδ complex upon contact with lipid membranes: Membrane delivery instead of extraction. *J. Am. Chem. Soc.* **134**, 11503–11510

28. Ismail, S. A., Chen, Y. X., Rusinova, A., Chandra, A., Bierbaum, M., Gremer, L., Triola, G., Waldmann, H., Bastiaens, P. I. H., and Wittinghofer, A. (2011) Arl2-GTP and Arl3-GTP regulate a GDI-like transport system for farnesylated cargo. *Nat. Chem. Biol.* **7**, 942–949

29. Chandra, A., Grecco, H. E., Pisupati, V., Perera, D., Cassidy, L., Skoulidis, F., Ismail, S. A., Hedberg, C., Hanzal-Bayer, M., Venkitaraman, A. R., Wittinghofer, A., and Bastiaens, P. I. H. (2012) The GDI-like solubilizing factor PDEδ sustains the spatial organization and signalling of Ras family proteins. *Nat. Cell Biol.* **14**, 148–158

30. Tnimov, Z., Abankwa, D., and Alexandrov, K. (2014) RhoGDI facilitates geranylgeranyltransferase-I-mediated RhoA prenylation. *Biochem. Biophys. Res. Commun.* **452**, 967–973

31. Robbe, K., Otto-Bruc, A., Chardin, P., and Antonny, B. (2003) Dissociation of GDP dissociation inhibitor and membrane translocation are required for efficient activation of Rac by the Dbl homology-pleckstrin homology region of Tiam. *J. Biol. Chem.* **278**, 4756–4762

32. Zhang, S. C., Gremer, L., Heise, H., Janning, P., Shymanets, A., Cirstea, I. C., Krause, E., Nürnberg, B., and Ahmadian, M. R. (2014) Liposome reconstitution and modulation of recombinant prenylated human Rac1 by GEFs, GDI1 and Pak1. *PLoS One*. 10.1371/journal.pone.0102425

33. Grizot, S., Fauré, J., Fieschi, F., Vignais, P. V., Dagher, M. C., and Pebay-Peyroula, E. (2001) Crystal structure of the Rac1 - RhoGDI complex involved in NADPH oxidase activation. *Biochemistry*. **40**, 10007–10013

34. Scheffzek, K., Stephan, I., Jensen, O. N., Illenberger, D., and Gierschik, P. (2000) The Rac-RhoGDI complex and the structural basis for the regulation of Rho proteins by RhoGDI. *Nat. Struct. Biol.* **7**, 122–126

35. Dransart, E., Olofsson, B., and Cherfils, J. (2005) RhoGDIs revisited: Novel roles in Rho regulation. *Traffic*. **6**, 957–966

36. Hoffman, G. R., Nassar, N., and Cerione, R. A. (2000) Structure of the Rho family GTP-binding protein Cdc42 in complex with the multifunctional regulator RhoGDI. *Cell*. **100**, 345–356

37. Longenecker, K., Read, P., Derewenda, U., Dauter, Z., Liu, X., Garrard, S., Walker, L., Somlyo, A. V., Nakamoto, R. K., Somlyo, A. P., and Derewenda, Z. S. (1999) How RhoGDI binds Rho. *Acta Crystallogr. Sect. D Biol. Crystallogr.* **55**, 1503–1515

38. Tnimov, Z., Guo, Z., Gambin, Y., Nguyen, U. T. T., Wu, Y. W., Abankwa, D., Stigter, A., Collins, B. M., Waldmann, H., Goody, R. S., and Alexandrov, K. (2012) Quantitative analysis of prenylated RhoA interaction with its chaperone, RhoGDI. *J. Biol. Chem.* **287**, 26549–26562

39. Sasaki, T., Kato, M., and Takai, Y. (1993) Consequences of weak interaction of rho GDI with the GTP-bound forms of rho p21 and rac p21. *J. Biol. Chem.* **268**, 23959–23963

40. Nomanbhoy, T. K., and Cerione, R. A. (1996) Characterization of the interaction between RhoGDI and Cdc42Hs using fluorescence spectroscopy. *J. Biol. Chem.* **271**, 10004–10009

41. Johnson, J. L., Erickson, J. W., and Cerione, R. A. (2009) New insights into how the Rho guanine nucleotide dissociation inhibitor regulates the interaction of Cdc42 with membranes. *J. Biol. Chem.* **284**, 23860–23871

42. Haeusler, L. C., Hemsath, L., Fiegen, D., Blumenstein, L., Herbrand, U., Stege, P., Dvorsky, R., and Ahmadian, M. R. (2006) Purification and biochemical properties of Rac1, 2, 3 and the splice variant Rac1b. *Methods Enzymol.* **406**, 1–11

43. Haeusler, L. C., Blumenstein, L., Stege, P., Dvorsky, R., and Ahmadian, M. R. (2003) Comparative functional analysis of the Rac GTPases. *FEBS Lett.* **555**, 556–560

44. Golovanov, A. P., Hawkins, D., Barsukov, I., Badii, R., Bokoch, G. M., Lian, L.-Y., and Roberts, G. C. K. (2001) Structural consequences of site-directed mutagenesis in flexible protein domains. *Eur. J. Biochem.* **268**, 2253–2260

45. Lam, B. D., and Hordijk, P. L. (2013) The Rac1 hyper variable region in targeting and signaling-a tail of many stories. *Small GTPases*. **4**, 78–89

46. Joseph, G., Gorzalczany, Y., Koshkin, V., and Pick, E. (1994) Inhibition of NADPH oxidase activation by synthetic peptides mapping within the carboxyl-terminal domain of small GTP-binding proteins. Lack of amino acid sequence specificity and importance of polybasic motif. *J. Biol. Chem.* **269**, 29024–29031

47. Maxwell, K. N., Zhou, Y., and Hancock, J. F. (2018) Rac1 Nanoscale Organization on the Plasma Membrane Is Driven by Lipid Binding Specificity Encoded in the Membrane Anchor. *Mol. Cell. Biol.* 10.1128/mcb.00186-18

48. Golovanov, A. P., Chuang, T. H., DerMardirossian, C., Barsukov, I., Hawkins, D., Badii, R., Bokoch, G. M., Lian, L. Y., and Roberts, G. C. K. (2001) Structure-activity relationships in flexible protein domains: Regulation of rho GTPases by RhoGDI and D4 GDI. *J. Mol. Biol.* **305**, 121–135

49. Lam, M. T., Coppola, S., Krumbach, O. H. F., Prencipe, G., Insalaco, A., Cifaldi, C., Brigida, I., Zara, E., Scala, S., Di Cesare, S., Martinelli, S., Di Rocco, M., Pascarella, A., Niceta, M., Pantaleoni, F., Ciolfi, A., Netter, P., Carisey, A. F., Diehl, M., Akbarzadeh, M., Cont, F., Merli, P., Pastore, A., Mortera, S. L., Camerini, S., Farina, L., Buchholzer, M., Pannone, L., Cao, T. N., Coban-Akdemir, Z. H., Jhangiani, S. N., Muzny, D. M., Gibbs, R. A., Basso-Ricci, L., Chiriaco, M., Dvorsky, R., Putignani, L., Carsetti, R., Janning, P., Stray-Pedersen, A., Erichsen, H. C., Horne, A. C., Bryceson, Y. T., Torralba-Raga, L., Ramme, K., Rosti, V., Bracaglia, C., Messia, V., Palma, P., Finocchi, A., Locatelli, F., Chinn, I. K., Lupski, J. R., MacE, E. M., Cancrini, C., Aiuti, A., Ahmadian, M. R., Orange, J. S., De Benedetti, F., and Tartaglia, M. (2019) A novel disorder involving dyshematopoiesis, inflammation, and HLH due to aberrant CDC42 function. *J. Exp. Med.* **216**, 2778–2799

50. Keep, N. H., Barnes, M., Barsukov, I., Badii, R., Lian, L. Y., Segal, A. W., Moody, P. C. E., and Roberts, G. C. K. (1997) A modulator of rho family G proteins, rhoGDI, binds these G

proteins via an immunoglobulin-like domain and a flexible N-terminal arm. *Structure*. **5**, 623–633

51. Hemsath, L., Dvorsky, R., Fiegen, D., Carlier, M. F., and Ahmadian, M. R. (2005) An electrostatic steering mechanism of Cdc42 recognition by Wiskott-Aldrich syndrome proteins. *Mol. Cell*. **20**, 313–324

52. Tetley, G. J. N., Szeto, A., Fountain, A. J., Mott, H. R., and Owen, D. (2018) Bond swapping from a charge cloud allows flexible coordination of upstream signals through WASP: Multiple regulatory roles for the WASP basic region. *J. Biol. Chem.* **293**, 15136–15151

53. Jiang, Y., Fu, H., Springer, T. A., and Wong, W. P. (2019) Electrostatic Steering Enables Flow-Activated Von Willebrand Factor to Bind Platelet Glycoprotein, Revealed by Single-Molecule Stretching and Imaging. *J. Mol. Biol.* **431**, 1380–1396

54. Olson, M. F. (2018) Rho GTPases, their post-translational modifications, disease-associated mutations and pharmacological inhibitors. *Small GTPases*. **9**, 203–215

55. Baran, P., Hansen, S., Waetzig, G. H., Akbarzadeh, M., Lamertz, L., Huber, H. J., Reza Ahmadian, M., Moll, J. M., and Scheller, J. (2018) The balance of interleukin (IL)-6, IL-6soluble IL-6 receptor (sIL-6R), and IL-6sIL-6Rsgp130 complexes allows simultaneous classic and trans-signaling. *J. Biol. Chem.* **293**, 6762–6775

56. Nouri, K., Fansa, E. K., Amin, E., Dvorsky, R., Gremer, L., Willbold, D., Schmitt, L., Timson, D. J., and Ahmadian, M. R. (2016) IQGAP1 interaction with RHO family proteins revisited kinetic and equilibrium evidence for multiple distinct binding sites. *J. Biol. Chem.* **291**, 26364–26376

57. Hall, T.A. (1999) BioEdit A User-Friendly Biological Sequence Alignment Editor and Analysis Program for Windows 95/98/NT. Nucleic Acids Symposium Series, 41, 95-98. - References - Scientific Research Publishing [online] https://www.scirp.org/(S(lz5mqp453edsnp55rrgjct55))/reference/ReferencesPapers.aspx?ReferenceID=1383440 (Accessed February 22, 2021)

58. Cock, P. J. A., Antao, T., Chang, J. T., Chapman, B. A., Cox, C. J., Dalke, A., Friedberg, I., Hamelryck, T., Kauff, F., Wilczynski, B., and de Hoon, M. J. L. (2009) Biopython: freely available Python tools for computational molecular biology and bioinformatics. *Bioinformatics*. **25**, 1422–1423

59. DeLano, W.L. (2002) The PyMOL Molecular Graphics System. Delano Scientific, San Carlos. - References - Scientific Research Publishing [online] https://www.scirp.org/(S(vtj3fa45qm1ean45vvffcz55))/reference/ReferencesPapers.aspx?ReferenceID=1958992 (Accessed February 22, 2021)

60. Kovačević, I., Sakaue, T., Majoleé, J., Pronk, M. C., Maekawa, M., Geerts, D., Fernandez-Borja, M., Higashiyama, S., and Hordijk, P. L. (2018) The Cullin-3-Rbx1-KCTD10 complex controls endothelial barrier function via K63 ubiquitination of RhoB. *J. Cell Biol.* **217**, 1015–1032

Figure legends

Figure 1. RAC1^{GG} and RAC1^{FL} bind with a similar affinity to GDI1. (**A**) Association of GDI1 (4 µM) with RAC1^{GG} and non-isoprenylated RAC1^{FL} (0.2 µM, respectively). (**B-D**) Quantitative measurements of GDI1 interaction with RAC1^{GG} and RAC1^{FL} led to the calculation of the individual binding constants, association rate constant or k_{on} (**B**), dissociation rate constant or k_{off} (**C**), and dissociation constant or K_d directly from the k_{off}/k_{on} ratio (**D**). (**E**) Titration of increasing GDI1 concentrations to RAC1^{GG} and non-isoprenylated RAC1^{FL} (0.2 µM, respectively), using fluorescence polarization, resulted in in the determination of the equilibrium K_d values. (**F-G**) SPR kinetics of the interaction of immobilized GST-GDI1 (0.2 µM) with increasing concentrations of RAC1^{GG} (**F**) and RAC1^{FL} (**G**). Note, the substantial difference in signal intensity between RAC1^{GG} and RAC1^{FL} can be attributed to the presence of geranylgeranyl moiety in RAC1^{GG}, that may be in close vicinity to the fluorescence reporter of mdGDP.

Figure 2. Biochemical and structural view into the RHO GTPase-GDI interactions. (**A**) Kinetics of association of 2 µM GDI proteins (GDI1, GDI2 and GDI3ΔN20) with 0.2 µM mdGDP-bound RHO GTPases (twelve different proteins) was only monitored for RAC1, RAC3, RHOG and RHOA using stopped-flow fluorimetry. GDI2 but not GDI1 and GDI3 associated with RAC2. No binding (n. b.) was observed for the other GTPases. The obtained data are the average of four to six independent measurements (mean ±S.D.). Kinetic data are shown in Figure S1. (**B**) Individual rate constants were determined, under the same conditions as shown in Figure 1A-C, for the interaction of GDI1 with RAC1, RAC3, RHOG and RHOA, and GDI2 with RAC2. Kinetic data are shown in Figure S2, were derived from the average of four to six independent measurements (mean ±S.D.). (**C**) Interaction matrix of the GDI proteins with twelve RHO family GTPases is generated to determine the frequency of contacts in respective structures (see Table S2; for more detail see Fig. S3). It comprises the amino acid sequence alignments of the RHO proteins (lower left panel) and the GDIs (upper right panel), respectively. Each element corresponds to a possible interaction of RHO residues (row; RAC numbering) and GDI residues (column; GDI1 numbering). The number of actual contact sites between RHO and GDI proteins (with distances of 4 Å or less) were calculated and are indicated with numbers for matrix elements between 1 and 9. (**D**) Schematic diagrams of the domain organizations of GDI1 and RAC1^{GG} illustrate their detailed boundaries. Amino acid sequence alignments of the N-terminal 25 amino acids and the C-terminal six residues of the GDI proteins (boxed) highlight negatively and positively charged residues (red and blue). (**E**) A detailed view into the structure (PDB code: 1HH4) of GDP-bound RAC1^{GG} (grey ribbon) in complex with GDI1 (surface representation) revealed that the basic HRV (blue) is sandwiched between a series of acidic residues of GDI1 supplied by NTA (purple) and GGBD (orange). Colors are the same in **D**.

Figure 3. RAC1 HRV generates a selective and high affinity interaction toward GDI1. (**A**) A sequence alignment of hypervariable region (HRV) of RHO GTPases shows significant differences in the frequency of the basic residues (blue). GDI-binding protein are shown in bold. Critical amino acid deviations in RAC2 are shown in magenta. The isoprenylation site (cysteine 198 in RAC1) is highlighted in bold. (**B**) Kinetics of GDI1 association were measured by mixing

RAC1 and RAC2 variants (0.2 µM, respectively) with 2 µM GDI1. (**C**) K_d values for the RHO GTPase-GDI1 interaction were determined by titrating RAC1 and RAC2 variants (0.2 µM, respectively) with increasing concentrations of GDI1 using fluorescence polarization (see Figure S4 for more details).

Figure 4. RHOGDI1 grasps basic HVR of RAC1 with multiple negatively charged residues. (**A**) Kinetics of association of 2 µM GDI1 variants with 0.2 µM mdGDP-bound RAC1 was monitored using stopped-flow fluorimetry. The obtained data are the average of four to six independent measurements (mean ±S.D.). Kinetic data are shown in Figure S5. (**B**) K_d values for the interaction between the GDI1 variants and mdGDP-bound RAC1 were determined by fluorescence polarization (see Figure S6 for more details). (**C**) GDI1 variants are, in contrast to GDI1 WT, impaired in extracting $RAC1^{GG}$ from PIP-enriched synthetic liposomes. The graphs represent densitometric analysis of three independent liposome sedimentation experiments (Fig. S7). Data are shown as mean ± SD. (**D**) FLAG-GDI1 variants were not able to extract GFP-RAC1 from the plasma membrane of HUVECs. All individual images are illustrated in Figure S8. Arrow point to colocalization of RAC1 and GDI1 at the plasma membrane.

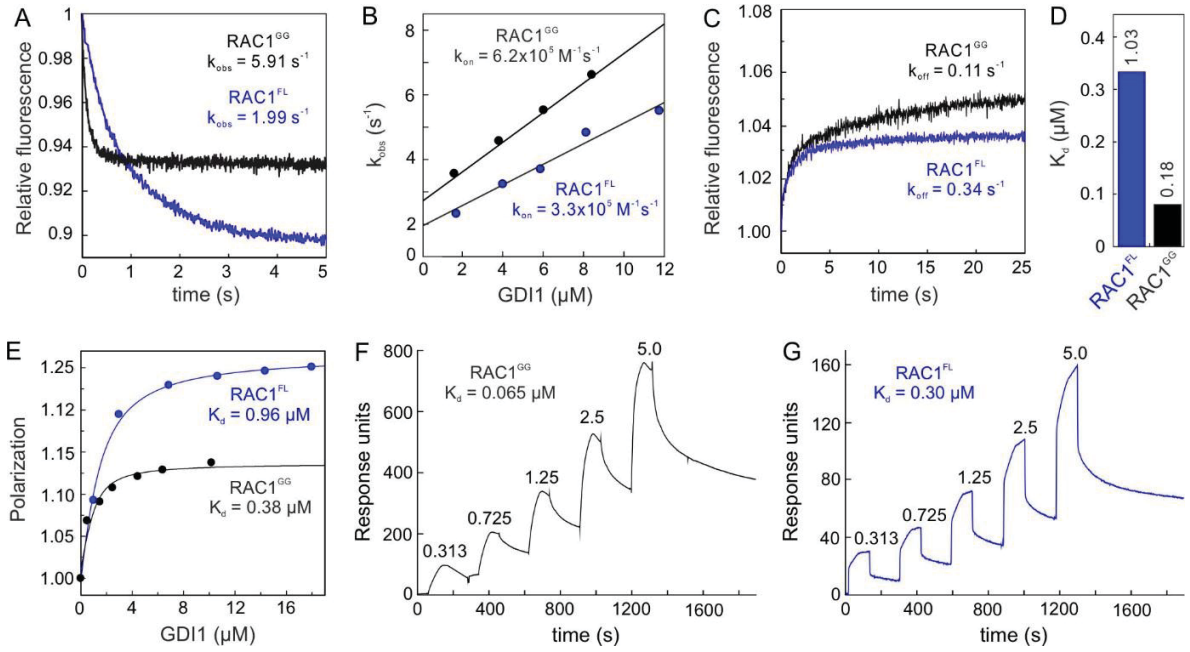
A
Relative fluorescence
time (s)
RAC1GG
kobs = 5.91 s-1
RAC1FL
kobs = 1.99 s-1
B
kobs (s-1)
GDI1 (μM)
RAC1GG
kon = 6.2x10^5 M-1s-1
RAC1FL
kon = 3.3x10^5 M-1s-1
C
Relative fluorescence
time (s)
RAC1GG
koff = 0.11 s-1
RAC1FL
koff = 0.34 s-1
D
Kd (μM)
1.03
0.18
RAC1FL
RAC1GG
E
Polarization
GDI1 (μM)
RAC1FL
Kd = 0.96 μM
RAC1GG
Kd = 0.38 μM
F
Response units
time (s)
RAC1GG
Kd = 0.065 μM
0.313
0.725
1.25
2.5
5.0
G
Response units
time (s)
RAC1FL
Kd = 0.30 μM
0.313
0.725
1.25
2.5
5.0

Figure 1

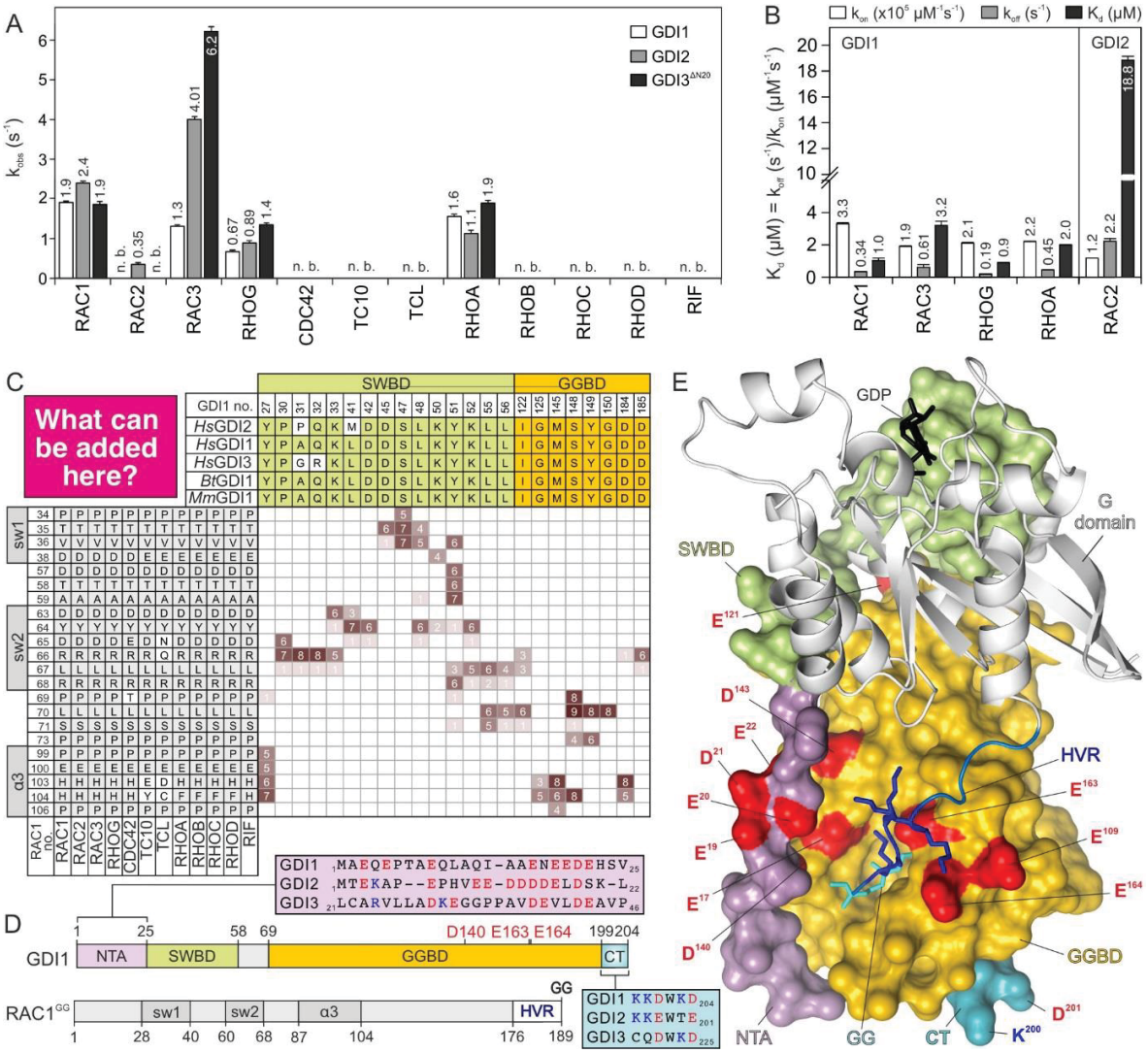

Figure 2

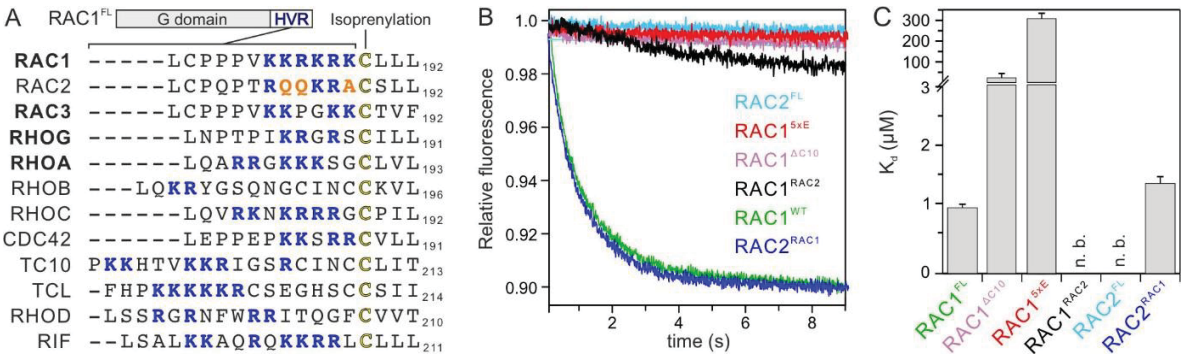

Figure 3

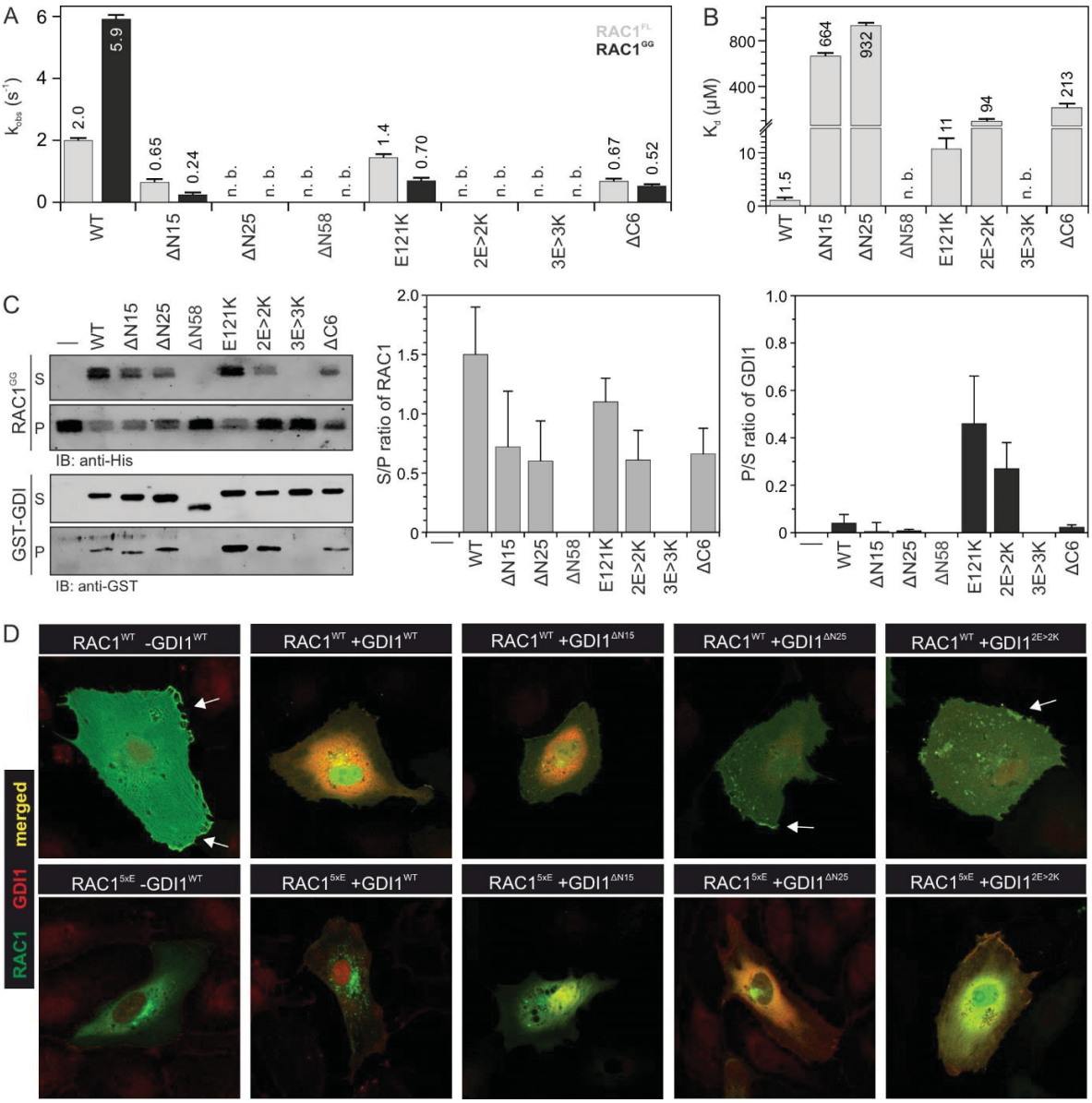
A
B
C
D
RAC1FL
RAC1GG
WT
ΔN15
ΔN25
ΔN58
E121K
2E>2K
3E>3K
ΔC6
n. b.
IB: anti-His
IB: anti-GST
GST-GDI
S/P ratio of RAC1
P/S ratio of GDI1
RAC1WT -GDI1WT
RAC1WT +GDI1WT
RAC1WT +GDI1ΔN15
RAC1WT +GDI1ΔN25
RAC1WT +GDI1 2E>2K
RAC15xE -GDI1WT
RAC15xE +GDI1WT
RAC15xE +GDI1ΔN15
RAC15xE +GDI1ΔN25
RAC15xE +GDI1 2E>2K
merged
GDI1
RAC1

Chapter VIII

Elucidation of cooperative mechanisms in the allosteric modulation of GRB2 interaction with SOS1

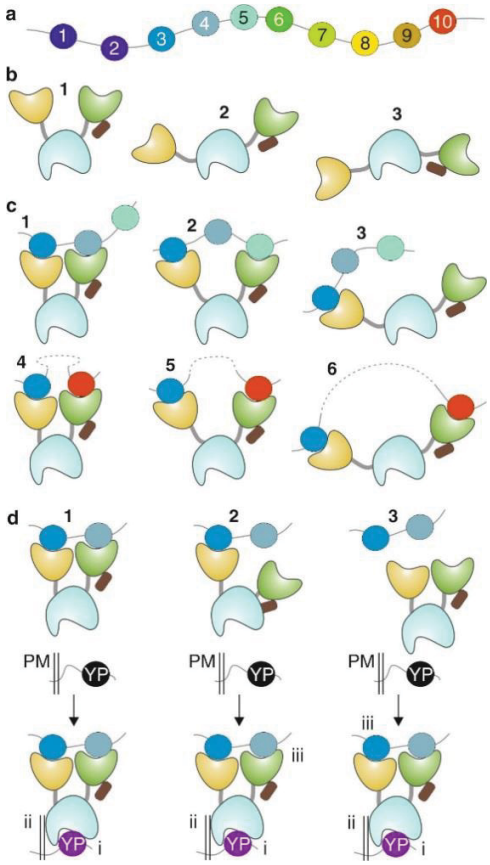

Under revision in : Biochemistry journal
Impact factor: 5.067 (2018)
Own Proportion to this work: 90%

Experimental design, mutational, bioinformatic and biophysical analysis, figure generation, writing and revising the manuscript

The intramolecular allostery of GRB2 governing its interaction with SOS1 is modulated by phosphotyrosine ligand

Neda S. Kazemein Jasemi[1], Christian Herrmann[2], Eva Magdalena Estirado[3], Radovan Dvorsky[1], Luc Brunsveld[3], Mohammad R. Ahmadian[1*]

[1]Institute of Biochemistry and Molecular Biology II, Medical Faculty of the Heinrich-Heine University, 40225 Düsseldorf, Germany

[2]Department of Physical Chemistry I, Ruhr University Bochum, Bochum, Germany

[3]Laboratory of Chemical Biology, Department of Biomedical Engineering and Institute for Complex Molecular Systems (ICMS), Eindhoven University of Technology, P.O. Box 513, 5600MB, Eindhoven, The Netherlands

Corresponding author: Reza Ahmadian (PhD), Institute of Biochemistry and Molecular Biology II, Medical faculty of the Heinrich Heine University, Universitätsstrasse 1, building 22.03.05, 40255 Düsseldorf, Germany; Tel.: +49-211-811 2384; Fax: +49-211-811 2726; E-mail: reza.ahmadian@hhu.de

Abstract

The growth factor receptor-bound protein 2 (GRB2) is a trivalent adaptor protein, and a key element in signal transduction. It interacts *via* its flanking SH3 domains with the proline-rich domain (PRD) of RAS activator SOS1, and *via* its central SH2 domain with phosphorylated tyrosine residues of receptor tyrosine kinases (RTKs; e.g., HER2). The elucidation of structural organization and mechanistic insights into GRB2 interactions, however, remain challenging due to its inherent flexibility. This study represents an important advance in our mechanistic understanding of how GRB2 links RTKs to SOS1. Accordingly, it can be proposed that (1) HER2 pYP-bound SH2 allosterically potentiates GRB2 SH3 domains interaction with SOS1 (an allosteric mechanism), (2) SH2 domain blocks cSH3 enabling nSH3 to bind SOS1 first before cSH3 follows (an avidity-based mechanism), and (3) allosteric behavior of cSH3 to other domains appears unidirectional although there is an allosteric effect between the SH2 and the SH3 domains.

Keywords: GRB2, HER2, proline-rich domain, proline-rich motif, RAS, SH2, SH3, SOS1

Introduction

Allosteric regulation of multivalent proteins is widespread in a variety of biological processes (*287*). In multivalent proteins, the signal can be propagated from one site to other sites by allosteric mechanisms. Allosteric sites facilitate the effectors binding to the protein, often by controlling the conformational changes within the protein enabled by protein dynamics (*288, 289*). The exact mechanism of allosteric regulation of proteins is still elusive, therefore, we aim to shed light on the allosteric behavior of the multivalent growth factor receptor-bound protein 2 (GRB2) and the impact on its interaction with Son of Sevenless 1 (SOS1).

GRB2 is a ubiquitously expressed and evolutionary conserved adaptor protein (*290*), which links extracellular signals to a variety of pathways, including the RAS signaling pathways, with diverse signaling molecules, including SOS1 (*106*). It is a 25-kDa protein and consists of three protein interaction modules, one SRC homology 2 (SH2) and two terminal SRC homology 3 domains (nSH3 and cSH3). The SH3 domains typically bind to the proline-rich motifs (PRMs) of target proteins, *e.g.*, RAS-specific exchange factor SOS1 and GRB2-associated-binding protein 1 (GAB1) (*106-108, 291-295*). The SH2 domain specifically binds to the tyrosylphosphate (pY)-containing proteins, such as activated receptor tyrosine kinases (RTKs; e.g., human epidermal growth factor receptor or HER2), and other transmembrane (*296-298*). The GRB2 SH2 domain has been shown to bind to a pY-Φ-N-Φ consensus motif (where Φ represents a hydrophobic residue) of activated receptors (*299*). The binding of the GRB2-SOS1 complex to the tyrosine phosphorylation sites on cell surface proteins has been proposed to translocate SOS1 to the plasma membrane in the vicinity of RAS. This enables the GDP/GTP exchange on RAS leading to activation of the mitogen-activated protein kinase (MAPK) cascade (*300, 301*). The GRB2-GAB1 complex is known to activate the protein tyrosine phosphatase SHP2. GRB2-GAB1-SHP2 complex downregulates the PI3K pathway and induces RAS activation (*110, 302*).

GRB2-SOS1 complex formation requires the interaction of GRB2 SH3 domains with the C-terminal proline-rich domain (PRD) of SOS1 (*303, 304*). SOS1 PRD contains more than ten PRMs, most of which seem not to bind GRB2 SH3 domains (*305-308*). The best-investigated SOS1 PRM is VPVPPPVPPRRR (here called reference peptide 1 or RP1). RP1 has been reported to bind GRB2 nSH3 more tightly than cSH3 (*293, 305, 309, 310*). RP1 binding has been recently shown to induce a closed conformation of nSH3 (*305*). Loss of PRM-binding variants of GRB2 SH3 domains (substitution of W36 and/or W193 for K) have been shown to abolish the critical role of GRB2 in ERK activation *via* the SOS1-RAS-RAF-MEK axis (*311, 312*). These mutations disrupt nSH3/cSH3 binding to SOS1. Thus, GRB2-SOS1 interaction is a key step towards proliferation in normal and cancer cells (*313*). Targeting GRB2−SOS1 interaction has been suggested to offer new venues for future therapeutic strategies for upstream mutations in cancer, such as in EGFR (*308*).

The notion that protein function is allosterically regulated by structural or dynamic changes in proteins has been extensively investigated for several proteins in solution (*287*). A quantitative description of the communication between two distinct sites in a multivalent protein is still very challenging. In the case of SH3 domains, whilst they have been often associated with allosteric mechanisms, the intra-domain communication between residues has been poorly explored to date (*314*). In this study, we have investigated GRB2 and its interaction with proline-rich peptides of SOS1 in the presence and absence of HER2 phosphotyrosine peptide (pYP). Our data clearly indicate an allosteric modulation of the GRB2-SOS1 interaction by HER2 pYP and a cooperative mechanism between cSH3 and nSH3 regarding binding to SOS1.

Results

Both functional GRB2 SH3 domains are required for the interaction with SOS1. The interaction of His-tagged SOS1 PRD with GST fusion proteins of GRB2 was analyzed in a pull-down assay. PRD equally bound to GRB2 FL, nSH3, and cSH3 but not at all if a conserved

tryptophan (W36 in nSH3 and W193 in cSH3; Fig. 1) was mutated to a lysine (K); W36K in nSH3, W193K in cSH3, and W36K/W193K in GRB2 FL abrogated their binding to SOS1 PRD (Fig. 2). Interestingly, however, single mutations in GRB2 FL (W36K or W193K) led also to a significant impairment of GRB2-RP1 interaction (Fig. 2). This was surprising because both GRB2 FL^{W36K} respectively GRB2 FL^{W193K} had one SH3 domain intact. This result indicates that functional interdomain interactions exist for GRB2.

GRB2 FL and isolated SH3 domains exhibit varying affinities for distinct sites of SOS1 PRD. Next, we analyzed the binding capacity of individual PRMs within SOS1 PRD. Binding of ten FITC-labelled peptides (P1 – P10; Table S1 and Fig. 3a) and two reference peptides (RP1 and RP2) to GST fusion proteins of GRB2 FL, nSH3, and cSH3, respectively, were qualitatively analyzed by combining GST pull-down and dot-blot assays. As shown in Figure 3b, SOS1 peptides P3, P4, and to a certain extent also P5, as well as the reference peptides PR1 and PR2, bound strongly GRB2-derived proteins. Signals observed for the other peptides were rather weak.

We next conducted fluorescence polarization measurements to obtain the affinities for the interaction between GRB2 and SOS1 PRMs. For this, increasing concentrations of the GRB2 proteins, FL, nSH3, and cSH3, respectively, were titrated to the fluorescent peptides at a constant concentration of 1 µM. We monitored an increase in polarization for P3, P4, P5, and the reference peptides (Fig. S2a) but not for the other SOS1 peptides (data not shown). All equilibrium dissociation constants (K_d) for the respective GRB2-SOS1 interactions are summarized in Table S3 and shown in Figure 3a as bar charts. The highest affinity exhibiting a K_d value of 1.2 µM was obtained for P3 binding to cSH3 which was 12.5-fold higher than that to nSH3. Relatively weak interactions with intermediate and low affinities were determined for P4 and P5 binding to cSH3 and nSH3, respectively. However, their dissociation constants of 15.5 µM and 13.2 µM, respectively, for GRB2 FL are still reasonable and suggest that P4 and P5 might constitute—in addition to P3—secondary binding sites for GRB2.

Isothermal titration calorimetry (ITC) measurements revealed that GRB2-SOS1 interaction exhibits a two-sites binding characteristic, with a first K_d of 1.2 µM and a second K_d of 4.0 µM, respectively (Fig. 5a). These observations provided two new insights on the GRB2-SOS1 interaction. First, GRB2 uses both SH3 domains to bind SOS1. Second, the binding affinity of the SH3 domains is considerably higher in the context of GRB2 FL as compared to the isolated domains suggesting intramolecular interaction and allosteric coupling between the domains.

Both functional SH3 domains of GRB2 FL are affected upon the interaction with SOS1. Based on our previous observation, the SOS1 PRD interaction with GRB2 FL was sufficiently compromised when only one of its two SH3 domains contained a loss of function mutation (W36K or W193K; Fig. 2 and Table S2). We set out to investigate the impact of additional mutations that are likely to alter the interaction with SOS1 as well as those that indirectly affect the affinity of GRB2 towards fluorescent SOS1 RP1. We hypothesized that such variations reside in the intramolecular and/or inter-domain interactions within the GRB2. To this end, we determined the K_d values for the binding of various GRB2 variants to SOS1 RP1 using fluorescence polarization under the same conditions as described above. The first analysis showed that indeed not only a double but also a single tryptophan mutation of GRB2 SH3 domains completely abolished SOS1

RP1 binding (Fig. 4a). In contrast, isolated nSH3 and cSH3 domains of GRB2 did bind strongly RP1 with K_d values of 3.4 and 11.5 µM, similar to the ITC results (Fig. 5a), respectively, but not their tryptophan to lysine mutations (Fig. 4b). Substitution of Trp193 for alanine and glutamic acid (W193A and W193D), respectively, also completely impaired RP1 interaction with cSH3 (Fig. 4b). Thus, a tryptophan at this position is essential for the interaction of SH3 domains with the RPMs.

These data indicate that there is a mutual influence of the two SH3 domains in the context of GRB2 FL. Hence, we systematically investigated in the following the impacts of the interconnecting regions, namely (i) the SH2 domain including its association with HER2, (ii) the linker regions of GRB2, and (iii) the allosteric interdomain communication of GRB2 on GRB2-SOS1 interaction.

GRB2 SH2 domain allosterically regulates GRB2-SOS1 interaction. Possible upstream effects of HER2 on GRB2-SOS1 interaction were examined. For mimicking such a signaling event, we designed fluorescent peptides, containing Tyr1193 (YP) and phospho-Tyr1193 (pYP) of human HER2 (Table S1), and determined their binding affinities for both GRB2 FL and its SH2 domain. Isolated SH2 and $GRB2^{FL}$ bound fluorescent pYP 16- and 106-fold more strongly than non-phosphorylated fluorescent YP (Fig. 4C). The intradomain interaction in $GRB2^{FL}$ strikingly enhances the HER2-GRB2 interaction, not only because of the high affinity of GRB2 FL for pYP but also because of the binding selectivity of pYP *vs.* YP.

Next, we addressed the impact of HER2 pYP binding to GRB2 FL on the SH3 interaction properties with SOS1 RP1. The experiments were conducted under the same conditions as before but in the presence of non-fluorescent HER2 pYP. Figure 4d shows that HER2 pYP binding to the GRB2 SH2 domain did not have any obvious effect on RP1 interaction with GRB2 FL. Remarkably, HER2 pYP induced a tight interaction of RP1 with $GRB2^{W36K}$ (Fig. 4d). As shown before, this GRB2 variant with one intact cSH3 domain was unable to bind SOS1 RP1 in the absence of HER pYP (Fig. 4a). This effect of pYP was marginal for $GRB2^{WT}$ and even absent for $GRB2^{W193K}$ and subsequently also for $GRB2^{W36K/W193K}$ (Fig. 4d). It seems that pYP association with SH2 uncouples potential interdomain interaction(s) within GRB2 suggesting, for the first time, an allosteric mechanism underlying the RTK-mediated regulation of SOS1 interaction with GRB2.

To further examine the impact of the SH2 domain on SOS1 RP1 binding affinity, we generated GRB2 ΔSH2 variants (Table S2) and measured their RP1 binding ability. The results showed that not only GRB2 ΔSH2 bound RP1 with a high affinity—higher than GRB2 FL in the absence and the presence of HER2 pYP (Fig. 4a and 4d)—but most remarkably also $\Delta SH2^{W36K}$ (Fig. 4e). Consistent with the data obtained with GRB2 FL, $\Delta SH2^{W193K}$ and $\Delta SH2^{W36K/W193K}$ did not show any RP1 binding.

These data indicate a modulatory impact of the pYP-SH2 complex on GRB2-SOS1 interaction and may rather challenge the existing paradigm of GRB2-mediated SOS1 activation.

Physical interdomain interactions control a structural and functional switch of GRB2. To inspect more deeply the interdependency between the three GRB2 domains associated with GRB2-SOS1 interaction we generated GRB2 variants lacking either cSH3 or nSH3 (Table S2) and performed fluorescence polarization experiments at the same setup as before. Figure 4f

shows that GRB2$^{\Delta cSH3}$ exhibited almost the same affinity for SOS1 RP1, as determined for GRB2^{FL} and that the presence of HER2 pYP did not show any meaningful increase in GRB2$^{\Delta cSH3}$-SOS1 interaction (Fig. 4f). In contrast and interestingly, a loss of SOS1 RP1 binding was observed for GRB2$^{\Delta nSH3}$ that was also disabled in SOS1 RP1 binding even in the presence of HER2 pYP (Fig. 4f).

To follow up on this observation, we next measured the impact of possible direct SH2-SH3 interactions on RP1 binding to individual SH3 domains. We carried out the fluorescence polarization measurements for the interaction of isolated cSH3 and nSH3 with SOS1 RP1 under the same condition as shown in (Fig. 4b) but in the presence of excess amounts of the SH2 domain. Figure 4g shows that the SH2 domain "*in trans*" significantly interfered with the binding of RP1 to both nSH3 and cSH3 domains. Whereas no binding was observed for nSH3, the binding affinity of cSH3 for SOS1 RP1 was reduced by 15-fold by the SH2 domain. Most remarkably, the presence of excess amounts of HER2 pYP-SH2 (200 μM respectively) actually enabled the nSH3 to bind RP1 (K_d = 11.3 μM) and strongly improved the cSH3-SOS1 RP1 interaction by 24-fold (Fig. 4g).

These data suggest that binding of activated RTK and possibly other transmembrane proteins to the SH2 domain change the overall conformation of the SH3 domains—most likely cSH3—and favor the association with SOS1.

As above data indicated unexpected interrelationship between GRB2 domains we have conducted a series of ITC experiments to uncover the direct or indirect interplay between isolated SH2 and SH3 domains as well as between isolated SH3 domains and SOS PR1 in the presence of the isolated SH2 domain. Data summarized in Figures 5d-g shows that the isolated SH3 domains bind with very low-affinity to the isolated SH2 of GRB2 and that the presence of HER2 pYP slightly attenuated these SH3-SH2 interactions. Moreover, in the presence of SOS1 RP1 the SH2 domain neither binds nSH3 nor cSH3 (Fig. 5h-i). Interestingly, a different scenario emerged from titrating SOS RP1 to a mixture of isolated SH3 and SH2 domains (Fig. 5j-m). While RP1 did not bind to the nSH3-SH2 complex, it exhibited a high affinity binding for the mixture of nSH3, SH2, and HER pYP (Fig. 5j and 5k). These results are consistent with the fluorescence polarization data (Fig. 3g) and support the idea that activated RTK or other phosphotyrosyl-containing proteins binding to GRB2 facilitates its interaction with SOS1. In contrast, cSH3 bound RP1 with a slightly higher affinity in the presence of SH2 as compared to the measurement in the absence of SH2 and the addition of pYP did not significantly strengthen the binding (Fig. 5l and 5m).

Taken together, above findings expand our understanding of the principles of modular domain organizations and the interdomain relationships of GRB2 and suggest a structural and functional switch that favors intramolecular interactions and allosteric coupling between its domains.

Interdomain linkers of GRB2 confer highly dynamic interactions with SOS1. We next addressed the question of whether the short linker segments of GRB2 interconnecting its globular domains (amino acids 54-63 and 149-159) plays a role in the allosteric mechanism of GRB2 action. A closer look at the structure of GRB2 (PDB ID: 1GRI) revealed a kind of antiparallel structural arrangement of these two linkers, especially in the central regions with sequences

^{57}PHP^{59} and ^{152}EQV^{154} (Fig. 1). To examine their impact, we generated deletion variants of GRB2, lacking both PHP and EQV, respectively. This variant was then combined with single and double tryptophan substitutions in the SH3 domains (Table S2). The data shown in Figure 4h indicate the critical role of the GRB2 linkers in the structural and functional features of GRB2 SH3 domains. Double truncation of the linkers, GRB2$^{\Delta PHP/\Delta EQV}$, led to an immense decrease of SOS1 RP1 binding affinity by 22.5-fold. This impairment was not reversed in the presence of HER2 pYP (Fig. 4h). In contrast to experiments with GRB2 FL shown in Figure 4a, PHP/EQV deletion restored SOS1 RP1 binding to GRB2^{W36K} and GRB2^{W193K}. These observations clearly underscore the critical role of the linker in the SH3-mediated interaction with SOS1.

To further analyze the effect of single linker truncation, we generated GRB2$^{\Delta PHP}$, and GRB2$^{\Delta EQV}$, respectively. Most remarkably, SOS1 RP1 binding was completely abolished upon PHP but not EQV deletion. GRB2$^{\Delta EQV}$ interaction with RP1 notably remained unchanged in the absence of HER2 pYP but 5-fold reduced in the presence of pYP (Fig. 4i).

These data emphasize the critical role of the linker segments, which give GRB2 domains freedom and space to move and to orient to each other in a most suitable way. This becomes more difficult when the linkers are shorter.

GRB2-SOS1 interaction underlies an allosteric mechanism. An inspection of the GRB2 structure (PDB ID: 1GRI) showed that Y37, K50, K195, T202 create an intra-molecular interaction network between the two SH3 domains (Fig. 1). We thought that replacing them with negatively charged aspartate residues may generate repulsive forces and thus abolish this interaction network. Another interesting contact site between the two SH3 domains is achieved by M1 in nSH3 and M186 in cSH3 (Fig. 1). The nature of this methionine interaction is more Van der Waals (hydrophobic) and their substitution by arginine or lysine may induce an interdomain electrostatic repulsion. To investigate possible allosteric effects of these sites on SOS1 RP1 binding we generated three sets of GRB2 variants, which are apart from the PRM binding site of the SH3 domains (Fig. 1; Table S2): (i) A sextuple variant with M1R, Y37D, K50D, M186R, K195D, and T202D substitutions (6allo); (ii) two triple variants with M1R, Y37D, and K50D substitutions (n3allo), and with M186R, K195D, and T202D (c3allo) substitutions, respectively; (iii) a triple variant with the substitutions of Met1, Met186, and Thr202 to arginines (M1R/M186R/T202R; called 1-2allo).

Fluorescence polarization data revealed that 6allo substitutions drastically impaired GRB2 SOS1 binding sites such that no RP1 association with GRB2^{6allo} was observed (Fig. 4j). This deficiency was slightly recovered in the presence of HER pYP. Curiously, isolated SH3 domains with the respective substitutions (3allo and 3allo, respectively) showed no binding with SOS1 RP1 either (Fig. 4k). This raises the question of whether a physical interaction between two SH3 domains in GBR2^{FL} is a prerequisite for their interactions with SOS1 RP1. The ITC measurements were performed to examine possible physical nSH3-cSH3 interaction. We observed that the two SH3 domains undergo a very low affinity binding (K_d = >200 µM), which was abolished when the 3allo variants of nSH3 and cSH3 were used (Fig. 5n, 5o, and S4). Moreover, analytical size exclusion chromatography of the SH3 proteins revealed that cSH3^{WT}, in contrast to monomeric nSH3^{WT} and nSH3^{3allo}, is a dimer and tetramer, and is shifted to monomeric/dimeric populations in the case of

monomeric 3allo variant (Fig. S5). These observations confirmed the notion that an inter-SH3 domain interaction forms an alliance of its own. Certainly, these allosteric sites are not primary binding sites but are obviously critical in the optimal control of SOS1 association with GRB2.

To further follow up on the impact of the allosteric site, we measured the RP1 binding activity of $GRB2^{n3allo}$ and $GRB2^{c3allo}$, respectively. $GRB2^{n3allo}$ showed a 30-fold reduced K_d value for SOS1 RP1. However, it was, contrary to $GRB2^{W36K}$, yet able to bind RP1 with a similar affinity in the background of W36K (Fig. 4l). RP1 binding was not observed for $GRB2^{n3allo/W193K}$. Most remarkably, $GRB2^{n3allo}$-SOS1RP1 interaction was greatly improved in the presence of HER pYP. This clearly supports the notion that HER pYP-SH2 interaction induces a reorientation of the SH3 domains and optimizes SH3-SOS1 interaction. In contrast, $GRB2^{c3allo}$ was able to efficiently bind RP1 with a K_d value of 1 µM, which remained unchanged in the background of W193K but was completely abolished in the background of W36K (Fig. 4m).

In order to reduce the number of substitutions at the allosteric sites, we generated and analyzed $GRB2^{1\text{-}2allo}$ using fluorescence polarization. As shown in Figure 4n, this protein binds SOS1 RP1 with high affinity but it is in comparison to $GRB2^{WT}$ able to bind RP1 with intermediate affinities in the background of W36K. The presence of HER pYP did not change these binding affinities. $GRB2^{1\text{-}2allo/W193K}$, however, exhibited K_d values of 2.2 for RP1 binding (Fig. 4N), which interestingly resembles the high binding affinities of $GRB2^{\Delta EQV}$ and $GRB2^{c3allo(W193K)}$, respectively (Fig. 4i and 4m).

These data strongly suggest that a cooperative nSH3-cSH3 interaction is required to facilitate SOS1 binding, and further support the idea of opposed impacts of the SH3 domains on their RP1 binding capabilities. It seems that nSH3 allosterically facilitates RP1 association with cSH3, and cSH3 allosterically precludes nSH3-RP1 interaction.

The unique C-terminal NRNV motif leverages GRB2 allostery. An inspection of the GRB2 structure revealed that the very C-terminal four amino acids consisting of NRNV undergoes contacts with the linker 2 and possibly also with the SH2 domain. It was tempting to investigate its impact on GRB2 interaction with SOS1 RP1 in the presence and absence of HER pYP. This was addressed by deleting this motif. As shown in Figure 4o, NRNV deletion led to a drastic attenuation of GRB2-RP1 interaction by more than 28-fold as compared to $GRB2^{FL}$ (Fig. 4a), which was recovered in the presence of HER2 pYP to the same extent as $GRB2^{FL}$ (Fig. 4d). Most remarkably, $GRB2^{\Delta NRNV}$ variants with W36K or W193K substitutions were, in contrast to $GRB2^{FL}$, able to bind RP1 even with higher affinities than without the tryptophan substitutions (Fig. 4o). Moreover, the addition of HER2 pYP resulted in loss of RP1 binding to $GRB2^{\Delta NRNV(W36K)}$ and gain of RP1 binding to $GRB2^{\Delta NRNV(W193K)}$. The very high affinity of the latter rather resembles the wild type $GRB2^{FL}$ in the presence of pYP (Fig. 4d).

With the very C-terminal NRNV, we have identified a sequence motif that seemingly leverages GRB2 allostery to direct RTK signaling towards SOS1 activation.

Discussion

One of the key steps in RAS activation at the plasma membrane is the bimodal interactions of GRB2 adaptor protein with the activated RTK and the RASGEF SOS1. GRB2 carries one SH2 domain for the association with a specific phosphotyrosine site of the activated RTK or non-receptor tyrosine kinases, and tyrosine-phosphorylated proteins, and two SH3 domains responsible for binding to proline-rich motifs, such as SOS1 PRD. This study provides comprehensive data on molecular interactions of PRD, PRMs, Y-/pY-peptides with GRB2 in an attempt to shed light on the mechanism underlying the linking RTKs with RASGEFs by GRB2. It demonstrates that the mechanism with which the GRB2 functions as adaptor protein is not based on a simple binding model. Using a systematic and unbiased approach we found that: (1) GBR2 binds, with P3, P4, and P5, the three out of ten SOS1 PRMs; (2) both functional GRB2 SH3 domains are required for the interaction with SOS1; (3) physical interdomain interactions of GRB2 structurally and functionally modulate a tight association with SOS1; (4) the two GRB2 linkers allow for highly dynamic interactions of the SH3 domains; (5) there is a reciprocal relationship between the two SH3 domains that determine their alternate interactions with SOS1; (6) the GRB2-SOS1 interaction underlies an allosteric mode of regulation that is leveraged by a unique C-terminal NRNV motif. Thus, GRB2 rather appears to undergo, upon upstream ligand binding (*e.g.*, HER2 pYP), a series of structural transitions from one site to a physically distinct site that may reinforce a stepwise association of downstream ligands (*e.g.*, SOS1 PRMs). Such a signal propagation is achieved *via* both intradomain structural changes and allosteric networks, on the one hand, induced by HER2 pYP binding to the SH2 domain, and on the other hand, modulated by specific domain–domain rearrangements, which ultimately results in the engagements of both SH3 domains in binding and eventually activating SOS1.

The interaction of GRB2 with SOS1 was first described in the early 1990s (*304, 315*). The first study by Lemmon et al. has shown that GRB2 undergoes a 1:2 complex with a SOS1 peptide, similar to P3, with a K_d value of 22 µM, and a 1:1 complex with a HER1 pYP with a K_d value of 0.4 µM (*316*). This study and Cussac et al. have proposed an independent ligand binding to the SH2 and SH3 domains of GRB2 (*310, 316*). Since then, many different groups have investigated GRB2 interactions with various SOS1 peptides with nanomolar to millimolar binding affinities for $GRB2^{FL}$, nSH3, and cSH3 using different methods and varying conditions (*293, 305-307, 317-320*). A detailed inspection of SOS1 PRD sequence revealed that the ten peptides, selected for this study (P1-P10; Fig. 6a), cover 13 out of 14 identified types of proline-rich consensus sequence motifs (Table S4). However, the majority of the studies have analyzed peptides with PXXPXR motif that were derived from P3 or quite similar to RP1 (see Table 1), and which has been proposed as a canonical GRB2-binding site. Moreover, GRB2 nSH3 has been generally appreciated as the main SOS1 binding module and the cSH3 may increase the overall stability of this protein complex. GRB2-SOS1 interaction has been very recently proposed to induce a closed conformation in nSH3 while the cSH3 conformation remains unchanged (*321*). McDonald et al. have proposed the formation of SOS1-GRB2-GAB1 complex (*108, 110*). Accordingly, SOS1 binding to nSH3 induces a conformational change in GRB2 allowing GAB1 to access the cSH3 domain in a non-competitive manner. This means that the association of one molecule GRB2 with its upstream ligands, *e.g.*, HER2 or LAT leads to activation of two distinct pathways, namely PI3K and MAPK pathways (*110, 300-302*).

In an NMR structural study, Yuzawa et al. have shown that GRB2 exists in multiple conformations in which two SH3 domains take different positions and orientations relative to the central SH2

domain (*322*). Figure 6b shows the randomly selected conformation of GRB2 with the tendency to form an inter-SH3 domain interaction, which is proposed in this study to be a prerequisite for SOS1 interaction. Disrupting the nSH3-cSH3 interaction by substitution of the interface residues (n3allo, c3allo or both) completely abolished their SOS1 binding capability. Moreover, there is reciprocal functional interdependence between SH3 domains that is required for SOS1 binding (Fig. 6b, 3ii). Substitution of one of the conserved tryptophan residues of the binding sites (W36K and W193K) has not only abolished own SOS1 binding activity but unexpectedly also SOS1 binding by WT SH3 domain.

Sehti et al. have calculated the intramolecular equilibrium constants for the interaction of GRB2 with SOS1 and determined a K_d value of 0.4 μM for GRB2-SOS1 complex with a stoichiometry of 1:1 (*323*). Liao et al. have very recently proposed two PRMs in SOS1 PRD, corresponding to P3 and P10 (Fig. 3a), as binding sites for GBR2 nSH3 and cSH3 domains, respectively (*305*). They have also considered but not favored P4 and P3 by reason of restricted structural flexibility as compared to the distance between P3 and P10 (Fig. 6c, 1-3). We found only P3, P4, and P5 peptides interacting with GRB2 SH3 domains confirming only partially this proposed model. We agree that GRB2-SOS1 interaction involves the successive binding of both SH3 domains and that GRB2 binding to one site may enhances its binding to the other. However, we think that the process of protein-protein interaction and complex formation correlates with the restricted/reduced structural flexibility, which is rather facilitated by adjacent or even tandem binding sites, such as P3-P5 or P3-P4 (Fig. 6c, 4-6). In this context, Vidal et al have demonstrated that the interaction of RP1 with GRB2 can be increased by 360- and 60-fold when RP1 covalently linked to identical RP1 (a double RP1) or to the different peptide (actually to PESPPLLPPR, the central part of P5; see Fig. 3a) was used (*324*). Similarly, Yuzawa et al. have shown that generated tandem peptides, consisting of RP1-RHY peptide with varying number of linker residues, exhibited much higher affinities, with K_d values between 0.01 and 0.5 μM, for $GRB2^{FL}$ as compared to single peptides (*322*). Accordingly, it has been suggested that GRB2 changes the relative position and orientation of the SH3 domains to enable efficient bivalent binding to non-continuous binding sites, and that binding affinity depends on the length of the linker between PRMs. We, thus, propose that GBR2 undergoes a stepwise, cooperative binding with SOS1, such as P3-P4 (Fig. 6c, 6).

Most multidomain proteins have at least some degree of segmental mobility facilitated by the flexibility of the interdomain linkers. This allows conformational changes that in some instances can be brought about by concerted domain movement from one distinct arrangement to another. The orientation of the globular domains in an SH3-SH2 or SH2-SH3 tandem may allow the formation of a compact rearrangement between them. Nussinov and colleagues have proposed that linker sequences and lengths are optimized in the course of evolution for efficiency of protein functions (*325*). They further argue that allosteric propagation of the energy that is generated by such perturbation events *via* flexible linkers can lead not only to conformational changes of a second binding site in another domain but also to a relatively large, allosterically driven reorientation of protein domains with respect to each other. A number of studies have shown that linker segments between SH3 and SH2 domains in various proteins, including ABL (*326*), CRK (*327*), FAK (*328*), LCK (*329*), NCK (*330*), and PLCγ (*331*), modulate the binding of these domains to their targets and thus regulating corresponding cellular processes. Accordingly, the present

study adds GRB2 to this list of proteins, whose domain arrangements and interaction dynamics are controlled, among others, by the flexibility of the linker segments. Our data revealed that truncation of one of the linkers or both affects GRB2 interaction with SOS1 most probably due to limited interdomain flexibility. An inspection of GRB2 structures (*322, 332*), revealed that both cSH3 and the very C-terminal NRNV motif are located in close proximity of linker 2, and may form stable intramolecular hydrogen bonds. GRB2 SUMOylation by SUMO1 at K56, which is located in the first linker segment, has been shown to result in an increase in the formation of the GRB2-SOS1 complex, sequentially in the activation of Ras/MEK/MAPK pathway (*333*). So, the linkers are not only flexible but are allosterically regulated. (*325*).

The crystal structure of $GRB2^{FL}$, determined by Maignan et al. (*332*), has revealed that it exists as a homodimer with accessible binding sites for both SH2 and SH3 domains. Ladbury and coworkers have found that monomer-dimer equilibrium determines its function in cells (*334*). Accordingly, the monomeric GRB2, the active form, associates with SOS1 whereas dimeric GRB2 represents its inactive inhibitory form. It has been suggested that dissociation of the dimer is facilitated by either phosphorylation of Y160 or through the binding of a tyrosylphosphate-containing ligands (*334*). Liao et al. have also proposed recently that the autoinhibited GRB2 dimer undergoes a conformational change, upon binding of its SH2 domain to a pYP, that releases the flanking SH3 domain for binding and recruiting SOS1 to the plasma membrane (*305*). Two assumptions are implied in this study (Fig. 6d, 1): (1) the autoinhibited GRB2 is disabled in binding PRM-containing ligands, including SOS1; (2) GRB2-SOS1 complex forms upon stimulation of cells by growth factor and the association of GRB2 with tyrosylphosphate-containing ligands.

The prevailing paradigm, however, suggests that SOS1 undergoes a stable interaction with GRB2 and resides in the cytoplasm and translocates to the plasma membrane upon stimulation (Fig. 6d, 2) (*335-341*). Chook et al. have shown that the GRB2-mSOS1 complex, co-purified from insect cells, forms a molar ratio of 1:1 and binds pY peptides with higher affinity than GRB2 alone, suggesting that the proximity of SOS1 to GRB2 facilitates the interaction of the GRB2 SH2 domain with the activated tyrosyl phosphorylated ligands (*342*). Welham et al. have yet reported that they did not detect GRB2 and SOS1 translocation to the plasma membrane upon cell stimulation by the different growth factors, including EGF (*343*). This raises the possibility of additional, yet unknown mechanisms by which GRB2 and SOS1 form a complex that ultimately results in SOS1 activation at the plasma membrane.

Whilst allosteric effects in SH3 domains have been previously explored to investigate the structural communication between contiguous domains in complex multidomain proteins (*314*), there is a lack of information regarding the interdomain allosteric crosstalk within the GRB2 molecule. Groves and coworkers have proposed an allosteric mechanism in which the binding affinity of LAT-GRB2 depends on the phosphorylation at remote tyrosine sites (*344*). As discussed above, it is still a matter of debate whether GRB2 association with its upstream pY molecules, such as HER2 or LAT, brings SOS1 `piggyback´ to the plasma membrane, where it binds and activates membrane-associated RAS. In another study, Groves and coworkers have demonstrated that the SOS1 catalytic RASGEF domain is inhibited by the PRD (*345*) suggesting

that GRB2 binding to the PRD may induce SOS1 activation. This autoinhibitory role of the PRD limits GRB2-independent recruitment of SOS to the membrane through binding of RAS•GTP in the SOS1 allosteric binding site (*346, 347*). Spatiotemporal specificity is further conferred by multiple intermolecular interactions on the membrane such as with lipids and GRB2 that bind to the N- and C-terminal domains, respectively (*53, 345*).

Taken together, three scenarios for GRB2-mediated SOS1 translocation to the plasma membrane can be postulated under growth factor-stimulated conditions (Fig. 6d): (1) A dimer-monomer equilibrium of GRB2 results in the SH2 association first with the tyrosylphosphate-containing ligands, and then upon a conformational change with the membrane phospholipids via surface cationic patches separate from pY-binding pockets (*348*), and ultimately with SOS1 PRD. (2) A cytoplasmic bivalent GRB2-SOS complex binds to its activated ligands (pYP and phospholipids), and thereby recruits SOS1 to the plasma membrane-associated RAS. This model may represent simple recruitment of cytoplasmic SOS1 to the plasma membrane. (3) A cytoplasmic monovalent GRB2-SOS complex binds to its activated ligands (pYP and phospholipids), which in turn allosterically induces a structural rearrangement and the release of a second SH3 domain of GRB2, its interaction with a second binding site on SOS1 PRD, and ultimately SOS1 activation. In this model, SOS1 recruitment to the plasma membrane is accompanied by the release for its autoinhibition.

Materials and Methods

Peptides. Peptides used in this study are listed in Table S1.

Constructs. Constructs used in this study are listed in Table S2.

Proteins. All proteins used in this study are listed in Table S2.

All methods are described in Supplementary information.

Acknowledgements

We are grateful to our colleagues from the Institute of Biochemistry and Molecular Biology II of the Medical Faculty of the Heinrich-Heine University Düsseldorf for their support, helpful advices, and stimulating discussions. This study was supported by the German Federal Ministry of Education and Research (BMBF) – German Network of RASopathy Research (GeNeRARe01GM1902C), the European Network on Noonan Syndrome and Related Disorders (NSEuroNet01GM1621B), and the Netherlands Organization for Scientific Research (NWO) through Gravity Program 024.001.035.

Author Contributions

MRA conceived and coordinated the study. NSKJ, MRA designed the study, wrote the manuscript, designed, performed and analyzed the experiments. LB and EME designed and synthesized the peptides. All authors reviewed the results and approved the final version of the manuscript.

Additional information

Supplementary Information accompanies this paper

Competing financial interests: The authors declare no competing financial interests.

References:

1. L. Laursen, J. Kliche, S. Gianni, P. Jemth, Supertertiary protein structure affects an allosteric network. *bioRxiv*, (2020).
2. G. Stock, P. Hamm, A non-equilibrium approach to allosteric communication. *Philosophical Transactions of the Royal Society B: Biological Sciences* **373**, 20170187 (2018).
3. K. Gunasekaran, B. Ma, R. Nussinov, Is allostery an intrinsic property of all dynamic proteins? *Proteins: Structure, Function, and Bioinformatics* **57**, 433-443 (2004).
4. K. Neumann, T. Oellerich, H. Urlaub, J. Wienands, The B-lymphoid Grb2 interaction code. *Immunological reviews* **232**, 135-149 (2009).
5. A. Giubellino, T. R. Burke, D. P. Bottaro, Grb2 signaling in cell motility and cancer. *Expert opinion on therapeutic targets* **12**, 1021-1033 (2008).
6. C. B. McDonald, K. L. Seldeen, B. J. Deegan, V. Bhat, A. Farooq, Assembly of the Sos1–Grb2–Gab1 ternary signaling complex is under allosteric control. *Archives of biochemistry and biophysics* **494**, 216-225 (2010).
7. E. Lowenstein *et al.*, The SH2 and SH3 domain-containing protein GRB2 links receptor tyrosine kinases to ras signaling. *Cell* **70**, 431-442 (1992).
8. P. G. Dharmawardana, B. Peruzzi, A. Giubellino, T. R. Burke Jr, D. P. Bottaro, Molecular targeting of growth factor receptor-bound 2 (Grb2) as an anti-cancer strategy. *Anti-cancer drugs* **17**, 13-20 (2006).
9. J. A. Simon, S. L. Schreiber, Grb2 SH3 binding to peptides from Sos: evaluation of a general model for SH3-ligand interactions. *Chemistry & biology* **2**, 53-60 (1995).
10. B. J. Mayer, D. Baltimore, Signalling through SH2 and SH3 domains. *Trends in cell biology* **3**, 8-13 (1993).
11. T. Pawson, J. Schlessingert, SH2 and SH3 domains. *Current Biology* **3**, 434-442 (1993).
12. A. Nimnual, D. Bar-Sagi, The two hats of SOS. *Science Signaling* **2002**, pe36-pe36 (2002).
13. J. Schlessinger, M. A. Lemmon, SH2 and PTB domains in tyrosine kinase signaling. *Sci. STKE* **2003**, re12-re12 (2003).
14. N. Bisson *et al.*, Selected reaction monitoring mass spectrometry reveals the dynamics of signaling through the GRB2 adaptor. *Nature biotechnology* **29**, 653-658 (2011).
15. Z. Ahmed *et al.*, Grb2 monomer–dimer equilibrium determines normal versus oncogenic function. *Nature communications* **6**, 1-11 (2015).
16. S. Zhou *et al.*, SH2 domains recognize specific phosphopeptide sequences. *Cell* **72**, 767-778 (1993).
17. M. J. Robinson, M. H. Cobb, Mitogen-activated protein kinase pathways. *Current opinion in cell biology* **9**, 180-186 (1997).
18. G. W. Reuther, C. J. Der, The Ras branch of small GTPases: Ras family members don't fall far from the tree. *Current opinion in cell biology* **12**, 157-165 (2000).
19. C. B. McDonald *et al.*, Allostery mediates ligand binding to Grb2 adaptor in a mutually exclusive manner. *Journal of molecular recognition* **26**, 92-103 (2013).
20. A. Montagner *et al.*, A novel role for Gab1 and SHP2 in epidermal growth factor-induced Ras activation. *Journal of Biological Chemistry* **280**, 5350-5360 (2005).
21. A. M. Tari, G. Lopez-Berestein, in *Seminars in oncology*. (Elsevier, 2001), vol. 28, pp. 142-147.
22. N. a. Li *et al.*, Guanine-nucleotide-releasing factor hSos1 binds to Grb2 and links receptor tyrosine kinases to Ras signalling. *Nature* **363**, 85-88 (1993).
23. T.-J. Liao, H. Jang, R. Nussinov, D. Fushman, High-affinity Interactions of the nSH3/cSH3 Domains of Grb2 with the C-terminal Proline-rich Domain of SOS1. *Journal of the American Chemical Society* **142**, 3401-3411 (2020).

24. C. B. McDonald, K. L. Seldeen, B. J. Deegan, A. Farooq, Structural basis of the differential binding of the SH3 domains of Grb2 adaptor to the guanine nucleotide exchange factor Sos1. *Archives of biochemistry and biophysics* **479**, 52-62 (2008).
25. C. B. McDonald, K. L. Seldeen, B. J. Deegan, A. Farooq, SH3 domains of Grb2 adaptor bind to PXψPXR motifs within the Sos1 nucleotide exchange factor in a discriminate manner. *Biochemistry* **48**, 4074-4085 (2009).
26. T.-J. Liao, H. Jang, R. Nussinov, D. Fushman, High-affinity Interactions of the nSH3/cSH3 Domains of Grb2 with the C-terminal Proline-rich Domain of SOS1. *Journal of the American Chemical Society*, (2020).
27. C. B. McDonald *et al.*, Structural landscape of the proline-rich domain of Sos1 nucleotide exchange factor. *Biophysical chemistry* **175**, 54-62 (2013).
28. D. Cussac, M. Frech, P. Chardin, Binding of the Grb2 SH2 domain to phosphotyrosine motifs does not change the affinity of its SH3 domains for Sos proline-rich motifs. *The EMBO Journal* **13**, 4011-4021 (1994).
29. M. Tanaka, R. Gupta, B. J. Mayer, Differential inhibition of signaling pathways by dominant-negative SH2/SH3 adapter proteins. *Molecular and cellular biology* **15**, 6829-6837 (1995).
30. A. Beigbeder, F. J. Chartier, N. Bisson, MPZL1 forms a signalling complex with GRB2 adaptor and PTPN11 phosphatase in HER2-positive breast cancer cells. *Scientific reports* **7**, 1-9 (2017).
31. T. Watanabe *et al.*, Significance of the Grb2 and son of sevenless (Sos) proteins in human bladder cancer cell lines. *IUBMB life* **49**, 317-320 (2000).
32. F. Malagrinò, F. Troilo, D. Bonetti, A. Toto, S. Gianni, Mapping the allosteric network within a SH3 domain. *Scientific reports* **9**, 1-6 (2019).
33. S. E. Egan *et al.*, Association of Sos Ras exchange protein with Grb2 is implicated in tyrosine kinase signal transduction and transformation. *Nature* **363**, 45-51 (1993).
34. M. A. Lemmon, J. E. Ladbury, V. Mandiyan, M. Zhou, J. Schlessinger, Independent binding of peptide ligands to the SH2 and SH3 domains of Grb2. *Journal of Biological Chemistry* **269**, 31653-31658 (1994).
35. J. C. Houtman *et al.*, Oligomerization of signaling complexes by the multipoint binding of GRB2 to both LAT and SOS1. *Nature structural & molecular biology* **13**, 798-805 (2006).
36. R. R. Bartelt *et al.*, Regions outside of conserved PxxPxR motifs drive the high affinity interaction of GRB2 with SH3 domain ligands. *Biochimica et Biophysica Acta (BBA)-Molecular Cell Research* **1853**, 2560-2569 (2015).
37. L. Sastry *et al.*, Quantitative analysis of Grb2-Sos1 interaction: the N-terminal SH3 domain of Grb2 mediates affinity. *Oncogene* **11**, 1107-1112 (1995).
38. M. Innocenti *et al.*, Mechanisms through which Sos-1 coordinates the activation of Ras and Rac. *Journal of Cell Biology* **156**, 125-136 (2002).
39. T.-J. Liao, H. Jang, D. Fushman, R. Nussinov, SOS1 interacts with Grb2 through regions that induce closed nSH3 conformations. *The Journal of Chemical Physics* **153**, 045106 (2020).
40. S. Yuzawa *et al.*, Solution structure of Grb2 reveals extensive flexibility necessary for target recognition. *Journal of molecular biology* **306**, 527-537 (2001).
41. A. Sethi, B. Goldstein, S. Gnanakaran, Quantifying intramolecular binding in multivalent interactions: a structure-based synergistic study on Grb2-Sos1 complex. *PLoS Comput. Biol.* **7**, e1002192 (2011).
42. M. Vidal *et al.*, Design of peptoid analogue dimers and measure of their affinity for Grb2 SH3 domains. *Biochemistry* **43**, 7336-7344 (2004).
43. B. Ma, C.-J. Tsai, T. Haliloğlu, R. Nussinov, Dynamic allostery: linkers are not merely flexible. *Structure* **19**, 907-917 (2011).

44. C. Corbi-Verge *et al.*, Two-state dynamics of the SH3–SH2 tandem of Abl kinase and the allosteric role of the N-cap. *Proceedings of the National Academy of Sciences* **110**, E3372-E3380 (2013).
45. Y. Kobashigawa *et al.*, Structural basis for the transforming activity of human cancer-related signaling adaptor protein CRK. *Nature structural & molecular biology* **14**, 503-510 (2007).
46. H. E. Lindfors, B. S. Venkata, J. W. Drijfhout, M. Ubbink, Linker length dependent binding of a focal adhesion kinase derived peptide to the Src SH3–SH2 domains. *FEBS letters* **585**, 601-605 (2011).
47. H. Meiselbach, H. Sticht, Effect of the SH3-SH2 domain linker sequence on the structure of Hck kinase. *Journal of molecular modeling* **17**, 1927-1934 (2011).
48. S. Banjade *et al.*, Conserved interdomain linker promotes phase separation of the multivalent adaptor protein Nck. *Proceedings of the National Academy of Sciences* **112**, E6426-E6435 (2015).
49. T. D. Bunney *et al.*, Structural and functional integration of the PLCγ interaction domains critical for regulatory mechanisms and signaling deregulation. *Structure* **20**, 2062-2075 (2012).
50. S. Maignan *et al.*, Crystal structure of the mammalian Grb2 adaptor. *Science* **268**, 291-293 (1995).
51. Y. Qu *et al.*, SUMOylation of Grb2 enhances the ERK activity by increasing its binding with Sos1. *Molecular cancer* **13**, 1-12 (2014).
52. Z. Ahmed *et al.*, Corrigendum: Grb2 monomer–dimer equilibrium determines normal versus oncogenic function. *Nature communications* **6**, (2015).
53. A. Nag, M. Monine, A. S. Perelson, B. Goldstein, Modeling and simulation of aggregation of membrane protein LAT with molecular variability in the number of binding sites for cytosolic Grb2-SOS1-Grb2. *PLoS One* **7**, e28758 (2012).
54. L. M. Luttrell *et al.*, G-protein-coupled receptors and their regulation: activation of the MAP kinase signaling pathway by G-protein-coupled receptors. *Advances in second messenger and phosphoprotein research* **31**, 263 (1997).
55. C. T. Baldari, J. L. Telford, Lymphocyte antigen receptor signal integration and regulation by the SHC adaptor. *Biological chemistry* **380**, 129-134 (1999).
56. A. Maffe, P. Comoglio, HGF controls branched morphogenesis in tubular glands. *European journal of morphology* **36**, 74-81 (1998).
57. R. Pai, A. Tarnawski, Signal transduction cascades triggered by EGF receptor activation: relevance to gastric injury repair and ulcer healing. *Digestive diseases and sciences* **43**, 14S-22S (1998).
58. K. L. Carraway, C. A. C. Carraway, Signaling, mitogenesis and the cytoskeleton: where the action is. *Bioessays* **17**, 171-175 (1995).
59. B. Margolis, E. Y. Skolnik, Activation of Ras by receptor tyrosine kinases. *Journal of the American Society of Nephrology* **5**, 1288-1299 (1994).
60. Y. M. Chook, G. D. Gish, C. M. Kay, E. F. Pai, T. Pawson, The Grb2-mSos1 complex binds phosphopeptides with higher affinity than Grb2. *Journal of Biological Chemistry* **271**, 30472-30478 (1996).
61. M. J. Welham, V. Duronio, K. B. Leslie, D. Bowtell, J. W. Schrader, Multiple hemopoietins, with the exception of interleukin-4, induce modification of Shc and mSos1, but not their translocation. *Journal of Biological Chemistry* **269**, 21165-21176 (1994).
62. W. Y. Huang, J. A. Ditlev, H.-K. Chiang, M. K. Rosen, J. T. Groves, Allosteric modulation of Grb2 recruitment to the intrinsically disordered scaffold protein, LAT, by remote site phosphorylation. *Journal of the American Chemical Society* **139**, 18009-18015 (2017).
63. Y. K. Lee *et al.*, Mechanism of SOS PR-domain autoinhibition revealed by single-molecule assays on native protein from lysate. *Nature communications* **8**, 1-11 (2017).

64. J. Gureasko *et al.*, Membrane-dependent signal integration by the Ras activator Son of sevenless. *Nature structural & molecular biology* **15**, 452 (2008).
65. L. Iversen *et al.*, Ras activation by SOS: Allosteric regulation by altered fluctuation dynamics. *Science* **345**, 50-54 (2014).
66. G. M. Findlay *et al.*, Interaction domains of Sos1/Grb2 are finely tuned for cooperative control of embryonic stem cell fate. *Cell* **152**, 1008-1020 (2013).
67. M.-J. Park *et al.*, SH2 domains serve as lipid-binding modules for pTyr-signaling proteins. *Molecular cell* **62**, 7-20 (2016).
68. E. Amin *et al.*, Deciphering the molecular and functional Basis of RHOGAP family proteins A systematic approach toward selective inactivation of rho family proteINS. *Journal of Biological Chemistry* **291**, 20353-20371 (2016).
69. K. Nouri *et al.*, IQGAP1 interaction with RHO family proteins revisited kinetic and equilibrium evidence for multiple distinct binding sites. *Journal of Biological Chemistry* **291**, 26364-26376 (2016).
70. T. Wiseman, S. Williston, J. F. Brandts, L.-N. Lin, Rapid measurement of binding constants and heats of binding using a new titration calorimeter. *Analytical biochemistry* **179**, 131-137 (1989).
71. M. G. Rudolph *et al.*, Thermodynamics of Ras/effector and Cdc42/effector interactions probed by isothermal titration calorimetry. *Journal of Biological Chemistry* **276**, 23914-23921 (2001).
72. N. N. Fang *et al.*, Rsp5/Nedd4 is the main ubiquitin ligase that targets cytosolic misfolded proteins following heat stress. *Nature cell biology* **16**, 1227-1237 (2014).
73. L. Peil *et al.*, Distinct XPPX sequence motifs induce ribosome stalling, which is rescued by the translation elongation factor EF-P. *Proceedings of the National Academy of Sciences* **110**, 15265-15270 (2013).
74. T. R. Hupp, M. Walkinshaw, Multienzyme assembly of a p53 transcription complex. *Nature structural & molecular biology* **14**, 885-887 (2007).
75. D. Dornan, H. Shimizu, L. Burch, A. J. Smith, T. R. Hupp, The proline repeat domain of p53 binds directly to the transcriptional coactivator p300 and allosterically controls DNA-dependent acetylation of p53. *Molecular and cellular biology* **23**, 8846-8861 (2003).
76. L. Guruprasad *et al.*, The crystal structure of the N-terminal SH3 domain of Grb2. *Journal of molecular biology* **248**, 856-866 (1995).
77. O. Aitio *et al.*, Structural basis of PxxDY motif recognition in SH3 binding. *Journal of molecular biology* **382**, 167-178 (2008).
78. H. Yu *et al.*, Structural basis for the binding of proline-rich peptides to SH3 domains. *Cell* **76**, 933-945 (1994).
79. S.-H. Tan, W. Hugo, W.-K. Sung, S.-K. Ng, A correlated motif approach for finding short linear motifs from protein interaction networks. *BMC bioinformatics* **7**, 502 (2006).
80. K. Rader, R. A. Orlando, X. Lou, M. G. Farquhar, Characterization of ANKRA, a novel ankyrin repeat protein that interacts with the cytoplasmic domain of megalin. *Journal of the American Society of Nephrology* **11**, 2167-2178 (2000).
81. R. P. Menon, R. C. Hughes, Determinants in the N-terminal domains of galectin-3 for secretion by a novel pathway circumventing the endoplasmic reticulum–Golgi complex. *European journal of biochemistry* **264**, 569-576 (1999).
82. P. Beltrao, L. Serrano, Comparative genomics and disorder prediction identify biologically relevant SH3 protein interactions. *PLoS computational biology* **1**, (2005).
83. K. Kowanetz *et al.*, CIN85 associates with multiple effectors controlling intracellular trafficking of epidermal growth factor receptors. *Molecular biology of the cell* **15**, 3155-3166 (2004).

84. A. D'erchia, G. Pesole, A. Tullo, C. Saccone, E. Sbisa, Guinea pig p53 mRNA: identification of new elements in coding and untranslated regions and their functional and evolutionary implications. *Genomics* **58**, 50-64 (1999).

Figure legends

Figure 1 | GRB2 structure highlights different regions, sites, and motifs investigated in this study. The upper panels represent the GRB2 structure (PDB code: 1GRI) from the front (left) and back side (right). The lower panels represent an open-book view of the two SH3 domains with the six interfacing residues. The SH2 domain (cyan) in complex with HER2 pYP peptide (magenta) links via linkers 1 (black pellets), and 2 (grey pellets) the flanking nSH2 (yellow), cSH3 (green), and the very C-terminal NRNV motif (brown). The SH3 domains are in complex with SOS1 RP1 peptide (blue). Different sites, relevant for this study, are the two tryptophans W36 in nSH3 and W193 in cSH3 (both in orange) at the SH3-RP1 interface, the two triplets, PHP from linker 1 and EQV from linker 2 (both in red), and the six residues in the nSH3-cSH3 interface.

Figure 2 | Inactivating mutation in one of the GRB2 SH3 domains also impairs SOS1 PRD interaction of the other SH3 domain. Purified SOS1 PRD was almost equally pulled down by GST fusion proteins of GRB2 FL, nSH3, and cSH3 but not by their mutants W36/W193, W36, and W193, respectively, or GST alone (negative control) and mmunoblotted with a polyclonal anti-SOS1 antibody (lower panel, output). Only single-point mutants of GRB2, either in nSH3 (W36K) or cSH3 (W193K) showed very weak binding to SOS1 PRD. The bottom panel (input) shows that equal amounts of SOS1 PRD proteins were used. Upper panel shows quantification of GRB2-PRD interaction (mean±s.e.m.; n = 3); ***, $p < 0.0001$(Student's t-test).

Figure 3 | The GRB2 binding properties for SOS1 PRMs. (**a**) The C-terminal PRD of SOS1 contains several PRMs, ten of which were investigated in this study, designated as peptide P1 to P10. As control was used the reference peptides RP1, a derivative of SOS1, and part of P1, and RP2, a derivative of the RHO GTPase WRCH1. Note that RP1 is part of P3. (**b**) GRB2 selectively interacts with three out of ten PRMs of SOS1. Dot-blot analysis of fluorescent SOS1 PRMs pulled down with GST-GRB2 proteins revealed high binding selectivity especially for GRB2 cSH3. (**c**) SOS1 P3 revealed the highest binding affinity for cSH3. Evaluated dissociation constants (K_d) of fluorescence polarization measurements for the SOS1 PRM-GRB2 interactions (Fig. S2A) are shown as bar. The colors of the bar charts highlight the K_d values (above the bars) for the SH3-PRM interaction, which are divided into high affinity (1 – 5 μM; green), intermediate affinity (6 – 20 μM; blue), and low affinity (>21 μM; red).

Figure 4 | SOS1 peptide binding by GRB2 FL depends on multiple factors. K_d values (in μM) for the interaction of various GRB2 variants with SOS1 RP1 in the presence and absence of HER2 pY peptide were obtained using fluorescence polarization and FITC-labelled peptides(**a-o**). Determined K_d values for the data shown in Figures S3, including the calculated error bars, were divided in high affinity (1 – 5 μM), intermediate affinity (6 – 20μM), and low affinity (21 – 90 μM).

Figure 5 | ITC measurements of the interdomain interactions of GRB2. Evaluated K_d values (**a-o**) for the data shown in Figure S4 were divided in high affinity (1 – 5 μM), intermediate affinity (6 – 20μM), and low affinity (21 – 90 μM) and very low-affinity (91 – >200 μM). The standard deviations for the whole K_d values ranged from 3 to 5%.

Figure 6 | Schematic models of GRB2 association with SOS1 and HER2. (**a**) Color-coded SOS1 PRD peptides P1-P10. (**b**) Selected GRB2 models (*322*), where the relative position and orientation of nSH3 and cSH3 domains are different. nSH3-cSH3-interaction (i) and the PRM interaction capability of the SH3 domains (ii) are likely to be a functional prerequisite. (**c**) The selectivity of GRB2-SOS1 PRD interaction. (**d**) HER2-GRB2-SOS1 complex formation at the plasma membrane (PM). (1) In this scenario, GRB2 exists in an autoinhibited state and does not bind SOS1. Growth factor stimulation induces a sequential interaction of GRB2 with HER2 (i) and PM (ii), which leads to GRB2 monomerization and subsequent binding to and translocation of SOS1 (iii). (2) Cytosolic GRB2-SOS1 complex translocates to phosphorylated HER2, where pYP binding of the SH2 domain (i) induces its association with the PM phospholipids (ii). (3) Another possible scenario, a cytosolic GRB2-SOS1 complex, formed only by one SH3 domain while the other SH3 domain (*e.g.*, cSH3) is blocked intramolecularly. The complex translocates to the membrane upon phosphorylation of HER2. pYP binding of the SH2 domain (i) induces not only the SH2-PM interaction (ii) but additionally induces a conformational change in GRB2 that releases cSH3, and is now able to contact SOS1 PRD at a second site (iii). In this model, HER2-GRB2 association may also confer to SOS1 activation.

Figure 1

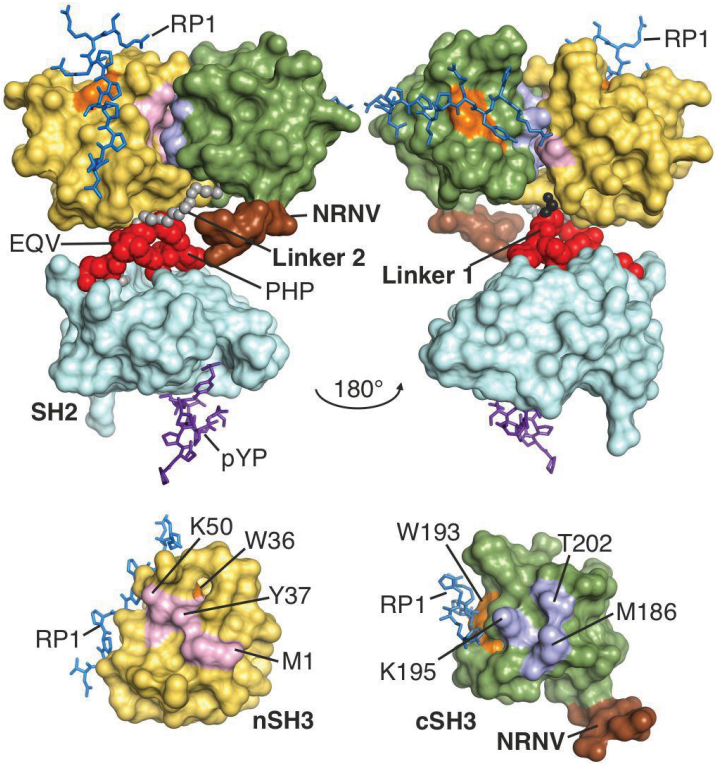

Figure 2

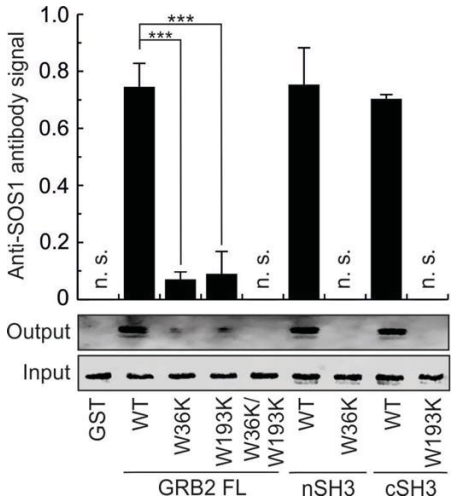

Figure 3

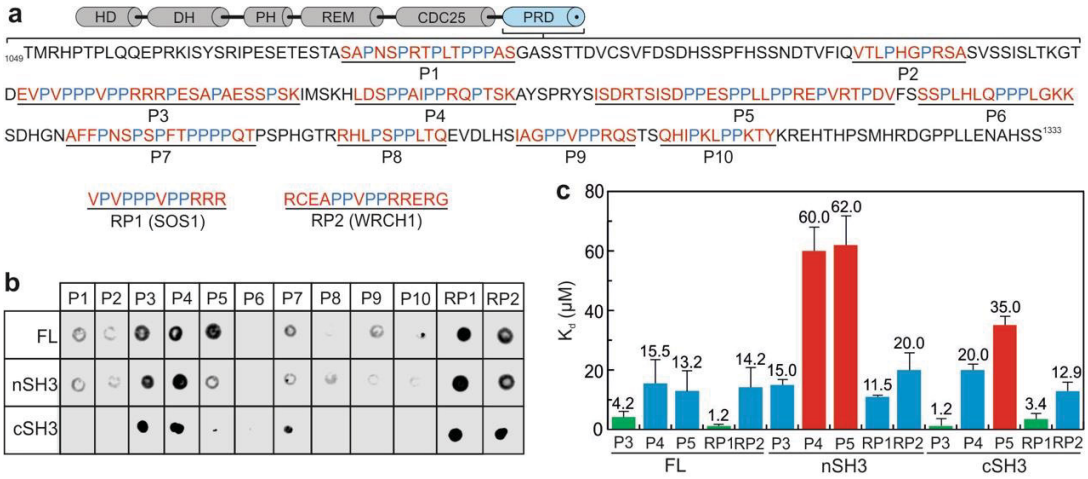

Figure 4

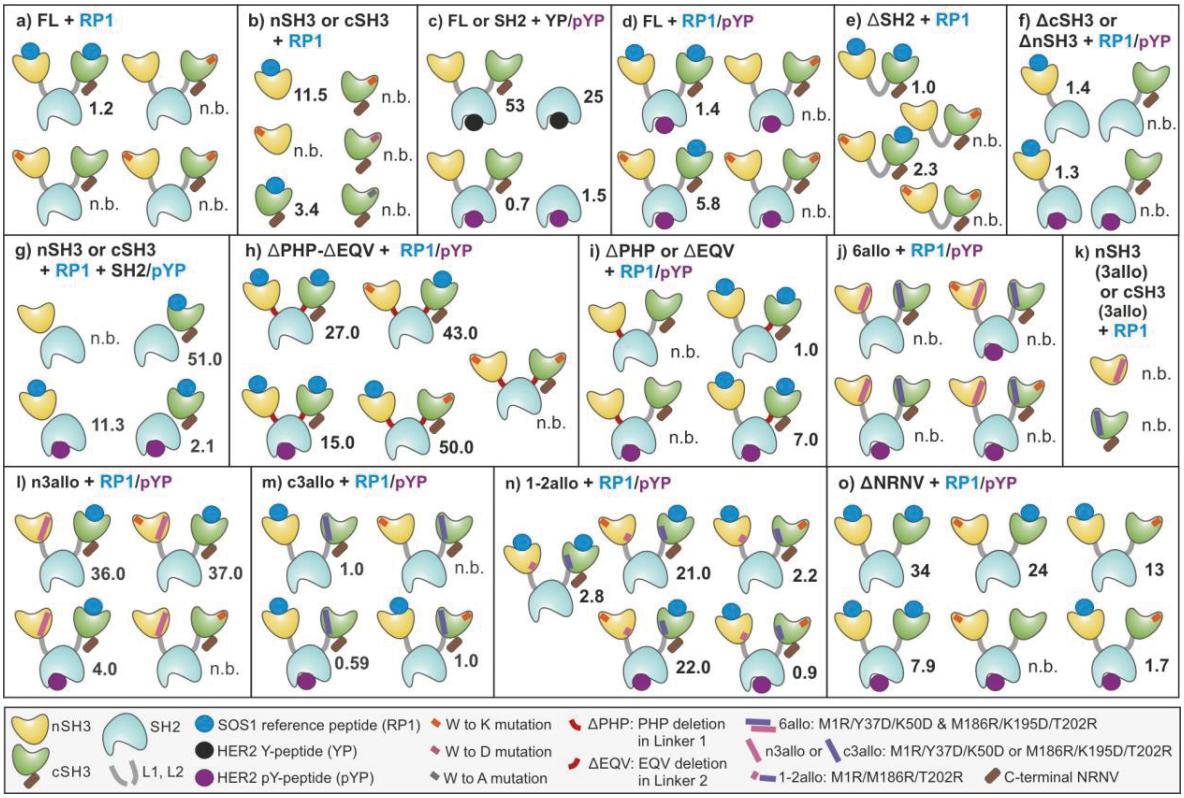
a) FL + RP1
1.2
n.b.
n.b.
n.b.
b) nSH3 or cSH3 + RP1
11.5
n.b.
n.b.
n.b.
3.4
n.b.
c) FL or SH2 + YP/pYP
53
25
0.7
1.5
d) FL + RP1/pYP
1.4
n.b.
5.8
n.b.
e) ΔSH2 + RP1
1.0
n.b.
2.3
n.b.
f) ΔcSH3 or ΔnSH3 + RP1/pYP
1.4
n.b.
1.3
n.b.
g) nSH3 or cSH3 + RP1 + SH2/pYP
n.b.
51.0
11.3
2.1
h) ΔPHP-ΔEQV + RP1/pYP
27.0
43.0
15.0
50.0
n.b.
i) ΔPHP or ΔEQV + RP1/pYP
n.b.
1.0
n.b.
7.0
j) 6allo + RP1/pYP
n.b.
n.b.
n.b.
n.b.
k) nSH3 (3allo) or cSH3 (3allo) + RP1
n.b.
n.b.
l) n3allo + RP1/pYP
36.0
37.0
4.0
n.b.
m) c3allo + RP1/pYP
1.0
n.b.
0.59
1.0
n) 1-2allo + RP1/pYP
2.8
21.0
2.2
22.0
0.9
o) ΔNRNV + RP1/pYP
34
24
13
7.9
n.b.
1.7
nSH3
cSH3
SH2
L1, L2
SOS1 reference peptide (RP1)
HER2 Y-peptide (YP)
HER2 pY-peptide (pYP)
W to K mutation
W to D mutation
W to A mutation
ΔPHP: PHP deletion in Linker 1
ΔEQV: EQV deletion in Linker 2
6allo: M1R/Y37D/K50D & M186R/K195D/T202R
n3allo or c3allo: M1R/Y37D/K50D or M186R/K195D/T202R
1-2allo: M1R/M186R/T202R
C-terminal NRNV

Figure 5

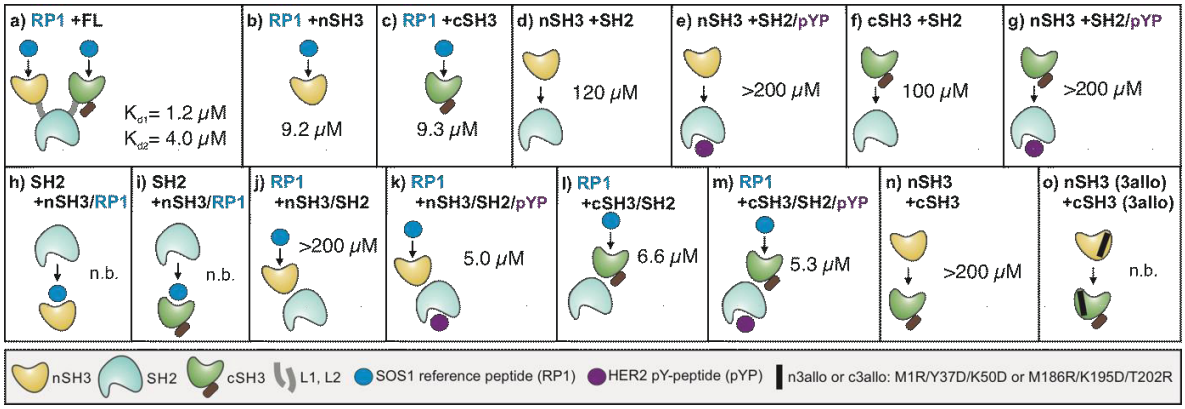

Figure 6

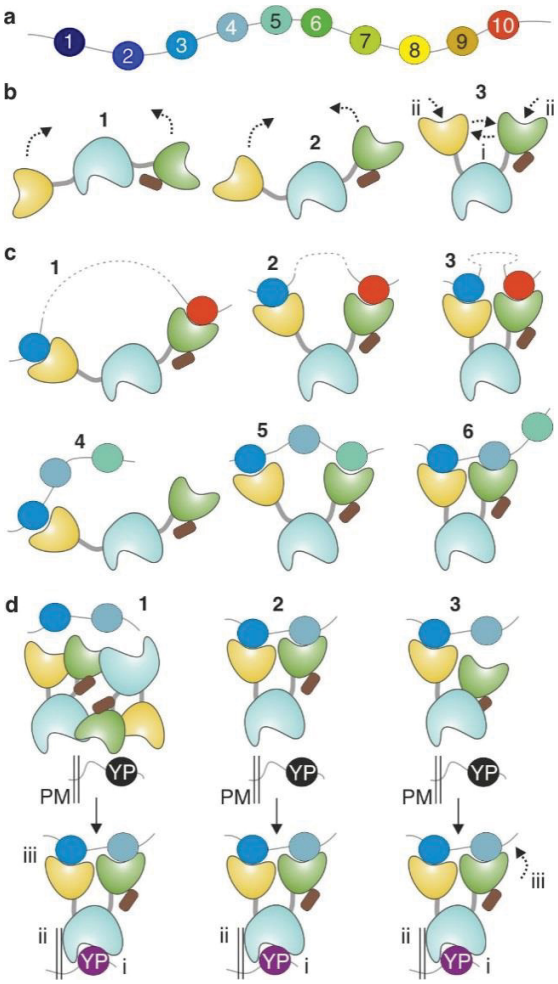

Supplementary Information

The intramolecular allostery of GRB2 governing its interaction with SOS1 is modulated by phosphotyrosine ligand

Neda S. Kazemein Jasemi, Christian Herrmann, Eva Magdalena Estirado, Radovan Dvorsky, Luc Brunsveld, Mohammad R. Ahmadian

Institute of Biochemistry and Molecular Biology II, Medical Faculty of the Heinrich-Heine University, 40225 Düsseldorf, Germany

Supplementary Methods

GST pull-down assay. Pull-down of SOS1 PRD was performed with GST fusion proteins of various GRB2 variants as previously described(*349*). Purified GST was used as a negative control. Briefly, 20 µM GST-GRB2 FL and the respective SH3 domains were incubated with 30 µM SOS1 PRD and GSH Sepharose beads (GE Healthcare, UK), in a buffer, containing 30mM Tris-HCl pH 7.5 pH 7.5, 3 mM Dithiothreitol, 5 mM $MgCl_2$, for 1 h, at 4°C. After 3x washing with the same buffer, the samples were denatured in Laemmli buffer for 10 min, at 95°C, and analyzed by SDS-PAGE and immunoblotting.

Fluorescence dot-blot analysis. Pull-down of 10 µM FITC-labelled peptides with 5 µM GST fusion proteins of various GRB2 variants was performed under the same conditions as described for GST pull-down assay. Purified GST was used as a negative control. After 3x washing, bound proteins were eluted by incubating in the same buffer, additionally containing 2 mM GSH, for 15 min, at 4°C, and the beads separated by centrifugation. Bound FITC-labelled peptides were detected by dot-blot analysis using 1µL eluent at an emission wavelength of 600 nm using Odyssey Fc Imaging System (LI-COR Biosciences). Detected signals were densitometrically quantified using the LI-COR Biosciences Image Studio version 5.2 imaging software.

Fluorescence polarization (FP). The interaction of FITC-labelled peptides (0.2 and 1 µM) with increasing concentration of the SH3 domains (0.2 to 200 µM) was measured by fluorescence polarization using a Fluoromax 4 fluorimeter as described (*189*). Excitation wavelength was 470 nm and emission wavelength 560 nm. The dissociation constants (K_d) were obtained by fitting the concentration dependent binding curve using a quadratic ligand binding equation.

Isothermal titration calorimetry (ITC). The thermodynamic parameters of GRB2-SOS1 and GRB2-GRB2 interactions were determined using an isothermal titration calorimeter (VP-ITC, MicroCal, Inc.) as described (*350*). In all experiments, the GRB2 proteins, including nSH3, cSH3, SH2, and FL, were placed into the sample cell at a concentration of 100 µM. The concentration of the proteins in the syringe was tenfold higher (1 mM) as compared to the protein concentrations in the cell. For data evaluation, the manufacturer's software was used as described (*351*). For all experiments a buffer, containing 50 mM Tris-HCl pH 7.4, 5 mM $MgCl_2$ and 2 mM dithiothreitol was used.

Analytical size-exclusion chromatography. The homogeneity of purified proteins was determined using a Superdex 200 (10/300) column (GE Healthcare), an ÄKTA purifier (GE Healthcare), and a buffer, containing 30mM Tris-HCl pH 7.5, 3 mM Dithiothreitol, 5 mM $MgCl_2$, in the presence and absence of 15 mM NaCl. The flow rate was sustained at 0.5 ml/min. The column was calibrated with a set of molecular weight protein standards (GE healthcare), comprising

aldolase (158 kDa), conalbumin (75 kDa), ovalbumin (44 kDa), Carbonic anhydrase (29 kDa) and RNase A (13.7 kDa). Fractions were collected at a volume of 0.5 ml and then peak fractions were visualized by 12.5% SDS-PAGE gel and staining using coomassie brilliant blue.

Table S1 | Peptides used in this study.

Source	Peptide[a]	Peptide sequence and position[d]
SOS1	**P1**	^{1078}SA**P**NS**P**RT**P**LT**PPP**AS^{1093}
	P2	^{1124}VTL**P**HG**P**RSA^{1133}
	P3	^{1146}E**V**P**V**P**PP**V**PP**RRR**P**ESA**P**AESS**P**SKI^{1171}
	P4	^{1176}LDS**PP**AI**PP**RQ**P**TSK^{1190}
	P5	^{1204}ISD**PP**ES**PP**LL**PP**RE**P**VRT**P**DV^{1225}
	P6	^{1227}SSS**P**LHLQ**PPP**LGKK^{1241}
	P7	^{1247}AFF**P**NS**P**S**P**FT**PPPP**QT**P**SPHGT^{1269}
	P8	^{1271}RHL**P**S**PP**LTQ^{1280}
	P9	^{1287}IAG**PP**V**PP**RQS^{1297}
	P10	^{1300}QHI**P**KL**PP**KTY^{1310}
HER2	**HER2 YP[b]**	^{1133}CSPQPE**Y**VNQPDV^{1145}
	HER2 pYP[b]	^{1133}CSPQPE**pY**VNQPDV^{1145}
Reference (SOS1)	**RP1[c]**	^{1147}VPV**PPP**V**PP**RRR^{1158}
Reference (WRCH1)	**RP2**	^{13}RCEA**PP**V**PP**RRERG^{26}

[a]All peptides were synthesized with and without fluorescein isothiocyanate (FITC) label using standard Fmoc solid-phase peptide synthesis (SPPS), by means of an automated peptide synthesizer (Intavis MultiPep Rsi) analogous to as described (Stevers *et al.* (2018) J Am Chem Soc. 140:14498-14510).

[b]These peptides were purchased from GenScript (Piscataway, USA).

[c]Reference peptide 1 (RP1) is derived from P3 (underlined).

[d]Peptides were selected according to all known proline-rich consensus sequence motifs and their incidence found in SOS1 PRD (see Table S4).

Table S2. | Constructs and proteins used in this study

Protein[a]	Nomenclature[b]	Construct/proteins[c]
SOS1	$SOS1^{PRD}$	aa 1049-1333
GRB2	$GRB2^{FL}$	aa 1-217
	$GRB2^{W36K}$	aa 1-217, W36K
	$GRB2^{W193K}$	aa 1-217, W193K
	$GRB2^{W193D}$	aa 1-217, W193D
	$GRB2^{W193A}$	aa 1-217, W193A
	$GRB2^{W36K/W193K}$	aa 1-217, W36K/W193K
	$GRB2^{6allo}$	aa 1-217, M1R/Y37D/K50D/M186R/K195D/T202D
	$GRB2^{6allo/W36K}$	aa 1-217, M1R/Y37D/K50D/M186R/K195D/T202D/W36K
	$GRB2^{6allo/W193K}$	aa 1-217, M1R/Y37D/K50D/M186R/K195D/T202D/W193K
	$GRB2^{n3allo}$	aa 1-217, M1R/Y37D/K50D
	$GRB2^{n3allo/W36K}$	aa 1-217, M1R/Y37D/K50D, W36K
	$GRB2^{n3allo/W193K}$	aa 1-217, M1R/Y37D/K50D, W193K
	$GRB2^{c3allo}$	aa 1-217, M186R/K195D/T202D
	$GRB2^{c3allo/W36K}$	aa 1-217, M186R/K195D/T202D, W36K
	$GRB2^{c3allo/W193K}$	aa 1-217, M186R/K195D/T202D, W193K
	$GRB2^{1\text{-}2allo}$	aa 1-217, M1R/M186R/T202R
	$GRB2^{1\text{-}2allo/W36K}$	aa 1-217, M1R/M186R/T202R, W36K
	$GRB2^{1\text{-}2allo/W193K}$	aa 1-217, M1R/M186R/T202R, W193K
	$GRB2^{\Delta PHP/\Delta EQV}$	aa 1-217, Δ57PHP/Δ152EQV
	$GRB2^{\Delta PHP/\Delta EQV/W36K}$	aa 1-217, Δ57PHP/Δ152EQV, W36K
	$GRB2^{\Delta PHP/\Delta EQV/W193K}$	aa 1-217, Δ57PHP/Δ152EQV, W193K
	$GRB2^{\Delta PHP/\Delta EQV\ /W36K/W193K}$	aa 1-217, Δ57PHP/Δ152EQV, W36K, W193K
	$GRB2^{\Delta PHP}$	aa 1-217, Δ57PHP
	$GRB2^{\Delta EQV}$	aa 1-217, Δ152EQV
	$GRB2^{\Delta SH2}$	Δ61-150

$GRB2^{\Delta SH2/W36K}$	Δ61-150, W36K
$GRB2^{\Delta SH2/W193K}$	Δ61-150, W193K
$GRB2^{\Delta SH2W36K/W193K}$	Δ61-150, W36K/W193K
$GRB2^{\Delta nSH3}$	aa 61-217
$GRB2^{\Delta CSH3}$	aa 1-149
$GRB2^{SH2}$	aa 61-150
$GRB2^{nSH3}$	aa 1–55
$GRB2^{nSH3/W36K}$	aa 1–55, W36K
$GRB2^{nSH3/3llo}$	aa 1–55, M1R/Y37D/K50D
$GRB2^{cSH3}$	aa 160–217
$GRB2^{cSH3/W193K}$	aa 160–217, W193K
$GRB2^{cSH3/3allo}$	aa 160–217, M186R/K195D/T202D

[a]Proteins used in this study were derived from human SOS1 (Acc. No.: Q07889), human RASGRF1 (Acc. No.: Q13972), and human GRB2 (Acc. No.: P62993).

[b]All GRB2 constructs were cloned into pGEX4T-1 *via BAM*H1 and *SAL*I restriction sites. SOS1 CAT and PRD constructs were cloned in PET23A *via SAL*I and *NOT*I restriction sites. RASGRF1 construct was cloned in pGEX4T1 *via BAM*H1 and *SAL*I restriction sites. SOS1 CAT-PRD was cloned in pFASTbac *via SAL*I and *NOT*I for a baculovirus-insect cell expression system. C, C-terminal; N, N-terminal; RDD, allosteric arginine-aspartic acid-aspartic acid variants of either nSH3, cSH3 or both; ΔPHP and ΔEQV, deletions in linker region 1 and 2; W36 and W193, residues critical for the PRM binding.

[c] All proteins were expressed in *Escherichia coli* and isolated as glutathione S-transferase (GST) fusion proteins *via* a glutathione (GSH) Sepharose column (GE Healthcare) and purified by size exclusion chromatography (Superdex 200; GE Healthcare) after thrombin cleavage of GST. Protein concentration of all fractions was determined by the Bradford assay (Bio-Rad, Hercules, CA). All proteins were stored at -80°C after analyzing by SDS-PAGE.

Table S3 | Dissociation constants (K_d)[a] determined for the SH3-PRP interactions.

GRB2 proteins		FL	nSH3	cSH3
SOS1 Peptides[b]	P1	-	-	-
	P2	-	-	-
	P3	4.2 ±2	15.0 ±2	1.2 ±0.25
	P4	15.5 ±8	60.0 ±8	20.0 ±2
	P5	13.2 ±7	62.0 ±10	35.0 ±3
	P6	-	-	-
	P7	-	-	-
	P8	-	-	-
	P9	-	-	-
	P10	-	-	-
Reference peptides[c]	RP1	1.2 ±0.1	11.5 ±0.8	3.4 ±0.21
	RP2	14.2 ±7	20 ±9	12.9 ±3

[a] Dissociation constant (K_d values in μM) were determined by evaluating the fluorescence polarization data (Figures S2) shown in Figure 3C as bar charts.

[b] The amino acid sequences of the peptides are listed in Table S1.

[c] RP1 is the best-studied peptide derivative of SOS1. RP2 is a derivative of the N-terminal extension of WRCH1.

Table S4 | Classification of published proline-rich consensus sequence motifs and their incidence found in SOS1 PRD.

No.	ID	Consensus sequences	Ref.	Peptides[a]											
				P1	P2	P3	P4	P5	P6	P7	P8	P9	P10	RP1	RP2
1	**0X1**	PPPP	(*352*)	-	-	-	-	-	-	+	-	-	-	-	-
2	**0X2**	XPPX	(*353*)	+	-	+	+	+	+	+	+	+	+	+	+
3	**1X1**	PXP	(*354*)	+	-	+	-	-	+	+	+	+	-	+	+
4	**1X2**	PXPXP	(*355*)	-	-	+	-	-	-	-	-	-	-	+	-
5	**1X3**	PPXPP	(*356*)	-	-	+	+	+	-	-	-	+	-	+	+
6	**2X1**	PXXDY	(*357*)	-	-	-	-	-	-	-	-	-	-	-	-
7	**2X2**	PXXP	(*358*)	+	+	+	+	+	-	+	+	+	+	+	+
8	**2X3**	PXXPX[KR]	(*359*)	-	-	+	+	+	-	-	-	+	-	+	+
9	**2X4**	[KR]XXPXXP	(*359*)	-	-	-	-	-	-	-	+	-	-	-	-
10	**2X5**	PXXPXXP	(*360*)	+	-	+	-	-	-	-	-	-	-	+	-
11	**3X1**	PXXXP	(*361*)	+	-	+	+	+	+	+	-	+	+	+	+
12	**3X2**	PXXXPXXXP	(*362*)	-	-	+	+	+	-	-	-	-	-	-	-
13	**3XP**	PXXXPR	(*363*)	-	-	+	+	+	-	-	-	+	-	+	+
14	**4XP**	PXXXXP	(*364*)	+	-	+	+	+	-	+	-	-	-	+	-

[a] The amino acid sequences of the peptides P1-P10 as well as PR1 and PR2 are listed in Table S1.

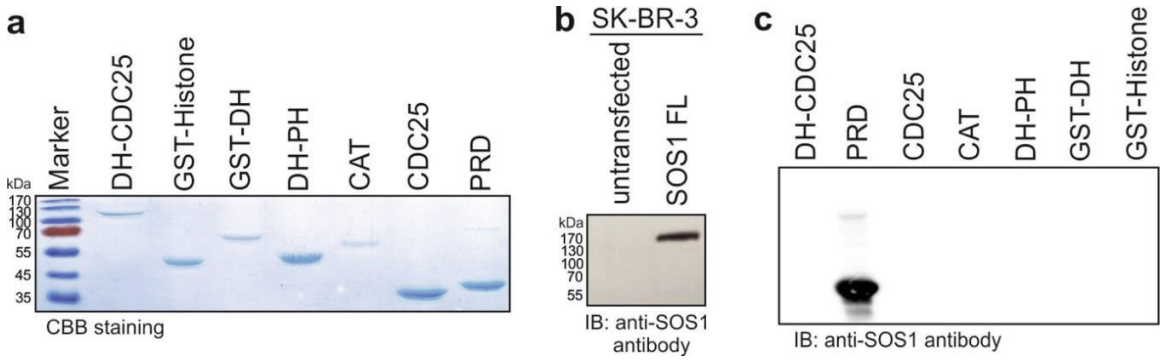

Figure S1 | SOS1 PRD recognition by an anti-SOS1 antibody. Various purified proteins, containing different SOS1 domains (**a**) along with the endogenous SOS1 FL in SK-BR-3 breast cancer cell line (**b**) were immunoblotted using a polyclonal anti-SOS1 antibody (#5890; Cell Signaling Technology). This antibody recognizes the proline-rich domain (PRD) of human SOS1 but not the other regions or domains (**c**).

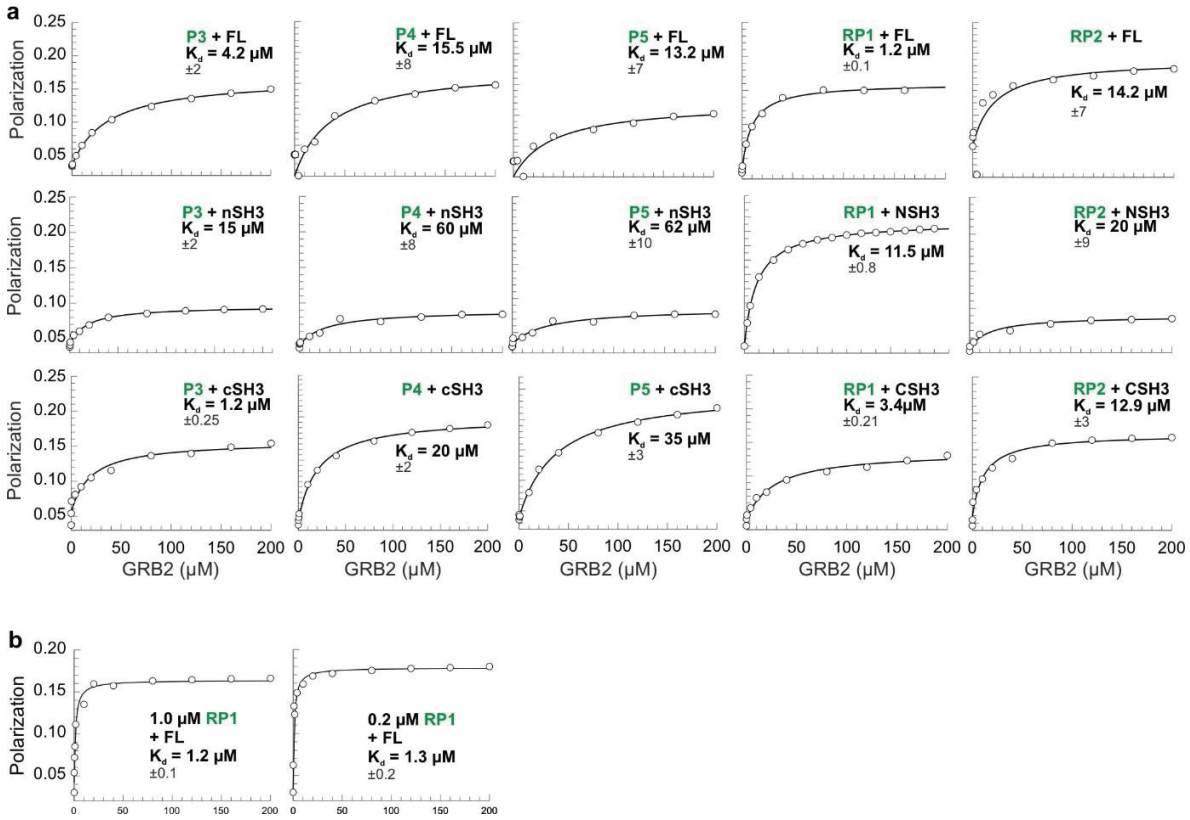

Figure S2 | Fluorescence polarization measurements of the interactions of the GRB2 proteins with the SOS1 and reference peptides. Fluorescence polarization experiments were performed to determine the dissociation constants (K_d) for the interactions of GRB2 FL, nSH3, and cSH3, respectively, (**a**) with FITC-peptides (green) from SOS1 PRD (P3, P4, P5, RP1 and RP2; See Fig. 3A and Table S1), and (**b**) with two different RP1 concentrations. The X-axis represents the concentration of GRB2-derived proteins in µM and Y-axis represents relative fluorescence polarization. Equilibrium K_d values for respective interactions were calculated by fitting data to a quadratic ligand-binding equation (solid lines). The K_d values are summarized in Table S3 and Figure 3C. The error bars were derived from the fitting errors.

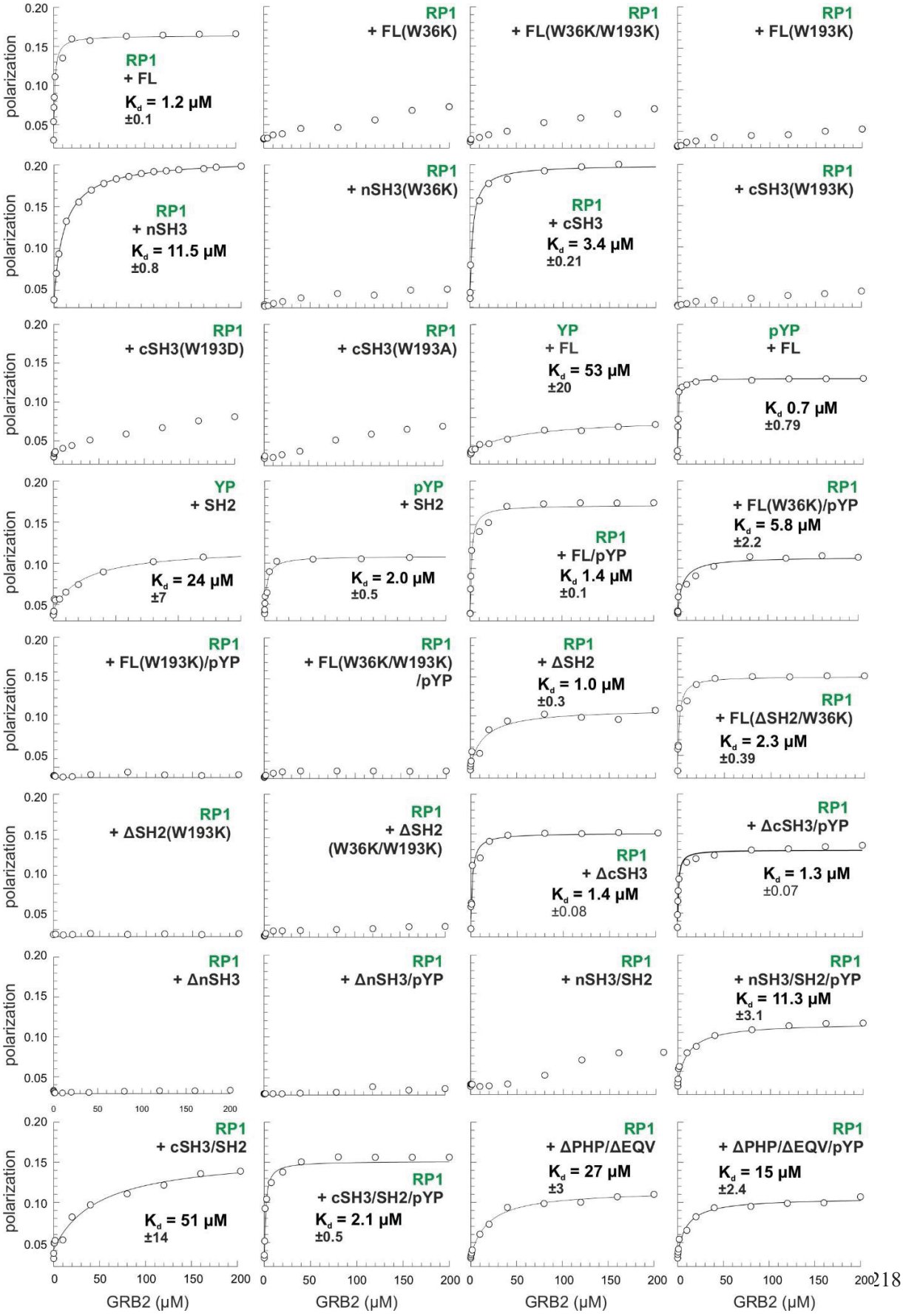
RP1
+ FL
K_d = 1.2 µM
±0.1
RP1
+ FL(W36K)
RP1
+ FL(W36K/W193K)
RP1
+ FL(W193K)
RP1
+ nSH3
K_d = 11.5 µM
±0.8
RP1
+ nSH3(W36K)
RP1
+ cSH3
K_d = 3.4 µM
±0.21
RP1
+ cSH3(W193K)
RP1
+ cSH3(W193D)
RP1
+ cSH3(W193A)
YP
+ FL
K_d = 53 µM
±20
pYP
+ FL
K_d 0.7 µM
±0.79
YP
+ SH2
K_d = 24 µM
±7
pYP
+ SH2
K_d = 2.0 µM
±0.5
RP1
+ FL/pYP
K_d 1.4 µM
±0.1
RP1
+ FL(W36K)/pYP
K_d = 5.8 µM
±2.2
RP1
+ FL(W193K)/pYP
RP1
+ FL(W36K/W193K)
/pYP
RP1
+ ΔSH2
K_d = 1.0 µM
±0.3
RP1
+ FL(ΔSH2/W36K)
K_d = 2.3 µM
±0.39
RP1
+ ΔSH2(W193K)
RP1
+ ΔSH2
(W36K/W193K)
RP1
+ ΔcSH3
K_d = 1.4 µM
±0.08
RP1
+ ΔcSH3/pYP
K_d = 1.3 µM
±0.07
RP1
+ ΔnSH3
RP1
+ ΔnSH3/pYP
RP1
+ nSH3/SH2
RP1
+ nSH3/SH2/pYP
K_d = 11.3 µM
±3.1
RP1
+ cSH3/SH2
K_d = 51 µM
±14
RP1
+ cSH3/SH2/pYP
K_d = 2.1 µM
±0.5
RP1
+ ΔPHP/ΔEQV
K_d = 27 µM
±3
RP1
+ ΔPHP/ΔEQV/pYP
K_d = 15 µM
±2.4
polarization
0.20
0.15
0.10
0.05
0
50
100
150
200
GRB2 (µM)

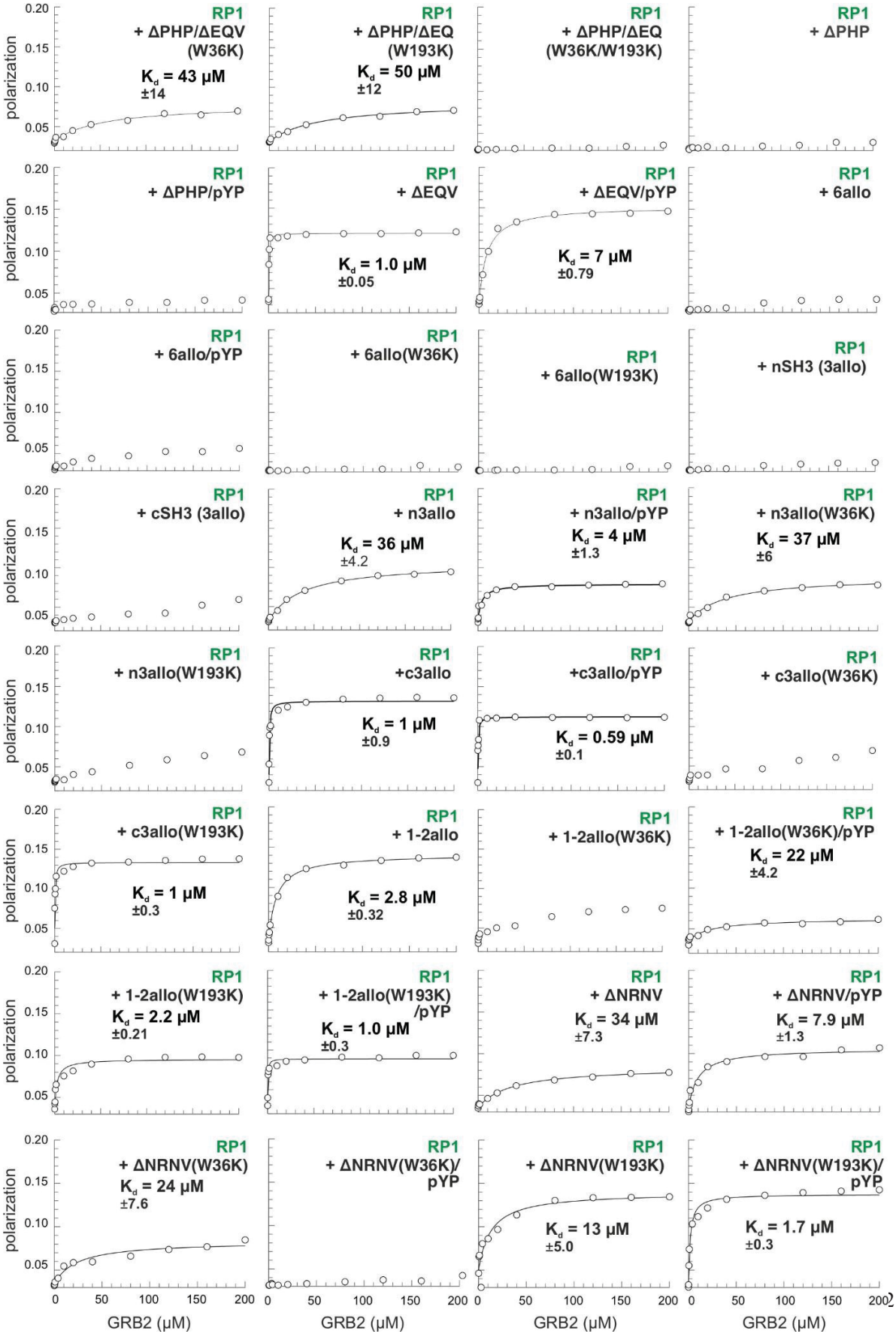
RP1 + ΔPHP/ΔEQV (W36K) Kd = 43 μM ±14
RP1 + ΔPHP/ΔEQ (W193K) Kd = 50 μM ±12
RP1 + ΔPHP/ΔEQ (W36K/W193K)
RP1 + ΔPHP
RP1 + ΔPHP/pYP
RP1 + ΔEQV Kd = 1.0 μM ±0.05
RP1 + ΔEQV/pYP Kd = 7 μM ±0.79
RP1 + 6allo
RP1 + 6allo/pYP
RP1 + 6allo(W36K)
RP1 + 6allo(W193K)
RP1 + nSH3 (3allo)
RP1 + cSH3 (3allo)
RP1 + n3allo Kd = 36 μM ±4.2
RP1 + n3allo/pYP Kd = 4 μM ±1.3
RP1 + n3allo(W36K) Kd = 37 μM ±6
RP1 + n3allo(W193K)
RP1 +c3allo Kd = 1 μM ±0.9
RP1 +c3allo/pYP Kd = 0.59 μM ±0.1
RP1 + c3allo(W36K)
RP1 + c3allo(W193K) Kd = 1 μM ±0.3
RP1 + 1-2allo Kd = 2.8 μM ±0.32
RP1 + 1-2allo(W36K)
RP1 + 1-2allo(W36K)/pYP Kd = 22 μM ±4.2
RP1 + 1-2allo(W193K) Kd = 2.2 μM ±0.21
RP1 + 1-2allo(W193K) /pYP Kd = 1.0 μM ±0.3
RP1 + ΔNRNV Kd = 34 μM ±7.3
RP1 + ΔNRNV/pYP Kd = 7.9 μM ±1.3
RP1 + ΔNRNV(W36K) Kd = 24 μM ±7.6
RP1 + ΔNRNV(W36K)/ pYP
RP1 + ΔNRNV(W193K) Kd = 13 μM ±5.0
RP1 + ΔNRNV(W193K)/ pYP Kd = 1.7 μM ±0.3
polarization
0.20
0.15
0.10
0.05
0
50
100
150
200
GRB2 (μM)

Figure S3 | Fluorescence Polarization measurements of GRB2 interactions with the SOS1 and reference peptides. Fluorescence polarization experiments were performed to determine the dissociation constants (K_d) for the interactions of different GRB2 variants (see Table S2) with FITC-peptides (green) derived from SOS1 (RP1) and HER2 (YP and pYP; see Table S1). The X-axis represents the concentration of GRB2-derived proteins in µM and the Y-axis represents relative fluorescence polarization. Equilibrium K_d values for the respective interactions were calculated by fitting data to a quadratic ligand-binding equation (solid lines). The K_d values are summarized in Figure 4. The error bars were derived from the fitting errors.

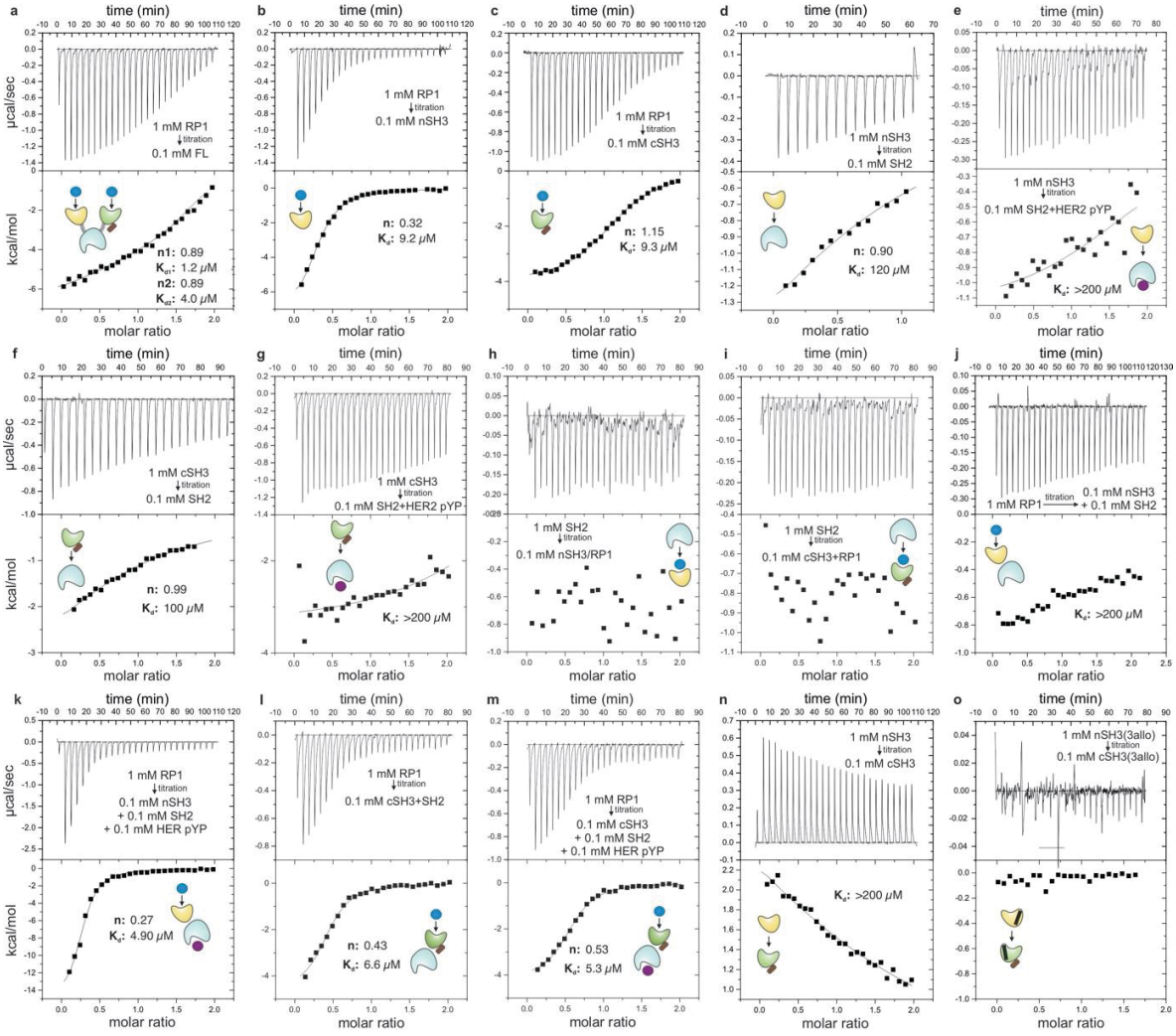

Figure S4 | ITC measurements of GRB2-SOS1 RP1 and GRB2 interdomain interactions. Isothermal titration calorimetry (ITC) was used as an independent method to measure the binding affinity and particularly also the stoichiometry of the SOS1 RP1 interaction with GRB2 FL, nSH3, and cSH3, respectively (**a-o**). The experiments were conducted by titrating protein or peptide solutions of 0.1 mM in the cell with a solution of 1 mM in the syringe as indicated in each panel. The buffer contained 30 mM Tris-HCl pH 7.4, 5 mM $MgCl_2$, and 2 mM dithiothreitol, at 25°C. The injection volumes were 10 µl (except for the first injection with a volume of 2 µl) and a delay of

150 s was set between the injections. The upper panels show heating power changes plotted versus the time. The lower panels represent the integrated heat changes referred to the concentration of injected protein and plotted against the increasing molar ratio of the interacting proteins. The solid lines in the lower panels represent the fit to the data by the manufacturer´s software according to a one site binding model, except for **a** where a two-sites binding model was applied. These fits yielded the K_d values of the complexes as indicated in the lower panels. The stoichiometry values (n) obtained from the fits range between 0.5 – 1.5 and particularly for the low affinity complexes these values exhibit large uncertainties. In addition, errors in the concentrations of proteins and peptides account for another contribution to this uncertainty. A reasonable fit using the two-sites binding model in panel a could only be obtained with the n-value for each of the two binding sites close to 1.

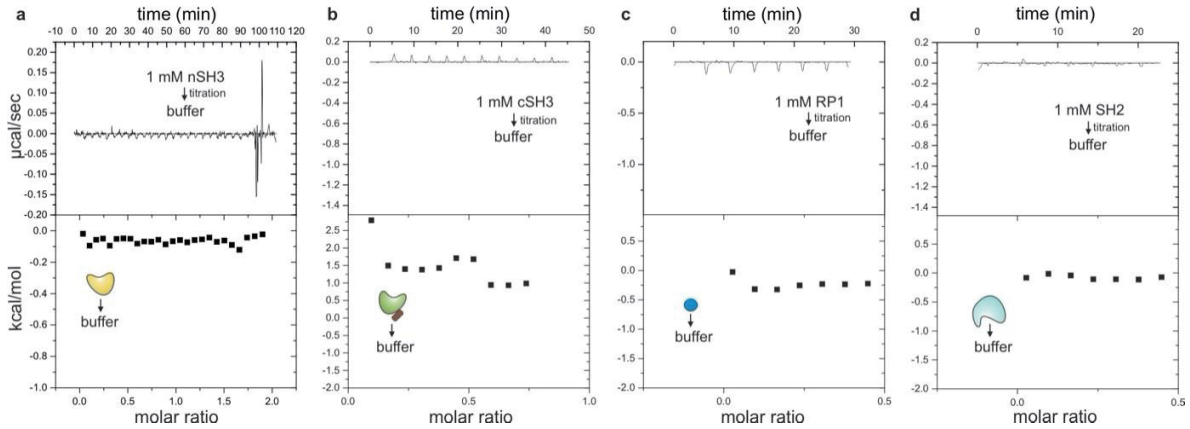

Figure S5 | ITC control measurements. Only small and constant heat changes were observed in the control experiments, which were conducted under the same condition as described in Figure S4. (**a**) nSH3 titrated to buffer; (**b**) cSH3 titrated to buffer; (**c**) RP1 titrated to buffer; (**d**) SH2 titrated to buffer. See Figure S4 legend for more information.

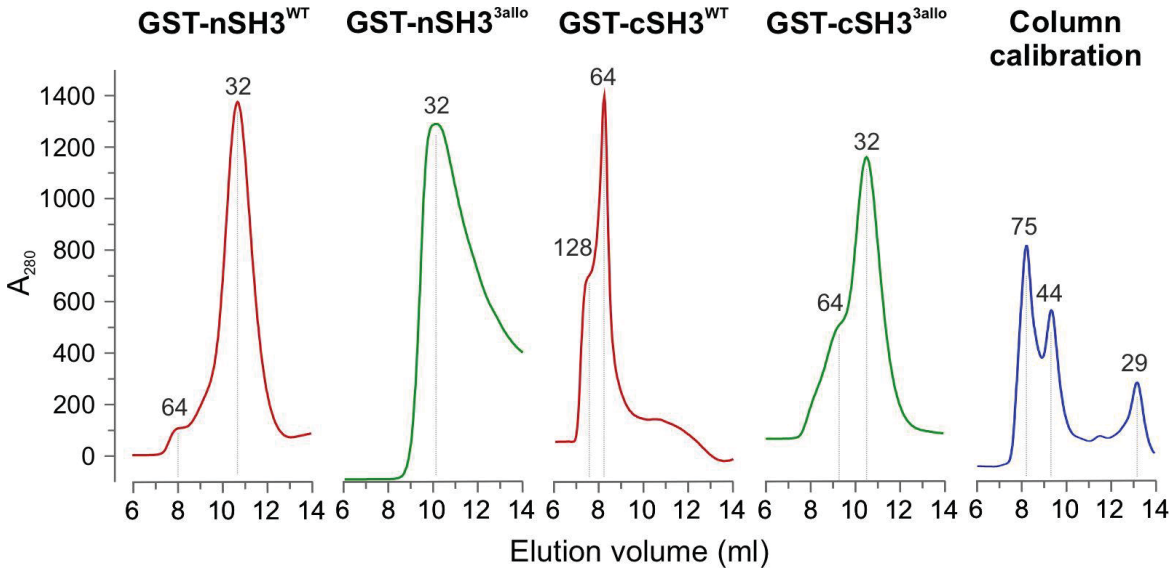

Figure S5 | Dimer-monomer shift of GRB2 HS3 domains upon allosteric substitution. Analytical size exclusion chromatography analysis of WT and 3allo nSH3 and cSH3 as GST fusion proteins on a Superdex 75 (10/300) revealed different elution profiles. nSH3 domains (WT and 3allo) predominantly eluted at monomers at 10-10.5 ml, which correspond to molecular weight (MW) of 32 kDa, respectively. A small dimeric population of $nSH3^{WT}$ eluted at 8 ml (64 kDa; 8.98 % population), which was not observed for $nSH3^{3allo}$. In contrast, $cSH3^{WT}$ eluted at 8.3 and 7. 3 ml, which correspond a dimer (64 kDa; 86% population) and tetramer (128 kDa; 14% population). Interestingly, $cSH3^{3allo}$ is mainly monomeric (32 kDa; 64% population) and showed under this condition also a dimeric (64 kDa) of 36%. Obtained MWs matches the theoretical MWs of 4,96 kDa for nSH3 and cSH3. The MWs of eluted peak fractions have calculated from calibration peaks (right panel) of conalbumin (75 kDa), ovalbumin (44 kDa), and carbonic anhydrase (29

Chapter IX

A genome-wide compilation of human SH3 superfamily proteins and their specificity for proline-rich motifs

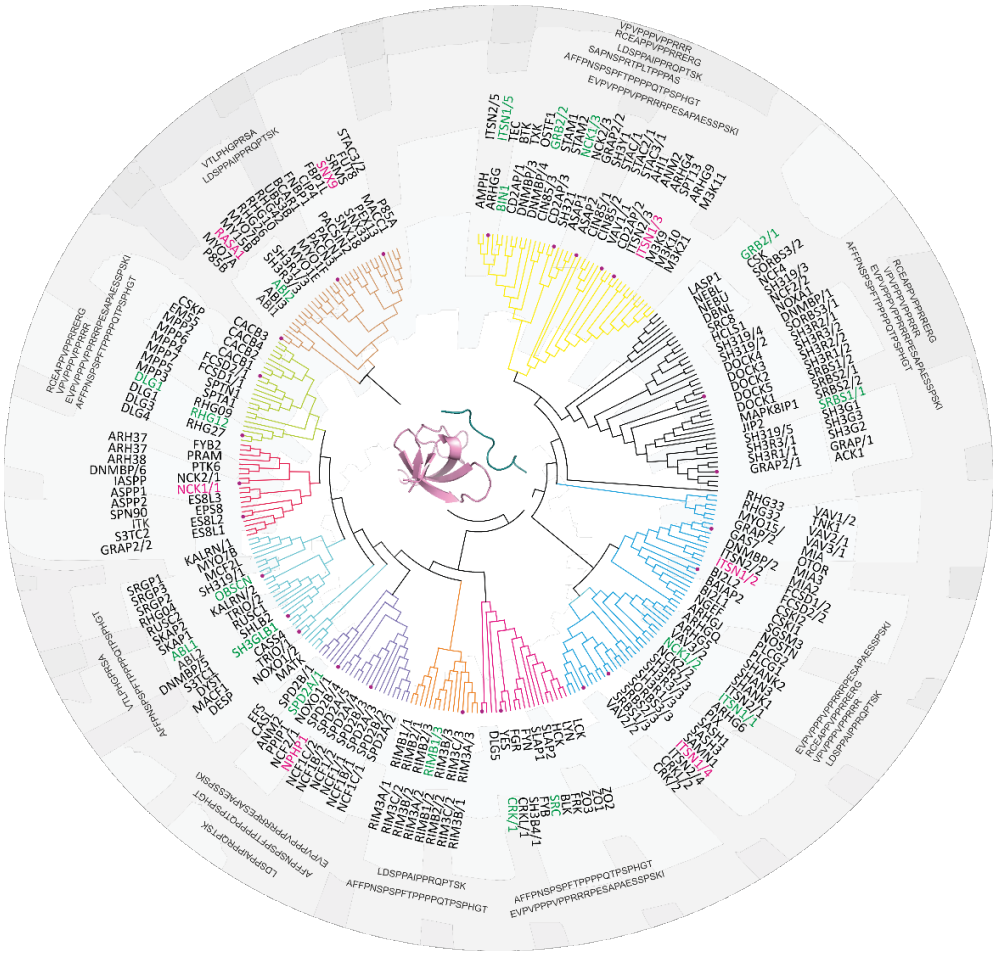

Status:	In preparation
Impact factor:	
Own Proportion to this work:	90%
	experimental design, cloning, protein purification, interaction analysis, figure generation, writing the manuscript

Genome-wide identification, functional classification and interaction selectivity landscape of human SH3 domain superfamily*

Neda S. Kazemein Jasemi[1], Mehrnaz Mehrabipour[1], Eva M. Estirado[2], Luc Brunsveld[2], Radovan Dvorsky[1], Mohammad R. Ahmadian[1@]

[1]Institute of Biochemistry and Molecular Biology II, Medical Faculty of the Heinrich-Heine University, 40225 Düsseldorf, Germany; [2]De Laboratory of Chemical Biology, Department of Biomedical Engineering and Institute of Complex Molecular Systems (ICMS), Eindhoven University of Technology, P.O. Box 513, 5600MB, Eindhoven, The Netherlands.

*Running title: Classification and selectivity of human SH3 superfamily

[@]Correspondences to reza.ahmadian@hhu.de

Abstract

SRC homology 3 (SH3) domains are critical for a wide range of biological processes. They selectively interact with a pool of ligands, the so-called proline-rich motifs (PRMs). A database search revealed a total of 298 SH3 domains in 221 reviewed SH3 domain-containing proteins in the human proteome. Phylogenetic analysis of all human SH3 domains, which can be obtained from the multiple sequence alignment, appeared to be most practical to classify them and determine their selectivity for defined proline-rich peptides (PRPs). Contrary to the whole-domain sequence analysis, the tree merely derived from the PRM-interacting residues extracted from SH3-PRP complex structures provided the proper functional classification of the SH3 domains into 11 families. The interaction of 25 representative SH3 domains with 12 peptides was determined using fluoro-dot blotting and fluorescence polarization. The peptides were derived from the proline-rich domain of the RAS activator SOS1 and also WRCH protein, and cover all 13 out of 14 reported proline-rich consensus sequence motifs. 41 out of 300 SH3-peptide pairs exhibited binding affinities ranging from 0.2 to 125 micromolar. Here, we provide an overview of the published structural and biochemical data of the peptide recognition specificity of the SH3 domain in human genome and we classified SH3 domains into ten classes regarding their

interaction with proline-rich motifs. This study provides a framework for bridging gaps between SH3-PRP pairs, and provides testable predictions about possible interaction of SH3 domains with proline rich motifs considering their sequence specifies. Our bioinformatics analysis was confirmed by the experimentally determined interactions, showing the effectiveness of our approach. This may serve as a framework for further/deeper understanding protein networks involving SH3-PRP interactions. This study could be considered as a general approach to be applicable to other domain-peptide interactions.

Keywords: ARHGAP12, GRB2, NCK1, proline-rich motifs, protein interaction, SH3 domain, signal transduction, SOS1, SRC homology 3

Introduction

SRC homology 3 (SH3) domain – was first described in 1988 (*365, 366*) – certainly belongs to the best-investigated modular building blocks across all five kingdoms of life and also viruses. They evidently provide, among other peptide-binding modules, multivalency by increasing the avidity of interactions and promoting phase transition upon physical interactions with a pool of ligands, the so-called proline-rich motifs (PRMs)(*367-369*). As selective SH3 domain-PRM interactions are fundamental to the assembly of multiprotein complexes, it is logical that the SH3-containing proteins are involved in a wide range of biological processes (*370-372*). Thus, they have a major influence on diseases, such as cancers, leukemia, osteoporosis, inflammation, Alzheimer disease, various infections(*373-379*).

A subset of five types of PRM-binding modules, including SH3, WW, EVH1, GYF, and UEV, have been reported to date (*371, 380-383*). Proline is a non-essential amino acid with an exceptional conformational rigidity due to its pyrrolidine ring as a side chain. Proline-containing sequences are often located on the surface of a protein, such as loops, turns, and random coils, which makes them accessible for the interaction with other proteins. The outstanding feature of PRMs is most probably the actual degree of combinatorial diversity that is determined by the presence of one or more proline residues(*96, 384*). They can bind in two opposite orientations defined by the relative positioning of non-proline residues, mostly a positively charged residue(*94, 97*). A canonical SH3 domain-PRP interaction describes a specific contact recognition of a positively charged PRP residue by a negatively charged residues of the SH3 domain (*385*).

SH3 domains are relatively short (~60 residues) protein modules and comprise a compact β-barrel made of five antiparallel β-strands(*386*). The amino acids that are conserved in the SH3 sequences are located close to each other on one side of the molecule. The PRM binding occurs on the surface at three major sites, involving the hydrophobic patch with conserved aromatic residues, flanked by the RT loop with conserved arginine and threonine residues and the n-SRC loop of the SH3 domain(*93, 94*). These variable loops account for the specificity and affinity in PRM binding(*95*). The specificity of the domain for particular short proline-rich peptides (PRPs) is generally modest, with affinities usually in the low micromolar range(*93, 94, 96, 97*). A comprehensive study on binding specificities for 115 SH3 domains has nicely shown that roughly half of the SH3 domains exhibit non-canonical specificities and collectively recognize a wide variety of peptide motifs (*387*).

Disruption of SH3-PRM interaction is associated with a variety of human diseases. This includes mutations in the SH3 domains of for example α-spectrin, MYO7A, SH3TC2, and CASK respectively cause neurodegenerative diseases caused by amyloid fibril formation (*98, 99*), deafness (*100, 101*), peripheral nerve inflammation (*102, 103*), and microcephaly and cerebellar hypoplasia(*104*). A missense mutation in the SH3-binding motif of STAMBP causes

microcephaly-capillary malformation syndrome(*105*). SH3-containing proteins, such as GBR2 and CRK/CRKL, are frequently associated with cancer(*388*). Moreover, proline-rich proteins that bind host-cell SH3 domains, such as GRB2, CRK/CRKL, C3G, have been identified in a variety of pathogenic microorganisms(*389, 390*). An intact PRM in viral proteins, such as HIV Nef, is essential for inducing an AIDS-like disease(*379, 391, 392*). Several SH3-containing proteins, including GRB2, FYN and NCK1, and HCK and ARHG7, has been suggested to play crucial roles in the host–virus relationship(*393*). Thus, SH3-PRM interaction has emerged as attractive therapeutic targets(*388, 390, 394, 395*).

Thus, biochemical processes regulated by SH3 domains raise important questions about the nature of specificity and the overall logic governing networks of protein interactions. Although SH3 domains share 25% sequence homology, still prediction of the PRM recognition specificity of SH3 domains has been challenging (*97, 372, 396*). The various number of SH3 domains in SH3-containing proteins and their sequence similarity raise the question of how specific is the SH3 domains-PRM interactions. In this study, we analyzed SH3 domains-PRMs interactions in human proteome and propose a specific interaction of SH3 domains with PRPs as a matrix which is an experts approach for prediction of SH3 domain-PRP interactions. *In the present study, we analyzed the protein characteristics, structures, phylogenetic relationships, and gene ontology (GO) annotations of SH3 domains to explain the evolution of SH3-PRMs interaction in the Human kingdom. Furthermore, we proposed the potential binding partners of SOS1 in the human proteome and may construct the SH3-mediated SOS1 function in signaling networks.*

Results

The SH3-containing proteins belong to versatile superfamily

SH3 domains are quite frequently identified in proteins by sequence similarity. 226,538 proteins contain SH3 domains in all organisms from which 1,171 are reviewed; in humans, a set of 244 out of 964 proteins are reviewed (https://www.uniprot.org). An advanced search combined with a detailed sequence comparison using multiple sequence alignments generated with the ClustalW algorithmyielded, in this study, 221 human SH3 domain-containing proteins with a total number of 298 SH3 domains (Table S1).

The presence of SH3 domains in a wide variety of proteins ranging from cytoskeletal components, such as myosin I and the chain of spectrin, to signal-transduction enzymes, such as non-receptor tyrosine kinases and phospholipase C suggest that they link signaling proteins (Fig. S7). SH3 domains mainly exist in adaptor proteins, docking proteins and scaffolding proteins with the role of complex formation and linker in signaling pathways (*101, 397*). SH3 domain-containing proteins mostly integrate in signaling pathways related to proliferation, differentiation, apoptosis and

cytoskeletal reorganization. Moreover, the interaction of the SH3 domains with their target PRMs also provide the basis the mechanism for compartmentalization in cells through liquid-liquid phase separation(*398-400*). The SH3 domain-containing proteins were classified into three ontologies: cellular component, molecular function, and biological process (Fig. S1). The vast majority of these proteins act at the interface between cytosol and membranes, especially plasma membranes, such as junctions and synapses. They are involved mostly in protein-protein interactions, particularly in signal transduction. They also control the enzyme and receptor activities, as well as transport processes. Their biological functions are versatile ranging from intracellular processes, biogenesis, regulatory and metabolic processes, subcellular localization and motility (Fig. S1).

The human SH3 domain-containing proteins can be classified based on their domain organization into the following three major groups: (i) lipid and membrane binding domains; (ii) peptide and protein interacting domains; and (iii) catalytic domains with enzyme activities (Fig. 1). They encompass a wide variety of protein families that are highly divergent in size and functions, and only partially well-characterized. The majority of the SH3 domain-containing proteins belong, for example, to the scaffold protein family (Intersectin1,SCHANK3, SH3RF3, CASKIN2 and Membrane-associated guanylate kinases (MAGUKs);(*401-405*)), the RHOGEF family (VAV1, TRIO, CZH, intersectin1 (*43, 406, 407*)), the RHOGAP family (SRGAP2, ARHGAP4, ARHGAP26, ARHGAP10, ARHGAP12, SNX26, RHOGAP10L, RHOGAO9 and RICS (*349, 408*)), adaptor protein family (CRK, GRB2 and NCK (*409, 410*)), and tyrosine kinase protein family (SRC, CSK, ABL, ITK, BTK, TEC, TXK, and BMX (*411-413*)). Thus, the numbers of other domains in many proteins are conspicuous, particularly the frequency of lipid membrane binding domains along with protein interaction domains, such as SH2, WW, and Ig-like domain, and the large number of catalytic and regulatory domains, such as kinase, REM, GAP and GEF domains. Notably, TUBA, a CDC42 guanine-nucleotide-exchange factor (GEF; also known as ARHGEF36 and DNMBP) contains six SH3 domains. It represents an important link between endocytosis, actin dynamics, and small GTPase signaling (*414*). Association of the very C-terminal SH3 domain of TUBA with the N-terminal cytoplasmic PRN of tricellulin (PLPPPPLPLQPP; aa 46–57) results in TUBA-mediated CDC42 activation that is required for the regulation the junctional tension of epithelial cells(*415*). Intersectin 1 and 2 (ITSN1/2) as well as SH3D19 and SH3PXD2A compose of five SH3 domains. These proteins are also involved in activities at the plasma membrane, such as endocytosis, podosome formation and transmembrane receptor processing (Table S1). The largest SH3 domain-containing protein is Obscurin (OBSCN; 868.5 kDa), a giant sacromeric, RHOGEF protein that interacts with calmodulin and titin (*416*).The smallest SH3 domain-containing protein are GRAPL (13.4 kDa) and OTOR (14.3 kDa). GRAPL is a GRB2-like protein with one SH3 and one SH2, respectively. OTOR (also known as MIAL1) belongs to a number of extracellular SH3 domain-containing proteins of the MIA family, including MIA1-3 proteins(*417, 418*).

Sequence-structure-function relationships of human SH3 domains

Comparative sequence-structure-function relationships of human SH3 domains can be obtained at three levels, that is, amino acid sequence, three-dimensional structures, and spatial configuration of the active site regions using in silico techniques. We first conducted a phylogenetic analysis of all human SH3 domains to delineate their PRM binding characteristics. Therefore, we retrieved the amino acid sequences of a collection of 298 human SH3 domains from the UniProt database, and used it to construct a phylogenetic tree of such a large domains family using MEGA 7 software (Version 7.0). The evolutionary relationship of human SH3 domains is illustrated in Figure 2A. An amino acid sequence alignment related to the first phylogenetic tree (tree #1) showed that major regions required for three-dimensional fold of the SH3 domains are highly conserved (Fig. S2). Thus, there is a strong sequence-structure relationship between different families. In contrast, we did not find a structure-function relationship when we extensively studied SH3-PRP interactions deduced from both SH3-PRP structures available in the protein data bank (Table S2) and published biochemical data about the SH3-PRP interactions (Table S3). So, PRPs do not cluster to defined SH3 domain family but rather distributed between the families that are distant to each other.

For this reason, we ran a separate phylogenetic analysis by focusing spatial configuration of the active site regions of the SH3 domain, which did not consider the full SH3 domain sequences as before but merely those residues of the SH3 domains that interact or are likely to interact with PRPs. Therefore, the sequence of 54 published structures of SH3 domains in complex with PRP (Table S2) were analyzed and the PRP interacting residues were extracted using an algorithm. The second phylogenetic tree, only constructed with PRP interacting residues (tree #2), now revealed 10 families/clusters of SH3 domains, and each family/cluster shares physiologically similar residues that determine a molecular environment responsible for recognizing particular PRPs (Fig. 2B; Table S3). Residues in another family/cluster define different environment suitable for interaction with another type of PRP. Such approach enabled us to decipher the way in which particular SH3 domains associate with particular PRPs (see below).

Verification of SH3 family/cluster-based PRP selectivity

To verify the functional classification of human SH3 domains assigned with studied PRPs, 25 SH3 domains from different SH3 families/clusters (Fig. 2B) were selected, cloned, purified as GST fusion proteins, and used for PRP binding analysis (see Materials and Methods).

To select PRPs, we reviewed the reported interactions between the SH3 domains and PRP-containing peptides. Specific SH3-PRP interactions were found within the phylogenic tree based on PRP interacting residues (Fig. 2B). Recently, a total of 154 peptide-binding specificities for 115

SH3 domains were grouped in nine classes (*387*). Accordingly, the SH3 domains of one family require similar pattern of PRP sequences for interaction. We collected 14 PRMs that have been identified in the previous studies (Table S4). Most of them belong to well-known PXXP motif. For this study, we selected 10 different PRPs from SOS1 proline-rich domain (RPD) because it encompasses all types of PRMs (Table S5). Two reference peptides RP1, a derivative of SOS1, and part of P3, and RP2, a derivative of the RHO GTPase WRCH1, were used a control peptide (Table S5). FITC-labelled derivatives of these 12 PRPs were used to analyze their binding capabilities to purified SH3 domains.

Binding of 10 FITC-labelled SOS1 peptides (P1 – P10; Table S2) and two reference peptides RP1 and RP2 to GST fusion proteins of 25 SH3 domains was qualitatively analyzed by combining GST pull-down and dot-blot assays. GST was used as a control protein. As shown in Figure 3A, peptides P2, P3, P4, P7 and P9 differentially associated with about 17 SH3 domains.

We next conducted fluorescence polarization measurements to determine the binding affinities for SH3-PRP interactions, which were observed in the GST pull-down and dot-blot analysis. For this, increasing concentrations of the SH3 proteins were titrated to the fluorescent peptides (1μM, respectively). We monitored increase in polarization for FITC tag of the proline rich peptides. (Fig. 3B; Table S6). The interaction of peptides P2, P3, P4, P7 and P9 associated with about 17 SH3 domains were confirmed using Fluorescent polarization. Despite all reported SH3-PRMs interaction which were shown to be in uM affinities, here we detected two interactions in nM affinity. The highest affinities were obtaining from the interaction of RHOGEF12 SH3 domain_ P7 SOS1 with 200 nM affinity and also the interaction of NCK1 SH3.3_ P9 with affinity of 900 nM. The newly reported SH3_PRMs interaction in nm range rai

SOS1 binding partners

Herein, using a battery of biophysical and bioinformatical tools, we provide evidence that PRMs of SOS1 interacts with CRK, SRC, GRB2, NCK1, Intersectin, ABI1, ABL2, BIN1, DLG2, SRBS1, SPD2A, Obscurin, RIM3B1 and RGH12. From those ABI1(*419*), intersectin (*420*), SRC (*421*), NCK1 (*422*) and GRB2 (*423*) were already clarified as a SOS1 binding partner in eukaryotic cell. Among them only the binding site GRB2 was reported before but not others. Here we clarified the binding site of known SOS1 binding partners and also reported a newly found SOS1 binding partners such as CRK, ABL2, BIN1, DLG2, SRBS1, SPD2A, and Obscurin. Although the interaction of the new SOS1 binding partners needs to be verified under cell-based condition.

Discussion

SH3 domains are the main player in various signaling pathways and they exist in divergent signaling proteins such as protein tyrosine kinases (PTKs) of the Src-family, myosin, cortactin, amphiphysin and spectrin (*101, 370*). Regulation of a broad of cellular functions by SH3 domains

raises the question about the specificity networks of SH3 domain interactions. Proline is the only N-substituted amino acid in Nature and it can form the PPII helix which forms a binding site packet for residues primarily from the RT and n-Src loops of SH3 domains (*382, 424, 425*). A couple of studies showed that SH3 domains binding motifs are proline-rich and identified PxxP motif (*92*). 14 proline-rich motifs are identified in human proteome and still, the specificity of the interaction of the SH3 domains with proline-rich motifs are unclear. Understanding the molecular basis representing the specific and diverse binding of SH3 domains to the PRMs would provide insights into the regulation of signaling pathways. To understand the specificity networks of SH3 domain interactions, we screened the published biochemical and structural analysis and by doing so, we reached hints on how to characterize the SH3 domains in human proteome based on their interaction with proline-rich motifs.

Different studies showed that SH3-PRMs interaction is transient and weak in micromolar range affinity(*426*). In some cases, SH3 containing protein increases the affinity of the interaction using multiple SH3 domains in an avidity based mechanism e.g. NCK1adaptor protein(*427*). Evanics et al. clarified that the Fyn SH3 domain-PRM (Arg-Ala-Leu-Pro-Pro-Leu-Pro) had an average exchange rate of 5200 s−1 between the free and bound states(*428*). Perfuming a molecular dynamics simulation of SH3-PRMs, Ahmad et al. proposed that SH3 domain-PRMs represent a bimodal binding mechanism to reduce the dimensionality. They also reported that electrostatic effects increase the complex formation and stabilize the transient of the SH3-PRMs complex(*429*). Mayer & Saksela reported that the limited specificity of peptide-SH3 binding means that SH3-mediated interactions can be highly dependent on their environment. As detailed below, additional surfaces on the peptide or SH3 domain, or other domains on the two potential binding partners or even on other members of a multiprotein complex, can all confer much greater overall specificity to a SH3-peptide interaction. They also reported that the moderate affinities also imply that the interactions they mediate are highly dynamic because off-rates are necessarily very rapid. This means that SH3-mediated interactions have the potential to quickly remodel, depending on subcellular localization and available binding partners(*430*).

Sequence-structure-function analysis using full-length SH3 domains was not successful because some SH3 containing protein include more than one SH3 domains. Each SH3 domain has a distinct binding specificity towards proline-rich motifs; therefore, characterization of SH3 domain-containing proteins was not possible. Consequently, the second generation of the phylogenetic tree was generated by aligning the SH3 domains sequences. The idea was to define the groups of SH3 domains within the phylogenetic tree as different subfamilies and each subfamily interacts with a specific sequence of proline-rich motifs. By comparing the distribution of published structural and biochemical data, the phylogenetic tree of SH3 domains failed to support our idea. Literature also revealed that certain proline rich containing proteins could have different binding sites e.g. amphiphysin SH3 domain recognizes the PxRPxR motif; the Itch proline-rich region (containing the “PSRPPRPSR” sequence) has two binding sites for the amphiphysin SH3 domain(*431*). The peptide library investigations also have reported that the recognition sites of SH3 domains are highly overlapping for proline-rich motifs(*384, 432, 433*). This shows that SH3 domains could interact differentially with different proline-rich motifs. Therefore, to have a comprehensive understanding of the interaction of the SH3 domains with PRMs, the principle of the phylogenetic tree was limited to the predicted interfacing residues instead of the complete

sequence of the SH3 domains. The interfacing residues of SH3 domains interacting proline-rich motifs were detected by comparing sequence alignment of published SH3 domains structure in complex with proline-rich motifs. The last version of the phylogenetic tree generated by alignment of interfacing residues of SH3 domains interacting proline-rich motifs were considered for further analysis. To define different subfamilies within the phylogenetic tree, we considered published structural and biochemical analysis of SH3 domains interacting proline-rich motifs. The structural and biochemical data were collected within the published papers and their distribution were studied within the phylogenetic tree.

10 subfamilies are made out of the SH3 domains in human by comparison of the distribution of the reported SH3 domains-PRMs structures and interactions. Insights gained from studies on show that each family interacts with a specific sequence of proline-rich motifs. To prove the in silico analysis and specificity of each family, we selected 25 representatives from the phylogenic tree and different proline-rich motifs for further in vitro investigation of their interaction.

Considering the general complex formation is crucial for the description of protein-protein interactions in complexes, and especially weak or transient protein complexes such as SH3 domain-PRMs(*426*). Zarrinpar mentioned that isolated SH3-domains are sufficient to encode interaction specificity among SH3 domains in yeast(*434*).

Having a protein model comprising different types of proline-rich motifs could explain the specificity of the various interactions with SH3 containing proteins because domain–ligand interactions take place in the context of folded proteins instead of binding to a short peptide sequence. SOS1 RAS GEF includes a variety of proline-rich motifs and it covers all yet known proline-rich motifs in the human proteome. Interaction of SOS1 with SH3 containing proteins including GRB2, Intersectin, NCK1, NCK2, and ABI1 was reported to be critical in various signaling pathways (*101, 315, 342, 355, 419, 423*). Therefore, SOS1 was selected as a poly-proline model.

Cesareni and coworkers have taken advantage of the high throughput analysis of the recognition specificity of a large number of human SH3 domains using new chip technology. They could characterize SH3 domains in three main families, 1)classical SH3 domains interacting with PXXP motifs, 2) Positive charge binders and 3)atypical SH3 domains using Insilco and high throughput qualitative measurements (*384, 417*). A comprehensive analysis of the SH3 domains interactions in evolution among four yeast species, *Saccharomyces cerevisiae*, *Ashbya gossypii*, *Candida albicans*, and *Schizosaccharomyces* revealed that each SH3 family within the generated phylogenic three had ~75% sequence homology over a large evolutionary distance. Furthermore, the SH3 domain family were predicted to interacts with the conserved binding specificity. (*435*). In this study, we covered all reviewed SH3 domains and also known proline-rich domains in low throughput analysis of pulldown assay combined with dot blotting. The interactions were providing via fluorescence polarization and the affinity of the interactions are determined. We reported novel SH3-PRMs interactions in nM affinities which were systematically explored in sequence-structure-property relationship analysis, and validated by mutational analysis.

Presence of the more than one proline in proline-rich motifs makes it complicated to find the key proline defining specificity. The current result shows that the residues -2, -1, +1, +2 are decisive

for the SH3-PRMs specificity. We found that the location of the proline residues is important for the SH3 domain recognition and provide a frame for the interaction and residues juxtapose the prolines act as a signature defining specificity. The importance of the juxtapose residues of the proline is not clearly described. Non proline residues consisting of combinations of arginine and leucine appeared to confer ligand specificity(*358*). Arginine was shown to be a crucial residue in proline-rich motifs for their interaction with SH3 domains. A single properly-positioned arginine is necessary and sufficient for Peptide recognition specificity of the SH3 domains(*436*). Although most of the SH3 domains interact with proline-rich motifs, there are some cases that are not associated with proline-rich motifs. Interaction of SH3 domain of p120, RHOGAP with the DLC1 RHOGAP domain was reported to not follow the classical P*XX*P-directed interaction. p120 SH3 domain targets the catalytic arginine finger of DLC1 and in a completion manner inhibits RHOGAP activity of DLC1 (*437*). SRC kinase-associated protein of 55 kDa (SKAP55) is an adaptor protein associated with the immune system. Its SH3 domains have been shown to bind to the RKxxYxxYP motif in a PRM-independent interaction(*385*).

Our study covers the SH3 domains-PRMs interactions in the human genome but the specificity and the mechanism of the PRM-independent interaction of SH3 domains remain to be investigated.

Materials and Methods

Peptides. Peptides used in this study are listed in Table S5.

Constructs. Constructs used in this study are listed in Table S7.

Bioinformatics and data bases. All sequences of the SH3 domains were obtained from Uniprot databank using the combination of full text search, information about available structures (https://www.uniprot.org). Sequences of SH3 domains were aligned using Bioedit (https://bioedit.software.informer.com/7.2/) and corresponding phylogenic tree was generated with the help of MEGA 7 software (https://www.megasoftware.net/dload_win_gui). The structural data were obtained from Protein data bank website (https://www.rcsb.org/). Pymol software was applied to analysis the SH3 domains structure and define their interface residues for the interaction with PRMs (https://pymol.org/2 /). An ontology classification of SH3 domains in human genome via online panther classification system (http://pantherdb.org).Proline rich motifs were collected within published articles from NCBI website (https://www.ncbi.nlm.nih.gov/protein).

Proteins. GST-SH3 domain proteins were isolated as glutathione S-transferase (GST) fusion proteins by affinity chromatography on a glutathione Sepharose column and purified in a second step, after proteolytic cleavage of GST, by size exclusion chromatography. His-tagged SOS1

PRD was purified via Ni-NTA affinity purification. All proteins were stored at -80°C after analyzing by SDS-PAGE.

Fluorescein labeled Proline-rich peptides. (see Table S5) P1: FITC-bAla-SAPNSPRTPLTPPPAS, P2: FITC-bAla-VTLPHGPRSA, P3: FITC-bAla-EVPVPPPVPPRRRPESAPAESSPSKI, P4: FITC-bAla-LDSPPAIPPRQPTSK, P5: FITC-bAla-ISDPPESPPLLPPREPVRTPDV, P6: FITC-bAla-SSSPLHLQPPPLGKK, P7: FITC-bAla-AFFPNSPSPFTPPPPQTPSPHGT, P8: FITC-bAla-RHLPSPPLTQ, P9: FITC-bAla-IAGPPVPPRQS, Pref1: FITC-bAla-VPVPPPVPPRRR, Pref2: FITC-bAla-RCEAPPVPPRRERG were synthesized using standard Fmoc solid-phase peptide synthesis (SPPS), by means of an automated peptide synthesizer (Intavis MultiPep Rsi) (*438*).

Cell based assay and GST-pull down assay. Pull-down of SOS1 in SKBR3 cell line were performed using GST-SH3 domains RHG12 and NCK1.3 coupled to the GSH sepharose beads (GE Healthcare, UK). After washing the beads three times with 1 ml buffer, containing 30 mM Tris/HCl pH 7.5, 3 mM DTT, 5mM MgCl2, 5 µM, 20 µM GST-SH3 and 600 µg SKBR3 cell lysate were added to the GSH Sepharose beads and incubated at 4°C for 1 h followed by three times washing step with 1 ml of Fish buffer. Purified GST was used as a negative control. Incubated at 4°C for 1 h followed by another three times washing with 1 ml of Fish buffer. Laemmli buffer was added into the samples followed by heat denaturation for 10 min at 95°C. All samples were analyzed by a 12.5 % SDS-PAGE and subsequent immunoblotting using monoclonal SOS1 antibody (5890s-cell signaling) recognizing proline rich domain.

Fluorescence dot-blot analysis. Pull-down of SOS1 PRM peptides using different GST-SH3 domains was performed by using GSH Sepharose beads (GE Healthcare, UK). After three times washing with a buffer, containing 30mM Tris pH 7.5, 3mM DTT, and 5mM $MgCl_2$, the GSH Sepharose beads were mixed with 5 µM GST-SH3 and 10 µM IL10R-peptides and incubated for 1 h, at 4°C. Purified GST was used as a negative control. After three times washing with 1 ml of above buffer bound proteins were eluted using a buffer, containing 30mM Tris pH 7.5, 100 mM NaCl, 3mM DTT, 5mM $MgCl_2$ and 2 mM glutathione for 15 min at 4°C. The SH3 domains–peptide interactions were analyzed by dot blotting using 1µL supernatant without beads and detected the fluorescence signal of FITC-labeled peptides at an emission wavelength 600 nm using Odyssey Fc Imaging System (LI-COR Biosciences]). Densitometric quantification of detected signals was performed on the LI-COR Biosciences Image Studio version 5.2 imaging software.

Fluorescence polarization. The interaction of Fluorescein labeled Proline rich peptides (1 μM) with increasing concentration of the SH3 domains (0_200 μM) were measured in a buffer containing 30 mM Tris/HCl (pH 7.5), 5 mM $MgCl_2$, and 3 mM DTT at 25°C using a Fluoromax 4 fluorimeter in polarization mode. Excitation wavelength was 470 nm and emission wavelength 560 nm. The dissociation constants (K_d) were obtained by fitting the concentration dependent binding curve using a quadratic ligand binding equation.

Acknowledgements

We are grateful to our colleagues from the Institute of Biochemistry and Molecular Biology II of the Medical Faculty of the Heinrich-Heine University Düsseldorf for their support, helpful advices, and stimulating discussions.

Author Contributions Statement

MRA conceived and coordinated the study. NSKJ, MRA designed the study and wrote the manuscript. E.M.E and L.B. Provided the fluorescein labelled peptides. NSKJ, RD, MRA designed, performed and analysed the experiments. All authors reviewed the results and approved the final version of the manuscript.

Conflict of Interest

The authors declare no competing financial interest.

Funding

This study was supported by the German Research Foundation (Deutsche Forschungsgemeinschaft or DFG; AH 92/8-1); the German Federal Ministry of Education and Research (BMBF) – German Network of RASopathy Research (GeNeRARe, 01GM1519D), and the European Network on Noonan Syndrome and Related Disorders (NSEuroNet, 01GM1602B).

References

1. Mayer, B.J., M. Hamaguchi, and H. Hanafusa, *A novel viral oncogene with structural similarity to phospholipase C.* Nature, 1988. **332**(6161): p. 272.
2. Stahl, M.L., et al., *Sequence similarity of phospholipase C with the non-catalytic region of src.* Nature, 1988. **332**(6161): p. 269-272.
3. Mayer, B.J., *The discovery of modular binding domains: building blocks of cell signalling.* Nature reviews Molecular cell biology, 2015. **16**(11): p. 691-698.
4. Case, L.B., et al., *Stoichiometry controls activity of phase-separated clusters of actin signaling proteins.* Science, 2019. **363**(6431): p. 1093-1097.
5. Huang, W.Y., et al., *A molecular assembly phase transition and kinetic proofreading modulate Ras activation by SOS.* Science, 2019. **363**(6431): p. 1098-1103.
6. Mayer, B.J., *SH3 domains: complexity in moderation.* Journal of cell science, 2001. **114**(7): p. 1253-1263.
7. Kaneko, T., L. Li, and S. Li, *The SH3 domain–a family of versatile peptide-and protein-recognition module.* Front Biosci, 2008. **13**: p. 4938-4952.
8. Kay, B.K., *SH3 domains come of age.* FEBS letters, 2012. **586**(17): p. 2606-2608.
9. Lucas, B. and J. Hardin, *Mind the (sr) GAP–roles of Slit–Robo GAPs in neurons, brains and beyond.* Journal of Cell Science, 2017. **130**(23): p. 3965-3974.
10. Richard, S., *Reaching for the STARs*, in *Post-Transcriptional Regulation by STAR Proteins*. 2010, Springer. p. 142-157.
11. Roskoski, R., *Michaelis-Menten Kinetics.* 2015.
12. Weisman, G.A., et al., *Molecular determinants of P2Y 2 nucleotide receptor function.* Molecular neurobiology, 2005. **31**(1-3): p. 169-183.
13. Bustelo, X.R., *Vav family exchange factors: an integrated regulatory and functional view.* Small GTPases, 2014. **5**(2): p. e973757.
14. Alexandrov, P.N., et al., *Deficits in the proline-rich synapse-associated Shank3 protein in multiple neuropsychiatric disorders.* Frontiers in neurology, 2017. **8**: p. 670.
15. Saksela, K., *Interactions of the HIV/SIV pathogenicity factor Nef with SH3 domain-containing host cell proteins.* Current HIV research, 2011. **9**(7): p. 531-542.
16. Holt, M.R. and A. Koffer, *Cell motility: proline-rich proteins promote protrusions.* Trends in cell biology, 2001. **11**(1): p. 38-46.
17. Zarrinpar, A., R.P. Bhattacharyya, and W.A. Lim, *The structure and function of proline recognition domains.* Science's STKE, 2003. **2003**(179): p. re8-re8.
18. Li, S.S.-C., *Specificity and versatility of SH3 and other proline-recognition domains: structural basis and implications for cellular signal transduction.* Biochemical Journal, 2005. **390**(3): p. 641-653.
19. Zafra-Ruano, A. and I. Luque, *Interfacial water molecules in SH3 interactions: Getting the full picture on polyproline recognition by protein–protein interaction domains.* FEBS letters, 2012. **586**(17): p. 2619-2630.
20. Cesareni, G., et al., *Can we infer peptide recognition specificity mediated by SH3 domains?* FEBS letters, 2002. **513**(1): p. 38-44.
21. Carducci, M., et al., *The protein interaction network mediated by human SH3 domains.* Biotechnology advances, 2012. **30**(1): p. 4-15.
22. Panni, S., L. Dente, and G. Cesareni, *In vitro evolution of recognition specificity mediated by SH3 domains reveals target recognition rules.* Journal of Biological Chemistry, 2002. **277**(24): p. 21666-21674.
23. Saksela, K. and P. Permi, *SH3 domain ligand binding: What's the consensus and where's the specificity?* FEBS letters, 2012. **586**(17): p. 2609-2614.

24. Kang, H., et al., *SH3 domain recognition of a proline-independent tyrosine-based RKxxYxxY motif in immune cell adaptor SKAP55.* The EMBO Journal, 2000. **19**(12): p. 2889-2899.
25. Musacchio, A., et al., *Crystal structure of a Src-homology 3 (SH3) domain.* Nature, 1992. **359**(6398): p. 851-855.
26. Mayer, B.J. and M.J. Eck, *SH3 domains: minding your p's and q's.* Current Biology, 1995. **5**(4): p. 364-367.
27. Cámara-Artigas, A., et al., *3D domain swapping in a chimeric c-Src SH3 domain takes place through two hinge loops.* Journal of structural biology, 2014. **186**(1): p. 195-203.
28. Teyra, J., et al., *Comprehensive analysis of the human SH3 domain family reveals a wide variety of non-canonical specificities.* Structure, 2017. **25**(10): p. 1598-1610. e3.
29. Morel, B., et al., *Environmental conditions affect the kinetics of nucleation of amyloid fibrils and determine their morphology.* Biophysical journal, 2010. **99**(11): p. 3801-3810.
30. Varela, L., et al., *A single mutation in an SH3 domain increases amyloid aggregation by accelerating nucleation, but not by destabilizing thermodynamically the native state.* FEBS letters, 2009. **583**(4): p. 801-806.
31. Wu, L., et al., *Structure of MyTH4-FERM domains in myosin VIIa tail bound to cargo.* Science, 2011. **331**(6018): p. 757-760.
32. Kurochkina, N. and U. Guha, *SH3 domains: modules of protein–protein interactions.* Biophysical reviews, 2013. **5**(1): p. 29-39.
33. Ichikawa, K., et al., *Novel mutations in SH 3 TC 2 in a young Japanese girl with Charcot-Marie-Tooth disease type 4C.* Pediatrics International, 2016. **58**(11): p. 1252-1254.
34. Lupo, V., et al., *Missense mutations in the SH3TC2 protein causing Charcot-Marie-Tooth disease type 4C affect its localization in the plasma membrane and endocytic pathway.* Human molecular genetics, 2009. **18**(23): p. 4603-4614.
35. LaConte, L.E., et al., *Two microcephaly-associated novel missense mutations in CASK specifically disrupt the CASK–neurexin interaction.* Human genetics, 2018. **137**(3): p. 231-246.
36. Hori, I., et al., *A novel homozygous missense mutation in the SH3-binding motif of STAMBP causing microcephaly-capillary malformation syndrome.* Journal of human genetics, 2018. **63**(9): p. 957-963.
37. Feller, S.M. and M. Lewitzky, *Potential disease targets for drugs that disrupt protein-protein interactions of Grb2 and Crk family adaptors.* Current pharmaceutical design, 2006. **12**(5): p. 529-548.
38. Bliska, J., *How pathogens expolit interactions mediated by SH3 domains.* Chemistry & biology, 1996. **3**(1): p. 7-11.
39. Ravi Chandra, B., et al., *Distribution of proline-rich (PxxP) motifs in distinct proteomes: functional and therapeutic implications for malaria and tuberculosis.* Protein Engineering Design and Selection, 2004. **17**(2): p. 175-182.
40. Hanna, Z., et al., *The pathogenicity of human immunodeficiency virus (HIV) type 1 Nef in CD4C/HIV transgenic mice is abolished by mutation of its SH3-binding domain, and disease development is delayed in the absence of Hck.* Journal of virology, 2001. **75**(19): p. 9378-9392.
41. Moroco, J.A., et al., *Remodeling of HIV-1 nef structure by Src-Family kinase binding.* Journal of molecular biology, 2018. **430**(3): p. 310-321.
42. Carducci, M., et al., *Enriching the viral–host interactomes with interactions mediated by SH3 domains.* Amino acids, 2010. **38**(5): p. 1541-1547.
43. Inglis, S.R., et al., *Identification and specificity studies of small-molecule ligands for SH3 protein domains.* Journal of medicinal chemistry, 2004. **47**(22): p. 5405-5417.
44. Vidal, M., V. Gigoux, and C. Garbay, *SH2 and SH3 domains as targets for anti-proliferative agents.* Critical reviews in oncology/hematology, 2001. **40**(2): p. 175-186.

45. Landgraf, C., et al., *Protein interaction networks by proteome peptide scanning.* PLoS Biol, 2004. **2**(1): p. e14.
46. Ingham, R.J., et al., *The Gab1 protein is a docking site for multiple proteins involved in signaling by the B cell antigen receptor.* Journal of Biological Chemistry, 1998. **273**(46): p. 30630-30637.
47. Pechstein, A., et al., *Vesicle Clustering in a Living Synapse Depends on a Synapsin Region that Mediates Phase Separation.* Cell Reports, 2020. **30**(8): p. 2594-2602. e3.
48. Ghosh, A., K. Mazarakos, and H.-X. Zhou, *Three archetypical classes of macromolecular regulators of protein liquid–liquid phase separation.* Proceedings of the National Academy of Sciences, 2019. **116**(39): p. 19474-19483.
49. Pak, C.W., et al., *Sequence determinants of intracellular phase separation by complex coacervation of a disordered protein.* Molecular cell, 2016. **63**(1): p. 72-85.
50. Russo, A. and J.P. O'Bryan, *Intersectin 1 is required for neuroblastoma tumorigenesis.* Oncogene, 2012. **31**(46): p. 4828-4834.
51. Ishida, H., et al., *Solution structures of the SH3 domains from Shank scaffold proteins and their interactions with Cav1. 3 calcium channels.* Febs Letters, 2018. **592**(16): p. 2786-2797.
52. Zhang, P., et al., *SH3RF3 promotes breast cancer stem-like properties via JNK activation and PTX3 upregulation.* Nature communications, 2020. **11**(1): p. 1-13.
53. Kwan, J.J. and L.W. Donaldson, *A lack of peptide binding and decreased thermostability suggests that the CASKIN2 scaffolding protein SH3 domain may be vestigial.* BMC structural biology, 2016. **16**(1): p. 1-6.
54. Zhu, J., et al., *Guanylate kinase domains of the MAGUK family scaffold proteins as specific phospho-protein-binding modules.* The EMBO journal, 2011. **30**(24): p. 4986-4997.
55. Jaiswal, M., R. Dvorsky, and M.R. Ahmadian, *Deciphering the Molecular and Functional Basis of Dbl Family Proteins A NOVEL SYSTEMATIC APPROACH TOWARD CLASSIFICATION OF SELECTIVE ACTIVATION OF THE Rho FAMILY PROTEINS.* Journal of Biological Chemistry, 2013. **288**(6): p. 4486-4500.
56. Estrach, S., et al., *The Human Rho-GEF trio and its target GTPase RhoG are involved in the NGF pathway, leading to neurite outgrowth.* Current biology, 2002. **12**(4): p. 307-312.
57. Humphries, A.C., S.K. Donnelly, and M. Way, *Cdc42 and the Rho GEF intersectin-1 collaborate with Nck to promote N-WASP-dependent actin polymerisation.* Journal of cell science, 2014. **127**(3): p. 673-685.
58. Amin, E., et al., *Deciphering the molecular and functional Basis of RHOGAP family proteins A systematic approach toward selective inactivation of rho family proteINS.* Journal of Biological Chemistry, 2016. **291**(39): p. 20353-20371.
59. Okada, H., et al., *Sh3 domain–based phototrapping in living cells reveals rho family gap signaling complexes.* Science signaling, 2011. **4**(201): p. rs13-rs13.
60. Birge, R.B., et al., *SH2 and SH3-containing adaptor proteins: redundant or independent mediators of intracellular signal transduction.* Genes to Cells, 1996. **1**(7): p. 595-613.
61. Roberts, J.M., et al., *Dynamics of the T ec-family tyrosine kinase SH 3 domains.* Protein Science, 2016. **25**(4): p. 852-864.
62. Levinson, N.M., P.R. Visperas, and J. Kuriyan, *The tyrosine kinase Csk dimerizes through Its SH3 domain.* PloS one, 2009. **4**(11): p. e7683.
63. Brown, M.T. and J.A. Cooper, *Regulation, substrates and functions of src.* Biochimica et Biophysica Acta (BBA)-Reviews on Cancer, 1996. **1287**(2-3): p. 121-149.
64. Zhu, J. and S.K. Shore, *c-ABL tyrosine kinase activity is regulated by association with a novel SH3-domain-binding protein.* Molecular and cellular biology, 1996. **16**(12): p. 7054-7062.

65. Salazar, M.A., et al., *Tuba, a novel protein containing bin/amphiphysin/Rvs and Dbl homology domains, links dynamin to regulation of the actin cytoskeleton.* Journal of Biological Chemistry, 2003. **278**(49): p. 49031-49043.
66. Oda, Y., et al., *Tricellulin regulates junctional tension of epithelial cells at tricellular contacts through Cdc42.* Journal of cell science, 2014. **127**(19): p. 4201-4212.
67. Young, P., E. Ehler, and M. Gautel, *Obscurin, a giant sarcomeric Rho guanine nucleotide exchange factor protein involved in sarcomere assembly.* The Journal of cell biology, 2001. **154**(1): p. 123-136.
68. Pubblicazioni, L.C., *Tinti M, Kiemer L, Costa S, Miller ML, Sacco F, Olsen JV, Carducci M, Paoluzi S, Langone F, Workman CT, Blom N, Machida K.* Mol Syst Biol, 2012. **8**(603): p. 22893001.
69. Stoll, R. and A. Bosserhoff, *Extracellular SH3 domain containing proteins-features of a new protein family.* Current Protein and Peptide Science, 2008. **9**(3): p. 221-226.
70. Fan, P.-D. and S.P. Goff, *Abl interactor 1 binds to sos and inhibits epidermal growth factor-and v-Abl-induced activation of extracellular signal-regulated kinases.* Molecular and cellular biology, 2000. **20**(20): p. 7591-7601.
71. Tong, X.K., et al., *The endocytic protein intersectin is a major binding partner for the Ras exchange factor mSos1 in rat brain.* The EMBO journal, 2000. **19**(6): p. 1263-1271.
72. Qian, X., et al., *The Sos1 and Sos2 Ras-specific exchange factors: differences in placental expression and signaling properties.* The EMBO journal, 2000. **19**(4): p. 642-654.
73. Hu, Q., D. Milfay, and L.T. Williams, *Binding of NCK to SOS and activation of ras-dependent gene expression.* Molecular and Cellular Biology, 1995. **15**(3): p. 1169-1174.
74. Chardin, P., et al., *Human Sos1: a guanine nucleotide exchange factor for Ras that binds to GRB2.* Science, 1993. **260**(5112): p. 1338-1343.
75. Nguyen, J.T., et al., *Exploiting the basis of proline recognition by SH3 and WW domains: design of N-substituted inhibitors.* Science, 1998. **282**(5396): p. 2088-2092.
76. Douangamath, A., et al., *Topography for independent binding of α-helical and PPII-helical ligands to a peroxisomal SH3 domain.* Molecular cell, 2002. **10**(5): p. 1007-1017.
77. Ren, R., et al., *Identification of a ten-amino acid proline-rich SH3 binding site.* Science, 1993. **259**(5098): p. 1157-1161.
78. Hahn, S. and D. Kim, *Transient protein-protein interaction of the SH3-peptide complex via closely located multiple binding sites.* PLoS One, 2012. **7**(3): p. e32804.
79. Hiipakka, M., K. Poikonen, and K. Saksela, *SH3 domains with high affinity and engineered ligand specificities targeted to HIV-1 Nef.* Journal of molecular biology, 1999. **293**(5): p. 1097-1106.
80. Evanics, F., et al., *19F NMR studies of solvent exposure and peptide binding to an SH3 domain.* Biochimica et Biophysica Acta (BBA)-General Subjects, 2007. **1770**(2): p. 221-230.
81. Ahmad, M., W. Gu, and V. Helms, *Mechanism of fast peptide recognition by SH3 domains.* Angewandte Chemie International Edition, 2008. **47**(40): p. 7626-7630.
82. Mayer, B.J. and K. Saksela, *SH3 domains.* Protein Science Encyclopedia: online, 2008.
83. Ladbury, J.E. and S. Arold, *Searching for specificity in SH domains.* Chemistry & biology, 2000. **7**(1): p. R3-R8.
84. Kay, B.K., M.P. Williamson, and M. Sudol, *The importance of being proline: the interaction of proline-rich motifs in signaling proteins with their cognate domains.* The FASEB journal, 2000. **14**(2): p. 231-241.
85. Sparks, A.B., et al., *Distinct ligand preferences of Src homology 3 domains from Src, Yes, Abl, cortactin, p53bp2, PLCgamma, Crk, and Grb2.* Proceedings of the National Academy of Sciences, 1996. **93**(4): p. 1540-1544.

86. Zarrinpar, A., S.-H. Park, and W.A. Lim, *Optimization of specificity in a cellular protein interaction network by negative selection.* Nature, 2003. **426**(6967): p. 676-680.
87. Egan, S.E., et al., *Association of Sos Ras exchange protein with Grb2 is implicated in tyrosine kinase signal transduction and transformation.* Nature, 1993. **363**(6424): p. 45-51.
88. Chook, Y.M., et al., *The Grb2-mSos1 complex binds phosphopeptides with higher affinity than Grb2.* Journal of Biological Chemistry, 1996. **271**(48): p. 30472-30478.
89. Dornan, D., et al., *The proline repeat domain of p53 binds directly to the transcriptional coactivator p300 and allosterically controls DNA-dependent acetylation of p53.* Molecular and cellular biology, 2003. **23**(23): p. 8846-8861.
90. Verschueren, E., et al., *Evolution of the SH3 domain specificity Landscape in Yeasts.* PloS one, 2015. **10**(6): p. e0129229.
91. Yu, H., et al., *Structural basis for the binding of proline-rich peptides to SH3 domains.* Cell, 1994. **76**(5): p. 933-945.
92. Balakrishnan, S., M.J. Scheuermann, and N.J. Zondlo, *Arginine Mimetics via α-Guanidino Acids: Introduction of Functional Groups and Stereochemistry Adjacent to Recognition Guanidiniums in Peptides.* Chembiochem: a European journal of chemical biology, 2012. **13**(2): p. 259.
93. Jaiswal, M., et al., *Functional cross-talk between ras and rho pathways: a Ras-specific GTPase-activating protein (p120RasGAP) competitively inhibits the RhoGAP activity of deleted in liver cancer (DLC) tumor suppressor by masking the catalytic arginine finger.* Journal of Biological Chemistry, 2014. **289**(10): p. 6839-6849.
94. Stevers, L.M., et al., *A thermodynamic model for multivalency in 14-3-3 protein–protein interactions.* Journal of the American Chemical Society, 2018. **140**(43): p. 14498-14510.
95. Vidal, M., et al., *Molecular and cellular analysis of Grb2 SH3 domain mutants: interaction with Sos and dynamin.* Journal of molecular biology, 1999. **290**(3): p. 717-730.
96. Hanawa-Suetsugu, K., et al., *Structural basis for mutual relief of the Rac guanine nucleotide exchange factor DOCK2 and its partner ELMO1 from their autoinhibited forms.* Proceedings of the National Academy of Sciences, 2012. **109**(9): p. 3305-3310.
97. Kami, K., et al., *Diverse recognition of non-PxxP peptide ligands by the SH3 domains from p67phox, Grb2 and Pex13p.* The EMBO journal, 2002. **21**(16): p. 4268-4276.
98. Massenet, C., et al., *Effects of p47phox C terminus phosphorylations on binding interactions with p40phox and p67phox: structural and functional comparison of p40phox and p67phox SH3 domains.* Journal of Biological Chemistry, 2005. **280**(14): p. 13752-13761.
99. Mott, H.R., et al., *Structural analysis of the SH3 domain of β-PIX and its interaction with α-p21 activated kinase (PAK).* Biochemistry, 2005. **44**(33): p. 10977-10983.
100. Jozic, D., et al., *Cbl promotes clustering of endocytic adaptor proteins.* Nature structural & molecular biology, 2005. **12**(11): p. 972-979.
101. Hashimoto, S., et al., *Targeting AMAP1 and cortactin binding bearing an atypical src homology 3/proline interface for prevention of breast cancer invasion and metastasis.* Proceedings of the National Academy of Sciences, 2006. **103**(18): p. 7036-7041.
102. Moncalián, G., et al., *Atypical polyproline recognition by the CMS N-terminal Src homology 3 domain.* Journal of Biological Chemistry, 2006. **281**(50): p. 38845-38853.
103. Takeuchi, K., et al., *Structural and functional evidence that Nck interaction with CD3ε regulates T-cell receptor activity.* Journal of molecular biology, 2008. **380**(4): p. 704-716.
104. Aitio, O., et al., *Recognition of tandem PxxP motifs as a unique Src homology 3-binding mode triggers pathogen-driven actin assembly.* Proceedings of the National Academy of Sciences, 2010. **107**(50): p. 21743-21748.
105. Gehmlich, K., et al., *Paxillin and ponsin interact in nascent costameres of muscle cells.* Journal of molecular biology, 2007. **369**(3): p. 665-682.

106. Schmidt, H., et al., *Solution structure of a Hck SH3 domain ligand complex reveals novel interaction modes.* Journal of molecular biology, 2007. **365**(5): p. 1517-1532.
107. Janz, J.M., T.P. Sakmar, and K.C. Min, *A novel interaction between atrophin-interacting protein 4 and β-p21-activated kinase-interactive exchange factor is mediated by an SH3 domain.* Journal of Biological Chemistry, 2007. **282**(39): p. 28893-28903.
108. Aitio, O., et al., *Structural basis of PxxDY motif recognition in SH3 binding.* Journal of molecular biology, 2008. **382**(1): p. 167-178.
109. Guettler, S., et al., *Structural basis and sequence rules for substrate recognition by Tankyrase explain the basis for cherubism disease.* Cell, 2011. **147**(6): p. 1340-1354.
110. Rouka, E., et al., *Differential recognition preferences of the three Src homology 3 (SH3) domains from the adaptor CD2-associated protein (CD2AP) and direct association with Ras and Rab interactor 3 (RIN3).* Journal of Biological Chemistry, 2015. **290**(42): p. 25275-25292.
111. Polle, L., et al., *Structural details of human tuba recruitment by InlC of Listeria monocytogenes elucidate bacterial cell-cell spreading.* Structure, 2014. **22**(2): p. 304-314.
112. Chen, Q. and M. Georgiadis, *Crystallization of and selenomethionine phasing strategy for a SETMAR–DNA complex.* Acta Crystallographica Section F: Structural Biology Communications, 2016. **72**(9): p. 713-719.
113. Eulitz, S., et al., *Identification of Xin-repeat proteins as novel ligands of the SH3 domains of nebulin and nebulette and analysis of their interaction during myofibril formation and remodeling.* Molecular biology of the cell, 2013. **24**(20): p. 3215-3226.
114. Zhao, D., et al., *Structural investigation of the interaction between the tandem SH3 domains of c-Cbl-associated protein and vinculin.* Journal of structural biology, 2014. **187**(2): p. 194-205.
115. Camara-Artigas, A., et al., *The role of water molecules in the binding of class I and II peptides to the SH3 domain of the Fyn tyrosine kinase.* Acta Crystallographica Section F: Structural Biology Communications, 2016. **72**(9): p. 707-712.
116. Shimada, A., A. Yamaguchi, and D. Kohda, *Structural basis for the recognition of two consecutive mutually interacting DPF motifs by the SGIP1 μ homology domain.* Scientific reports, 2016. **6**(1): p. 1-14.
117. Bhatt, V.S., et al., *Binding mechanism of the N-terminal SH3 domain of CrkII and proline-rich motifs in cAbl.* Biophysical journal, 2016. **110**(12): p. 2630-2641.
118. Hologne, M., et al., *NMR reveals the interplay among the AMSH SH3 binding motif, STAM2, and Lys63-linked diubiquitin.* Journal of molecular biology, 2016. **428**(22): p. 4544-4558.
119. Desrochers, G., et al., *Molecular basis of interactions between SH3 domain-containing proteins and the proline-rich region of the ubiquitin ligase Itch.* Journal of Biological Chemistry, 2017. **292**(15): p. 6325-6338.
120. Lemmon, M.A., et al., *Independent binding of peptide ligands to the SH2 and SH3 domains of Grb2.* Journal of Biological Chemistry, 1994. **269**(50): p. 31653-31658.
121. Houtman, J.C., et al., *Oligomerization of signaling complexes by the multipoint binding of GRB2 to both LAT and SOS1.* Nature structural & molecular biology, 2006. **13**(9): p. 798-805.
122. Bartelt, R.R., et al., *Regions outside of conserved PxxPxR motifs drive the high affinity interaction of GRB2 with SH3 domain ligands.* Biochimica et Biophysica Acta (BBA)-Molecular Cell Research, 2015. **1853**(10): p. 2560-2569.
123. Sastry, L., et al., *Quantitative analysis of Grb2-Sos1 interaction: the N-terminal SH3 domain of Grb2 mediates affinity.* Oncogene, 1995. **11**(6): p. 1107-1112.

124. McDonald, C.B., et al., *SH3 domains of Grb2 adaptor bind to PXψPXR motifs within the Sos1 nucleotide exchange factor in a discriminate manner.* Biochemistry, 2009. **48**(19): p. 4074-4085.
125. McDonald, C.B., et al., *Structural basis of the differential binding of the SH3 domains of Grb2 adaptor to the guanine nucleotide exchange factor Sos1.* Archives of biochemistry and biophysics, 2008. **479**(1): p. 52-62.
126. Innocenti, M., et al., *Mechanisms through which Sos-1 coordinates the activation of Ras and Rac.* Journal of Cell Biology, 2002. **156**(1): p. 125-136.
127. Liao, T.-J., et al., *High-affinity Interactions of the nSH3/cSH3 Domains of Grb2 with the C-terminal Proline-rich Domain of SOS1.* Journal of the American Chemical Society, 2020. **142**(7): p. 3401-3411.
128. Fang, N.N., et al., *Rsp5/Nedd4 is the main ubiquitin ligase that targets cytosolic misfolded proteins following heat stress.* Nature cell biology, 2014. **16**(12): p. 1227-1237.
129. Peil, L., et al., *Distinct XPPX sequence motifs induce ribosome stalling, which is rescued by the translation elongation factor EF-P.* Proceedings of the National Academy of Sciences, 2013. **110**(38): p. 15265-15270.
130. Hupp, T.R. and M. Walkinshaw, *Multienzyme assembly of a p53 transcription complex.* Nature structural & molecular biology, 2007. **14**(10): p. 885-887.
131. Guruprasad, L., et al., *The crystal structure of the N-terminal SH3 domain of Grb2.* Journal of molecular biology, 1995. **248**(4): p. 856-866.
132. Tan, S.-H., et al., *A correlated motif approach for finding short linear motifs from protein interaction networks.* BMC bioinformatics, 2006. **7**(1): p. 502.
133. Rader, K., et al., *Characterization of ANKRA, a novel ankyrin repeat protein that interacts with the cytoplasmic domain of megalin.* Journal of the American Society of Nephrology, 2000. **11**(12): p. 2167-2178.
134. Menon, R.P. and R.C. Hughes, *Determinants in the N-terminal domains of galectin-3 for secretion by a novel pathway circumventing the endoplasmic reticulum–Golgi complex.* European journal of biochemistry, 1999. **264**(2): p. 569-576.
135. Beltrao, P. and L. Serrano, *Comparative genomics and disorder prediction identify biologically relevant SH3 protein interactions.* PLoS computational biology, 2005. **1**(3).
136. Kowanetz, K., et al., *CIN85 associates with multiple effectors controlling intracellular trafficking of epidermal growth factor receptors.* Molecular biology of the cell, 2004. **15**(7): p. 3155-3166.
137. D'erchia, A., et al., *Guinea pig p53 mRNA: identification of new elements in coding and untranslated regions and their functional and evolutionary implications.* Genomics, 1999. **58**(1): p. 50-64.

Figure legends

Figure 1/ Graphical representations of overall structure and domain organization of SH3 domain-containing proteins. Domain composition and organization of 221 human SH3-containing proteins is presented in an alphabetical order. Functional domains other than SH3 (red) are membrane lipid binding domains (blue), peptide and protein interaction domains (green), and domains with enzymatic and regulatory activities (orange).

Figure 2/ Evolutionary sequence-structure-function relationships of the SH3 domains. Whole-sequence phylogenetic tree of 298 human SH3 domains was generated using MEGA7 program. The specificity of the SH3 domains for distinct PRMs (colored dots) is highlighted according to available structural and biochemical studies [28] (Table S2). The tree shows a well distributed of published structures (Table S2) of the SH3 domains (red) in complex with the assigned proline-rich peptides.

Figure 3/ Evolutionary sequence-structure-function relationships of the PRM interfacing residues of SH3 domains. (A) The phylogenic tree of extracted PRM-interacting residues of 298 human SH3 domains was generated using MEGA7 program. The specificity of the SH3 domains for distinct PRMs (colored dots) is highlighted according to available structural and biochemical studies [28] (Table S2). The tree shows a well distributed of published structures (Table S2) of the SH3 domains (red) in complex with the assigned proline-rich peptides. The SH3 domains are grouped in ten different families to which were defined PRMs are assigned. (B) The interfacing residues of the representatives were aligned using ClustalW multiple alignment in BioEdit software. The order of the sequences starts with family 1 in yellow and ends with family 10 in brown. The identical sequences are shown in light orange boxes.

Figure 4/The binding selectivities of SH3 domain representatives to different PRP types. (A) Dot-blot analysis of 12 fluorescent PRPs pulled down with GST-SH3 domains. The PRPs P1 to P10 were derived from SOS1 PRD. The reference peptide RP1 is a derivative of SOS1, and RP2 a derivative of the RHO GTPase WRCH1. Note that RP1 is part of P3. The dot intensities were divided in five groups from 10 (red) to 100 (green). (B) Bar charts illustrating evaluated dissociation constants (K_d) for the SH3-PRP interactions (Table S6; Fig. S5). The colors of the bar charts highlight the K_d values (above the bars), which are divided in high affinity (0.2 – 5 µM; green), intermediate affinity (6 – 20 µM; blue), and low affinity (>21 µM; red).

Figure5/ The conserved residues of SH3 domain subfamilies defines their specificity towards proline-rich motifs. (A) The conserved residues between SH3 domains interacting with specific proline-rich peptide were defined by aligning of interfacing residues. (B) Mutational analysis of the conserved residues defining specificity were perfumed considering the higher

affinities in the SH3-PRMs interactions. NCK1.3 and RHG12 were selected for the mutational analysis. The reported residues important for the interaction of RHG12 and NCK1 with P7 and P9, respectively, were mutated to alanine. (C) The physiological relevance of the SH3-PRMs with affinities in nM range were investigated in HEK293. HA. SOS1 were transfected into HEK293. GST pulldown assay was performed for the interaction analysis of the His-tagged MBP-RA domains of RASSF proteins with HA-SOS1 and GST-RHG12 and GST-NCK1.3. GST-SH3 proteins were coupled to the bead and after incubation for one hour and washing steps, the HA-SOS1, overexpressed in HEK 293T cells as cell lysate was added to the GST-SH3 domains coupled to the beads. Anti-GST antibody was used for the detection of GST-tagged SH3 domains of RHG12 and NCK1.3 as input and output control. Input and output samples on one gel helps to show the functionality of the pulldown assay and having comparable levels of RASSF5 vs RASSF7 vs RASSF9 in input samples and also having comparable levels of RASSF5 vs RASSF7 vs RASSF9 bound to the beads in output samples. Immunoblots of total cell lysates (TCL) were served as a loading control to show the equal amount of used cell lysate for each pulldown. SOS1 level were analyzed by immunoblotting (IB) using anti-HA antibody.

Figure 1

Figure 2

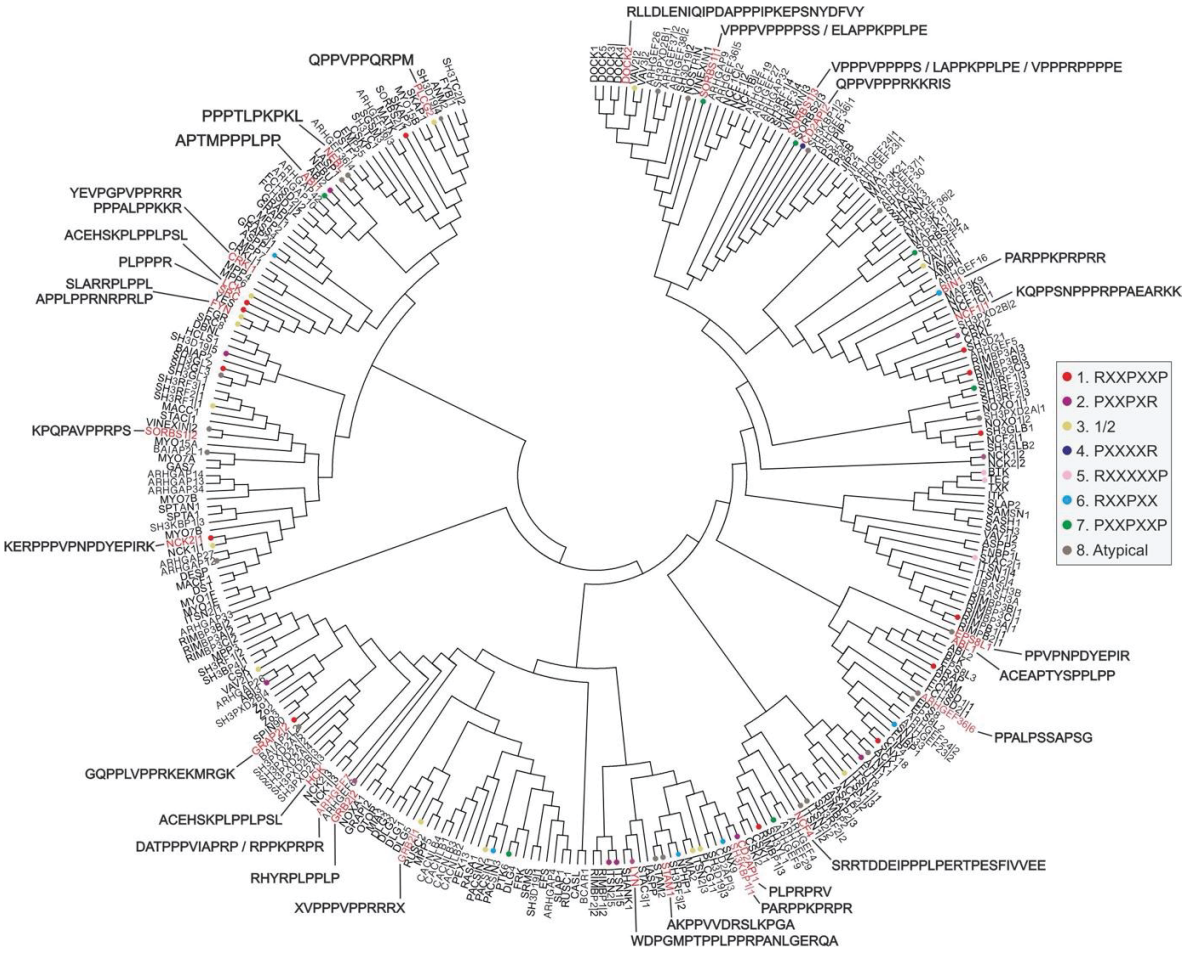
RLLDLENIQIPDAPPPIPKEPSNYDFVY
VPPPVPPPPSS / ELAPPKPPLPE
VPPPVPPPPS / LAPPKPPLPE / VPPPRPPPPE
QPPVPPPRKKRIS
PARPPKPRPRR
KQPPSNPPPRPPAEARKK
PPVPNPDYEPIR
ACEAPTYSPPLPP
PPALPSSAPSG
SRRTDDEIPPPLPERTPESFIVVEE
PLPRPRV
PARPPKPRPR
AKPPVVDRSLKPGA
WDPGMPTPPLPPRPANLGERQA
XVPPPVPPRRRX
RHYRPLPPLP
DATPPPVIAPRP / RPPKPRPR
ACEHSKPLPPLPSL
GQPPLVPPRKEKMRGK
KERPPPVPNPDYEPIRK
KPQPAVPPRPS
APLPPRNRPRLP
SLARRPLPPL
PLPPPR
ACEHSKPLPPLPSL
PPPALPPKKR
YEVPGPVPPRRR
APTMPPPLPP
PPPTLPKPKL
QPPVPPQRPM
1. RXXPXXP
2. PXXPXR
3. 1/2
4. PXXXXR
5. RXXXXXP
6. RXXPXX
7. PXXPXXP
8. Atypical

Figure 3

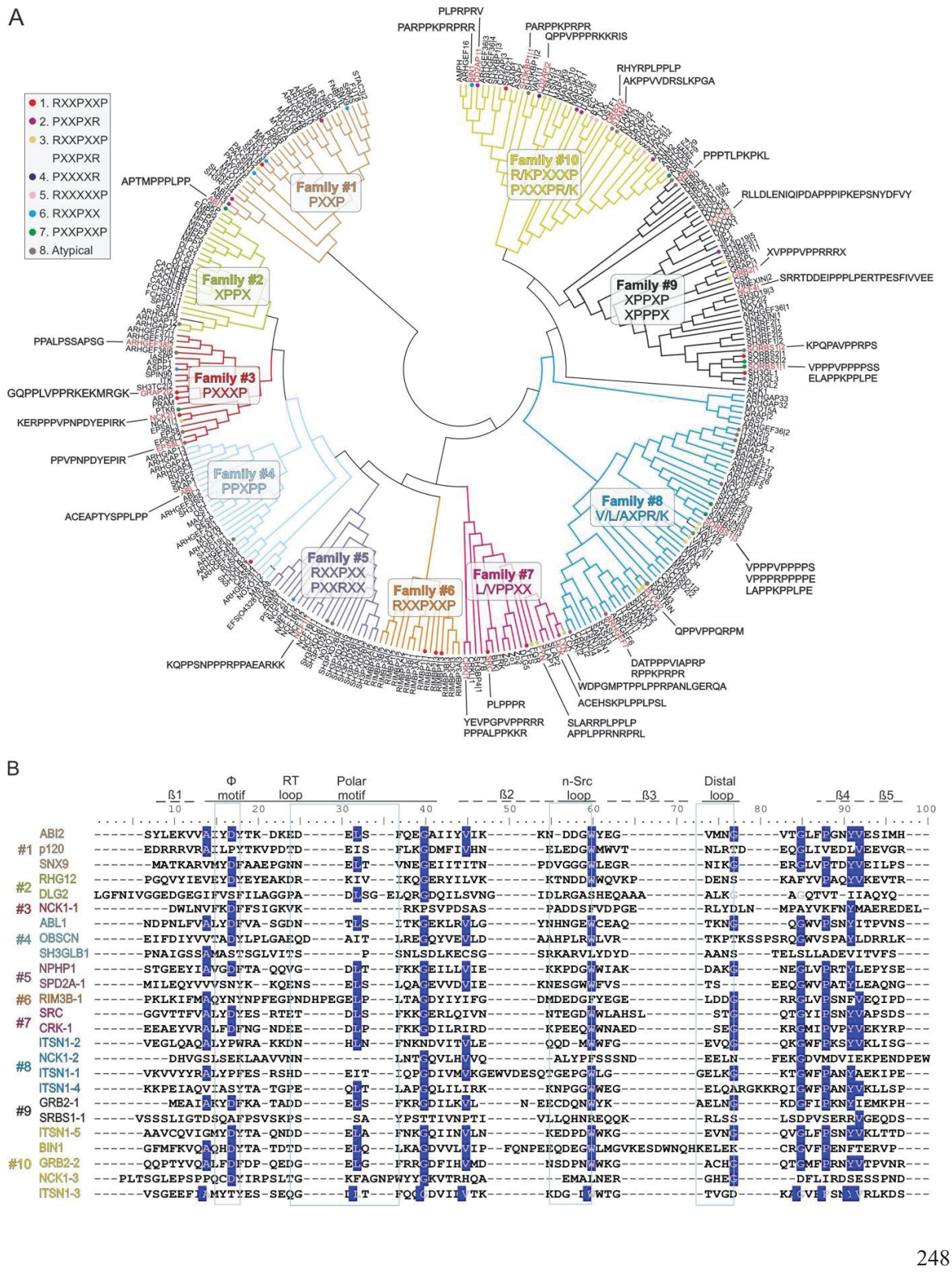
A
1. RXXPXXP
2. PXXPXR
3. RXXPXXP
PXXPXR
4. PXXXXR
5. RXXXXXP
6. RXXPXX
7. PXXPXXP
8. Atypical
Family #1
PXXP
Family #2
XPPX
Family #3
PXXXP
Family #4
PPXPP
Family #5
RXXPXX
PXXRXX
Family #6
RXXPXXP
Family #7
L/VPPXX
Family #8
V/L/AXPR/K
Family #9
XPPXP
XPPPX
Family #10
R/KPXXXP
PXXXPR/K
APTMPPPLPP
PPALPSSAPSG
GQPPLVPPRKEKMRGK
KERPPPVPNPDYEPIRK
PPVPNPDYEPIR
ACEAPTYSPPLPP
KQPPSNPPPRPPAEARKK
PLPRPRV
PARPPKPRPRR
PARPPKPRPR
QPPVPPPRKKRIS
RHYRPLPPLP
AKPPVVDRSLKPGA
PPPTLPKPKL
RLLDLENIQIPDAPPPIPKEPSNYDFVY
XVPPPVPPRRRX
SRRTDDEIPPPLPERTPESFIVVEE
KPQPAVPPRPS
VPPPVPPPPSS
ELAPPKPPLPE
VPPPVPPPPS
VPPPRPPPPE
LAPPKPPLPE
QPPVPPQRPM
DATPPPVIAPRP
RPPKPRPR
WDPGMPTPPLPPRPANLGERQA
ACEHSKPLPPLPSL
PLPPPR
YEVPGPVPPRRR
PPPALPPKKR
SLARRPLPPLP
APPLPPRNRPRL
B
ß1
Φ motif
RT loop
Polar motif
ß2
n-Src loop
ß3
Distal loop
ß4
ß5
ABI2
#1 p120
SNX9
#2 RHG12
DLG2
#3 NCK1-1
ABL1
#4 OBSCN
SH3GLB1
#5 NPHP1
SPD2A-1
#6 RIM3B-1
#7 SRC
CRK-1
ITSN1-2
#8 NCK1-2
ITSN1-1
ITSN1-4
#9 GRB2-1
SRBS1-1
ITSN1-5
BIN1
#10 GRB2-2
NCK1-3
ITSN1-3

Figure 4

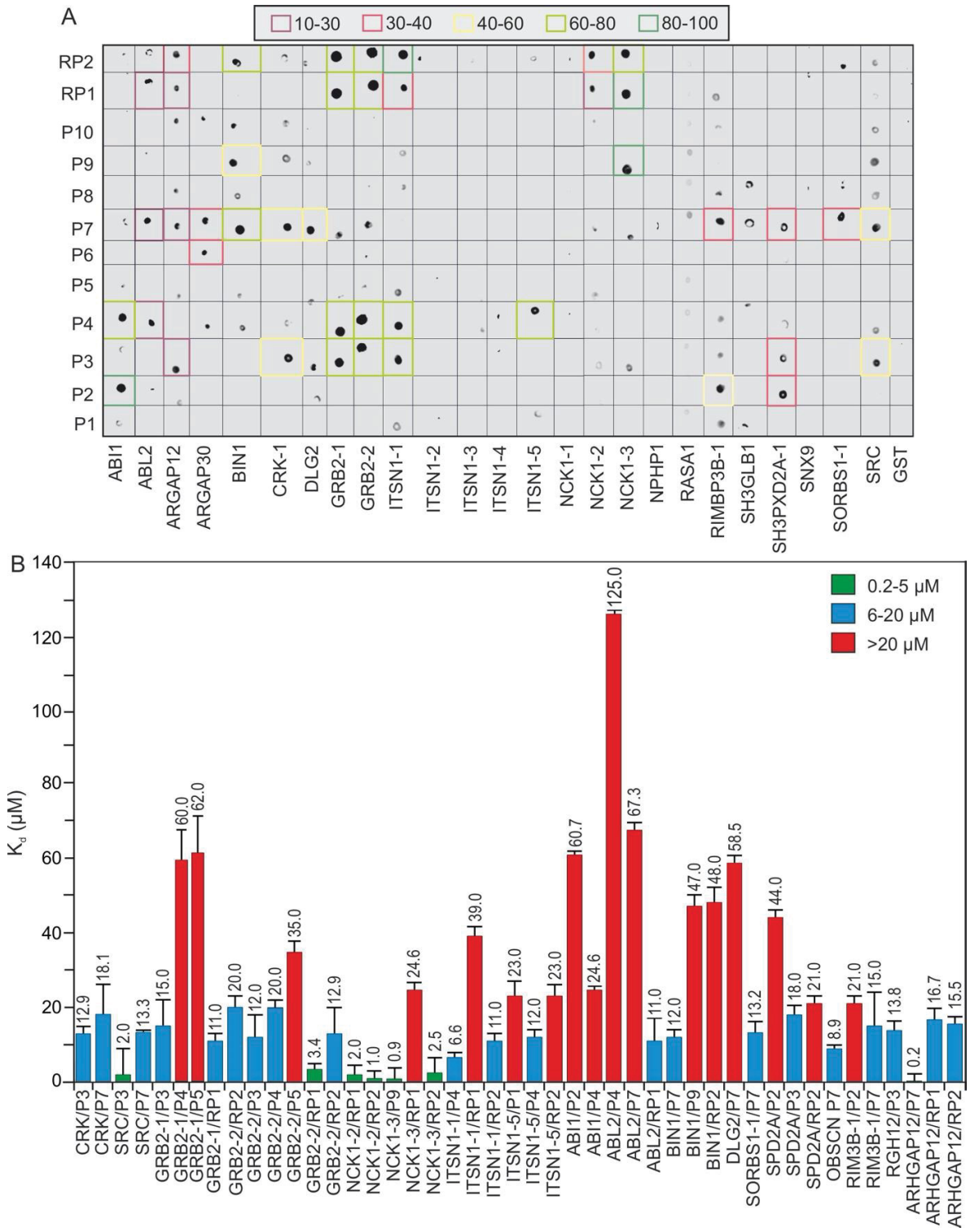
A
10-30
30-40
40-60
60-80
80-100
RP2
RP1
P10
P9
P8
P7
P6
P5
P4
P3
P2
P1
ABI1
ABL2
ARGAP12
ARGAP30
BIN1
CRK-1
DLG2
GRB2-1
GRB2-2
ITSN1-1
ITSN1-2
ITSN1-3
ITSN1-4
ITSN1-5
NCK1-1
NCK1-2
NCK1-3
NPHP1
RASA1
RIMBP3B-1
SH3GLB1
SH3PXD2A-1
SNX9
SORBS1-1
SRC
GST
B
0.2-5 μM
6-20 μM
>20 μM
K_d (μM)
0
20
40
60
80
100
120
140
12.9
18.1
2.0
13.3
15.0
60.0
62.0
11.0
20.0
12.0
20.0
35.0
3.4
12.9
2.0
1.0
0.9
24.6
2.5
6.6
39.0
11.0
23.0
12.0
23.0
60.7
24.6
125.0
67.3
11.0
12.0
47.0
48.0
58.5
13.2
44.0
18.0
21.0
8.9
21.0
15.0
13.8
0.2
16.7
15.5
CRK/P3
CRK/P7
SRC/P3
SRC/P7
GRB2-1/P3
GRB2-1/P4
GRB2-1/P5
GRB2-1/RP1
GRB2-2/RP2
GRB2-2/P3
GRB2-2/P4
GRB2-2/P5
GRB2-2/RP1
GRB2-2/RP2
NCK1-2/RP1
NCK1-2/RP2
NCK1-3/P9
NCK1-3/RP1
NCK1-3/RP2
ITSN1-1/P4
ITSN1-1/RP1
ITSN1-1/RP2
ITSN1-5/P1
ITSN1-5/P4
ITSN1-5/RP2
ABI1/P2
ABI1/P4
ABL2/P4
ABL2/P7
ABL2/RP1
BIN1/P7
BIN1/P9
BIN1/RP2
DLG2/P7
SORBS1-1/P7
SPD2A/P2
SPD2A/P3
SPD2A/RP2
OBSCN P7
RIM3B-1/P2
RIM3B-1/P7
RGH12/P3
ARHGAP12/P7
ARHGAP12/RP1
ARHGAP12/RP2

Figure 5

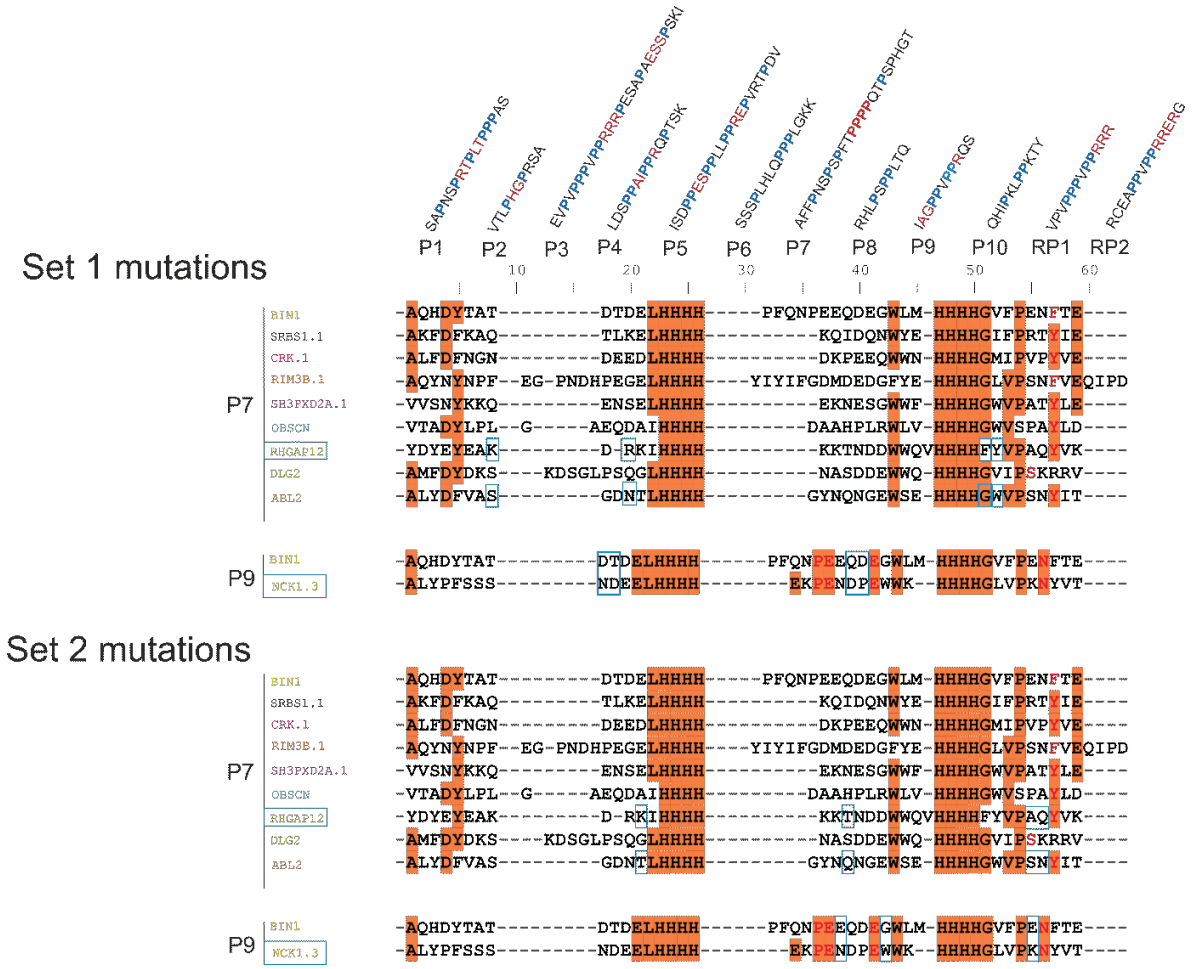
Set 1 mutations
Set 2 mutations
P1
P2
P3
P4
P5
P6
P7
P8
P9
P10
RP1
RP2
BIN1
SRBS1.1
CRK.1
RIM3B.1
SH3PXD2A.1
OBSCN
RHGAP12
DLG2
ABL2
NCK1.3

Supplementary information

Genome-wide identification, functional classification and interaction selectivity landscape of human SH3 domain superfamily*

Neda S. Kazemein Jasemi[1], Mehrnaz Mehrabipour[1], Eva M. Estirado[2], Luc Brunsveld[2], Radovan Dvorsky[1], Mohammad R. Ahmadian[1]

[1]Institute of Biochemistry and Molecular Biology II, Medical Faculty of the Heinrich-Heine University, 40225 Düsseldorf, Germany; [2]De Laboratory of Chemical Biology, Department of Biomedical Engineering and Institute of Complex Molecular Systems (ICMS), Eindhoven University of Technology, P.O. Box 513, 5600MB, Eindhoven, The Netherlands.

Table S1. The superfamily of human SH3 domain-containing protein (1-50)

Entry name (No. of SH3)	Aliases, interactions & functions	Uniprot ID
ABI1 (1)	E3B1; binds Abl, spectrin & EPS8; regulate the dendritic outgrowth & branching	Q8IZP0
ABI2 (1)	ArgBP1; component of the WAVE complex; involved in cell motility & adhesion	Q9NYB9
ABI3 (1)	NESH; component of the WAVE complex, regulates dendritic Spine Morphology	Q9P2A4
ABL1 (1)	Proto-oncogene tyrosine-protein kinase; regulates adhesion, motility & differentiation	P00519
ABL2 (1)	Proto-oncogene tyrosine-Protein kinase; regulates adhesion, motility & differentiation	P42684
ACK1 (1)	TNK2; phosphorylates AKT1, AR, WASP; mediates CDC42-dependent cell migration	Q07912
AHI1 (1)	JBTS3; involved in vesicle trafficking, ciliogenesis & WNT signaling	Q8N157
AMPH (1)	Amphiphysin; involved in regulated exocytosis	P49418
ANM2 (1)	PRMT2; methylates the arginines in STAT3, FBL, & H4; involved in growth regulation	P55345
ARAP (1)	**2 FYB2; T-cell receptor signaling & integrin-mediated adhesion**	Q5VWT5
ARHGAP4 (1)	RGC1; SRGAP4; acts as RHOGAP in hematopoietic cells	P98171
ARHGAP9 (1)	RGL1; acts as a CDC42/RAC1 GAP; regulates matrix adhesion of hematopoietic cells	Q9BRR9
ARHGAP10 (1)	GRAF2; PSGAP; acts as a GAP on CDC42 & RHOA; involved in actin organization	A1A4S6
ARHGAP12 (1)	Acts as a GAP on RHO family proteins, maybe downstream of the GPCR Signaling	Q8IWW6
ARHGAP13 (1)	SRGAP1; Acts as RhoA/CDC42GAP in neuronal migration	Q7Z6B7
ARHGAP14 (1)	SRGAP3; WRP; MEGAP; WAVE-associated Rac1/CDC42GAP	O43295
ARHGAP26 (1)	GRAF1; acts as a GAP on RHO family proteins in pathways related focal adhesion	Q9UNA1
ARHGAP27 (1)	CAMGAP1; SH3D20; acts as a GAP on RHO family proteins in endocytosis	Q6ZUM4
ARHGAP32 (1)	p200; GRIT; acts as a RHOGAP in the differentiation of neuronal cells	A7KAX9
ARHGAP33 (1)	SNX26; TCGAP; acts as a GAP on RHO family proteins in intracellular trafficking	O14559
ARHGAP34 (1)	SRGAP2; regulates as a RAC1GAP cell migration and differentiation	O75044
ARHGAP42 (1)	GRAF3; acts as a GAP on RHO family proteins in vascular smooth muscle	A6NI28
ARHGEF4 (1)	ASEF1; STM6; a CDC42 GEF, involved in cell-cell adhesion & migration	Q9NR80
ARHGEF5 (1)	Ephexin-3; p60TIM; RHOAGEF; involved in SRC-induced podosome formation	Q12774
ARHGEF6 (1)	αPIX; COOL2; RAC/CDC42GEF; associated with X-linked intellectual disability	Q15052
ARHGEF7 (1)	βPIX, CCOL1; RAC/CDC42GEF; cell adhesion, spreading & migration	Q14155
ARHGEF9 (1)	HPEM1; Collybistin; RAC/CDC42GEF; formation of GABAergic & glycinergic synapses	O43307
ARHGEF14 (1)	MCF2L; RHOA/CDC42GEF associated with osteoarthritis	O15068
ARHGEF16 (1)	Ephexin4; RHOG/CDC42GEF; cell migration	Q5VV41
ARHGEF19 (1)	Ephexin2; WGEF; RHOAGEF; interacts with BRAF & activates MAPK pathway	Q8IW93
ARHGEF23 (2)	TRIO, MRD44; acts as a dual RAC1/RHOAGEF in hippocampal neurons	O75962
ARHGEF24 (2)	KALRN; DUO; TRAD; regulate as a RHOGEF neuronal shape, growth & plasticity	O60229
ARHGEF26 (1)	SGEF; RHOGGEF; macropinocytosis; trans-endothelial migration of leukocytes	Q96DR7
ARHGEF27 (1)	NGEF; EPHEXIN1; acts as a RHOGEF ephrin-induced axon & spine morphogenesis	Q8N5V2
ARHGEF29 (1)	ASEF2; SPATA13; acts as a CDC42GEF in cell migration & adhesion	Q96N96
ARHGEF30 (1)	OBSCN; Obscurin; a giant sacromeric protein; calmodulin and titin binding	Q5VST9
ARHGEF36 (6)	TUBA; DNMBP; links dynamin to actin regulatory proteins & is involved in adhesion	Q6XZF7
ARHGEF37 (2)	**3 FLJ41603; RHOGEF; clathrin-mediated endocytosis, GPCR & p75-NRT signaling**	A1IGU5
ARHGEF38 (1)	FLJ20184; RHOGEF; GPCR & p75-NRT signaling	Q9NXL2
ASAP1 (1)	AMAP1; Centaurinβ4; ARF1/ARF5GAP; coordinate membrane trafficking; ciliogenesis	Q9ULH1
ASAP2 (1)	AMAP2; Centaurinβ3; ARFGAP; PYK2 & SRC substrate; regulates vesicular transport	O43150
ASPP1 (1)	PPP1R13B; regulates the DNA binding & transactivation function of p53	Q96KQ4
ASPP2 (1)	TP53BP2; P53BP2; regulates cell growth & apoptosis by binding to p53 & BCL2	Q13625
BAIAP2 (1)	IRS58; links RAC1/CDC42 to downstream effectors; promotes filopodial protrusions	Q9UQB8
BAIAP2L1 (1)	IRTKS; IR substrate; RAC1 binding; promotes actin assembly & membrane protrusions	Q9UHR4
BAIAP2L2 (1)	Pinkbar; formation of curved membrane structures	Q6UXY1
BCAR1 (1)	p130CAS; CAS1; CASS1; regulates cell adhesion & migration	P56945

BIN1 (1)	AMPHL; SH3P9; membrane curvature & remodeling; negative regulator of endocytosis	O00499
BLK (1)	MODY11; p55; B-cell receptor signaling & development	P51451
BTK (1)	ATK; BPK; XLA; B-cell development & differentiation & signaling	Q06187

Table S1. The superfamily of human SH3 domain-containing protein (51-100)

Entry name (No. of SH3)	Aliases, interactions & functions	Uniprot ID
CACNLB1 (1)	CAB1; CCHLB1; regulates the activity of L-type calcium channels	Q02641
CACNLB2 (1)	CAVB2; MYSB; a subunit of voltage-dependent calcium channels	Q08289
CACNLB3 (1)	CAB3; a regulatory subunit of the voltage-gated calcium channel	P54284
CACNLB4 (1)	CAB4, EJM4; EIG4; a dihydropyridine-sensitive subunit of L-type calcium channel	O00305
CASL (1)	CAS2; NEDD9; CASS2; regulates cell adhesion & migration	Q14511
CASS4 (1)	CAS4; HEFL; regulates focal adhesion integrity & cell spreading	Q9NQ75
CD2AP (3)	CMS; involved in receptor clustering & cytoskeletal polarity	Q9Y5K6
CIP4 (1)	TRIP10; STP; promotes CDC42(WASP-induced actin polymerization	Q15642
CRK (2)	CRKII; regulates cell adhesion, spreading & migration	P46108
CRKL (2)	CRK-like adaptor protein that activate the RAS & JUN kinase signaling pathways	P46109
CSK (1)	CYL; regulates cell growth, migration & immune response	P41240
CSKI1 (1)	CASKIN1; ANKS5A; links CASK to downstream intracellular effectors	Q8WXD9
CSKI2 (1)	CASKIN2; ANKS5B; links CASK to downstream intracellular effectors	Q8WXE0
CSKP (1)	CASK; FGS4; LIN2; HCASK; a Ca2+/CAM-dependent kinase involved in neurogenesis	O14936
DBNL (1)	SH3P7; ABP1; CMAP; HIP55; involved endocytic pathways & podosome formation	Q9UJU6
DESP (1)	DSP; Desmoplakin; is part of the desmosomal cadherin-plakoglobin complexes	P15924
DLG1 (1)	SAP97; DLGH1; involved in synaptogenesis & lymphocyte activation	Q12959
DLG2 (1)	PSD93; binds NMDA receptor subunits & regulates excitatory synapses	Q15700
DLG3 (1)	MRX90; SAP102; XLMR; involved in NMDA receptor-mediated synaptic plasticity	Q92796
DLG4 (1)	PSD95; SAP90; required for synaptic plasticity associated with NMDA receptor signaling	P78352
DLG5 (1)	PDLG; involved in dendritic spine formation & synaptogenesis as well as ciliogenesis	Q8TDM6
DOCK1 (1)	DOCK180; as a GEF regulates cell spreading & migration	Q14185
DOCK2 (1)	IMD40; involved as RAC1/2 GEF in lymphocyte migration	Q92608
DOCK3 (1)	MOCA; PBP; activates as a RACGEF the WAVE complex & induces axonal outgrowth	Q8IZD9
DOCK4 (1)	KIAA0716; with its RHOGEF function regulates cell migration	Q8N1I0
DOCK5 (1)	Associates with CRK/CRKL, & regulates epithelial cell spreading & migration	Q9H7D0
DST (1)	BP240; HSAN6; MACF2; acts as a cytoskeletal linker protein on axonal transport	Q03001
EFS (1)	HEFS, CAS3; SIN; acts as SRC activator on cell adhesion	O43281
EMP55 (1)	MPP1; AAG12; EMP55; as a MAGUK family proteins regulates neutrophil polarity	Q00013
EPS8 (1)	DFNB102; regulates in complex with SOS1/ABI1 cell migration & invasion	Q12929
EPS8L1 (1)	DRC3; EPS8R1; involved in membrane ruffling & remodeling of the actin cytoskeleton	Q8TE68
EPS8L2 (1)	DFNB106; required for stereocilia maintenance in adult hair cells	Q9H6S3
EPS8L3 (1)	EPS8R3; function unknown	Q8TE67
FCHSD1 (2)	NWK2; promotes SNX9WASL-mediated actin polymerization.	Q86WN1
FCHSD2 (2)	NWK1; SH3MD3; promotes actin polymerization & internalization of surface receptors	O94868
FGR (1)	SRC2; regulates immune responses via AKT1, ABL1, CBL, CTTN, FAK1, PYK2 & VAV2	P09769
FNBP1 (1)	FBP17; Rapostlin; links RND2 signaling to F-actin & spine morphogenesis	Q96RU3
FNBP1L (1)	TOCA1; binds CDC42/WASP; promote membrane tubulation & F-actin reorganization	Q5T0N5
FRK (1)	PTK5; RAK; GTL; stabilizes PTEN & negatively regulates cell proliferation	P42685
FUT8 (1)	CDGF1; a Golgi associated enzyme regulates adhesion, migration & invasion	Q9BYC5
FYB (1)	SLAP130; THC3; binds FYN and LCP2 & regulates actin cytoskeleton in T-cells	O15117
FYN (1)	SLK; SYN; regulates cell growth and survival, adhesion, motility, & axon guidance	P06241
GAS7 (1)	KIAA0394; promotes maturation & morphological differentiation of cerebellar neurons	O60861
GRAP (2)	DFN114; a BCR-ABL binding enzyme involved in RAS signaling pathway	Q13588
GRAP2 (2)	GRID; MONA; binds SHC, GAB1, LCP2, SLP76; involved in NF-AT activation	O75791
GRAPL (1)	Involved in GPCR & RET signaling	Q8TC17
GRB2 (2)	ASH; NCKAP2; binds SHC, GAB1, FRS2, CBL; links surface receptors to RAS signaling	P62993
HCK (1)	p59; targets ADAM15, BCR, ELMO1, GAB1", RAPGEF1, STAT5B, TP73, VAV1 & WAS	P08631
HCLS1 (1)	LCKBP1; HS1; CTTNL; involves in antigen receptor signaling in lymphoid cells	P14317
IASPP (1)	PPP1R13L; NKIP1; RIA4; inhibits p53 & NFκB; regulates apoptosis and transcription	Q8WUF5

Table S1. The superfamily of human SH3 domain-containing protein (101-150)

Entry name (No. of SH3)	Aliases, interactions & functions	Uniprot ID
ITK (1)	LYK; EMT; binds GATA3; regulates T-cell development, function & differentiation	Q08881
ITSN1 (5)	SH3D1A; SH3P17; acts as a CDC42GEF on actin nucleation & endocytosis	Q15811
ITSN2 (5)	SH3P18; SH3P18; SWAP; acts as a CDC42GEF on actin nucleation & endocytosis	Q9NZM3
JIP1 (1)	MAPK8IP1; IB1; involved as MAPK component in survival response	Q9UQF2
JIP2 (1)	MAPK8IP2; IB2; involved as MAPK component in survival response	Q13387
LASP1 (1)	MLN50; LASP1; regulates actin-associated ion transport activities	Q14847
LCK (1)	LSK; YT16; targets RUNX3, PYK2, MAPT, RHOH and TYROBP in T-cell regulation	P06239
LYN (1)	JTK8; regulates growth factor/cytokine/integrin-mediated innate immune responses	P07948
MACC1 (1)	SH3BP4L; 7A5; promotes HGF-MET signaling & cell motility, proliferation & metastasis	Q6ZN28
MACF1 (1)	ACF7, LIS9; OFC4; involved in AXIN1/APC/CTNNB1/GSK3B complex translocation	Q9UPN3
MAP3K9 (1)	MLK1; MEKK9; activates JNK pathway; involved in the cyt c release & apoptosis	P80192
MAP3K10 (1)	MLK2; MST; MEKK10; activates JNK & SEK1 pathways	Q02779
MAP3K11 (1)	MLK3; PTK1; MEKK11; SPRK; activates BRAF, ERK, p38 and JNK1 pathways	Q16584
MAP3K21 (1)	MLK4; negative regulator of TLR4 signaling	Q5TCX8
MATK (1)	CHK; CTK, HYL; LSK; has an inhibitory role in the control of T-cell proliferation	P42679
MIA1 (1)	Associated with melanoma, glioma and neuroectodermal tumors	Q16674
MIA2 (1)	MGEA11; TALI; MEA6; involved in cholesterol & TAG homeostasis, & OL7A1 secretion	Q96PC5
MIA3 (1)	TANGO; ARNT; required for membrane-bound ER-resident complexes consisting of MIA2	Q5JRA6
MPP2 (1)	DLG2; negatively regulates SRC function in epithelial cells	Q14168
MPP3 (1)	DLG3; interact with the cytoskeleton & regulates intracellular junctions & cell proliferation	Q13368
MPP4 (1)	DLG6; plays a role in retinal photoreceptors development.	Q96JB8
MPP5 (1)	PALS1; involved in adherens junction biogenesis & localization of the exocyst complex	Q8N3R9
MPP6 (1)	PALS2; VAM1; act on receptor clustering by forming multiprotein complexes	Q9NZW5
MPP7 (1)	Promotes epithelial cell polarity and tight junction formation	Q5T2T1
MYO15A (1)	DFNB3; unconventional MYO15 required for stereocilia formation in mature hair bundles.	Q9UKN7
MYO15B (1)	MYO15BP; no functional motor domain	Q96JP2
MYO1E (1)	FSGS6; HUNCM-IC; controls the movement of class II-containing cytoplasmic vesicles	Q12965
MYO1F (1)	Acts with MYO1E on innate immunity in cell migration & phagocytosis	O00160
MYO7A (1)	DFNB2; NSRD2; mediates in complex with USH1C/G & CDH23 mechanotransduction	Q13402
MYO7B (2)	MYOVIIb; acts in the intermicrovillar adhesion complex on microvilli organization & length	Q6PIF6
NCF1 (2)	p47phox; NOXO2; NCF1A; required for activation of the latent NADPH oxidase	P14598
NCF1B (2)	NCF1B; required for activation of the latent NADPH oxidase	A6NI72
NCF1C (2)	NCF1C; required for activation of the latent NADPH oxidase	A8MVU1
NCF2 (2)	p67phox; NOXA2; required for activation of the latent NADPH oxidase	P19878
NCF4 (1)	p40phox; SH3PXD4; involved assembly & activation of the NADPH oxidase complex	Q15080
NCK1 (3)	Acts as an RTK-associated protein on RAS signaling & dsRNA-induced PKR activation	P16333
NCK2 (3)	GRB4; acts as an RTK-associated protein on RAS signaling & translational initiation	O43639
NEBL (1)	LASP2; LIM-Nebulette; links sarcomeric actin to desmin around the Z-disk	O76041
NEBU (1)	NEM2; NEB177B; binds & stabilize F-actin; involved in sarcomeric integrity	P20929
NOSTRIN (1)	Multivalent adapter protein involved in NO metabolism by sequestering NOS3	Q8IVI9
NOXA1 (1)	p51NOX; activates as a p67phox-like factor NOX1/3 in the host defense & oxygen sensing	Q86UR1
NOXO1 (2)	SH3PXD5; p41NOX; activates together with NOX2 NOX1/3	Q8NFA2
NPHP1 (1)	NPH1; Nephrocystin-1; control together with PTK2B/PYK2 the epithelial cell polarity	O15259
OSTF1 (1)	SH3P2; OSF; induces bone resorption & enhances osteoclast formation & activity	Q92882
OTOR (1)	Otoraplin; MIAL1; FDP; functions in cartilage development and maintenance	Q9NRC9
p85α (1)	PIK3R1; AMG7; regulates membrane binding & activity of p110 catalytic subunit of PI3K	P27986
P85β (1)	PIK3R2; MPPH1; regulates membrane binding & activity of p110 catalytic subunit of PI3K	O00459
PACSIN1 (1)	SYNDAPIN1; recruits DNM1/2/3 to membranes; regulates neurite formation & branching	Q9BY11
PACSIN2 (1)	SYNDAPIN2; involved in plasma membrane protein internalization by endocytosis	Q9UNF0
PACSIN3 (1)	SYNDAPIN3; involved in cell-surface receptor internalization by endocytosis	Q9UKS6

Table S1. The superfamily of human SH3 domain-containing protein (151-200)

Entry name (No. of SH3)	Aliases, interactions & functions	Uniprot ID
PEX13 (1)	PEROXIN13; NALD; involved in the import of peroxisomal biogenesis factors PTS1/2	Q92968
PLCG1 (1)	PLC1; PLC148; NCKAP3; catalyzes DAG & IP3 production	P19174
PLCG2 (1)	PLCIV; APLAID; FCAS3; catalyzes DAG & IP3 production	P16885
PRAM (1)	PRAM1; PMLRAR; involved in myeloid differentiation & integrin signaling in neutrophils	Q96QH2
PSTPIP1 (1)	CD2BP1L; PAPAS; regulates WAS actin-bundling activity, endocytosis and cell migration	O43586
PTK6 (1)	BRK; controls the differentiation and maintenance of normal epithelia & tumor growth	Q13882
RASA1 (1)	p120RASGAP; CMAVM1; acts as a GAP of RAS	P20936
RIMBP1 (3)	RBP1; PRAX1; synchronizes and couples cynaptic vesicle to the sites of exocytosis	O95153
RIMBP2 (3)	RBP2; PPP1R133; synchronizes and couples cynaptic vesicle to the sites of exocytosis	O15034
RIMBP3A (3)	Plays a key role in sperm head morphogenesis during late stages of sperm development	Q9UFD9
RIMBP3B (3)	Plays a key role in sperm head morphogenesis during late stages of sperm development	A6NNM3
RIMBP3C (3)	Plays a key role in sperm head morphogenesis during late stages of sperm development	A6NJZ7
RUSC1 (1)	NESCA; regulates MAPK & NFκB pathways, & NGF-dependent neurite outgrowth	Q9BVN2
RUSC2 (1)	MRT61; IPORIN; acts as a RAB35 effector on intracellular vesicular trafficking	Q8N2Y8
SAMSN1 (1)	HACS1; SH3D6B; acts on RAC1-dependent cell spreading & polarization	Q9NSI8
SASH1 (1)	PEPE1; SH3D6A; Acts on TLR4/NFκB signaling & LPS-induced endothel. cell migration	O94885
SASH3 (1)	HACS2; SH3D6C; functions as a signaling adapter protein in lymphocytes	O75995
SGSM3 (1)	MAP; RUSC3; RABGAP5; involved in NF2-mediated growth suppression of cells	Q96HU1
SH3BP4 (1)	EHB10; TTP; BOG25; controls clathrin-mediated endocytosis	Q9P0V3
SH3D19 (5)	EBP; EVE-1; acts on ADAMs/EGFR axis & suppresses RAS-induced cell transformation	Q5HYK7
SH3D21 (3)	Unknown function	A4FU49
SH3GL1 (1)	Endophilin A2; SH3D2B; acts on membrane shaping & clathrin-independent endocytosis	Q99961
SH3GL2 (1)	Endophilin 1; SH3D2A; acts on membrane shaping & synaptic vesicle endocytosis	Q99962
SH3GL3 (1)	Endophilin 3; SH3D2C; implicated in membrane shaping & endocytosis	Q99963
SH3GLB1 (1)	BIF1; involved in membrane fusion & in the regulation of autophagy	Q9Y371
SH3GLB2 (1)	RRIG1; Endophilin-B2; involved in endocytosis	Q9NR46
SH3KBP1 (1)	CD2BP3; CIN85; HSB1; controls cell shape & migration, & stimulates B cell activation	Q96B97
SH3PXD2A (5)	TKS5; SH3MD1; involved in ROS generation, podosome formation & ECM degradation	Q5TCZ1
SH3PXD2B (4)	TSK4; FAD49; involved in ROS generation, podosome formation & ECM degradation	A1X283
SH3RF1 (4)	POSH1; SH3MD2; involved in dynamin-dependent endocytosis & JNK activation	Q7Z6J0
SH3RF2 (3)	POSH3; HEPP1; mediates TNFα signaling & proteasomal degradation	Q8TEC5
SH3RF3 (4)	POSH2; SH3MD4; is a RAC effector & mediates proteasomal degradation	Q8TEJ3
SH3TC1 (1)	Unknown function	Q8TE82
SH3TC2 (1)	CMT4C; MNMN; involved as a RAB11 effector in axoglial interactions myelination	Q8TF17
SH3YL1 (1)	RAY; involved in hair follicle development, cell migration, & dorsal ruffle formation	Q96HL8
SHANK1 (1)	SSTRIP; acts in GKAP/PSD95/HOMER complex on dendritic spine organization	Q9Y566
SHANK2 (1)	CORTBP1; involved in structural and functional organization of the dendritic spine	Q9UPX8
SHANK3 (1)	PSAP2; acts on th dendritic spine and synapse formation, maturation and maintenance	Q9BYB0
SKAP1 (1)	SCAP1; positively regulates T-cell receptor signaling by enhancing the MAPK pathway	Q86WV1
SKAP2 (1)	SCAP2; PRAP; SAPS; involved in B-cell and macrophage adhesion processes	O75563
SLAP1 (1)	SLA1; links ZAP70 with CBL & negatively regulates T-cell receptor signaling	Q13239
SLAP2 (1)	SLA2; MARS; links ZAP70 with CBL & negatively regulates T-cell receptor signaling	Q9H6Q3
SNX9 (1)	SH3PX1; SDP1; WISP; stimulates DNM2 GTPase activity; involved in endocytosis	Q9Y5X1
SNX18 (1)	SNAG1; SH3PX2; stimulates DNM2 GTPase activity; involved in endocytosis	Q96RF0
SNX33 (1)	SH3PX2; reorganizes the cytoskeleton, endocytosis and cellular vesicle trafficking	Q8WV41
SORBS1 (3)	SH3P12; FLAF2; CAP; involved in formation of actin stress fibers and focal adhesions	Q9BX66
SORBS2 (3)	ARGBP2; forms complex with ABL1/CBL & promotes ABL1 ubiquitination & degradation	O94875
SPIN90 (1)	NCKIPSD; WISH; WASLBP; stimulates N-WASP-induced ARP2/3 complex activation	Q9NZQ3
SPTA1 (1)	SPH3; EL2; forms the cytoskeletal superstructure of the erythrocyte plasma membrane	P02549
SPTAN1 (1)	NEAS; EIEE5; involved in calcium-dependent cytoskeleton movement at the membrane	Q13813

Table S1. The superfamily of human SH3 domain-containing protein (201-221)

Entry name (No. of SH3)	Aliases, interactions & functions	Uniprot ID
SRC (1)	THC6; ASV; participates in transcription, immunity, adhesion, apoptosis, migration	P12931
SRC8 (1)	CTTN; EMS1; Amplaxin; involved in the formation of lamellipodia and in cell migration	Q14247
SRMS (1)	PTK70; phosphorylates DOK1, KHDRBS1/SAM68 and VIM	Q9H3Y6
STAC (1)	Involved in the modulation of calcium channel at the cell membrane	Q99469
STAC2 (1)	24B2; involved in the modulation of calcium channel at the cell membrane	Q6ZMT1
STAC3 (1)	MYPBB; NAM; Required for excitation-contraction coupling in skeletal muscle	Q96MF2
STAM1 (1)	HSE1H; involved in signal transduction mediated by cytokines and growth factors	Q92783
STAM2 (1)	HBP; involved in signal transduction mediated by cytokines and growth factors	O75886
TEC (1)	PSCTK4; regulates the development, function and differentiation of diverse cell types	P42680
TNK1 (1)	Negative regulates the RAS-MAPK pathway; utilized broadly during fetal development	Q13470
TXK (1)	PTK4; BTKL; RKL; regulates the development and differentiation of conventional T-cells	P42681
UBASH3A	TULA1, STS2; as a T-cell ubiquitin ligand family member negatively act on T-cell signaling	P57075
UBASH3B (1)	TULA2; STS1; as a T-cell ubiquitin ligand family member negatively act on T-cell signaling	Q8TF42
VAV1 (2)	Acts as a RAC1/RHOAGEF; involved in cell differentiation & proliferation	P15498
VAV2 (2)	Acts as a RAC1GEF; involved in angiogenesis & endothelial cell migration	P52735
VAV3 (2)	Acts a RHOA/RHOGGEF; involved in angiogenesis & endothelial cell migration	Q9UKW4
VINEXIN (3)	SORBS3; SH3D4; SCAM1; plays a role in cell spreading	O60504
YES (1)	HST441; regulates cell growth, adhesion, cytoskeleton remodeling, and differentiation	P07947
ZO1 (1)	TJP1; involved in tight junction organization, epithelial polarization and barrier formation	Q07157
ZO2 (1)	TJP2; PFIC4; DFNA51; plays a role in tight junctions and adherens junctions	Q9UDY2
ZO3 (1)	TJP3; links tight junction transmembrane proteins	O95049

Table S2. Published structures of the SH3-PRM complexes.

No.	SH3/PRM structures	PRM sequence	PDB code	Ref.
1	GRB2-1(Y7V,C32S)/SOS1	PVPPPVPPRRRP	1AZE	(*439*)
2	GRB2-2/synthetic peptide	RHYRPLPPLP	1IO6	tbp
3	DOCK2/ELMO1	RLLDLENIQIPDAPPPIPKEPSNYDFVY	2RQR	(*440*)
4	ITSN2-2/synthetic peptide	ACEWRGSLSYLKGPL	4IIO	tbp
5	ABL/synthetic peptide	ACEAPTYSPPLPP	4J9E	tbp
6	CD2AP-2/ARAP1	PTPRPVPMKRHIFR	4X1V	tbp
7	CRKII-1/RAPGEF1	DNSPPPALPPKKRQS	5L23	tbp
8	$p67^{phox}$-c/$p47^{phox}$	SKPQPAVPPRPSADLILNRCSESTKRKLASAV	1K4U	(*441*)
9	NCF4/NCF1	KPQPAVPPRPS	1W70	(*442*)
10	betaPIX/alphaPAK	DATPPPVIAPRPEHTKSVYTRS	1ZSG	(*443*)
11	betaPIX/CBL-b	RPPKPRPRR	2AK5	(*444*)
12	CIN85/CBL-b	PARPPKPRPR	2BZ8	(*444*)
13	Cortactin/ ASAP1	KRPPPPPPG	2D1X	(*445*)
14	CMS-1/CD2	PLPRPRV	2J6O	(*446*)
15	NCK2-1/CD3epsilon	KERPPPVPNPDYEPIRKGQRDLYS	2JXB	(*447*)
16	IRTKS/EspFu-R47	HIPPAPNWPAPTPPVQN	2kxc	(*448*)
17	SRBS1-2/ Paxillin	VPPPVPPPPSS	2O9V	(*449*)
18	HCK/synthetic peptide	ACEHSKPLPPLPSL	2OJ2	(*450*)
19	betaPIX/AIP4	RPPRPSRPPPPTPRRP	2P4R	(*451*)
20	betaPIX/AIP4	PSRPPRPSRPPPPTPR	2P4R	(*451*)
21	EPS8L1/CD3epsilon	PPVPNPDYEPIR	2ROL	(*357*)
22	DOCK2/ELMO1	PDAPPPIP	3A98	(*440*)
23	DOCK2/ELMO1	EIKLRLLDLENIQIPDAPPPIPKEPSNYDFVYDCN	3A98	(*440*)
24	ARC4/SH3BP2	LQRSPPDGQSFR	3TWR	(*452*)
25	ARC4/SH3BP2	QRSPPDGQSFR	3TWR	(*452*)
26	CD2AP-2/ RIN3	QPPVPPPRKKRIS	3U23	(*453*)
27	TUBA-3/NWASP	PPALPSSAPSG	4CC2	(*454*)
28	TUBA-3/MENA	PPPPLPSGPAYA	4CC3	(*454*)
29	TUBA-3/MENA	PPPPALPSSAPSG	4CC7	(*454*)
30	FYN/synthetic peptide	SLARRPLPPLP	4EIK	(*455*)
31	NEBEL/XIRP2	PPPTLPKPKLP	4F14	(*456*)
32	SRBS1-2/Vinculin	LAPPKPPLPE	4LN2	(*457*)
33	CBL/Vinculin	VPPPRPPPPE	4LNP	(*457*)
34	SRBS1-1/Vinculin	VPPPRPPPP	4LNP	(*457*)
35	CD2AP-1/RIN3	KNLPTAPPRR	4WCI	(*453*)
36	FYN/synthetic peptide	APPLPPRNR	4ZNX	(*458*)
37	SGIP1/Eps15	DPFGGDPFK	5AWT	(*459*)
38	CRKII-n/ABL	SEKPALPRKR	5IH2	(*460*)
39	STAM2/AMSH	AKPPVVDRSLKPG	5IXF	(*461*)
40	betaPIX/ITCH	RPPRPSRPPPPTPRRP	5SXP	(*462*)

Table S3. Published dissociation constants (K_d) determined for the SH3-PRP interactions.

GRB2	SOS peptide	K_d (μM)	Method	Reference
FL	GTDEVPVPPPVPPRRRP	22		(*316*)
	GRB2 injection into SOS1	170 nM	ITC	(*317*)
	SOS1 injection into GRB2	480 nM	ITC	(*317*)
	SOS1 proline rich domain	360 nM	ITC	(*318*)
	N-Terminal PR SOS1	260 nM	ITC	(*317*)
	C-Terminal PR SOS1	510 nM	ITC	(*317*)
	SOS1	1.48 nM	SPR	(*463*)
nSH3	VPVPPPVPPRRR (RP1)	39	ITC	(*307*)
	LDSPPAIPPRQPTSK (P4)	56	ITC	(*307*)
	ISDPPESPPLLPPREPVRTPDV(P5)	182	ITC	(*307*)
	VPVPPPVPPRRR (RP1)	1.68 nM	SPR	(*463*)
	VPVPPPVPPRRR (RP1)	38.64	ITC	(*306*)
	SOS1 proline rich domain	7.8 nM	SPR	(*320*)
cSH3	VPVPPPVPPRRR (RP1)	125	ITC	(*307*)
	LDSPPAIPPRQPTSK (P4)	1396	ITC	(*307*)
	ISDPPESPPLLPPREPVRTPDV(P5)	1718	ITC	(*307*)
	VPVPPPVPPRRR (RP1)	142	NMR	(*305*)
	VPVPPPVPPRRR (RP1)	117.10	ITC	(*306*)

Table S4. Classification of published proline-rich consensus sequence motifs and their incidence found in SOS1 PRD.

No.	ID	Consensus sequences	Ref.	Peptides[a]											
				P1	P2	P3	P4	P5	P6	P7	P8	P9	P10	RP1	RP2
1	0X1	PPPP	(*352*)	-	-	-	-	-	-	+	-	-	-	-	-
2	0X2	XPPX	(*353*)	+	-	+	+	+	+	+	+	+	+	+	+
3	1X1	PXP	(*354*)	+	-	+	-	-	+	+	+	+	-	+	+
4	1X2	PXPXP	(*355*)	-	-	+	-	-	-	-	-	-	-	+	-
5	1X3	PPXPP	(*356*)	-	-	+	+	+	-	-	-	+	-	+	+
6	2X1	PXXDY	(*357*)	-	-	-	-	-	-	-	-	-	-	-	-
7	2X2	PXXP	(*358*)	+	+	+	+	+	-	+	+	+	+	+	+
8	2X3	PXXPX[KR]	(*359*)	-	-	+	+	+	-	-	-	+	-	+	+
9	2X4	[KR]XXPXXP	(*359*)	-	-	-	-	-	-	-	+	-	-	-	-
10	2X5	PXXPXXP	(*360*)	+	-	+	-	-	-	-	-	-	-	+	-
11	3X1	PXXXP	(*361*)	+	-	+	+	+	+	+	-	+	+	+	+
12	3X2	PXXXPXXXP	(*362*)	-	-	+	+	+	-	-	-	-	-	-	-
13	3XP	PXXXPR	(*363*)	-	-	+	+	+	-	-	-	+	-	+	+
14	4XP	PXXXXP	(*364*)	+	-	+	+	+	-	+	-	-	-	+	-

[a] The amino acid sequences of the peptides are listed in Table S5.

Table S5. Peptide used in this study

Peptide name	Peptide sequence
P1[a]	^{1078}SAPNSPRTPLTPPPAS^{1093}
P2	^{1124}VTLPHGPRSA^{1133}
P3	^{1146}EVPVPPPVPPRRRPESAPAESSPSKI^{1171}
P4	^{1176}LDSPPAIPPRQPTSK^{1190}
P5	^{1204}ISDPPESPPLLPPREPVRTPDV^{1225}
P6	^{1227}SSSPLHLQPPPLGKK^{1241}
P7	^{1247}AFFPNSPSPFTPPPPQTPSPHGT^{1269}
P8	^{1271}RHLPSPPLTQ^{1280}
P9	^{1287}IAGPPVPPRQS^{1297}
P10	^{1300}QHIPKLPPKTY^{1310}
RP1[b]	^{1147}VPVPPPVPPRRR^{1158}
RP2[c]	^{13}RCEAPPVPPRRERG^{26}

[a] P stands for peptides derived from SOS1.

[b] Reference peptide 1 (RP1) is derived from peptide 3 (P3).

[c] Reference peptide 2 (RP2) is derived from WRCH.

Table S6. Dissociation constants (K_d)[a] determined for the SH3-PRP interactions.

SH3 Domains[b]	Peptides[c]											
	P1	P2	P3	P4	P5	P6	P7	P8	P9	P10	RP1	RP2
ABI1	-	60.7	-	24.6	-	-	-	-	-	-	-	-
ABL2	-	-	-	125	-	-	67.3	-	-	-	11	-
ARHGAP12	-	-	13.8	-	-	-	0.2	-	-	-	16.7	15.5
Obscurin	-	-	-	-	-	-	8.9	-	-	-	-	-
BIN1	-	-	-	-	-	-	12.0	-	47.0	-	-	48.0
CRK-1	-	-	12.9	-	-	-	18.1	-	-	-	-	-
DLG2	-	-	-	-	-	-	58.5	-	-	-	-	-
GRB2-1	-	-	15.0	60	62	-	-	-	-	-	11.0	20.0
GRB2-2	-	-	12.0	20	35	-	-	-	-	-	3.4	12.9
INTS1-1	-	-	-	6.6	-	-	-	-	-	-	39	11.0
INTS1-2	-	-	-	-	-	-	-	-	-	-	-	-
INTS1-3	-	-	-	-	-	-	-	-	-	-	-	-
INTS1-4	-	-	-	-	-	-	-	-	-	-	-	-
INTS1-5	23.0	-	-	12.0	-	-	-	-	-	-	-	23.0
NCK1-1	-	-	-	-	-	-	-	-	-	-	-	-
NCK1-2	-	-	-	-	-	-	-	-	-	-	2.0	1.0
NCK1-3	-	-	-	-	-	-	-	-	0.9	-	24.6	2.5
NPHP1	-	-	-	-	-	-	-	-	-	-	-	-
RASA1	-	-	-	-	-	-	-	-	-	-	-	-
RIMBP3B-1	-	21.0	-	-	-	-	15.0	-	-	-	-	-
SH3GLB1	-	-	-	-	-	-	-	-	-	-	-	-
SH3PXD2A-1	-	44.0	18.0	-	-	-	-	-	-	-	-	21.0
SNX9	-	-	-	-	-	-	-	-	-	-	-	-
SORBS1-1	-	-	-	-	-	-	13.2	-	-	-	-	-
SRC	-	-	2.0	-	-	-	13.3	-	-	-	-	-

[a] Dissociation constant (K_d values) were determined by evaluating the fluorescence polarization data (Figures x, xx) shown in Figure x as bar charts. Evaluated K_d values were divided in high affinity (0.1 to 1.0 μM; green), intermediate affinity (1.1 to 5 μM; blue), low affinity (5 to 25 μM; red) and very low affinity (26 to 125 μM; black). No binding (-) stands for K_d values higher than 126 μM.

[b] SH3 domains from SH3-containing proteins with two or more SH3 domains are highlighted with a dash and the number of the SH3 domain.

[c] The amino acid sequences of the peptides are listed in Table S3.

Table S7. Constructs used in this study

Domains	Protein	Construct (aa)	UniProt ID
SH3[a]	ABI1	446-505	Q8IZP0
	ABL2	107-167	P42684
	ARHGAP12	12-74	Q8IWW6
	ARHGAP12(K28S, R30N, F62G, Y63W)	12-74	
	ARHGAP12(K31T, T46Q,A66S, Q67N)	12-74	
	ARHGAP30	5600-5667	Q5VST9
	BIN1	520-593	O00499
	CRK	132-192	P46108
	DLG2	536-606	Q15700
	GRB2-1	1-58	P62993
	GRB2-2	158-215	P62993
	ITSN1-1	740-806	Q15811
	ITSN1-2	913-971	Q15811
	ITSN1-3	1002-1060	Q15811
	ITSN1-4	1070-1138	Q15811
	ITSN1-5	1155-1214	Q15811
	NCK1-1	2-61	P16333
	NCK1-2	106-165	
	NCK1-3	190–252	
	NCK1-3(N205D, D206T,D226Q, P227D)	190–252	
	NCK1-3(N225E, W229G, K244E)	190–252	
	RASA1	279–341	P20936
	RIMBP3B-1	832-899	A6NNM3
	SRC	218-306	P12931
	SH3GLB1	305-365	Q9Y371

	SH3PXD2A-1	166-225	Q5TCZ1
	SORBS1-1	793-852	Q9BX66
	SNX9	1-62	Q9Y5X1
SOS1	SOS1(FL)[b]	1-1333	Q07889
	SOS1(PRD)	1049-1333	

[a] These are in pGEX4T-1 vector for an expression in E. coli.

[b] These are in pFastbac vector for expression in insect cells

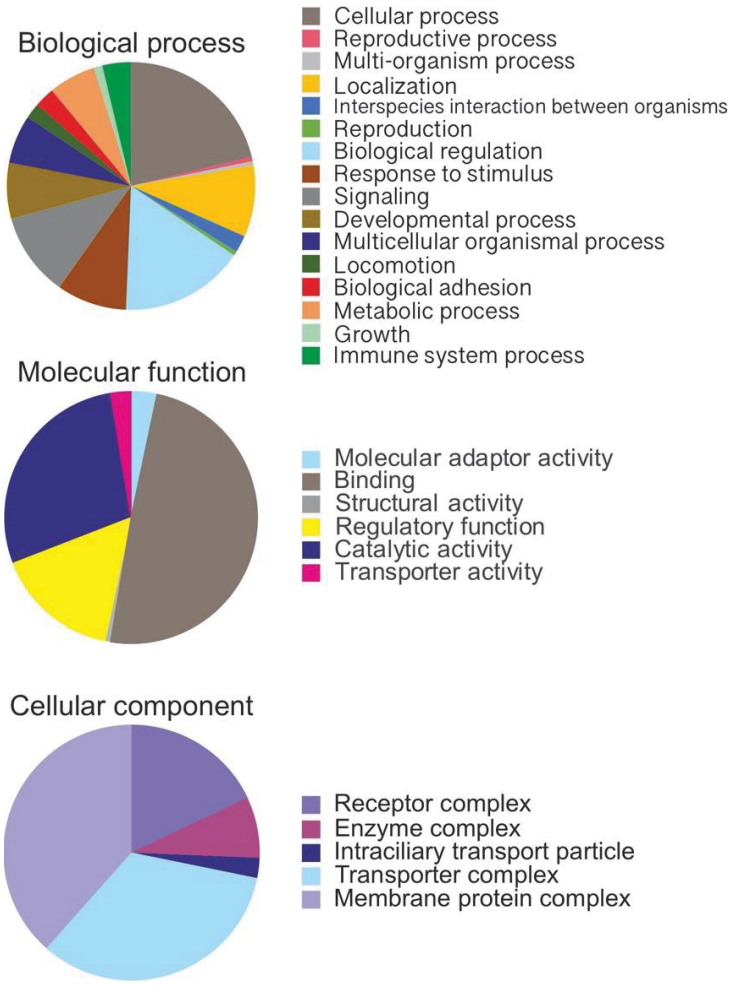

Figure S1. Gene Ontology analysis of the superfamily of human SH3 domain-containing protein. Gene Ontology (GO) terms for the biological process, molecular function, and cellular components of human SH3 domain-containing protein were identified using the PANTHER database (Mi H, Huang X, Muruganujan A, Tang H, Mills C, Kang D & Thomas PD (2017) PANTHER version 11: expanded annotation data from Gene Ontology and Reactome pathways, and data analysis tool enhancements. Nucleic Acids Res 45, D183–D189.)

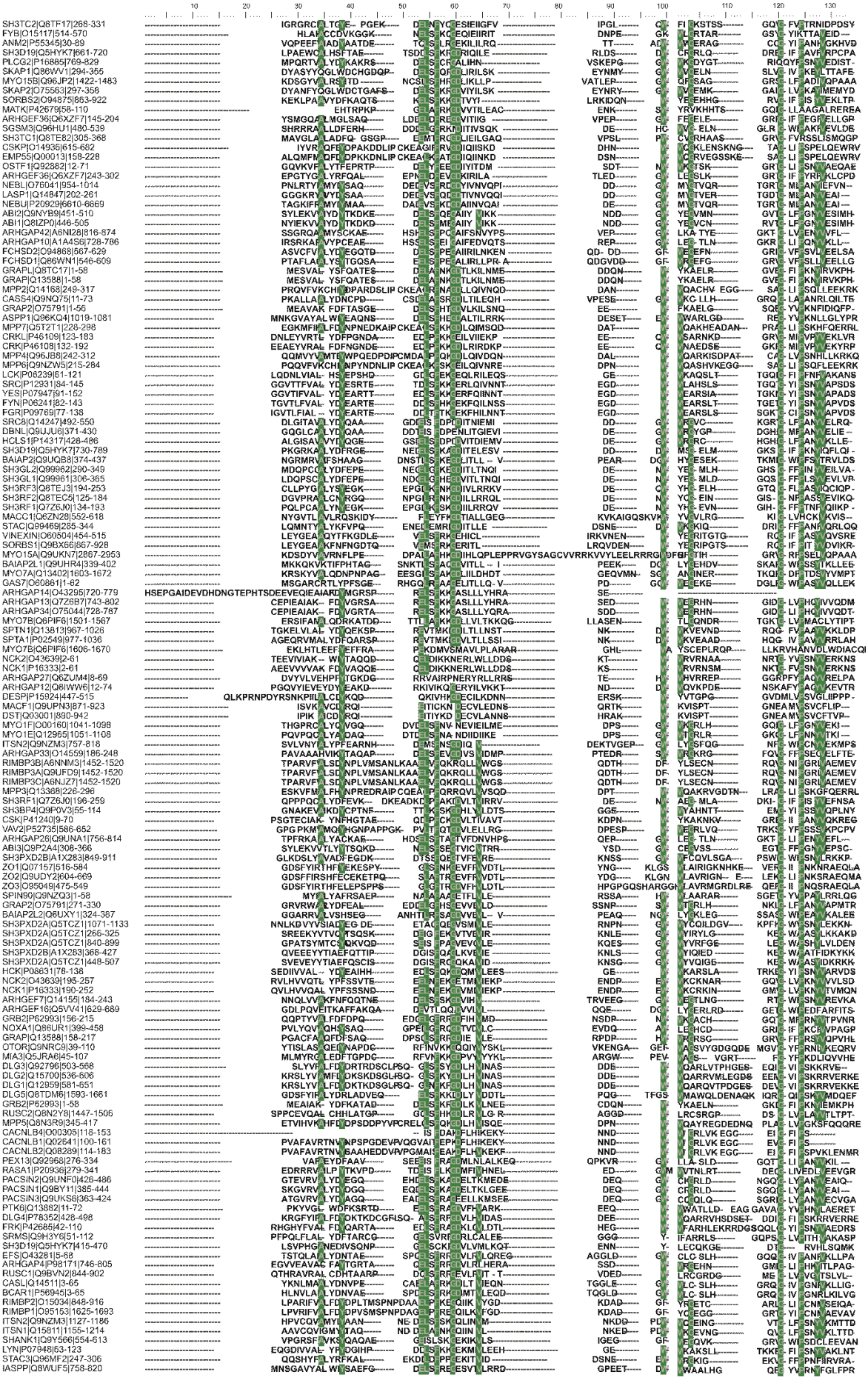

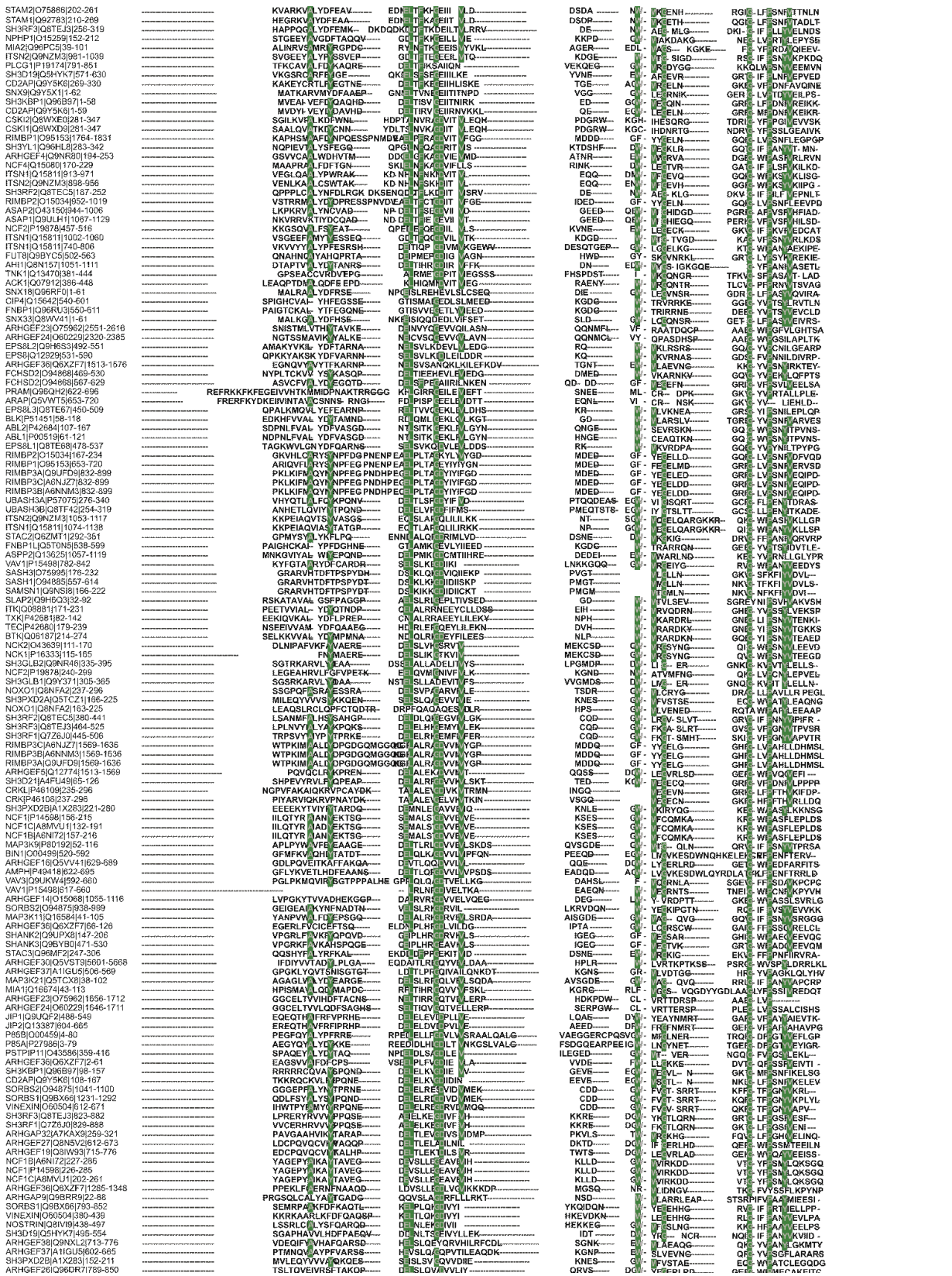

Figure S3 SH3 domain sequence alignment. The multiple sequence alignment of SH3 domains is generated using BioEdite program. The identical residues are shown in green.

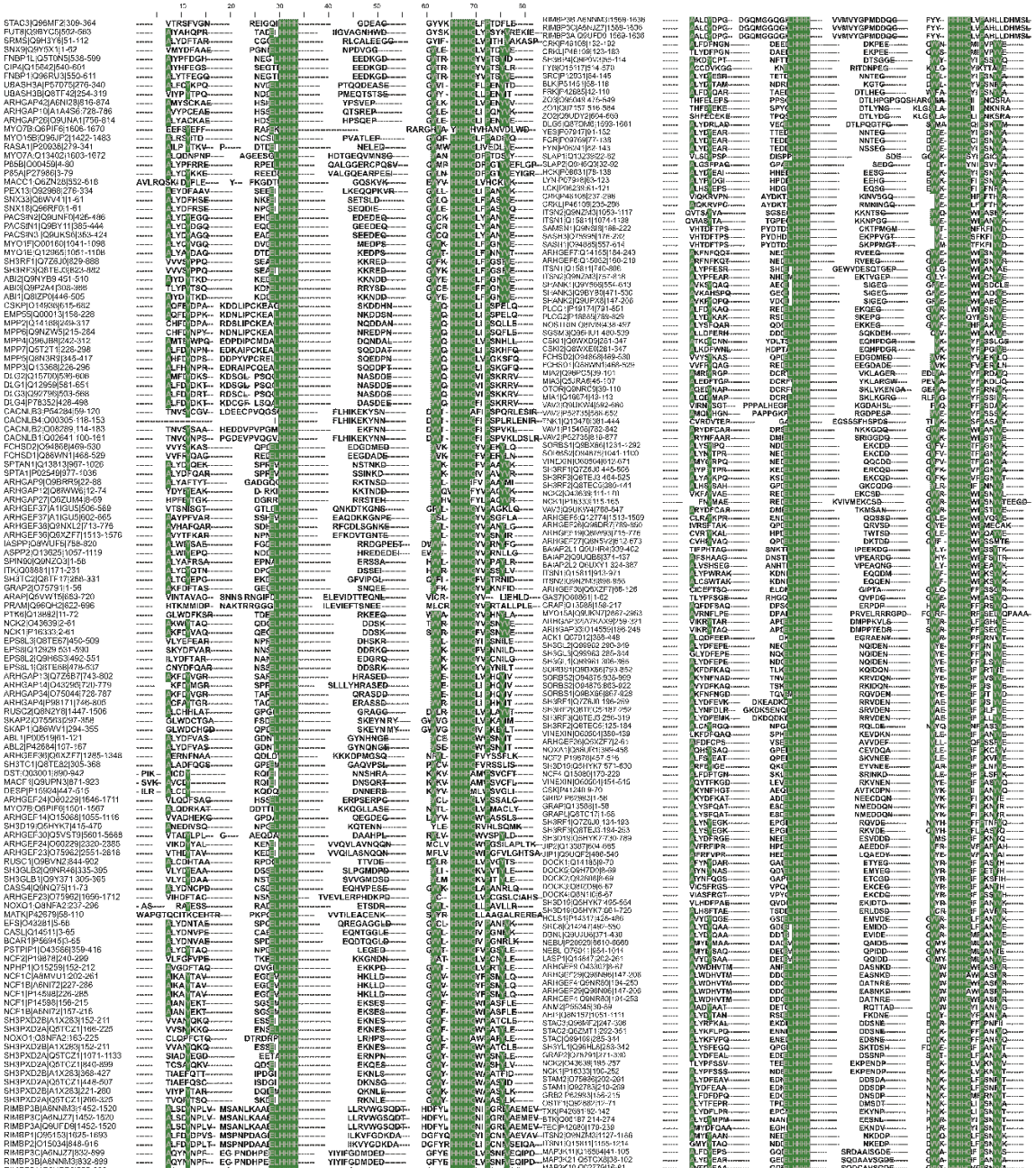

Figure S4. PRM binding residues of all human SH3 domains. The multiple sequence alignment of interfacing residues of SH3 domains responsible for their interaction with proline-

rich motifs is generated using BioEdite program. The identical residues are shown in green. H repeats shows the deletion part of the SH3 domains.

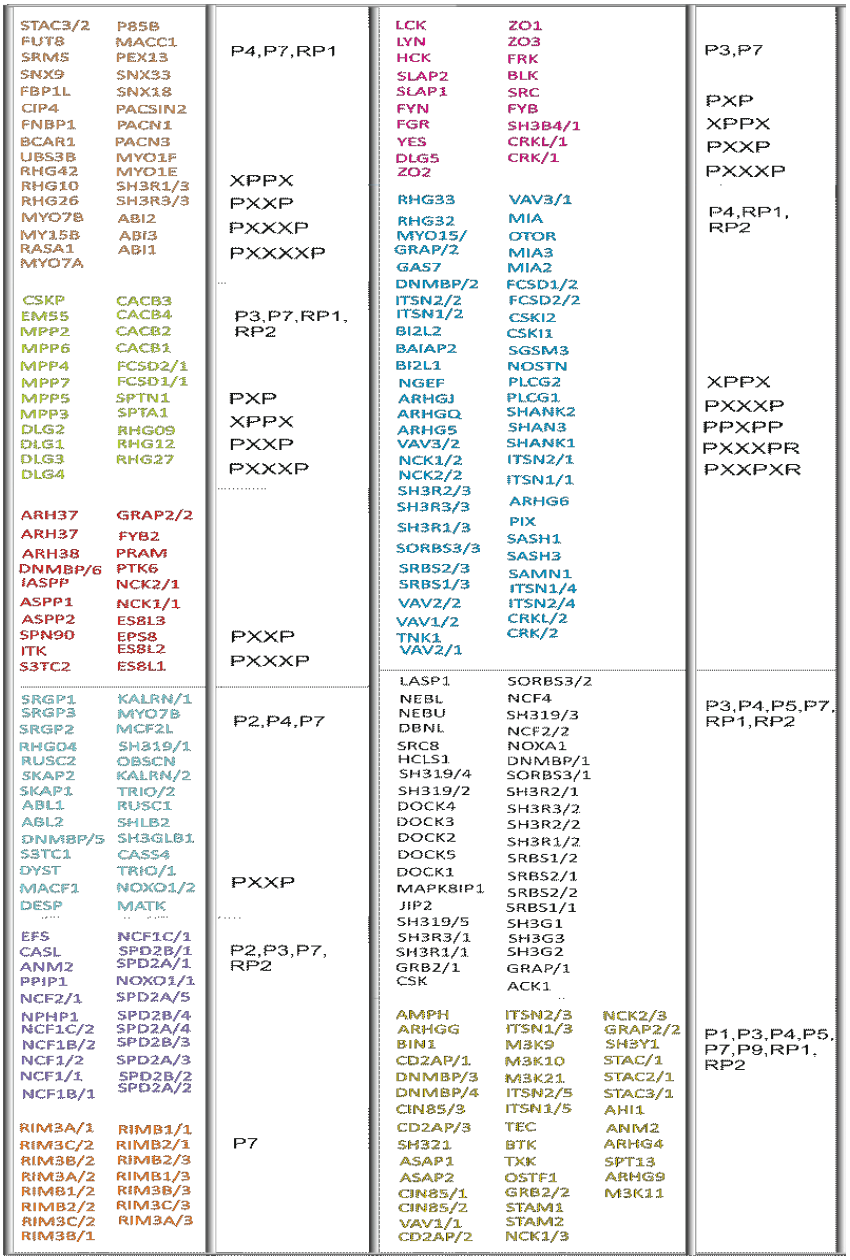

Figure S5. Specificity of the SH3-PRMs interaction analyzed for different SH3 domains families in human genome. The specific of proline-rich motifs that may interact with each family are defined for each family by comparing the sequence-structure and functional analysis of SH3 domains in complex with PRMs.

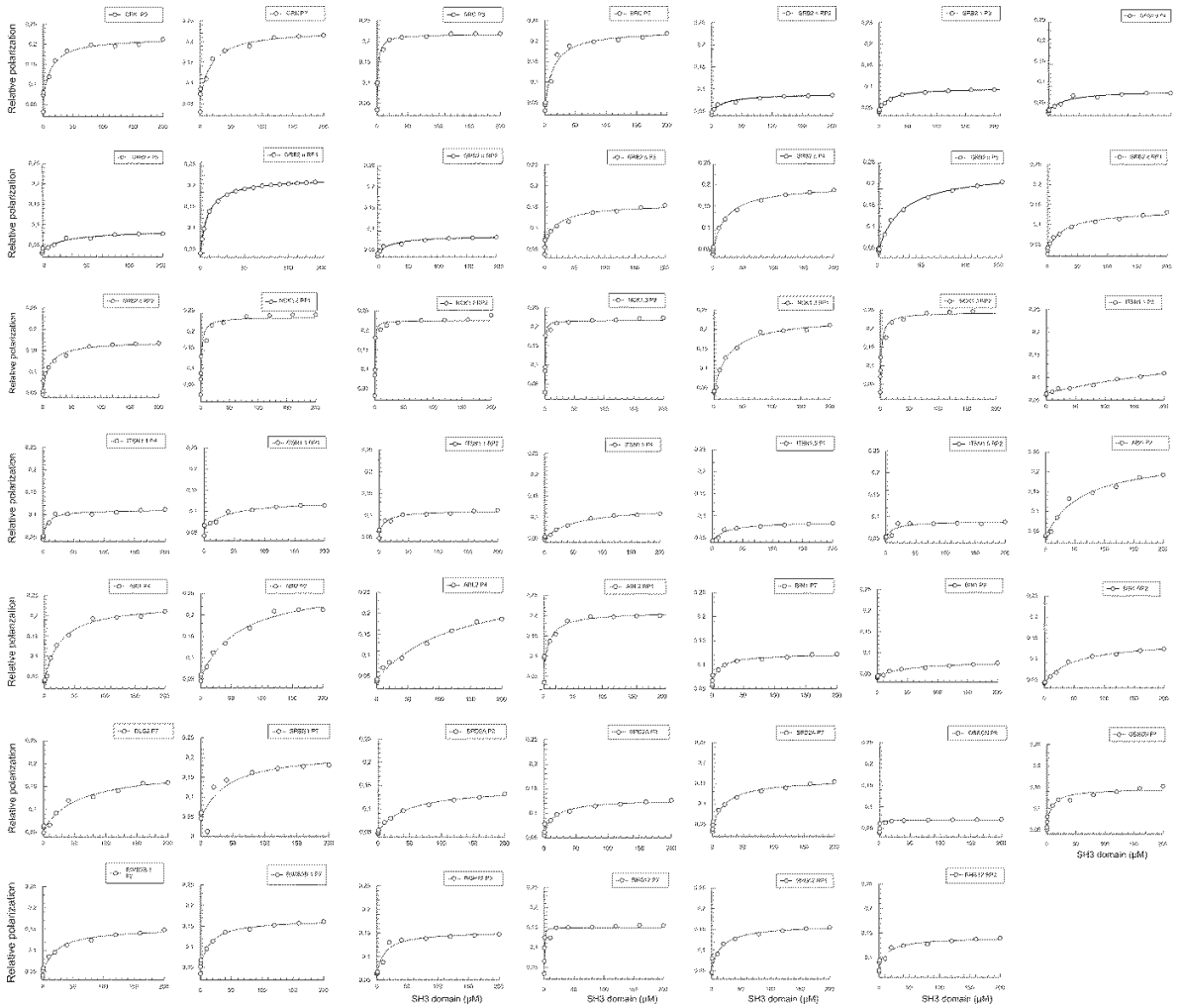

Figure S6. Fluorescence Polarization measurements of SH3 domain interactions with the SOS1 and reference peptides. Fluorescence polarization experiments were conducted to determine the dissociation constants (K_d) by titrating fluorescent peptides (0.2 μM, respectively) with increasing concentrations of the respective SH3 domains. The X-axis represents the concentration of the SH3 domain as GST fusion proteins in μM and Y-axis represents fluorescence polarization. The lines through the data points indicate that equilibrium K_d values have been determined for the respective measurements. The K_d values are summarized in Figure 3b and Table S6.

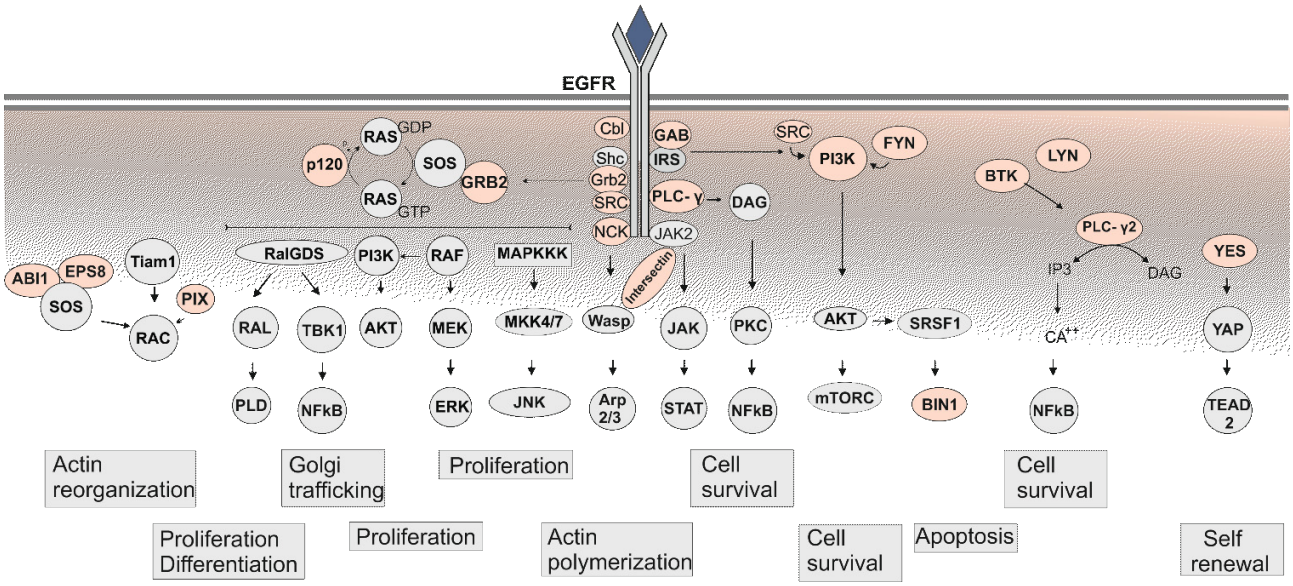

Figure S7. Schematic diagram of SH3 domain-containing proteins in transduction signaling pathways. SH3-containing proteins are important signaling proteins including adaptor proteins, kinases, RAS GEFs, RAS GAPs, scaffold proteins and effectors. SH3 containing proteins are involved in the processes of various transduction pathways in the cell (ERK, p38, JUNK, PKC). See Discussion for more details!

Chapter X

Accessory proteins of the RAS-MAPK pathway: Moving from the sideline to the front line

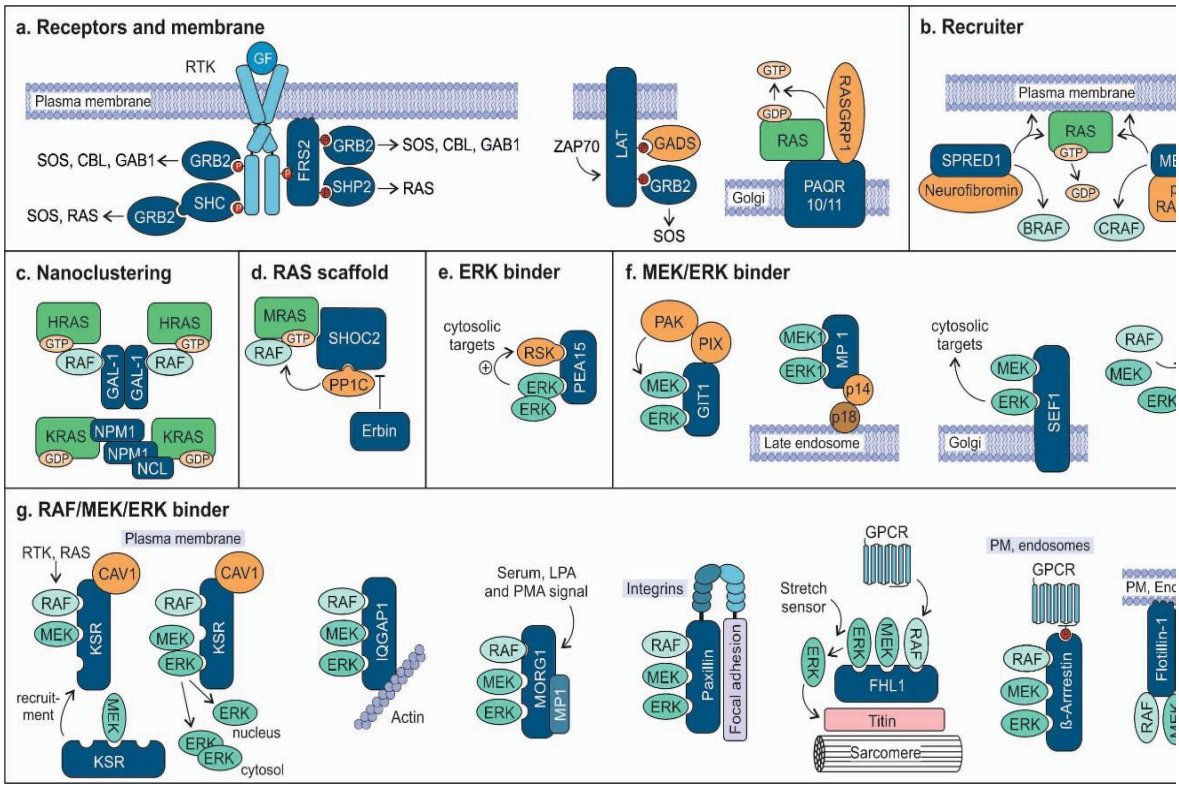

Published in:	Journal of communication Biology
Impact factor:	38.42 (2019)
Own Proportion to this work:	20%
	Compilation of the literature about related to the adaptor proteins of MAPK pathways, writing and revising the manuscript

Accessory proteins of the RAS-MAPK pathway: Moving from the sideline to the front line

Silke Pudewell, Christoph Wittig, Neda S. Kazemein Jasemi, Farhad Bazgir, Mohammad R. Ahmadian

Institute of Biochemistry and Molecular Biology II, Medical Faculty of the Heinrich-Heine University, 40225 Düsseldorf, Germany; reza.ahmadian@hhu.de

Abstract. Health and disease are directly related to the RTK-RAS-MAPK signalling cascade. After more than three decades of intensive research, understanding its spatiotemporal features is afflicted with major conceptual shortcomings. The compilation of a vast array of accessory proteins may resolve some parts of the puzzles in this field, as they safeguard the strength, efficiency and specificity of signal transduction. Targeting such modulators, rather than the constituent components of the RTK-RAS-MAPK signalling cascade may attenuate instead of inhibit disease-relevant signalling pathways.

General introduction

Nature has evolved sophisticated, cell type-specific mechanisms to sense, amplify and integrate diverse external signals, and ultimately generate the appropriate cellular response. Signals are processed by evolutionary conserved signalling cassettes that comprise specific constituent components that act as receptors, mediators, effectors, and regulatory proteins. Activated receptor tyrosine kinases (RTKs), for instance, link the RAS activator SOS1 to RAS paralogs, *e.g.*, the protooncogene KRAS4B, which in turn regulate various signalling pathways, including the mitogen-activated protein kinase (MAPK) pathway.[1] This pathway contains a three-tiered kinase cascade comprising the serine/threonine kinases BRAF/CRAF, the dual specificity kinase MEK1/2, and the serine/threonine kinases ERK1/2.[1,2] The RTK-RAS-MAPK axis is a highly conserved, intracellular signalling pathway that plays an essential role throughout mammalian development, from embryogenesis to tissue-specific cellular homeostasis in the adult.[3] Dysregulation of components or regulators of this cascade is frequently associated with tumour growth and a distinct subset of developmental disorders called the RAS-MAPK syndromes or RASopathies.[4–6] This signalling cascade has rapidly taken centre stage in cancer and RASopathy therapies (see below).

However, the strength, efficiency, specificity and accuracy of signal transduction are controlled by mechanisms that increase the connectivity of the signalling molecules and thus increase their local concentration and reduce their dimensionality. This state can be achieved by liquid-liquid phase separation (LLPS), a mechanism in which two separate liquid phases with different protein composition emerge from one mixed solution.[7] A large number of proteins, hereafter collectively designated as the `accessory proteins´, fulfil the requirements to drive LLPS and have been reported to act as adaptor, anchoring, docking or scaffold proteins. Accessory proteins link constituent components of individual signal transduction pathways by forming physical complexes. What the functions of the accessory proteins are, why they are crucial for signal transduction, and whether they represent better therapeutic targets for different human diseases are questions which we will address in this article mainly in the context of the RTK-RAS-MAPK signalling pathway.

Structural and functional variety of accessory proteins

Rapidly emerging reports on signalling networks support the idea that various signalling molecules operate together in functional protein complexes. For example, activated protein nanoclusters in specialized membrane microdomains selectively connect with and subsequently turn on cytosolic signalling components or complexes.[8,9] Also RAS-nanoclusters form and locally increase the concentration of RAS paralogs in membrane microdomains.[10]

Membrane-resident signalling proteins, such as transmembrane and membrane-associated proteins, are predominantly trafficked to the plasma membrane *via* the secretory pathway.[11] But how are the cytosolic proteins trafficked to their cognate membrane nanoclusters? Mounting evidence has emerged recently that a large number of membraneless compartments (also called non-membrane-bound organelles or biomacromolecular condensates) are assembled *via* LLPS.[12] The formation of cytosolic signalling condensates is based on two processes. First multivalent molecules undergo phase separation, while in a second step other proteins are able to diffuse into the phase without considerably contributing to the stability of the phase. This process can increase local concentrations of molecules manifold. One example is the enrichment of kinases in membrane-associated liquid droplets around T-cell receptors while phosphatases are excluded.[13]

An essential group of proteins that are themselves not constituent components of signal transduction but allow assembly and spatiotemporal organization of a signalling cascade are accessory proteins. These proteins have the features to interact with and assemble other biomolecules, ranging from lipids, over proteins to nucleic acids. They mostly lack enzymatic activity, but are equipped with different types of protein-protein interaction domains, motifs, and intrinsically disordered regions (IDRs). Thus, accessory proteins dictate the local formation of macromolecular protein complexes through modular multivalent interactions, and thereby organize and facilitate signal transduction.

Accessory proteins bind and connect at least two constituent components to orchestrate their spatiotemporal localization and enhance their assembly *via* reducing dimensionality of interactions and/or increasing local concentrations of interacting proteins.[14–16] They can be categorized in four distinct groups based on their structure and mode of action: (1) **Scaffold proteins** are cytosolic multi-domain proteins that bind two or more distinct components to organize them in a functional unit and modulate their function. (2) **Adaptor proteins** link two partners usually *via* SH2 and/or SH3 domains and may also regulate their specific downstream signalling pathways. (3) **Anchoring proteins** bind to the membrane and other proteins, which are usually protein kinases, and therefore, bring them to their site of action. (4) **Docking proteins** assemble signalling complexes by binding to effectors and receptor tyrosine kinases or G-proteins at the membrane.

Accessory proteins of the RTK-RAS-MAPK pathway

New discoveries and concepts regarding the receptor-driven RAS-MAPK signal transduction have emerged during the last three decades: Novel pathway components, structure elucidation, biophysical principles, biomimetic strategies, and clinical drug candidates. By focusing particularly

on the signalling process itself, the emphasis of this article is on the implementation of the accessory proteins, which bind molecular components and orchestrate their assembly and eventually activity in a context-dependent manner. We believe that the spatial arrangements of such biophysical features over time determine specificity, efficiency, fidelity of signal transduction, and safeguard against any deleterious effects.

A multitude of accessory proteins, which largely vary in size and domain architecture (Figure 1), are involved in orchestrating RTK-RAS-MAPK signal transduction (Supplemental Table S1). The high variability of scaffold proteins is—due to their high interaction specificity—comprehensible. Certain domains or repeats frequently exist in individual proteins, for example LDs (repeated leucine-rich sequence) in Paxillin, WDs (WD-repeat) in MORG1, RRMs (RNA recognition motif) in NCL, and LIMs in FHL1/2. Furthermore, IDRs are found in several proteins, which may fold upon interaction with their binding partner. IDRs are also involved in oligomerization for example in Galectin-3.[17] Anchoring proteins contain membrane-binding domains, such as the PH domain in CNK1 and GAB1/2, and transmembrane (TM) segment, *e.g.*, in LAT, NTAL and SEF1. PAQR10/11 contain 7 TM segments and anchor RAS to the Golgi apparatus *via* their N-terminal cytoplasmic tail.[18] The PHB domain of FLOT1 has been reported to be a membrane association domain as it is post-translationally modified by palmitoylation.[19] This leads to FLOT1 association with lipid rafts of phagosomes and the plasma membrane. Docking proteins frequently possess both PH domains, which increase their residence time at the membrane, and PTB domains, which enable them to interact specifically with activated RTKs. Adaptor proteins are specialized in linking usually activated RTKs *via* SH2 domains with their downstream signalling molecules, in most cases, *via* SH3 domains.

Linking transmembrane receptors to RAS

GRB2 links activated RTKs or anchoring proteins, such as LAT, with SOS1/2 to activate RAS paralogs (Figure 2a). The adaptor protein function of GRB2 is accomplished by a central SH2 domain that binds to the tyrosine-phosphorylated RTK and two flanking SH3 domains, which bind to the C-terminal proline-rich domain of SOS1 and translocate it to the plasma membrane.[20,21] Activated SOS1, in turn, stimulates, as a RASGEF, the GDP/GTP exchange of RAS paralogs and thereby activate amongst others the MAPK cascade.[22]

Furthermore, direct GRB2 association with activated RTKs leads to the recruitment of GAB1 and CBL. GAB1 provides a docking platform for several signalling molecules, *e.g.*, SHP2, PLCγ, and PI3K, thereby cross-linking different signalling pathways.[23] CBL was originally described to acts as an adaptor protein as it contains several domains and motifs for protein-protein interactions (Figure 1). Later it was identified as an RING-dependent E3-ubiquitin-protein-ligase that transfers the ubiquitin to RTKs for endocytic internalization, and recycling or degradation.[24] It also regulates signalling processes of the non-receptor tyrosine kinases SYK, ZAP70, and SRC.[25] CBL constitutively interacts with GRB2, mediating hematopoietic cell proliferation[26], and T cell and B cell receptor and cytokine receptor signalling via interaction with CRKL SH2 domain.[27] As CBL and SOS1 bind to the same region of GRB2, the overexpression of CBL inhibits complex formation between SOS1 and GRB2 underlining the fine-tuning mechanism of accessry proteins by binding other pathway modulators.[28]

Engagement of GRB2 is versatile and depends on the cellular context. GRB2 can bind indirectly to RTKs *via* interaction with the tyrosine-phosphorylated adaptor proteins and FRS2. SHC links activated TRKA receptors to GRB2 in PC12nnr5 cells,[20,21,29] which can recruit SOS to the PM and control the extend of RAS activation.[22] Upon activation of the B-cell antigen receptor (BCR) in B-lymphocytes, the tyrosine kinase SYK phosphorylates SHC which leads to translocation of GRB2-SOS1 and activation of membrane-associated RAS signalling.[30] The SHC-GRB2 complex, downstream of cytokine receptors, also activates the PI3K pathway to control cell survival and/or proliferation.[31] A similar mechanism of GRB2-SOS-RAS activation is operated *via* FRS2, which acts downstream of TRKA in neurons,[20] and FGFR in embryonic stem cells.[32,33] FRS2 has multiple tyrosine phosphorylation sites to activate, in response to a wide range of agonists, PI3K and RAS-MAPK pathways in various cell types *via* binding to GRB2 and SHP2, respectively.[34–38] Binding of the ubiquitous protein tyrosine phosphatase SHP2 to GRB2, induces recruitment by the FRS2-SHP2 complex which controls retinal precursor proliferation and lens development.[39]

Modulating the RAS cycle

The RAS cycle between an inactive, GDP-bound state and an active, GTP bound state is strictly controlled by multidomain regulatory proteins.[40–43] Unlike the well-understood cellular process of RAS activation by RASGEFs, such as SOS1 little is known about the recruitment and activation of RASGAPs. The first evidence has emerged that the RASGAPs Neurofibromin and p120 are recruited to the plasma membrane and RAS•GTP by two distinct scaffold proteins, SPRED1 and Merlin (Figure 2b). The EVH domain of SPRED1, a member of the sprouty family, binds the GAP domain of Neurofibromin without interfering with its GAP function.[44,45] SPRED1 appears to directly contact BRAF and thus to interfere with KRAS signalling.[46] Merlin, a member of the ERM family, directly binds to, on the one hand, p120 and RAS (probably KRAS4B), a mechanism that potentiates RAS inactivation in Schwann cells, and on the other hand, CRAF and blocks its interaction with RAS.[47,48] p120 modulates many regulatory and signalling proteins *via* its N-terminal protein interaction domains, apparently independent of its GAP function.[49,50]

RAS-RAF connection

Lipidation and clustering of the RAS paralogs are critical steps for a tight control of signal transduction through the MAPK pathway. This process connects two distinct macromolecular clusters, plasma membrane-associated RAS-containing clusters[9] and cytosolic RAF/MEK/ERK-containing clusters.[51]

The scaffold proteins are Galectin 1 and 3 are carbohydrate-binding proteins that are involved in many physiological functions. While Galectin 1 homodimer binds to HRAS-RAF complex and stabilizes HRAS•GTP at the plasma membrane,[10,52] Galectin 3 selectively binds and clusters KRAS4B•GTP (Figure 2c).[53] The nucleolar phosphoproteins Nucleophosmin and Nucleolin shuttle between nucleus and PM and are different types of RAS scaffold proteins, which have been reported to stabilize KRAS4B levels in a nucleotide-independent manner at the plasma membrane. Nucleophosmin also increases the KRAS4B•GTP clusters and enhances MAPK signal transduction.[54]

Another type of clustering is performed by the scaffold protein SHOC2 (also known as SUR8), which connects activated RAS with the RAF kinases (Figure 2d). SHOC2 is an integral element of a heterotrimeric holoenzyme complex with PP1 and MRAS, which dephosphorylates and releases RAF from its inhibited state,[55,56] and subsequently activates the MAPK pathway.[57] The scaffold protein Erbin interferes with this process.[58] It binds and sequesters SHOC2 from its RAS/RAF complex, and inhibits ERK activation.[59] Erbin is a large scaffold protein (Figure 1). As such, it links different pathways by binding, besides SHOC2, also various other accessory proteins, including GRB2,[60] CBL,[61] Merlin,[62] and KSR1.[2,63]

RAF/MEK/ERK cascade

RAF kinase translocation to the plasma membrane and activation by direct interaction with RAS•GTP is well described.[2,64–66] Activated BRAF/CRAF heterodimer phosphorylates MEK1/2, which in turn phosphorylates ERK1/2 at the TEY motif in the activation loop.[67,68] Activated ERK1/2 are ultimately recruited to their substrates in various subcellular compartments.[69,70] The assembly of macromolecular complexes of the MAPK components and their connection with RAS nanoclusters at the membrane, which constitutes the RAS-ERK axis, is arranged by homo- and hetero-dimerization of the members of this pathway.[67] To achieve signal diversity, specificity, and fine-tuning, the spatiotemporal flux through the pathway is organized by various distinct accessory proteins, which bind either ERK, MEK/ERK or RAF/MEK/ERK.[1,69,71]

PEA15 modulates ERK activity towards its cytosolic substrates, including RSK2. It enhances ERK-dependent phosphorylation of RSK2 by binding both of them independently (Figure 2e).[72] PEA15 phosphorylation by PKC, AKT or CaMKII inhibits this process. In addition, PEA15 steers subcellular localization of ERK by facilitating its nucleocytoplasmic export.[73]

The MEK/ERK accessory proteins are illustrated in Figure 2f. GIT1 binds MEK1 and ERK1 in response to integrin, RTK and GPCR activation. Its activity is directly regulated by different downstream effectors, such as PIX/PAK complex.[74] MP1 binds and translocates MEK1 and ERK1 to late endosomes by associating with p14 and p18.[75,76] The anchoring protein SEF binds activated MEK on the Golgi apparatus, and subsequently ERK, leading to activation of ERK and finally its cytosolic substrates such as RSK2.[77] The latter phosphorylates SEF and induces its translocation to the plasma membrane, where it directly inhibits FGFRs, and enhances EGFR signalling instead.[78] RKIP acts as a competitive inhibitor of MEK phosphorylation. It binds ERK and mutually exclusively RAF or MEK, and thus, dissociates active RAF/MEK complexes.[79] The phosphorylation of RKIP by PKC results in release of RAF1 and enable the activation of MAPK pathway.[80]

The scaffolding of RAF/MEK/ERK is dependent on several factors, including the tissue specificity, cellular localization of the signalling complexes and the type of upstream signals (Figure 2g). KSR1 is one of the best studied scaffolds that binds to all three members of the RAF/MEK/ERK cascade.[71] KSR1 translocates, upon RTK-RAS activation, in a complex with MEK to CAV1-rich microdomains in the plasma membrane to bind activated RAF and modulate MEK and ERK activation. Feedback phosphorylation of KSR1 and BRAF by ERK promotes their dissociation and results in the release of KSR1/MEK from the plasma membrane.[81] In this way, MEK is sequestered from upstream signals and cannot itself regulate ERK activation.

The multidomain protein IQGAP1 scaffolds and activates the RAF/MEK/ERK kinases by directly associating with the EGF receptor.[82,83] With over one hundred binding partners, the localization and effect of IQGAP interaction reaches from actin cytoskeleton reorganization in the context of neurite outgrowth, migration or vascular barrier integrity to insulin secretion *via* exocytosis or cell proliferation and differentiation *via* ERK signalling. The extensive interactions of IQGAP vary according to cell types and environmental conditions.[84] In contrast, MORG1, FHL1, Paxillin and β-Arrestin act EGF-independent (Figure 2g). MORG1 exists in a complex with MP1, and facilitates ERK1/2 activation in response to LPA and PMA, and GPCR activation.[85] The focal-adhesion protein Paxillin modulates the activation of the RAF/MEK/ERK complex through binding of other proteins, controlling the remodelling of the actin cytoskeleton.[86] FHL1 scaffolds RAF/MEK/ERK on the N2B domain of the giant protein titin at the sarcomere of the mammalian muscle cells.[87] β-Arrestin stimulates ERK signalling in response to receptor activation, including GPCRs on the plasma membrane but also endosomes. FLOT1/2 are membrane raft associated proteins which form heterodimers. They are not only involved in the EGF receptor clustering and activation, but also directly bind CRAF, MEK and ERK enhancing their activity upon stimulation.[88] CNK1 physically interacts with RAF facilitating its activation through assisting RAF membrane localization and oligomerization upon RAS activation,[89] while being able to interact with RAS as well via the N-terminal regions.[90]

Accessory proteins as in human disease

Even if dysregulated constituent components of the RTK-RAS-MAPK pathway are amongst the most intensively studied target structures for disease treatment, new emphasis should be laid on accessory proteins (Figure 3). Their loss-of-function or gain-of-function mutations are mostly and frequently associated with the initiation and progression of human diseases and disorders. The hyperactivation of the RTK-RAS-MAPK pathway is a known cause of many diseases, including cancer and developmental disorders, including RASopathies.

Cancer

The upregulation of activating proteins or the downregulation of inhibiting proteins lead to gain-of-function of the RTK-RAS-MAPK pathway in almost all types of cancer (Figure 3a). The expression of accessory proteins is tightly controlled and often dysregulated in tumours. Paxillin is a scaffold protein, which is involved in focal adhesion. A gain-of-function mutation in Paxillin has been found in 9% of all non-small-cell lung cancers (1).[91] Furthermore, amplification of Paxillin gene in lung cancer promotes tumour growth, invasion and migration.[92] SPRED1/2, negative modulators of RAS signalling, are downregulated in 84% of patients with hepatocellular carcinoma (2).[93] The scaffold protein IQGAP1 promotes tumour formation, transformation, invasion and metastasis in various cancer types (3).[94] A study of a KSR $^{-/-}$ mouse model proves the resistance against RAS-dependent tumour formation,[95] highlighting the pro-oncogenic function of KSR in RAS-driven cancers (4). SHOC2 mediates tumourigenesis and metastasis in different cancer types *via* tethering RAS and CRAF proteins in close proximity and thus promoting RAS-mediated CRAF activation.[96,97] Knock-out models of SHOC2 in KRAS mutated lung adenocarcinoma in

mice have revealed a significant reduction of tumour growth, as well as a prolonged survival, accentuating the scaffold protein as a potential therapeutic target (5).[98] GAB2 has been implicated as a central modulator for oncogenic BCR-ABL signalling.[99] GAB2 deficient mice have exhibited resistance against cancer cell transformation of myeloid progenitors in the presence of BCR-ABL, which is found in 90% of patients with chronic myeloid leukaemia (6).[99,100] SHP2 is not only associated with a large number of cancers but plays a central role PD-L1/PD-1 singling that inhibits the TCR-activated pathways, including RAS-MAPK, in T-cells (Figure 3b (7)).[101] Thus, SHP2 inhibitors provide a possible effective therapy against these cancers.

RASopathies

RASopathies or RAS-MAPK syndromes are defined as a group of developmental disorders that are caused by mild gain-of-function germline mutations in genes related to not only the constituent members of the RTK-RAS-MAPK pathway[102] but also various accessory proteins, including CBL, SHP2, SPRED1, and SHOC2 (Figure 3a).[102]

Germline CBL mutations exhibit a wide phenotypic variability related to Noonan syndrome, which is characterized by a relatively high frequency of neurological features, predisposition to juvenile myelomonocytic leukaemia, and low prevalence of cardiac defects, reduced growth, and cryptorchidism.[103] The mutations are mainly located in the central region of CBL, which is known to abolish the ubiquitination of RTKs by impairing CBLs E3 ligase activity .[103] Legius syndrome-associated mutations in SPRED1, mostly result in loss-of-function of the scaffold protein, and gain-of-function of the RAS-MAPK pathway.[104,105] In contrast, mutations in genes encoding SHP2 and SHOC2 lead to a gain of function and contribute to MAPK signalling upregulation that causes diverse developmental phenotypes.[55,58,106] A recurrent activating mutation at the very N-terminus of SHOC2 (Ser-2 to Gly) leads to N-myristoylation of SHOC2, confers continuous membrane association and consequently causes Mazzanti syndrome, a RASopathy characterized by features resembling Noonan syndrome.[106,107] Another RASopathy-causing SHOC2 mutation (Gln-269 to His and His-270 to Tyr) has been recently identified to be associated with prenatal-onset hypertrophic cardiomyopathy.[106] This mutation changes the relative orientation of the two leucine-rich repeat domains of SHOC2 and enhances its binding to MRAS and PPP1CB, two other RASopathy genes,[108] and thus, increased signalling through the MAPK cascade.[106]

Other diseases

Moyamoya angiopathy (MMA) is characterized by progressive stenosis of the terminal portion of the internal carotid arteries and the development of a network of abnormal collateral vessels. This is a rare condition that is caused by *de novo* CBL mutations even in the absence of obvious signs of RASopathy.[109] Evidence linking CNK1 dysfunction to autosomal recessive intellectual disability (ARID) in patients emphasizes the importance of this anchoring protein in the orchestration of the RTK-RAS-MAPK signalling in brain development and cognition.[110] The scaffold proteins FHL1/2 link RAS-MAPK signalling to the sarcomere and is a critical component of the hypertrophy signalling in cardiac cells (Figure 3c).[87] FHL mutations are associated with cardiac diseases.[111] FLOT1 has been implicated in the development of Alzheimer and type 2 diabetes and could be a promising proteomic biomarker.[112,113]

Accessory proteins as therapeutic targets

Direct targeting of constituent members of the RTK-RAS-MAPK axis in the context of disease treatment, such as cancer, is a big challenge. Therapies for KRAS cancers remain a major clinical need, despite allele-specific inhibitors that trap and inactivate mutant KRAS(G12C).[114,115] Three decades of research led to significant advances in tumour treatment.[116] However the side-effects can still be severe and more specific treatments could ease patient suffering. Unfortunately, many of the expectations for RAS pathway-targeted drugs have not been fulfilled. High toxicity and resistance acquisition have hampered many of the drugs developed to date.[116,117] An alternative therapeutic strategy to treat KRAS mutant cancers aims at protein degradation *via* proteolysis targeting chimeras (PROTACs).[118] The ablation of CRAF in advanced tumours driven by KRAS oncogene leads to significant tumour regression with no detectable appearance of resistance mechanisms and limited toxicities.[119] In this context, a recent study has reported first progress to develop degrader molecules that target KRAS oncogene in non-small-cell lung carcinomas.[120]

Emerging evidence suggests that constituent signalling proteins assemble into macromolecular complexes and co-operate in clusters at specific sites of the cell. Therefore, it is important to note that the stoichiometric imbalance of each subunit of a complex—either by gene overexpression on the one side, and depletion, knockout or targeted protein degradation on the other—perturbs the equilibrium, and interferes at some level with the function of the protein or its complex.[121] With accessory proteins being of immense relevance for the whole signalling machinery and operating particularly from the sideline, we propose that functional interference with a defined site of accessory proteins may attenuate rather than inhibit the signalling of hyperactivated RTK-RAS-MAPK axis.

The knock-out or knock-down of accessory proteins in cell-based or animal models could already show the importance of these modulators in cancer signalling. The scaffold protein SHOC2 has an important role in embryogenesis, therefore, loss of SHOC2 is embryonically lethal. In contrast, the systemic knock-out in adult mice as well as in human cell lines is quite well tolerated and leads to growth inhibition of RAS-mutated NSCLC cell lines.[98] Furthermore, the depletion of SHOC2 leads to a sensitization towards MEK-inhibitor treatment, by interfering with the feedback-loop of MEK inhibition *via* BRAF/CRAF dimerization, which is SHOC2 dependent.[98] Therefore, dual targeting of SHOC2 and MEK appears as a promising treatment strategy in RAS-mutated cancers. Another approach deals the scaffold protein GIT1. The knock-down of GIT1 in human osteosarcoma cells has shown *in vivo* and *in vitro* reduced tumour cell growth, invasion and angiogenesis, which could make GIT1 a potential target in gene therapy.[122]

There is a number of approaches of targeting specific functions of accessory proteins. The CNK1 inhibitor PHT-7.3 binds to its PH domain and prevents the co-localization with prenylated KRAS4B on the plasma membrane.[123] PHT-7.3 successfully inhibits growth of tumour cells incudes by mutated but not wild type KRAS4B. The interference of GRB2 mRNA by liposome-incorporated nuclease-resistant antisense oligodeoxynucleotides in BCR-ABL fusion protein positive cancer cells, leads to reduced tumour growth in Xenograft models.[124] It interferes with RAS/MAPK pathway and the cross-talk towards AKT pathway *via* GAB2. A WW-peptide of IQGAP1 binds ERK and competes with endogenous IQGAP1, which leads to attenuation of ERK activation.[125]

This treatment together with the BRAF inhibitor Vemurafenib (PLX-4032), was very successful in tumour mouse models.[125] It has been later shown that not the WW-domain but the IQ domain is necessary to bind ERK.[126] The effects on the tumour growth suppression may stem from the interference with another yet unknown binding partner of IQGAP1 as an integral elements of its complex scaffolding function. Another interesting example of an accessory proteins as therapeutic target is the small molecule APS-2-79, which binds KSR in its inactive state and interferes with RAF binding and thus block MEK phosphorylation.[127] The cell-based experiments with APS-2-79 have shown not only reduced ERK activation and growth inhibition in combination with the MEK-inhibitor Trametinib, but also antagonizing its resistance mechanism.[128] Besides active site inhibitors, an allosteric inhibitor of SHP2 SHP099 stabilizes the autoinhibited state and interferes with the enzyme activity as well as its adaptor protein function to bind, for example, GRB2-SOS complex.[129] A combination of SHP099 with a MEK inhibitor and has been shown to interfere with the feedback mechanism *via* SHP2 and to block the resistance initiation observed in KRAS4B-driven cancer therapy.[129–131] Additionally, SHP2 inhibition by SHP099 has been shown to have a positive effect on anti-tumour immunity in colon cancer xenograft models, especially in a co-treatment with anti-PD-1 antibody.[132]

Given that the majority of accessory proteins are now emerging as attractive therapeutic targets, still a very small number of accessory inhibitors are discovered yet.

Concluding remarks

Accessory proteins tightly control signal transduction by finetuning spatiotemporal organization of signalling components and maintaining specificity and function of the pathway. They operate from the sideline, from which they specifically leverage their multivalent domains on the formation of macromolecular clusters, as highlighted in this article. Even though interest in accessory proteins has grown in the past few years, the possibilities to practically visualize them, track their pathway, and experimentally and selectively affect their functions in human cells are keys to addressing questions about their cell type specificities, subcellular distribution, and interactions in a context-dependent manner at the `endogenous´ levels. The major challenges faced and likely to be faced in near future are the difficult task of the direct use of antibodies post-purchase without careful validation,[133] and the overexpression studies in spite of their experimental advantages.[121] A barrier that is even more difficult to assess is the misinformed opinion that it is difficult to glean meaningful biological insights when genes are expressed at nonphysiological levels. A prominent example is KSR overexpression that has been erroneously identified as a suppressor of RAS signalling. Thus, exploring these concepts in greater detail will provide the framework for the future research that will fill existing gaps in our knowledge and expand our understanding of more effective therapies.

References

1. McKay, M. M. & Morrison, D. K. Integrating signals from RTKs to ERK/MAPK. **Oncogene** 2007 26: 3113–3121

2. Lavoie, H. & Therrien, M. Regulation of RAF protein kinases in ERK signalling. **Nat. Rev. Mol. Cell Biol.** 2015 16: 281–298

3. Nakhaei-Rad, S., Haghighi, F., Nouri, P., Rezaei Adariani, S., Lissy, J., Kazemein Jasemi, N. S., Dvorsky, R. & Ahmadian, M. R. Structural fingerprints, interactions, and signaling networks of RAS family proteins beyond RAS isoforms. **Crit. Rev. Biochem. Mol. Biol.** 2018 53: 130–156

4. Tartaglia, M. & Gelb, B. D. Disorders of dysregulated signal traffic through the RAS-MAPK pathway: Phenotypic spectrum and molecular mechanisms. **Ann. N. Y. Acad. Sci.** 2010 1214: 99–121

5. Dhillon, A. S., Hagan, S., Rath, O. & Kolch, W. MAP kinase signalling pathways in cancer. **Oncogene** 2007 26: 3279–3290

6. Castel, P., Rauen, K. A. & McCormick, F. The duality of human oncoproteins: drivers of cancer and congenital disorders. **Nat. Rev. Cancer** 2020 20: 383–397

7. Lyon, A. S., Peeples, W. B. & Rosen, M. K. A framework for understanding the functions of biomolecular condensates across scales. **Nat. Rev. Mol. Cell Biol.** 2020 doi:10.1038/s41580-020-00303-z

8. Kholodenko, B. N., Hancock, J. F. & Kolch, W. Signalling ballet in space and time. **Nat. Rev. Mol. Cell Biol.** 2010 11: 414–426

9. Zhou, Y., Prakash, P., Gorfe, A. A. & Hancock, J. F. Ras and the Plasma Membrane: A Complicated Relationship. **Cold Spring Harb. Perspect. Med.** 2018 8:

10. Blaževitš, O., Mideksa, Y. G., Šolman, M., Ligabue, A., Ariotti, N., Nakhaeizadeh, H., Fansa, E. K., Papageorgiou, A. C., Wittinghofer, A., Ahmadian, M. R. & Abankwa, D. Galectin-1 dimers can scaffold Raf-effectors to increase H-ras nanoclustering. **Sci. Rep.** 2016 6: 24165

11. Omerovic, J. & Prior, I. A. Compartmentalized signalling: Ras proteins and signalling nanoclusters. **FEBS J.** 2009 276: 1817–1825

12. Banani, S. F., Lee, H. O., Hyman, A. A. & Rosen, M. K. Biomolecular condensates: Organizers of cellular biochemistry. **Nat. Rev. Mol. Cell Biol.** 2017 18: 285–298

13. Su, X., Ditlev, J. A., Hui, E., Xing, W., Banjade, S., Okrut, J., King, D. S., Taunton, J., Rosen, M. K. & Vale, R. D. Phase separation of signaling molecules promotes T cell receptor signal transduction. **Science (80-.).** 2016 352: 595–599

14. Hunter, T. Signaling - 2000 and beyond. **Cell** 2000 100: 113–127

15. Tian, T., Harding, A., Inder, K., Plowman, S., Parton, R. G. & Hancock, J. F. Plasma membrane nanoswitches generate high-fidelity Ras signal transduction. **Nat. Cell Biol.** 2007 9: 905–914

16. Ivakhno, S. & Armstrong, J. D. Non-linear dimensionality reduction of signaling networks. **BMC Syst. Biol.** 2007 1: 1–17

17. Lin, Y. H., Qiu, D. C., Chang, W. H., Yeh, Y. Q., Jeng, U. S., Liu, F. T. & Huang, J. rong. The intrinsically disordered N-terminal domain of galectin-3 dynamically mediates multisite self-association of the protein through fuzzy interactions. **J. Biol. Chem.** 2017 292: 17845–17856

18. Jin, T., Ding, Q., Huang, H., Xu, D., Jiang, Y., Zhou, B., Li, Z., Jiang, X., He, J., Liu, W., Zhang, Y., Pan, Y., Wang, Z., Thomas, W. G. & Chen, Y. PAQR10 and PAQR11 mediate Ras signaling in the Golgi apparatus. **Cell Res.** 2012 22: 661–676

19. Morrow, I. C., Rea, S., Martin, S., Prior, I. A., Prohaska, R., Hancock, J. F., James, D. E. & Parton, R. G. Flotillin-1/reggie-2 traffics to surface raft domains via a novel Golgi-independent pathway. Identification of a novel membrane targeting domain and a role for palmitoylation. **J. Biol. Chem.** 2002 277: 48834–48841

20. MacDonald, J. I. S., Gryz, E. A., Kubu, C. J., Verdi, J. M. & Meakin, S. O. Direct binding of the signaling adapter protein Grb2 to the activation loop tyrosines on the nerve growth factor receptor tyrosine kinase, TrkA. **J. Biol. Chem.** 2000 275: 18225–18233

21. Biernat, W. Epidermal growth factor receptor in glioblastoma. **Folia Neuropathol** 2005 43: 123–132

22. Ravichandran, K. S., Lorenz, U., Shoelson, S. E. & Burakoff, S. J. Interaction of Shc with Grb2 regulates association of Grb2 with mSOS. **Mol. Cell. Biol.** 1995 15: 593–600

23. Wöhrle, F. U., Daly, R. J. & Brummer, T. Function, regulation and pathological roles of the Gab/DOS docking proteins. **Cell Commun. Signal.** 2009 7: 22

24. Joazeiro, C. A. P., Wing, S. S., Huang, H. K., Leverson, J. D., Hunter, T. & Liu, Y. C. The tyrosine kinase negative regulator c-Cbl as a RING-type, E2- dependent ubiquitin-protein ligase. **Science (80-.).** 1999 286: 309–312

25. Sanjay, A., Horne, W. C. & Baron, R. The Cbl Family: Ubiquitin Ligases Regulating Signaling by Tyrosine Kinases. **Sci. Signal.** 2001 2001: pe40–pe40

26. Brizzi, M. F., Dentelli, P., Lanfrancone, L., Rosso, A., Pelicci, P. G. & Pegoraro, L. Discrete protein interactions with the Grb2/c-Cbl complex in SCF- and TPO-mediated myeloid cell proliferation. **Oncogene** 1996 13: 2067–2076

27. Elly, C., Witte, S., Zhang, Z., Rosnet, O., Lipkowitz, S., Altman, A. & Liu, Y. C. Tyrosine phosphorylation and complex formation of Cbl-b upon T cell receptor stimulation. **Oncogene** 1999 18: 1147–1156

28. Wong, A., Lamothe, B., Lee, A., Schlessinger, J. & Lax, I. FRS2α attenuates FGF receptor signaling by Grb2-mediated recruitment of the ubiquitin ligase Cbl. **Proc. Natl. Acad. Sci. U. S. A.** 2002 99: 6684–6689

29. Stephens, RM ; Loeb, DM ; Copeland, TD ; Pawson, Tony ; Greene, LA ; Kaplan, D. Trk receptors use redundant signal transduction pathways involving SHC and PLC-gamma 1 to mediate NGF responses | TSpace Repository. **Neuron** 1994 3: 691–705

30. Harmer, S. L. & DeFranco, A. L. Shc contains two Grb2 binding sites needed for efficient formation of complexes with SOS in B lymphocytes. **Mol. Cell. Biol.** 1997 17: 4087–4095

31. Gu, H., Maeda, H., Moon, J. J., Lord, J. D., Yoakim, M., Nelson, B. H. & Neel, B. G. New Role for Shc in Activation of the Phosphatidylinositol 3-Kinase/Akt Pathway. **Mol. Cell. Biol.** 2000 20: 7109–7120

32. Kouhara, H., Hadari, Y. R., Spivak-Kroizman, T., Schilling, J., Bar-Sagi, D., Lax, I. & Schlessinger, J. A lipid-anchored Grb2-binding protein that links FGF-receptor activation

to the Ras/MAPK signaling pathway. **Cell** 1997 89: 693–702

33. Murohashi, M., Nakamura, T., Tanaka, S., Ichise, T., Yoshida, N., Yamamoto, T., Shibuya, M., Schlessinger, J. & Gotoh, N. An FGF4-FRS2α-Cdx2 axis in trophoblast stem cells induces Bmp4 to regulate proper growth of early mouse embryos. **Stem Cells** 2010 28: 113–121

34. Zhang, S. Q., Yang, W., Kontaridis, M. I., Bivona, T. G., Wen, G., Araki, T., Luo, J., Thompson, J. A., Schraven, B. L., Philips, M. R. & Neel, B. G. Shp2 Regulates Src Family Kinase Activity and Ras/Erk Activation by Controlling Csk Recruitment. **Mol. Cell** 2004 13: 341–355

35. Hadari, Y. R., Kouhara, H., Lax, I. & Schlessinger, J. Binding of Shp2 Tyrosine Phosphatase to FRS2 Is Essential for Fibroblast Growth Factor-Induced PC12 Cell Differentiation. **Mol. Cell. Biol.** 1998 18: 3966–3973

36. Dance, M., Montagner, A., Salles, J. P., Yart, A. & Raynal, P. The molecular functions of Shp2 in the Ras/Mitogen-activated protein kinase (ERK1/2) pathway. **Cell. Signal.** 2008 20: 453–459

37. Tajan, M., de Rocca Serra, A., Valet, P., Edouard, T. & Yart, A. SHP2 sails from physiology to pathology. **Eur. J. Med. Genet.** 2015 58: 509–525

38. Chen, P. Y. & Friesel, R. FGFR1 forms an FRS2-dependent complex with mTOR to regulate smooth muscle marker gene expression. **Biochem. Biophys. Res. Commun.** 2009 382: 424–429

39. Gotoh, N., Ito, M., Yamamoto, S., Yoshìno, I., Song, N., Wang, Y., Lax, I., Schlessinger, J., Shibuya, M. & Lang, R. A. Tyrosine phosphorylation sites on FRS2α responsible for Shp2 recruitment are critical for induction of lens and retina. **Proc. Natl. Acad. Sci. U. S. A.** 2004 101: 17144–17149

40. Quilliam, L. A., Rebhun, J. F. & Castro, A. F. A growing family of guanine nucleotide exchange factors is responsible for activation of ras-family GTPases. **Prog. Nucleic Acid Res. Mol. Biol.** 2002 71: 391–444

41. Scheffzek, K. & Shivalingaiah, G. Ras-specific gtpase-activating proteins— structures, mechanisms, and interactions. **Cold Spring Harb. Perspect. Med.** 2019 9:

42. Simanshu, D. K., Nissley, D. V. & McCormick, F. RAS Proteins and Their Regulators in Human Disease. **Cell** 2017 170: 17–33

43. Haghighi, F., Dahlmann, J., Nakhaei-Rad, S., Lang, A., Kutschka, I., Zenker, M., Kensah, G., Piekorz, R. P. & Ahmadian, M. R. bFGF-mediated pluripotency maintenance in human induced pluripotent stem cells is associated with NRAS-MAPK signaling. **Cell Commun. Signal.** 2018 16: 96

44. Stowe, I. B., Mercado, E. L., Stowe, T. R., Bell, E. L., Oses-Prieto, J. A., Hernández, H., Burlingame, A. L. & McCormick, F. A shared molecular mechanism underlies the human rasopathies Legius syndrome and Neurofibromatosis-1. **Genes Dev.** 2012 26: 1421–1426

45. Dunzendorfer-Matt, T., Mercado, E. L., Maly, K., McCormick, F. & Scheffzek, K. The neurofibromin recruitment factor Spred1 binds to the GAP related domain without affecting

Ras inactivation. **Proc. Natl. Acad. Sci. U. S. A.** 2016 113: 7497–7502

46. Siljamäki, E. & Abankwa, D. SPRED1 Interferes with K-ras but Not H-ras Membrane Anchorage and Signaling. **Mol. Cell. Biol.** 2016 36: 2612–2625

47. Cui, Y., Groth, S., Troutman, S., Carlstedt, A., Sperka, T., Riecken, L. B., Kissil, J. L., Jin, H. & Morrison, H. The NF2 tumor suppressor merlin interacts with Ras and RasGAP, which may modulate Ras signaling. **Oncogene** 2019 38: 6370–6381

48. Cui, Y., Ma, L., Schacke, S., Yin, J. C., Hsueh, Y.-P., Jin, H. & Morrison, H. Merlin cooperates with neurofibromin and Spred1 to suppress the Ras–Erk pathway. **Hum. Mol. Genet.** 2020 ddaa263:

49. Pamonsinlapatham, P., Hadj-Slimane, R., Lepelletier, Y., Allain, B., Toccafondi, M., Garbay, C. & Raynaud, F. P120-Ras GTPase activating protein (RasGAP): A multi-interacting protein in downstream signaling. **Biochimie** 2009 91: 320–328

50. Jaiswal, M., Dvorsky, R., Amin, E., Risse, S. L., Fansa, E. K., Zhang, S. C., Taha, M. S., Gauhar, A. R., Nakhaei-Rad, S., Kordes, C., Koessmeier, K. T., Cirstea, I. C., Olayioye, M. A., Häussinger, D. & Ahmadian, M. R. Functional cross-talk between ras and rho pathways: A ras-specific gtpase-activating protein (p120RasGAP) competitively inhibits the rhogap activity of deleted in liver cancer (DLC) tumor suppressor by masking the catalytic arginine finger. **J. Biol. Chem.** 2014 289: 6839–6849

51. An, S., Yang, Y., Ward, R., Liu, Y., Guo, X. X. & Xu, T. R. Raf-interactome in tuning the complexity and diversity of Raf function. **FEBS J.** 2015 282: 32–53

52. Belanis, L., Plowman, S. J., Rotblat, B., Hancock, J. F. & Kloog, Y. Galectin-1 is a novel structural component and a major regulator of H-Ras nanoclusters. **Mol. Biol. Cell** 2008 19: 1404–1414

53. Shalom-Feuerstein, R., Plowman, S. J., Rotblat, B., Ariotti, N., Tian, T., Hancock, J. F. & Kloog, Y. K-Ras nanoclustering is subverted by overexpression of the scaffold protein galectin-3. **Cancer Res.** 2008 68: 6608–6616

54. Inder, K. L., Lau, C., Loo, D., Chaudhary, N., Goodall, A., Martin, S., Jones, A., Van der Hoeven, D., Parton, R. G., Hill, M. M. & Hancock, J. F. Nucleophosmin and nucleolin regulate K-ras plasma membrane interactions and MAPK signal transduction. **J. Biol. Chem.** 2009 284: 28410–28419

55. Young, L. C., Hartig, N., Boned Del Río, I., Sari, S., Ringham-Terry, B., Wainwright, J. R., Jones, G. G., McCormick, F. & Rodriguez-Viciana, P. SHOC2-MRAS-PP1 complex positively regulates RAF activity and contributes to Noonan syndrome pathogenesis. **Proc. Natl. Acad. Sci. U. S. A.** 2018 115: E10576–E10585

56. Rodriguez-Viciana, P., Oses-Prieto, J., Burlingame, A., Fried, M. & McCormick, F. A Phosphatase Holoenzyme Comprised of Shoc2/Sur8 and the Catalytic Subunit of PP1 Functions as an M-Ras Effector to Modulate Raf Activity. **Mol. Cell** 2006 22: 217–230

57. del Río, I. B., Young, L. C., Sari, S., Jones, G. G., Ringham-Terry, B., Hartig, N., Rejnowicz, E., Lei, W., Bhamra, A., Surinova, S. & Rodriguez-Viciana, P. SHOC2 complex-driven RAF dimerization selectively contributes to ERK pathway dynamics. **Proc. Natl. Acad. Sci. U. S. A.** 2019 116: 13330–13339

58. Jang, H., Stevens, P., Gao, T. & Galperin, E. The leucine-rich repeat signaling scaffolds Shoc2 and Erbin: cellular mechanism and role in disease. **FEBS J.** 2020 febs.15450 doi:10.1111/febs.15450

59. Dai, P., Xiong, W. C. & Mei, L. Erbin inhibits RAF activation by disrupting the Sur-8-Ras-Raf complex. **J. Biol. Chem.** 2006 281: 927–933

60. Zheng, Z., Zheng, X., Zhu, Y., Gu, X., Gu, W., Xie, X., Hu, W. & Jiang, J. miR-183-5p Inhibits Occurrence and Progression of Acute Myeloid Leukemia via Targeting Erbin. **Mol. Ther.** 2019 27: 542–558

61. Yao, S., Zheng, P., Wu, H., Song, L. M., Ying, X. F., Xing, C., Li, Y., Xiao, Z. Q., Zhou, X. N., Shen, T., Chen, L., Liu, Y. H., Lai, M. De, Mei, L., Gao, T. M. & Li, J. M. Erbin interacts with c-Cbl and promotes tumourigenesis and tumour growth in colorectal cancer by preventing c-Cbl-mediated ubiquitination and down-regulation of EGFR. **J. Pathol.** 2015 236: 65–77

62. Wilkes, M. C., Repellin, C. E., Hong, M., Bracamonte, M., Penheiter, S. G., Borg, J. P. & Leof, E. B. Erbin and the NF2 Tumor Suppressor Merlin Cooperatively Regulate Cell-Type-Specific Activation of PAK2 by TGF-β. **Dev. Cell** 2009 16: 433–444

63. Stevens, P. D., Wen, Y. A., Xiong, X., Zaytseva, Y. Y., Li, A. T., Wang, C., Stevens, A. T., Farmer, T. N., Gan, T., Weiss, H. L., Inagaki, M., Marchetto, S., Borg, J. P. & Gao, T. Erbin suppresses KSR1-mediated RaS/RAF signaling and tumorigenesis in colorectal cancer. **Cancer Res.** 2018 78: 4839–4852

64. Matallanas, D., Birtwistle, M., Romano, D., Zebisch, A., Rauch, J., von Kriegsheim, A. & Kolch, W. Raf family kinases: old dogs have learned new tricks. **Genes Cancer** 2011 2: 232–60

65. Rezaei Adariani, S., Buchholzer, M., Akbarzadeh, M., Nakhaei-Rad, S., Dvorsky, R. & Ahmadian, M. R. Structural snapshots of RAF kinase interactions. **Biochem. Soc. Trans.** 2018 46: 1393–1406

66. Terrell, E. M. & Morrison, D. K. Ras-mediated activation of the Raf family kinases. **Cold Spring Harb. Perspect. Med.** 2019 9:

67. Santos, E. & Crespo, P. The RAS-ERK pathway: A route for couples. **Sci. Signal.** 2018 11:

68. Roskoski, R. ERK1/2 MAP kinases: Structure, function, and regulation. **Pharmacol. Res.** 2012 66: 105–143

69. Wortzel, I. & Seger, R. The ERK cascade: Distinct functions within various subcellular organelles. **Genes and Cancer** 2011 2: 195–209

70. Kolch, W. Meaningful relationships: The regulation of the Ras/Raf/MEK/ERK pathway by protein interactions. **Biochem. J.** 2000 351: 289–305

71. Kolch, W. Coordinating ERK/MAPK signalling through scaffolds and inhibitors. **Nat. Rev. Mol. Cell Biol.** 2005 6: 827–837

72. Vaidyanathan, H., Opoku-Ansah, J., Pastorino, S., Renganathan, H., Matter, M. L. & Ramos, J. W. ERK MAP kinase is targeted to RSK2 by the phosphoprotein PEA-15. **Proc.**

Natl. Acad. Sci. U. S. A. 2007 104: 19837–19842

73. Formstecher, E., Ramos, J. W., Fauquet, M., Calderwood, D. A., Hsieh, J. C., Canton, B., Nguyen, X. T., Barnier, J. V., Camonis, J., Ginsberg, M. H. & Chneiweiss, H. PEA-15 Mediates Cytoplasmic Sequestration of ERK MAP Kinase. **Dev. Cell** 2001 1: 239–250

74. Zhang, N., Cai, W., Ma, Y., Yin, G., Nagel, D. & Berk, B. GIT1 is a Novel MEK1-ERK1/2 Scaffold that Localizes to Focal Adhesions. **Cell Biol. Int.** 2009 34: 41–47

75. Teis, D., Wunderlich, W. & Huber, L. A. Localization of the MP1-MAPK Scaffold Complex to Endosomes Is Mediated by p14 and Required for Signal Transduction. **Dev. Cell** 2002 3: 803–814

76. Nada, S., Hondo, A., Kasai, A., Koike, M., Saito, K., Uchiyama, Y. & Okada, M. The novel lipid raft adaptor p18 controls endosome dynamics by anchoring the MEK-ERK pathway to late endosomes. **EMBO J.** 2009 28: 477–489

77. Kovalenko, D., Yang, X., Nadeau, R. J., Harkins, L. K. & Friesel, R. Sef inhibits fibroblast growth factor signaling by inhibiting FGFR1 tyrosine phosphorylation and subsequent ERK activation. **J. Biol. Chem.** 2003 278: 14087–14091

78. Ren, Y., Li, Z., Rong, Z., Cheng, L., Li, Y., Wang, Z. & Chang, Z. Tyrosine 330 in hSef is critical for the localization and the inhibitory effect on FGF signaling. **Biochem. Biophys. Res. Commun.** 2007 354: 741–746

79. Yeung, K., Seitz, T., Li, S., Janosch, P., McFerran, B., Kaiser, C., Fee, F., Katsanakis, K. D., Rose, D. W., Mischak, H., Sedivy, J. M. & Kolch, W. Suppression of Raf-1 kinase activity and MAP kinase signalling by RKIP. **Nature** 1999 401: 173–177

80. Keller, E. T., Fu, Z. & Brennan, M. The role of Raf kinase inhibitor protein (RKIP) in health and disease. **Biochem. Pharmacol.** 2004 68: 1049–1053

81. McKay, M. M., Ritt, D. A. & Morrison, D. K. Signaling dynamics of the KSR1 scaffold complex. **Proc. Natl. Acad. Sci. U. S. A.** 2009 106: 11022–11027

82. McNulty, D. E., Li, Z., White, C. D., Sacks, D. B. & Annan, R. S. MAPK scaffold IQGAP1 binds the EGF receptor and modulates its activation. **J. Biol. Chem.** 2011 286: 15010–15021

83. Bañón-Rodríguez, I., Gálvez-Santisteban, M., Vergarajauregui, S., Bosch, M., Borreguero-Pascual, A. & Martín-Belmonte, F. EGFR controls IQGAP basolateral membrane localization and mitotic spindle orientation during epithelial morphogenesis. **EMBO J.** 2014 33: 129–145

84. Hedman, A. C., Smith, J. M. & Sacks, D. B. The biology of IQGAP proteins: beyond the cytoskeleton. **EMBO Rep.** 2015 16: 427–446

85. Vomastek, T., Schaeffer, H. J., Tarcsafalvi, A., Smolkin, M. E., Bissonette, E. A. & Weber, M. J. Modular construction of a signaling scaffold: MORG1 interacts with components of the ERK cascade and links ERK signaling to specific agonists. **Proc. Natl. Acad. Sci. U. S. A.** 2004 101: 6981–6986

86. Turner, C. E. Paxillin and focal adhesion signalling. **Nat. Cell Biol.** 2000 2:

87. Sheikh, F., Raskin, A., Chu, P. H., Lange, S., Domenighetti, A. A., Zheng, M., Liang, X., Zhang, T., Yajima, T., Gu, Y., Dalton, N. D., Mahata, S. K., Dorn, G. W., Heller-Brown, J., Peterson, K. L., Omens, J. H., McCulloch, A. D. & Chen, J. An FHL1-containing complex within the cardiomyocyte sarcomere mediates hypertrophic biomechanical stress responses in mice. **J. Clin. Invest.** 2008 118: 3870–3880

88. Amaddii, M., Meister, M., Banning, A., Tomasovic, A., Mooz, J., Rajalingam, K. & Tikkanen, R. Flotillin-1/Reggie-2 protein plays dual role in activation of receptor-tyrosine kinase/mitogen-activated protein kinase signaling. **J. Biol. Chem.** 2012 287: 7265–7278

89. Therrien, M., Wong, A. M. & Rubin, G. M. CNK, a RAF-binding multidomain protein required for RAS signaling. **Cell** 1998 95: 343–353

90. Therrien, M., Wong, A. M., Kwan, E. & Rubin, G. M. Functional analysis of CNK in RAS signaling. **Proc. Natl. Acad. Sci. U. S. A.** 1999 96: 13259–13263

91. Mackinnon, A. C., Tretiakova, M., Henderson, L., Mehta, R. G., Yan, B. C., Joseph, L., Krausz, T., Husain, A. N., Reid, M. E. & Salgia, R. Paxillin expression and amplification in early lung lesions of high-risk patients, lung adenocarcinoma and metastatic disease. **J. Clin. Pathol.** 2011 64: 16–24

92. Jagadeeswaran, R., Surawska, H., Krishnaswamy, S., Janamanchi, V., Mackinnon, A. C., Seiwert, T. Y., Loganathan, S., Kanteti, R., Reichman, T., Nallasura, V., Schwartz, S., Faoro, L., Wang, Y. C., Girard, L., Tretiakova, M. S., Ahmed, S., Zumba, O., Soulii, L., Bindokas, V. P., Szeto, L. L., Gordon, G. J., Bueno, R., Sugarbaker, D., Lingen, M. W., Sattler, M., Krausz, T., Vigneswaran, W., Natarajan, V., Minna, J., Vokes, E. E., Ferguson, M. K., Husain, A. N. & Salgia, R. Paxillin is a target for somatic mutations in lung cancer: Implications for cell growth and invasion. **Cancer Res.** 2008 68: 132–142

93. Yoshida, T., Hisamoto, T., Akiba, J., Koga, H., Nakamura, K., Tokunaga, Y., Hanada, S., Kumemura, H., Maeyama, M., Harada, M., Ogata, H., Yano, H., Kojiro, M., Ueno, T., Yoshimura, A. & Sata, M. Spreds, inhibitors of the Ras/ERK signal transduction, are dysregulated in human hepatocellular carcinoma and linked to the malignant phenotype of tumors. **Oncogene** 2006 25: 6056–6066

94. White, C. D., Brown, M. D. & Sacks, D. B. IQGAPs in cancer: A family of scaffold proteins underlying tumorigenesis. **FEBS Lett.** 2009 583: 1817–1824

95. Nguyen, A., Burack, W. R., Stock, J. L., Kortum, R., Chaika, O. V., Afkarian, M., Muller, W. J., Murphy, K. M., Morrison, D. K., Lewis, R. E., McNeish, J. & Shaw, A. S. Kinase Suppressor of Ras (KSR) Is a Scaffold Which Facilitates Mitogen-Activated Protein Kinase Activation In Vivo. **Mol. Cell. Biol.** 2002 22: 3035–3045

96. Kaduwal, S., Jeong, W. J., Park, J. C., Lee, K. H., Lee, Y. M., Jeon, S. H., Lim, Y. beom, Min, D. S. & Choi, K. Y. Sur8/Shoc2 promotes cell motility and metastasis through activation of Ras-PI3K signaling. **Oncotarget** 2015 6: 33091–33105

97. Lee, Y. M., Kaduwal, S., Lee, K. H., Park, J. C., Jeong, W. J. & Choi, K. Y. Sur8 mediates tumorigenesis and metastasis in colorectal cancer. **Exp. Mol. Med.** 2016 48: e249

98. Jones, G. G., del Río, I. B., Sari, S., Sekerim, A., Young, L. C., Hartig, N., Areso Zubiaur, I., El-Bahrawy, M. A., Hynds, R. E., Lei, W., Molina-Arcas, M., Downward, J. & Rodriguez-Viciana, P. SHOC2 phosphatase-dependent RAF dimerization mediates resistance to MEK

inhibition in RAS-mutant cancers. **Nat. Commun.** 2019 10:

99. Gu, S., Chan, W. W., Mohi, G., Rosenbaum, J., Sayad, A., Lu, Z., Virtanen, C., Li, S., Neel, B. G. & Van Etten, R. A. Distinct GAB2 signaling pathways are essential for myeloid and lymphoid transformation and leukemogenesis by BCR-ABL1. **Blood** 2016 127: 1803–1813

100. Shtivelman, E., Lifshitz, B., Gale, R. P. & Canaani, E. Fused transcript of abl and bcr genes in chronic myelogenous leukaemia. **Nature** 1985 315: 550–554

101. Patsoukis, N., Brown, J., Petkova, V., Liu, F., Li, L. & Boussiotis, V. A. Selective effects of PD-1 on Akt and ras pathways regulate molecular components of the cell cycle and inhibit T cell proliferation. **Sci. Signal.** 2012 5:

102. Tajan, M., Paccoud, R., Branka, S., Edouard, T. & Yart, A. The RASopathy family: Consequences of germline activation of the RAS/MAPK pathway. **Endocr. Rev.** 2018 39: 676–700

103. Martinelli, S., Stellacci, E., Pannone, L., D'Agostino, D., Consoli, F., Lissewski, C., Silvano, M., Cencelli, G., Lepri, F., Maitz, S., Pauli, S., Rauch, A., Zampino, G., Selicorni, A., Melançon, S., Digilio, M. C., Gelb, B. D., De Luca, A., Dallapiccola, B., Zenker, M. & Tartaglia, M. Molecular Diversity and Associated Phenotypic Spectrum of Germline CBL Mutations. **Hum. Mutat.** 2015 36: 787–796

104. Brems, H. & Legius, E. Legius syndrome, an update. molecular pathology of mutations in SPRED1. **Keio J. Med.** 2013 62: 107–112

105. Yan, W., Markegard, E., Dharmaiah, S., Urisman, A., Drew, M., Esposito, D., Scheffzek, K., Nissley, D. V., McCormick, F. & Simanshu, D. K. Structural Insights into the SPRED1-Neurofibromin-KRAS Complex and Disruption of SPRED1-Neurofibromin Interaction by Oncogenic EGFR. **Cell Rep.** 2020 32: 107909

106. Motta, M., Giancotti, A., Mastromoro, G., Chandramouli, B., Pinna, V., Pantaleoni, F., Di Giosaffatte, N., Petrini, S., Mazza, T., D'Ambrosio, V., Versacci, P., Ventriglia, F., Chillemi, G., Pizzuti, A., Tartaglia, M. & Luca, A. Clinical and functional characterization of a novel RASopathy-causing *SHOC2* mutation associated with prenatal-onset hypertrophic cardiomyopathy. **Hum. Mutat.** 2019 40: humu.23767

107. Cordeddu, V., Di Schiavi, E., Pennacchio, L. A., Ma'ayan, A., Sarkozy, A., Fodale, V., Cecchetti, S., Cardinale, A., Martin, J., Schackwitz, W., Lipzen, A., Zampino, G., Mazzanti, L., Digilio, M. C., Martinelli, S., Flex, E., Lepri, F., Bartholdi, D., Kutsche, K., Ferrero, G. B., Anichini, C., Selicorni, A., Rossi, C., Tenconi, R., Zenker, M., Merlo, D., Dallapiccola, B., Iyengar, R., Bazzicalupo, P., Gelb, B. D. & Tartaglia, M. Mutation of SHOC2 promotes aberrant protein N-myristoylation and causes Noonan-like syndrome with loose anagen hair. **Nat. Genet.** 2009 41: 1022–1026

108. Motta, M., Sagi-Dain, L., Krumbach, O. H. F., Hahn, A., Peleg, A., German, A., Lissewski, C., Coppola, S., Pantaleoni, F., Kocherscheid, L., Altmüller, F., Schanze, D., Logeswaran, T., Chahrokh-Zadeh, S., Munzig, A., Nakhaei-Rad, S., Cavé, H., Ahmadian, M. R., Tartaglia, M. & Zenker, M. Activating MRAS mutations cause Noonan syndrome associated with hypertrophic cardiomyopathy. **Hum. Mol. Genet.** 2019 doi:10.1093/hmg/ddz108

109. Guey, S., Grangeon, L., Brunelle, F., Bergametti, F., Amiel, J., Lyonnet, S., Delaforge, A.,

Arnould, M., Desnous, B., Bellesme, C., Hervé, D., Schwitalla, J. C., Kraemer, M., Tournier-Lasserve, E. & Kossorotoff, M. De novo mutations in CBL causing early-onset paediatric moyamoya angiopathy. **J. Med. Genet.** 2017 54: 550–557

110. Kazeminasab, S., Taskiran, I. I., Fattahi, Z., Bazazzadegan, N., Hosseini, M., Rahimi, M., Oladnabi, M., Haddadi, M., Celik, A., Ropers, H. H., Najmabadi, H. & Kahrizi, K. CNKSR1 gene defect can cause syndromic autosomal recessive intellectual disability. **Am. J. Med. Genet. Part B Neuropsychiatr. Genet.** 2018 177: 691–699

111. Liang, Y., Bradford, W. H., Zhang, J. & Sheikh, F. Four and a half LIM domain protein signaling and cardiomyopathy. **Biophys. Rev.** 2018 10: 1073–1085

112. Angelopoulou, E., Paudel, Y. N., Shaikh, M. F. & Piperi, C. Flotillin: A promising biomarker for alzheimer's disease. **J. Pers. Med.** 2020 10:

113. Galazis, N., Afxentiou, T., Xenophontos, M., Diamanti-Kandarakis, E. & Atiomo, W. Proteomic biomarkers of type 2 diabetes mellitus risk in women with polycystic ovary syndrome. **Eur. J. Endocrinol.** 2013 168:

114. Moore, A. R., Rosenberg, S. C., McCormick, F. & Malek, S. RAS-targeted therapies: is the undruggable drugged? **Nat. Rev. Drug Discov.** 2020 19: 533–552

115. Ostrem, J. M., Peters, U., Sos, M. L., Wells, J. A. & Shokat, K. M. K-Ras(G12C) inhibitors allosterically control GTP affinity and effector interactions. **Nature** 2013 503: 548–551

116. Matallanas, D. & Crespo, P. New druggable targets in the Ras pathway? . **Curr Opin Mol Ther.** 2010 674–683

117. Vasan, N., Baselga, J. & Hyman, D. M. A view on drug resistance in cancer. **Nature** 2019 575: 299–309

118. Khan, S., He, Y., Zhang, X., Yuan, Y., Pu, S., Kong, Q., Zheng, G. & Zhou, D. PROteolysis TArgeting Chimeras (PROTACs) as emerging anticancer therapeutics. **Oncogene** 2020 39: 4909–4924

119. Sanclemente, M., Francoz, S., Esteban-Burgos, L., Bousquet-Mur, E., Djurec, M., Lopez-Casas, P. P., Hidalgo, M., Guerra, C., Drosten, M., Musteanu, M. & Barbacid, M. c-RAF Ablation Induces Regression of Advanced Kras/Trp53 Mutant Lung Adenocarcinomas by a Mechanism Independent of MAPK Signaling. **Cancer Cell** 2018 33: 217-228.e4

120. Zeng, M., Xiong, Y., Safaee, N., Nowak, R. P., Donovan, K. A., Yuan, C. J., Nabet, B., Gero, T. W., Feru, F., Li, L., Gondi, S., Ombelets, L. J., Quan, C., Jänne, P. A., Kostic, M., Scott, D. A., Westover, K. D., Fischer, E. S. & Gray, N. S. Exploring Targeted Degradation Strategy for Oncogenic KRASG12C. **Cell Chem. Biol.** 2020 27: 19-31.e6

121. Prelich, G. Gene overexpression: Uses, mechanisms, and interpretation. **Genetics** 2012 190: 841–854

122. Zhang, Z., Hu, P., Xiong, J. & Wang, S. Inhibiting GIT1 reduces the growth, invasion and angiogenesis of osteosarcoma. **Cancer Manag. Res.** 2018 10: 6445–6455

123. Indarte, M., Puentes, R., Maruggi, M., Ihle, N. T., Grandjean, G., Scott, M., Ahmed, Z., Meuillet, E. J., Zang, S., Lemos, R., Du-Cuny, L., Layng, F. I. A. L., Correa, R. G., Bankston, L. A., Liddington, R. C., Kirkpatrick, L. & Powis, G. An inhibitor of the pleckstrin homology

domain of CNK1 selectively blocks the growth of mutant KRAS cells and tumors. **Cancer Res.** 2019 79: 3100–3111

124. Tari, A. M., Gutiérrez-Puente, Y., Monaco, G., Stephens, C., Sun, T., Rosenblum, M., Belmont, J., Arlinghaus, R. & Lopez-Berestein, G. Liposome-incorporated Grb2 antisense oligodeoxynucleotide increases the survival of mice bearing bcr-abl-positive leukemia xenografts. **Int. J. Oncol.** 2007 31: 1243–1250

125. Jameson, K. L., Mazur, P. K., Zehnder, A. M., Zhang, J., Zarnegar, B., Sage, J. & Khavari, P. A. IQGAP1 scaffold-kinase interaction blockade selectively targets RAS-MAP kinase-driven tumors. **Nat. Med.** 2013 19: 626–630

126. Bardwell, A. J., Lagunes, L., Zebarjedi, R. & Bardwell, L. TheWWdomain of the scaffolding protein IQGAP1 is neither necessary nor sufficient for binding to the MAPKs ERK1 and ERK2. **J. Biol. Chem.** 2017 292: 8750–8761

127. Dhawan, N. S., Scopton, A. P. & Dar, A. C. Small molecule stabilization of the KSR inactive state antagonizes oncogenic Ras signalling. **Nature** 2016 537: 112–116

128. Neilsen, B. K., Frodyma, D. E., Lewis, R. E. & Fisher, K. W. KSR as a therapeutic target for Ras-dependent cancers. **Expert Opin. Ther. Targets** 2017 21: 499–509

129. Xie, J., Si, X., Gu, S., Wang, M., Shen, J., Li, H., Li, D., Fang, Y., Liu, C. & Zhu, J. Allosteric Inhibitors of SHP2 with Therapeutic Potential for Cancer Treatment. **J. Med. Chem.** 2017 60: 10205–10219

130. Mainardi, S., Mulero-Sánchez, A., Prahallad, A., Germano, G., Bosma, A., Krimpenfort, P., Lieftink, C., Steinberg, J. D., De Wit, N., Gonçalves-Ribeiro, S., Nadal, E., Bardelli, A., Villanueva, A. & Bernards, R. SHP2 is required for growth of KRAS-mutant non-small-cell lung cancer in vivo letter. **Nat. Med.** 2018 24: 961–967

131. Ruess, D. A., Heynen, G. J., Ciecielski, K. J., Ai, J., Berninger, A., Kabacaoglu, D., Görgülü, K., Dantes, Z., Wörmann, S. M., Diakopoulos, K. N., Karpathaki, A. F., Kowalska, M., Kaya-Aksoy, E., Song, L., Van Der Laan, E. A. Z., López-Alberca, M. P., Nazaré, M., Reichert, M., Saur, D., Erkan, M. M., Hopt, U. T., Sainz, B., Birchmeier, W., Schmid, R. M., Lesina, M. & Algül, H. Mutant KRAS-driven cancers depend on PTPN11/SHP2 phosphatase. **Nat. Med.** 2018 24: 954–960

132. Zhao, M., Guo, W., Wu, Y., Yang, C., Zhong, L., Deng, G., Zhu, Y., Liu, W., Gu, Y., Lu, Y., Kong, L., Meng, X., Xu, Q. & Sun, Y. SHP2 inhibition triggers anti-tumor immunity and synergizes with PD-1 blockade. **Acta Pharm. Sin. B** 2019 9: 304–315

133. Acharya, P., Quinlan, A. & Neumeister, V. The ABCs of finding a good antibody: How to find a good antibody, validate it, and publish meaningful data. **F1000Research** 2017 6:

Acknowledgements. We are grateful to our colleagues Ehsan Amin, Ion C. Cirstea, Oliver Krumbach, Niloufar Mosaddeghzadeh, Saeideh Nakhaei-Rad, K. Nouri, and for stimulating discussion.

Author Contributions. S.P., N.S.K.J., F.B. and C.W. systematically searched and read the literature using the PubMed database, and compiled Table S1; C.W. made Figure 1, and S.P. Figures 2 and 3; All authors designed, wrote and approved the final version of the manuscript.

Conflicts of interest. The authors declare no competing financial interest.

Funding. This study was supported by the the German Research Foundation (Deutsche Forschungsgemeinschaft or DFG; AH 92/8-1), the German Research Foundation (Deutsche Forschungsgemeinschaft or DFG) through the International Research Training Group “Intra- and interorgan communication of the cardiovascular system” (grant number: IRTG 1902-p6), the European Network on Noonan Syndrome and Related Disorders (NSEuroNet, grant number: 01GM1621B); the German Federal Ministry of Education and Research (BMBF) – German Network of RASopathy Research (GeNeRARe, grant numbers: 01GM1902C).

Keywords. Adaptor proteins, anchoring proteins, docking proteins, MAPK pathway, RAS GTPase, scaffolding proteins, signal transduction

Abbreviations

ANK, ankyrin repeats

ASPP, Apoptosis-stimulating of p53 protein

ARR N, arrestin N-terminal domain

ARR C, arrestin C-terminal domain

C, cysteine-rich

CaM, Calmodulin

CBL, Casitas B-lineage lymphoma proto-oncogene

CC, coiled coil

CHD, calponin homology domain

CNK1, Connector enhancer of kinase suppressor of ras 1

CRD, carbohydrate-recognition domain

CRIC, conserved region in CNK

CRKL, Crk-like protein

CT, C-terminal domain

DE, aspartic acid and glutamic acid-rich

DED, death effector domain

DHR, DLG homologous region

DOK, Docking protein

EF, EF-hand

EGF, epidermal growth factor

EGFR, EGF receptor

Erbin, Erbb2-interacting protein

ERK, extracellular signal regulated kinase

ERM, ezrin-radixin-moesin

EVH, Ena-VASP homology

FERM, 4.1 protein,/ezrin/radixin/moesin domain

FGF, fibroblast growth factor

FHL, Four and a half LIM domains protein

FLOT, Flotillin

FRS2, Fibroblast growth factor receptor substrate 2

GAB, GRB2-associated-binding protein

GAL, Galectin

GAP, GTPase-activating protein

GAR, GAS2-related domain

GDP/GTP, guanosine di/triphosphate

GEF, guanine nucleotide exchange factor

GPCR, G protein-coupled receptor

GPR, G-protein regulator

GRB2, growth factor receptor binding protein 2

GRD, GAP-related domain

GRF1, Guanine nucleotide release factor 1

GRK2BD, GRK2 binding domain

HBD, Histone binding domain

IDRs, Intrinsically disordered regions

IRS, Insulin receptor substrate

IQ, IQ motif

KBD, KIT-binding domain

KSR1, Kinase suppressor of RAS-1

L, leucine-rich

LAT, Linker for activation of T-cells family member 1

LD, leucine-rich sequence motif

LIM, LIN-11/Isl-1/MEC-3 domain

LRR, leucine-rich-repeats

MAPK, mitogen activated protein kinase

MORG1, WD repeat domain-containing protein 83

MP1, MEK-binding partner 1

MTB, microtubule-binding region

NCL, Nucleolin

NES, nuclear export signal

NF1, neurofibromatosis type 1

NLS, nuclear localization signal

NoLS, nucleolar localization signal

NPM, Neucleophosmin

NTAL, Non-T-cell activation linker

OD, oligomerization Domain

P, proline-rich

PAQR, Progestin and adipoQ receptor family member

PBS, paxillin binding site

PDZ, PSD95/discs-large/zona occludens-1

PEA15, phosphoprotein enriched in astrocytes

PH, pleckstrin homology

PHB, prohibitin homologues

PI3K, phosphoinositide 3-kinase

PP1, protein phosphatase 1

PPP1CB, Protein phosphatase 1 catalytic subunit beta

PTB, phosphotyrosine binding

PTP, phosphotyrosin phosphatase

Q, glutamine-rich

RAF, rapidly accelerated fibrosarcoma

RAS, rat sarcoma

RBD, RAS binding domain

RGCT, RASGAP C-terminus

RGS, regulators of G protein signalling

RING, Really Interesting New Gene finger domain

RKIP, RAF kinase inhibitor protein

RNA-BD, RNA binding domain

RRM, RNA recognition motif

RTK, receptor tyrosine kinase

S, serine-rich

SAM, Sterile alpha motif

SEFIR, SEFs and IL17Rs domain

SH, SRC homology domain

SH2, SRC homology 2

SH3, SRC homology 3

SHC, SRC homology and collagen domain protein

SHD, SPA2 homology domain

SHP2, SH2 domain-containing tyrosine phosphatase 2

SID, SIN3 interaction domain

SOS, Son of sevenless homolog protein

SPFH, Stomatin/ Prohibitin/ Flotillin/HflK/C

SPR, cysteine-rich sprouty domain

SPRED, Sprouty-related, EVH1 domain-containing protein

SPRY, Sprouty

TM, transmembrane domain

TRKA, tyrosine kinase receptor A

UBA, ubiquitin associated domain

UBL, ubiquitin-like domain

WDs, WD repeats

WH1, WASP Homology domain 1

WW, two tryptophan containing β-sheets

4H, four-helix bundle

Table 1. Accessory proteins as attractive therapeutic targets.

Accessory protein	Disease	Drug	State of art	Comment	Ref.
CNK1	Cancers with KRAS4B mutations	PHT-7.3	Cell-based model	PHT-7.3 binds selectively to CNK1 PH domain, interferes its co-localisation with KRAS4B on the plasma membrane, and dimishes RAF/MEK/ERK signalling	[123]
GRB2	BCR-ABL-positive leukaemia	Anti-miDNA L-GRB2	Xenograft model	L-GRB2 selectively targets GRB2 mRNA and inhibits its translation	[124]
IQGAP1	Cancers with KRAS4B mutations	WW-competitive peptide	Mouse model	WW competitive peptide antagonist of IQGAP1 is applied in combination with the BRAF inhibitor Vemurafenib (PLX-4032) against KRAS4B oncogene	[125]
KSR	Cancers with KRAS4B mutations	APS-2-79	Cell-based model	APS-2-79 binds and stabilizes KSR in its inactive state, interferes with KSR/RAF heterodimerization, and inhibit oncogenic KRAS4B signalling	[127,128]
SHP2	Cancers	SHP099	Xenograft model	SHP099 binds SHP2 as an allosteric inhibitor, stabilizes its autoinhibited state, and inhibit oncogenic Ras signalling	[129–132]

Figure legends

Figure 1. Domain organization and crucial interactions of RTK-RAS-MAPK accessory proteins. Schematic representation of relevant domains. Direct binding partners, which are part of the RTK-RAS-MAPK pathway, are mentioned next to the amino acid numbers at the right side of the proteins. Please check list of abbreviations for more details.

Figure 2. Involvement of RTK-RAS-MAPK accessory proteins in signal transduction.

Accessory proteins are involved in every step of the RTK-RAS-MAPK pathway and increase the connectivity between signalling components. Docking proteins like FRS2 and adaptor proteins like SHC, GRB2 and SHP2 interact with receptors at the plasma membrane and facilitate the transmission of extracellular signals. Anchoring proteins like LAT and PAQR10/11 localize the RAS/MAPK signalling members towards specific cellular compartments (a). The scaffold proteins SPREAD1 and MERLIN recruit their binding partner to the PM by binding RAS-GTP and BRAF or CRAF respectively (b). Nanoclustering can be induced by Galectin1 or Nucleophosmin and Nucleolin, which increase the concentration of HRAS-GTP or KRAS-GDP in membrane rafts (c). RAS scaffold proteins like SHOC2 enhance RAS-RAF interaction, which can be antagonized by the other accessory proteins like ERBIN (d). Other docking, scaffold and anchoring proteins bind one, two or all three members of the MAPKs, bringing them close together, regulate their activity and determine their localization (e-f). For more detailed information, please see text.

More general: Accessory proteins are involved in every step of the RTK-RAS-MAPK pathway and increase the connectivity between signalling components. Adaptor proteins and docking proteins interact with phosphorylated receptors, in contrast to anchoring proteins, which are directly associated with the membrane (a). Recruiter translocate binding partner towards the site of action, e.g. a GTPase activating protein to activated RAS at the plasma membrane (b). Scaffold proteins which induce nanoclustering, increase the local concentration of their binding partner in lipid rafts (c). RAS scaffold proteins, bind RAS and other components of the RTK-RAS-MAPK pathway (d), whereas ERK binder (e), MEK/ERK binder (f), and RAF/MEK/ERK binder can connect one, two or all three members of the MAPKs, bringing them close together, regulate their activity and determine their localization. For more detailed information, please see text and list of abbreviations.

Figure 3. Involvement of accessory proteins in diseases. The canonical RAS/MAPK-pathway is tightly regulated by many proteins, attenuators and negative feedback mechanisms. Mutations in regulators like accessory proteins can lead to a dysregulated RAS/MAPK-pathway and therefore to a variety of diseases as cancer and RASopathies (a).

The genomic amplification of Paxillin is found in many non-small cell lung cancer (NSCLC) patients and activates the focal adhesion complex downstream of intergins (1). Loss-of-function mutations of SPRED1 activates the RAS-MAPK pathway and leads to Legius syndrome (germline) and hepatocellular carcinoma (somatic) (2). IQGAP1 mutations are often associated with tumour formation and metastasis (3), whereas KSR is a central player in KRAS-driven cancers inducing proliferation and survival (4). Mild gain-of-function mutations of SHOC2 lead to Noonan-like syndrome with loose anagen hair or Mazzanti syndrome, other somatic mutations

can lead to hypertrophic cardiomyopathy or tumourigenesis (5). The signalling of BCR-ABL positive cells in chronic myeloid leukaemia is also dependent on GAB2 activation, cross-linking AKT and RAS pathway (6). The adaptor protein SHP2 is of major importance in the activation of T-cells, connecting the programmed death 1 receptor (PD-1) with ZAP-70 at the T-cell receptor (TCR) (b). FHL1 is involved in the development of cardiac hypertrophy. which is caused by a gain-of-function mutation, leading to increased ERK signalling (c).

Figure 1

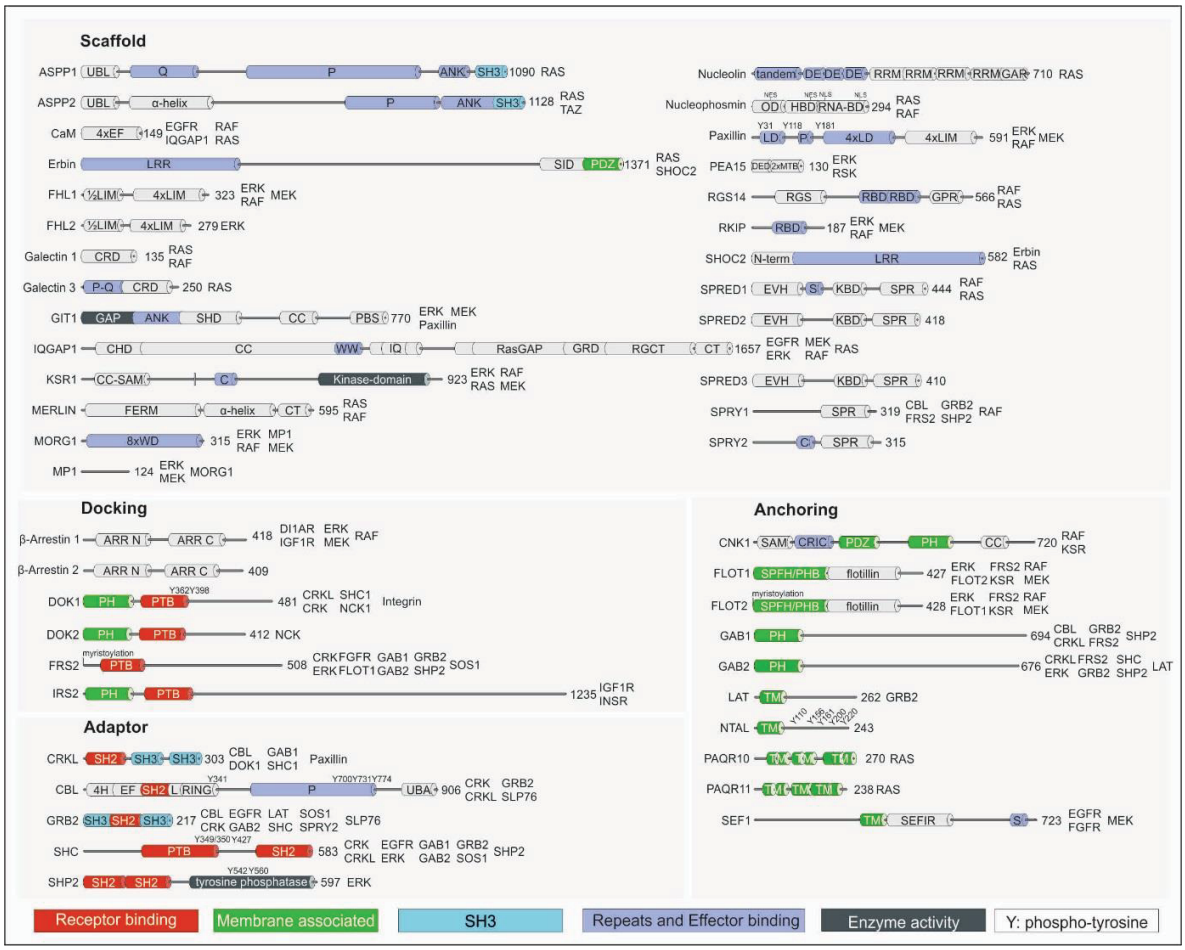
Scaffold
ASPP1 UBL Q P ANK SH3 1090 RAS
ASPP2 UBL α-helix P ANK SH3 1128 RAS TAZ
CaM 4xEF 149 EGFR IQGAP1 RAF RAS
Erbin LRR SID PDZ 1371 RAS SHOC2
FHL1 ½LIM 4xLIM 323 ERK RAF MEK
FHL2 ½LIM 4xLIM 279 ERK
Galectin 1 CRD 135 RAS RAF
Galectin 3 P-Q CRD 250 RAS
GIT1 GAP ANK SHD CC PBS 770 ERK MEK Paxillin
IQGAP1 CHD CC WW IQ RasGAP GRD RGCT CT 1657 EGFR ERK MEK RAF RAS
KSR1 CC-SAM C Kinase-domain 923 ERK RAS RAF MEK
MERLIN FERM α-helix CT 595 RAS RAF
MORG1 8xWD 315 ERK RAF MP1 MEK
MP1 124 ERK MEK MORG1
Nucleolin tandem DE DE DE RRM RRM RRM RRM GAR 710 RAS
Nucleophosmin OD HBD RNA-BD 294 RAS RAF
Paxillin LD P 4xLD 4xLIM 591 ERK RAF MEK
PEA15 DED 2xMTB 130 ERK RSK
RGS14 RGS RBD RBD GPR 566 RAF RAS
RKIP RBD 187 ERK RAF MEK
SHOC2 N-term LRR 582 Erbin RAS
SPRED1 EVH S KBD SPR 444 RAF RAS
SPRED2 EVH KBD SPR 418
SPRED3 EVH KBD SPR 410
SPRY1 SPR 319 CBL FRS2 GRB2 SHP2 RAF
SPRY2 C SPR 315
Docking
β-Arrestin 1 ARR N ARR C 418 DI1AR IGF1R ERK MEK RAF
β-Arrestin 2 ARR N ARR C 409
DOK1 PH PTB 481 CRKL CRK SHC1 NCK1 Integrin
DOK2 PH PTB 412 NCK
FRS2 PTB 508 CRK FGFR ERK FLOT1 GAB1 GRB2 GAB2 SHP2 SOS1
IRS2 PH PTB 1235 IGF1R INSR
Adaptor
CRKL SH2 SH3 SH3 303 CBL DOK1 GAB1 SHC1 Paxillin
CBL 4H EF SH2 L RING P UBA 906 CRK CRKL GRB2 SLP76
GRB2 SH3 SH2 SH3 217 CBL CRK EGFR GAB2 LAT SHC SOS1 SPRY2 SLP76
SHC PTB SH2 583 CRK CRKL EGFR ERK GAB1 GAB2 GRB2 SOS1 SHP2
SHP2 SH2 SH2 tyrosine phosphatase 597 ERK
Anchoring
CNK1 SAM CRIC PDZ PH CC 720 RAF KSR
FLOT1 SPFH/PHB flotillin 427 ERK FLOT2 FRS2 KSR RAF MEK
FLOT2 SPFH/PHB flotillin 428 ERK FLOT1 FRS2 KSR RAF MEK
GAB1 PH 694 CBL CRKL GRB2 FRS2 SHP2
GAB2 PH 676 CRKL ERK FRS2 GRB2 SHC SHP2 LAT
LAT TM 262 GRB2
NTAL TM 243
PAQR10 TM TM TM 270 RAS
PAQR11 TM TM TM 238 RAS
SEF1 TM SEFIR S 723 EGFR FGFR MEK
Receptor binding
Membrane associated
SH3
Repeats and Effector binding
Enzyme activity
Y: phospho-tyrosine

Figure 2

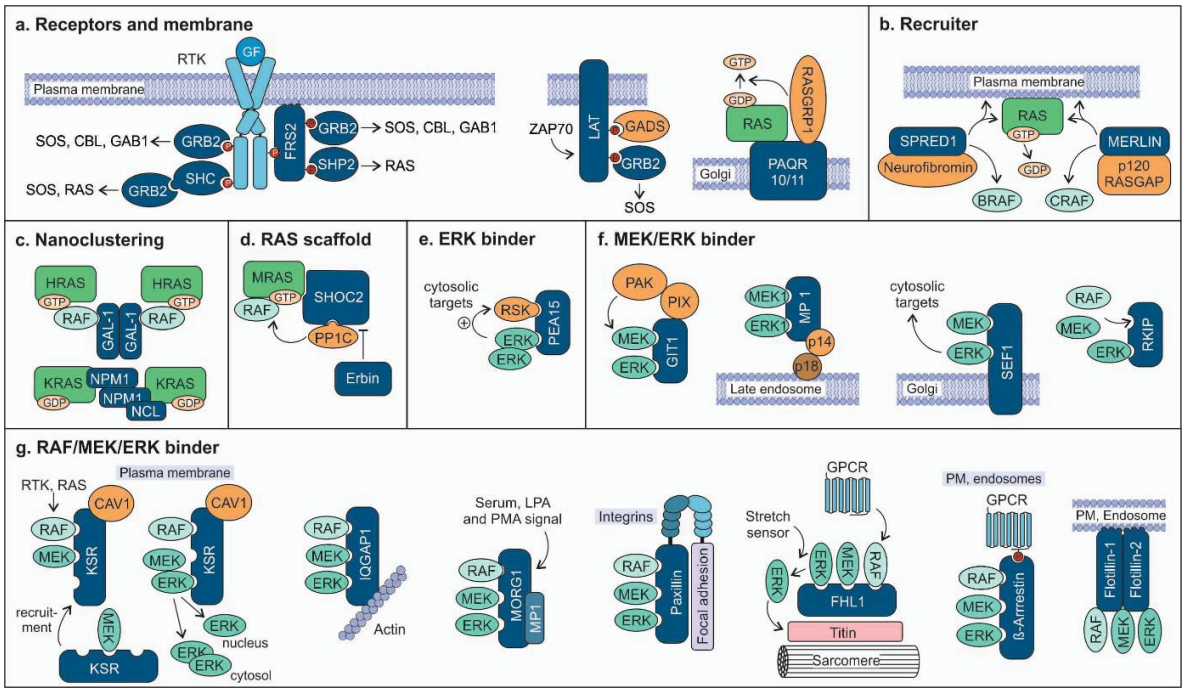

Figure 3

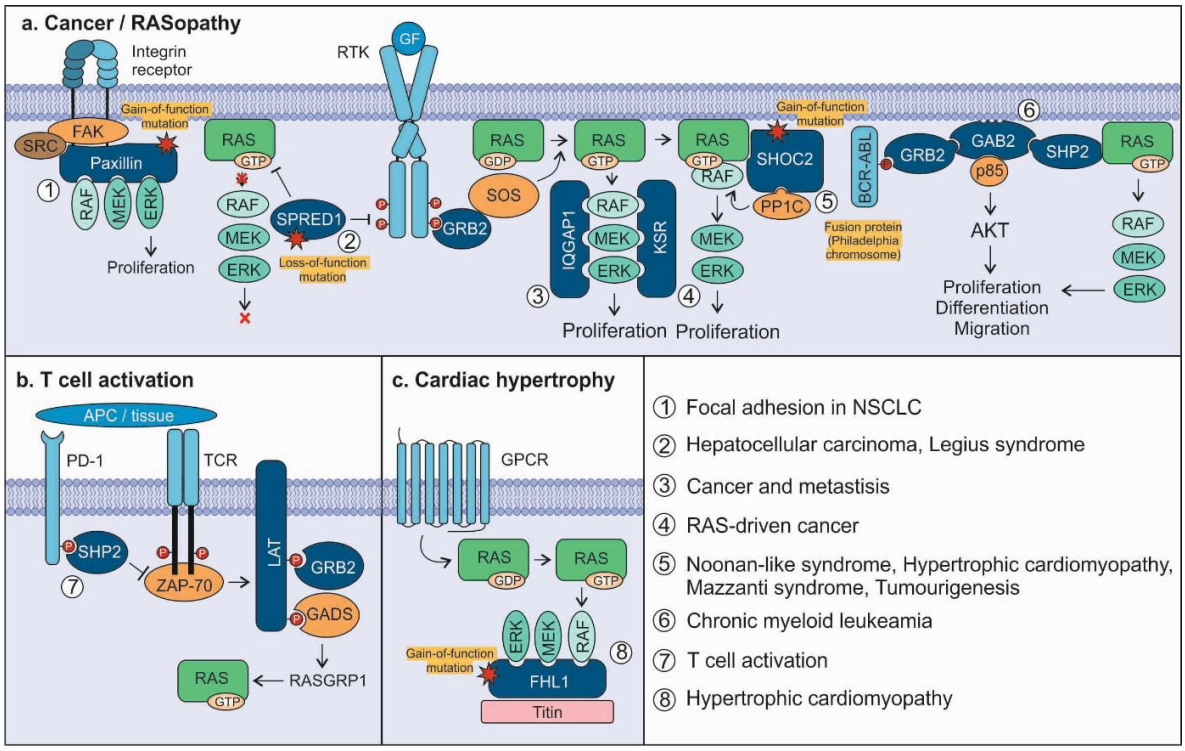

Discussion

Small G-proteins, or the RAS superfamily proteins control different cell biology aspects. They are influenced by upstream regulatory signals and they regulate broad effector outputs. RAS is a member of RAS superfamily and regulates mainly proliferation and apoptosis, respectively, by cycling as molecular switches between active and inactive states (*23*).
Dys-regulation of RAS activation has been notably associated with human diseases especially; cancer, neurodegenerative diseases, and major cardiovascular disorders (*464-466*). The development of pharmacological inhibitors interfering with RAS signal transduction is well investigated in the last 30 years. A wide range of studies has suggested different RAS MAPK pathway inhibitors such as geranyl geranyl transferase inhibitors (GGTIs), farnesyl transferase inhibitors (FIs) and RAS, RAF, MEK and ERK inhibitors (*467*). Nevertheless, none of the approaches of RAS inhibition was successful and specific targeting of RAS signal transduction remained to be investigated. Identification of the upstream mechanism of RAS activation or downstream mechanisms of RAS interactions may offer great potential for a more selective therapeutic intervention of RAS GTPases. In this work, we have tried to understand the mechanism of Receptor triggered activation of SOS1 RAS GEF, consequently RAS GTPases regulation, activation and RAS-effector interactions.

3.1 Mechanism of receptor triggered SOS1 activity

GRB2 adaptor protein interaction with the activated RTK and the RAS GEF SOS1 is one of the key steps in RAS activation at the plasma membrane (*107*). GRB2 comprises one SH2 domain, interacting with a specific phosphotyrosine site of the activated receptor tyrosine kinases (RTKs) or non-receptor tyrosine kinases and tyrosine-phosphorylated proteins, and two SH3 domains responsible for the binding to the Proline-rich motifs e.g. SOS1 RAS GEF. The mechanism of GRB2_SOS1 interaction is not clearly understood so far. Here, we shed light on the mechanism underlying the role of GRB2 in linking RTKs with RAS GEF and show that the GRB2 interaction with SOS1 is not based on a reported simple binding model (*304, 305*). Our findings showed that: (1) GBR2 interacts with three PRPs (3, 4 and 5) out of ten SOS1 PRPs; (2) Both GRB2 SH3 domains are needed for GRB2 interaction with SOS1; (3) Interdomain interactions of GRB2 controls GRB2-SOS1 interaction; (4) Dynamic interactions and flexibility of the GRB2 SH3 domains are caused via GRB2 linkers; (5) SH3 domains reciprocal relationship effect SH3 domains interactions with SOS1; (6) A unique C-terminal NRNV motif of GRB2 allosterically affects the GRB2-SOS1 interaction. Our results proposed that upon upstream ligand binding (e.g., HER2 pYP), GRB2 undergoes a series of structural transitions from one site, SH2 domain, to a physically distinct site, SH3 domains, that bolster up a stepwise association of downstream ligands (e.g., SOS1 PRMs). Intradomain structural changes and allosteric networks are induced by HER2 pYP binding to the SH2 domain. Eventually, both SH3 domains are engaged in binding and activating SOS1. GRB2 interaction with SOS1 was described for the first time in the 1990s (*304, 315*). Lemmon et al. for the first time has shown that GRB2 forms a 1:2 complex with a SOS1 peptide, Kd value of 22 μM, and a 1:1 complex with a HER1 phosphorylated peptide with, Kd value of 0.4 μM (*316*). In this study, we showed that both SH3 domains of GRB2 interact with SOS1 and CSH3 has a higher affinity, and we proposed that GBR2 undergoes a stepwise binding with SOS1, most likely it interacts mainly with P3-P4 of SOS1. Yuzawa et al. provided the crystal

structure of GRB2 and showed that GRB2 exists in multiple conformations with different positions of SH3 domains and their orientations relative to the central SH2 domain (*322*). A closer look at the GRB2 structure provides us with more information on which there could be interdomain interactions between SH3 domains. We proposed that SH3 domains interactions are a prerequisite for SOS1 interaction. The capability of GRB2 interaction with SOS1 was completely abolished by substitution of the interface residues of SH3 domains.

Most of the mobility of the multidomain proteins is facilitated by the flexibility of the interdomain linkers. Mobility of the proteins allows the conformational changes which are the regulator of proteins functions (*468*). The present study showed that truncation of one of the linkers or both affects GRB2 interaction with SOS1. All in all, GRB2 undergoes allosteric intradomain interactions which are required for the overall function and interaction of GRB2 with SOS1.

3.2 Genome-wide identification, functional classification and interaction selectivity analysis of human SH3 domain superfamily

SRC homology 3 (SH3) domain was introduced in 1988 (*365, 366*). SH3 domains are one of the best-investigated modular building blocks across all five kingdoms. They provide peptide-binding modules for proline-rich motifs (PRMs) (*367-369*). SH3-containing proteins are involved in a wide range of biological processes because of their critical interaction with PRMs which are fundamental to the assembly of protein complexes (Figure S7) (*370-372*). Mutations in the SH3 domains have been reported to be associated with human diseases, such as cancers, leukemia, osteoporosis, inflammation, Alzheimer disease, and various infections (*373-379*).

The wide contribution of SH3 domains in signaling pathways prompted us to perform sequence-structure-function analysis using 298 different SH3 domains. Therefore, we aimed to characterize the SH3 domain-PRM interactions by considering their sequences, structures and interaction specificities. Phylogenetic analysis of complete amino acid sequences of these SH3 domains (65 amino acids in average) was conducted to generate a first phylogenetic tree. To further define the SH3 families from this tree, we collected published structural and biochemical data about the SH3 domains and their interactions with different PRMs. Accordingly, our analysis with the full-length SH3 domains was not successful in assigning studied SH3-PRM interactions to the respective families derived from the first phylogenetic tree. Therefore, we generated a second phylogenetic tree based on the interfacing residues between the SH3 domains and the PRMs, which were defined by comparing the sequence alignment of published structures of the SH3 domain-PRM complexes. The distribution of the published SH3-PRMs structures within the second tree enabled us to classify human SH3 superfamily into 10 families based on their interaction with PRMs. The orientation of the prolines and also specific amino acids other than prolines within the PRMs appeared to define the specificity of the SH3 domain-PRM interactions. Our data explain why one peptide uses different residues to interact with different groups of SH3 domains. To prove our findings and further specify the SH3-PRM interactions, we generated 10 peptides from the C-terminal region of SOS1 and analyzed their binding capabilities with 25 selected representatives from each SH3 domain family. Two methods were established for these analysis. One was combined pulldown and dot blot analysis and the other fluorescence polarization using fluoresceinated SOS1 PMR peptides. In this study, we found several new SOS1 binding partners,

including ARHGAP12 and NCK1, which showed unexpectedly high affinities of 0.9 and 0.2 μM towards P7 and 9, respectively.

3.3 The RAS binding selectivity of the RAS-association domain family proteins

RAS GTPases regulate a variety of cellular processes, including survival, growth, adhesion, migration, and differentiation. Signal transduction relies on a physical association of activated RAS proteins with and activation of assorted downstream effectors, *e.g.*, CRAF, PI3Kα, TIAM1, RALGDS, PLCε and RASSF5 (*23, 119, 122-125, 469-471*). Interaction of the effectors with the activated RAS essentially requires RAS binding domains of effectors interaction with the switch I and switch II regions in RAS GTPases. RAS-effector interaction only occurs when RAS proteins are in GTP-bound form. In GTP-bound form, the switch regions of the RAS proteins have a suitable conformation acting as a platform for the association of the effector proteins(*6, 130-133*).

There are two types of RAS binding domains, called RAS binding (RB) and RAS association (RA) domains, in RAS effectors which share common structural characteristics (*122, 134-136*). In this study, 41 RA domains in 39 proteins and 16 RB domains in 14 proteins were extracted using database searches in the human proteome. Most of the RA domain containing proteins interaction with RAS GTPases still are uncharacterized. Therefore, we analyzed the sequence-structure and interaction relation between the different representative's RA domain family proteins (RASSFs) and two RB domain-containing proteins, CRAF and TIAM1 with the representative of the RAS family, HRAS, RRAS, RALA, RAP1B, RAP2A, RHEB1, and RIT1.

The best investigated RB domain containing RAS effector is CRAF which interact with classical RAS proteins; HRAS, NRAS and KRAS (*134*). This study showed interaction of CRAF RB domain with RAP1B and RHEB1 but not for RIT1 or RAP2A. CRAF interaction with RIT1 has been proposed to be associated with RASopathy (*173*). We observed a very low affinity for these two proteins and it could be because of the sequence deviation between RIT1 and HRAS in their switch I region. Andres and coworkers have shown that RIT1 does not interact with the CRAF RB domain (*174*). It was also reported that RIT1 binds and activates BRAF but not CRAF (*175*). Therefore, additional regions may exist outside the conserved RB domains of the RAF paralogs, which differently facilitate the interaction with the RAS proteins.

We determined the hotspots (distinct regions at the interface of RAS-effector complexes) throughout the RA/RB domains from an average of 19 RAS-binding residues considering the sequence and structural analysis of the available structural data, RAS-effector interactions. We could also show new interactions of RRAS1, RIT1, and RALA for RASSF7, RASSF9, and RASSF1, which were proposed to have the possibility of the interaction in our sequence-structural analysis. Although the RAS-effector interaction in biological conditions remained to be analyzed. RASSF1 and RASSF5 are the only member of RASSF family which interact in high or intermediate affinities with all investigated RAS family members but not RIT1 (*472, 473*). Sequence analysis shows that the sequence similarity of RASSF7-9 RA domains is close to each other and different from other RASSFs RA domains. K/R241 and K/R308 hotspots are the common residues in RASSF RA domains

We reported the affinity for RAS-effector interactions, ranged between high (0.3 μM) and very low (500 μM) affinities. The central concern of the biophysical investigation in protein-protein interactions is the biological relevance of low (> 10 μM) affinity interactions in the regulation of cellular

processes. Protein complexes formation requires weak and transient interactions to be controllable in response to external stimuli. Cellular membranes are an important place for the protein complexes orientation and consequently signal transduction (*176*). RAS activity implies by RAS interaction with membrane. KRAS4B interaction analysis with the lipid bilayer membrane has shown that the association of the ARAF RB domain with active KRAS4B facilitates membrane binding of ARAF RBD (*177*). Protein complex formation is a multistep process in which the first step could be the increase of local protein concentrations in a complex and driving the cytoplasmic phase separations (*213-215*). In the second step, specific sites of proteins interact and assemble protein complex associated with the membrane, such as RAS proteins (*28, 214, 215*). Since the final complex formation comes among multivalent interactions (*216*); therefore, it increases significantly the uM affinity by orders of magnitude (*28*). The nanomolar affinity is often characterized by fast association and slow dissociation rates forming stable protein complexes (*217-219*).

3.4 Activating mutations of *RRAS2* are a rare cause of Noonan syndrome

RAS and MAPK signaling control a variety of cell decisions in response to extracellular stimuli (*474*). Aberrant MAPK signaling and its upregulation constitute a central theme in disorders affecting the development such as; Noonan syndrome (NS) (*475*). Noonan syndrome is a developmental disorder characterized by cardiac defects, short stature, variable cognitive impairment, and predisposition to malignancies (*476*). Mutation in more than ten genes have been reported to underlie this disorder which is mostly related to the MAPK pathway and only about 10%-20% of affected individuals of NS do not have mutations in known RASopathy-associated genes (*477*). By using exome sequencing and functional candidacy, we introduced RRAS2 as a gene associated with NS. RRAS2 mutations causing NS occurs highly in conserved residues localized around the nucleotide binding pocket which display variably effect on RRAS2 biochemical behaviors, comprising nucleotide binding, GTP hydrolysis, and is effector interactions. Increased activation of the MAPK cascade was observed in all pathogenic variants but their impact on cell morphology and cytoskeletal rearrangement was variable.

RRAS2 reveals the highest amino acid identity to the classical GTPes (HRAS, KRAS, and NRAS) compare to other GTPases (*478*). RRAS2 Somatic mutations like classical RAS proteins have been contributed to the oncogenesis but less frequently compared to HRAS, KRAS, and NRAS (*479*). A noticeable finding of this study is that hyperactivation of the MAPK pathway resulting in the unaltered binding to CRAF and impaired binding of this mutant to RASSF5 was observed for the NS-causing RRAS2 Ala70Thr protein. RASSF5 is known as a tumor suppressor protein that negatively modulates YAP1 levels by activation of the Hippo pathway. YAP1 is a transcriptional cofactor promoting cell proliferation, which undergoes RASSF5-mediated phosphorylation and degradation (*480*). Therefore, impaired RASSF5 interaction with RRAS2 increases the possibility of a less effective Hippo-mediated control of YAP1 levels. Further studies are demanded investigating the precise mechanisms linking upregulated RRAS2 function with the RAS MAPK signaling dysregulation.

3.5 The Pseudo Natural Product Rhonin Targets RHOGDI1

The discovery of new bioactive compounds controlling protein function and their interaction is a challenging topic that requires efficient strategies. The structure and activity of natural products (NP) have proven their efficiency as Biology Oriented Synthesis compounds (*481, 482*). The NP-

related compound is only focused on areas of chemical space and biological target space. While fragment-based design enables efficient and wider coverage of biologically relevant which is highly desirable. Combination of fragment-based design and the synthesis of NP-inspired compound collections are called de novo combinations of NP fragments (*483*). Here we designed, synthesised and evaluated "pseudo natural product Rhonin" from a compound collection that combines five-membered N-heterocycles (i.e. pyrrolidines, pyrrolines and succinimides). The compound collection had a different structure and a different biosynthetic origin with different connectivities.

We found that the novel pseudo-NP Rhonin is an inhibitor of the Hedgehog (Hh) signalling. The Hh pathway is involved in organ development during embryogenesis. The Hh dysregulation is associated with different types of cancers. SMO is the main player of Hh signalling and the most druggable target in Hh signalling and most of the drugs often affect SMO ciliary localization (*484-486*). There are two types of Hh signalling, SMO-dependent and –independent non-canonical Hh-pathways which drugs have rarely been developed (*485, 486*). We showed that Rhonin targets RHOGDI1, which RHO GTPases regulator and displace RHO GTPases from the membrane to the cytoplasm. Interaction of Rhonin with RHOGDI1 causes the stability of GTP-bound RHO GTPases in membrane and link between RHOGDI1 and Hh signalling. Deletion of RHOGDI1 completely abrogated the inhibitory effect of Rhonin on Hh signaling and proved that RHOGDI1 is a potential target of Hh pathway inhibition. Till now, there is only one reported small molecule related to RHOGDI1 function is secramine A, which inhibits CDC42-mediated actin polymerization. The only reported small molecule related to RHOGDI1 function is secramine A, which inhibits CDC42-mediated actin polymerization in a RHOGDI1-dependent manner (*487*).

RHOGDI1 negatively regulates the RHO GTPases RHOA, RAC1 and CDC42 (*488*) which eventually affect the actin cytoskeleton and cell adhesion (*488*). RHOGDI1 interacts and translocates RHO GTPases from the membrane to the cytosol and preventing their activation. It extracts RHO GTPases from the membrane and sequesters them to the cytosol, thus preventing their activation at the target membrane (*489*). RHO GTPases act in a SMO-dependent manner as a non-canonical Hh signalling and SMO-RHOA pathway suppresses the SMO-GLI pathway (*485*).

Our study provided evidence that Rhonin affects the canonical Hh signaling via a non-canonical route. Our findings are in agreement that Rhonin binds to RHOGDI1 and prevents the extraction of RHO GTPases from membranes resulting in an increase of GTP-bound RHO GTPases and bound to the membrane. We show that inhibition of RHOGDI1 with Rhonin increases RHOA activity causing stress fiber formation. We could also clarify the link between Increased actin polymerization and impaired cilia-related function (*490*) and this link could explain the link between RHOA activity and Hh-GLI pathway inhibition.

3.6 Novel molecular and functional insights into the regulation of the RAC1-membrane interaction by GDI1

RHO proteins regulation is dependent on a variety of regulators which act together. GDI is one of RHO GTPases regulator that displace them from membrane and inhibit their activation at plasma membrane or proteasomal degradation

(13). HVR of RHO GTPases associate with the membrane and determines the kinetic of membrane localization of RHO GTPases (47) and promote various intracellular trafficking, compartmentalization, subcellular localization, interactions, and membrane association by interacting with a variety of proteins (45). The specific mechanism of RHO GDI interaction and function towards RHO GTPases is not elucidated so far. Here we revealed the multi-step mechanism of the RHOGDI1 interaction with RAC1 that smooth the path of membrane extraction and inhibition of RAC1 activation, by for example TIAM1 (32). We showed that GDI1 interact with switch regions of $RAC1^{GG}$ on the membrane (*247*) next it interacts with RAC1 HVR associated with the negatively charged phospholipids (47) as an electrostatic steering mechanism. Electrostatic steering mechanism has been already reported for different protein-protein interactions such as, the interaction of CDC42 and WASP(51, 52), VWF and GPIbα(53). Electrostatic steering forces control the fast association reaction of two molecules but not the association reaction (51). The electrostatic steering interactions between GDI1 and RAC1 pull the geranylgeranyl moiety of RAC1 from the membrane and keep it into the GGBD hydrophobic pocket of GDI1. And at the end, $RAC1^{GG}$-GDI1 interaction is locked by the last interaction between the very terminal residues of GDI1 NTA and CT. Our study revealed crucial and modulatory mechanisms, controlling RAC1 regulation and function via GDI1. Understanding the molecular mechanism of RAC1 regulation could be considered as a therapeutic target of RAC1 which its deregulation and dysfunction is implicated in a variety of diseases, such as atherosclerosis, diabetes and cancer (54).

3.7 Novel FMRP interaction networks linked to *cellular* stress

Silencing of the fragile X mental retardation 1 (FMR1) gene is associated with fragile X syndrome, an inherited intellectual disability (*491*). FMRP also is involved in the increased viral infection, liver disease, and reduced risk of cancer (*492-495*). FMRP has a broad biological role in RNA binding, chromatin dynamics, mRNA transport, and translation (*496-499*). The molecular mechanisms of FMRP and its protein networks remained elusive. Therefore, we analyzed the protein complexes of FMRP. We found that FMRP interacts with 180 proteins by employing affinity pull-down and quantitative LC-MS/MS analyses. Of these, 28 proteins interacted with its N-terminus ,102 proteins with the C-terminus, and 48 proteins interacted with both terminuses of FMRP. Although some of the FMRP binding partners were already known, including the ribosomal proteins FXR1P, NUFIP2, Caprin-1, but the rest were novel FMRP candidate interacting proteins. Here we reported that CARF, LARP1, LEO1, NOG2, G3BP1, NONO, NPM1, SKIP, SND1, SQSTM1, and TRIM28 are novel FMRP candidate interacting proteins. Our data related to the new binding partner of FMRP suggest that FMRP could play role in transcription, RNA metabolism, ribonucleoprotein stress granule formation, translation, DNA damage response, chromatin dynamics, cell cycle regulation, ribosome biogenesis, miRNA biogenesis, and mitochondrial organization.

References

1. J. Harvey, An unidentified virus which causes the rapid production of tumours in mice. *Nature* **204**, 1104 (1964).
2. W. Kirsten, V. Schauf, J. McCoy, in *Comparative Leukemia Research 1969*. (Karger Publishers, 1970), vol. 36, pp. 246-249.
3. L. F. Parada, C. J. Tabin, C. Shih, R. A. Weinberg, Human EJ bladder carcinoma oncogene is homologue of Harvey sarcoma virus ras gene. *Nature* **297**, 474 (1982).
4. T. M. Cabrera-Vera *et al.*, Insights into G protein structure, function, and regulation. *Endocrine reviews* **24**, 765-781 (2003).
5. G. M. Cooper, Cellular transforming genes. *Science* **217**, 801-806 (1982).
6. I. R. Vetter, A. Wittinghofer, The guanine nucleotide-binding switch in three dimensions. *Science* **294**, 1299-1304 (2001).
7. P. B. Wedegaertner, P. T. Wilson, H. R. Bourne, Lipid modifications of trimeric G proteins. *J Biol Chem* **270**, 503-506 (1995).
8. A. J. Ridley, Rho family proteins: coordinating cell responses. *Trends Cell Biol* **11**, 471-477 (2001).
9. A. Schmidt, A. Hall, Guanine nucleotide exchange factors for Rho GTPases: turning on the switch. *Genes Dev* **16**, 1587-1609 (2002).
10. S. Y. Moon, Y. Zheng, Rho GTPase-activating proteins in cell regulation. *Trends Cell Biol* **13**, 13-22 (2003).
11. J. Colicelli, Human RAS superfamily proteins and related GTPases. *Sci STKE* **2004**, RE13 (2004).
12. M. Zerial, H. McBride, Rab proteins as membrane organizers. *Nat Rev Mol Cell Biol* **2**, 107-117 (2001).
13. A. R. Memon, The role of ADP-ribosylation factor and SAR1 in vesicular trafficking in plants. *Biochim Biophys Acta* **1664**, 9-30 (2004).
14. Z. Nie, D. S. Hirsch, P. A. Randazzo, Arf and its many interactors. *Curr Opin Cell Biol* **15**, 396-404 (2003).
15. J. B. Pereira-Leal, M. C. Seabra, Evolution of the Rab family of small GTP-binding proteins. *J Mol Biol* **313**, 889-901 (2001).
16. K. Weis, Regulating access to the genome: nucleocytoplasmic transport throughout the cell cycle. *Cell* **112**, 441-451 (2003).
17. H. Y. Li, K. Cao, Y. Zheng, Ran in the spindle checkpoint: a new function for a versatile GTPase. *Trends Cell Biol* **13**, 553-557 (2003).
18. K. Wennerberg, K. L. Rossman, C. J. Der, The Ras superfamily at a glance. *J cell Sci* **118**, 843-846 (2005).
19. S. Clarke, J. P. Vogel, R. J. Deschenes, J. Stock, Posttranslational modification of the Ha-ras oncogene protein: evidence for a third class of protein carboxyl methyltransferases. *Proc Natl Acad Sci U S A* **85**, 4643-4647 (1988).
20. K. Wennerberg, K. L. Rossman, C. J. Der, The Ras superfamily at a glance. *J Cell Sci* **118**, 843-846 (2005).
21. D. Vigil, J. Cherfils, K. L. Rossman, C. J. Der, Ras superfamily GEFs and GAPs: validated and tractable targets for cancer therapy? *Nat Rev Cancer* **10**, 842-857 (2010).
22. C. Kiel, L. Serrano, The ubiquitin domain superfold: structure-based sequence alignments and characterization of binding epitopes. *Journal of molecular biology* **355**, 821-844 (2006).

23. C. Herrmann, Ras–effector interactions: after one decade. *Current opinion in structural biology* **13**, 122-129 (2003).
24. M. Malumbres, M. Barbacid, RAS oncogenes: the first 30 years. *Nature Reviews Cancer* **3**, 459-465 (2003).
25. L. van der Weyden, D. J. Adams, The Ras-association domain family (RASSF) members and their role in human tumourigenesis. *Biochimica et Biophysica Acta (BBA)-Reviews on Cancer* **1776**, 58-85 (2007).
26. A. Agathanggelou, W. N. Cooper, F. Latif, Role of the Ras-association domain family 1 tumor suppressor gene in human cancers. *Cancer research* **65**, 3497-3508 (2005).
27. R. Dammann *et al.*, Epigenetic inactivation of a RAS association domain family protein from the lung tumour suppressor locus 3p21. 3. *Nature genetics* **25**, 315-319 (2000).
28. V. Ibáňez Gaspar, S. Catozzi, C. Ternet, P. J. Luthert, C. Kiel, Analysis of Ras-effector interaction competition in large intestine and colorectal cancer context. *Small GTPases*, 1-17 (2020).
29. U. Krengel *et al.*, Three-dimensional structures of H-ras p21 mutants: molecular basis for their inability to function as signal switch molecules. *Cell* **62**, 539-548 (1990).
30. E. F. Pai *et al.*, Refined crystal structure of the triphosphate conformation of H-ras p21 at 1.35 A resolution: implications for the mechanism of GTP hydrolysis. *The EMBO journal* **9**, 2351-2359 (1990).
31. A. F. Overbeck *et al.*, Guanine nucleotide exchange factors: activators of Ras superfamily proteins. *Mol Reprod Dev* **42**, 468-476 (1995).
32. M. R. Ahmadian, P. Stege, K. Scheffzek, A. Wittinghofer, Confirmation of the arginine-finger hypothesis for the GAP-stimulated GTP-hydrolysis reaction of Ras. *Nat Struct Biol* **4**, 686-689 (1997).
33. A. Dovas, J. R. Couchman, RhoGDI: multiple functions in the regulation of Rho family GTPase activities. *Biochemical Journal* **390**, 1-9 (2005).
34. T. Sasaki, Y. Takai, The Rho small G protein family-Rho GDI system as a temporal and spatial determinant for cytoskeletal control. *Biochem Biophys Res Commun* **245**, 641-645 (1998).
35. B. Olofsson, Rho guanine dissociation inhibitors: pivotal molecules in cellular signalling. *Cellular signalling* **11**, 545-554 (1999).
36. A. Chandra *et al.*, The GDI-like solubilizing factor PDEδ sustains the spatial organization and signalling of Ras family proteins. *Nature cell biology* **14**, 148-158 (2012).
37. W. Baehr, Membrane protein transport in photoreceptors: the function of pdeδ. *Investigative ophthalmology & visual science* **55**, 8653-8666 (2014).
38. H. Zhang *et al.*, Photoreceptor cGMP phosphodiesterase δ subunit (PDEδ) functions as a prenyl-binding protein. *Journal of Biological Chemistry* **279**, 407-413 (2004).
39. L. Renault, J. Kuhlmann, A. Henkel, A. Wittinghofer, Structural basis for guanine nucleotide exchange on Ran by the regulator of chromosome condensation (RCC1). *Cell* **105**, 245-255 (2001).
40. B. Zhang, Y. Zhang, E. Shacter, Y. Zheng, Mechanism of the guanine nucleotide exchange reaction of Ras GTPase--evidence for a GTP/GDP displacement model. *Biochemistry* **44**, 2566-2576 (2005).
41. B. Zhang, Y. Zhang, Z. Wang, Y. Zheng, The role of Mg2+ cofactor in the guanine nucleotide exchange and GTP hydrolysis reactions of Rho family GTP-binding proteins. *J Biol Chem* **275**, 25299-25307 (2000).
42. Z. Guo, M. R. Ahmadian, R. S. Goody, Guanine nucleotide exchange factors operate by a simple allosteric competitive mechanism. *Biochemistry* **44**, 15423-15429 (2005).
43. M. Jaiswal, R. Dvorsky, M. R. Ahmadian, Deciphering the Molecular and Functional Basis of Dbl Family Proteins A NOVEL SYSTEMATIC APPROACH TOWARD CLASSIFICATION OF SELECTIVE

ACTIVATION OF THE Rho FAMILY PROTEINS. *Journal of Biological Chemistry* **288**, 4486-4500 (2013).
44. J. L. Bos, H. Rehmann, A. Wittinghofer, GEFs and GAPs: critical elements in the control of small G proteins. *Cell* **129**, 865-877 (2007).
45. A. S. Nimnual, B. A. Yatsula, D. Bar-Sagi, Coupling of Ras and Rac guanosine triphosphatases through the Ras exchanger Sos. *Science* **279**, 560-563 (1998).
46. L. Bonfini, C. A. Karlovich, C. Dasgupta, U. Banerjee, The Son of sevenless gene product: a putative activator of Ras. *Science* **255**, 603-606 (1992).
47. L. Bonfini, C. A. Karlovich, C. Dasgupta, U. Banerjee, The Son of sevenless gene product: a putative activator of Ras. *Science* **255**, 603-606 (1992).
48. S. Pierre, A. S. Bats, X. Coumoul, Understanding SOS (Son of Sevenless). *Biochem Pharmacol* **82**, 1049-1056 (2011).
49. B. S. Bausenwein, M. Schmidt, B. Mielke, T. Raabe, In vivo functional analysis of the daughter of sevenless protein in receptor tyrosine kinase signaling. *Mech Dev* **90**, 205-215 (2000).
50. M. A. Simon, G. S. Dodson, G. M. Rubin, An SH3-SH2-SH3 protein is required for p21Ras1 activation and binds to sevenless and Sos proteins in vitro. *Cell* **73**, 169-177 (1993).
51. D. Bar-Sagi, The Sos (Son of sevenless) protein. *Trends Endocrinol Metab* **5**, 165-169 (1994).
52. R. L. Kortum *et al.*, Targeted Sos1 deletion reveals its critical role in early T-cell development. *Proc Natl Acad Sci U S A* **108**, 12407-12412 (2011).
53. G. M. Findlay *et al.*, Interaction domains of Sos1/Grb2 are finely tuned for cooperative control of embryonic stem cell fate. *Cell* **152**, 1008-1020 (2013).
54. S. Corbalan-Garcia, S. M. Margarit, D. Galron, S.-s. Yang, D. Bar-Sagi, Regulation of Sos activity by intramolecular interactions. *Molecular and cellular biology* **18**, 880-886 (1998).
55. X. Qian, W. C. Vass, A. G. Papageorge, P. H. Anborgh, D. R. Lowy, N terminus of Sos1 Ras exchange factor: critical roles for the Dbl and pleckstrin homology domains. *Molecular and Cellular Biology* **18**, 771-778 (1998).
56. Y. K. Lee *et al.*, Mechanism of SOS PR-domain autoinhibition revealed by single-molecule assays on native protein from lysate. *Nature communications* **8**, 15061 (2017).
57. J. Gureasko *et al.*, Role of the histone domain in the autoinhibition and activation of the Ras activator Son of Sevenless. *Proceedings of the National Academy of Sciences* **107**, 3430-3435 (2010).
58. H. Sondermann, S. M. Soisson, D. Bar-Sagi, J. Kuriyan, Tandem histone folds in the structure of the N-terminal segment of the ras activator Son of Sevenless. *Structure* **11**, 1583-1593 (2003).
59. S. A. Sullivan, L. Aravind, I. Makalowska, A. D. Baxevanis, D. Landsman, The histone database: a comprehensive WWW resource for histones and histone fold-containing proteins. *Nucleic Acids Res* **28**, 320-322 (2000).
60. J. M. Rojas, J. L. Oliva, E. Santos, Mammalian son of sevenless Guanine nucleotide exchange factors: old concepts and new perspectives. *Genes & cancer* **2**, 298-305 (2011).
61. T. Noguchi, F. Galland, M. Batoz, M. Mattei, D. Birnbaum, Activation of a mcf. 2 oncogene by deletion of amino-terminal coding sequences. *Oncogene* **3**, 709-715 (1988).
62. A. Eva, S. A. Aaronson, Isolation of a new human oncogene from a diffuse B-cell lymphoma. *Nature* **316**, 273 (1985).
63. M. J. Hart, A. Eva, T. Evans, S. A. Aaronson, R. A. Cerione, Catalysis of guanine nucleotide exchange on the CDC42Hs protein by the dbloncogene product. *Nature* **354**, 311 (1991).
64. M. A. Lemmon, Phosphoinositide recognition domains. *Traffic* **4**, 201-213 (2003).
65. J. M. Kavran *et al.*, Specificity and promiscuity in phosphoinositide binding by pleckstrin homology domains. *Journal of Biological Chemistry* **273**, 30497-30508 (1998).

66. J. T. Snyder *et al.*, Quantitative analysis of the effect of phosphoinositide interactions on the function of Dbl family proteins. *Journal of Biological Chemistry* **276**, 45868-45875 (2001).
67. J. Roose *et al.*, One-way membrane trafficking of SOS in receptor-triggered Ras activation. (2016).
68. J. L. Byrne, H. F. Paterson, C. J. Marshall, p21Ras activation by the guanine nucleotide exchange factor Sos, requires the Sos/Grb2 interaction and a second ligand-dependent signal involving the Sos N-terminus. *Oncogene* **13**, 2055-2065 (1996).
69. S. M. Margarit *et al.*, Structural evidence for feedback activation by Ras· GTP of the Ras-specific nucleotide exchange factor SOS. *Cell* **112**, 685-695 (2003).
70. D. Broek *et al.*, The S. cerevisiae CDC25 gene product regulates the RAS/adenylate cyclase pathway. *Cell* **48**, 789-799 (1987).
71. P. A. Boriack-Sjodin, S. M. Margarit, D. Bar-Sagi, J. Kuriyan, The structural basis of the activation of Ras by Sos. *Nature* **394**, 337 (1998).
72. D. Bar-Sagi, D. Rotin, A. Batzer, V. Mandiyan, J. Schlessinger, SH3 domains direct cellular localization of signaling molecules. *Cell* **74**, 83-91 (1993).
73. A. Musacchio, M. Wilmanns, M. Saraste, Structure and function of the SH3 domain. *Prog Biophys Mol Biol* **61**, 283-297 (1994).
74. A. Nimnual, D. Bar-Sagi, The two hats of SOS. *Sci STKE* **2002**, pe36 (2002).
75. N. Li *et al.*, Guanine-nucleotide-releasing factor hSos1 binds to Grb2 and links receptor tyrosine kinases to Ras signalling. *Nature* **363**, 85-88 (1993).
76. H. Sondermann *et al.*, Structural analysis of autoinhibition in the Ras activator Son of sevenless. *Cell* **119**, 393-405 (2004).
77. J. Gureasko *et al.*, Membrane-dependent signal integration by the Ras activator Son of sevenless. *Nat Struct Mol Biol* **15**, 452-461 (2008).
78. R. H. Chen, S. Corbalan-Garcia, D. Bar-Sagi, The role of the PH domain in the signal-dependent membrane targeting of Sos. *EMBO J* **16**, 1351-1359 (1997).
79. T. S. Freedman *et al.*, A Ras-induced conformational switch in the Ras activator Son of sevenless. *Proceedings of the National Academy of Sciences* **103**, 16692-16697 (2006).
80. H. Chen, X. Wu, Z. K. Pan, S. Huang, Integrity of SOS1/EPS8/ABI1 tri-complex determines ovarian cancer metastasis. *Cancer Res* **70**, 9979-9990 (2010).
81. O. A. Timofeeva *et al.*, Enhanced expression of SOS1 is detected in prostate cancer epithelial cells from African-American men. *Int J Oncol* **35**, 751-760 (2009).
82. M. Tartaglia *et al.*, Gain-of-function SOS1 mutations cause a distinctive form of Noonan syndrome. *Nat Genet* **39**, 75-79 (2007).
83. F. Lepri *et al.*, SOS1 mutations in Noonan syndrome: molecular spectrum, structural insights on pathogenic effects, and genotype-phenotype correlations. *Hum Mutat* **32**, 760-772 (2011).
84. M. Zenker *et al.*, SOS1 is the second most common Noonan gene but plays no major role in cardio-facio-cutaneous syndrome. *Journal of medical genetics* **44**, 651-656 (2007).
85. T. C. Hart *et al.*, A mutation in the SOS1 gene causes hereditary gingival fibromatosis type 1. *Am J Hum Genet* **70**, 943-954 (2002).
86. R. I. Marshall, P. M. Bartold, A clinical review of drug-induced gingival overgrowths. *Australian dental journal* **44**, 219-232 (1999).
87. Y. S. Wang, L. Wu, Enhanced expression of son of sevenless homolog 1 is predictive of poor prognosis in uveal malignant melanoma patients. *Ophthalmic Genet* **40**, 22-28 (2019).
88. S. Kaliki, C. L. Shields, J. A. Shields, Uveal melanoma: estimating prognosis. *Indian J Ophthalmol* **63**, 93-102 (2015).
89. B. J. Mayer, M. Hamaguchi, H. Hanafusa, A novel viral oncogene with structural similarity to phospholipase C. *Nature* **332**, 272-275 (1988).

90. H. Yu *et al.*, Solution structure of the SH3 domain of Src and identification of its ligand-binding site. *Science* **258**, 1665-1668 (1992).
91. P. Cicchetti, B. J. Mayer, G. Thiel, D. Baltimore, Identification of a protein that binds to the SH3 region of Abl and is similar to Bcr and GAP-rho. *Science* **257**, 803-806 (1992).
92. R. Ren, B. J. Mayer, P. Cicchetti, D. Baltimore, Identification of a ten-amino acid proline-rich SH3 binding site. *Science* **259**, 1157-1161 (1993).
93. B. J. Mayer, M. J. Eck, SH3 domains: minding your p's and q's. *Current Biology* **5**, 364-367 (1995).
94. K. Saksela, P. Permi, SH3 domain ligand binding: What's the consensus and where's the specificity? *FEBS letters* **586**, 2609-2614 (2012).
95. A. Cámara-Artigas, S. Martínez-Rodríguez, E. Ortiz-Salmerón, J. M. Martín-García, 3D domain swapping in a chimeric c-Src SH3 domain takes place through two hinge loops. *Journal of structural biology* **186**, 195-203 (2014).
96. M. Carducci *et al.*, The protein interaction network mediated by human SH3 domains. *Biotechnology advances* **30**, 4-15 (2012).
97. S. Panni, L. Dente, G. Cesareni, In vitro evolution of recognition specificity mediated by SH3 domains reveals target recognition rules. *Journal of Biological Chemistry* **277**, 21666-21674 (2002).
98. B. Morel, L. Varela, A. I. Azuaga, F. Conejero-Lara, Environmental conditions affect the kinetics of nucleation of amyloid fibrils and determine their morphology. *Biophysical journal* **99**, 3801-3810 (2010).
99. L. Varela, B. Morel, A. I. Azuaga, F. Conejero-Lara, A single mutation in an SH3 domain increases amyloid aggregation by accelerating nucleation, but not by destabilizing thermodynamically the native state. *FEBS letters* **583**, 801-806 (2009).
100. L. Wu, L. Pan, Z. Wei, M. Zhang, Structure of MyTH4-FERM domains in myosin VIIa tail bound to cargo. *Science* **331**, 757-760 (2011).
101. N. Kurochkina, U. Guha, SH3 domains: modules of protein–protein interactions. *Biophysical reviews* **5**, 29-39 (2013).
102. K. Ichikawa, K. Numasawa, S. Takeshita, A. Hashiguchi, H. Takashima, Novel mutations in SH 3 TC 2 in a young Japanese girl with Charcot-Marie-Tooth disease type 4C. *Pediatrics International* **58**, 1252-1254 (2016).
103. V. Lupo *et al.*, Missense mutations in the SH3TC2 protein causing Charcot-Marie-Tooth disease type 4C affect its localization in the plasma membrane and endocytic pathway. *Human molecular genetics* **18**, 4603-4614 (2009).
104. L. E. LaConte *et al.*, Two microcephaly-associated novel missense mutations in CASK specifically disrupt the CASK–neurexin interaction. *Human genetics* **137**, 231-246 (2018).
105. I. Hori *et al.*, A novel homozygous missense mutation in the SH3-binding motif of STAMBP causing microcephaly-capillary malformation syndrome. *Journal of human genetics* **63**, 957-963 (2018).
106. A. Giubellino, T. R. Burke, D. P. Bottaro, Grb2 signaling in cell motility and cancer. *Expert opinion on therapeutic targets* **12**, 1021-1033 (2008).
107. A. Nimnual, D. Bar-Sagi, The two hats of SOS. *Science Signaling* **2002**, pe36-pe36 (2002).
108. C. B. McDonald, K. L. Seldeen, B. J. Deegan, V. Bhat, A. Farooq, Assembly of the Sos1–Grb2–Gab1 ternary signaling complex is under allosteric control. *Archives of biochemistry and biophysics* **494**, 216-225 (2010).
109. W. Wang, S. Xu, M. Yin, Z. G. Jin, Essential roles of Gab1 tyrosine phosphorylation in growth factor-mediated signaling and angiogenesis. *International journal of cardiology* **181**, 180-184 (2015).

110. C. B. McDonald *et al.*, Allostery mediates ligand binding to Grb2 adaptor in a mutually exclusive manner. *Journal of molecular recognition* **26**, 92-103 (2013).
111. G. Song, G. Ouyang, S. Bao, The activation of Akt/PKB signaling pathway and cell survival. *Journal of cellular and molecular medicine* **9**, 59-71 (2005).
112. J. I. MacDonald, E. A. Gryz, C. J. Kubu, J. M. Verdi, S. O. Meakin, Direct binding of the signaling adapter protein Grb2 to the activation loop tyrosines on the nerve growth factor receptor tyrosine kinase, TrkA. *Journal of Biological Chemistry* **275**, 18225-18233 (2000).
113. H. Kouhara *et al.*, A lipid-anchored Grb2-binding protein that links FGF-receptor activation to the Ras/MAPK signaling pathway. *Cell* **89**, 693-702 (1997).
114. A. Żawrocki, W. Biernat, Epidermal growth factor receptor in glioblastoma. *Folia neuropathologica* **43**, (2005).
115. K. S. Ravichandran, U. Lorenz, S. E. Shoelson, S. J. Burakoff, Interaction of Shc with Grb2 regulates association of Grb2 with mSOS. *Molecular and Cellular Biology* **15**, 593-600 (1995).
116. M. Jaiswal *et al.*, Functional cross-talk between ras and rho pathways: a Ras-specific GTPase-activating protein (p120RasGAP) competitively inhibits the RhoGAP activity of deleted in liver cancer (DLC) tumor suppressor by masking the catalytic arginine finger. *J Biol Chem* **289**, 6839-6849 (2014).
117. D. K. Simanshu, D. V. Nissley, F. McCormick, RAS proteins and their regulators in human disease. *Cell* **170**, 17-33 (2017).
118. S. Gutierrez-Erlandsson *et al.*, R-RAS2 overexpression in tumors of the human central nervous system. *Molecular cancer* **12**, 127 (2013).
119. A. E. Karnoub, R. A. Weinberg, Ras oncogenes: split personalities. *Nature reviews Molecular cell biology* **9**, 517-531 (2008).
120. S. Nakhaei-Rad *et al.*, The role of embryonic stem cell-expressed RAS (ERAS) in the maintenance of quiescent hepatic stellate cells. *Journal of Biological Chemistry*, jbc. M115. 700088 (2016).
121. E. Castellano, J. Downward, in *Phosphoinositide 3-kinase in Health and Disease*. (Springer, 2010), pp. 143-169.
122. J. J. Chan *et al.*, Comparative analysis of interactions of RASSF1-10. *Advances in biological regulation* **53**, 190-201 (2013).
123. T. D. Bunney, M. Katan, PLC regulation: emerging pictures for molecular mechanisms. *Trends in biochemical sciences* **36**, 88-96 (2011).
124. E. Ferro, L. Trabalzini, RalGDS family members couple Ras to Ral signalling and that's not all. *Cellular signalling* **22**, 1804-1810 (2010).
125. K. Rajalingam, R. Schreck, U. R. Rapp, Š. Albert, Ras oncogenes and their downstream targets. *Biochimica et Biophysica Acta (BBA)-Molecular Cell Research* **1773**, 1177-1195 (2007).
126. R. Nussinov *et al.*, Principles of K-Ras effector organization and the role of oncogenic K-Ras in cancer initiation through G1 cell cycle deregulation. *Expert review of proteomics* **12**, 669-682 (2015).
127. I. M. Ahearn, K. Haigis, D. Bar-Sagi, M. R. Philips, Regulating the regulator: post-translational modification of RAS. *Nature reviews Molecular cell biology* **13**, 39 (2012).
128. A. Hennig, R. Markwart, M. A. Esparza-Franco, G. Ladds, I. Rubio, Ras activation revisited: role of GEF and GAP systems. *Biological chemistry* **396**, 831-848 (2015).
129. A. Fischer *et al.*, B-and C-RAF Display Essential Differences in Their Binding to Ras THE ISOTYPE-SPECIFIC N TERMINUS OF B-RAF FACILITATES RAS BINDING. *Journal of Biological Chemistry* **282**, 26503-26516 (2007).
130. H. R. Mott, D. Owen, Structures of Ras superfamily effector complexes: What have we learnt in two decades? *Critical reviews in biochemistry and molecular biology* **50**, 85-133 (2015).

131. D. Filchtinski *et al.*, What makes Ras an efficient molecular switch: a computational, biophysical, and structural study of Ras-GDP interactions with mutants of Raf. *Journal of molecular biology* **399**, 422-435 (2010).
132. A. Erijman, J. M Shifman, RAS/effector interactions from structural and biophysical perspective. *Mini reviews in medicinal chemistry* **16**, 370-375 (2016).
133. N. Nassar *et al.*, Ras/Rap effector specificity determined by charge reversal. *Nature structural biology* **3**, 723-729 (1996).
134. H. Nakhaeizadeh, E. Amin, S. Nakhaei-Rad, R. Dvorsky, M. R. Ahmadian, The RAS-effector interface: isoform-specific differences in the effector binding regions. *PLoS One* **11**, e0167145 (2016).
135. G. A. Repasky, E. J. Chenette, C. J. Der, Renewing the conspiracy theory debate: does Raf function alone to mediate Ras oncogenesis? *Trends in cell biology* **14**, 639-647 (2004).
136. S. Wohlgemuth *et al.*, Recognizing and defining true Ras binding domains I: biochemical analysis. *Journal of molecular biology* **348**, 741-758 (2005).
137. T. Dhanaraman *et al.*, RASSF effectors couple diverse RAS subfamily GTPases to the Hippo pathway. *Science Signaling* **13**, (2020).
138. T. D. Goddard *et al.*, UCSF ChimeraX: Meeting modern challenges in visualization and analysis. *Protein Science* **27**, 14-25 (2018).
139. N. Nassar *et al.*, The 2.2 Å crystal structure of the Ras-binding domain of the serine/threonine kinase c-Raf1 in complex with RaplA and a GTP analogue. *Nature* **375**, 554 (1995).
140. T. D. Bunney *et al.*, Structural and mechanistic insights into ras association domains of phospholipase C epsilon. *Molecular cell* **21**, 495-507 (2006).
141. B. Stieglitz *et al.*, Novel type of Ras effector interaction established between tumour suppressor NORE1A and Ras switch II. *The EMBO journal* **27**, 1995-2005 (2008).
142. M. E. Pacold *et al.*, Crystal structure and functional analysis of Ras binding to its effector phosphoinositide 3-kinase γ. *Cell* **103**, 931-944 (2000).
143. M. J. Smith *et al.*, Evolution of AF6-RAS association and its implications in mixed-lineage leukemia. *Nature communications* **8**, 1-13 (2017).
144. C. Kiel *et al.*, Recognizing and defining true Ras binding domains II: in silico prediction based on homology modelling and energy calculations. *Journal of molecular biology* **348**, 759-775 (2005).
145. H. Donninger, M. L. Schmidt, J. Mezzanotte, T. Barnoud, G. J. Clark, in *Seminars in cell & developmental biology*. (Elsevier, 2016), vol. 58, pp. 86-95.
146. S. Rezaei Adariani *et al.*, Structural snapshots of RAF kinase interactions. *Biochemical Society Transactions* **46**, 1393-1406 (2018).
147. F. Haghighi *et al.*, bFGF-mediated pluripotency maintenance in human induced pluripotent stem cells is associated with NRAS-MAPK signaling. *Cell Communication and Signaling* **16**, 96 (2018).
148. E. Desideri, A. L. Cavallo, M. Baccarini, Alike but different: RAF paralogs and their signaling outputs. *Cell* **161**, 967-970 (2015).
149. E. Castellano, J. Downward, RAS interaction with PI3K: more than just another effector pathway. *Genes & cancer* **2**, 261-274 (2011).
150. E. M. Ross, T. M. Wilkie, GTPase-activating proteins for heterotrimeric G proteins: regulators of G protein signaling (RGS) and RGS-like proteins. *Annual review of biochemistry* **69**, 795-827 (2000).
151. F. S. Willard *et al.*, Regulator of G-protein signaling 14 (RGS14) is a selective H-Ras effector. *PloS one* **4**, (2009).
152. A. Malliri, J. G. Collard, Role of Rho-family proteins in cell adhesion and cancer. *Current opinion in cell biology* **15**, 583-589 (2003).

153. C. Rooney *et al.*, The Rac activator STEF (Tiam2) regulates cell migration by microtubule-mediated focal adhesion disassembly. *EMBO reports* **11**, 292-298 (2010).
154. J. Yamauchi, Y. Miyamoto, A. Tanoue, E. M. Shooter, J. R. Chan, Ras activation of a Rac1 exchange factor, Tiam1, mediates neurotrophin-3-induced Schwann cell migration. *Proceedings of the National Academy of Sciences* **102**, 14889-14894 (2005).
155. S. Nakhaei-Rad *et al.*, Structural fingerprints, interactions, and signaling networks of RAS family proteins beyond RAS isoforms. *Critical reviews in biochemistry and molecular biology* **53**, 130-156 (2018).
156. C. Kiel, M. Foglierini, N. Kuemmerer, P. Beltrao, L. Serrano, A genome-wide Ras-effector interaction network. *Journal of molecular biology* **370**, 1020-1032 (2007).
157. R. Ghai *et al.*, Phox homology band 4.1/ezrin/radixin/moesin-like proteins function as molecular scaffolds that interact with cargo receptors and Ras GTPases. *Proceedings of the National Academy of Sciences* **108**, 7763-7768 (2011).
158. R. Ghai, B. Collins, PX-FERM proteins: A link between endosomal trafficking and signaling? *Small GTPases* **2**, 7763-7768 (2011).
159. C. R. Amendola *et al.*, KRAS4A directly regulates hexokinase 1. *Nature* **576**, 482-486 (2019).
160. D. Chowdhury, J. W. Hell, How CBP/Shank3 Guards Rap and H-Ras. *Structure* **28**, 274-276 (2020).
161. Q. Cai, T. Hosokawa, M. Zeng, Y. Hayashi, M. Zhang, Shank3 Binds to and Stabilizes the Active Form of Rap1 and HRas GTPases via Its NTD-ANK Tandem with Distinct Mechanisms. *Structure* **28**, 290-300. e294 (2020).
162. J. Miyan *et al.*, Direct physical interaction of active Ras with mSIN1 regulates mTORC2 signaling. *BMC cancer* **19**, 1-16 (2019).
163. H. Iwasa, S. Hossain, Y. Hata, Tumor suppressor C-RASSF proteins. *Cellular and Molecular Life Sciences* **75**, 1773-1787 (2018).
164. M. Gordon, S. Baksh, RASSF1A: not a prototypical Ras effector. *Small GTPases* **2**, 5729-5740 (2011).
165. D. Thillaivillalan *et al.*, RASSF effectors couple diverse RAS subfamily GTPases to the Hippo pathway. *bioRxiv*, (2020).
166. B. Bauer *et al.*, Effector recognition by the small GTP-binding proteins Ras and Ral. *Journal of Biological Chemistry* **274**, 17763-17770 (1999).
167. N. Nelson, G. J. Clark, Rheb may complex with RASSF1A to coordinate Hippo and TOR signaling. *Oncotarget* **7**, 33821 (2016).
168. T. Devanand, P. Venkatraman, S. Vemparala, Phosphorylation promotes binding affinity of Rap-Raf complex by allosteric modulation of switch loop dynamics. *Scientific reports* **8**, 1-15 (2018).
169. T. Devanand, S. Krishnaswamy, S. Vemparala, Interdigitation of Lipids Induced by Membrane–Active Proteins. *The Journal of membrane biology* **252**, 331-342 (2019).
170. W. M. Yee, P. F. Worley, Rheb interacts with Raf-1 kinase and may function to integrate growth factor-and protein kinase A-dependent signals. *Molecular and cellular biology* **17**, 921-933 (1997).
171. M. Karbowniczek, G. P. Robertson, E. P. Henske, Rheb inhibits C-raf activity and B-raf/C-raf heterodimerization. *Journal of Biological Chemistry* **281**, 25447-25456 (2006).
172. J. J. Heard, I. Phung, M. I. Potes, F. Tamanoi, An oncogenic mutant of RHEB, RHEB Y35N, exhibits an altered interaction with BRAF resulting in cancer transformation. *BMC cancer* **18**, 69 (2018).
173. M. Yaoita *et al.*, Spectrum of mutations and genotype–phenotype analysis in Noonan syndrome patients with RIT1 mutations. *Human genetics* **135**, 209-222 (2016).
174. H. Shao, K. Kadono-Okuda, B. S. Finlin, D. A. Andres, Biochemical characterization of the Ras-related GTPases Rit and Rin. *Archives of biochemistry and biophysics* **371**, 207-219 (1999).

175. G.-X. Shi, D. A. Andres, Rit contributes to nerve growth factor-induced neuronal differentiation via activation of B-Raf-extracellular signal-regulated kinase and p38 mitogen-activated protein kinase cascades. *Molecular and cellular biology* **25**, 830-846 (2005).
176. T. S. Chavan *et al.*, Plasma membrane regulates Ras signaling networks. *Cellular logistics* **5**, e1136374 (2015).
177. M. T. Mazhab-Jafari *et al.*, Oncogenic and RASopathy-associated K-RAS mutations relieve membrane-dependent occlusion of the effector-binding site. *Proceedings of the National Academy of Sciences* **112**, 6625-6630 (2015).
178. D. Abankwa, A. A. Gorfe, J. F. Hancock, Ras nanoclusters: molecular structure and assembly. *Semin Cell Dev Biol* **18**, 599-607 (2007).
179. D. Abankwa, A. A. Gorfe, K. Inder, J. F. Hancock, Ras membrane orientation and nanodomain localization generate isoform diversity. *Proc Natl Acad Sci U S A* **107**, 1130-1135 (2010).
180. I. C. Cirstea *et al.*, A restricted spectrum of NRAS mutations causes Noonan syndrome. *Nat Genet* **42**, 27-29 (2010).
181. Y. Zhou, J. F. Hancock, Deciphering lipid codes: K-Ras as a paradigm. *Traffic* **19**, 157-165 (2018).
182. S. Kapoor *et al.*, Revealing conformational substates of lipidated N-Ras protein by pressure modulation. *Proc Natl Acad Sci U S A* **109**, 460-465 (2012).
183. A. Vogel *et al.*, Interaction of the human N-Ras protein with lipid raft model membranes of varying degrees of complexity. *Biol Chem* **395**, 779-789 (2014).
184. B. Sperlich, S. Kapoor, H. Waldmann, R. Winter, K. Weise, Regulation of K-Ras4B Membrane Binding by Calmodulin. *Biophys J* **111**, 113-122 (2016).
185. N. Erwin, S. Patra, M. Dwivedi, K. Weise, R. Winter, Influence of isoform-specific Ras lipidation motifs on protein partitioning and dynamics in model membrane systems of various complexity. *Biol Chem* **398**, 547-563 (2017).
186. D. Abankwa, A. A. Gorfe, K. Inder, J. F. Hancock, Ras membrane orientation and nanodomain localization generate isoform diversity. *Proceedings of the National Academy of Sciences* **107**, 1130-1135 (2010).
187. I. C. Cirstea *et al.*, A restricted spectrum of NRAS mutations causes Noonan syndrome. *Nature genetics* **42**, 27-29 (2010).
188. D. Abankwa, A. A. Gorfe, J. F. Hancock, in *Seminars in cell & developmental biology*. (Elsevier, 2007), vol. 18, pp. 599-607.
189. K. Nouri *et al.*, IQGAP1 interaction with RHO family proteins revisited kinetic and equilibrium evidence for multiple distinct binding sites. *Journal of Biological Chemistry* **291**, 26364-26376 (2016).
190. S. Y. Yoon, A. Tefferi, C. Y. Li, Cellular distribution of platelet-derived growth factor, transforming growth factor-beta, basic fibroblast growth factor, and their receptors in normal bone marrow. *Acta Haematol* **104**, 151-157 (2000).
191. Y. Zhou, J. F. Hancock, Deciphering lipid codes: K-Ras as a paradigm. *Traffic* **19**, 157-165 (2018).
192. S. Kapoor *et al.*, Revealing conformational substates of lipidated N-Ras protein by pressure modulation. *Proceedings of the National Academy of Sciences* **109**, 460-465 (2012).
193. M. T. Mazhab-Jafari *et al.*, Oncogenic and RASopathy-associated K-RAS mutations relieve membrane-dependent occlusion of the effector-binding site. *Proc Natl Acad Sci U S A* **112**, 6625-6630 (2015).
194. R. Nussinov, C. J. Tsai, H. Jang, Is Nanoclustering essential for all oncogenic KRas pathways? Can it explain why wild-type KRas can inhibit its oncogenic variant? *Semin Cancer Biol*, (2018).
195. R. Nussinov, C.-J. Tsai, H. Jang, Ras assemblies and signaling at the membrane. *Current Opinion in Structural Biology* **62**, 140-148 (2020).

196. R. Thurman, E. Siraliev-Perez, S. L. Campbell, RAS ubiquitylation modulates effector interactions. *Small GTPases*, 1-6 (2017).
197. C. Barceló *et al.*, Phosphorylation at Ser-181 of oncogenic KRAS is required for tumor growth. *Cancer research* **74**, 1190-1199 (2014).
198. R. Thapar, J. G. Williams, S. L. Campbell, NMR characterization of full-length farnesylated and non-farnesylated H-Ras and its implications for Raf activation. *Journal of molecular biology* **343**, 1391-1408 (2004).
199. Z.-L. Li, P. Prakash, M. Buck, A "tug of war" maintains a dynamic protein–membrane complex: molecular dynamics simulations of C-Raf RBD-CRD bound to K-Ras4B at an anionic membrane. *ACS central science* **4**, 298-305 (2018).
200. S. Li, H. Jang, J. Zhang, R. Nussinov, Raf-1 cysteine-rich domain increases the affinity of K-Ras/Raf at the membrane, promoting MAPK signaling. *Structure* **26**, 513-525. e512 (2018).
201. C.-D. Hu *et al.*, Cysteine-rich region of Raf-1 interacts with activator domain of post-translationally modified Ha-Ras. *Journal of Biological Chemistry* **270**, 30274-30277 (1995).
202. J. G. Williams *et al.*, Elucidation of binding determinants and functional consequences of Ras/Raf-cysteine-rich domain interactions. *Journal of Biological Chemistry* **275**, 22172-22179 (2000).
203. H. Ke *et al.*, Structural basis for intramolecular interaction of post-translationally modified H-Ras• GTP prepared by protein ligation. *FEBS letters* **591**, 2470-2481 (2017).
204. S. Bunda *et al.*, Src promotes GTPase activity of Ras via tyrosine 32 phosphorylation. *Proceedings of the National Academy of Sciences* **111**, E3785-E3794 (2014).
205. Y. Kano *et al.*, Tyrosyl phosphorylation of KRAS stalls GTPase cycle via alteration of switch I and II conformation. *Nature communications* **10**, 1-14 (2019).
206. F. Shima *et al.*, Association of yeast adenylyl cyclase with cyclase-associated protein CAP forms a second Ras-binding site which mediates its Ras-dependent activation. *Molecular and cellular biology* **20**, 26-33 (2000).
207. G. G. Kelley, S. E. Reks, J. M. Ondrako, A. V. Smrcka, Phospholipase Cε: a novel Ras effector. *The EMBO journal* **20**, 743-754 (2001).
208. T. Travers *et al.*, Molecular recognition of RAS/RAF complex at the membrane: Role of RAF cysteine-rich domain. *Scientific reports* **8**, 1-15 (2018).
209. B. Lakshman *et al.*, Quantitative biophysical analysis defines key components modulating recruitment of the GTPase KRAS to the plasma membrane. *Journal of Biological Chemistry* **294**, 2193-2207 (2019).
210. E. Park *et al.*, Architecture of autoinhibited and active BRAF–MEK1–14-3-3 complexes. *Nature* **575**, 545-550 (2019).
211. H. Jang, M. Zhang, R. Nussinov, The quaternary assembly of KRas4B with Raf-1 at the membrane. *Computational and Structural Biotechnology Journal*, (2020).
212. B. N. Kholodenko, J. B. Hoek, H. V. Westerhoff, Why cytoplasmic signalling proteins should be recruited to cell membranes. *Trends in cell biology* **10**, 173-178 (2000).
213. S. Sukenik, P. Ren, M. Gruebele, Weak protein–protein interactions in live cells are quantified by cell-volume modulation. *Proceedings of the National Academy of Sciences* **114**, 6776-6781 (2017).
214. L. B. Case, J. A. Ditlev, M. K. Rosen, Regulation of transmembrane signaling by phase separation. *Annual Review of Biophysics* **48**, 465-494 (2019).
215. A. Bratek-Skicki, R. Pancsa, B. Meszaros, J. Van Lindt, P. Tompa, A guide to regulation of the formation of biomolecular condensates. *The FEBS Journal*, (2020).
216. S. F. Banani, H. O. Lee, A. A. Hyman, M. K. Rosen, Biomolecular condensates: organizers of cellular biochemistry. *Nature reviews Molecular cell biology* **18**, 285-298 (2017).

217. C. Kiel, T. Selzer, Y. Shaul, G. Schreiber, C. Herrmann, Electrostatically optimized Ras-binding Ral guanine dissociation stimulator mutants increase the rate of association by stabilizing the encounter complex. *Proceedings of the National Academy of Sciences* **101**, 9223-9228 (2004).
218. C. Kiel *et al.*, Improved binding of Raf to Ras· GDP is correlated with biological activity. *Journal of Biological Chemistry* **284**, 31893-31902 (2009).
219. G. Schreiber, G. Haran, H.-X. Zhou, Fundamental aspects of protein− protein association kinetics. *Chemical reviews* **109**, 839-860 (2009).
220. L. Gremer *et al.*, Germline KRAS mutations cause aberrant biochemical and physical properties leading to developmental disorders. *Human mutation* **32**, 33-43 (2011).
221. T. A. Hall, in *Nucleic acids symposium series*. ([London]: Information Retrieval Ltd., c1979-c2000., 1999), vol. 41, pp. 95-98.
222. P. J. Cock *et al.*, Biopython: freely available Python tools for computational molecular biology and bioinformatics. *Bioinformatics* **25**, 1422-1423 (2009).
223. W. L. DeLano, The PyMOL molecular graphics system. *http://www. pymol. org*, (2002).
224. A. Ursu, H. Waldmann, Hide and seek: Identification and confirmation of small molecule protein targets. *Bioorganic & medicinal chemistry letters* **25**, 3079-3086 (2015).
225. B. K. Wagner, S. L. Schreiber, The Power of Sophisticated Phenotypic Screening and Modern Mechanism-of-Action Methods. *Cell chemical biology* **23**, 3-9 (2016).
226. F. Vincent *et al.*, Developing predictive assays: the phenotypic screening "rule of 3". *Science translational medicine* **7**, 293ps215 (2015).
227. H. van Hattum, H. Waldmann, Biology-oriented synthesis: harnessing the power of evolution. *Journal of the American Chemical Society* **136**, 11853-11859 (2014).
228. G. Karageorgis *et al.*, Chromopynones are pseudo natural product glucose uptake inhibitors targeting glucose transporters GLUT-1 and -3. *Nature chemistry*, (2018).
229. B. Over *et al.*, Natural-product-derived fragments for fragment-based ligand discovery. *Nat Chem* **5**, 21-28 (2013).
230. M. J. Uddin, S. Kokubo, K. Ueda, K. Suenaga, D. Uemura, Haterumaimides F–I, Four New Cytotoxic Diterpene Alkaloids from an Ascidian Lissoclinum Species. *Journal of Natural Products* **64**, 1169-1173 (2001).
231. M. Isaka *et al.*, Hirsutellones A–E, antimycobacterial alkaloids from the insect pathogenic fungus Hirsutella nivea BCC 2594. *Tetrahedron* **61**, 5577-5583 (2005).
232. J. i. Kobayashi, H. Nakamura, Y. Ohizumi, Y. Hirata, Eudistomidin-A, a novel calmodulin antagonist from the okinawan tunicate eudistoma glaucus. *Tetrahedron Letters* **27**, 1191-1194 (1986).
233. S. Tyroller, W. Zwickenpflug, E. Richter, New Sources of Dietary Myosmine Uptake from Cereals, Fruits, Vegetables, and Milk. *Journal of Agricultural and Food Chemistry* **50**, 4909-4915 (2002).
234. T. L. Lohr, T. J. Marks, Orthogonal tandem catalysis. *Nature chemistry* **7**, 477-482 (2015).
235. A. D. Melhado, G. W. Amarante, Z. J. Wang, M. Luparia, F. D. Toste, Gold(I)-Catalyzed Diastereo- and Enantioselective 1,3-Dipolar Cycloaddition and Mannich Reactions of Azlactones. *Journal of the American Chemical Society* **133**, 3517-3527 (2011).
236. W. Sun *et al.*, Organocatalytic Diastereo- and Enantioselective 1,3-Dipolar Cycloaddition of Azlactones and Methyleneindolinones. **52**, 8633-8637 (2013).
237. A. P. Antonchick *et al.*, Highly enantioselective synthesis and cellular evaluation of spirooxindoles inspired by natural products. *Nature chemistry* **2**, 735 (2010).
238. R. Narayan, M. Potowski, Z.-J. Jia, A. P. Antonchick, H. Waldmann, Catalytic Enantioselective 1,3-Dipolar Cycloadditions of Azomethine Ylides for Biology-Oriented Synthesis. *Accounts of chemical research* **47**, 1296-1310 (2014).

239. P. Ertl, S. Roggo, A. Schuffenhauer, Natural Product-likeness Score and Its Application for Prioritization of Compound Libraries. *Journal of Chemical Information and Modeling* **48**, 68-74 (2008).
240. A. P. Bento *et al.*, The ChEMBL bioactivity database: an update. *Nucleic Acids Research* **42**, D1083-D1090 (2014).
241. V. Law *et al.*, DrugBank 4.0: shedding new light on drug metabolism. *Nucleic Acids Research* **42**, D1091-D1097 (2014).
242. W. H. B. Sauer, M. K. Schwarz, Molecular Shape Diversity of Combinatorial Libraries: A Prerequisite for Broad Bioactivity. *Journal of Chemical Information and Computer Sciences* **43**, 987-1003 (2003).
243. I. Colomer *et al.*, A divergent synthetic approach to diverse molecular scaffolds: assessment of lead-likeness using LLAMA, an open-access computational tool. *Chemical Communications* **52**, 7209-7212 (2016).
244. T. L. Lin, W. Matsui, Hedgehog pathway as a drug target: Smoothened inhibitors in development. *OncoTargets and therapy* **5**, 47-58 (2012).
245. R. Garcia-Mata, E. Boulter, K. Burridge, The 'invisible hand': regulation of RHO GTPases by RHOGDIs. *Nature reviews. Molecular cell biology* **12**, 493-504 (2011).
246. E. Boulter *et al.*, Regulation of Rho GTPase crosstalk, degradation and activity by RhoGDI1. *Nature cell biology* **12**, 477-483 (2010).
247. S.-C. Zhang *et al.*, Liposome Reconstitution and Modulation of Recombinant Prenylated Human Rac1 by GEFs, GDI1 and Pak1. *PloS one* **9**, e102425 (2014).
248. J. Bigay, J. F. Casella, G. Drin, B. Mesmin, B. Antonny, ArfGAP1 responds to membrane curvature through the folding of a lipid packing sensor motif. *The EMBO journal* **24**, 2244-2253 (2005).
249. A. R. Newcombe, R. W. Stockley, J. L. Hunter, M. R. Webb, The Interaction between Rac1 and Its Guanine Nucleotide Dissociation Inhibitor (GDI), Monitored by a Single Fluorescent Coumarin Attached to GDI. *Biochemistry* **38**, 6879-6886 (1999).
250. T. Mejuch *et al.*, Small-Molecule Inhibition of the UNC119-Cargo Interaction. *Angewandte Chemie (International ed. in English)* **56**, 6181-6186 (2017).
251. Z. Tnimov *et al.*, Quantitative analysis of prenylated RhoA interaction with its chaperone, RhoGDI. *The Journal of biological chemistry* **287**, 26549-26562 (2012).
252. J. R. Silvius, F. l'Heureux, Fluorimetric evaluation of the affinities of isoprenylated peptides for lipid bilayers. *Biochemistry* **33**, 3014-3022 (1994).
253. A. R. Shepard *et al.*, Identification of PDE6D as a molecular target of anecortave acetate via a methotrexate-anchored yeast three-hybrid screen. *ACS chemical biology* **8**, 549-558 (2013).
254. C. Guilluy, R. Garcia-Mata, K. Burridge, Rho protein crosstalk: another social network? *Trends in cell biology* **21**, 718-726 (2011).
255. A. J. Ridley, A. Hall, The small GTP-binding protein rho regulates the assembly of focal adhesions and actin stress fibers in response to growth factors. *Cell* **70**, 389-399 (1992).
256. A. J. Ridley, H. F. Paterson, C. L. Johnston, D. Diekmann, A. Hall, The small GTP-binding protein rac regulates growth factor-induced membrane ruffling. *Cell* **70**, 401-410 (1992).
257. R. S. Bon, H. Waldmann, Bioactivity-guided navigation of chemical space. *Accounts of chemical research* **43**, 1103-1114 (2010).
258. S. Wetzel, R. S. Bon, K. Kumar, H. Waldmann, Biology-oriented synthesis. *Angewandte Chemie (International ed. in English)* **50**, 10800-10826 (2011).
259. R. W. Huigens *et al.*, A ring-distortion strategy to construct stereochemically complex and structurally diverse compounds from natural products. *Nature Chemistry* **5**, 195-202 (2013).
260. R. J. Rafferty, R. W. Hicklin, K. A. Maloof, P. J. Hergenrother, Synthesis of Complex and Diverse Compounds through Ring Distortion of Abietic Acid. *Angew Chem Int Edit* **53**, 220-224 (2014).

261. Y. Goto, Y. Ito, Y. Kato, S. Tsunoda, H. Suga, One-Pot Synthesis of Azoline-Containing Peptides in a Cell-free Translation System Integrated with a Posttranslational Cyclodehydratase. *Chem Biol* **21**, 766-774 (2014).
262. T. Ozaki *et al.*, Dissection of goadsporin biosynthesis by in vitro reconstitution leading to designer analogues expressed in vivo. *Nat Commun* **8**, (2017).
263. T. Asai *et al.*, Use of a biosynthetic intermediate to explore the chemical diversity of pseudo-natural fungal polyketides. *Nature Chemistry* **7**, 737-743 (2015).
264. H. Kikuchi *et al.*, Monoterpene Indole Alkaloid-Like Compounds Based on Diversity-Enhanced Extracts of Iridoid-Containing Plants and Their Immune Checkpoint Inhibitory Activity. *Org Lett* **18**, 5948-5951 (2016).
265. D. R. Cook, K. L. Rossman, C. J. Der, Rho guanine nucleotide exchange factors: regulators of Rho GTPase activity in development and disease. *Oncogene* **33**, 4021-4035 (2014).
266. R. Teperino, F. Aberger, H. Esterbauer, N. Riobo, J. A. Pospisilik, Canonical and non-canonical Hedgehog signalling and the control of metabolism. *Semin Cell Dev Biol* **33**, 81-92 (2014).
267. D. J. Robbins, D. L. Fei, N. A. Riobo, The Hedgehog signal transduction network. *Sci Signal* **5**, re6 (2012).
268. H. E. Pelish *et al.*, Secramine inhibits Cdc42-dependent functions in cells and Cdc42 activation in vitro. *Nature Chemical Biology* **2**, 39 (2005).
269. R. G. Hodge, A. J. Ridley, Regulating Rho GTPases and their regulators. *Nature Reviews Molecular Cell Biology* **17**, 496-510 (2016).
270. J. L. Arnst *et al.*, Discovery and characterization of small molecule Rac1 inhibitors. *Oncotarget* **8**, 34586-34600 (2017).
271. L. Hong *et al.*, Characterization of a Cdc42 protein inhibitor and its use as a molecular probe. *The Journal of biological chemistry* **288**, 8531-8543 (2013).
272. M. Gorovoy *et al.*, RhoGDI-1 modulation of the activity of monomeric RhoGTPase RhoA regulates endothelial barrier function in mouse lungs. *Circ Res* **101**, 50-58 (2007).
273. A. Schaefer, N. R. Reinhard, P. L. Hordijk, Toward understanding RhoGTPase specificity: structure, function and local activation. *Small GTPases* **5**, 6 (2014).
274. G. B. Carballo, J. R. Honorato, G. P. F. de Lopes, T. C. L. D. E. Spohr, A highlight on Sonic hedgehog pathway. *Cell Commun Signal* **16**, (2018).
275. T. Pandit, S. K. Ogden, Contributions of Noncanonical Smoothened Signaling During Embryonic Development. *J Dev Biol* **5**, (2017).
276. P. Chinchilla, L. Xiao, M. G. Kazanietz, N. A. Riobo, Hedgehog proteins activate pro-angiogenic responses in endothelial cells through non-canonical signaling pathways. *Cell cycle (Georgetown, Tex.)* **9**, 570-579 (2010).
277. A. H. Polizio *et al.*, Heterotrimeric G(i) Proteins Link Hedgehog Signaling to Activation of Rho Small GTPases to Promote Fibroblast Migration. *Journal of Biological Chemistry* **286**, 19589-19596 (2011).
278. K. Kasai *et al.*, The G12 family of heterotrimeric G proteins and Rho GTPase mediate Sonic hedgehog signalling. *Genes to cells : devoted to molecular & cellular mechanisms* **9**, 49-58 (2004).
279. A. E. Douglas *et al.*, The alpha Subunit of the G Protein G(13) Regulates Activity of One or More Gli Transcription Factors Independently of Smoothened. *Journal of Biological Chemistry* **286**, 30714-30722 (2011).
280. S. S. Choi *et al.*, Activation of Rac1 promotes hedgehog-mediated acquisition of the myofibroblastic phenotype in rat and human hepatic stellate cells. *Hepatology (Baltimore, Md.)* **52**, 278-290 (2010).

281. X. Yuan *et al.*, Ciliary IFT80 balances canonical versus non-canonical hedgehog signalling for osteoblast differentiation. *Nat Commun* **7**, (2016).
282. J. Kim *et al.*, Functional genomic screen for modulators of ciliogenesis and cilium length. *Nature* **464**, 1048-U1114 (2010).
283. M. L. Drummond *et al.*, Actin polymerization controls cilia-mediated signaling. *J Cell Biol* **217**, 3255-3266 (2018).
284. Z. A. Knight, K. M. Shokat, Chemical genetics: Where genetics and pharmacology meet. *Cell* **128**, 425-430 (2007).
285. W. A. Weiss, S. S. Taylor, K. M. Shokat, Recognizing and exploiting differences between RNAi and small-molecule inhibitors. *Nature Chemical Biology* **3**, 739-744 (2007).
286. M. Mirvis, T. Stearns, W. J. Nelson, Cilium structure, assembly, and disassembly regulated by the cytoskeleton. *Biochem J* **475**, 2329-2353 (2018).
287. L. Laursen, J. Kliche, S. Gianni, P. Jemth, Supertertiary protein structure affects an allosteric network. *bioRxiv*, (2020).
288. G. Stock, P. Hamm, A non-equilibrium approach to allosteric communication. *Philosophical Transactions of the Royal Society B: Biological Sciences* **373**, 20170187 (2018).
289. K. Gunasekaran, B. Ma, R. Nussinov, Is allostery an intrinsic property of all dynamic proteins? *Proteins: Structure, Function, and Bioinformatics* **57**, 433-443 (2004).
290. K. Neumann, T. Oellerich, H. Urlaub, J. Wienands, The B-lymphoid Grb2 interaction code. *Immunological reviews* **232**, 135-149 (2009).
291. E. Lowenstein *et al.*, The SH2 and SH3 domain-containing protein GRB2 links receptor tyrosine kinases to ras signaling. *Cell* **70**, 431-442 (1992).
292. P. G. Dharmawardana, B. Peruzzi, A. Giubellino, T. R. Burke Jr, D. P. Bottaro, Molecular targeting of growth factor receptor-bound 2 (Grb2) as an anti-cancer strategy. *Anti-cancer drugs* **17**, 13-20 (2006).
293. J. A. Simon, S. L. Schreiber, Grb2 SH3 binding to peptides from Sos: evaluation of a general model for SH3-ligand interactions. *Chemistry & biology* **2**, 53-60 (1995).
294. B. J. Mayer, D. Baltimore, Signalling through SH2 and SH3 domains. *Trends in cell biology* **3**, 8-13 (1993).
295. T. Pawson, J. Schlessingert, SH2 and SH3 domains. *Current Biology* **3**, 434-442 (1993).
296. J. Schlessinger, M. A. Lemmon, SH2 and PTB domains in tyrosine kinase signaling. *Sci. STKE* **2003**, re12-re12 (2003).
297. N. Bisson *et al.*, Selected reaction monitoring mass spectrometry reveals the dynamics of signaling through the GRB2 adaptor. *Nature biotechnology* **29**, 653-658 (2011).
298. Z. Ahmed *et al.*, Grb2 monomer–dimer equilibrium determines normal versus oncogenic function. *Nature communications* **6**, 1-11 (2015).
299. S. Zhou *et al.*, SH2 domains recognize specific phosphopeptide sequences. *Cell* **72**, 767-778 (1993).
300. M. J. Robinson, M. H. Cobb, Mitogen-activated protein kinase pathways. *Current opinion in cell biology* **9**, 180-186 (1997).
301. G. W. Reuther, C. J. Der, The Ras branch of small GTPases: Ras family members don't fall far from the tree. *Current opinion in cell biology* **12**, 157-165 (2000).
302. A. Montagner *et al.*, A novel role for Gab1 and SHP2 in epidermal growth factor-induced Ras activation. *Journal of Biological Chemistry* **280**, 5350-5360 (2005).
303. A. M. Tari, G. Lopez-Berestein, in *Seminars in oncology*. (Elsevier, 2001), vol. 28, pp. 142-147.
304. N. a. Li *et al.*, Guanine-nucleotide-releasing factor hSos1 binds to Grb2 and links receptor tyrosine kinases to Ras signalling. *Nature* **363**, 85-88 (1993).

305. T.-J. Liao, H. Jang, R. Nussinov, D. Fushman, High-affinity interactions of the nSH3/cSH3 domains of Grb2 with the C-terminal proline-rich domain of SOS1. *Journal of the American Chemical Society* **142**, 3401-3411 (2020).
306. C. B. McDonald, K. L. Seldeen, B. J. Deegan, A. Farooq, Structural basis of the differential binding of the SH3 domains of Grb2 adaptor to the guanine nucleotide exchange factor Sos1. *Archives of biochemistry and biophysics* **479**, 52-62 (2008).
307. C. B. McDonald, K. L. Seldeen, B. J. Deegan, A. Farooq, SH3 domains of Grb2 adaptor bind to PXψPXR motifs within the Sos1 nucleotide exchange factor in a discriminate manner. *Biochemistry* **48**, 4074-4085 (2009).
308. T.-J. Liao, H. Jang, R. Nussinov, D. Fushman, High-affinity Interactions of the nSH3/cSH3 Domains of Grb2 with the C-terminal Proline-rich Domain of SOS1. *Journal of the American Chemical Society*, (2020).
309. C. B. McDonald *et al.*, Structural landscape of the proline-rich domain of Sos1 nucleotide exchange factor. *Biophysical chemistry* **175**, 54-62 (2013).
310. D. Cussac, M. Frech, P. Chardin, Binding of the Grb2 SH2 domain to phosphotyrosine motifs does not change the affinity of its SH3 domains for Sos proline-rich motifs. *The EMBO Journal* **13**, 4011-4021 (1994).
311. M. Tanaka, R. Gupta, B. J. Mayer, Differential inhibition of signaling pathways by dominant-negative SH2/SH3 adapter proteins. *Molecular and cellular biology* **15**, 6829-6837 (1995).
312. A. Beigbeder, F. J. Chartier, N. Bisson, MPZL1 forms a signalling complex with GRB2 adaptor and PTPN11 phosphatase in HER2-positive breast cancer cells. *Scientific reports* **7**, 1-9 (2017).
313. T. Watanabe *et al.*, Significance of the Grb2 and son of sevenless (Sos) proteins in human bladder cancer cell lines. *IUBMB life* **49**, 317-320 (2000).
314. F. Malagrinò, F. Troilo, D. Bonetti, A. Toto, S. Gianni, Mapping the allosteric network within a SH3 domain. *Scientific reports* **9**, 1-6 (2019).
315. S. E. Egan *et al.*, Association of Sos Ras exchange protein with Grb2 is implicated in tyrosine kinase signal transduction and transformation. *Nature* **363**, 45-51 (1993).
316. M. A. Lemmon, J. E. Ladbury, V. Mandiyan, M. Zhou, J. Schlessinger, Independent binding of peptide ligands to the SH2 and SH3 domains of Grb2. *Journal of Biological Chemistry* **269**, 31653-31658 (1994).
317. J. C. Houtman *et al.*, Oligomerization of signaling complexes by the multipoint binding of GRB2 to both LAT and SOS1. *Nature structural & molecular biology* **13**, 798-805 (2006).
318. R. R. Bartelt *et al.*, Regions outside of conserved PxxPxR motifs drive the high affinity interaction of GRB2 with SH3 domain ligands. *Biochimica et Biophysica Acta (BBA)-Molecular Cell Research* **1853**, 2560-2569 (2015).
319. L. Sastry *et al.*, Quantitative analysis of Grb2-Sos1 interaction: the N-terminal SH3 domain of Grb2 mediates affinity. *Oncogene* **11**, 1107-1112 (1995).
320. M. Innocenti *et al.*, Mechanisms through which Sos-1 coordinates the activation of Ras and Rac. *Journal of Cell Biology* **156**, 125-136 (2002).
321. T.-J. Liao, H. Jang, D. Fushman, R. Nussinov, SOS1 interacts with Grb2 through regions that induce closed nSH3 conformations. *The Journal of Chemical Physics* **153**, 045106 (2020).
322. S. Yuzawa *et al.*, Solution structure of Grb2 reveals extensive flexibility necessary for target recognition. *Journal of molecular biology* **306**, 527-537 (2001).
323. A. Sethi, B. Goldstein, S. Gnanakaran, Quantifying intramolecular binding in multivalent interactions: a structure-based synergistic study on Grb2-Sos1 complex. *PLoS Comput. Biol.* **7**, e1002192 (2011).
324. M. Vidal *et al.*, Design of peptoid analogue dimers and measure of their affinity for Grb2 SH3 domains. *Biochemistry* **43**, 7336-7344 (2004).

325. B. Ma, C.-J. Tsai, T. Haliloğlu, R. Nussinov, Dynamic allostery: linkers are not merely flexible. *Structure* **19**, 907-917 (2011).
326. C. Corbi-Verge *et al.*, Two-state dynamics of the SH3–SH2 tandem of Abl kinase and the allosteric role of the N-cap. *Proceedings of the National Academy of Sciences* **110**, E3372-E3380 (2013).
327. Y. Kobashigawa *et al.*, Structural basis for the transforming activity of human cancer-related signaling adaptor protein CRK. *Nature structural & molecular biology* **14**, 503-510 (2007).
328. H. E. Lindfors, B. S. Venkata, J. W. Drijfhout, M. Ubbink, Linker length dependent binding of a focal adhesion kinase derived peptide to the Src SH3–SH2 domains. *FEBS letters* **585**, 601-605 (2011).
329. H. Meiselbach, H. Sticht, Effect of the SH3-SH2 domain linker sequence on the structure of Hck kinase. *Journal of molecular modeling* **17**, 1927-1934 (2011).
330. S. Banjade *et al.*, Conserved interdomain linker promotes phase separation of the multivalent adaptor protein Nck. *Proceedings of the National Academy of Sciences* **112**, E6426-E6435 (2015).
331. T. D. Bunney *et al.*, Structural and functional integration of the PLCγ interaction domains critical for regulatory mechanisms and signaling deregulation. *Structure* **20**, 2062-2075 (2012).
332. S. Maignan *et al.*, Crystal structure of the mammalian Grb2 adaptor. *Science* **268**, 291-293 (1995).
333. Y. Qu *et al.*, SUMOylation of Grb2 enhances the ERK activity by increasing its binding with Sos1. *Molecular cancer* **13**, 1-12 (2014).
334. Z. Ahmed *et al.*, Corrigendum: Grb2 monomer–dimer equilibrium determines normal versus oncogenic function. *Nature communications* **6**, (2015).
335. A. Nag, M. Monine, A. S. Perelson, B. Goldstein, Modeling and simulation of aggregation of membrane protein LAT with molecular variability in the number of binding sites for cytosolic Grb2-SOS1-Grb2. *PLoS One* **7**, e28758 (2012).
336. L. M. Luttrell *et al.*, G-protein-coupled receptors and their regulation: activation of the MAP kinase signaling pathway by G-protein-coupled receptors. *Advances in second messenger and phosphoprotein research* **31**, 263 (1997).
337. C. T. Baldari, J. L. Telford, Lymphocyte antigen receptor signal integration and regulation by the SHC adaptor. *Biological chemistry* **380**, 129-134 (1999).
338. A. Maffe, P. Comoglio, HGF controls branched morphogenesis in tubular glands. *European journal of morphology* **36**, 74-81 (1998).
339. R. Pai, A. Tarnawski, Signal transduction cascades triggered by EGF receptor activation: relevance to gastric injury repair and ulcer healing. *Digestive diseases and sciences* **43**, 14S-22S (1998).
340. K. L. Carraway, C. A. C. Carraway, Signaling, mitogenesis and the cytoskeleton: where the action is. *Bioessays* **17**, 171-175 (1995).
341. B. Margolis, E. Y. Skolnik, Activation of Ras by receptor tyrosine kinases. *Journal of the American Society of Nephrology* **5**, 1288-1299 (1994).
342. Y. M. Chook, G. D. Gish, C. M. Kay, E. F. Pai, T. Pawson, The Grb2-mSos1 complex binds phosphopeptides with higher affinity than Grb2. *Journal of Biological Chemistry* **271**, 30472-30478 (1996).
343. M. J. Welham, V. Duronio, K. B. Leslie, D. Bowtell, J. W. Schrader, Multiple hemopoietins, with the exception of interleukin-4, induce modification of Shc and mSos1, but not their translocation. *Journal of Biological Chemistry* **269**, 21165-21176 (1994).
344. W. Y. Huang, J. A. Ditlev, H.-K. Chiang, M. K. Rosen, J. T. Groves, Allosteric modulation of Grb2 recruitment to the intrinsically disordered scaffold protein, LAT, by remote site phosphorylation. *Journal of the American Chemical Society* **139**, 18009-18015 (2017).

345. Y. K. Lee *et al.*, Mechanism of SOS PR-domain autoinhibition revealed by single-molecule assays on native protein from lysate. *Nature communications* **8**, 1-11 (2017).
346. J. Gureasko *et al.*, Membrane-dependent signal integration by the Ras activator Son of sevenless. *Nature structural & molecular biology* **15**, 452 (2008).
347. L. Iversen *et al.*, Ras activation by SOS: Allosteric regulation by altered fluctuation dynamics. *Science* **345**, 50-54 (2014).
348. M.-J. Park *et al.*, SH2 domains serve as lipid-binding modules for pTyr-signaling proteins. *Molecular cell* **62**, 7-20 (2016).
349. E. Amin *et al.*, Deciphering the molecular and functional Basis of RHOGAP family proteins A systematic approach toward selective inactivation of rho family proteINS. *Journal of Biological Chemistry* **291**, 20353-20371 (2016).
350. T. Wiseman, S. Williston, J. F. Brandts, L.-N. Lin, Rapid measurement of binding constants and heats of binding using a new titration calorimeter. *Analytical biochemistry* **179**, 131-137 (1989).
351. M. G. Rudolph *et al.*, Thermodynamics of Ras/effector and Cdc42/effector interactions probed by isothermal titration calorimetry. *Journal of Biological Chemistry* **276**, 23914-23921 (2001).
352. N. N. Fang *et al.*, Rsp5/Nedd4 is the main ubiquitin ligase that targets cytosolic misfolded proteins following heat stress. *Nature cell biology* **16**, 1227-1237 (2014).
353. L. Peil *et al.*, Distinct XPPX sequence motifs induce ribosome stalling, which is rescued by the translation elongation factor EF-P. *Proceedings of the National Academy of Sciences* **110**, 15265-15270 (2013).
354. T. R. Hupp, M. Walkinshaw, Multienzyme assembly of a p53 transcription complex. *Nature structural & molecular biology* **14**, 885-887 (2007).
355. D. Dornan, H. Shimizu, L. Burch, A. J. Smith, T. R. Hupp, The proline repeat domain of p53 binds directly to the transcriptional coactivator p300 and allosterically controls DNA-dependent acetylation of p53. *Molecular and cellular biology* **23**, 8846-8861 (2003).
356. L. Guruprasad *et al.*, The crystal structure of the N-terminal SH3 domain of Grb2. *Journal of molecular biology* **248**, 856-866 (1995).
357. O. Aitio *et al.*, Structural basis of PxxDY motif recognition in SH3 binding. *Journal of molecular biology* **382**, 167-178 (2008).
358. H. Yu *et al.*, Structural basis for the binding of proline-rich peptides to SH3 domains. *Cell* **76**, 933-945 (1994).
359. S.-H. Tan, W. Hugo, W.-K. Sung, S.-K. Ng, A correlated motif approach for finding short linear motifs from protein interaction networks. *BMC bioinformatics* **7**, 502 (2006).
360. K. Rader, R. A. Orlando, X. Lou, M. G. Farquhar, Characterization of ANKRA, a novel ankyrin repeat protein that interacts with the cytoplasmic domain of megalin. *Journal of the American Society of Nephrology* **11**, 2167-2178 (2000).
361. R. P. Menon, R. C. Hughes, Determinants in the N-terminal domains of galectin-3 for secretion by a novel pathway circumventing the endoplasmic reticulum–Golgi complex. *European journal of biochemistry* **264**, 569-576 (1999).
362. P. Beltrao, L. Serrano, Comparative genomics and disorder prediction identify biologically relevant SH3 protein interactions. *PLoS computational biology* **1**, (2005).
363. K. Kowanetz *et al.*, CIN85 associates with multiple effectors controlling intracellular trafficking of epidermal growth factor receptors. *Molecular biology of the cell* **15**, 3155-3166 (2004).
364. A. D'erchia, G. Pesole, A. Tullo, C. Saccone, E. Sbisa, Guinea pig p53 mRNA: identification of new elements in coding and untranslated regions and their functional and evolutionary implications. *Genomics* **58**, 50-64 (1999).
365. B. J. Mayer, M. Hamaguchi, H. Hanafusa, A novel viral oncogene with structural similarity to phospholipase C. *Nature* **332**, 272 (1988).

366. M. L. Stahl, C. R. Ferenz, K. L. Kelleher, R. W. Kriz, J. L. Knopf, Sequence similarity of phospholipase C with the non-catalytic region of src. *Nature* **332**, 269-272 (1988).
367. B. J. Mayer, The discovery of modular binding domains: building blocks of cell signalling. *Nature reviews Molecular cell biology* **16**, 691-698 (2015).
368. L. B. Case, X. Zhang, J. A. Ditlev, M. K. Rosen, Stoichiometry controls activity of phase-separated clusters of actin signaling proteins. *Science* **363**, 1093-1097 (2019).
369. W. Y. Huang *et al.*, A molecular assembly phase transition and kinetic proofreading modulate Ras activation by SOS. *Science* **363**, 1098-1103 (2019).
370. B. J. Mayer, SH3 domains: complexity in moderation. *Journal of cell science* **114**, 1253-1263 (2001).
371. T. Kaneko, L. Li, S. Li, The SH3 domain–a family of versatile peptide-and protein-recognition module. *Front Biosci* **13**, 4938-4952 (2008).
372. B. K. Kay, SH3 domains come of age. *FEBS letters* **586**, 2606-2608 (2012).
373. B. Lucas, J. Hardin, Mind the (sr) GAP–roles of Slit–Robo GAPs in neurons, brains and beyond. *Journal of Cell Science* **130**, 3965-3974 (2017).
374. S. Richard, in *Post-Transcriptional Regulation by STAR Proteins*. (Springer, 2010), pp. 142-157.
375. R. Roskoski, Michaelis-Menten Kinetics. (2015).
376. G. A. Weisman *et al.*, Molecular determinants of P2Y 2 nucleotide receptor function. *Molecular neurobiology* **31**, 169-183 (2005).
377. X. R. Bustelo, Vav family exchange factors: an integrated regulatory and functional view. *Small GTPases* **5**, e973757 (2014).
378. P. N. Alexandrov, Y. Zhao, V. Jaber, L. Cong, W. J. Lukiw, Deficits in the proline-rich synapse-associated Shank3 protein in multiple neuropsychiatric disorders. *Frontiers in neurology* **8**, 670 (2017).
379. K. Saksela, Interactions of the HIV/SIV pathogenicity factor Nef with SH3 domain-containing host cell proteins. *Current HIV research* **9**, 531-542 (2011).
380. M. R. Holt, A. Koffer, Cell motility: proline-rich proteins promote protrusions. *Trends in cell biology* **11**, 38-46 (2001).
381. A. Zarrinpar, R. P. Bhattacharyya, W. A. Lim, The structure and function of proline recognition domains. *Science's STKE* **2003**, re8-re8 (2003).
382. S. S.-C. Li, Specificity and versatility of SH3 and other proline-recognition domains: structural basis and implications for cellular signal transduction. *Biochemical Journal* **390**, 641-653 (2005).
383. A. Zafra-Ruano, I. Luque, Interfacial water molecules in SH3 interactions: Getting the full picture on polyproline recognition by protein–protein interaction domains. *FEBS letters* **586**, 2619-2630 (2012).
384. G. Cesareni, S. Panni, G. Nardelli, L. Castagnoli, Can we infer peptide recognition specificity mediated by SH3 domains? *FEBS letters* **513**, 38-44 (2002).
385. H. Kang *et al.*, SH3 domain recognition of a proline-independent tyrosine-based RKxxYxxY motif in immune cell adaptor SKAP55. *The EMBO Journal* **19**, 2889-2899 (2000).
386. A. Musacchio, M. Noble, R. Pauptit, R. Wierenga, M. Saraste, Crystal structure of a Src-homology 3 (SH3) domain. *Nature* **359**, 851-855 (1992).
387. J. Teyra *et al.*, Comprehensive analysis of the human SH3 domain family reveals a wide variety of non-canonical specificities. *Structure* **25**, 1598-1610. e1593 (2017).
388. S. M. Feller, M. Lewitzky, Potential disease targets for drugs that disrupt protein-protein interactions of Grb2 and Crk family adaptors. *Current pharmaceutical design* **12**, 529-548 (2006).
389. J. Bliska, How pathogens expolit interactions mediated by SH3 domains. *Chemistry & biology* **3**, 7-11 (1996).

390. B. Ravi Chandra, R. Gowthaman, R. Raj Akhouri, D. Gupta, A. Sharma, Distribution of proline-rich (PxxP) motifs in distinct proteomes: functional and therapeutic implications for malaria and tuberculosis. *Protein Engineering Design and Selection* **17**, 175-182 (2004).
391. Z. Hanna *et al.*, The pathogenicity of human immunodeficiency virus (HIV) type 1 Nef in CD4C/HIV transgenic mice is abolished by mutation of its SH3-binding domain, and disease development is delayed in the absence of Hck. *Journal of virology* **75**, 9378-9392 (2001).
392. J. A. Moroco *et al.*, Remodeling of HIV-1 nef structure by Src-Family kinase binding. *Journal of molecular biology* **430**, 310-321 (2018).
393. M. Carducci, L. Licata, D. Peluso, L. Castagnoli, G. Cesareni, Enriching the viral–host interactomes with interactions mediated by SH3 domains. *Amino acids* **38**, 1541-1547 (2010).
394. S. R. Inglis *et al.*, Identification and specificity studies of small-molecule ligands for SH3 protein domains. *Journal of medicinal chemistry* **47**, 5405-5417 (2004).
395. M. Vidal, V. Gigoux, C. Garbay, SH2 and SH3 domains as targets for anti-proliferative agents. *Critical reviews in oncology/hematology* **40**, 175-186 (2001).
396. C. Landgraf *et al.*, Protein interaction networks by proteome peptide scanning. *PLoS Biol* **2**, e14 (2004).
397. R. J. Ingham, M. Holgado-Madruga, C. Siu, A. J. Wong, M. R. Gold, The Gab1 protein is a docking site for multiple proteins involved in signaling by the B cell antigen receptor. *Journal of Biological Chemistry* **273**, 30630-30637 (1998).
398. A. Pechstein *et al.*, Vesicle Clustering in a Living Synapse Depends on a Synapsin Region that Mediates Phase Separation. *Cell Reports* **30**, 2594-2602. e2593 (2020).
399. A. Ghosh, K. Mazarakos, H.-X. Zhou, Three archetypical classes of macromolecular regulators of protein liquid–liquid phase separation. *Proceedings of the National Academy of Sciences* **116**, 19474-19483 (2019).
400. C. W. Pak *et al.*, Sequence determinants of intracellular phase separation by complex coacervation of a disordered protein. *Molecular cell* **63**, 72-85 (2016).
401. A. Russo, J. P. O'Bryan, Intersectin 1 is required for neuroblastoma tumorigenesis. *Oncogene* **31**, 4828-4834 (2012).
402. H. Ishida, A. Skorobogatov, A. P. Yamniuk, H. J. Vogel, Solution structures of the SH3 domains from Shank scaffold proteins and their interactions with Cav1. 3 calcium channels. *Febs Letters* **592**, 2786-2797 (2018).
403. P. Zhang *et al.*, SH3RF3 promotes breast cancer stem-like properties via JNK activation and PTX3 upregulation. *Nature communications* **11**, 1-13 (2020).
404. J. J. Kwan, L. W. Donaldson, A lack of peptide binding and decreased thermostability suggests that the CASKIN2 scaffolding protein SH3 domain may be vestigial. *BMC structural biology* **16**, 1-6 (2016).
405. J. Zhu *et al.*, Guanylate kinase domains of the MAGUK family scaffold proteins as specific phospho-protein-binding modules. *The EMBO journal* **30**, 4986-4997 (2011).
406. S. Estrach *et al.*, The Human Rho-GEF trio and its target GTPase RhoG are involved in the NGF pathway, leading to neurite outgrowth. *Current biology* **12**, 307-312 (2002).
407. A. C. Humphries, S. K. Donnelly, M. Way, Cdc42 and the Rho GEF intersectin-1 collaborate with Nck to promote N-WASP-dependent actin polymerisation. *Journal of cell science* **127**, 673-685 (2014).
408. H. Okada *et al.*, Sh3 domain–based phototrapping in living cells reveals rho family gap signaling complexes. *Science signaling* **4**, rs13-rs13 (2011).
409. R. B. Birge, B. S. Knudsen, D. Besser, H. Hanafusa, SH2 and SH3-containing adaptor proteins: redundant or independent mediators of intracellular signal transduction. *Genes to Cells* **1**, 595-613 (1996).

410. J. M. Roberts *et al.*, Dynamics of the T ec-family tyrosine kinase SH 3 domains. *Protein Science* **25**, 852-864 (2016).
411. N. M. Levinson, P. R. Visperas, J. Kuriyan, The tyrosine kinase Csk dimerizes through Its SH3 domain. *PloS one* **4**, e7683 (2009).
412. M. T. Brown, J. A. Cooper, Regulation, substrates and functions of src. *Biochimica et Biophysica Acta (BBA)-Reviews on Cancer* **1287**, 121-149 (1996).
413. J. Zhu, S. K. Shore, c-ABL tyrosine kinase activity is regulated by association with a novel SH3-domain-binding protein. *Molecular and cellular biology* **16**, 7054-7062 (1996).
414. M. A. Salazar *et al.*, Tuba, a novel protein containing bin/amphiphysin/Rvs and Dbl homology domains, links dynamin to regulation of the actin cytoskeleton. *Journal of Biological Chemistry* **278**, 49031-49043 (2003).
415. Y. Oda, T. Otani, J. Ikenouchi, M. Furuse, Tricellulin regulates junctional tension of epithelial cells at tricellular contacts through Cdc42. *Journal of cell science* **127**, 4201-4212 (2014).
416. P. Young, E. Ehler, M. Gautel, Obscurin, a giant sarcomeric Rho guanine nucleotide exchange factor protein involved in sarcomere assembly. *The Journal of cell biology* **154**, 123-136 (2001).
417. L. C. Pubblicazioni, Tinti M, Kiemer L, Costa S, Miller ML, Sacco F, Olsen JV, Carducci M, Paoluzi S, Langone F, Workman CT, Blom N, Machida K. *Mol Syst Biol* **8**, 22893001 (2012).
418. R. Stoll, A. Bosserhoff, Extracellular SH3 domain containing proteins-features of a new protein family. *Current Protein and Peptide Science* **9**, 221-226 (2008).
419. P.-D. Fan, S. P. Goff, Abl interactor 1 binds to sos and inhibits epidermal growth factor-and v-Abl-induced activation of extracellular signal-regulated kinases. *Molecular and cellular biology* **20**, 7591-7601 (2000).
420. X. K. Tong *et al.*, The endocytic protein intersectin is a major binding partner for the Ras exchange factor mSos1 in rat brain. *The EMBO journal* **19**, 1263-1271 (2000).
421. X. Qian *et al.*, The Sos1 and Sos2 Ras-specific exchange factors: differences in placental expression and signaling properties. *The EMBO journal* **19**, 642-654 (2000).
422. Q. Hu, D. Milfay, L. T. Williams, Binding of NCK to SOS and activation of ras-dependent gene expression. *Molecular and Cellular Biology* **15**, 1169-1174 (1995).
423. P. Chardin *et al.*, Human Sos1: a guanine nucleotide exchange factor for Ras that binds to GRB2. *Science* **260**, 1338-1343 (1993).
424. J. T. Nguyen, C. W. Turck, F. E. Cohen, R. N. Zuckermann, W. A. Lim, Exploiting the basis of proline recognition by SH3 and WW domains: design of N-substituted inhibitors. *Science* **282**, 2088-2092 (1998).
425. A. Douangamath *et al.*, Topography for independent binding of α-helical and PPII-helical ligands to a peroxisomal SH3 domain. *Molecular cell* **10**, 1007-1017 (2002).
426. S. Hahn, D. Kim, Transient protein-protein interaction of the SH3-peptide complex via closely located multiple binding sites. *PLoS One* **7**, e32804 (2012).
427. M. Hiipakka, K. Poikonen, K. Saksela, SH3 domains with high affinity and engineered ligand specificities targeted to HIV-1 Nef. *Journal of molecular biology* **293**, 1097-1106 (1999).
428. F. Evanics, J. L. Kitevski, I. Bezsonova, J. Forman-Kay, R. S. Prosser, 19F NMR studies of solvent exposure and peptide binding to an SH3 domain. *Biochimica et Biophysica Acta (BBA)-General Subjects* **1770**, 221-230 (2007).
429. M. Ahmad, W. Gu, V. Helms, Mechanism of fast peptide recognition by SH3 domains. *Angewandte Chemie International Edition* **47**, 7626-7630 (2008).
430. B. J. Mayer, K. Saksela, SH3 domains. *Protein Science Encyclopedia: online*, (2008).
431. J. E. Ladbury, S. Arold, Searching for specificity in SH domains. *Chemistry & biology* **7**, R3-R8 (2000).

432. B. K. Kay, M. P. Williamson, M. Sudol, The importance of being proline: the interaction of proline-rich motifs in signaling proteins with their cognate domains. *The FASEB journal* **14**, 231-241 (2000).
433. A. B. Sparks *et al.*, Distinct ligand preferences of Src homology 3 domains from Src, Yes, Abl, cortactin, p53bp2, PLCgamma, Crk, and Grb2. *Proceedings of the National Academy of Sciences* **93**, 1540-1544 (1996).
434. A. Zarrinpar, S.-H. Park, W. A. Lim, Optimization of specificity in a cellular protein interaction network by negative selection. *Nature* **426**, 676-680 (2003).
435. E. Verschueren *et al.*, Evolution of the SH3 domain specificity Landscape in Yeasts. *PLoS One* **10**, e0129229 (2015).
436. S. Balakrishnan, M. J. Scheuermann, N. J. Zondlo, Arginine Mimetics via α-Guanidino Acids: Introduction of Functional Groups and Stereochemistry Adjacent to Recognition Guanidiniums in Peptides. *Chembiochem: a European journal of chemical biology* **13**, 259 (2012).
437. M. Jaiswal *et al.*, Functional cross-talk between ras and rho pathways: a Ras-specific GTPase-activating protein (p120RasGAP) competitively inhibits the RhoGAP activity of deleted in liver cancer (DLC) tumor suppressor by masking the catalytic arginine finger. *Journal of Biological Chemistry* **289**, 6839-6849 (2014).
438. L. M. Stevers, P. J. De Vink, C. Ottmann, J. Huskens, L. Brunsveld, A thermodynamic model for multivalency in 14-3-3 protein–protein interactions. *Journal of the American Chemical Society* **140**, 14498-14510 (2018).
439. M. Vidal *et al.*, Molecular and cellular analysis of Grb2 SH3 domain mutants: interaction with Sos and dynamin. *Journal of molecular biology* **290**, 717-730 (1999).
440. K. Hanawa-Suetsugu *et al.*, Structural basis for mutual relief of the Rac guanine nucleotide exchange factor DOCK2 and its partner ELMO1 from their autoinhibited forms. *Proceedings of the National Academy of Sciences* **109**, 3305-3310 (2012).
441. K. Kami, R. Takeya, H. Sumimoto, D. Kohda, Diverse recognition of non-PxxP peptide ligands by the SH3 domains from p67phox, Grb2 and Pex13p. *The EMBO journal* **21**, 4268-4276 (2002).
442. C. Massenet *et al.*, Effects of p47phox C terminus phosphorylations on binding interactions with p40phox and p67phox: structural and functional comparison of p40phox and p67phox SH3 domains. *Journal of Biological Chemistry* **280**, 13752-13761 (2005).
443. H. R. Mott, D. Nietlispach, K. A. Evetts, D. Owen, Structural analysis of the SH3 domain of β-PIX and its interaction with α-p21 activated kinase (PAK). *Biochemistry* **44**, 10977-10983 (2005).
444. D. Jozic *et al.*, Cbl promotes clustering of endocytic adaptor proteins. *Nature structural & molecular biology* **12**, 972-979 (2005).
445. S. Hashimoto *et al.*, Targeting AMAP1 and cortactin binding bearing an atypical src homology 3/proline interface for prevention of breast cancer invasion and metastasis. *Proceedings of the National Academy of Sciences* **103**, 7036-7041 (2006).
446. G. Moncalián *et al.*, Atypical polyproline recognition by the CMS N-terminal Src homology 3 domain. *Journal of Biological Chemistry* **281**, 38845-38853 (2006).
447. K. Takeuchi *et al.*, Structural and functional evidence that Nck interaction with CD3ε regulates T-cell receptor activity. *Journal of molecular biology* **380**, 704-716 (2008).
448. O. Aitio *et al.*, Recognition of tandem PxxP motifs as a unique Src homology 3-binding mode triggers pathogen-driven actin assembly. *Proceedings of the National Academy of Sciences* **107**, 21743-21748 (2010).
449. K. Gehmlich *et al.*, Paxillin and ponsin interact in nascent costameres of muscle cells. *Journal of molecular biology* **369**, 665-682 (2007).
450. H. Schmidt *et al.*, Solution structure of a Hck SH3 domain ligand complex reveals novel interaction modes. *Journal of molecular biology* **365**, 1517-1532 (2007).

451. J. M. Janz, T. P. Sakmar, K. C. Min, A novel interaction between atrophin-interacting protein 4 and β-p21-activated kinase-interactive exchange factor is mediated by an SH3 domain. *Journal of Biological Chemistry* **282**, 28893-28903 (2007).
452. S. Guettler *et al.*, Structural basis and sequence rules for substrate recognition by Tankyrase explain the basis for cherubism disease. *Cell* **147**, 1340-1354 (2011).
453. E. Rouka *et al.*, Differential recognition preferences of the three Src homology 3 (SH3) domains from the adaptor CD2-associated protein (CD2AP) and direct association with Ras and Rab interactor 3 (RIN3). *Journal of Biological Chemistry* **290**, 25275-25292 (2015).
454. L. Polle, L. A. Rigano, R. Julian, K. Ireton, W.-D. Schubert, Structural details of human tuba recruitment by InlC of Listeria monocytogenes elucidate bacterial cell-cell spreading. *Structure* **22**, 304-314 (2014).
455. Q. Chen, M. Georgiadis, Crystallization of and selenomethionine phasing strategy for a SETMAR–DNA complex. *Acta Crystallographica Section F: Structural Biology Communications* **72**, 713-719 (2016).
456. S. Eulitz *et al.*, Identification of Xin-repeat proteins as novel ligands of the SH3 domains of nebulin and nebulette and analysis of their interaction during myofibril formation and remodeling. *Molecular biology of the cell* **24**, 3215-3226 (2013).
457. D. Zhao *et al.*, Structural investigation of the interaction between the tandem SH3 domains of c-Cbl-associated protein and vinculin. *Journal of structural biology* **187**, 194-205 (2014).
458. A. Camara-Artigas, E. Ortiz-Salmeron, M. Andujar-Sánchez, J. Bacarizo, J. M. Martin-Garcia, The role of water molecules in the binding of class I and II peptides to the SH3 domain of the Fyn tyrosine kinase. *Acta Crystallographica Section F: Structural Biology Communications* **72**, 707-712 (2016).
459. A. Shimada, A. Yamaguchi, D. Kohda, Structural basis for the recognition of two consecutive mutually interacting DPF motifs by the SGIP1 μ homology domain. *Scientific reports* **6**, 1-14 (2016).
460. V. S. Bhatt, D. Zeng, I. Krieger, J. C. Sacchettini, J.-H. Cho, Binding mechanism of the N-terminal SH3 domain of CrkII and proline-rich motifs in cAbl. *Biophysical journal* **110**, 2630-2641 (2016).
461. M. Hologne *et al.*, NMR reveals the interplay among the AMSH SH3 binding motif, STAM2, and Lys63-linked diubiquitin. *Journal of molecular biology* **428**, 4544-4558 (2016).
462. G. Desrochers *et al.*, Molecular basis of interactions between SH3 domain-containing proteins and the proline-rich region of the ubiquitin ligase Itch. *Journal of Biological Chemistry* **292**, 6325-6338 (2017).
463. L. Sastry *et al.*, Quantitative analysis of Grb2-Sos1 interaction: the N-terminal SH3 domain of Grb2 mediates affinity. *Oncogene* **11**, 1107-1112 (1995).
464. I. A. Prior, F. E. Hood, J. L. Hartley, The frequency of Ras mutations in cancer. *Cancer Research*, (2020).
465. A. Arrazola Sastre *et al.*, Small GTPases of the Ras and Rho families switch on/off signaling pathways in neurodegenerative diseases. *International Journal of Molecular Sciences* **21**, 6312 (2020).
466. K. R. Chien, M. Hoshijima, Unravelling Ras signals in cardiovascular disease. *Nature cell biology* **6**, 807-808 (2004).
467. L. Santarpia, S. M. Lippman, A. K. El-Naggar, Targeting the MAPK–RAS–RAF signaling pathway in cancer therapy. *Expert opinion on therapeutic targets* **16**, 103-119 (2012).
468. P. Bernado, D. I. Svergun, Structural analysis of intrinsically disordered proteins by small-angle X-ray scattering. *Molecular biosystems* **8**, 151-167 (2012).
469. S. Gutierrez-Erlandsson *et al.*, R-RAS2 overexpression in tumors of the human central nervous system. *Molecular cancer* **12**, 1-12 (2013).

470. S. Nakhaei-Rad *et al.*, The role of embryonic stem cell-expressed RAS (ERAS) in the maintenance of quiescent hepatic stellate cells. *Journal of Biological Chemistry* **291**, 8399-8413 (2016).
471. E. Castellano, J. Downward, Role of RAS in the regulation of PI 3-kinase. *Phosphoinositide 3-kinase in Health and Disease*, 143-169 (2010).
472. G. Pfeifer, R. Dammann, Methylation of the tumor suppressor gene RASSF1A in human tumors. *Biochemistry (Moscow)* **70**, 576-583 (2005).
473. J. Park *et al.*, Tumor suppressor ras association domain family 5 (RASSF5/NORE1) mediates death receptor ligand-induced apoptosis. *Journal of Biological Chemistry* **285**, 35029-35038 (2010).
474. J. R. Molina, A. A. Adjei, The ras/raf/mapk pathway. *Journal of Thoracic Oncology* **1**, 7-9 (2006).
475. A. A. Jorge, A. C. Malaquias, I. J. Arnhold, B. B. Mendonca, Noonan syndrome and related disorders: a review of clinical features and mutations in genes of the RAS/MAPK pathway. *Hormone Research in Paediatrics* **71**, 185-193 (2009).
476. G. Binder, Noonan syndrome, the Ras–MAPK signalling pathway and short stature. *Hormone Research in Paediatrics* **71**, 64-70 (2009).
477. Y. Capri *et al.*, Activating mutations of RRAS2 are a rare cause of Noonan syndrome. *The American Journal of Human Genetics* **104**, 1223-1232 (2019).
478. T. Niihori *et al.*, Germline-activating RRAS2 mutations cause Noonan syndrome. *The American Journal of Human Genetics* **104**, 1233-1240 (2019).
479. S. M. Graham *et al.*, Aberrant function of the Ras-related protein TC21/R-Ras2 triggers malignant transformation. *Molecular and Cellular Biology* **14**, 4108-4115 (1994).
480. R. Nussinov *et al.*, Autoinhibition in Ras effectors Raf, PI3Kα, and RASSF5: a comprehensive review underscoring the challenges in pharmacological intervention. *Biophysical reviews* **10**, 1263-1282 (2018).
481. R. S. Bon, H. Waldmann, Bioactivity-guided navigation of chemical space. *Accounts of chemical research* **43**, 1103-1114 (2010).
482. S. Wetzel, R. S. Bon, K. Kumar, H. Waldmann, Biology-oriented synthesis. *Angewandte Chemie International Edition* **50**, 10800-10826 (2011).
483. B. Over *et al.*, Natural-product-derived fragments for fragment-based ligand discovery. *Nature chemistry* **5**, 21-28 (2013).
484. D. R. Cook, K. L. Rossman, C. J. Der, Rho guanine nucleotide exchange factors: regulators of Rho GTPase activity in development and disease. *Oncogene* **33**, 4021-4035 (2014).
485. R. Teperino, F. Aberger, H. Esterbauer, N. Riobo, J. A. Pospisilik, in *Seminars in cell & developmental biology*. (Elsevier, 2014), vol. 33, pp. 81-92.
486. D. J. Robbins, D. L. Fei, N. A. Riobo, The Hedgehog signal transduction network. *Science signaling* **5**, re6-re6 (2012).
487. H. E. Pelish *et al.*, Secramine inhibits Cdc42-dependent functions in cells and Cdc42 activation in vitro. *Nature chemical biology* **2**, 39-46 (2006).
488. R. G. Hodge, A. J. Ridley, Regulating Rho GTPases and their regulators. *Nature reviews Molecular cell biology* **17**, 496 (2016).
489. R. Garcia-Mata, E. Boulter, K. Burridge, The'invisible hand': regulation of RHO GTPases by RHOGDIs. *Nature reviews Molecular cell biology* **12**, 493-504 (2011).
490. M. Mirvis, T. Stearns, W. James Nelson, Cilium structure, assembly, and disassembly regulated by the cytoskeleton. *Biochemical Journal* **475**, 2329-2353 (2018).
491. T. Maurin, S. Zongaro, B. Bardoni, Fragile X syndrome: from molecular pathology to therapy. *Neuroscience & Biobehavioral Reviews* **46**, 242-255 (2014).
492. I. Ferder *et al.*, Expression of fragile X mental retardation protein and Fmr1 mRNA during folliculogenesis in the rat. *Reproduction* **145**, 335-343 (2013).

493. H. Tian *et al.*, The targeting and functions of miRNA-383 are mediated by FMRP during spermatogenesis. *Cell death & disease* **4**, e617-e617 (2013).
494. S. M. Novak, A. Joardar, C. C. Gregorio, D. C. Zarnescu, Regulation of heart rate in drosophila via fragile X mental retardation protein. *PLoS One* **10**, e0142836 (2015).
495. X. Zhao, Y. Wang, C. Meng, N. Fang, FMRP regulates endothelial cell proliferation and angiogenesis via the miR-181a-CaM-CaMKII pathway. *Cell biology international* **42**, 1432-1444 (2018).
496. M. Ascano *et al.*, FMRP targets distinct mRNA sequence elements to regulate protein expression. *Nature* **492**, 382-386 (2012).
497. V. Brown *et al.*, Microarray identification of FMRP-associated brain mRNAs and altered mRNA translational profiles in fragile X syndrome. *Cell* **107**, 477-487 (2001).
498. J. C. Darnell, E. Klann, The translation of translational control by FMRP: therapeutic targets for FXS. *Nature neuroscience* **16**, 1530-1536 (2013).
499. J. C. Darnell *et al.*, FMRP stalls ribosomal translocation on mRNAs linked to synaptic function and autism. *Cell* **146**, 247-261 (2011).

Acknowledgments

Firstly, I would like to express my sincere gratitude to my advisor Prof. Reza ahmadian who accepted me to join his research group and for the continuous support of my Ph.D. study and related research, for his patience, motivation, and immense knowledge. His guidances helped me in all the time of research and writing of this thesis. I could not have imagined having a better advisor and mentor for my PhD study.

In addition, I would like to thank the rest of my co-supervisor Prof. Georg Groth, and Prof. Jürgen Scheller and Dr. Roland Piekorz from the Institute of Biochemistry and Molecular Biology II for their insightful comments and encouragement, but also for the hard question in seminars and workshops, which invented me to widen my research from various perspectives.

My sincere thanks also go to Dr. Radovan Dvorsky who provided me the opportunity to learn bioinformatics. Without his precious support, it would not be possible to conduct this research.

My sincere thanks go to the European Commission (ERARE) and Bundesministerium für Bildung und Forschung (BMBF) for generous sponsoring of this thesis.

I would like to thank my parents and sisters for allowing me to realize my own potential. Also, I need to thank especially my sister Dr. Vida Kazemein Jasemi, who taught me the value of hard work and an education. All the supports she has provided me over the years were the greatest gift anyone has ever given me. Without her support, I may never have gotten to where I am today.

CURRICULUM VITEA

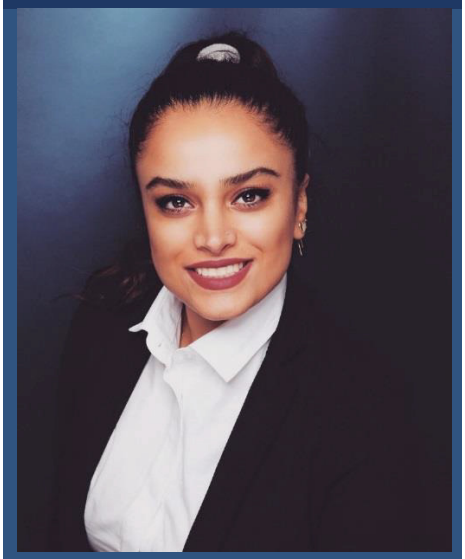

Neda Sadat Kazemein Jasemi
PhD, Biochemistry

Personal data

Date of birth:
November 26st 1990
Place of birth:
Kermanshah/Iran

Address

Düsseldorf Germany

Contact

Email: Kazemein@hhu.de

Language

Persian: Native
German: Intermediate
English: Fluent

RESEARCH INTERESTS

- Structural and dynamic properties of protein-protein interactions
- Phase separation, protein macromolecular clustering and networks
- Cell-based protein interaction network analysis
- The effects of misfolding and subsequent aggregation of proteins in for example neurodegenerative diseases
- Identification and validation of disease-relevant, native protein complexes

ACADEMIC EDUCATION

2017- 2021 **Dr. rer. nat. in Biochemistry**
Ahmadian Lab, Heinrich Heine University, Düsseldorf, Germany. Title: Understanding of the mechanism of SOS1 interactions and activation towards RAS GTPases.

2014 - 2016 **MSc in Biochemistry** Riazi Lab, Institute of Biochemistry and Biophysics (IBB), University of Tehran, Iran. Title: Design of Nano catalyst based on Zinc metal in micellar environment

2011- 2014 **BSc in Biology**
Razi University, Kermanshah, Iran

SKILLS

Biotechnology

- Recombinant gene expression using *Escherichia coli* and Baculovirus/insect cell systems
- Large-scale protein purification (ÄKTA systems)

Bioanalytics

- Unbiased, detergent-free cell fractionation
- Isolation and identification of native protein complexes
- Chromatographic techniques, *e.g.*, analytical size exclusion chromatography (Superdex 75/200, Superose 6)
- Ligand analysis *via* reversed-face HPLC
- Blue native-PAGE of native protein complexes up to 6 mDa

Biophysical Techniques

- Fluorescence-based Stopped-flow technique
- Fluorescent polarization
- Isothermal titration calorimetry
- Surface plasmon resonance (Biacore)

Liposomology

- *In vitro* liposome reconstitution (classical sonication and extruder methods, using synthetic lipids and monitoring of liposome-protein interaction)

Molecular and Cellular Biology

- Culturing various eukaryotic cell lines (*e.g.*, NIH 3T3, SK-BR-3, COS-7 and HEK-293)
- DNA recombination techniques (PCR, site-directed mutagenesis, sub-cloning, RNA/DNA isolation)
- Quantitative real-time-PCR
- Confocal laser scanning microscopy

Protein Biochemical Analysis

- Pull down assay
- Immunoprecipitation
- Immunoblotting (LI-COR Odyssey Infrared Imaging System)

Bioinformatics Software

- SnapGene
- CorelDraw
- EndNote
- GraFit
- Bioedit
- PyMol
- Image Studio

Conferences

- Annual Satellite meeting, Erlangen (2016)
- First SGSH annual symposium (2017)

Awards

- The 3th score in overall entrance exam of M.Sc. programs in Biochemistry of over 7000 applicants in the Iranian national exam (2013)
- The 3rd score in biochemistry department, University of Tehran, Iran (2014-2015)

PUBLICATIONS

Published

- Asadollahi K, **Kazemein Jasemi NS**, Riazi GH, Hedayati Katuli F, Yazdani F, Sartipnia N, Moosavi MA, Rahimie A, Falahati M. A bio-mimetic zinc/tau protein as an artificial catalase. *Int j biolmacromol* (2016):1307-1312.

- Nakhaei-Rad S, Highlight F, Nouri P, Rezaei Adariani S, Lissy J, **Kazemein Jasemi NS**, Dvorsky R, Ahmadian MR. Structural fingerprints, interactions, and signaling networks of RAS family proteins beyond RAS isoforms. *Crit Rev Biochem Mol Biol.* (2018): 130-156.

- Capri Y, Flex E, Krumbach OHF, Carpentieri G, Cecchetti S, Lißewski C, Rezaei Adariani S, Schanze D, Brinkmann J, Piard J, Pantaleoni F, Lepri FR, Goh ES, Chong K, Stieglitz E, Meyer J, Kuechler A, Bramswig NC, Sacharow S, Strullu M, Vial Y, Vignal C, Kensah G, Cuturilo G, **Kazemein Jasemi NS**, Dvorsky R, Monaghan KG, Vincent LM, Cavé H, Verloes A, Ahmadian MR, Tartaglia M, Zenker M. Activating mutations of RRAS2 are a rare cause of Noonan syndrome. *Am J Hum Genet*. (2019): 1223-1232.

- Taha MS, Haghighi F, Stefanski A, Nakhaei-Rad S, **Kazemein Jasemi NS**, Al Kabbani MA, Görg B, Fujii M, Lang PA, Häussinger D, Piekorz RP, Stühler K, Ahmadian MR. Novel FMRP interaction networks linked to cellular stress. *FEBS J* (2020): 837-860.

- Rezaei S*, **Kazemein Jasemi NS***, Wittig C**,** Bazgir F, Amin E, Seidel CAM, Dvorsky R, Ahmadian MR. The selectivity of RAS-RASSF protein interactions. *J Biol Chem* (accepted).

- Pudewell S, Wittig C, **Kazemein Jasemi NS,** Bazgir F, Ahmadian MR. Accessory proteins of the RAS/MAPK pathway. *Nat rev mol cell biol* (accepted).

Submitted/under revision

- **Kazemein Jasemi NS**, Dvorsky R, Estirado EM, Brunsveld L, Ahmadian MR. The intramolecular allostery of GRB2 governing its interaction with SOS1 is modulated by phosphotyrosine ligand. *Proc Natl Acad Sci U S A* (under revision).

- Patil S, Shang E, Narayan R, Akbarzadeh M, **Kazemein Jasemi NS**, Buchholzer M, Potowski M, Karatas H, Karageorgis G, Marten C, Golz C, Strohmann C, Antonchick AP, Janning P, Goody RS, Ahmadian MR, Ziegler S, Waldmann H. The Pseudo Natural Product Rhonin Targets RHOGDI1. *Nat Chem Biol* (revised).

In preparation

- Mosadeghzadeh N, **Kazemein Jasemi NS,** Akbarzadeh M, Majolee J, Zhang SC, Hordijk P, Dvorsky R. Ahmadian MR. Novel insights into the regulation of the RAC1-membrane interaction by RHOGDI1: an electrostatic force mechanism (to be submitted).

- **Kazemein Jasemi NS**, Dvorsky R, Estirado EM, Brunsveld L, Ahmadian MR. Genome-wide identification, functional classification and interaction selectivity landscape of human SH3 domain superfamily (in preparation).

REFERENCES

- **Reza Ahmadian**, Institute of Biochemistry and Molecular Biology II, Heinrich Heine University, Düsseldorf, (Reza.ahmadian@hhu.de)
- **Jürgen Scheller**, Institute of Biochemistry and Molecular Biology II, Heinrich Heine University, Düsseldorf, (jscheller@hhu.de)
- **Roland Piekorz**, Institute of Biochemistry and Molecular Biology II Heinrich Heine University, Düsseldorf, (roland.piekorz@hhu.de)
- **Gholam Hossein Riazi**, Institute of Biochemistry and Biophysics (IBB), Tehran University, Tehran, Iran, (ghriazi@ut.ac.ir)

4 Declaration

I do solemnly declare that my thesis is presentation of original research performed according to the “Principles of Good Scientific Practice” set out by Heinrich-Heine University of Düsseldorf. This thesis does not contain the data already published in public domain and it has never been submitted or accepted by any other institutions for the award of any other degrees.

Düsseldorf, April 2021

Neda Sadat Kazemein jasemi